British Journal of Pharmacology

March 1995

Volume 114 Number 6 pages 1105–1326

British Journal of Pharmacology (1995) 114, 1105-1106

SPECIAL REPORT

Inhibition by sodium nitroprusside of the expression of inducible nitric oxide synthase in rat neutrophils

S. Mariotto, *L. Cuzzolin, *A. Adami, †P. Del Soldato, [1]H. Suzuki & *G. Benoni

Istituto di Chimica Biologica and *Istituto di Farmacologia, Università di Verona and †Pharmaceutical Discovery Service, Milano, Italy

A well-known nitric oxide (NO)-releasing compound, sodium nitroprusside (SNP), decreases in a dose-dependent manner NO synthase (NOS) activity induced in rat neutrophils by treatment with lipopolysaccharide (LPS). This inhibitory action of SNP seems not to be due to its direct effect on the enzyme activity. The strong nitrosonium ion (NO^+) character of SNP could be responsible for its inhibition of NOS induction in neutrophils.

Keywords: Nitric oxide; nitric oxide synthase; sodium nitroprusside; neutrophil; nitrite/nitrate

Introduction The expression of inducible nitric oxide synthase (iNOS), present in various cells including macrophages, neutrophils and hepatocytes, is induced by lipopolysaccharide (LPS) and some lymphokines such as interferon gamma. The promoter region of iNOS gene has been shown to contain a number of regulatory sequences. Recently a feedback inhibition of NOS by NO· has been also reported in the macrophage (Assreuy *et al.*, 1993). There is little information available on a possible effect of NO on the induction of iNOS gene expression.

In this work we present data suggesting that a NO-releasing compound, sodium nitroprusside (SNP), acts as an inhibitor of iNOS expression in neutrophils of LPS-treated rats.

Methods *Animal treatment* Female Sprague-Dawley rats (Charles River, Italy) weighing 220–240 g, which had been fasted overnight but allowed free access to water, were treated with SNP (1, 5 and 10 mg kg^{-1} body weight) suspended in saline solution and administered orally in a volume of 1 ml 100 g^{-1} body weight; control rats received the vehicle. LPS (5 mg kg^{-1} body weight) was given via the tail vein 1 h after the drug administration. Four hours later, rats were anaesthetized with sodium pentobarbitone (60 mg kg^{-1} body weight) i.p. and blood samples were collected in EDTA-containing tubes.

Separation of neutrophils Neutrophils were separated by Ficoll-Hypaque density gradient centrifugation and erythrocytes removed by dextran sedimentation followed by lysis with NaCl 0.2% and then with NaCl 1.6%. Cell viability was 97%, as determined by Trypan blue exclusion, and the suspension contained less than 2% contaminating leukocytes.

Assay of NOS activity in the neutrophils NOS activity was estimated by measuring the conversion of L-[2,3,4,5-^{3}H]-arginine to L-[2,3,4,5-^{3}H]-citrulline according to a modification of the method described by Bredt & Snyder (1990).

Protein determination Protein concentration was measured by the method of Bradford (1976).

Quantitation of nitrite/nitrate Nitrite was assayed colorimetrically after reaction with the Griess reagent (Green *et al.*, 1982); nitrate was reduced to nitrite using a bacterial nitrate reductase according to a modification of the method described by Bartholomew (1984).

Chemicals L-[2,3,4,5-^{3}H]-arginine monohydrochloride (specific activity: 60 Ci/mmol^{-1}; 1 Ci = 37 GBq) was supplied by Amersham Life Science. (6**R**)-5,6,7,8-tetrahydro-l-biopterin was purchased from Dr B. Schircks Lab., Jona, Switzerland. Lipopolysaccharide from *E. coli* (serotype 026:B6) and sodium nitroprusside were Sigma products.

Statistical analysis The statistical analysis of data was performed by one-way analysis of variance followed by Dunnett's multicomparison test. $P<0.05$ or less was considered as indicative of significance.

Results As shown in Figure 1, in control rats NOS activity was not detectable under our assay conditions. LPS treat-

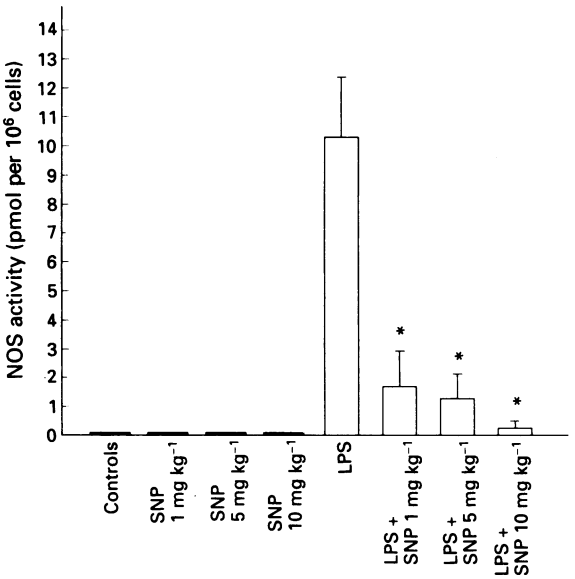

Figure 1 Changes in nitric oxide synthase (NOS) activity in rat neutrophils after treatment with sodium nitroprusside (SNP) or lipopolysaccharide (LPS) or both. The values are expressed as mean ± s.e. ($n = 6$). *$P<0.005$ significance compared to values obtained from LPS-treated rats.

[1] Author for correspondence.

ment induced a consistent increase of NOS activity in purified neutrophils. The co-administration to rats of LPS and SNP caused a dose-dependent decrease of NOS activity, while SNP alone did not induce NOS activity. SNP, at least up to a concentration of 100 μM, had no effect on the neutrophil NOS activity under the assay conditions used in this work (data not shown).

Plasma NO_2^-/NO_3^- levels are shown in Figure 2. LPS administration produced a 7 fold increase of NO_2^-/NO_3^- concentrations. No significant changes were observed in rats treated with SNP before LPS administration. On the contrary, plasma NO_2^-/NO_3^- levels increased in a dose-dependent manner in rats to which only SNP was administered.

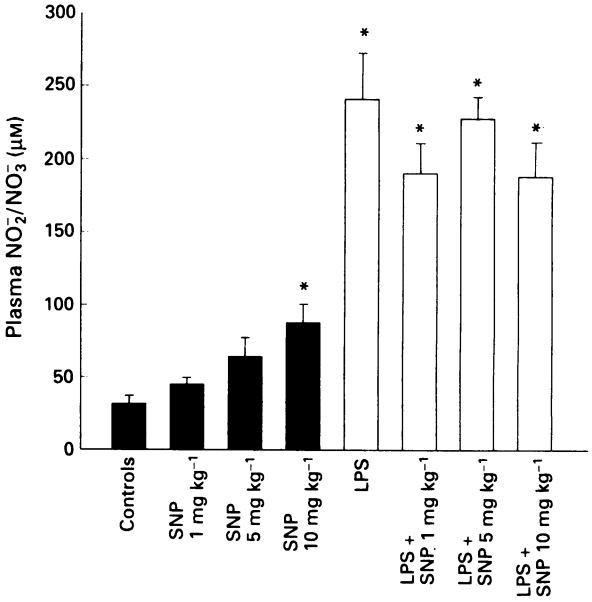

Figure 2 Plasma NO_2^-/NO_3^- levels in rats to which lipopolysaccharide (LPS) and sodium nitroprusside (SNP) had been administered. The values are expressed as mean ± s.e. ($n = 6$). *$P < 0.005$ significance compared to control rats.

Discussion In the present study, SNP has been shown to inhibit, in a dose-dependent manner, neutrophil NOS activity induced by LPS. In animals treated with SNP alone, no modification in NOS activity could be detected, while a dose-dependent increase in plasma NO_2^-/NO_3^- levels was observed, suggesting the gastrointestinal absorption of the drug. The decrease in NOS activity in neutrophils of rats co-treated with LPS and various doses of SNP should not be due to a direct inhibitory effect of the drug on NOS, since 100 μM SNP added to the assay mixture did not affect the neutrophil NOS activity (data not shown). This is in contrast with the data of Assreuy *et al.* (1993), that suggest a direct inhibitory effect of NO-releasing compounds on macrophage NOS. The results reported here raise the question how SNP could decrease NOS activity in the neutrophils. A possible answer could be found in a recent paper of Lipton *et al.* (1993) on the different effects shown by nitrogen monoxide when it was used in different redox states. SNP is a nitroso-compound with a strong nitrosonium ion (NO^+) character. Although it can also readily generate NO·, a reductive activation is required for this. An increased level of NOS activity induced by LPS treatment and the consequent increase of plasma NO_2^-/NO_3^- concentration suggest that endogenous NO did not exert, at least under our experimental conditions, an inhibitory effect on the induction of neutrophil NOS. In this context, the data presented here seem to support the hypothesis that NO exogenously released from SNP could act because of its strong NO^+ character, as an inhibitory agent on iNOS expression, while endogenous NO might not have a significant effect on this event. The absence of significant differences between plasma NO_2^-/NO_3^- levels in rats treated with LPS alone and in those treated also with the drug could be explained in the following two ways: (a) a decrease in endogenous NO· production due to an inhibition of iNOS expression in the neutrophils caused by NO^+ which derives from SNP or, (b) an increase in NO· plasma concentration, which could be released directly from SNP under appropriate physiological conditions.

In conclusion, the results obtained by us in an *in vivo* system suggest an inhibitory action of the NO- releasing compound SNP on the iNOS expression in rat neutrophils; this inhibitory action should be ascribed to a strong nitrosonium ion character.

References

ASSREUY, J., CUNHA, F.Q., LIEW, F.Y. & MONCADA, S. (1993). Feedback inhibition of nitric oxide synthase activity by nitric oxide. *Br. J. Pharmacol.*, **108**, 833–837.

BARTHOLOMEW, B. (1984). A rapid method for the assay of nitrate in urine using the nitrate reductase enzyme of E.coli. *Food Chem. Toxicol.*, **22**, 541–543.

BRADFORD, M.M. (1976). A rapid and sensitive method for the quantification of microgram of protein utilizing the principle of protein binding. *Anal. Biochem.*, **72**, 248–254.

BREDT, D.S., & SNYDER, S.H. (1990). Isolation of nitric oxide synthase, a calmodulin-requiring enzyme. *Proc. Natl. Acad. Sci. U.S.A.*, **87**, 682–685.

GREEN, L.C., WAGNER, D.A., GLOGOWSKI, J., SKIPPER, P.L., WISHNOK, J.S. & TANNENBAUM, S.R. (1982). Analysis of nitrate, nitrite and ^{15}N nitrate in biological fluids. *Anal. Biochem.*, **126**, 131–138.

LIPTON, S.A., CHOI, Y., PAN, Z., LEI, S.Z., CHEN, H.V., SUCHER, N.J., LOSCALZO, J., SINGEL, D.J. & STAMLER, J.S. (1993). A redox-based mechanism for the neuroprotective and neurodestructive effects of nitric oxide and related nitroso compounds. *Nature*, **364**, 626–632.

(Received November 21, 1994
Accepted December 15, 1994)

British Journal of Pharmacology (1995) 114, 1107-1109

SPECIAL REPORT

Evidence that 5-hydroxytryptamine release in rat dorsal raphé nucleus is controlled by 5-HT_{1A}, 5-HT_{1B} and 5-HT_{1D} autoreceptors

Colin Davidson & [1]Jonathan A. Stamford

Anaesthetics Unit (Neurotransmission Laboratory), London Hospital Medical College, Alexandra Wing, Royal London Hospital, Whitechapel, London E1 1BB.

Electrically stimulated 5-hydroxytryptamine (5-HT) release was monitored in slices of rat dorsal raphé nucleus (DRN) by fast cylic voltammetry. Pseudo-single pulse stimulations (5 pulses at 100 Hz) were used to enable the effect of various receptor agonists to be seen without competition from endogenously released transmitter. The selective 5-HT_{1A} receptor agonist, (+)-8-OH-DPAT (1.0 μM) decreased stimulated 5-HT release to 31 ± 3% of controls. This decrease was inhibited by the 5-HT_{1A} receptor antagonists, (+)-WAY-100135 (1.0 μM) and WAY-100635 (0.1 μM) but not by the 5-$HT_{1D/B}$ antagonist, GR127935 (0.05 μM). The selective 5-HT_{1B} receptor agonist, CP-93129 (0.3 μM) decreased stimulated 5-HT release to 61 ± 4% of control. This effect was antagonized by the 5-HT_{1B} receptor antagonist, isamoltane (0.5 μM) but not by (+)-WAY-100135. The 5-HT_{1D} agonist, sumatriptan (0.5 μM) decreased stimulated 5-HT release to 52 ± 2 % of controls. This decrease was blocked by GR-127935 but not by WAY-100635. These results suggest that 5-HT release in the rat DRN is under the control of 5-HT_{1A}, 5-HT_{1B} and 5-HT_{1D} autoreceptors.

Keywords: Dorsal raphé nucleus; 5-hydroxytryptamine; 5-HT_{1A} autoreceptor; 5-HT_{1B} autoreceptor; 5-HT_{1D} autoreceptor; fast cyclic voltammetry; brain slice

Introduction The dorsal raphé nucleus (DRN) is one of the primary 5-hydroxytryptamine (5-HT) cell body areas and projects to most parts of the brain. Traditionally 5-HT neurotransmission in the DRN is thought to be under 5-HT_{1A} receptor control: Stimulation of 5-HT_{1A} autoreceptors slows raphé cell firing (Sprouse & Aghajanian, 1987) and decreases 5-HT release (Davidson & Stamford, 1994).

Recently however, studies in the guinea-pig have shown that 5-HT_{1D} autoreceptors can also influence 5-HT release in the DRN (Starkey & Skingle, 1994). The rat homologue of the 5-$HT_{1D\beta}$ receptor is the 5-HT_{1B} receptor (Hoyer *et al.*, 1994) and we have now shown (Davidson & Stamford, 1994) that 5-HT release in the rat DRN may also be reduced by the 5-$HT_{1B/D}$ agonist, CP-94253 (3-1,2,3,5,6-tetrahydro-4-pyridyl)-5-propoxypyrrolo[3,2-*b*]pyridine).

The rat is not generally held to have functional 5-HT_{1D} receptors, although mRNA for the rat homologue of the 5-$HT_{1D\alpha}$ receptor is found in the DRN (Hamblin *et al.*, 1992) and it has been tentatively suggested that there may be functional 5-HT_{1D} receptors in the rat DRN (Pineyro *et al.*, 1994). However these conclusions were largely based on the use of mianserin as a 5-HT_{1D} antagonist, a drug with only modest selectivity over 5-HT_{1B} receptors (Hoyer *et al.*, 1994). In this study we have used selective agonists and antagonists for 5-HT_{1A}, 5-HT_{1B} and 5-HT_{1D} receptors to determine which autoreceptors are involved in the control of electrically stimulated 5-HT release in the rat DRN.

Methods *Brain slices* Male Wistar rats (100-150 g) were killed by cervical dislocation. Brains were rapidly removed under ice-cold artificial cerebrospinal fluid (ACSF). Coronal slices (350 μm) of DRN were taken at +4.8 mm versus the interaural line (Paxinos & Watson, 1986) and placed in a standard brain slice chamber. Slices were superfused with warmed (32°C) oxygenated (95% O_2/5% CO_2) ACSF at 1.2 ml min^{-1} and allowed to equilibrate for 1 h before electrical stimulation.

[1] Author for correspondence.

Fast cyclic voltammetry Fast cyclic voltammetry was used to monitor 5-HT release: a triangular voltage waveform, −1.0 to +1.4 V, 480 V/s, was applied to a carbon fibre microelectrode (CFM: tip size 40 × 8 μm) twice per second. A sample and hold circuit was set to monitor current at the 5-HT oxidation potential, +0.6 V versus Ag/AgCl and its output stored on computer.

Stimulation protocol The CFM was placed in the centre of the DRN and a bipolar stimulating electrode located 200 μm ventrally. Pseudo-single pulse electrical stimulations consisting of five 0.1 ms duration pulses (100 Hz, 10 mA) were applied every 5 min. Stimulations were applied until 4 stable 5-HT release events were recorded, at which point the agonist was added for 40 min. Where an antagonist was also used, it was added to the superfusate at least 80 min before the agonist to allow any effect to reach a stable plateau.

Statistical analysis Each group of drugs was analysed by one-way ANOVA, followed by *post-hoc* application of the Tukey-Kramer test to locate significant differences. Probability levels of $P<0.05$ were deemed significant.

Drugs N-[2-[4-(2-methoxyphenyl)-1-piperazinyl]ethyl]-N-(2-pyridinyl)cyclohexanecarboxamide trihydrochloride (WAY-100635), (+)-8-hydroxy-2-(di-*n*-propylamino)tetralin ((+)-8-OH-DPAT), 3-(1,2,5,6-tetrahydropyrid-4-yl)pyrrolo[3,2-*b*]pyrid-5-one (CP-93129), N-[4-methoxy-3-(4-methyl-1-piperazinyl)phenyl]-2'-methyl-4'-(5-methyl-1,2,4-oxadiozol-3-yl)[1,1-biphenyl]-4-carboxamide (GR-127935), (+)-N-tert-butyl-3-(4-[2-methoxyphenyl]piperazin-1-yl)-2-phenylpropanamide ((+)-WAY-100135), sumatriptan and isamoltane were initially dissolved in distilled water to make 1 mM stock solutions. A few drops of dimethyl sulphoxide were initially used to dissolve GR-127935. Further dilutions were made in ACSF.

Results The selective 5-HT_{1A} agonist, (+)-8-OH-DPAT (1.0 μM) significantly ($P<0.05$ to 0.001) decreased stimulated 5-HT release to 31 ± 3% of controls (Figure 1a). This

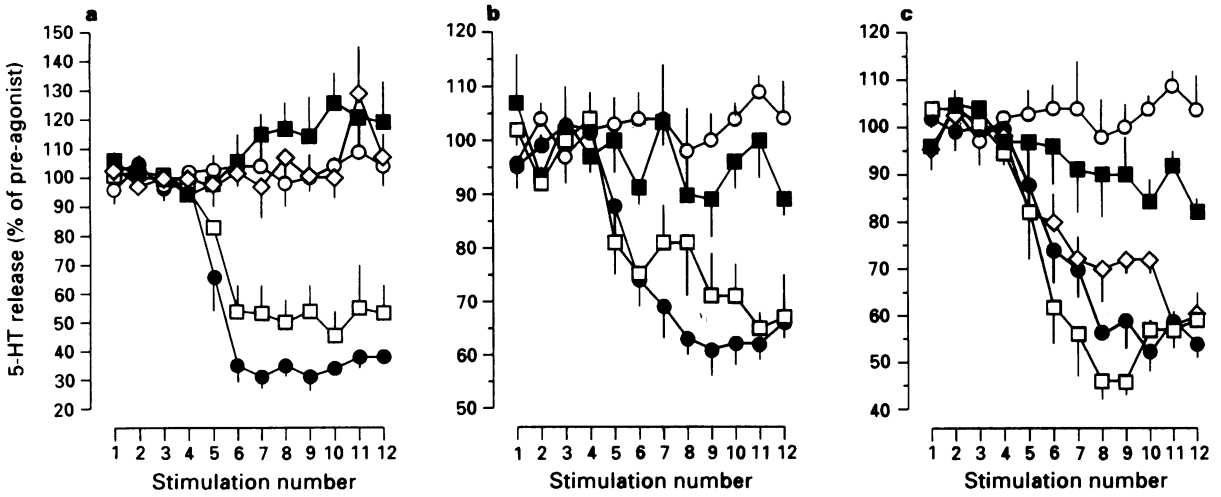

Figure 1 (a) Effects of 8-OH-DPAT (1.0 μM) on stimulated 5-HT release in the DRN either alone (●) or after WAY-100635 (0.1 μM: ◇), (+)-WAY-100135 (1.0 μM: ■) or GR-127935 (0.05 μM: □). Controls (○) are also shown for comparison. 8-OH-DPAT was significantly ($P<0.05$ to 0.001) different from controls (stimulation 5 onward) and from 8-OH-DPAT in the presence of (+)-WAY-100135 and WAY-100635 (stimulation 6 onward). 8-OH-DPAT was not significantly different from GR-127935 at any time point. (b) Effects of CP-93129 (0.3 μM) on stimulated 5-HT release either alone (●) or after (+)-WAY-100135 (1.0 μM: □) or isamoltane (0.5 μM: ■). Controls (○) are also shown for comparison. CP-93129 was significantly ($P<0.05$ to 0.001) different from controls (stimulation 6 onward) and from CP-93129 in the presence of isamoltane (stimulations 7,10 and 11). CP-93129 was not significantly different from (+)-WAY-100135 at any time point. (c) Effects of sumatriptan (0.5 μM) on stimulated 5-HT release either alone (●) or after isamoltane (0.5 μM: ◇), WAY-100635 (0.1 μM: □) or GR-127935 (0.05 μM: ■). Controls (○) are also shown for comparison. Sumatriptan was significantly ($P<0.05$ to 0.001) different from controls (stimulation 8 onward), from sumatriptan in the presence of GR-127935 (stimulation 8 onward) and isamoltane (stimulation 10). Sumatriptan was not significantly different from WAY-100635 at any time point. All values are means (± s.e.mean, $n=4$). Agonists were given immediately after stimulation 4. For abbreviations, see text.

decrease was prevented by (+)-WAY-100135 (1.0 μM) and WAY-100635 (0.1 μM). GR-127935 (0.05 μM) had no effect on the response to (+)-8-OH-DPAT. CP-93129 (0.3 μM) also decreased stimulated 5-HT release ($P<0.05$ to 0.001), to 61 ± 4% of control (Figure 1b), an effect antagonised by isamoltane (0.5 μM) but not by (+)-WAY-100135 (1.0 μM). Figure 1c shows that sumatriptan (0.5 μM) also decreased stimulated 5-HT release to 52 ± 2% of controls ($P<0.01$ to 0.001). This effect was inhibited by GR-127935 but not by WAY-100635 or isamoltane.

Discussion Figure 1a shows that the selective 5-HT_{1A} agonist, (+) 8-OH-DPAT, inhibits 5-HT release in the DRN. The complete antagonism of (+)-8-OH-DPAT by the selective 5-HT_{1A} antagonists (+)-WAY-100135 and WAY-100635 confirms that this effect is wholly mediated via 5-HT_{1A} receptors.

Figure 1b shows that the selective 5-HT_{1B} agonist, CP-93129 (Koe *et al.*, 1992) also inhibits 5-HT release. Since the effect is blocked by the selective 5-HT_{1B} antagonist, isamoltane but not by (+)-WAY-100135, the data suggest that there is a functional 5-HT_{1B} autoreceptor in the rat DRN. This is directly analogous to the finding of a 5-HT_{1D} receptor in the guinea-pig DRN by Starkey & Skingle (1994) and may suggest a parallel role for the 5-HT_{1B} site in the rat.

Most interestingly, the selective 5-HT_{1D} agonist, sumatriptan, also inhibits 5-HT release in the DRN and the absence of effect of (+)-WAY-100135 (at a concentration that blocks (+)-8-OH-DPAT) excludes an action via 5-HT_{1A} receptors. Conversely, the 5-$HT_{1D/B}$ antagonist, GR-127935 shows good antagonism of sumatriptan, while isamoltane, which has a pK_B for 5-HT_{1D} receptors of 4.4 compared with 7.3 at the 5-HT_{1B} receptor (Hoyer *et al.*, 1994), had no significant effect. Although it is possible that, at this concentration (0.5 μM), sumatriptan has a small effect at the 5-HT_{1B} receptor ($pK_B = 6.0$: Hoyer *et al.*, 1994), the absence of effect of isamoltane makes this unlikely. The 5-HT_{1E} subtype is also unlikely to explain the actions of sumatriptan and GR-127935 since their affinity at this site is at least 2 orders of magnitude lower than at the 5-HT_{1D} receptor (Starkey & Skingle, 1994).

The observation of multiple functional 5-HT_1 subtypes in the DRN begs the question: where are these receptors located? The 5-HT_{1B} receptor is often assumed to be a terminal autoreceptor and may therefore be located on terminals in the DRN from other 5-hydroxytryptaminergic nuclei (Kalen *et al.*, 1985) or from axon collaterals within the DRN itself (Chazel & Ralston, 1987). The presence of 5-HT_{1D} mRNA in the DRN (Hamblin *et al.*, 1992) may suggest that DRN 5-HT_{1D} receptors are on dendrites or recurrent collaterals. Further work is in progress to clarify these matters.

This work was supported by SmithKline Beecham Pharmaceuticals. We also thank Wyeth for the gift of (+)-WAY-100135.

References

CHAZEL, G. & RALSTON III, H.J. (1987). Serotonin-containing structures in the nucleus raphe dorsalis of the cat: an ultrastructural analysis of dendrites, presynaptic dendrites, and axon terminals, *J. Comp. Neurol.*, **259**, 317–329.

DAVIDSON, C. & STAMFORD, J.A. (1994). Not only 5-HT_{1A} but also 5-HT_{1B} receptors modulate serotonin efflux in the rat dorsal raphe nucleus. In *Monitoring Molecules in Neuroscience*. ed. Louilot, A., Durkin, T., Spampinato, U. & Cador, M. pp. 195–6. Seignosse: Univ. Bordeaux.

HAMBLIN, M.W., MCGUFFIN, R.W., METCALF, M.A., DORSA, D.M., & MERCHANT, K.M. (1992). Distinct 5-HT_{1B} and 5-HT_{1D} serotonin receptors in rat: Structural and pharmacological comparison of the two cloned receptors. *Mol. Cell. Neurosci.*, **3**, 578–587.

HOYER, D., CLARKE, D.E., FOZARD, J.R., HARTIG, P.R., MARTIN, G.R., MYLECHARANE, E.J. SAXENA, P.R. & HUMPHREY, P.P.A. (1994). VII. International Union of Pharmacology classification of receptors for 5-hydroxytryptamine (serotonin). *Pharmacol. Rev.*, **46**, 157–203.

KALEN, P., KARLSON, M., & WIKLUND, L. (1985). Possible excitatory amino acid afferents to nucleus raphe dorsalis of the rat investigated with retrograde wheat germ agglutinin and D-(^{3}H)aspartate tracing. *Brain Res.*, **360**, 285–297.

KOE, B.K., NIELSON, J.A., MACOR, J.E., & HEYM, J. (1992). Biochemical and behavioural studies of the 5-HT_{1B} receptor agonist, CP-94253. *Drug. Dev. Res.*, **26**, 241–250.

PAXINOS, G. & WATSON, C. (1986). *The Rat Brain in Stereotaxic Coordinates.*, London: Academic Press.

PINEYRO, G., DEMONTIGNY, C., & BLIER, P. (1994). 5-HT_{1D} receptors control somatodendritic release of 5-HT in the rat: Electrophysiological and voltammetry studies in the dorsal raphe nucleus. *Neuropsychopharmacol.*, **10**, 269S.

SPROUSE, J.S., & AGHAJANIAN, G.K. (1987). Electrophysiological responses of serotonergic dorsal raphe neurones to 5-HT_{1A} and 5-HT_{1B} agonists. *Synapse*, **1**, 3–9.

STARKEY, S.J. & SKINGLE, M. (1994). 5-HT_{1D} as well as 5-HT_{1A} autoreceptors modulate 5-HT release in the guinea-pig dorsal raphe nucleus. *Neuropharmacol.*, **33**, 393–402.

(Received November 25, 1994
Accepted December 19, 1994)

British Journal of Pharmacology (1995) 114, 1110-1116

Endothelin ET_A and ET_B mRNA and receptors expressed by smooth muscle in the human vasculature: majority of the ET_A sub-type

[1]Anthony P. Davenport, Gillian O'Reilly & Rhoda E. Kuc

Clinical Pharmacology Unit, University of Cambridge, Addenbrooke's Hospital, Cambridge CB2 2QQ

1 We measured the ratio of ET_A and ET_B sub-types in the media (containing mainly smooth muscle) of human cardiac arteries (aorta, pulmonary and coronary), internal mammary arteries and saphenous veins.

2 In saturation experiments, [^{125}I]-endothelin-1 ([^{125}I]-ET-1) bound with high affinity to the media of each vessel ($n = 3$ individuals or homogenate preparations ± s.e.mean):coronary artery, $K_D = 0.14 \pm 0.02$ nM, $B_{max} = 71.0 \pm 21.0$ fmol mg^{-1} protein; pulmonary artery, $K_D = 0.85 \pm 0.25$ nM, $B_{max} = 15.2 \pm 10.3$ fmol mg^{-1} protein; aorta, $K_D = 0.51 \pm 0.02$ nM, $B_{max} = 9.4 \pm 4.4$ fmol mg^{-1} protein; internal mammary artery, $K_D = 0.34 \pm 0.31$ nM, $B_{max} = 2.0 \pm 0.5$ fmol mg^{-1} protein and saphenous vein, $K_D = 0.28 \pm 0.05$ nM, $B_{max} = 52.8 \pm 1.0$ fmol mg^{-1} protein. In each vessel, over the concentration-range tested, Hill slopes were close to unity and a one site fit was preferred to a two site model.

3 In competition binding assays, the ET_A selective ligand, BQ123 inhibited the binding of 0.1 nM [^{125}I]-ET-1 to the media in a biphasic manner. In each case, a two site fit was preferred to a one or three site model: coronary artery, $K_D ET_A = 0.85 \pm 0.03$ nM, $K_D ET_B = 7.58 \pm 2.27$ μM, ratio = 89:11%; pulmonary artery, $K_D ET_A = 0.27 \pm 0.05$ nM, $K_D ET_B = 24.60 \pm 5.34$ μM, ratio = 92:8%; aorta, $K_D ET_A = 0.80 \pm 0.40$ nM, $K_D ET_B = 2.67 \pm 2.60$ μM ratio = 89:11%; saphenous vein, $K_D ET_A = 0.55 \pm 0.17$ nM, $K_D ET_B = 14.4 \pm 0.26$ μM, 85:15% ($n = 3$ individuals or homogenate preparations ± s.e.mean). BQ123 showed up to 18000 fold selectivity for the ET_A over the ET_B sub-type. The ET_A-selective ligand, [^{125}I]-PD151242 labelled 85% of the receptors detected by a fixed concentration of [^{125}I]-ET-1 in media of internal mammary artery, measured by quantitative autoradiography. In contrast, the density of ET_B receptors detected with [^{125}I]-BQ3020 was 7.0 ± 1.5 amol mm^{-2}, representing about 8% of [^{125}I]-ET-1.

4 A single band corresponding to the expected position for mRNA encoding the ET_A receptor (299 base pairs) was found in the media in each of the five vessels ($n = 3$ individuals) using reverse-transcriptase polymerase chain reaction assays. A single band corresponding to the ET_B sub-type (428 base pairs) was also always detected.

5 ^{35}S-labelled antisense probes to ET_A and ET_B hybridised to the media of epicardial coronary arteries as well as intramyocardial vessels, confirming the presence of mRNA encoding both sub-types in the vascular smooth muscle of the vessel wall.

6 Although mRNA for both receptors was detected, competition binding using BQ123 demonstrated that the majority (at least 85%) of ET receptors present in smooth muscle are the ET_A sub-type. These results provide further support for the hypothesis that the ET_A sub-type is the receptor that must be blocked in humans to produce a beneficial vasodilatation in pathophysiological conditions where there is an increase in peptide concentration or receptor density.

Keywords: Endothelin; PD151242; BQ123; BQ3020; ET_A mRNA; ET_B mRNA; autoradiography; polymerase chain reaction; aorta; coronary artery; internal mammary artery; pulmonary artery; saphenous vein

Introduction

In man, three genes have been predicted to encode three endothelin (ET) peptides, ET-1, ET-2 and ET-3. Biochemical analysis by radioimmunoassay and high performance liquid chromatography has shown that ET-1 and ET-2 are the most abundant isoforms expressed by the human cardiovascular system (Plumpton *et al.*, 1993). ET-1 and ET-2 (but not ET-3) mRNA has been detected in human endothelial cells (O'Reilly *et al.*, 1993a,b). Immunoreactive mature ET, and the precursors big ET-1 and big ET-2 (but not big ET-3) have been localized to the cytoplasm of endothelial cells from a range of human vascular beds including internal mammary artery and saphenous vein (Howard *et al.*, 1992). The widespread distribution of ET-1 (and possibly ET-2) is consistent with a proposed role as a ubiquitous endothelium-derived vasoactive peptide and a corresponding general expression of ET receptors in smooth muscle of the vessel wall would be expected. ET-3 is the only endogenous isoform that is able to distinguish between the two receptor sub-types having low affinity for the ET_A receptor compared to ET-1 but a similar affinity for the ET_B sub-type. Since ET-3 is a poor agonist at ET_A receptors, the predominance of this subtype in the smooth muscle of the human vasculature would be consistent with the lack of expression of ET-3 by endothelial cells of blood vessels.

In support of this hypothesis, in isolated epicardial coronary arteries (Davenport *et al.*, 1993) and renal vessels (Maguire *et al.*, 1994b) ET-1-induced vasoconstriction appears to be mediated mainly by the ET_A sub-type since ET-3 is about two orders of magnitude less potent than ET-1. Secondly, the ET_A-selective antagonists cause a rightward and parallel shift of the ET-1-induced constriction in these vessels. However, mRNA encoding both sub-types have been detected and binding assays using sub-type selective ligands suggest ET_B as well as ET_A receptors are present.

[1] Author for correspondence.

In animals, ET-1 can elicit constriction through both ET_A and ET_B receptors although the pattern is complex: the sub-type ratio varies in different vascular beds in the same species and in the same vascular bed in different species (Davenport & Maguire, 1994). For example, constriction appears to be mediated only by ET_A receptors in rat aorta (Sumner *et al.*, 1992) but by ET_B receptors in rabbit pulmonary artery (White *et al.*, 1994a). In porcine coronary artery, the ET_A selective antagonist, BQ123 does not block all of the ET-1-induced contraction, indicating activation of both sub-types (Ihara *et al.*, 1992).

ET-1 is a potent constrictor of human isolated vessels. The peptide has an EC_{50} of 15 nM in aorta (Maguire & Davenport, 1995). In pulmonary arteries, EC_{50} values have a range of 0.1–17 nM (Hay *et al.*, 1993; Fukuroda *et al.*, 1994; Maguire & Davenport, 1995) and in coronary arteries the range is 1–130 nM (Franco-Cereceda, 1989; Davenport *et al.*, 1989b; Godfraind *et al.*, 1993; Maguire & Davenport, 1993; 1994; 1995; Opgaard *et al.*, 1994). In the internal mammary artery, EC_{50} values range from 4–10 nM (Costello *et al.*, 1990; Luscher *et al.*, 1990; Bax *et al.*, 1993; Maguire & Davenport, 1993, 1994; 1995; White *et al.*, 1994b) and 3–18 nM in the sapheneous vein (Luscher *et al.*, 1990; Costello *et al.*, 1990; Maguire & Davenport, 1993; 1994; 1995; Seo *et al.*, 1994; Akar *et al.*, 1994). However, whether the media of all of these vessels express ET_A and ET_B mRNA as well as the corresponding receptor protein has not been examined in detail.

Our aim was to use ligand binding to measure the ratio of ET_A and ET_B sub-types in the media (containing mainly smooth muscle) of human cardiac arteries where animal studies suggest ET-1 constriction occurs only via ET_A (rat aorta), ET_B (rabbit pulmonary artery) or both sub-types (porcine coronary artery). We also compared the internal mammary artery and saphenous veins where ET_B-mediated constrictor responses have been reported (White *et al.*, 1994b; Seo *et al.*, 1994). These results were correlated with the expression of mRNA encoding each receptor using reverse-transcriptase polymerase chain reaction (RT-PCR) assays.

Methods

Vessels

Aorta, pulmonary arteries, left and right main stem coronary arteries were obtained at the time of operation from male and female patients undergoing heart transplantation (age range 43–56 years) for ischaemic heart disease. Saphenous vein and left internal mammary artery were obtained from male and female patients undergoing coronary artery bypass grafts. The endothelial layer was scraped off and the adventitia separated from the media (confirmed by microscopy of haematoxylin and eosin stained sections). Tissue was snap frozen immediately in liquid nitrogen and stored at − 70°C until use.

Saturation binding assays: slide mounted sections

For ligand binding in larger vessels (aorta, pulmonary and coronary arteries), sections (10 μm thick) were cut on a cryostat microtome and mounted onto gelatin-coated microscope slides. In saturation experiments, tissue sections were pre-incubated for 15 min in HEPES buffer as previously described (Davenport *et al.*, 1989a,b; 1991; Karet & Davenport, 1993). Briefly, sections were then incubated with increasing concentrations (8 pM–8 nM) of [^{125}I]-ET-1 in incubation buffer for 2 h at 23°C. Non-specific binding was defined with 1 μM of unlabelled ET-1. Sections were rinsed in Tris-HCl buffer (0.05 M, pH 7.4) at 4°C (3 × 5 min) and the amount of radioactivity measured in a gamma counter.

Homogenate binding

Frozen saphenous veins and internal mammary arteries (typically from a minimum of 30 individuals to obtain sufficient tissue) were homogenized in ice cold 50 mM Tris-HCl buffer, pH 7.4 (containing 5 mM $MgCl_2$, 5 mM EDTA, 1 mM EGTA, 10,000 units ml^{-1} aprotinin). The homogenate was centrifuged at 1000 *g* for 1 min at 4°C, the pellet discarded and the supernatant re-centrifuged at 40,000 *g* for 30 min. The resulting pellet was washed and resuspended three times in the Tris-HCl buffer. The final pellet was resuspended in 50 mM HEPES buffer, pH 7.4 (containing 5 mM $MgCl_2$, 0.3% wt/vol bovine serum albumen). After measuring the protein, the membranes were diluted to give typical concentrations of about 6 mg ml^{-1} protein.

Aliquots (100 μl) were added to tubes containing increasing amounts of [^{125}I]-ET-1 (8 pM–8 nM) in HEPES incubation buffer for 2 h at 23°C. Non-specific binding was determined with 1 μM unlabelled ET-1. The final protein concentration was 2 mg ml^{-1}. Each assay was terminated by centrifugation (20,000 *g*, 10 min, 4°C) to separate bound from free radioligand. The supernatants were discarded and the pellets resuspended in 1 ml ice cold 50 mM Tris-HCl buffer (pH 7.4 at 4°C). The tubes were re-centrifuged (20,000 *g*, 10 min, 4°C), the supernatants discarded and the pellets counted in a gamma counter.

Competition experiments

Competition assays were carried out under the conditions described above. Sections of aorta, pulmonary and coronary artery or homogenate of saphenous vein were incubated with 0.1 pM [^{125}I]-ET-1 and increasing concentrations (20 pM–100 μM) of BQ123. Non-specific binding was defined by use of 1 μM unlabelled ET-1. The results of binding experiments were analysed with EBDA and LIGAND programmes as previously described (Molenaar *et al.*, 1992; 1993; Davenport *et al.*, 1994a). The presence of 1, 2 or 3 sites was tested by the *F*-ratio test in LIGAND. The model adopted was that which provided the best fit ($P < 0.05$).

Autoradiography

Quantitative autoradiography was used to compare the density of ET_A and ET_B receptors in the internal mammary artery, as there was insufficient material for competition binding assays. Sections of internal mammary artery (as well as aorta, pulmonary, coronary arteries and saphenous veins) from three individuals were incubated in buffer containing either 0.1 nM [^{125}I]-ET-1 to visualize all ET receptors, 0.1 nM [^{125}I]-PD151242 to visualize ET_A (Davenport *et al.*, 1994a,c; Peter & Davenport, 1994; 1995) or 0.1 nM [^{125}I]-BQ3020 (Molenaar *et al.*, 1992; 1993) to detect the ET_B sub-type. [^{125}I]-PD151242 has previously been shown to be highly selective for the human ET_A sub-type and the unlabelled compound is a competitive antagonist causing a parallel rightward shift of the ET-1 concentration-response curve in human isolated coronary arteries (Davenport *et al.*, 1994a). [^{125}I]-BQ3020 is selective for the human ET_B sub-type (Molenaar *et al.*, 1992; 1993) and a potent agonist at animal ET_B receptors (Gardiner *et al.*, 1994). In each case, non-specific binding was determined by incubating adjacent consecutive sections in the presence of 1 μM of the corresponding unlabelled peptides. Sections were exposed to radiation-sensitive film (Hyperfilm βmax) with radioactive standards and quantified by computer-assisted densitometry as previously described (Davenport *et al.*, 1988).

Reverse-transcriptase polymerase chain reaction (RT-PCR) assays

Total RNA was extracted from the media of aorta, pulmonary, coronary, internal mammary arteries and saphenous

veins from three individuals by a single step guanidinium isothiocyanate method. cDNA synthesis and RT-PCR assays were carried out as previously described (O'Reilly *et al.*, 1992; 1993a,b; Karet *et al.*, 1994). Avian myoblastosis virus reverse transcriptase was used to synthesize first strand cDNA from 2.5 μg RNA. Nested PCR amplification was carried out using 1 μl cDNA template, 5 μl reaction buffer (100 nM Tris-HCl, pH 8.3 at 25°C, 500 mM KCl and 15 mM $MgCl_2$), 5 μl dNTPs (2 mM), 5 μl of each of the appropriate oligonucleotide primer pairs (designed from published nucleotide sequences) and 2.5 U *Taq* DNA polymerase. PCR products were separated by agarose gel electrophoresis and the bands stained with ethidium bromide. These previously cloned and sequenced PCR products show 100% homology with published sequences for ET_A or ET_B (O'Reilly *et al.*, 1992).

In situ *hybridization*

The distribution of ET_A and ET_B mRNA was compared in more detail in coronary arteries by *in situ* hybridization. Assays were carried out as previously described (Molenaar *et al.*, 1993). Briefly, ET_A (bases 439–737) and ET_B (bases 497–924) PCR amplified DNA bands were cloned into pBluescript II KS (Stratagene Inc., La Jolla, California, U.S.A.) and the linearised inserts used as a template to generate ^{35}S labelled sense and antisense RNA probes. Sections of epicardial coronary artery and intra-ventricular septum containing intra-myocardial vessels were exposed to radiation-sensitive film together with standards. The amount of probe specifically hybridized was determined by digitally subtracting the autoradiographical image of the sense control probe from that of the antisense probe by computer-assisted densitometry as previously described (Davenport & Nunez, 1990).

Table 1 Dissociation constants (K_D), maximal density of receptors (B_{max}) and Hill coefficients (n_H) for [^{125}I]-endothelin-1 ([^{125}I]-ET-1) binding in human vessels

	K_D (nM)	B_{max} (fmol mg^{-1} protein)	n_H
Arteries:			
Coronary	0.14 ± 0.02	71.0 ± 21.0	0.99 ± 0.01
Pulmonary	0.85 ± 0.25	15.2 ± 10.3	0.85 ± 0.08
Aorta	0.51 ± 0.02	9.4 ± 4.4	0.85 ± 0.11
Internal mammary	0.34 ± 0.31	2.0 ± 0.5	0.92 ± 0.10
Vein:			
Saphenous	0.28 ± 0.05	52.8 ± 1.0	0.89 ± 0.01

For aorta, coronary and pulmonary arteries values are the mean ± s.e.mean of three individuals; for saphenous vein and internal mammary artery values are the mean ± s.e.mean of three separate experiments using vessels pooled from about 30 individuals.

Drugs

BQ123, (cyclo [D-Asp-L-Pro-D-Val-L-Leu-D-Trp-], Ihara *et al.*, 1992) and BQ3020, [$Ala^{11,15}$]Ac-ET-$1_{(6-21)}$ (Molenaar *et al.*, 1992) were synthesized by solid phase t-Boc chemistry. PD151242, (N-[(hexahydro-1-azepinyl)carbonyl]L-Leu(1-Me) D-Trp-D-Tyr (Davenport *et al.*, 1994a,c) was synthesized and supplied by Dr A.M. Doherty (Parke-Davis Pharmaceutical Research Division). Peptide concentrations were determined by u.v. spectrophotometry. [^{125}I]-ET-1, [^{125}I]-PD151242 and [^{125}I]-BQ3020 were from Amersham International plc, (Amersham, UK); unlabelled ET-1 from Novabiochem (Nottingham, UK). Taq polymerase was from Perkin-Elmer Cetus (London, UK), reverse-transcriptase from Anglian Biotech (Essex, UK). All other reagents were from Sigma Chemical Co. (Poole, Dorset, UK), BDH (Poole, Dorset, UK) or Fisons (Loughborough, Leicester, UK).

Results

Ligand binding

[^{125}I]-ET-1 bound with a similar sub-nanomolar affinity to the media of all of the vessels examined (Table 1). In each vessel, over the concentration-range tested, Hill slopes were close to unity and a one site fit was preferred to a two site model. The highest densities of ET receptors were present in the coronary arteries; lowest levels were detected in the internal mammary artery.

BQ123 competed for the binding of a fixed concentration of [^{125}I]-ET-1 in a biphasic manner in the media of all vessels (Table 2, Figure 1). In each case, a one site model could not be fitted to these data and a two site fit was preferred to a three site model, giving a high nanomolar affinity corresponding to the ET_A receptor and a low, micromolar site corresponding to the ET_B receptor. BQ123 showed up to 18 000 fold selectivity for the ET_A over the ET_B sub-type. In each case ET_A receptors predominated, with the ET_B subtype representing less than 15% of the ET receptors in smooth muscle cells of the human vasculature.

Autoradiography

Owing to the small size of internal mammary arteries obtained following surgery it was not possible to obtain sufficient receptor protein to carry out competition assays and relative densities were compared by quantitative autoradiography. The density of ET_A binding in the media of internal mammary artery following incubation with a fixed concentration of [^{125}I]-PD151242 was 78.7 ± 5.9 amol mm^{-2}, representing about 85% of the [^{125}I]-ET-1 binding (92.9 ± 4.6 amol mm^{-2}). In contrast, the density of ET_B receptors detected with [^{125}I]-BQ3020 was 7.0 ± 1.5 amol mm^{-2}, representing about 8% of [^{125}I]-ET-1. As expected from the competition binding assays, a similar pattern was observed in the media from aorta, pulmonary and coronary arteries as well

Table 2 Inhibition of [^{125}I]-endothelin-1 ([^{125}I]-ET-1) binding to media from human vessels by the ET_A selective BQ123

	K_D ET_A (nM)	ET_B (μM)	B_{max} ET_A (fmol mg^{-1}protein)	ET_B	*Ratio* ET_A:ET_B
Arteries:					
Coronary	0.85 ± 0.03	7.58 ± 2.27	15.4 ± 4.1	1.7 ± 0.5	89:11
Pulmonary	0.27 ± 0.05	24.60 ± 5.34	27.2 ± 3.0	2.4 ± 0.6	92:8
Aorta	0.80 ± 0.40	2.67 ± 2.60	9.4 ± 1.7	1.1 ± 0.4	89:11
Vein:					
Saphenous	0.55 ± 0.17	14.4 ± 0.26	35.3 ± 20.2	6.5 ± 1.5	85:15

Values are mean ± s.e.mean of 3 individuals.

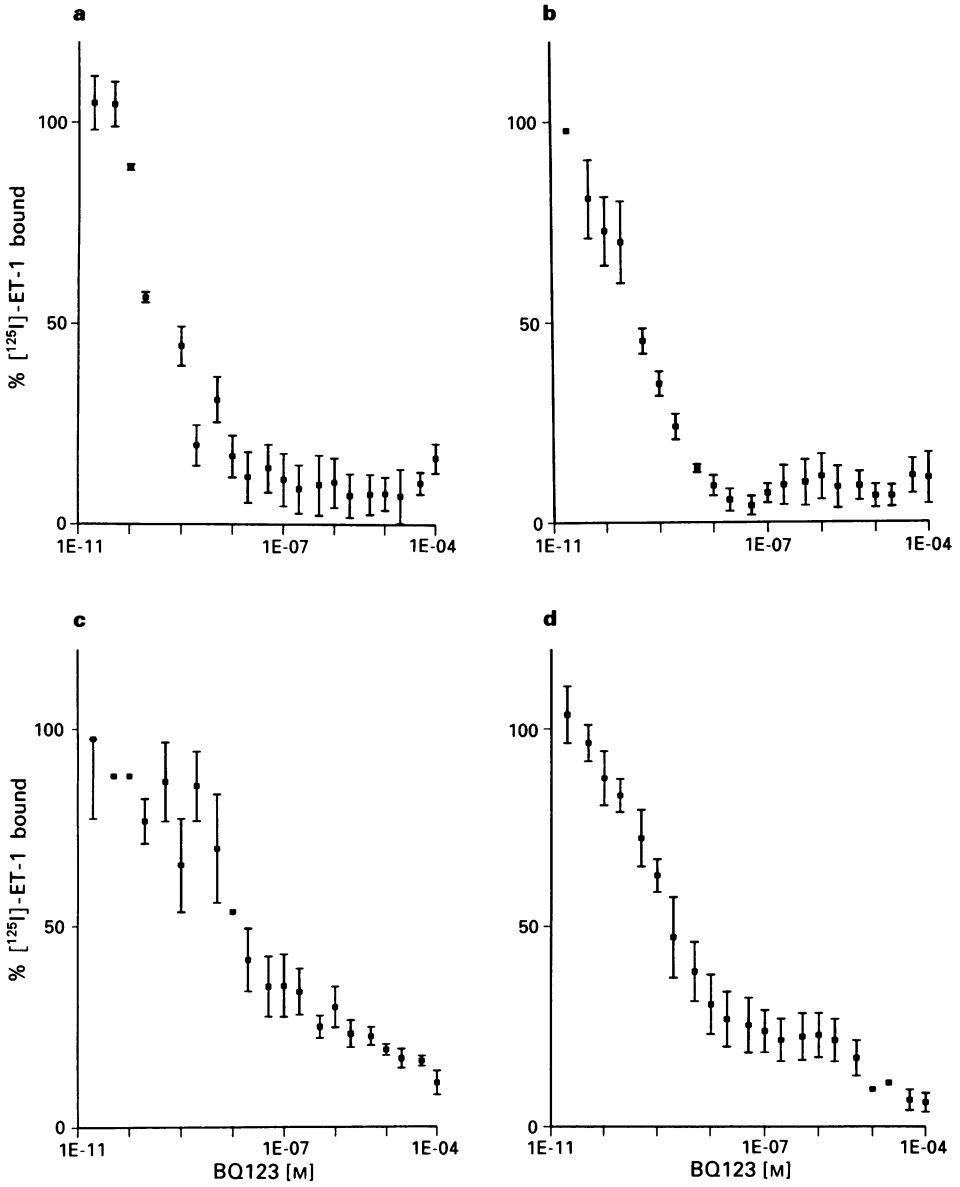

Figure 1 Inhibition of 0.1 nM [^{125}I]-endothelin-1 ([^{125}I]-ET-1) binding by BQ123 to slide mounted sections of main stem aorta (a), pulmonary artery (b), coronary artery (c) and saphenous vein (d). In each case, with the exception of the aorta, over the concentration-range tested, BQ123 competed in a biphasic manner and a two site fit was preferred to a one site or three site model. (Each value represents the mean ± s.e.mean of three individuals except for saphenous vein where homogenates were prepared from about 30 vessels).

as the saphenous vein, with the density of ET_B receptors being much lower in the smooth muscle than densities of the ET_A sub-type localized by [^{125}I]-PD151242.

Molecular biology

Agarose gels showing the presence of PCR products of the expected size corresponding to mRNA encoding both the ET_A receptor (299 base pairs) and ET_B receptor (428 bases pairs) were detected in the media obtained from three individuals in each of the four arteries and saphenous vein. Bands were not detected in the negative control lane in which the template had been omitted (Figure 2).

In situ *hybridization*

The ^{35}S-labelled antisense ET_A probe hybridized to the media of epicardial coronary arteries as well as intramyocardial vessels. The autoradiographic image of the sense control probe was digitally subtracted from that of the antisense probe to give the amount specifically hybridized of 90 ± 8 amol mm^{-2} in epicardial coronary arteries and 50.0 ± 3 amol mm^{-2} in intramyocardial vessels (mean ± s.e.mean of at least 3 vessels). The amount of non-specific hybridization detected by the sense control probe was higher for the ET_B receptor but specific hybridization could still be detected, 34.3 ± 3 amol mm^{-2} and 43.0 ± 8 amol mm^{-2} in epicardial and intra-myocardial vessels respectively.

Discussion

[^{125}I]-ET-1 bound with a similar sub-nanomolar affinity to the media containing mainly vascular smooth muscle, in all of the human blood vessels examined. Over the concentration-range tested, Hill slopes were close to unity and a one site fit was preferred to a two site model. These results suggest the presence of either a single population of receptors or a

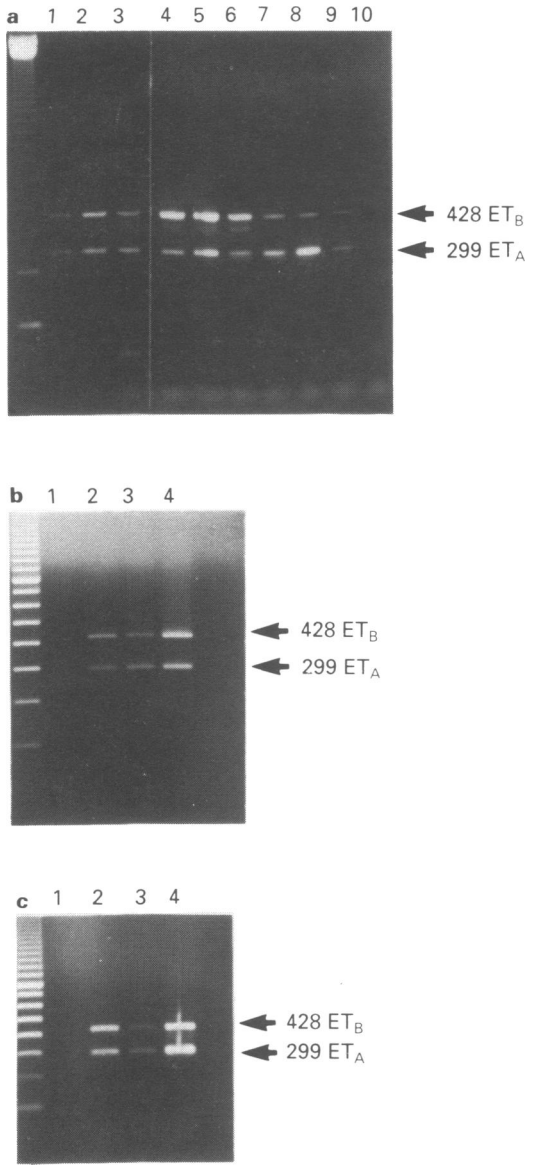

Figure 2 Detection of ET_A and ET_B mRNA in human vessels. Agarose gel electrophoresis of reverse-transcriptase polymerase chain reaction (RT-PCR) products from the media (containing mainly vascular smooth muscle cells) of vessels obtained from different vascular beds. The presence of PCR bands corresponding to size predicted for ET_A (299 base pairs) and ET_B (428 base pairs) mRNA was detected in the media of all vessels examined. (a) Lane 1–3, aorta from three individuals; lane 4–6, pulmonary artery from three individuals; lane 7–9, coronary artery from three individuals. Lane 10, negative control where cDNA template had been omitted. The marker is a 123-base pair ladder. (b) Lane 1, negative control where cDNA template had been omitted. Lane 2–4, saphenous vein from three individuals. The marker is a 100-base pair ladder. (c) Lane 1, negative control where cDNA template had been omitted. Lane 2–4, internal mammary artery from three individuals. The marker is a 100-base pair ladder.

heterogeneous population with the same affinity for the peptide. In the majority of human tissues examined using homogenates or slide mounted sections, labelled ET-1 binds monophasically with affinities ranging from about 0.01–10 nM, with receptor densities of about 10 to 10 000 fmol mg^{-1} protein (Davenport *et al.*, 1994d). The range of K_D values in the media of these five vessels (0.14–0.85 nM) compare with values estimated by the same technique in other types of human muscle. For example, in human myometrium (consisting of mainly non-vascular smooth muscle), K_D values were 1.2 nM (Bacon *et al.*, 1993). In cardiac muscle, K_D values of 0.60 and 0.35 nM were obtained in atria and ventricle (Molenaar *et al.*, 1993). The range of affinities for [^{125}I]-ET-1 binding to homogenates of placental arteries and veins (presumed to contain media, adventitia and endothelium) was 0.026–0.045 nM (Robaut *et al.*, 1991). Thus [^{125}I]-ET-1 binds with high affinity in the media of these vessels although the density of binding is comparatively low compared to other human tissue. The affinities calculated by ligand binding for the five vessels show a positive correlation with the EC_{50} values for the contractile effects of this peptide on the isolated vessels denuded of endothelium (Maguire & Davenport, 1995).

A consistent pattern emerged with the detection in all vessels of receptor mRNA using RT-PCR. A single PCR product corresponding to the expected position for ET_A mRNA was detected in media of each of these vessels. A single band corresponding to ET_B mRNA was also always found. Localization of ET_B as well as ET_A mRNA to vascular smooth muscle cells was confirmed by *in situ* hybridization in sections of coronary arteries. Single bands corresponding to ET_A and ET_B mRNA have also been found in renal veins and arteries by RT-PCR (Maguire *et al.*, 1994b) and by Northern analysis in internal mammary artery (Seo *et al.*, 1994). Expression of mRNA encoding both sub-types has been found in a range of human tissues including ventricle (Molenaar *et al.*, 1993), endometrium (O'Reilly *et al.*, 1992) and kidney (Davenport *et al.*, 1993b). In these studies, detection of mRNA correlates with expression of receptor protein. Using the same RT-PCR assay conditions with isolated cells, only ET_B mRNA was detected in human vascular endothelial cells whereas rat aortic smooth muscle cells express ET_A mRNA (Molenaar *et al.*, 1993) and only the ET_A receptor protein could be detected (Davenport *et al.*, 1994b). However, in isolated myocytes mRNA encoding both sub-types was found and BQ123 inhibited binding of iodinated ET-1 biphasically, confirming that both receptor sub-types were present in these cells (Molenaar *et al.*, 1993).

The ET_A selective ligand, BQ123, inhibited [^{125}I]-ET-1 binding in a biphasic manner in both arteries (aorta, pulmonary and coronary arteries) as well as saphenous vein in agreement with the molecular biology studies. Quantitative autoradiography showed that while a small population of ET_B receptors could be detected in the internal mammary artery, the ET_A sub-type was again more abundant. Similar results have been obtained with other human vessels. In human kidney, ET_A receptors detected with [^{125}I]-PD151242 were mainly localized to the vasculature and micro-autoradiography demonstrated smaller vessels such as arterioles expressed the ET_A sub-type (Karet *et al.*, 1993).

BQ123 competes for [^{125}I]-ET-1 binding for an ET_A site in the nanomolar range and ET_B site at micromolar concentrations in a number of human tissues including cardiac muscle (Molenaar *et al.*, 1993), myometrium (Bacon *et al.*, 1993) and kidney cortex and medulla (Karet *et al.*, 1993). Intriguingly, Bax *et al.* (1993) found while BQ123 competed in a biphasic manner for [^{125}I]-ET-1 binding in human cardiac muscle the compound detected only one site in coronary arteries. Two sites were detected when BQ123 competed for [^{125}I]-sarafotoxin S6b in this artery. This was interpreted as evidence of a non-ET_A/ET_B site. The RT-PCR assays used in this study have not revealed the presence of additional bands. In competition binding assys, BQ123 competed with similar affinities in coronary artery as all other vessels where Schild slopes of unity have also been found (Maguire & Davenport, 1995).

These studies show that human vessels express a small population of ET_B receptors. In animals, a complex pattern of ET-1-induced vasoconstriction has emerged, with a significant ET_B component in some vessels (see for example, Davis *et al.*, 1991; Clozel *et al.*, 1992; Sumner *et al.*, 1992; Cristol *et al.*, 1993; Gardiner *et al.*, 1994; Pollock & Opgenorth, 1993; 1994; Wellings *et al.*, 1994; White *et al.*, 1994a) whereas constriction appears to be mediated only by ET_A receptors in rat aorta (Sumner *et al.*, 1992) or rabbit

renal artery (Telemarque *et al.*, 1993) but both sub-types are activated in porcine coronary artery (Ihara *et al.*, 1992).

Although the ET_B agonists BQ3020 and [$Ala^{1,3,11,15}$]-ET-1 are potent constrictors of some rat vascular beds (Bigaud & Pelton, 1992; Gardiner *et al.*, 1994), they had no detectable action on the isolated vessels used in this study at concentrations up to 3 μM (Davenport *et al.*, 1993; Maguire & Davenport, 1995). The non-endogenous ET_B agonist in mammals, sarafotoxin S6c, was also inactive in aorta and pulmonary artery (Maguire & Davenport, 1995). This peptide does cause vasoconstriction in some human vessels such as saphenous vein (White *et al.*, 1994b, Maguire & Davenport, 1995), internal mammary artery (Seo *et al.*, 1994; Maguire & Davenport, 1995) and vein (Seo *et al.*, 1994), omental arteries and veins (Riezebos *et al.*, 1994) and pulmonary arteries (Hay *et al.*, 1993; Maguire & Davenport, 1995). Where responses did occur, these can be variable, for example a response was detected in saphenous vein in only about 50% (White *et al.*, 1994) of individuals or less (Maguire & Davenport, 1995). Although the constrictor actions of this snake venom are potent, the magnitude of the response is much less than that of ET-1. Therefore whilst some individuals may have functional constrictor ET_B receptors, the poor response to ET-3 in these vessels (Maguire & Davenport, 1994, Davenport & Maguire, 1995) would suggest that these receptors may have limited physiological importance in the cardiovascular system.

Ligand binding has demonstrated that the majority (at least 85%) of ET receptors present in smooth muscle from the five vessels are of the ET_A sub-type. Functional studies have shown that ET_A-selective antagonists in these vessels cause a parallel, rightward shift of the ET-1 concentration-response curve and Schild slopes were not significantly different from unity (Maguire & Davenport, 1995; Maguire *et al.*, 1994a,c). This contrasts with porcine coronary artery, where a portion of the ET-1 response mediated via presumed ET_B receptors is not blocked by BQ123 (Ihara *et al.*, 1992).

In other human vessels, ET-1 is always more potent, with the ET-3 dose-response curve shifted to the right. ET-3 is at least 100 fold less potent that ET-1 in omental veins (Riezebos *et al.*, 1994), renal arteries and veins (Maguire *et al.*, 1994b), umbilical artery (Bodelsson & Stjernquist, 1993) or inactive in omental arteries (Riezebos *et al.*, 1994). Where full concentration-response curves have been carried out comparing ET-1 and ET-3, human vessels have not yet been identified in which ET-3 is equipotent to ET-1 as in the rabbit pulmonary artery (White *et al.*, 1994a).

In the human vasculature, a consistent pattern is emerging: although both receptors can be detected by ligand binding, *in vitro* pharmacological experiments suggest that vasoconstriction in man is mediated predominantly via the ET_A sub-type. Taken together, these results provide further support for the hypothesis that the ET_A sub-type is the receptor that must be blocked in human patients to produce a beneficial vasodilatation in pathophysiological conditions where there are elevated concentrations of the peptide or increases in receptor density. ET_A selective drugs may have an additional advantage in avoiding blockade of the ET_B sub-type present on endothelial cells since activation of these receptors by ET-1 is thought to release endothelium-derived relaxing factors.

We thank the surgeons and theatre staff of Papworth Hospital for their co-operation in obtaining tissue and Dr A.M. Doherty (Parke-Davis Pharmaceutical Research Division) for synthesizing and supplying PD151242. Supported by grants from the British Heart Foundation, Royal Society, BBSRC, Isaac Newton Trust.

References

AKAR, F. UYDES, B.S., AYRANCIOGLU, K., YENER, A., ASLAMACI, S., ARSAN, M., TORUNER, A. & KANZIK, I. (1994). Endothelial function of human gastroepiploic artery in comparison with saphenous vein. *Cardiovasc. Res.*, **28,** 500–504.

BACON, C.R., O'REILLY, G., CAMERON, I.T. & DAVENPORT, A.P. (1993). Endothelin receptors in human myometrium characterized by BQ123 and BQ3020. *Br. J. Pharmacol.*, **110,** P45.

BAX, W.A., BRUINVELS, A.T., VAN-SUYLEN, R.J., SAXENA, P.R. & HOYER, D. (1993). Endothelin receptors in the human coronary artery, ventricle and atrium. A quantitative autoradiographic analysis. *Naunyn-Schmied. Arch. Pharmacol.*, **348,** 403–410.

BIGAUD, M. & PELTON, J.T. (1992). Discrimination between ET_A- and ET_B-receptor mediated effects of endothelin-1 and [$Ala^{1,3,11,15}$]endothelin-1 by BQ123 in the anaesthetised rat. *Br. J. Pharmacol.*, **107,** 912–917.

BODELSSON, G. & STJERNQUIST, M. (1993). Characterization of endothelin receptors and localization of 125I-endothelin-1 binding sites in human umbilical artery. *Eur. J. Pharmacol.*, **249,** 299–305.

CLOZEL, M., GRAY, G.A., BREU, V., LÖFFLET, B.-M. & OSTERWALDER, R. (1992). The endothelin ET_B receptor mediates both vasodilation and vasoconstriction *in vivo*. *Biochem. Biophys. Res. Commun.*, **186,** 867–873.

COSTELLO, K.B., STEWART, D.J. & BAFFOUR, R. (1990). Endothelin is a potent constrictor of human vessels used in coronary revascularization surgery. *Eur. J. Pharmacol.*, **186,** 311–314.

CRISTOL, J.-P., WARNER, T.D., THIEMERMANN, C. & VANE, J.R. (1993). Mediation via different receptors of the vasoconstrictor effects of endothelins and sarafotoxins in the systemic circulation and renal vasculature of the anaesthetised rat. *Br. J. Pharmacol.*, **108,** 776–779.

DAVENPORT, A.P., BERESFORD, I.J.M., HALL, M.D., HILL, R.G. & HUGHES, J. (1988). Quantitative autoradiography. In *Molecular Neuroanatomy*, Vol. III, pp. 121–145 ed. Van Leeuwen, F.W., Buijs, R.M., Pool, C.W. & Pach, O. Amsterdam: Elsevier.

DAVENPORT, A., KUC, R.E., FITZGERALD, F., MAGUIRE, J.J., BERRYMAN, K. & DOHERTY, A.M. (1994a). [^{125}I]-PD151242: a selective radioligand for human ET_A receptors. *Br. J. Pharmacol.*, **111,** 4–6.

DAVENPORT, A.P., KUC, R.E., HOSKINS, S.L., KARET, F.E. & FITZGERALD, F. (1994b). [^{125}I]-PD151242 is selective for endothelin ET_A receptors in human kidney and localises to renal vasculature. *Br. J. Pharmacol.*, **113,** 1303–1310.

DAVENPORT, A.P., KUC, R.E., HOSKINS, S.L. & KARET, F.E. (1994c). [^{125}I]-PD151242 is a selective endothelin ET_A receptors in human kidney and localises to the vasculature. *Br. J. Pharmacol.*, **112,** 554P.

DAVENPORT, A.P. & MAGUIRE, J.J. (1994). Is endothelin-induced vasoconstriction mediated only by ET_A receptors in humans? *Trends Pharmacol. Sci.*, **15,** 9–11.

DAVENPORT, A.P., MAGUIRE, J.J. & KARET, F.E. (1994d). Endothelin receptors and their subtypes. In *Endothelin: Role in Health and Disease*. ed. A. Gulati, pp. 13–23. Amsterdam: Harwood Academic Publishers.

DAVENPORT, A.P., MORTON, A.J. & BROWN, M.J. (1991). Localisation of endothelin (1–3), mouse VIC and sarafotoxin S6b binding sites in mammalian heart and kidney. *J. Cardiovasc. Pharmacol.*, **17,7,** S152–S155.

DAVENPORT, A.P. & NUNEZ, D.J. (1990). Quantification in *in situ* hybridisation. In *In Situ Hybridization* ed. Polak, J.M. & McGee, J.O.D. pp. 95–111. Oxford: Oxford University Press.

DAVENPORT, A.P., NUNEZ, D.J. & BROWN, M.J. (1989a). Quantitative autoradiography reveals binding sites for [125I] endothelin-1 in kidneys with a differential distribution among rat, pig and man. *Clin. Sci.*, **77,** 129–131.

DAVENPORT, A.P., NUNEZ, D.J., HALL, J.A, KAUMANN, A.J. & BROWN, M.J. (1989b). Autoradiographical localisation of binding sites for [125I] endothelin-1 in humans, pigs and rats: functional relevance in man. *J. Cardiovasc. Pharmacol.*, **13,5,** S166–170.

DAVENPORT, A.P., O'REILLY, G., MOLENAAR, P., MAGUIRE, J.J., KUC, R.E., SHARKEY, A., BACON, C.R. & FERRO, A. (1993). Human endothelin receptors characterised using reverse transcriptase-polymerase chain reaction, *in situ* hybridization and sub-type selective ligands BQ123 and BQ3020: evidence for expression of ET_B receptors in human vascular smooth muscle. *J. Cardiovasc. Pharmacol.*, **22(S8),** 22–25.

DAVIS, L.S., LADOUCEUR, D.M., KEISER, J.A. & HALEEN, S.J. (1991). Relative vasodilator and vasoconstrictor activity of endothelin-1 (ET-1), endothelin-3 (ET-3) and sarafotoxin 6c (SFTX-6c) on regional arterial beds of the anaesthetized rat: relationship to ET_A and ET_B receptor agonist activity. *FASEB J.*, **6**, 391.

FRANCO-CERECEDA, A. (1989). Endothelin- and neuropeptide Y-induced vasoconstriction of human epicardial coronary arteries in vitro. *Br. J. Pharmacol.*, **97**, 968–972.

FUKURODA, T., KOBAYASHI, M., OZAKI, S., YANO, M., MIYAUCHI, T., ONIZUKA, M., SUGISHITA, Y., GOTO, K. & NISHIKIBE, M. (1994). Endothelin receptor subtypes in human versus rabbit pulmonary arteries. *J. Appl. Physiol.*, **76**, 1976–1982.

GARDINER, S.M., KEMP, P.A., MARCH, J.E., BENNETT, T., DAVENPORT, A.P. & EDVINSSON, L. (1994). Effects of an ET_1-receptor antagonist, FR139317 on regional haemodynamic responses to endothelin-1 and [$Ala^{11,15}$] Ac-endothelin-1 (6–21) in conscious rats. *Br. J. Pharmacol.*, **112**, 477–486.

GODFRAIND, T. (1993). Evidence for heterogeneity of endothelin receptor distribution in human coronary artery. *Br. J. Pharmacol.*, **110**, 1201–1205.

HAY, D.W.P., LUTTMANN, M.A., HUBBARD, W.C. & UNDEM, B.J. (1993). Endothelin receptor subtypes in human and guinea-pig pulmonary tissues. *Br. J. Pharmacol.*, **110**, 1175–1183.

HOWARD, P.G., PLUMPTON, C. & DAVENPORT, A.P. (1992). Anatomical localisation and pharmacological activity of mature endothelins and their precursors in human vascular tissue. *J. Hypertens*, **10**, 1379–1386.

IHARA, M., NOGUCHI, K., SAEKI, T., FUKURODA, T., TSUCHIDA, S., KIMURA, S., FUKAMI, T., ISHIKAWA, K., NISHIKIBE, M. & YANO, M. (1992). Biological profiles of highly potent novel endothelin antagonists selective for the ETA receptor. *Life Sci.*, **50**, 247–255.

KARET, F.E. & DAVENPORT, A.P. (1993). Human kidney: Endothelin isoforms revealed by HPLC with radioimmunoassay, and receptor sub-types detected using ligands BQ123 and BQ3020. *J. Cardiovasc. Pharmacol.*, **22(S8)**, 29–33.

KARET, F.E., JONES, D.S.C., HARRISON-WOOLRYCH, M., O'REILLY, G.R., DAVENPORT, A.P. & SMITH, S.K. (1994). Validation of mRNA quantification using a novel fluorescent nested reverse transcriptase polymerase chain reaction. *Anal. Biochem.*, **220**, 384–390.

KARET, F.E., KUC, R.E. & DAVENPORT, A.P. (1993). Novel ligands BQ123 and BQ3020 characterize endothelin receptor subtypes ET_A and ET_B in human kidney. *Kidney Int.*, **44**, 36–42.

LUSCHER, T.F., YANG, Z., BAUER, E., TSCHUDI, M., VON-SEGESSER, L., STULZ, P., BOULANGER, C., SIEBENMANN, R., TURINA, M. & BUHLER, F.R. (1990). Interaction between endothelin-1 and endothelium-derived relaxing factor in human arteries and veins. *Circ. Res.*, **66**, 1088–1094.

MAGUIRE, J.J., BACON, C.R., FUIJIMOTO, M. & DAVENPORT, A.P. (1994a). Myricerone caffeoyl ester 50-235, is a non-peptide antagonist selective for human ET_A receptors. *J. Hypertens.*, **12**, 675–680.

MAGUIRE, J.J. & DAVENPORT, A.P. (1993). Endothelin-induced vasoconstriction in human isolated vasculature is mediated predominantly via activation of ET_A receptors. *Br. J. Pharmacol.*, **110**, P47.

MAGUIRE, J.J. & DAVENPORT, A.P. (1994). Pre-administration or post-administration of BQ123 and FR129317 antagonizes endothelin-1 (ET-1)-induced contraction of human blood vessels *in vitro*. *Br. J. Pharmacol.*, **111**, P149.

MAGUIRE, J.J. & DAVENPORT, A.P. (1995). ET_A receptors mediate the constrictor responses to endothelin peptides in human blood vessels *in vitro*. *Br. J. Pharmacol.* (in press).

MAGUIRE, J.J., KUC, R.E., O'REILLY, G. & DAVENPORT, A.P. (1994b). Vasoconstrictor endothelin receptors characterised in human renal artery and vein *in vitro*. *Br. J. Pharmacol.*, **113**, 49–54.

MAGUIRE, J.J., KUC, R.E., O'REILLY, G. & DAVENPORT, A.P. (1994c). Potency of the novel orally active antagonist Ro46-2005 for endothelin receptors in human vascular smooth muscle. *Br. J. Pharmacol.*, **112**, 552P.

MOLENAAR, P., KUC, R.E. & DAVENPORT, A.P. (1992). Characterization of two new ET_B selective radioligands. [^{125}I]-BQ3020 and [^{125}I]-[$Ala^{1,3,11,15}$]-ET-1 in human heart. *Br. J. Pharmacol.*, **107**, 637–639.

MOLENAAR, P., O'REILLY, G., SHARKEY, A., KUC, R.E., HARDING, D.P., PLUMPTON, P., GRESHAM, G.A. & DAVENPORT, A.P. (1993). Characterization and localization of endothelium receptor sub-types in the human atrioventricular conducting system and myocardium. *Circ. Res.*, **72**, 526–538.

OPGAARD, O.S., ADNER, M., GULBENKIAN, S. & EDVINSSON, L. (1994). Localization of endothelin immunoreactivity and demonstration of constrictory endothelin-A receptors in human coronary arteries and veins. *J. Cardiovasc. Pharmacol.*, **23**, 576–583.

O'REILLY, G., CHARNOCK-JONES, D.S., CAMERON, I.T., SMITH, S.K. & DAVENPORT, A.P. (1993a). Endothelin-2 mRNA splice variants detected by RT-PCR in cultured human vascular smooth muscle and endothelial cells. *J. Cardiovasc. Pharmacol.*, **22 (S8)**, 18–21.

O'REILLY, G., CHARNOCK-JONES, D.S., DAVENPORT, A.P., CAMERON, I.T. & SMITH, S.K. (1992). Presence of mRNA for endothelin-1, endothelin-2, and endothelin-3 in human endometrium, and a change in the ratio of ET_A and ET_B receptor subtype across the menstrual cycle. *J. Clin. Endocrinol. Metab.*, **75**, 1545–1549.

O'REILLY, G., CHARNOCK-JONES, D.S., MORRISON, J.J., CAMERON, I.T., DAVENPORT, A.P. & SMITH, S.K. (1993a,b). Alternatively spliced mRNAs for human endothelin-2 and their tissue distribution. *Biochem. Biophys. Res. Commun.*, **193**, 834–840.

PETER, M.G. & DAVENPORT, A.P. (1994). [^{125}I]-PD151242 as an endothelin ET_A selective radioligand in the human, rat and porcine heart. *Br. J. Pharmacol.*, **112**, 494P.

PETER, M.G. & DAVENPORT, A.P. (1995). Selectivity of [^{125}I]-PD 151242 for the human, rat and porcine endothelin ET_A receptors in the heart. *Br. J. Pharmacol.*, **114**, 297–302.

PLUMPTON, C., CHAMPENEY, R., ASHBY, M.J., KUC, R.E. & DAVENPORT, A.P. (1993). Characterisation of endothelin isoforms in human heart: Endothelin 2 demonstrated. *J. Cardiovasc. Pharmacol.*, **22 (S8)**, 26–28.

POLLOCK, D.M. & OPGENORTH, J. (1993). Evidence for endothelin-induced renal vasoconstriction independent of ET_A receptor activation. *Am. J. Physiol.*, **264**, R222–R226.

POLLOCK, D.M. & OPGENORTH, J. (1994). ET_A receptor-mediated responses to endothelin-1 and big endothelin-1 in the rat kidney. *Br. J. Pharmacol.*, **111**, 729–732.

RIEZEBOS, J., WATTS, I.S. & VALLANCE, P.J.T. (1994). Endothelin receptors mediating functional responses in human small arteries and veins. *Br. J. Pharmacol.*, **111**, 609–615.

ROBAUT, C., MONDON, F., BANDET, J., FERRE, F. & CAVERO, I. (1991). Regional distribution and pharmacological characterization of [^{125}I]endothelin-1 binding sites in human fetal placental vessels. *Placenta*, **12**, 55–67.

SEO, B., OEMAR, B.S., SIEBENMANN, R., VON-SEGESSER, L. & LUSCHER, T.F. (1994). Both ET(A) and ET(B) receptors mediate contraction to endothelin-1 in human blood vessels. *Circulation*, **89**, 1203–1208.

SUMNER, M.J., CANNON, T.R., GARRATT, H., MUNDIN, J.W., WHITE, D.G. & WATTS, I.S. (1992). Endothelin ET(A) and ET(B) receptors mediate vascular smooth muscle contraction. *Br. J. Pharmacol.*, **107**, 858–860.

TELEMAQUE, S., GRATTON, J.-P., CLAING, A. & D'ORLEANS-JUSTE, P. (1993). Endothelin-1 induces vasoconstriction and prostacyclin release via the activation of endothelin ET_A receptors in the perfused rabbit kidney. *Eur. J. Pharmacol.*, **237**, 275–281.

WELLINGS, R.P., CORDER, R., WARNER, T.D., CRISTOL, J.-P., THIEMERMANN, C. & VANE, J.R. (1994). Evidence from receptor antagonists for an important role for ET_B-mediated vasoconstrictor effects of endothelin-1 in the rat kidney. *Br. J. Pharmacol.*, **111**, 515–520.

WHITE, D.G., CANNON, T.R., GARRATT, H., MUNDIN, J.W., SUMNER, M.J. & WATTS, I.S. (1994a). Endothelin ET_A and ET_B receptors mediate vascular smooth-muscle contraction. *J. Cardiovasc. Pharmacol.*, **22**, S144–S148.

WHITE, D.G., GARRATT, H., MUNDIN, J.W., SUMNER, M.J., VALLANCE, P.J. & WATTS, I.S. (1994b). Human saphenous vein contains both endothelin ET(A) and ET(B) contractile receptors. *Eur. J. Pharmacol.*, **257**, 307–310.

(Received August 3, 1994
Revised November 9, 1994
Accepted November 10, 1994)

British Journal of Pharmacology (1995) 114, 1117-1124

Pharmacology of LR-B/081, a new highly potent, selective and orally active, nonpeptide angiotensin II AT_1 receptor antagonist

[1]R. Cirillo, A.R. Renzetti, P. Cucchi, M. Guelfi, *A. Salimbeni, *S. Caliari, †A. Castellucci, †S. Evangelista, A. Subissi & **A. Giachetti

Departments of Pharmacology of Laboratori Guidotti, Pisa, *Lusofarmaco, Milan, †Malesci, Florence and **Menarini, Florence, Italy

1 The pharmacological profile of LR-B/081, (methyl 2-[[4-butyl-2-methyl-6-oxo-5-[[2'-(1H-tetrazol-5-yl)[1,1'-biphenyl]-4-yl]methyl]-1(6H)-pyrimidinyl]methyl]-3-thiophenecarboxylate), a novel antagonist at the angiotensin II (AII) AT_1-receptor, was studied *in vitro* and *in vivo*.

2 In rabbit aortic strips incubated with LR-B/081 (1-1,000 nM), the concentration-response curve to AII was displaced to the right in a nonparallel fashion and the maximal contraction was progressively reduced, indicating that the compound is an insurmountable antagonist in this preparation (apparent $pK_B = 9.50 \pm 0.23$). However, the interaction of LR-B/081 with AII receptors was found to be reversible, since the maximal response to AII was restored by coincubation with losartan, a surmountable AII AT_1-antagonist. Contractions elicited by KCl or phenylephrine were not affected by 10 μM LR-B/081.

3 In rat isolated perfused kidney, LR-B/081 and losartan antagonized the AII-induced vasoconstriction [IC_{50} (95% confidence limits) = 17(13-24) and 39(32-54) nM, respectively]. The LR-B/081 antagonism was incompletely reversed by excess AII, while losartan was fully displaced. The IC_{50} values of LR-B/081 and losartan obtained against vasoconstriction induced by endothelin-1 and noradrenaline were two orders of magnitude higher.

4 In pithed rats, the intravenous administration of LR-B/081 (0.2-2 μmol kg^{-1}) dose-dependently shifted to the right in a nonparallel fashion the dose-pressor response curve to AII. The maximal pressor response to AII was reduced by LR-B/081 in a dose-dependent fashion. The coadministration of losartan induced a progressive recovery of the maximal pressor response to AII, indicating that *in vivo* the interaction of LR-B/081 with AII receptors is reversible. LR-B/081 at 6 μmol kg^{-1}, i.v. also did not affect the vasopressor response induced by noradrenaline in the pithed rat.

5 In conscious normotensive rats, single oral administration of LR-B/081 at 6 μmol kg^{-1} markedly inhibited the AII-induced pressor response; the inhibition lasted more than 24 h.

6 In conscious renal hypertensive rats, intravenous LR-B/081 appeared as potent as losartan (ED_{40mmHg} (95% confidence limits) = 0.50(0.36-0.70) and 0.86(0.57-1.3) μmol kg^{-1}, respectively). A single intravenous (2 μmol kg^{-1}) or oral (6 μmol kg^{-1}) administration of LR-B/081 induced a marked fall in blood pressure which lasted for at least 12 h.

7 In conscious spontaneously hypertensive rats, LR-B/081 at 20 μmol kg^{-1}, p.o., induced a marked and sustained fall in blood pressure. The duration of the antihypertensive effect was longer than 12 h. Heart rate was not modified by LR-B/081 treatment. Repeated oral administration of 17 μmol kg^{-1} LR-B/081 for 16 days did not result in the development of tolerance.

8 These results demonstrate that LR-B/081 is a potent, selective and orally active antagonist of AII at the AT_1-receptor subtype, which markedly lowers the blood-pressure in conscious renal and spontaneously hypertensive rats.

Keywords: AT_1 receptor antagonists; LR-B/081; hypertension; losartan; insurmountable antagonism; angiotensin II

Introduction

The renin-angiotensin system (RAS) is important for the regulation of cardiovascular functions and body fluid composition. Angiotensin II (AII), the biologically active peptide hormone of the RAS, elicits multiple pharmacological effects, most of which seem to be mediated by the AII AT_1 receptor subtype, while the functions of the AT_2 subtype receptors are poorly understood (Philipps, 1987; Herblin *et al.*, 1991; Timmermans *et al.*, 1991). The clinical use of inhibitors of angiotensin converting enzyme (ACE) has demonstrated the relevance of the RAS in controlling blood pressure and fluid balance under physiological and pathophysiological conditions (Dzau *et al.*, 1980; Williams, 1988). It has been proposed that the limited specificity of these agents for the RAS system may account for some of their clinical side-effects such as dry cough and angioedema (Williams, 1988; Chin & Buchan, 1990). Moreover, it has been recently shown that AII can also be formed in man by a chymotrypsin-like proteinase which is not affected by ACE inhibitors (Kinoshita *et al.*, 1991).

One of the possible approaches to overcome these limitations of ACE inhibitors is the specific blockade of AII receptors. The recent discovery of selective nonpeptide AII receptor antagonists (Timmermans *et al.*, 1993) provides a more selective means to control and manage hypertension. Losartan represents the prototype of this new class of agents, which is selective for the AII AT_1 receptor subtype (Chiu *et al.*, 1990; Wong *et al.*, 1990a).

[1] Author for correspondence at: Department of Pharmacology, Laboratori Guidotti Via Livornese, 897 56122 S.Piero a Grado (Pisa), Italy.

In this paper, we describe the pharmacological profile of LR-B/081 (methyl 2-[[4-butyl-2-methyl-6-oxo-5-[[2'-(1H-tetrazol-5-yl)[1,1'-biphenyl]-4-yl]methyl]-1(6H)-pyrimidinyl] methyl]-3-thiophenecarboxylate; Figure 1), which belongs to a series of novel 4-pyrimidinones which are potent and selective AT_1 antagonists (Renzetti *et al.*, 1994a,b).

Methods

AII-induced contraction in rabbit isolated aorta

New Zealand White male rabbits (Pampaloni, Fauglia, Italy) weighing 2 to 3 kg were killed by cervical dislocation and exsanguinated. The thoracic aorta was removed and cleaned of adherent fat and connective tissue. The vascular endothelium was removed by gently rubbing the intimal surface of the vessel. Aortic strips (2–3 mm wide and 30 mm long) were then prepared according to Furchgott & Bhadrakom (1953) and mounted in 5 ml organ baths containing Krebs solution (composition in mM: NaCl 118, KCl 4.7, KH_2PO_4 1.18, $CaCl_2$ 2.52, $NaHCO_3$ 25 and glucose 11.1; pH = 7.4). Strips were attached to isometric transducers connected to an 8-channel polygraph (mod. 614/2; Biomedica Mangoni, Pisa, Italy) and a resting tension of 1 g was applied to each strip. Changes in contraction were analyzed with a digital computer (IDAS BM 10000, Biomedica Mangoni). Aortic strips were allowed to equilibrate for 1 h and washed every 15 min. Two consecutive contractile-response curves to cumulative addition of AII (0.1–300 mM) were constructed. After each curve the strips were washed 4 times and allowed to relax to the baseline tension. Afterwards, each strip was incubated for 30 min with the vehicle or with a single concentration of LR-B/081 (1–10–100–1000 nM) or losartan (10–100–1000 nM) before a third concentration-response curve to AII was obtained. The results are expressed as a percentage of the maximal AII response obtained with the second curve, which served as control.

A separate series of experiments was performed in order to study the interaction between LR-B/081 and losartan. After the two AII-response curves, the tissue was incubated with 0.1 μM LR-B/081 or its vehicle. After 30 min, 1 μM losartan or vehicle was added to each experimental group and incubated for an additional 30 min. The concentration-response curve for AII was then repeated.

Pharmacological selectivity towards AII receptors was assessed by using phenylephrine (1 nM–100 μM) or KCl (10–70 mM) in the absence or in the presence of 10 μM LR-B/081 with a similar protocol.

AII-induced vasoconstriction in rat isolated perfused kidney

Male Sprague–Dawley rats (Charles River, Calco, Italy) weighing 350–400 g were anaesthetized with 10% urethane i.p. Laparotomy was performed via a midline incision, one of the kidneys exposed for less than 10 min and the renal artery cannulated with a PE G-022 tubing (0.8 mm in diameter; Clay Adams, Parsippany, NJ, U.S.A.). The kidney was then removed and placed in a humid organ chamber where it was perfused with Tyrode solution (KCl 2.7, $CaCl_2$ 1.8, $MgCl_2$ 1.04, $NaHCO_3$ 11.9, NaH_2PO_4 0.42, NaCl 136.9 and glucose 11.1 mM) at 37°C and at a constant rate of 4.5 ml min^{-1} by means of a peristaltic pump (model T 6.5, Sigmamotor, Middleport, NJ, U.S.A.). Perfusion pressure was measured with a Bentley-Trantec pressure transducer (model 60/800, American Edwards Labs., Santa Ana, CA, U.S.A.) coupled to a recorder (Unirecord 7050, U.Basile, Comerio, Italy). After a 30 min stabilization period, the Tyrode solution was replaced with a solution containing 30 nM AII, as the minimum concentration able to produce a constant and permanent increase (at least 50 mmHg) in perfusion pressure. When a stable pressure plateau was reached, increasing concentrations of LR-B/081 or losartan (10–300 nM) were progressively added.

To assess reversibility of the antagonism, an excess of AII (1 μM) was added to the perfusate at the end of the antagonist concentration-response curve. In separate experiments, vasoconstriction was induced by submaximal concentrations of endothelin-1 (3 nM) or noradrenaline (3 μM) (Castellucci *et al.*, 1993) to assess the selectivity of the antagonism of LR-B/081 in this preparation.

AII-induced pressor response in pithed rats

Male Sprague–Dawley rats (Charles River, Calco, Italy) weighing 250–350 g were anaesthetized with sodium pentobarbitone (60 mg kg^{-1}, i.p.) and artificially ventilated with room air (70 strokes min^{-1}; 1 ml 100 g^{-1}, body wt.). Animals were maintained at 37°C by means of a heating pad. Subsequently, the animals were pithed through the orbit with a steel rod and the jugular and the femoral vein were cannulated for AII infusion and for vehicle or drug administration, respectively. Blood pressure was measured by means of a polyethylene catheter, inserted in the right carotid artery, connected to a pressure transducer (Transpac II, Abbot, Campoverde, Italy) coupled to a 2-channel 7070 Gemini recorder (U.Basile, Comerio, Italy).

Cumulative dose-response curves to AII (0.003–30 μg kg^{-1}; 0.5 ml kg^{-1}) were obtained after the intravenous administration of vehicle, LR-B/081 (0.2, 0.6 and 2 μmol kg^{-1}) or losartan (2, 6, 13 and 20 μmol kg^{-1}). The time interval between the administration of test compounds and the beginning of the AII dose-response curve was 5 min for LR-B/081 and 15 min for losartan. Only one full dose-response curve was obtained in each rat.

In separate experiments, the interaction between LR-B/081 and losartan was investigated. Animals were treated intravenously with LR-B/081 at 0.6 μmol kg^{-1} and, 10 min later, with losartan at 6 or 13 μmol kg^{-1}. After an additional 5 min a dose-pressor response curve to AII was obtained.

To assess selectivity, the effects of 6 μmol kg^{-1} LR-B/081 were tested against cumulative increasing noradrenaline (0.01–300 μg kg^{-1}, i.v.) vasopressor responses.

AII-induced pressor response in conscious normotensive rats

Male Sprague–Dawley rats (Charles River, Calco, Italy) weighing 280–340 g, were premedicated with i.p. fentanyl (0.024 mg kg^{-1}) plus fluanisone (1.2 mg kg^{-1}) (Hypnorm) and anaesthetized with sodium pentobarbitone (30–35 mg kg^{-1}, i.v.). Polyethylene catheters were inserted into the left carotid artery and right jugular vein and exteriorized behind the head through a single channel swivel (U. Danuso,

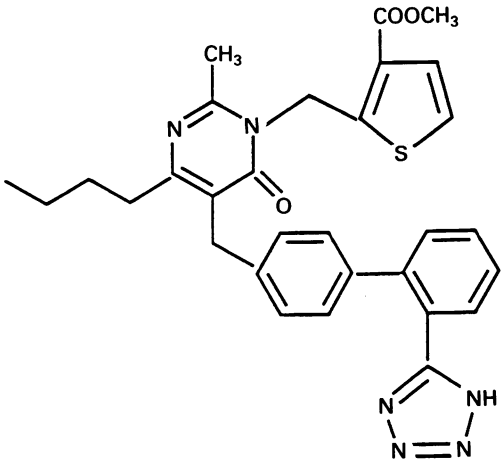

Figure 1 Chemical structure of LR-B/081.

Milano, Italy). The carotid catheter was connected to a Transpac II transducer (Abbott, Campoverde, Italy) connected to a 8805 D preamplifier (Hewlett-Packard, Milan, Italy), and blood pressure and heart rate were recorded by a 7758 D polygraph (Hewlett-Packard). Data samples of variables were taken using a IDAS BM 9000 (Biomedica Mangoni) coupled to a Compaq 386/20e computer. Eighteen hours after surgery, following an overnight fast with water *ad libitum*, a submaximal pressor dose of AII (0.105 nmol kg^{-1} i.v.) was injected three times at 20 min intervals to establish the baseline response. Then vehicle, LR-B/081 or losartan (6 μmol kg^{-1}) was administered orally by stomach tube and AII bolus injections were performed every hour for 24 h by means of a computer-controlled infusion pump (mod. 22 Harvard, South Natick, MA, U.S.A.) connected to a Compaq Prolinea 3/25s personal computer.

Conscious renal hypertensive rats (RHRs)

The method of unilateral ligation of the left renal artery for development of renal hypertension in the rat has been previously described in detail (Cangiano *et al.*, 1979). Briefly, male Sprague–Dawley rats (Charles River, Calco, Italy) weighing 270–300 g were anaesthetized with sodium pentobarbitone (45 mg kg^{-1}, i.p.) and a midline abdominal incision (about 2 cm long) was made to expose the left kidney. The renal artery was separated with care from the vein and then closed with sterile 4-0 silk. The incision was closed by careful suturing of the muscle layer and skin. Five days later, the rats were anaesthetized and instrumented as described previously. Eighteen hours after surgery, only animals with a mean arterial pressure value greater than 150 mmHg were included in the study. To evaluate the antihypertensive effect, vehicle or increasing intravenous doses (0.06, 0.2, 0.6, 2 and 6 μmol kg^{-1}) of LR-B/081 or losartan were cumulatively injected at appropriate time intervals (15–60 min).

To assess the efficacy and the duration of action of a single intravenous (2 μmol kg^{-1}) and oral (6 μmol kg^{-1}) dose of LR-B/081 or losartan, the respective effects on blood pressure and heart rate were monitored for 24 h following treatment.

Conscious spontaneously hypertensive rats (SHRs)

For the single dose study, male SHRs (Charles River, Calco, Italy; 22–24 weeks old) weighing 280–320 g were instrumented as described previously. Eighteen hours later, rats were treated orally with vehicle or LR-B/081 or losartan (20 μmol kg^{-1}). The effects on blood pressure and heart rate were monitored for 24 h following drug administration.

For the repeated dose study, male SHRs (Charles River, Calco, Italy; 12 weeks old) weighing 200–240 g were used. Systolic blood pressure was measured by means of the indirect tail cuff method (Digital Pressure Meter LE 5000, Letica, Barcelona, Spain). Animals were treated orally once a day for 16 days with vehicle, 17 μmol kg^{-1} LR-B/081 or 22 μmol kg^{-1} losartan. Blood pressure was measured 3 h after administration of test compounds on days 1, 4, 8, 12 and 16.

Conscious normotensive rats

Male Sprague–Dawley rats (Charles River, Calco, Italy) weighing 270–370 g were instrumented as described in paragraph 2.4. Eighteen hours later, the animals were treated intravenously every 15 min with increasing doses of LR-B/081 (0.6 to 20 μmol kg^{-1}).

Data analysis

Data in the text or figures are reported as means ± s.e.mean. The pA_2 value for losartan was determined by the method of Arunlakshana & Schild (1959). An apparent pK_B value for LR-B/081 was derived by a double-reciprocal regression plot from at least 3–4 couples of curves (control and in the presence of the antagonist) for those concentrations of antagonist (10–100–1000 nM LR-B/081) that resulted in at least 40–50% suppression of maximal response (Kenakin, 1987). IC_{50} values and 95% confidence limits were calculated from regression lines by means of the least squares method. ED_{50}s of AII-induced pressor response in the pithed rat were determined, considering as 100% the maximum response achieved in each group. ED_{40mmHg} and 95% confidence limits in renal hypertensive rats were calculated using the peak of the blood pressure lowering effect. Significance was assessed by the one-way analysis of variance followed by Bonferroni's test. A P value less than 0.05 indicated a significant difference between means.

Chemicals

LR-B/081 was synthesized by Lusofarmaco, Dept. of Medicinal Chemistry, Milan, Italy. Losartan was a gift from Dr R.D. Smith (DuPont, Wilmington, DE, U.S.A.). Angiotensin II, noradrenaline and phenylephrine were purchased from Sigma Chemical Co. (St. Louis, MO, U.S.A.) and endothelin-1 from Peninsula (Belmont, CA, U.S.A.). The antagonists were dissolved in 1% dimethylsulphoxide (DMSO) (water solution) and a stoichiometric amount of 0.01 N NaOH was added. The pH of the solution was then adjusted to 7.4–7.6 with 0.1 N HCl.

Results

Effects on AII-induced contraction in rabbit isolated aorta

The cumulative addition of AII (0.1–300 nM) caused a concentration-dependent contraction of rabbit aortic strips. The preincubation with LR-B/081 (1–1,000 nM) induced concentration-related nonparallel shifts to the right of the response curve to AII and decreased the maximal contraction achievable up to 50%, yielding an apparent pK_B value of 9.50 ± 0.23 ($n = 11$) (Figure 2). No agonist activity was found with LR-B/081 at any concentration employed (data not shown). In contrast, losartan shifted to the right in a parallel fashion the concentration-response curve to AII, while leaving the maximal contraction unchanged. The Schild plot produced a pA_2 value of 8.03 ± 0.21 with a slope of 1.3 ± 0.1 (data not shown).

To investigate the nature of the insurmountable antagonism, LR-B/081 was coincubated with the surmountable

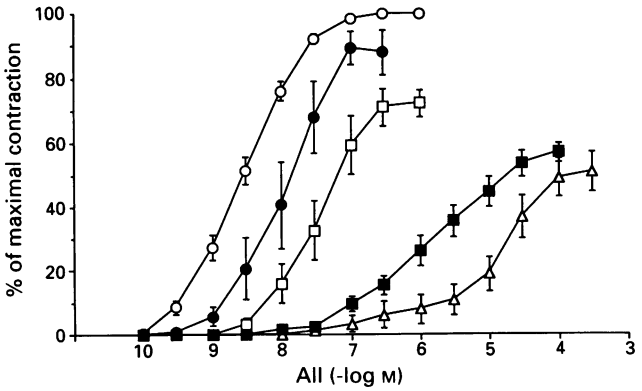

Figure 2 Effect of 1 (●, $n = 6$), 10 (□, $n = 5$), 100 (■, $n = 14$) and 1000 nM (△, $n = 8$) LR-B/081 on the contractions induced by angiotensin II (AII) in rabbit aortic strips. Results are expressed as percentage of the maximum response obtained with AII in control preparations (○, $n = 33$). Values represent the means ± s.e.mean.

antagonist losartan. LR-B/081 0.1 μM reduced the maximum contractile response to 61 ± 3.6% ($n = 12$). Addition of 1 μM losartan partly restored it to 81 ± 0.1 ($n = 7$; $P < 0.01$; Figure 3).

LR-B/081 (10 μM) did not affect the concentration-contraction curves obtained with either KCl or phenylephrine (data not shown).

Effects on AII-induced vasoconstriction in rat isolated perfused kidney

Mean resting perfusion pressure of rat isolated perfused kidney was 91 ± 6 mmHg ($n = 15$). The addition of 30 nM AII caused a sustained vasoconstriction that increased perfusion pressure by 48 ± 6 mmHg ($n = 15$) over baseline and was stable for at least 60–90 min in the control group (final value: 43 ± 5 mmHg; $n = 6$). The addition of increasing concentrations of LR-B/081 ($n = 5$) or losartan ($n = 5$) to the perfusion medium caused a progressive inhibition of AII-induced vasoconstriction. IC_{50} (95% confidence limits) values were 17(13–24) and 39(32–54) nM for LR-B/081 and losartan, respectively. The inhibition of AII-induced vasoconstriction exerted by losartan was fully reversible, since an excess of AII (1 μM) in the medium following the highest dose of antagonist caused a full recovery of the perfusion pressure. Conversely, the inhibition induced by LR-B/081 was only partially reversed by excess AII (Figure 4).

Furthermore, LR-B/081 was a weak inhibitor of vasoconstriction induced by endothelin-1 or adrenaline in this preparation: the respective IC_{50} values were 3.5 (2.6–5.2) and 2.9 (2.2–4.0) μM (data not shown).

Effects on AII-induced pressor response in pithed rats

In control rats the basal mean diastolic pressure was 40 ± 1.5 mmHg ($n = 10$) before vehicle administration and 44 ± 1.5 mmHg after 15 min. LR-B/081 at 0.2, 0.6 and 2 μmol kg^{-1}, i.v., dose-dependently decreased diastolic blood pressure (DBP) from 41 ± 0.8 ($n = 17$) to 34 ± 2.0 ($n = 6$), 29 ± 1.5 ($n = 6$) and 27 ± 1.6 mmHg ($n = 5$), 5 min after administration. No agonist activity was found with any dose employed. Losartan at 2, 6, 13 and 20 μmol kg^{-1}, i.v., lowered DBP from 41 ± 1.2 ($n = 22$) to 32 ± 4.3 ($n = 6$), 28 ± 2.8 ($n = 5$), 28 ± 1.1 ($n = 5$) and 27 ± 1.3 ($n = 6$) mmHg, respectively, 15 min after administration (data not shown).

The cumulative infusion of AII (0.003–30 μg kg^{-1}) caused a dose-dependent increase in DBP up to 108 ± 2.0 mmHg with an ED_{50} of 0.11 (0.05–0.21) μg kg^{-1}. The administration of LR-B/081 at 0.2, 0.6 and 2 μmol kg^{-1}, i.v., caused non-parallel shifts to the right of the dose-response curve to AII and increased the ED_{50} (95% confidence limits) value to 1.5 (0.74–2.7), 5.0 (3.6–7.0) and 95 (82–111) μg kg^{-1}, respectively (Figure 5). The maximal value of DBP was progressively decreased with increasing doses of LR-B/081 (Figure 5). In contrast, losartan at 2, 6, 13 and 20 μmol kg^{-1}, i.v. induced parallel shifts to the right of the dose-response curve to AII, with ED_{50} values of 3.2 (2.4–4.3), 7.6 (4.7–9.6), 29 (14–48) and 179 (135–236) μg kg^{-1}, respectively. The maximum increase in DBP after each dose of losartan was not significantly different from that obtained with the vehicle (data not shown).

As shown in Figure 6, when 6 μmol kg^{-1} losartan was coadministered with 0.6 μmol kg^{-1} LR-B/081, a progressive recovery of the maximal AII-induced pressor response was observed. In the presence of 13 μmol kg^{-1} losartan the AII-induced pressor response curve was further shifted to the right.

Noradrenaline-induced pressor responses were not affected by LR-B/081 at 6 μmol kg^{-1}, i.v. (data not shown).

Effects on AII-induced pressor response in conscious normotensive rats

In the vehicle-treated group ($n = 9$), mean basal arterial blood pressure was 113 ± 2.3 mmHg. Intravenous AII (0.105 nmol kg^{-1}) induced a pressor response (43 ± 2.3 mmHg over basal after the first injection) that

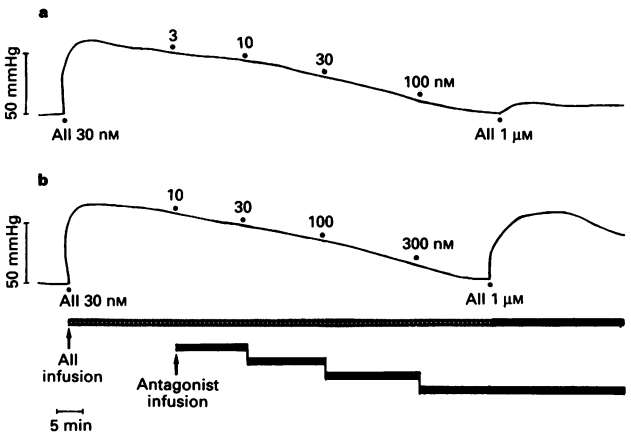

Figure 4 Representative experiments of the effects of increasing concentrations of LR-B/081 (a) and losartan (b) on angiotensin II (AII)-induced vasoconstriction in the rat isolated perfused kidney. At the end of the experiment, an excess of AII (1 μM) was added to the perfusate to test for reversibility.

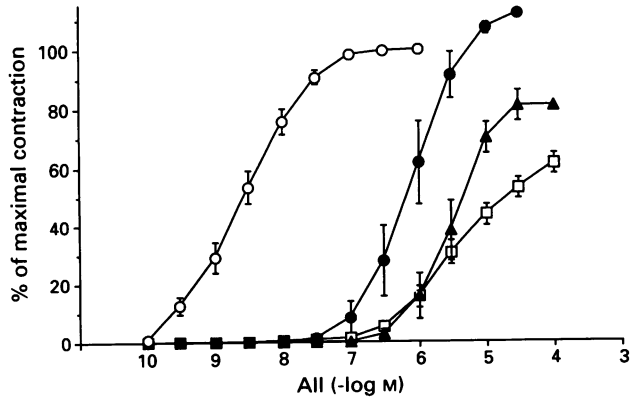

Figure 3 Effect of 1 μM losartan (●, $n = 6$), 0.1 μM LR-B/081 (□, $n = 12$) and 0.1 μM LR-B/081 coincubated with 1 μM losartan (▲, $n = 7$) on the contractions induced by angiotensin II (AII) in rabbit aortic strips. Results are expressed as percentage of the maximum response obtained with AII in control preparations (○, $n = 25$). Values represent the means ± s.e.mean.

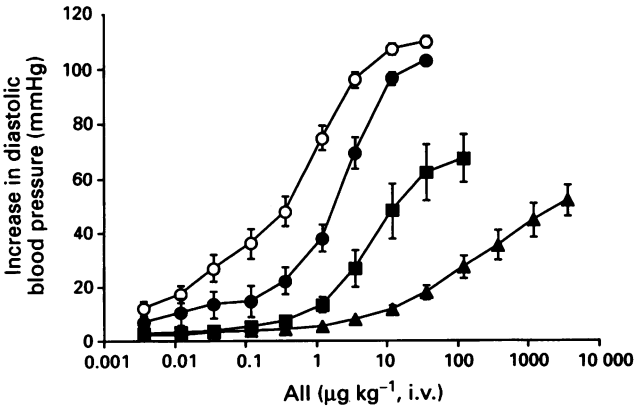

Figure 5 Effect of intravenous vehicle (○, $n = 10$), 0.2 (●, $n = 6$), 0.6 (■, $n = 6$) and 2 μmol kg^{-1} (▲, $n = 5$) LR-B/081 on angiotensin II (AII)-induced (0.003–3,000 μg kg^{-1}, i.v.) pressor response in the pithed rat. Data represent mean values ± s.e.mean.

showed a very slow tendency to decrease during the course of the experiment (Figure 7). In LR-B/081 ($n = 8$) and losartan ($n = 8$) groups, mean basal arterial blood pressure was 113 ± 1.9 and 116 ± 2.2 mmHg and pretreatment responses to AII were 44 ± 2.4 and 40 ± 2.7 mmHg, respectively. LR-B/081 and losartan at 6 μmol kg^{-1}, p.o., exerted a marked inhibitory effect on AII-induced pressor responses. Maximum inhibition was reached after 2 h with LR-B/081 ($82 \pm 3\%$) and after 4 h with losartan ($83 \pm 1.5\%$). Both compounds showed a long lasting effect, which was still significant ($P < 0.05$) 24 h after the oral dosing (Figure 7).

Effects in conscious renal hypertensive rats

Cumulative intravenous injections of LR-B/081 ($n = 6$) or losartan ($n = 12$) caused a dose-dependent decrease in mean arterial pressure in conscious RHRs. The ED_{40mmHg} values (95% confidence limits) were 0.50 (0.36–0.70) and 0.86 (0.57–1.30) μmol kg^{-1} for LR-B/081 and losartan, respectively (data not shown). A single intravenous administration of 2 μmol kg^{-1} LR-B/081 ($n = 10$) or losartan ($n = 8$) exerted a prolonged fall in blood pressure that lasted more than 12 h (Figure 8).

When given orally at 6 μmol kg^{-1} LR-B/081 ($n = 8$) produced a marked drop in MAP that lasted more than 12 h. A similar result was found with 6 μmol kg^{-1} losartan ($n = 6$; Figure 9a). Heart rate was not modified by either LR-B/081 or losartan treatment (Figure 9b).

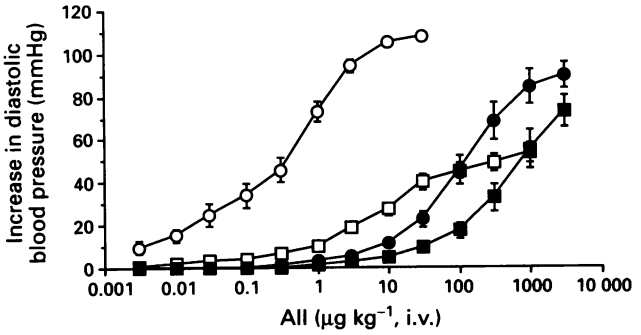

Figure 6 Effect of intravenous vehicle (○, $n = 10$), 0.6 μmol kg^{-1} LR-B/081 alone (□, $n = 6$) and coadministered with 6 (●, $n = 8$) and 13 μmol kg^{-1} (■, $n = 6$) losartan on angiotensin II (AII)-induced (0.003–3,000 μg kg^{-1}, i.v.) pressor response in the pithed rat. Data represent mean values ± s.e.mean.

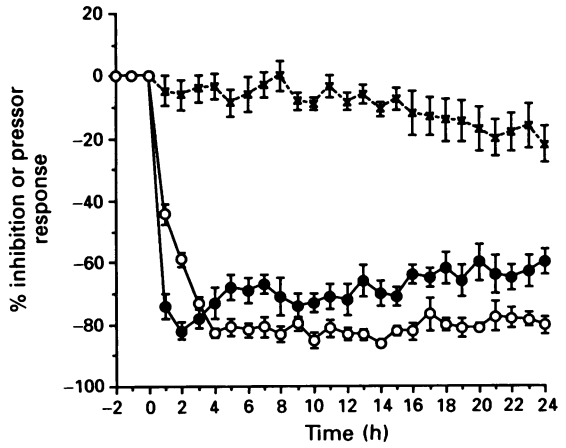

Figure 7 Effect of orally administered vehicle (x, $n = 9$), 6 μmol kg^{-1} LR-B/081 (●, $n = 8$) or losartan (○, $n = 8$) on angiotensin II-induced (0.105 nmol kg^{-1}, i.v.) pressor response in conscious normotensive rats. Values represent the means ± s.e. mean.

Effects in conscious spontaneously hypertensive rats (SHRs)

LR-B/081 at 20 μmol kg^{-1}, p.o. ($n = 7$) caused a fall in blood pressure similar to that produced by 20 μmol kg^{-1} losartan ($n = 7$). The duration of action for both compounds exceeded

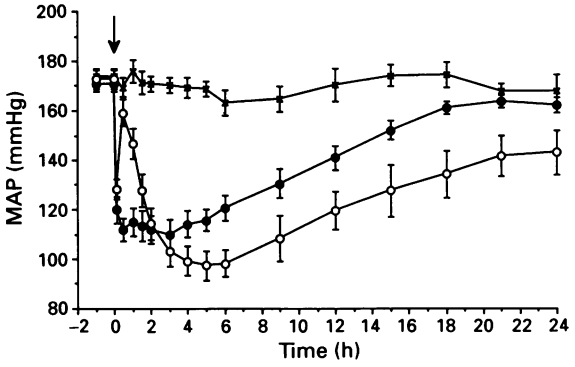

Figure 8 Effect of intravenous administration of vehicle (x, $n = 6$), 2 μmol kg^{-1} LR-B/081 (●, $n = 10$) and losartan (○, $n = 8$) on mean arterial pressure in conscious renal hypertensive rats. Data represent the means ± s.e. mean.

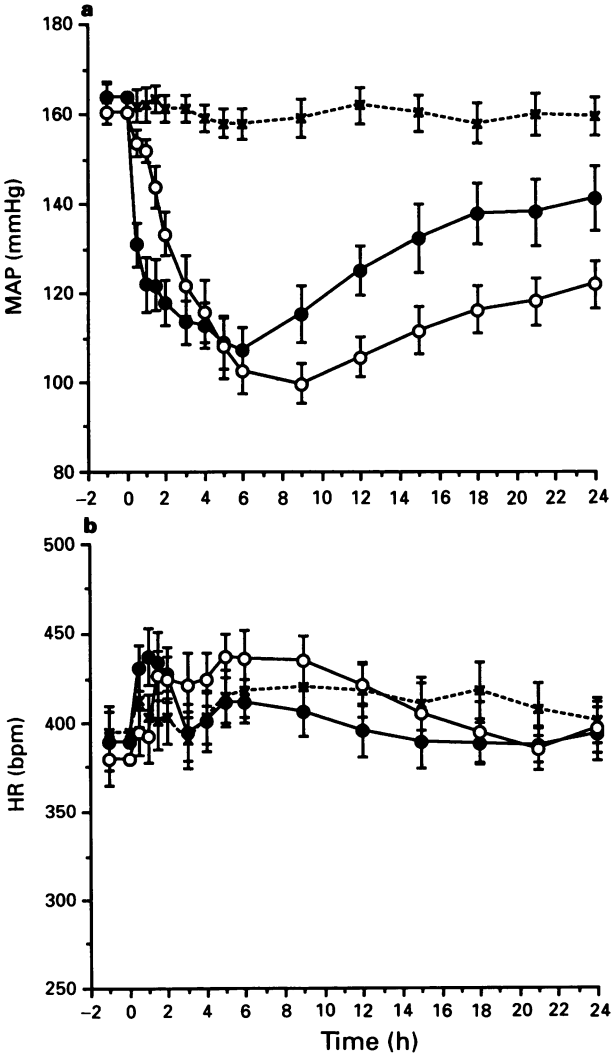

Figure 9 Effect of a single oral administration of vehicle (x, $n = 11$), 6 μmol kg^{-1} LR-B/081 (●, $n = 8$) and losartan (○, $n = 6$) on mean arterial pressure (a) and heart rate (b) in conscious renal hypertensive rats. Values represent the means ± s.e.mean.

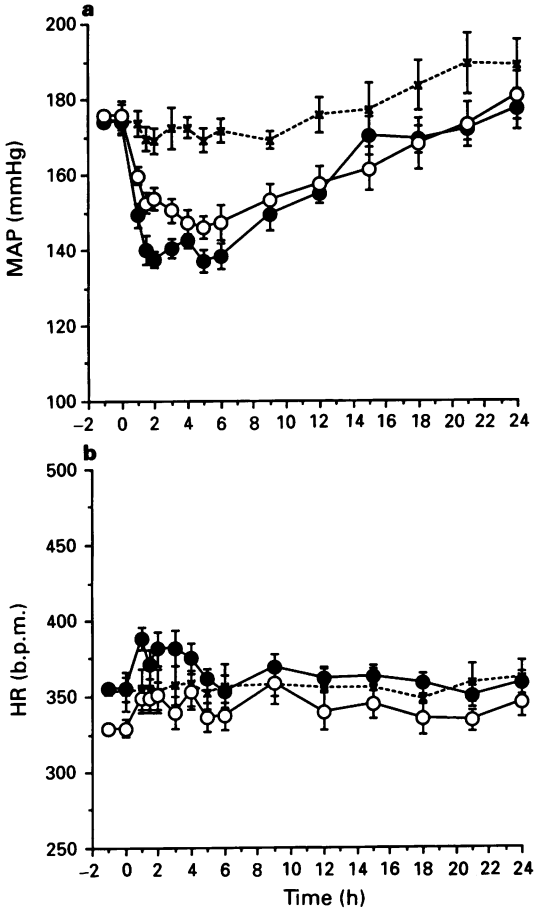

Figure 10 Effect of single oral administration of vehicle (x, $n = 6$), 20 μmol kg^{-1} LR-B/081 (●, $n = 7$) and losartan (○, $n = 7$) on mean arterial pressure (a) and heart rate (b) in conscious spontaneously hypertensive rats. Values represent the means ± s.e.mean.

12 h (Figure 10a). Heart rate was not significantly modified by either drug (Figure 10b).

Daily oral administration of 17 μmol kg^{-1} LR-B/081 ($n = 10$) or 22 μmol kg^{-1} losartan ($n = 10$) for 16 days induced a similar sustained fall in systolic blood pressure. The decrease in systolic blood pressure measured with both compounds on the first day was not significantly different from that obtained at day 16 (Figure 11).

Effects in conscious normotensive rats

No significant difference between the effects of vehicle ($n = 6$) or cumulative dose injections of LR-B/081 (0.6–20 μmol kg^{-1}; $n = 6$) on mean arterial pressure and heart rate were found (data not shown).

Discussion

LR-B/081 has been recently characterized in *in vitro* binding studies as a potent and selective AT_1 receptor antagonist: its affinity for receptors of rat adrenal cortex membranes ($K_i = 0.9 \pm 0.2$ nM) was about tenfold higher than that of losartan, whereas its binding to the AT_2 receptor of bovine cerebellum membranes was negligible (Renzetti *et al.*, 1994b). In saturation experiments, LR-B/081 decreased the number of binding sites without affecting the K_D for AII. However, the compound did not influence the rate of dissociation of tritiated AII from these receptors, indicating that LR-B/081 differs from both classical competitive and allosteric antagonists (Renzetti *et al.*, 1994b).

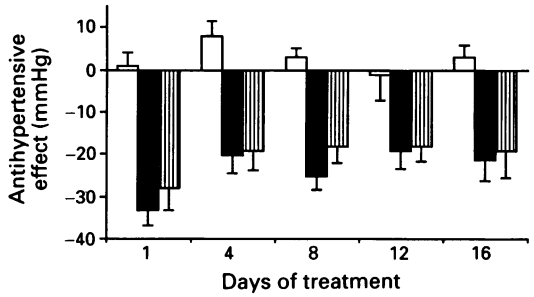

Figure 11 Effect of repeated oral dosing of vehicle (open columns, $n = 10$), 17 μmol kg^{-1} LR-B/081 (solid columns; $n = 10$) and 22 μmol kg^{-1} losartan (hatched columns; $n = 10$) on systolic blood pressure in conscious spontaneously hypertensive rats. Figure shows the antihypertensive effect measured 3 h after treatment on days 1, 4, 8, 12 and 16. Values represent the means ± s.e.mean.

The present data agree with the above observations. Indeed, LR-B/081 appears to be an insurmountable antagonist of AII in rabbit aorta as shown by nonparallel shifts of the dose-response curves to AII and by the depression of the maximal contractile responses. Wash-out procedures for up to 2 h of rabbit aorta incubated with 10 nM LR-B/081 did not result in any recovery of the maximal contraction (unpublished data). A similar behaviour was observed in rat isolated perfused kidney, in which LR-B/081 potently inhibited the AII-induced vasoconstriction, but an excess of AII was not able to restore the perfusion pressure to the pretreatment value. Similarly, in the pithed rat, increasing intravenous doses of LR-B/081 resulted in nonparallel shifts of the dose-pressor curves to AII with a decrease of maximal response, a behaviour consistent with insurmountable antagonism. However, the interaction of LR-B/081 with AT_1-receptors of the vasculature appears to be reversible, since the coincubation or coadministration of losartan, a surmountable AII AT_1 antagonist, was capable of restoring the maximal response to AII both in rabbit aorta and in pithed rats, suggesting that LR-B/081 and losartan interact with the same binding site both *in vitro* or *in vivo* (Wong & Timmermans, 1991; Robertson *et al.*, 1992; Wienen *et al.*, 1992).

The molecular mechanisms that underlie this insurmountable antagonism are not clear, although a slow displacement rate of LR-B/081 from its binding sites, in tissues believed to have little or no receptor reserve for AII, is likely to be involved (Liu *et al.*, 1992; Wienen *et al.*, 1992). An insurmountable antagonism similar to that exerted by LR-B/081 has been observed for other nonpeptide AT_1 antagonists such as EXP 3174 (Wong *et al.*, 1990b), GR 117289 (Robertson *et al.*, 1992), BIBR 277 (Wienen *et al.*, 1993), CV 11974 (Shibouta *et al.*, 1993), valsartan (Criscione *et al.*, 1993) and DuP 532 (Chiu *et al.*, 1991).

In terms of potency, a precise comparison between LR-B/081 and losartan is precluded by the different nature of the antagonism, surmountable for the latter, insurmountable for the former. However, LR-B/081 appears considerably more potent in rabbit aorta and in pithed rats, in agreement with binding studies (Renzetti *et al.*, 1994b), while it was only twice as potent on rat kidney vasculature.

A selective interaction of LR-B/081 with AII receptors was substantiated by the observation that the compound was unable to affect vasoconstriction induced by either KCl or phenylephrine on rabbit aorta and inhibited the vasoconstriction induced by noradrenaline and endothelin-1 in the rat isolated perfused kidney only at high concentrations. Also *in vitro*, the antagonism of LR-B/081 appeared to be specific since vasopressor responses to noradrenaline in the pithed rat were not affected by LR-B/081.

LR-B/081, administered intravenously, lowered blood pres-

sure in the pithed rat, but did not affect blood pressure in conscious normotensive rats. The hypotensive effect is presumably due to the suppression by AT_1 antagonists of the vasoconstrictor influence of endogenous AII in the pithed rat, a model in which blood pressure is highly dependent upon activation of the renin-angiotensin system (De Jonge *et al.*, 1982). Furthermore, LR-B/081 was devoid of any agonist activity either *in vitro* or *in vivo*.

When tested orally for potency and duration of action, LR-B/081 was found to be as active as losartan either in inhibiting AII-induced pressor response or in lowering blood pressure in conscious renal and spontaneously hypertensive rats. The onset of the effect was generally shorter than that of losartan. The pressure lowering effect was not accompanied by tachycardia. Repeated administration of LR-B/081 did not result in any phenomenon of tolerance and its efficacy was retained after 16 days of treatment.

It should be noted that the maximal antihypertensive effect of LR-B/081 in RHRs did not occur concomitantly with the maximal inhibitory effect on the AII pressor response. As suggested by others (Roccon *et al.*, 1994), the AT_1 receptor antagonists, might require some time to penetrate completely into the vascular compartment to exert a maximal blockade of endogenous AII-induced vasoconstriction. Differences in inhibiting the vasoconstriction induced by exogenous or endogenous AII may involve AT_1 receptors in different layers of the vascular wall.

Although LR-B/081 was found to be more potent than losartan both in binding studies and in rabbit aortic strips or the pithed rat, its antihypertensive effects in rat models was similar to that exhibited by losartan. The reason for this discrepancy may be related to the *in vivo* effects of losartan which are attributed to the hepatically-generated metabolite, EXP 3174 (Wong *et al.*, 1990b), while LR-B/081 is active *per se in vivo*.

In summary, the data presented demonstrate that LR-B/081 is a highly selective, potent and orally active nonpeptide AII AT_1-receptor antagonist. Given orally, LR-B/081 is an effective antihypertensive agent, particularly in animals in which blood pressure is elevated as a result of activation of the renin-angiotensin system or by sustained infusion of AII. The comparison of the profile over time of the inhibitory effect of LR-B/081 on AII pressor response in normotensive rats with its antihypertensive effects in RHRs, suggests that the blockade of the vasoconstrictor effect of AII by LR-B/081 is the likely primary mechanism of its antihypertensive effect. The therapeutic potential of the LR-B/081 will be evaluated in clinical studies.

This work was supported by IMI, Rome (grant No. 53092). The authors wish to thank Dr M. Criscuoli for the helpful suggestions and critical reading of the manuscript and Mr M. Bachi and Mrs F. Giuntini for their excellent technical assistance.

References

ARUNLAKSHANA, A.D. & SCHILD, H.O. (1959). Some quantitative uses of drug agonists. *Br. J. Pharmacol. Chemother.*, **14**, 48–58.

CANGIANO, J.L., RODRIGUEZ-SARGENT, C. & MARTINEZ-MALDONADO, M. (1979). Effects of antihypertensive treatment on systolic blood pressure and renin in experimental hypertension in rats. *J. Pharmacol. Exp. Ther.*, **208**, 310–313.

CASTELLUCI, A., MANZINI, S. & EVANGELISTA, S. (1993). A new method for assessing Ca^{2+} requirements for vasoconstriction in the rat isolated perfused kidney. Effect of norepinephrine and endothelin. *J. Pharmacol. Methods*, **29**, 17–20.

CHIN, H.L. & BUCHAN, D.A. (1990). Severe angioedema after long-term use of an angiotensin-converting enzyme inhibitor. *Ann. Intern. Med.*, **112**, 312–313.

CHIU, A.T., CARINI, D.J., DUNCIA, J.V., LEUNG, K.H., MCCALL, D.E., PRICE, J.W.A., WONG, P.C., SMITH, R.D., WEXLER, R.R. & TIMMERMANS, P.B.M.W.M. (1991). DuP 532: a second generation of nonpeptide angiotensin II receptor antagonists. *Bioch. Biophys. Res. Commun.*, **177**, 209–217.

CHIU, A.T., MCCALL, D.E., PRICE, W.A., WONG, P.C., CARINI, D.J. DUNCIA, J.V., WEXLER, R.R., YOO, S.E., JOHNSON, A.L. & TIMMERMANS, P.B.M.W.M. (1990). Nonpeptide angiotensin II receptor antagonists. VII. Cellular and biochemical pharmacology of DuP 753, an orally active antihypertensive agent. *J. Pharmacol. Exp. Ther.*, **252**, 711–718.

CRISCIONE, L., DE GASPARO, M., BUHLMAYER, P., WHITEBREAD, S., RAMJOUE', H.P.R. & WOOD, J. (1993). Pharmacological profile of valsartan: a potent, orally active, nonpeptide antagonist of the angiotensin II AT_1-receptor subtype. *Br. J. Pharmacol.*, **110**, 761–771.

DE JONGE, A., KNAPE, J.T.A., VAN MEEL, J.C.A., KALKAN, H.O., WILFFERT, B., THOOLEN, M.J.M.C., TIMMERMANS, P.B.M.W.M. & VAN ZWIETEN, P.A. (1982). Effect of converting enzyme inhibition and angiotensin receptor blockade on the vasoconstriction mediated by alpha-1 and alpha-2 adrenoceptors in pithed normotensive rats. *Naunyn-Schmied. Arch. Pharmacol.*, **321**, 309–321.

DZAU, V.J., KOPELMAN, R.I., BARGER, A.C. & HABER, E. (1980). Renin-specific antibody for study of cardiovascular homeostasis. *Science*, **207**, 1091–1093.

FURCHGOTT, R.F. & BHADRAKOM, S. (1953). Reactions of strips of rabbit aorta to ephinephrine, isopropylarterenol, sodium nitrite and other drugs. *J. Pharmacol. Exp. Ther.*, **108**, 129–143.

HERBLIN, W.F., CHIU, A.T., MCCALL, D.E., ARDECKY, R.J., CARINI, D.J., DUNCIA, J.V., PEASE, L.J., WONG, P.C., WEXLER, R.R., JOHNSON, A.L. & TIMMERMANS, P.B.M.W.M. (1991). Angiotensin II receptor heterogeneity. *Am. J. Hypertens.*, **4** (Suppl.), 299S–302S.

KENAKIN, T.P. (1987). Drug antagonism. In *Pharmacological Analysis of Drug-Receptor Interaction.*, ed. Kenakin T.P., pp. 205–244. New York: Raven Press.

KINOSHITA, A., URATU, H., BUMPUS, F.M. & HUSAIN, A. (1991). Multiple determinants for the high substrate specificity of an angiotensin II-forming chimase from human heart. *J. Biol. Chem.*, **266**, 19192–19197.

LIU, Y.J., SHANKLEY, N.P., WELSH, N.J. & BLACK, J.W. (1992). Evidence that the apparent complexity of receptor antagonism by angiotensin II analogues is due to a reversible and synntopic action. *Br. J. Pharmacol.*, **106**, 233–241.

PHILIPPS, P.I. (1987). Functions of angiotensin in the central nervous system. *Annu. Rev. Physiol.*, **49**, 413–435.

RENZETTI, A.R., CUCCHI, P., GUELFI, M., SALIMBENI, A. & SUBISSI, A. (1994a). LR-B/057: a novel orally active AT_1 receptor antagonist. *Br. J. Pharmacol.*, **111**, 267P.

RENZETTI, A.R., SALIMBENI, A., SUBISSI, A. & GIACHETTI, A. (1994b). Receptor binding pharmacology of LR-B/081, a novel AT_1 receptor antagonist. *J. Hypertension*, **12** (Suppl. 3), S96.

ROBERTSON, M.J., BARNES, J.C., DREW, G.M., CLARK, K.L., MARSHALL, F.H., MICHEL, A., MIDDLEMISS, D., ROSS, B.C., SCOPES, D. & DOWLE, M.D. (1992). Pharmacological profile of GR 117289 *in vitro*: a novel non-peptide angiotensin AT_1-receptor antagonist. *Br. J. Pharmacol.*, **107**, 1173–1180.

ROCCON, A., MARCHIONNI, D., DONAT, F., SEGONDY, D., CAZAUBON, C. & NISATO, D. (1994). A pharmacodynamic study of SR 47436, a selective AT_1 receptor antagonist, on blood pressure in conscious cynomolgus monkeys. *Br. J. Pharmacol.*, **111**, 145–150.

SHIBOUTA, Y., INADA, Y., OJIMA, M., WADA, T., NODA, M., SANADA, T., KUBO, K., KOHARA, Y., NAKA, T. & NISHIKAWA, K. (1993). Pharmacological profile of a highly potent and long-acting angiotensin II receptor antagonist, 2-ethoxy-1-[[2'- (1H-tetrazol-5-yl)biphenyl-4-yl]methyl]-1H-benzimidazole-7-carboxylic acid (CV-11974), and its prodrug, (±)-1-(cyclohexyloxycarbonyloxy)-ethyl 2-ethoxy-1-[[2'-(1H-tetrazol-5-yl)biphenyl-4-yl]methyl]-1H-benzimidazole-7-carboxylate (TCV-116). *J. Pharmacol. Exp. Ther.*, **266**, 114–120.

TIMMERMANS, P.B.M.W.M., WONG, P.C., CHIU, A.T. & HERBLIN, W.F. (1991). Nonpeptide angiotensin II receptor antagonists. *Trends Pharmacol. Sci.*, **12,** 55–62.

TIMMERMANS, P.B.M.W.M., WONG, P.C., CHIU, A.T. HERBLIN, W.F., BENFIELD, P., CARINI, D.J., LEE, R.J., WEXLER, R.R., SAYE, J.A.M. & SMITH, R.D. (1993). Angiotensin II receptors and angiotensin II receptor antagonists. *Pharmacol. Rev.*, **45,** 205–251.

WIENEN, W., HAVEL, N., VAN MEEL, J.C.A., NARR, B., RIES, U. & ENTZEROTH, M. (1993). Pharmacological characterization of the novel nonpeptide angiotensin II receptor antagonist, BIBR 277. *Br. J. Pharmacol.*, **110,** 245–252.

WIENEN, W., MAUZ, A.B.M., VAN MEEL, J.C.A. & ENTZEROTH, M. (1992). Different types of receptor interaction of peptide and nonpeptide angiotensin II antagonists revealed by receptor binding and functional studies. *Mol. Pharmacol.*, **41,** 1081–1088.

WILLIAMS, H.G. (1988). Converting enzyme inhibitors in the treatment of hypertension. *N. Engl. J. Med.*, **319,** 1517–1525.

WONG, P.C., PRICE, W.A., CHIU, A.T., DUNCIA, J.V., CARINI, D.J., WEXLER, R.R., JOHNSON, A.L. & TIMMERMANS, P.B.M.W.M. (1990a). Nonpeptide angiotensin II receptor antagonists. VIII. characterization of functional antagonism displaced by DuP 753, an orally active antihypertensive agent. *J. Pharmacol. Exp. Ther.*, **252,** 719–725.

WONG, P.C., PRICE, W.A., CHIU, A.T., DUNCIA, J.V., CARINI, D.J., WEXLER, R.R., JOHNSON, A.L. & TIMMERMANS, P.B.M.W.M. (1990b). Nonpeptide angiotensin II receptor antagonists. XI. Pharmacology of EXP 3174: an active metabolite of DuP 753, an orally active antihypertensive agent. *J. Pharmacol. Exp. Ther.*, **255,** 211–217.

WONG, P.C. & TIMMERMANS, P.B.M.W.M. (1991). Nonpeptide angiotensin II receptor antagonists: insurmountable angiotensin II antagonism of EXP 3892 is reversed by the surmountable antagonist DuP 753. *J. Pharmacol. Exp. Ther.*, **258,** 49–57.

(Received June 28, 1994
Revised October 12, 1994
Accepted November 9, 1994)

British Journal of Pharmacology (1995) 114, 1125-1132

Effects of suramin on contractions of the guinea-pig vas deferens induced by analogues of adenosine 5'-triphosphate

S.J. Bailey & [1]S.M.O. Hourani

Receptors and Cellular Regulation Research Group, School of Biological Sciences, University of Surrey, Guildford, Surrey GU2 5XH

1 Adenosine 5'-triphosphate (ATP) and some of its analogues contract the guinea-pig vas deferens, acting via receptors which have been classified as P_{2X}-purinoceptors. We have recently shown, however, that the effects of ATP are enhanced, rather than inhibited, by the non-selective P_2 antagonist, suramin, and that this enhancement could not easily be explained in terms of inhibition by suramin of the breakdown of ATP. We therefore investigated the effects of suramin on contractions induced by ATP analogues, to define the structure-activity relationships of the suramin-resistant response.

2 In the absence of suramin, the order of potency for ATP analogues was adenosine 5'-(α,β-methylene)triphosphonate (AMPCPP) = P^1,P^5-diadenosine pentaphosphate (Ap_5A) = adenosine 5'-tetraphosphate (Ap_4) > adenosine 5'-O-(3-thiotriphosphate) (ATPγS) = adenylyl 5'-(β,γ-methylene) diphosphonate (AMPPCP) > P^1,P^5-diadenosine tetraphosphate (Ap_4A) > adenosine 5'-O-(2-thiodiphosphate) (ADPβS) > 2-methylthioadenosine 5'-triphosphate (MeSATP) ≥ ATP > adenosine 5'-diphosphate (ADP). This is generally in agreement with previously reported structure-activity relationships in this tissue.

3 In the presence of suramin (1 mM), responses to Ap_5A, Ap_4A, AMPPCP, ADPβS and ADP were abolished or greatly reduced, and contractions induced by AMPCPP, Ap_4 and ATPγS were inhibited. Contractions induced by MeSATP however, like those induced by ATP itself, were not reduced, but at concentrations above 100 μM were enhanced. In the presence of suramin (1 mM) the order of potency of analogues was therefore AMPCPP = Ap_4 > ATP = MeSATP > ATPγS, with all other analogues tested being essentially inactive at concentrations up to 500 μM.

4 Contractile responses of the vas deferens to transmural nerve stimulation (1-50 Hz) in the presence of the α-adrenoceptor antagonist, phentolamine (10 μM), were abolished by suramin (1 mM). This is in agreement with previous reports that suramin inhibits the excitatory junction potential, a response thought to be mediated by P_2 purinoceptors. It is however hard to reconcile the evidence implicating ATP as the non-adrenergic transmitter responsible for this response with the failure of suramin to inhibit the contractions induced by ATP itself while abolishing nerve-mediated contractions.

5 In conclusion, these results confirm our previous findings of a suramin-resistant component to the ATP-induced contraction in the guinea-pig vas deferens, and show that the structure-activity relationships of this response are not identical to those of any known P_2-purinoceptor subclass. Although the inhibition by suramin of the breakdown of ATP may contribute to the suramin-resistance of some of the ATP analogues, it does not appear to provide the full explanation.

Keywords: P_2-purinoceptors; guinea-pig vas deferens; ATP; suramin; adenine nucleotides; adenine dinucleotides

Introduction

The rodent vas deferens had been extensively used as a model tissue in which to study purinoceptor pharmacology and indeed was one of the first tissues in which adenosine 5'-triphosphate (ATP) was convincingly shown to have a role as a co-transmitter with noradrenaline (NA) in sympathetic nerves. The response to nerve stimulation is a biphasic contraction, and the first phase is thought to be due largely to ATP whereas the second, slower phase is due to released NA (Fedan *et al.*, 1981; see Burnstock, 1990; Morris & Gibbins, 1992; Hoyle, 1992 for reviews). The receptor population at which ATP acts in this tissue has the structure-activity relationships of a P_{2X}-purinoceptor and indeed the original division of ATP receptors into P_{2X} mediating contraction and P_{2Y} mediating relaxation of smooth muscle was made partly on the basis of the effects of analogues in the vas deferens (Burnstock & Kennedy, 1985). Analogues of ATP with a relatively stable methylene linkage in the triphosphate chain, such as adenylyl 5'-(β,γ-methylene)diphosphonate (AMPPCP) and adenosine 5'-(α,β-methylene)triphosphonate (AMPCPP) are more potent than ATP at causing contraction while 2-substituted analogues such as 2-methylthioadenosine 5'-triphosphate (MeSATP) are equipotent. In relaxant tissues, however, the order of potency is MeSATP > ATP > AMPCPP, AMPPCP. This division of P_2-purinoceptors in smooth muscle has become widely accepted, and additional subtypes have also been proposed in other tissues: the receptor for ATP^{4-} causing reversible permeabilization of mast cells and some other immune cells (P_{2Z}) and the ADP receptor on blood platelets (P_{2T}) (Gordon, 1986; Cusack & Hourani, 1990). The trypanocidal drug, suramin, has been shown to act as an antagonist at P_{2X}, P_{2Y} and P_{2T} receptors, and is a very useful pharmacological tool although it is a relatively weak antagonist (pA_2 approximately 5) and may not be simply competitive (Dunn & Blakely, 1988; Den Hertog *et al.*, 1989a;b; Hoyle *et al.*, 1990; Leff *et al.*, 1990; Von Kügelgen *et al.*, 1990; Hourani *et al.*, 1992). In addition, it inhibits the breakdown of ATP by ectonucleotidases present on the surface of cells (Hourani & Chown, 1989), which may complicate its use as an antagonist. More recently it has become apparent that in addition to P_{2Y}-purinoceptors, another class of receptor exists with similar actions, which has been called the P_{2U} or nucleotide receptor, at which ATP and uridine 5'-triphosphate (UTP) are agonists but MeSATP is inactive (O'Connor *et al.*, 1991; Dubyak & El-Moatassim, 1993). Two distinct G protein-coupled receptors with the

[1] Author for correspondence.

characteristics expected of P_{2Y} and P_{2U} receptors have recently been cloned, confirming the pharmacological evidence for these subtypes (Webb *et al.*, 1993; Lustig *et al.*, 1993). The P_{2X} receptor has not yet been cloned, but a receptor binding radiolabelled AMPCPP with high affinity has been solubilized from the rat vas deferens and has the expected characteristics of the P_{2X}-purinoceptor, in that the order of potency for displacing binding was AMPCPP = AMPPCP > ATP > MeSATP (Bo *et al.*, 1992). These authors also reported that the binding studies using this radioligand in the membrane preparations derived from the rat vas deferens revealed the presence of both low and high affinity sites, although the significance of this is not clear.

In spite of the structure-activity relationships which clearly define the ATP receptor on the vas deferens as P_{2X}, the actions of ATP and its analogues in this tissue are surprisingly complex and are still not fully understood. On the mouse and rat vas deferens there is evidence for the presence of relaxant P_{2Y}-purinoceptors in addition to the contractile P_{2X} (Blakely *et al.*, 1991; Boland *et al.*, 1992; Mallard *et al.*, 1992), which complicates interpretation of structure-activity relationships. Indeed, on the basis of measurements of intracellular calcium concentrations, it has been proposed that the true rank order of potency for the P_{2X}-purinoceptor in the mouse vas deferens is ATP = MeSATP > AMPPCP, and that the observed low potency of ATP in causing contraction is simply a reflection of its lack of selectivity for P_{2X} receptors and its ability to activate simultaneously P_{2Y} receptors (Boland *et al.*, 1992). Suramin has been reported to increase the maximal response to AMPCPP in rat and mouse vas deferens in addition to shifting the concentration-response curve to the right, which has been attributed to antagonism of inhibitory P_2-purinoceptors, presumably P_{2Y} (Blakely *et al.*, 1991; Mallard *et al.*, 1992). Suramin has also been reported to be unable to inhibit competitively the responses to high concentrations of ATP (> 1 μM) in the mouse vas deferens, although it inhibited responses to AMPCPP, adenosine 5′-O-(3-thiotriphosphate) (ATPγS) and low concentrations of ATP (0.1–1 μM) in an apparently competitive manner (Von Kügelgen *et al.*, 1990). These authors therefore suggested the presence of a suramin-resistant component to the contractile response to ATP of the mouse vas deferens. A suramin-resistant component of the responses to ATP in the rat vas deferens, not mediated by P_{2X} or P_{2Y}-purinoceptors, has also recently been reported (Bültmann & Starke, 1994).

We have recently shown that suramin even at a concentration of 1 mM does not inhibit contractions of the guinea-pig vas deferens induced by ATP at any concentration tested (1–500 μM), and indeed at high concentrations (> 100 μM) enhances contractions induced by high concentrations of ATP (> 100 μM). This concentration of suramin almost abolished ATP-induced contractions of the guinea-pig urinary bladder, another tissue thought to contain P_{2X}-purinoceptors, as well as contractions of the vas deferens induced by the other naturally-occurring nucleoside triphosphates. As the rate of breakdown of ATP was, if anything, faster in the bladder than in the vas deferens, and the other triphosphates have been shown (Welford *et al.*, 1986; 1987; Beukers *et al.*, 1993) to be broken down at the same rate as ATP, differential inhibition of ATP breakdown by suramin in the two tissues appeared unlikely to explain its differential effect as an inhibitor. Desensitization of the P_{2X}-purinoceptors of the vas deferens with AMPCPP abolished ATP-induced contractions in the absence of suramin, as previously reported by Meldrum & Burnstock (1983), but did not affect those induced in the presence of suramin. These findings suggested the presence of an additional suramin-resistant contractile ATP receptor on the vas deferens, whose presence is revealed by suramin, possibly due to concomitant blockade of inhibitory P_{2Y}-purinoceptors (Bailey & Hourani, 1994). The existence of two dissociable phases of contractions induced by ATP in the guinea-pig vas deferens has previously been proposed based, on a series of experiments by Fedan and coworkers (see Fedan & Lamport, 1990a for review). In addition to the normal rapid contraction induced by ATP, at high concentrations (> 100 μM) a second slower phase was observed, and the two phases were inhibited selectively by the two irreversible inhibitors, 3′-O-arylazidoaminopropionyl ATP ($ANAPP_3$) and 2′,3′-dialdehyde ATP (P-ATP) respectively (Fedan *et al.*, 1982b; Fedan & Lamport, 1990b). ATP analogues without methylene substituents in the triphosphate chain, such as ATPγS and adenosine 5′-tetraphosphate (Ap_4) also had a discernible tonic phase, whereas AMPPCP and AMPCPP did not (Fedan *et al.*, 1982a,b), and it was suggested that the second phase might involve a transient transfer of phosphate (or thiophosphate) to the tissue (Lamport-Vrana *et al.*, 1991). We have therefore investigated the ability of suramin to inhibit contractions of the guinea-pig vas deferens induced by a series of analogues of ATP, to define the structure-activity relationships of the suramin-resistant site and to see if the suramin-sensitive and -insensitive components correspond to the two phases discussed by Fedan & Lamport (1990a).

Methods

Male guinea-pigs, 300–350 g, were killed by cervical dislocation and the vasa deferentia were removed. The vasa (15–20 mm long) were mounted in 3 ml organ baths and maintained at 35°C in Krebs solution of the following composition (mM): NaCl 120, KCl 5.9, $MgCl_2$ 1.2, $NaHCO_3$ 15.4, $NaHPO_4$ 1.2, $CaCl_2$ 2.5 and glucose 11.5, gassed with 95%O_2/5%CO_2. A resting tension of 0.5 g was applied to the tissues, and contractions were recorded isometrically with Grass FT03 transducers connected to Grass 79D polygraphs. The tissues were allowed to equilibrate for 1 h, suramin was added (or water for the controls) and the tissues were incubated for another hour, after which non-cumulative concentration-response curves were constructed by giving increasing concentrations of agonists with at least 15 min between doses. In the case of AMPCPP, which caused a long-lasting desensitization, only one concentration was tested on each tissue, at the end of an experiment in which another analogue had been used. To investigate the effect of suramin on non-adrenergic nerve stimulation in the vas deferens, the tissues were electrically field-stimulated in the presence of phentolamine (10 μM) via platinum electrodes (1 cm apart) with a train of pulses at a voltage of 40 V, a duration of 0.5 ms and at a variable frequency, using a Grass S88 stimulator. The stimulus was applied until the contraction had reached a peak and started to decline (approximately 5 s). In one experiment using four tissues an attempt was made to investigate the effect of suramin (1 mM) on the two phases of the response to nerve stimulation in the absence of phentolamine. The tissues were stimulated for 20 s at a frequency of 8 Hz, with the chart recorder running at a fast speed to allow the shape of the response to be seen more clearly. Control responses were recorded, followed by responses in the same tissue after incubation with suramin for 30 min. All other experiments using suramin were carried out in parallel with control experiments, using paired tissues from the same animal, with only one concentration-response curve carried out on each tissue. All contractions were expressed as a percentage of the contraction induced by ATP (500 μM) applied at the start of the experiment, before incubation of the tissues with suramin.

Drugs

MeSATP was obtained from Research Biochemicals, Natick, MA, U.S.A., and ATP, AMPPCP, AMPCPP, Ap_4, ATPγS, P_1,P_5-diadenosine pentaphosphate (Ap_5A), P_1,P_4-diadenosine tetraphosphate (Ap_4A), adenosine 5′-diphosphate (ADP), adenosine 5′-(α,β-methylene)diphosphonate (AMPCP) and

adenosine 5'-O-(2-thiodiphosphate) (ADPβS) were obtained from Sigma Chemical Co., Poole, Dorset. Phentolamine mesylate (Rogitine) was obtained from Ciba-Geigy, and suramin was a generous gift from Bayer, UK. All drugs were dissolved in water, and stored frozen.

Results

All nucleotides tested induced contraction of the guinea-pig vas deferens with the exception of AMPCP, which was inactive at concentrations up to 500 μM. The concentration-response curves were not parallel and the maximal contraction induced varied considerably, which makes calculation of potency ratios difficult, but by estimation of the concentration required to induce 100% contraction (i.e. equal to that induced by 500 μM ATP) the order of potency was AMPCPP = Ap_5A = Ap_4 > ATPγS = AMPPCP > Ap_4A > ADPβS > MeSATP ≥ ATP > ADP. Concentration-response curves for all these agonists are shown in Figure 1a. In the presence of suramin (1 mM), responses to Ap_5A, Ap_4A, AMPPCP, ADPβS and ADP at concentrations up to 500 μM were abolished or greatly reduced (Figure 2; ADP results not shown). Although dose-ratios clearly cannot be calculated, inspection of the figures show that dose-ratios must be greater than 100 for AMPPCP and Ap_4A and greater than 1000 for Ap_5A. Contractions induced by AMPCPP, Ap_4 and ATPγS were inhibited by suramin (1 mM), which caused a shift in the concentration-response curves, but because of the non-sigmoidal shape of the curves and the lack of a clearly defined maximal response dose-ratios cannot be calculated with any accuracy. However, by estimation of the concentrations required to cause 100% contraction in the absence and presence of suramin, dose-ratios of approximately 60 for AMPCPP and Ap_4 and 30 for ATPγS can be derived (Figure 3). Contractions induced by MeSATP were not inhibited by suramin (1 mM), and at concentrations greater than 100 μM were enhanced (Figure 4), in a similar manner to those induced by ATP (results not shown). In the presence of suramin (1 mM) the order of potency for inducing contractions was AMPCPP = Ap_4 ≥ ATP = MeSATP > ATPγS, with all other analogues tested being essentially inactive at concentrations up to 500 μM. Concentration-response curves for those analogues causing contraction in the presence of suramin (1 mM) are shown for comparison in Figure 1b. The contractions induced by these agonists in the presence or absence of suramin (1 mM) did not differ qualitatively, and in each case were extremely rapid and transient. In the case of ATPγS, at high concentrations (e.g. 500 μM) a sustained contraction was sometimes observed following the phasic twitch, but this was inconsistent and again there was no obvious difference in the occurence of this type of response in the absence or presence of suramin (results not shown).

Contractions induced by field stimulation of the tissue (1–50 Hz) in the presence of phentolamine (10 μM) were abolished by suramin (1 mM) (Figure 5). Contractions induced by ATP (0.1–500 μM) in the presence of suramin (1 mM) were not inhibited by phentolamine (10 μM) (results not shown). In the absence of phentolamine, biphasic responses to field stimulation at 8 Hz were observed, but suramin (1 mM) essentially abolished both phases (Figure 6). Suramin (1 mM) did not affect contractions induced by noradrenaline (1–500 μM) (results not shown).

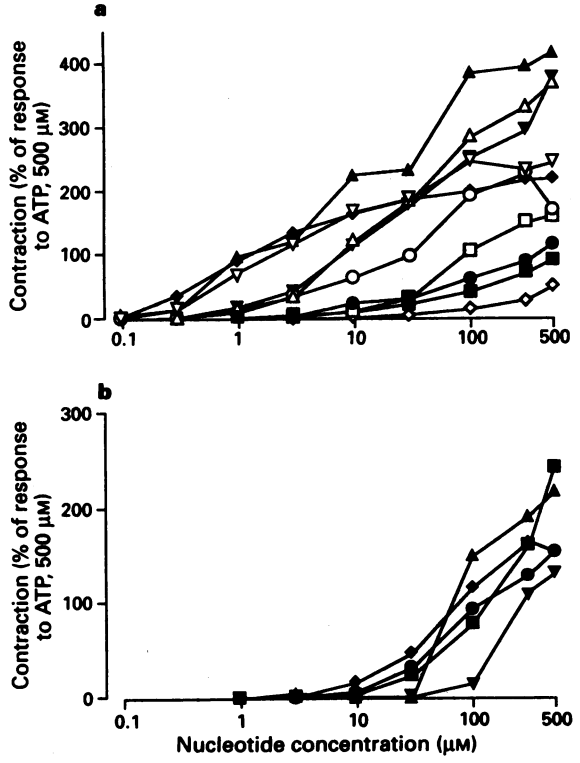

Figure 1 Contractions of the guinea-pig vas deferens induced by ATP (■), ADP (◇), AMPCPP (▲), ATPγS (▼), ADPβS (□), Ap_4 (◆), Ap_4A (○), AMPPCP (△), Ap_5A (▽) or MeSATP (●) in (a) the absence or (b) the presence of suramin (1 mM). Each point is the mean of at least 4 determinations and error bars have been omitted for clarity. For abbreviations see text.

Discussion

In the absence of suramin, the structure-activity relationships of the contractile response were, as previously reported, consistent with the interaction of ATP and its analogues with a P_{2X}-purinoceptor (Burnstock & Kennedy, 1985). The potencies of the analogues tested were generally in agreement with those previously reported, in that AMPPCP, AMPCPP, Ap_5A, Ap_4, ATPγS and ADPβS were all more potent than ATP (Stone, 1981; 1985; Fedan *et al.*, 1982a; MacKenzie *et al.*, 1988), and that Ap_4A was less potent than AMPCPP and Ap_5A (MacKenzie *et al.*, 1988). Fedan and coworkers (1982a,b) have reported that the concentration-response curve for AMPCPP is bell-shaped in that the response decreases at concentrations above 10 μM, and we also found this to be the case if full concentration-response curves using increasing concentrations of this agonist were carried out on each tissue (results not shown). This analogue appeared to cause a much more long-lasting desensitization than any of the others tested, and for this reason only one concentration was tested on each tissue. When this protocol was followed the concentration-response curve was not bell-shaped (see Figures 1a and 3). It has previously been reported that the desensitization of the guinea-pig vas deferens caused by AMPCPP is more long-lasting than that of Ap_5A, and this has been interpreted as indicating a difference in the mechanism of action of these two compounds at their receptor (MacKenzie *et al.*, 1988). In a preliminary study on the rat vas deferens however, desensitization by AMPCPP and Ap_5A has been reported to reduce selectively the slow and fast phases respectively of the response to ATP, and this was interpreted as indicating the possible existence of subtypes of receptor in this tissue (Stone & Paton, 1989). The low potency of ADP and inactivity of AMPCP is also as previously reported (Fedan *et al.*, 1982a), although these workers showed some contractile effects of AMPCP at concentrations of 300 μM and above. MeSATP was roughly equipotent with ATP, in agreement with previous reports (Burnstock *et al.*, 1985), and this is as expected for a P_{2X}-purinoceptor (Burnstock & Kennedy, 1985).

In the presence of 1 mM suramin however, the potency order of the analogues changed, and the effect of suramin was not consistent but depended on the analogue used. It

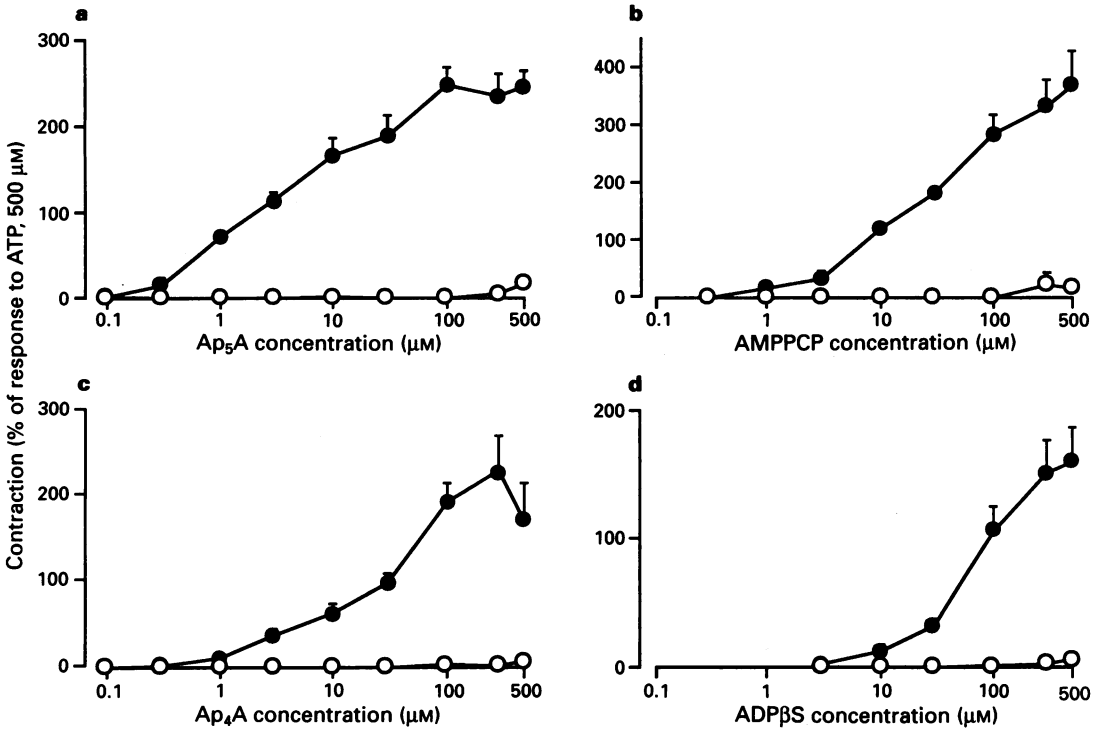

Figure 2 Contractions of the guinea-pig vas deferens induced by (a) Ap_5A, (b) AMPPCP, (c) Ap_4A or (d) ADPβS in the absence (●) or presence (○) of suramin (1 mM). Each point is the mean of at least 4 determinations and the vertical bars show the s.e.mean. For abbreviations see text.

should be noted that although in some systems suramin behaves as a pure competitive antagonist (Von Kügelgen *et al.*, 1990), it has limited specificity and usually displays pronounced noncompetitive effects, with a very steep Schild plot slope or depression of the maximal response to agonists (Hoyle *et al.*, 1990; Leff *et al.*, 1990; Hourani *et al.*, 1992; Bailey & Hourani, 1994). It has been described as a very slowly equilibrating competitive antagonist in the rabbit ear artery (Leff *et al.*, 1990), although in other systems this cannot explain its kinetics (Hourani *et al.*, 1992). This complication means that even though its pA_2 has been measured in some systems and has been reported to be in the region of 5 (Hoyle *et al.*, 1990; Leff *et al.*, 1990; Von Kügelgen *et al.*, 1990; Hourani *et al.*, 1992), it is not a straightforward matter to predict the dose-ratio observed with any concentration of suramin. If it were a simple competitive antagonist, suramin at a concentration of 1 mM should give a dose-ratio in the region of 100. However, it almost abolishes contractile responses of the guinea-pig urinary bladder, which also contains P_{2X}-purinoceptors (Burnstock & Kennedy, 1985) to both ATP itself (up to 1 mM, corresponding to a dose-ratio in excess of 100) (Bailey & Hourani, 1994) and to AMPCPP (up to 1 mM, corresponding to a dose-ratio in excess of 1000) (Hoyle *et al.*, 1990). The 'dose-ratio' of approximately 60 observed against AMPCPP and Ap_4A might not appear inconsistent with a pA_2 in the region of 5, but the effect of suramin on other analogues suggests that in this tissue too, suramin is behaving non-competitively and that 1 mM suramin essentially abolishes responses mediated via P_{2X}-purinoceptors. For example, AMPPCP and ATPγS were equipotent in causing contractions in the absence of suramin, but in the presence of 1 mM suramin AMPPCP was completely inactive at concentrations up to 500 μM (equivalent to a dose-ratio in excess of 100) whereas ATPγS retained activity. Similarly, Ap_5A and Ap_4 were equipotent in the absence of suramin but only Ap_4 could cause contraction in the presence of 1 mM suramin, responses to Ap_5A being abolished (corresponding to a dose-ratio in excess of 1000). Most strikingly, the contractions induced by MeSATP were enhanced by suramin, in the same way that those of ATP are enhanced (Bailey & Hourani, 1994). This may reflect the presence of an inhibitory P_2-purinoceptor (presumably P_{2Y}) on the tissue, as has been proposed for the mouse (Blakely *et al.*, 1991; Boland *et al.*, 1992) and rat (Mallard *et al.*, 1992) vas deferens. Suramin-resistant responses to MeSATP have also been reported in the rat vagus nerve, where responses to ATP are also enhanced by suramin (Trezise *et al.*, 1993).

Overall however, the structure-activity relationships observed in the presence of 1 mM suramin are not the same as those observed in its absence, and cannot be explained in terms of a shift of the concentration-response curves of all the agonists to the right by a constant factor. Although it is hard to rule out any effect via P_{2X}-purinoceptors in the presence of suramin (1 mM), it seems likely that in fact it effectively blocks these receptors and that the responses observed in its presence are mediated by another site, with distinct structure-activity relationships. This site cannot be a P_{2U} or nucleotide receptor, at which UTP is equipotent with ATP and MeSATP is inactive (O'Connor *et al.*, 1990), as contractile responses to UTP are abolished by suramin (Bailey & Hourani, 1994), whereas those to MeSATP were enhanced. The structure-activity relationships are also not compatible with this contractile site being a P_{2T}-,P_{2Y}- or P_{2Z}-purinoceptor: at P_{2T} receptors ATP is an antagonist, at P_{2Y} receptors MeSATP is considerably more potent than ATP, and at P_{2Z} receptors AMPCPP is inactive (see Cusack & Hourani, 1990; Cusack, 1993 for review). In any case, suramin is as potent an antagonist at the first two of these subtypes as it is at P_{2X}-purinoceptors (Hoyle *et al.*, 1990; Hourani *et al.*, 1992), and has also been reported to inhibit the effects of ATP on mast cells (Jaffar & Pearce, 1990), which contain P_2-purinoceptors of the P_{2Z} subtype (Gordon, 1986). A suramin-resistant contractile P_2-purinoceptor responding to ATP but not identical to P_{2X} or to P_{2Y} has recently been proposed in the rat vas deferens, on the basis of studies of the effects of various putative P_2-purinoceptor antagonists (Bültmann & Starke, 1994). The structure-activity relationships for agonists at this receptor in the rat vas deferens have however not yet been reported.

The suramin-resistant response also did not seem to corres-

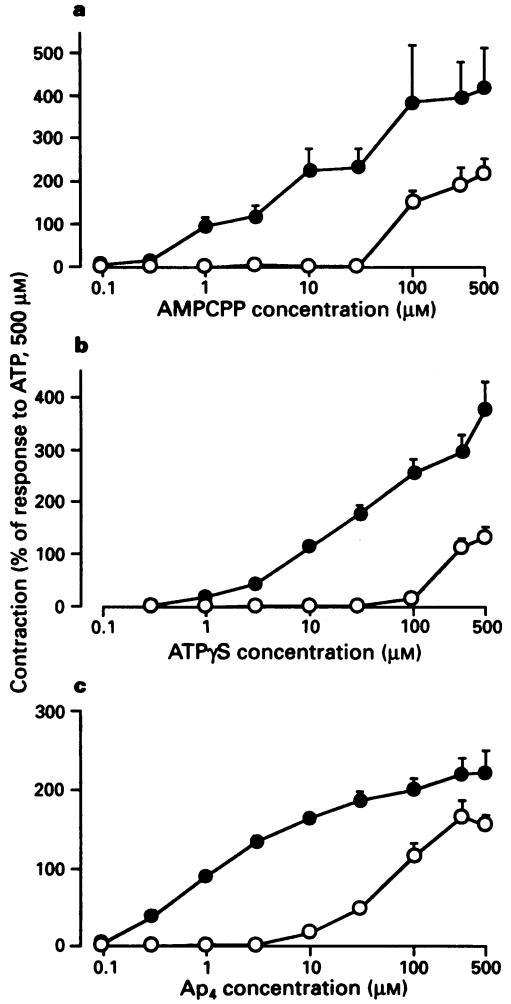

Figure 3 Contractions of the guinea-pig vas deferens induced by (a) AMPCPP, (b) ATPγS or (c) Ap_4 in the absence (●) or presence (○) of suramin (1 mM). Each point is the mean of at least 4 determinations and the vertical bars show the s.e.mean. For abbreviations see text.

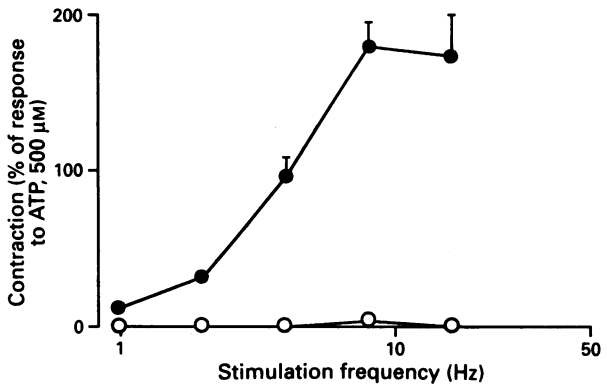

Figure 5 Contractions of the guinea-pig vas deferens induced by electrical field stimulation in the presence of phentolamine (10 μM), in the absence (●) or presence (○) of suramin (1 mM). Each point is the mean of at least 3 determinations and the vertical bars show the s.e.mean.

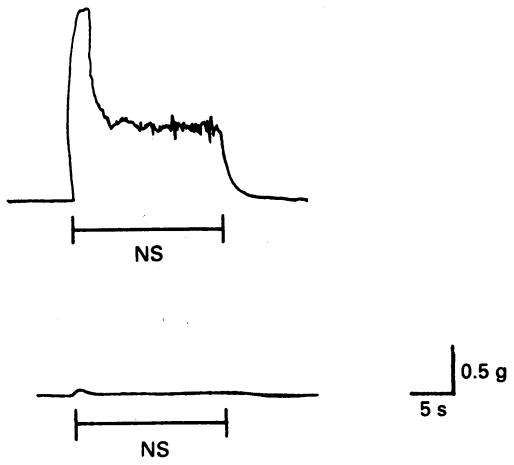

Figure 6 Representative traces showing contraction of the guinea-pig vas deferens in response to nerve stimulation (NS) (8 Hz, 70 V, 0.5 ms for 20 s) in the absence (top trace) and presence (bottom trace) of suramin (1 mM, 30 min incubation).

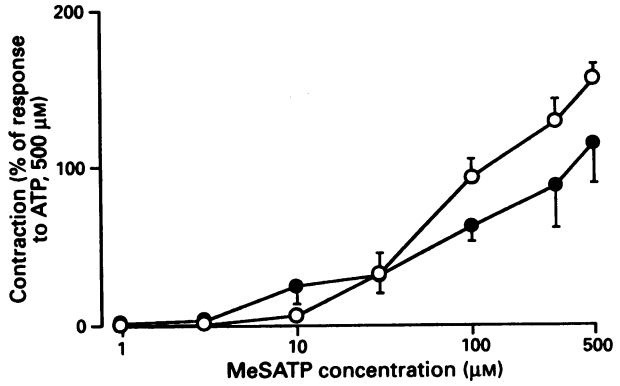

Figure 4 Contractions of the guinea-pig vas deferens induced by MeSATP in the absence (●) or presence (○) of suramin (1 mM). Each point is the mean of at least 4 determinations and the vertical bars show the s.e.mean. For abbreviations see text.

pond clearly to the second phase of the contractions observed by Fedan and coworkers, who concluded that the response of the guinea-pig vas deferens consisted of a receptor-mediated phasic twitch followed in some cases at high concentrations by a more sustained contraction, which they suggested was due to phosphorylation of the tissue (Fedan *et al.*, 1982a,b; Fedan & Lamport, 1990a,b; Vrana-Lamport *et al.*, 1991). Although it appeared possible that the effect of suramin might be to inhibit selectively the initial phasic contraction and leave the second phase unchanged or enhanced, our results suggest the explanation is not as simple. For those analogues which caused contractions in the presence of suramin, the nature of the responses was unchanged, and was still characterized by a rapid twitch. Indeed, at the concentrations used in our study it was hard to distinguish a second phase, except for ATPγS which clearly caused a more sustained contraction than ATP, as reported by Fedan *et al.* (1982a). Even for this analogue this second phase was not consistently present and was no more apparent in the presence of suramin than in its absence. More importantly, the structure-activity relationships of the suramin-resistant response did not correlate exactly with the expected structure-activity relationships of the second phase. Of the agonists we used, ATPγS, Ap_4, ADP and ATP were reported to have a distinct tonic phase, whereas AMPCPP and AMPPCP did not (Fedan *et al.*, 1982). However, AMPCPP appeared to have a suramin-resistant component to its action, and was clearly different in this respect from AMPPCP, which was almost abolished by suramin. However, Stone & Paton (1989) reported in the rat vas deferens that AMPCPP selectively desensitized the second phase of responses to ATP, suggesting that it may after all interact with this second site. Indeed, although this analogue is generally regarded as being metabolically more stable than ATP, it can

lose its terminal phosphate, but the product of this reaction, AMPCP, is much more stable than is ADP (see e.g. Bailey & Hourani, 1992). With this in mind, the overall conclusions of Fedan and coworkers, that analogues capable of transferring a terminal phosphate to the tissue elicit the second phase of contraction (Fedan & Lamport, 1990a,b), are not incompatible with our findings, in that the analogues for which it is clear that there is no suramin resistant phase, i.e. AMPPCP, Ap_5A and Ap_4A, are unlikely to be able to transfer a phosphate to the tissue. In the case of AMPPCP the terminal phosphate is linked by the very stable methylene linkage, and in the case of the dinucleotides the phosphates are protected by adenosine moieties and so are not 'terminal' and available for transfer. In the rat vas deferens, the dinucleotides were reported to be able to desensitize selectively the first phase of the ATP-induced contraction (Stone & Paton, 1989), which would again be in agreement with the suggestion of Fedan & Lamport (1990a,b). Suramin has however been reported to inhibit ectonucleotidases in the guinea-pig bladder (Hourani & Chown, 1989), and a number of nucleotide-binding enzymes (see Voogd *et al.*, 1993 for review), and it seems quite likely that it would also inhibit whichever enzyme may be responsible for the phosphate transfer in the guinea-pig vas deferens.

Another complication in the interpretation of the nature of the responses to ATP was raised recently by an interesting report by Sneddon & Machaly (1992), suggesting that the observed response to agonists in the vas deferens may depend on the part of the tissue responding, with the prostatic end responding with a phasic twitch whereas the epididymal end responds with a more sustained contraction. The biphasic responses observed by Fedan *et al.* (1982a) in response to ATP may therefore reflect interaction with receptors on the two ends of the tissue, with the mechanism of the contractile response being different at the two ends. The differential inhibition by $ANAPP_3$ and P-ATP of the two phases of the response (Fedan & Lamport, 1990a,b) may therefore in turn reflect inhibition of responses mediated by the two ends of the tissue.

A complication with the use of suramin is its ability to inhibit the breakdown of ATP as well as to act as antagonist (Hourani & Chown, 1989). This breakdown may reduce the observed potency of ATP and its degradable analogues in some tissues (Welford *et al.*, 1986;1987), so blockade of breakdown may oppose any antagonistic action of suramin. Indeed, electrophysiological studies on isolated smooth muscle cells from rat tail artery (Evans & Kennedy, 1994) as well as studies on intracellular calcium levels in mouse vas deferens (Boland *et al.*, 1992) have suggested that the true order of potency at P_{2X} receptors is MeSATP = ATP > AMPPCP/AMPCPP. In electrophysiological studies using isolated cells from the rat and guinea-pig vas deferens, ATP has also been reported to be more potent than AMPPCP/AMPCPP (Friel, 1988; Inoue & Brading, 1990). The discrepancy between this order of potency and that observed when studying contractions in the whole tissues has been attributed by Inoue & Brading (1990) and by Evans & Kennedy (1994) to a greater influence of breakdown in the whole tissue compared to single cells. This cannot be a factor in the studies by Boland *et al.* (1992) which were on whole tissues, and these authors convincingly explained their results in terms of the coexistence of relaxant P_{2Y} receptors in the tissue. However, in a recent abstract describing work in which a newly-developed selective ectonucleotidase inhibitor was used, Leff *et al.* (1994) have reported enhancement of responses to ATP but not to AMPCPP in the rabbit ear artery. In another abstract, this group have also reported that responses to ATP in this tissue are enhanced by suramin, while those to AMPCPP are inhibited, and have attributed this to concomitant inhibition by suramin of ATP breakdown (Crack *et al.*, 1994). This is similar to the results presented here in the vas deferens, in that suramin enhanced responses to ATP and MeSATP, which are both rapidly degraded, while abolishing those to AMPPCP, which is not degraded (Welford *et al.*, 1986; 1987). However, in our initial studies comparing the vas deferens and the bladder (Bailey & Hourani, 1994), we directly investigated this possibility and measured the breakdown of ATP in both tissues and its inhibition by suramin, but were unable to explain the differential effects of suramin in these tissues on this basis. Our previous finding of the inhibition by suramin of responses to the other naturally-occurring nucleotides in the vas deferens is also not easy to explain in this way, as these compounds are just as susceptible to breakdown as is ATP itself (Welford *et al.*, 1986; 1987; Beukers *et al.*, 1993). In addition, in the present study the dinucleotide Ap_4A was shown to have no suramin-resistant phase, yet has been reported to be very rapidly degraded by ectonucleotidases present on a variety of cells, including smooth muscle (Ogilvie, 1992). Thus while inhibition of breakdown by suramin may contribute to the anomolous effects of suramin in the vas deferens, it is unlikely to be the only factor. It is of course not possible at the moment to measure the breakdown at ATP in the vicinity of the receptors but only that detectable in the bulk phase of the buffer, so it is difficult to judge accurately the contribution of breakdown to observed potency. With the development of selective ectonucleotidase inhibitors (Leff *et al.*, 1994), it may become possible in the future to investigate this directly.

Contractions induced by nerve stimulation in the presence of the α-adrenoceptor antagonist, phentolamine, were abolished by suramin, and this is consistent with a recent report by Sneddon (1992) that suramin inhibited the excitatory junction potential, a response which is thought to be mediated by ATP. In view of the wealth of other evidence that ATP is a cotransmitter in this tissue (Morris & Gibbins, 1992; Hoyle *et al.*, 1992), it is perhaps surprising that suramin blocks contractile responses induced by nonadrenergic (purinergic) nerve stimulation but enhances contractions induced by ATP (Bailey & Hourani, 1994). One difference between these experiments was that the contractions induced by nerve stimulation were carried out in the presence of 10 μM phentolamine to block the effects of noradrenaline, but this cannot account for the difference in the effects of suramin as contractions induced by ATP in the presence of suramin were, as expected, not inhibited by phentolamine. Indeed, even in the absence of phentolamine, suramin (1 mM) abolished nerve-mediated contractions, and there was no sparing of the second, sustained phase which has been suggested to be due to released noradrenaline (Fedan *et al.*, 1981). Given that suramin has been shown not to inhibit NA release in rat and mouse vas deferens (Von Kügelgen *et al.*, 1989; 1994), this could imply a nonspecific inhibition of contraction by suramin, but this is unlikely because suramin did not inhibit contractions induced by noradrenaline. A more plausible explanation is that the suramin-sensitive purinergic transmitter can contribute to both phases of the contraction induced by a train of pulses. This has been shown to be the case for the rat vas deferens, where suramin inhibits selectively the first phase of the contraction induced by a single pulse, but both suramin and desensitization with AMPCPP reduce both phases of the much more sustained contraction induced by a train of pulses (Major *et al.*, 1989; Bourreau *et al.*, 1991; Mallard *et al.*, 1992). We were not able, using our equipment, to investigate the contraction induced by a single pulse.

The simplest explanation for the discrepancy between the effect of suramin on ATP and its effect on nerve-mediated contractions is that neuronally released ATP does not have access to the suramin-resistant sites on the tissue, and such a suggestion has also been made for the mouse vas deferens, in which there is also a suramin-resistant contractile response to ATP (Von Kügelgen *et al.*, 1990), although it is less marked than in the guinea-pig vas deferens. Alternatively, if the suramin-resistance of the response to ATP is explainable in terms of the inhibition of its breakdown, then ATP released

from nerves may not be as susceptible to breakdown as that added to the bath. There is unequivocal evidence that ATP, detected with the specific luciferase assay, is rapidly released from nerves into the surrounding medium when the guinea-pig vas deferens is electrically stimulated (Lew & White, 1987). However, diadenosine polyphosphates such as Ap_4A and Ap_5A have recently been proposed as neurotransmitters (Hoyle, 1990; Pintor & Miras-Portugal, 1993), and can be cleaved by ectoenzymes asymmetrically to form ATP (see Ogilvie, 1992 for review). An alternative explanation for the discrepancy between the effects of suramin on exogenously added ATP (Bailey & Hourani, 1994) and nerve-stimulated contractions could be that one of these dinucleotides, which lack a suramin-resistant component, is responsible for the nerve-mediated contraction. This explanation would also account for the well-known discrepancy in the size of the contraction induced by ATP and by nerve stimulation, as the dinucleotides are considerably more potent than ATP and better match the nerve-mediated contraction (see Figures 1 and 5). There is however no direct evidence for the release of these compounds from smooth muscle preparations, although they have been shown to be released, together with larger amounts of ATP, from chromaffin cells and rat brain synaptosomes (see Pintor & Miras-Portugal, 1993 for review). This explanation must therefore be regarded as speculative and would need considerably more evidence to confirm it.

Overall, these results confirm our previous findings (Bailey & Hourani, 1994) of a suramin-resistant component in the contractile response to ATP of the guinea-pig vas deferens, and show that the structure-activity relationships of this response are not identical to those of the other P_2-purinoceptor subclasses.

We thank the Wellcome Trust for support for S.J.B. (Grant Ref. 034852/Z/91/Z).

References

BAILEY, S.J. & HOURANI, S.M.O. (1992). Effects of purines on the longitudinal muscle of the rat colon. *Br. J. Pharmacol.*, **105**, 885–892.

BAILEY, S.J. & HOURANI, S.M.O. (1994). Differential effects of suramin on P_2-purinoceptors mediating contractions of the guinea-pig vas deferens and urinary bladder. *Br. J. Pharmacol.*, **112**, 219–225.

BEUKERS, M.W., PIROVANO, I.M., VAN WEERT, A., KERKHOF, C.J.M., IJZERMAN, A.P. & SOUDIJN, W. (1993). Characterization of ecto-ATPase on human blood cells. *Biochem. Pharmacol.*, **46**, 1959–1966.

BLAKELY, A.G.H., BROCKBANK, J.E., KELLY, S.S. & PETERSEN, S.A. (1991). Effects of suramin on the concentration-response relationship of α,β-methylene-ATP on the mouse vas deferens. *J. Auton. Pharmacol.*, **11**, 45–49.

BO, X., SIMON, J., BURNSTOCK, G. & BARNARD, E.A. (1992). Solubilization and molecular size determination of the P_{2x} purinoceptor from rat vas deferens. *J. Biol. Chem.*, **267**, 17581–17587.

BOLAND, B., HIMPENS, B., VINCENT, M.F., GILLIS, J.-M. & CASTEELS, R. (1992). ATP activates P_{2X}-contracting and P_{2Y}-relaxing purinoceptors in the smooth muscle of the mouse vas deferens. *Br. J. Pharmacol.*, **107**, 1152–1158.

BOURREAU, J.P., ZHANG, Z.D., LOW, A.M., KWAN, C.Y. & DANIEL, E.E. (1991). Ryanodine and the adrenergic, purinergic stimulation in the rat vas deferens smooth muscle: functional and radioligand binding studies. *J. Pharmacol. Exp. Ther.*, **256**, 1063–1071.

BÜLTMANN, R. & STARKE, K. (1994). P_2-Purinoceptor antagonists discriminate three contraction-mediating receptors for ATP in rat vas deferens. *Naunyn-Schmied. Arch. Pharmacol.*, **349**, 74–80.

BURNSTOCK, G. (1990). Noradrenaline and ATP as cotransmitters in sympathetic nerves. *Neurochem. Int.*, **17**, 357–368.

BURNSTOCK, N.J., CUSACK, N.J. & MELDRUM, L.A. (1985). Studies on the stereoselectivity of the P_2-purinoceptor on the guinea-pig vas deferens. *Br. J. Pharmacol.*, **84**, 431–434.

BURNSTOCK, G. & KENNEDY, C. (1985). Is there a basis for distinguishing two types of P_2-purinoceptor? *Gen. Pharmacol.*, **16**, 433–440.

CRACK, B.B., BEUKERS, M.W., IJZERMAN, A.P., MCKECHNIE, K.C.W. & LEFF, P. (1994). Inhibition of ATP degradation by L-2-methylthio-β,γ-bromomethylene-ATP and suramin. *Drug Dev. Res.*, **31**, 259.

CUSACK, N.J. (1993). P_2 receptor: subclassification and structure-activity relationships. *Drug Dev. Research*, **28**, 244–252.

CUSACK, N.J. & HOURANI, S.M.O. (1990). Subtypes of P_2-purinoceptors. Studies using analogues of ATP. *Ann. N.Y. Acad. Sci.*, **603**, 172–181.

DEN HERTOG, A., HELEMANS, A. & VAN DEN AKKER, J. (1989a). The inhibitory action of suramin on the P_2-purinoceptor in smooth muscle cells of guinea-pig taenia caeci. *Eur. J. Pharmacol.*, **166**, 531–534.

DEN HERTOG, A., VAN DEN AKKER, J. & NELEMANS, A. (1989b). Suramin and the inhibitory junction potential in taenia caeci of the guinea-pig. *Eur. J. Pharmacol.*, **173**, 207–209.

DUBYAK, G.R. & EL-MOATASSIM, C. (1993). Signal transduction via P_2-purinergic receptors for extracellular ATP and other nucleotides. *Am. J. Physiol.*, **265**, C577–C606.

DUNN, P.M. & BLAKELY, A.G.H. (1988). Suramin: a reversible P_2-purinoceptor antagonist in the mouse vas deferens. *Br. J. Pharmacol.*, **93**, 243–245.

EVANS, R.J. & KENNEDY, C. (1994). Characterization of P_2-purinoceptors in the smooth muscle of the rat tail artery: a comparison between contractile and electrophysiological responses. *Br. J. Pharmacol.*, **113**, 853–860.

FEDAN, J.S., HOGABOOM, G.K., O'DONNELL, J.P., COLBY, J. & WESTFALL, D.P. (1981). Contribution by purines to the neurogenic response of the vas deferens of the guinea-pig. *Eur. J. Pharmacol.*, **69**, 41–53.

FEDAN, J.S., HOGABOOM, G.K., WESTFALL, D.P. & O'DONNELL, J.P. (1982a). Comparison of contractions of the smooth muscle of the guinea-pig vas deferens induced by ATP and related nucleotides. *Eur. J. Pharmacol.*, **81**, 193–204.

FEDAN, J.S., HOGABOOM, G.K., WESTFALL, D.P. & O'DONNELL, J.P. (1982b). Comparison of the effects of arylazido aminopropionyl ATP ($ANAPP_3$), and ATP antagonist, on responses of the smooth muscle of the guinea-pig vas deferens to ATP and related nucleotides. *Eur. J. Pharmacol.*, **85**, 277–290.

FEDAN, J.S. & LAMPORT, S.J. (1990a). P_2-purinoceptor antagonists. In *Purines in Cellular Signalling*. ed. Jacobson, K.A., Daly, J.W. & Manganiello, V., pp. 182–197. New York: Springer-Verlag.

FEDAN, J.S. & LAMPORT, S.J. (1990b). Two dissociable phases in the contractile response of the guinea-pig isolated vas deferens to adenosine triphosphate. *J. Pharmacol. Exp. Ther.*, **253**, 993–1001.

FRIEL, D.D. (1988). An ATP-sensitive conductance in single smooth muscle cells from the rat vas deferens. *J. Physiol.*, **401**, 361–380.

GORDON, J.L. (1986). Extracellular ATP: effects, sources and fate. *Biochem. J.*, **233**, 309–319.

HOURANI, S.M.O. & CHOWN, J.A. (1989). The effects of some possible inhibitors of ectonucleotidases on the breakdown and pharmacological effects of ATP in the guinea-pig urinary bladder. *Gen. Pharmacol.*, **20**, 413–416.

HOURANI, S.M.O., HALL, D.A. & NIEMAN, C.J. (1992). Effects of the P_2-purinoceptor antagonist suramin on human platelet aggregation induced by adenosine 5'-diphosphate. *Br. J. Pharmacol.*, **105**, 453–457.

HOYLE, C.H.V. (1990). Pharmacological activity of adenine dinucleotides in the periphery: possible receptor classes and transmitter function. *Gen. Pharmacol.*, **21**, 827–831.

HOYLE, C.H.V. (1992). Transmission: Purines. In *Autonomic Neuroeffector Mechanisms*. ed. Burnstock, G. & Hoyle, C.H.V. pp. 367–407. Reading: Harwood Academic Publishers.

HOYLE, C.H.V., KNIGHT, G.E. & BURNSTOCK, G. (1990). Suramin antagonizes responses to P_2-purinoceptor agonists and purinergic nerve stimulation in the guinea-pig urinary bladder and taenia coli. *Br. J. Pharmacol.*, **99**, 617–621.

INOUE, R. & BRADING, A.F. (1990). The properties of the ATP-induced depolarization and current in single cells isolated from the guinea-pig urinary bladder. *Br. J. Pharmacol.*, **100**, 619–625.

JAFFAR, Z.H. & PEARCE, F.L. (1990). Histamine secretion from mast cells stimulated with ATP. *Agents Actions*, **30**, 64–66.

LAMPORT-VRANA, S.J., VRANA, K.E. & FEDAN, J.S. (1991). Involvement of ecto-phosphoryl transfer in contractions of the smooth muscle of the guinea-pig vas deferens to adenosine 5'-triphosphate. *J. Pharmacol. Exp. Ther.*, **258**, 339–348.

LEFF, P., HUMPHRIES, R.G., CRACK, B.E., POLLARD, C.E. & MCKECHNIE, K. (1994). New ATP analogues: pharmacological tools and potential drugs. *Drug Dev. Res.*, **31**, 290.

LEFF, P., WOOD, B.E. & O'CONNOR, S.E. (1990). Suramin is a slowly-equilibrating but competitive antagonist at P_{2X}-receptors in the rabbit isolated ear artery. *Br. J. Pharmacol.*, **101**, 645–649.

LEW, M.J. & WHITE, T.D. (1987). Release of endogenous ATP during sympathetic nerve stimulation. *Br. J. Pharmacol.*, **92**, 349–355.

LUSTIG, K.D., SHIAU, A.K., BRAKE, A.J. & JULIUS, D. (1993). Expression cloning of an ATP receptor from mouse neuroblastoma cells. *Proc. Natl. Acad. Sci. U.S.A.*, **90**, 5113–5117.

MACKENZIE, I., KIRKPATRICK, K.A. & BURNSTOCK, G. (1988). Comparative study of the actions of AP_5A and α,β-methylene ATP on nonadrenergic, noncholinergic neurogenic excitation in the guinea-pig vas deferens. *Br. J. Pharmacol.*, **94**, 699–706.

MAJOR, T.C., WEISHARR, R.E. & TAYLOR, D.G. (1989). Two phases of contractile response in rat isolated vas deferens and their regulation by adenosine and α-receptors. *Eur. J. Pharmacol.*, **167**, 323–331.

MALLARD, N., MARSHALL, R., SITHERS, A. & SPRIGGS, B. (1992). Suramin: a selective inhibitor of purinergic neurotransmission in the rat isolated vas deferens. *Eur. J. Pharmacol.*, **220**, 1–10.

MELDRUM, L.A. & BURNSTOCK, G. (1983). Evidence that ATP acts as a co-transmitter with noradrenaline in sympathetic nerves supplying the guinea-pig vas deferens. *Eur. J. Pharmacol.*, **92**, 161–163.

MORRIS, J.L. & GIBBINS, I.L. (1992). Co-transmission and neuromodulation. In *Autonomic Neuroeffector Mechanisms*. ed. Burnstock, G. & Hoyle, C.H.V. pp. 33–119. Reading: Harwood Academic Publishers.

O'CONNOR, S.E., DAINTY, I.A. & LEFF, P. (1991). Further subclassification of ATP receptors based on agonist studies. *Trends Pharmacol. Sci.*, **12**, 137–141.

OGILVIE, A. (1992). Extracellular functions for Ap_nA. In *Ap_4A and Other Dinucleoside Polyphosphates*. ed. McLennan, A.G. pp. 229–273. Boca Ratan FL: CRC Press.

PINTOR, J. & MIRAS-PORTUGAL, M.T (1993). Diadenosine polyphosphates (Ap_XA) as new neurotransmitters. *Drug Dev. Res.*, **28**, 259–262.

SNEDDON, P. (1992). Suramin inhibits excitatory junction potentials in guinea-pig isolated vas deferens. *Br. J. Pharmacol.*, **107**, 101–103.

SNEDDON, P. & MACHALY, M. (1992). Regional variation in purinergic and adrenergic responses in isolated vas deferens of rat, rabbit and guinea-pig. *J. Auton. Pharmacol.*, **12**, 421–428.

STONE, T.W. (1981). Actions of adenine dinucleotides on the vas deferens, guinea-pig taena caeci and bladder. *Eur. J. Pharmacol.*, **75**, 93–102.

STONE, T.W. (1985). The activity of phosphorothioate analogues of ATP in various smooth muscle systems. *Br. J. Pharmacol.*, **84**, 165–173.

STONE, T.W. & PATON, D.M. (1989). Possible subtypes of ATP receptor producing contraction of rat vas deferens, revealed by cross-desensitization. *Gen. Pharmacol.*, **20**, 61–64.

TREZISE, D.J., KENNEDY, I. & HUMPHREY, P.P.A. (1993). Characterization of purinoceptors mediating depolarization of rat isolated vagus nerve. *Br. J. Pharmacol.*, **110**, 1055–1060.

VON KÜGELGEN, I., BULTMAN, R. & STARKE, K. (1990). Interaction of adenine nucleotides, UTP and suramin in mouse vas deferens: suramin-sensitive and suramin-insensitive components in the contractile effect of ATP. *Naunyn-Schmied Arch. Pharmacol.*, **342**, 198–205.

VON KÜGELGEN, I., KURZ, K. & STARKE, K. (1994). P_2-purinoceptor-mediated autoinhibition of sympathetic transmitter release in mouse and rat vas deferens. *Naunyn-Schmied Arch. Pharmacol.*, **349**, 125–132.

VON KÜGELGEN, I., SCHÖFFEL, E. & STARKE, K. (1989). Inhibition by nucleotides acting at presynaptic P_2-receptors of sympathetic neuro-effector transmission in the mouse isolated vas deferens. *Naunyn-Schmied. Arch. Pharmacol.*, **340**, 522–532.

VOOGD, T.E., VANSTERKENBURG, E.L.M., WILTING, J. & JANSSEN, L.H.M. (1993). Recent research on the biological activity of suramin. *Pharmacol. Rev.*, **45**, 177–203.

WEBB, T.E., SIMON, J., KRISHAK, B.J, BATESON, A.N., SMART, T.G., KING, B.F., BURNSTOCK, G. & BARNARD, E.A. (1993). Cloning and functional expression of a brain G-protein-coupled ATP receptor. *FEBS Lett.*, **324**, 219–225.

WELFORD, L.A., CUSACK, N.J. & HOURANI, S.M.O. (1986). ATP analogues and the guinea-pig taenia coli: a comparison of the structure-activity relationships of ectonucleotidases with those of the P_2-purinoceptor. *Eur. J. Pharmacol.*, **129**, 217–224.

WELFORD, L.A., CUSACK, N.J. & HOURANI, S.M.O. (1987). The structure-activity relationships of ectonucleotidases and of excitatory P_2-purinoceptors: evidence that dephosphorylation of ATP analogues reduces pharmacological potency. *Eur. J. Pharmacol.*, **141**, 123–130.

(Received March 29, 1994
Revised November 9, 1994
Accepted November 15, 1994).

British Journal of Pharmacology (1995) 114, 1133-1142

Quantitative comparisons of muscarinic and bradykinin receptor-mediated Ins (1,4,5)P_3 accumulation and Ca^{2+} signalling in human neuroblastoma cells

[1]G.B. Willars & S.R. Nahorski

Department of Cell Physiology and Pharmacology, University of Leicester, University Road, Leicester LE1 9HN

1 Muscarinic and bradykinin receptor-mediated Ins(1,4,5)P_3 accumulation, Ca^{2+} mobilization and Ca^{2+} entry have been examined in human SH-SY5Y neuroblastoma cells. This has allowed both direct comparison of signalling events by two receptor types potentially linked to the same transduction pathway and an investigation of the interactions between the components of this pathway.

2 Stimulation of muscarinic receptors with carbachol produced biphasic accumulations of Ins(1,4,5)P_3 consisting of a rapid peak followed by a lower sustained phase. Both phases were dose-dependent but the potency of elevation at peak was significantly less than that of the sustained phase. Bradykinin also dose-dependently stimulated Ins(1,4,5)P_3 accumulation but responses were smaller and not sustained.

3 Lowering of $[Ca^{2+}]_e$ reduced basal Ins(1,4,5)P_3 levels. Peak Ins(1,4,5)P_3 elevation in response to carbachol and bradykinin were lowered by an amount approximating this reduction over the entire dose-response curves. Sustained Ins(1,4,5)P_3 elevation in response to carbachol showed a more marked absolute reduction. Agonist potencies were unaffected by lowering $[Ca^{2+}]_e$. Thus, a consistent but small amount of PLC activity during rapid activation appears to be sensitive to lowered $[Ca^{2+}]_e$, whilst activity during sustained stimulation is greatly facilitated by external Ca^{2+}, probably through Ca^{2+} entry.

4 The temporal- and dose-dependency of carbachol-mediated Ins(1,4,5)P_3 accumulations were unaffected by loading cells with fura-2, thus allowing direct comparison of Ins(1,4,5)P_3 and $[Ca^{2+}]_i$ changes monitored by fura-2.

5 Changes in $[Ca^{2+}]_i$ by both agonists revealed temporal patterns that were similar to Ins(1,4,5)P_3 accumulations. Only carbachol stimulated a marked sustained $[Ca^{2+}]_i$ signal and this was fully dependent on external Ca^{2+}.

6 All agonist-mediated $[Ca^{2+}]_i$ elevations occurred with significantly greater potency than that of the respective Ins(1,4,5)P_3 accumulations. Further examination of peak elevations in response to carbachol indicated that this was independent of Ca^{2+} entry. Thus, a major site for amplification of the potency of rapid agonist-mediated responses lies at the level of the Ins(1,4,5)P_3 receptor.

7 The transient nature of Ins(1,4,5)P_3 and $[Ca^{2+}]_i$ peaks followed by either lower but sustained levels with carbachol or a return to basal levels with bradykinin suggests rapid but partial desensitization of the muscarinic receptor and complete desensitization of the bradykinin receptor. This indicates receptor-specific desensitization. Further analysis of this was provided by detecting accumulations of [^{3}H]-inositol phosphates ([^{3}H]-InsPs) in Li^+-blocked, *myo*-[^{3}H]-inositol labelled cells. Carbachol produced a rapid accumulation over the first minute, followed by a slower linear accumulation for at least 29 min. At this point accumulations were dose-related with a potency similar to that of sustained Ins(1,4,5)P_3 accumulation. However, bradykinin produced a minor accumulation of [^{3}H]-InsPs, maximal by 1 min. Thus, analysis of PLC activation by measurement of [^{3}H]-InsPs over relatively long time frames will indicate the ability of agonists for predominantly sustained PLC activation, potentially driven by a partially desensitized receptor, as opposed to rapid activation by a fully sensitized receptor.

8 These data provide quantitative comparisons between and within components of the receptor-mediated phosphoinositide and Ca^{2+} signalling pathway, provide mechanistic insights into regulation of these components and characterize a model system in which heterologous interaction between two receptors linked to the same transduction pathway may be examined.

Keywords: Inositol 1,4,5-trisphosphate; intracellular calcium; desensitization; muscarinic receptor; bradykinin receptor; human neuroblastoma cells

Introduction

Upon agonist binding, a variety of cell surface receptors increase the activity of specific isoforms of phospholipase C (PLC), via GTP-binding proteins, to increase the hydrolysis of phosphatidylinositol 4,5-bisphosphate. This liberates both diacylglycerol and inositol 1,4,5-trisphosphate (Ins(1,4,5)P_3) which activate various isoforms of protein kinase C (PKC) and mobilize Ca^{2+} from intracellular stores respectively (Berridge, 1993; Putney & Bird, 1993) providing the means for regulation of cellular events. Although the sequence of events following receptor activation is known, much remains to be uncovered regarding the nature and generality of regulatory features within the pathway. It is clear, for example, that the dose-response curves for many cellular and tissue responses in PLC-linked systems lie to the left of the PLC activation curve, which in turn may lie to the left of the apparent receptor occupation curve (Kenakin, 1987). However, mechanistic aspects of such amplification are unclear and, given the possible unsuitability of the commonly used measurement of total [^{3}H]-inositol phosphates ([^{3}H]-InsPs) in

[1] Author for correspondence.

lithium-blocked cells for the determination of rapid PLC activation (see below), these fundamental relationships may require reassessment.

In a series of recent studies we have examined phosphoinositide signalling in the human neuroblastoma cell line SH-SY5Y that displays many of the characteristics of human foetal sympathetic ganglion cells (Ross *et al.*, 1983). These cells possess a predominant (Lambert *et al.*, 1989), although probably not exclusive (Wall *et al.*, 1991) M_3 receptor population and muscarinic receptor agonists stimulate phosphatidylinositol 4,5-bisphosphate hydrolysis via a pertussis-toxin insensitive G-protein (Lambert & Nahorski, 1990a) probably involving a member of the $G_{q/11}$ family (Rhee & Choi, 1992). Activated SH-SY5Y cells display a rapid peak of Ins(1,4,5)P_3 followed by a lower sustained phase which is dependent upon extracellular Ca^{2+} (Lambert & Nahorski, 1990b; Lambert *et al.*, 1991). Consistent with agonist-induced increases in $[Ca^{2+}]_i$ in many cell types (Putney & Bird, 1993), the pattern of muscarinic-induced $[Ca^{2+}]_i$ elevation is also biphasic in SH-SY5Y cells and parallels the changes in Ins(1,4,5)P_3 levels. The initial peak arises predominantly from Ins(1,4,5)P_3-mediated liberation of Ca^{2+} from intracellular stores and the sustained phase is dependent upon Ca^{2+} entry (Lambert & Nahorski, 1990b; Murphy *et al.*, 1991).

Using muscarinic receptor stimulation in the SH-SY5Y cell line as a model phosphoinositide-linked receptor system, the present study sought to compare the determination of PLC activity by measurement of accumulation of [^{3}H]-InsPs and Ins(1,4,5)P_3 mass and allow direct quantitative comparison with components of the Ca^{2+} signalling pathway. In addition, this work revealed a bradykinin receptor linked to activation of PLC in these cells, and this has, therefore, allowed the examination of these relationships for two PLC-linked receptors in the same cell type to assess the receptor specificity of such phenomena. Given both the reported Ca^{2+}-sensitivity of some PLC isoforms (Rhee & Choi, 1992) and the Ca^{2+} influx across the plasma membrane caused by many agonists (Putney & Bird, 1993) we have also examined the influence of reductions in the extracellular $[Ca^{2+}]$ ($[Ca^{2+}]_e$) on both $[Ca^{2+}]_i$ elevation and Ins(1,4,5)P_3 generation to assess further potential regulatory elements of the signalling pathway.

We provide evidence that measurement of accumulation of [^{3}H]-InsPs reflects reduced but sustained PLC activity which may be indicative of a desensitized agonist-mediated process. Additionally we demonstrate a clear dissociation between the dose-response relationships for agonist-mediated Ins(1,4,5)P_3 generation and components of $[Ca^{2+}]_i$ elevation and highlight the complex interactions between Ins(1,4,5)P_3-induced Ca^{2+} mobilization, Ca^{2+} entry across the plasma membrance and the role of the latter in facilitating Ins(1,4,5)P_3 generation.

Methods

Cell culture

Cultures of the human neuroblastoma cell line, SH-SY5Y (originally given by Dr J. Biedler, Sloan-Kettering Institute, New York, U.S.A.) were maintained in Minimum Essential Medium supplemented with 50 iu ml^{-1} penicillin, 50 μg ml^{-1} streptomycin, 2.5 μg ml^{-1} amphotericin B, 2 mM L-glutamine and 10% (v/v) newborn-calf serum. Cultures were maintained at 37°C in 5% CO_2/humidified air. Stock cultures were passaged weekly at a 1:4–6 split following harvesting with 10 mM HEPES, 154 mM NaCl, 0.54 mM EDTA pH7.4 (harvesting buffer) and fed or refed alternately 2–3 times per week.

Population $[Ca^{2+}]_i$ measurement

Confluent cultures of SH-SY5Y cells (P70-90) were harvested and reseeded in 3 ml of media at an equivalent density on 11 × 22 mm coverslips in 8 well multidishes. After leaving overnight to allow cell attachment, coverslips were placed in 3 ml Krebs/HEPES buffer (composition (mM): HEPES 10, $NaHCO_3$ 4.2, glucose 10, $MgSO_4$ 1.2, KH_2PO_4 1.2, KCl 4.7, NaCl 118 and $CaCl_2$ 2) within acrylic cuvettes constructed to hold them diagonally across the cuvette. Cuvettes were placed in a Perkin-Elmer LS-5B spectrofluorimeter with a water jacket to maintain cuvette temperature at 37°C and aligned to minimize reflectance. Buffer was stirred continually with a magnetic follower. Excitation wavelengths were 340 and 380 nm, with a 3.8 s changeover time, and emission was recorded at 509 nm. Following determination of autofluorescence, 10 μl of fura-2-AM in DMSO was added (final fura-2-AM concentration 3.3 μM). After 40 min at room temperature with continual stirring, buffer was removed, the cuvette washed 3 times with 3 ml buffer at 37°C and left in 3 ml of buffer for 5 min at 37°C. When $[Ca^{2+}]_i$) was to be examined at reduced $[Ca^{2+}]_e$, cuvettes were then washed 3 times with 3 ml of nominally Ca^{2+}-free (low $[Ca^{2+}]_e$) buffer and left for a further 5 min at 37°C in 3 ml of buffer. The $[Ca^{2+}]$ of low $[Ca^{2+}]_e$ buffer was approximately 2 μM as determined with fura-2 (Grynkiewicz *et al.*, 1985). The $[Ca^{2+}]_e$ of standard buffer was 2 mM and this was defined as normal $[Ca^{2+}]_e$. Agonists were added in 50 μl aliquots. With emission determined at 509 nm, the 340 nm/380 nm ratio was recorded as an index of $[Ca^{2+}]_i$. However, the relationship between the 340 nm/380 nm ratio and $[Ca^{2+}]_i$ is non-linear and in particular will underestimate the magnitude of changes in $[Ca^{2+}]_i$ as the ratio approaches R_{max} (Grynkiewicz *et al.*, 1985) thus invalidating EC_{50} determination or direct comparison of changes at different ratio values. An *in situ* calibration was therefore performed in separate experiments, deriving R_{max} with either ionomycin or Br-A23187 (6–33 μM) and elevated $[Ca^{2+}]_e$ of up to 10 mM followed by EGTA to determine R_{min}. These values were used to convert all population 340/380 ratios to $[Ca^{2+}]_i$ (Grynkiewicz *et al.*, 1985).

Measurement of D-Ins(1,4,5)P_3 mass

This was done by modification of a radioreceptor method previously assessed for stereo- and positional specificity (Challiss *et al.*, 1990). Confluent cultures (P70-90) were harvested and reseeded at an equivalent density in 24 well multidishes. After incubating overnight to allow cell attachment, wells were washed with 1 ml of Krebs/HEPES at 37°C and left for 30 min at 37°C with 1 ml of buffer per well. When Ins(1,4,5)P_3 generation was to be examined at low $[Ca^{2+}]_e$, standard buffer was replaced by low $[Ca^{2+}]_e$ buffer for the last 5 min. Multidishes were maintained at 37°C, wells aspirated individually and 100 μl of buffer with the appropriate agonist concentration added immediately. Reactions were stopped with 100 μl of ice-cold 1 M TCA. For zero time, TCA was added prior to agonist. Multidishes were left at 4°C for at least 15 min and 40 μl of 10 mM EDTA added to 160 μl aliquots, followed by 200 μl of a 1:1 (v:v) mixture of tri-n-octyl-amine and 1,1,2-trichloro-trifluoro-ethane. After vortexing, samples were left at room temperature for 15 min then microfuged (10,000 g, 2 min) and 100 μl of the upper aqueous phase was taken to which 50 μl of 25 mM $NaHCO_3$ was added. Samples were stored at 4°C until assay of Ins(1,4,5)P_3 (<3 days).

D-Ins(1,4,5)P_3 was quantified in single 30 μl aliquots of duplicate generations in a final volume of 120 μl (25 mM Tris-HCl, 1 mM EDTA, pH 8.0) at 4°C using bovine adrenal cortical binding protein (~0.6 mg protein per tube) and D-*myo*-[^{3}H]-inositol 1,4,5-trisphosphate (specific activity 44 Ci $mmol^{-1}$, 3.6 nCi per tube) as radioligand. Authentic D-Ins(1,4,5)P_3 (0.1 nM–3 μM) was used as a standard with non specific binding (<10% of total) defined by 10 μM Ins(1,4,5)P_3. Following a 30 min incubation, protein was collected with 2 ml of ice-cold buffer (25 mM Tris-HCl, 1 mM EDTA, 5 mM $NaHCO_3$, pH8.0) and rapid filtration (Brandel Cell Harvester) onto Whatman GF/B glass fibre filters. After two

rapid 5 ml washes, filters were counted by liquid-scintillation spectrometry in 4 ml Emulsifier-Safe scintillation cocktail.

Protein content of wells (typically 100–200 μg) was determined in 0.1 M NaOH digests of at least two wells per multidish by the Bradford method using an acidic Coomassie Brilliant Blue G-250 solution and bovine albumin fraction V as standard. When n is given, this represents the number of duplicate generations of Ins(1,4,5)P_3.

Measurement of inositol phosphate accumulation

Cells were prelabelled with 3 μCi ml^{-1} of *myo*-[^{3}H]-inositol (86 Ci $mmol^{-1}$) for 48 h in 24 well multidishes. Following a 10 min preincubation in 250 μl Krebs/HEPES with 5 mM Li^+, a further 250 μl of buffer containing agonist was added. Following incubation at 37°C, reactions were stopped with 500 μl 1 M TCA. An 800 μl aliquot was removed and 200 μl of 10 mM EDTA added. After vortexing with 1 ml of a 1:1 (v:v) mixture of tri-n-octyl-amine and 1,1,2-trichloro-trifluoro-ethane, 50 μl of 250 mM $NaHCO_3$ was added to 800 μl of the aqueous phase. This was applied to a Dowex AG1X8, 200–400 mesh column which was then washed with 10 ml of 25 mM ammonium formate. Inositol phosphates were washed off with 10 ml of 1M ammonium formate/0.1 M formic acid (Baird *et al.*, 1989). A 2 ml aliquot of this was counted by liquid scintillation spectrometry following addition of 8 ml Floscint.

Materials

Reagents of analytical grade and highly purified Elgastat water were used throughout. Minimum Essential Medium, penicillin/streptomycin, amphotericin B, glutamine, newborn calf serum and tissue culture flasks were from Gibco. Multidishes were from Nunc. Fura-2-AM (pentaacetoxymethyl ester), ionomycin free acid and 4-Br-A23187 were from Calbiochem. Anhydrous dimethyl sulphoxide (DMSO) was from Aldrich. Tri-n-octylamine, 1,2,3-trichloro-trifluoro-ethane, N-[2-hydroxyethyl]piperazine-N'-[2-ethanesulphonic acid (HEPES), Tris-HCl, atropine, carbachol, ethylene glycol-*bis* (β-aminoethylether) *N,N,N',N'*-tetraacetic acid (EGTA), ethylenediaminetetraacetic acid (EDTA), bradykinin, N-adamantaneacetyl-D-Arg, [Hyp^3, Thi^{5,8},D-Phe^7]-bradykinin and bovine alumin fraction V were from Sigma. Triton X-100 was from Boehringer. Coomassie reagent was from Pierce. D-Ins(,1,4,5)P_3 (K^+ Salt) was from University of Rhode Island Foundation, U.S.A. D-*myo*-[^{3}H]-inositol 1,4,5-trisphosphate and *myo*-[^{3}H]-inositol were from Amersham. Emulsifier-Safe Scintillation Cocktail and Flo Scint IV were from Packard. Trichloroacetic acid (TCA) and all other reagents were from Fisons.

Statistical analysis

Dose-response curves were fitted by Graph-PAD (Academic Press Inc. 1986) using a standard four-parameter logistic equation. EC_{50} mean values and standard errors of the Ins(1,4,5)P_3 data were generated from the mean ± standard error of the mean (s.e.mean) of $\log_{10}$ EC_{50} values generated from separate curves. However, for the $[Ca^{2+}]_i$ data, where individual data points were from different coverslips, EC_{50} values were from curves fitted with mean data for each concentration and the s.e.mean quoted therefore reflects the standard error determined by the curve fitting routine. The degrees of freedom associated with comparisons of these data were taken as the mean number of values contributing to each data point minus 2. The lines representing the dose-response curves in the figures represent the best fit curves with uniform weighting to all points. Comparison of full dose-response curves was by two-way analysis of variance with $\log_{10}$ transformations to account for heteroscedastic data where required. Other statistical comparisons were by Student's two-tailed unpaired *t* test. Acceptance of significance for all tests was at $P<0.05$. EC_{50} values are presented as $\log_{10}$ M mean ± s.e.mean (*n*). All other data are presented as mean ± s.e.mean (*n*).

Results

Carbachol- and bradykinin-mediated Ins(1,4,5)P_3 accumulation

Carbachol and bradykinin both increased Ins(1,4,5)P_3 levels. Following 1 mM carbachol there was a biphasic elevation consisting of a peak at 10 s followed by a reduction over the next 50 s to a lower, but sustained phase (Figure 1a). Following 10 μM bradykinin there was also a peak of Ins(1,4,5)P_3 at 10 s, which decreased rapidly over the next 50 s and then more slowly over the next 2–3 min to approximately basal levels (Figure 1a). Peak Ins(1,4,5)P_3 responses to carbachol and bradykinin were dose-dependent with EC_{50} values of −4.63 ± 0.07 (11) (24 μM) and −6.58 ± 0.13 (9) (264 nM) respectively (Figure 2a and 2b). The sustained phase of Ins(1,4,5)P_3, determined at 300 s following carbachol addition, was also dose-dependent (not shown) with an EC_{50} of −5.37 ± 0.23 (6) (4.3 μM), this being significantly ($P<0.02$) lower than that of the peak EC_{50}. A maximal (10 μM)

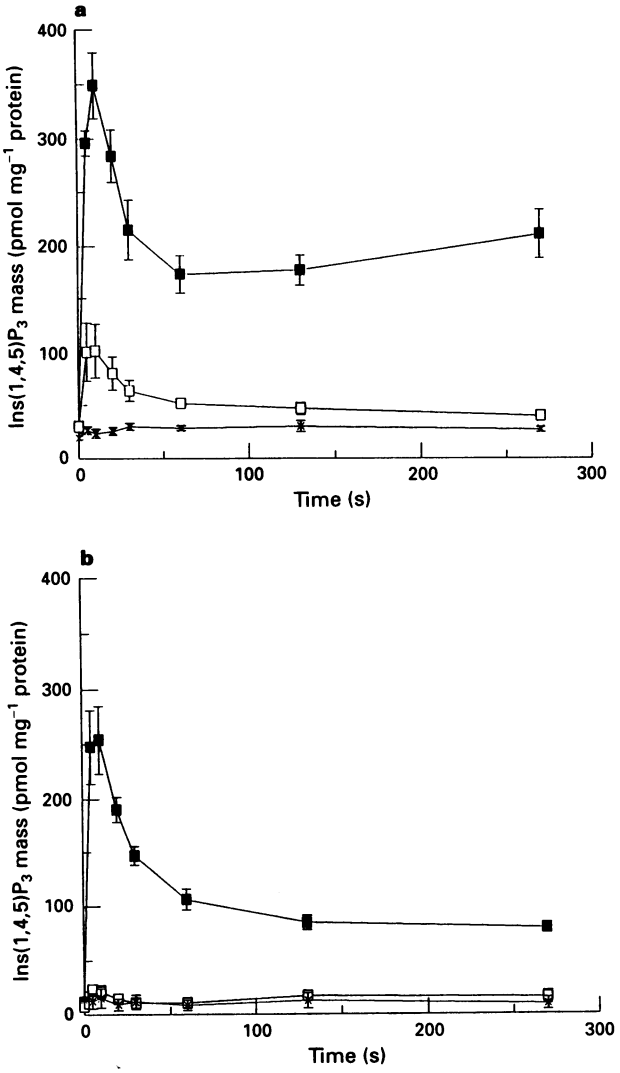

Figure 1 Time course of changes in inositol 1,4,5-trisphosphate (Ins(1,4,5)P_3) mass following addition of 1 mM carbachol (■), 10 μM bradykinin (□) or buffer alone (x) to adherent SH-SY5Y cells at normal (a) or low (b) $[Ca^{2+}]_e$. Data are mean ± s.e.mean, $n = 3–5$.

bradykinin challenge produced only a small (2.32±0.27 (10) fold) increase in Ins(1,4,5)P_3 levels at 10 s compared to that in response to carbachol (8.75±0.78 (11) fold) (Figures 1 and 2). The sustained phase of Ins(1,4,5)P_3 elevation in response to carbachol was 5.75±0.78 fold (68% of peak response) compared to only 0.47±0.25 fold (20% of peak response) for bradykinin.

Sensitivity of carbachol- and bradykinin-mediated Ins(1,4,5)P_3 accumulation to reductions in $[Ca^{2+}]_e$

A 5 min preincubation of cells in low $[Ca^{2+}]_e$ buffer prior to agonist challenge significantly reduced the resting level of Ins(1,4,5)P_3 from 36.2±4.8 (18) pmol mg^{-1} protein to 9.0±2.2 (6) pmol mg^{-1} protein. This preincubation did not affect the time course of the responses to carbachol or bradykinin (Figure 1a and b). The reduction in the peak response to carbachol was of a similar absolute magnitude over the entire dose-response. However, as a proportion of the response in the presence of extracellular Ca^{2+} the reduction varied over the carbachol dose-response curve, decreasing from approximately 80% at 1 nM to approximately 20% at 1 mM. The EC_{50} at low $[Ca^{2+}]_e$ was not significantly different from that in the presence of a normal $[Ca^{2+}]_e$ (−4.59±0.23 (3) (26 μM) and −4.63±0.07 (11) (24 μM) respectively) (Figure 2a). The elevation of Ins(1,4,5)P_3 during the sustained phase at low $[Ca^{2+}]_e$ was also dose-dependent with an EC_{50} of −5.38±0.11 (3) (4 μM) (data not shown). This was not significantly different from the EC_{50} determined in the presence of normal $[Ca^{2+}]_e$ (−5.37±0.23 (6) (4.3 μM)) but was significantly ($P<0.05$) less than that of peak Ins(1,4,5)P_3 elevation at low $[Ca^{2+}]_e$ (−4.59±0.23 (3) (26 μM)). The accumulation of Ins(1,4,5)P_3 at 10 s in response to bradykinin was markedly reduced at low $[Ca^{2+}]_e$ (Figures 1b and 2b). Compared to the direct addition of TCA, the addition of buffer alone provoked an increase of 14.8±0.4 (26) pmol mg^{-1} protein at 10 s which remained elevated for the duration of stimulation (Figure 1a and b). This increase was virtually abolished in low $[Ca^{2+}]_e$ buffer (0.81±0.84 (3) pmol mg^{-1} protein) (Figure 1a and b).

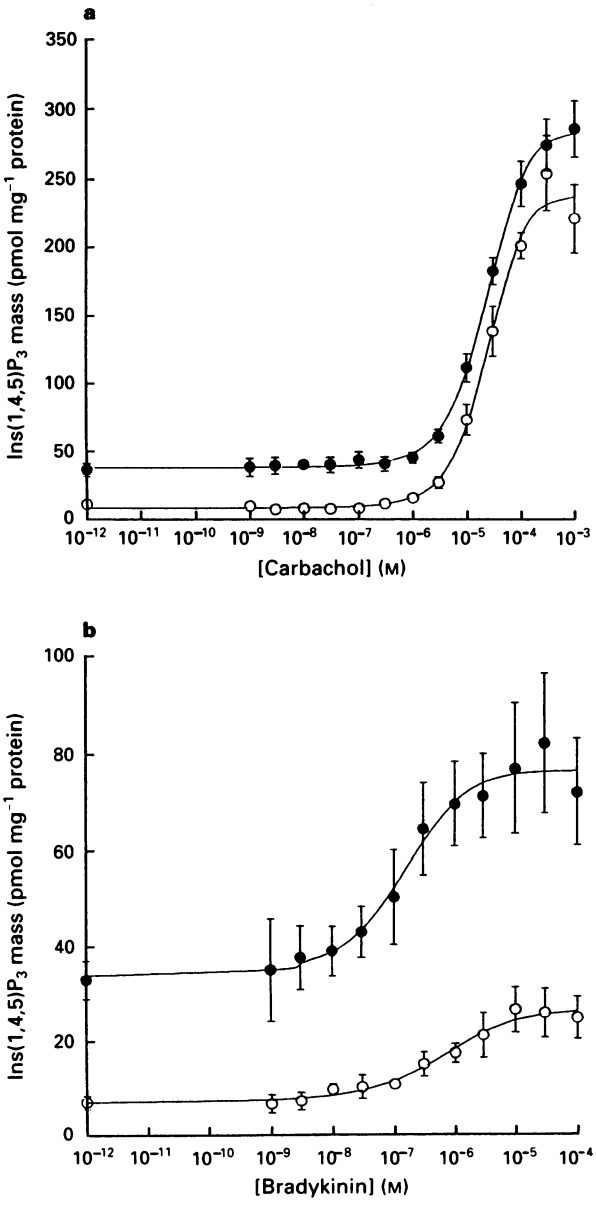

Figure 2 Dose-response relationship for carbachol (a) and bradykinin (b) mediated peak changes in inositol 1,4,5-trisphosphate (Ins(1,4,5)P_3) mass in adherent SH-SY5Y cells at normal (●) or low (○) $[Ca^{2+}]_e$. Data points are mean ± s.e.mean, $n = 7-11$ for carbachol, $n = 6-9$ for bradykinin at normal $[Ca^{2+}]_e$ and $n = 3$ for bradykinin at low $[Ca^{2+}]_e$. EC_{50} ($\log_{10}$ M, mean ± s.e.mean (n)) were clearly not different whether determined in the presence of normal or low $[Ca^{2+}]_e$ for either carbachol (−4.63 ± 0.07 (11) (24 μM) and −4.59 ± 0.23 (3) (26 μM) respectively) or bradykinin (−6.58 ± 0.13 (9) (264nM) and −6.17 ± 0.16 (3) (673 nM) respectively).

Pertussis toxin sensitivity of carbachol- and bradykinin-mediated Ins(1,4,5)P_3 accumulation

Pretreatment of cells for 24 h with 100 ng ml^{-1} pertussis toxin (added at the time of seeding of cells into multiwells) had no effect on the levels of Ins(1,4,5)P_3 during the sustained phase in response to carbachol (data not shown). However, there was a small but significant effect of pertussis toxin on the Ins(1,4,5)P_3 response to carbachol at 10 s, ($P<0.01$ by two-way analysis of variance of dose-response curves). Thus, 1 mM carbachol elevated Ins(1,4,5)P_3 levels from 29.2±5.1 (5) pmol mg^{-1} protein to 290.3±49.2 (5) pmol mg^{-1} protein in untreated compared to 25.8±2.1 (5) pmol mg^{-1} protein to 210.9±41.4 (5) pmol mg^{-1} protein in pertussis toxin-treated cells. The EC_{50} was, however, unaffected (data not shown). There was no significant effect of pertussis toxin on the Ins(1,4,5)P_3 response to bradykinin at 10 s (data not shown).

Ins(1,4,5)P_3 accumulation in fura-2 loaded cells

To allow direct comparison of dose-response curves for elevation of Ins(1,4,5)P_3 and $[Ca^{2+}]_i$, carbachol stimulation of Ins(1,4,5)P_3 accumulation was determined in fura-2 loaded cells. Cells preloaded with fura-2, by incubation in 1 ml Krebs/HEPES containing 3.3 μM fura-2-AM for 40 min at room temperature prior to carbachol stimulation, displayed time-course and dose-response relationships for Ins(1,4,5)P_3 generation that were identical to those in unloaded cells (data not shown). Thus any potential influence of cellular fura-2 on Ins(1,4,5)P_3 generation via Ca^{2+} buffering was not apparent over the full range of Ins(1,4,5)P_3 levels.

Carbachol- and bradykinin-mediated accumulation of [^{3}H]-InsPs

In response to 1 mM carbachol, [^{3}H]-InsPs showed a biphasic accumulation, being more rapid over the initial minute compared to a slower but still linear accumulation between 1 min and 30 min. By 1 min, accumulation was 133±7% (3) over basal compared with 1501±139% (3) at 30 min (Figure 3a). The response at 30 min was dose-related (Figure 3b) with an EC_{50} of −5.54±0.16 (3) (2.9 μM) which was not significantly different from the sustained phase of Ins(1,4,5)P_3 accumulation (−5.37±0.23 (6) (4.3 μM)). In contrast, in response to 10 μM bradykinin, [^{3}H]-InsPs increased by 47±14% (3) over basal by 1 min and showed no further increase over the subsequent 29 min (Figure 3a).

Carbachol and bradykinin mediated elevations of $[Ca^{2+}]_i$

At normal $[Ca^{2+}]_e$ carbachol at 100 nM or greater produced a characteristic rapid peak of $[Ca^{2+}]_i$ followed by a sustained phase (Figure 4). At 10 nM carbachol and below, although there was no characteristic $[Ca^{2+}]_i$ peak, there was evidence for the generation of a sustained component but this represented changes of less than 10 nM $[Ca^{2+}]_i$. Changes in $[Ca^{2+}]_i$ were dose-dependent and the EC_{50} values were not significantly different between peak (-6.26 ± 0.16 (0.55 M) and sustained phases (-6.64 ± 0.22 (0.23 μM)) (Figure 5). Responses to maximal (1 mM) carbachol stimulation were prevented by 10 μM atropine while addition of atropine during the plateau phase returned $[Ca^{2+}]_i$ levels to basal (data now shown).

Challenge with bradykinin also resulted in an immediate, concentration dependent, increase in $[Ca^{2+}]_i$ with an EC_{50} of -7.80 ± 0.11 (16 nM) (Figures 6 and 7). There was little evidence for a sustained phase of $[Ca^{2+}]_i$ elevation at maximal (1 μM) bradykinin concentrations, basal levels being attained after approximately 1 min (Figure 6). At 130 s following bradykinin addition, the $[Ca^{2+}]_i$ was $10.4 \pm 23.3\%$ (16) of the peak response compared to $33.1 \pm 4.1\%$ (7) and $12.6 \pm 1.5\%$ (8) for the sustained carbachol response at normal and low $[Ca^{2+}]_e$ respectively. However, at sub-maximal concentrations, particularly 10 nM, the $[Ca^{2+}]_i$ response to bradykinin showed a rapid elevation followed by a slow decline such that at 130 s following stimulation (the point for sustained response determination) $[Ca^{2+}]_i$ was still elevated above basal but declining (Figure 6 inset). Those populations of cells which did respond to bradykinin at a concentration of 1 nM or below showed very small (5–10 nM) sustained

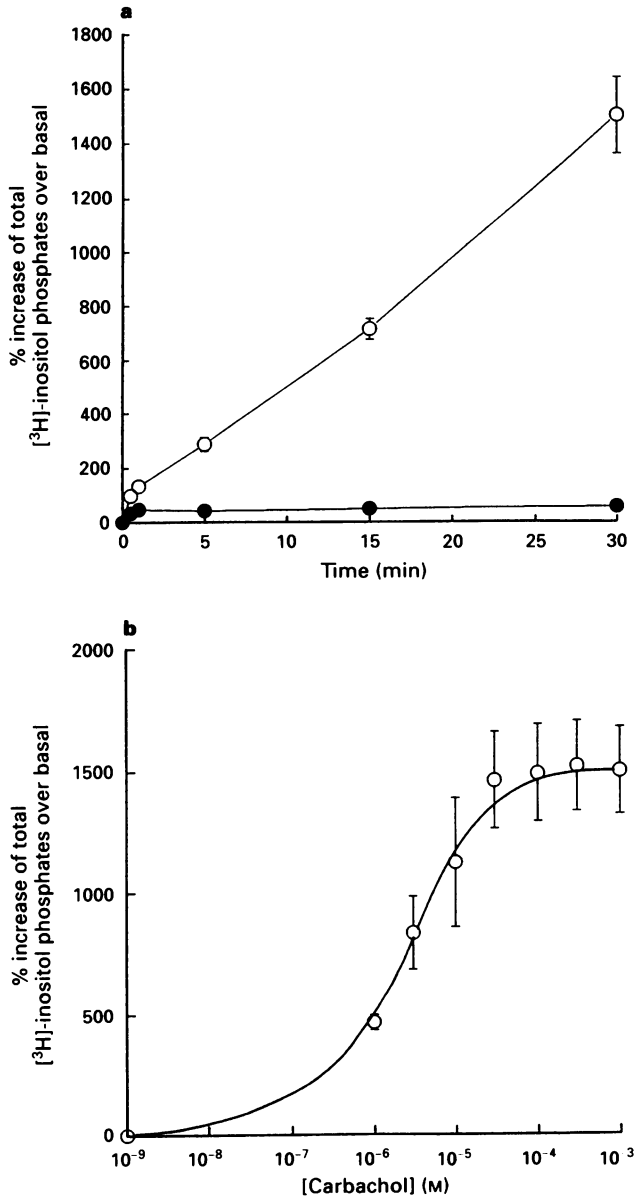

Figure 3 Time course of accumulation of [^{3}H]-inositol phosphates ([^{3}H]-InsPs) in adherent SH-SY5Y cells in response to 1 mM carbachol (○) and 10 μM bradykinin (●) (a) and the dose-response relationship for carbachol-mediated accumulation of [^{3}H]InsPs after 30 min of agonist exposure (b): EC_{50} value (mean ± s.e.mean (n) $\log_{10}$ M) of -5.54 ± 0.16 (3) (2.9 μM). Data points are mean ± s.e.mean $n = 3$.

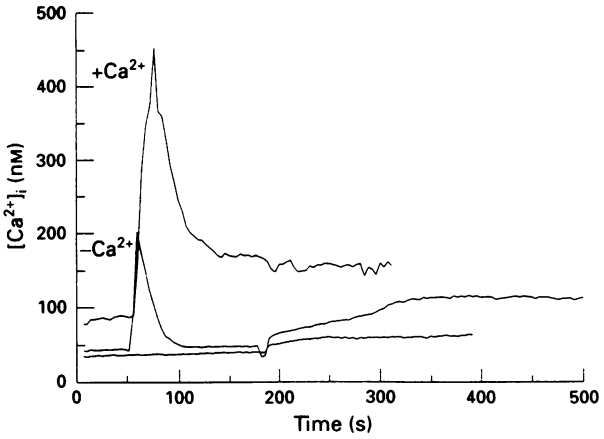

Figure 4 Representative traces of the time course of $[Ca^{2+}]_i$ elevation in populations of adherent SH-SY5Y cells in response to 1 mM carbachol, added at 50 s, at normal (upper peak) or low $[Ca^{2+}]_e$ (lower peak). At 180 s Ca^{2+} was added back to cells stimulated at low $[Ca^{2+}]_e$. The bottom trace demonstrates the effect of Ca^{2+} readdition to cells incubated, but not stimulated, at low $[Ca^{2+}]_e$.

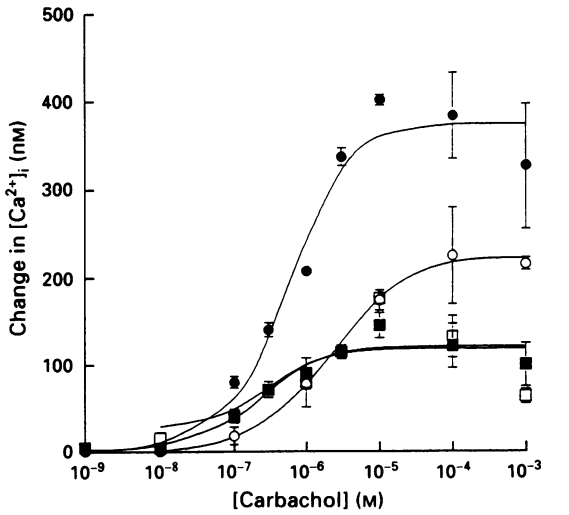

Figure 5 Dose-response relationships for carbachol mediated elevation of $[Ca^{2+}]_e$ in populations of adherent SH-SY5Y cells at peak (●) and sustained phase (■) in the presence of normal $[Ca^{2+}]_e$ and peak (○) at low $[Ca^{2+}]_e$ with Ca^{2+} readdition for determination of sustained phase (□). EC_{50} values ($\log_{10}$ M, mean ± s.e.mean) for peak and sustained phases were not significantly different whether determined in the presence of normal $[Ca^{2+}]_e$ (-6.26 ± 0.16 (0.55 μM) and -6.64 ± 0.22 (0.23 μM) respectively) or at low $[Ca^{2+}]_e$ with Ca^{2+} readdition (-5.68 ± 0.10 (2.1 μM) and -5.91 ± 0.18 (1.2 μM respectively). All data are mean ± s.e.mean, $n = 3$.

elevations of $[Ca^{2+}]_i$ (data not shown). The response to 10 nM bradykinin was fully inhibited by the bradykinin B_2 receptor antagonist, N-adamantaneacetyl-D-Arg[Hyp^3, Thi^{5,8}, D-Phe^7]-bradykinin at 10 μM with recovery of response after removal of antagonist by washing (data not shown).

Sensitivity of carbachol- and bradykinin-mediated elevation of $[Ca^{2+}]_i$ to reductions in $[Ca^{2+}]_e$

Basal $[Ca^{2+}]_i$ was 59±10 nM (8) at normal $[Ca^{2+}]_e$. Preincubation of cells in low $[Ca^{2+}]_e$ buffer at 37°C for 5 min prior to agonist challenge had a small but not statistically significant effect on basal $[Ca^{2+}]_i$ (47±7nM (8)). Subsequently, 1 mM carbachol increased $[Ca^{2+}]_i$ by 221±35 nM (8) representing a numerical but not significant reduction of 38% compared to the response at normal $[Ca^{2+}]_e$ (358±93 nM (7)). The response during the sustained phase was, however, more severely (73%) and significantly ($P<0.01$) reduced from an elevation of 73±12 nM (8) at normal to 20±5 nM (7) at low $[Ca^{2+}]_e$ (see Figure 4 for example traces). Thus, the sustained phase of $[Ca^{2+}]_i$ elevation was very dependent upon Ca^{2+} entry. To ensure determination of agonist potency for intracellular Ca^{2+} mobilization, independent of Ca^{2+} entry, the dose-dependence of carbachol elevation of $[Ca^{2+}]_i$ at peak was determined at low $[Ca^{2+}]_e$. In addition, the potency of carbachol for sustained elevation of $[Ca^{2+}]_i$ was evaluated by Ca^{2+} readdition to these cells (Figures 4 and 5). Determined by these methods, the EC_{50} values for peak (−5.68±0.10 (2.1 μM)) and sustained (−5.91±0.18 (1.2 μM)) phases were not significantly different from each other or their respective values determined at normal $[Ca^{2+}]_e$ (−6.26±0.16 (0.55 μM) and −6.64±0.22 (0.23 μM)) (Figures 4 and 5).

Under conditions of normal $[Ca^{2+}]_e$ a maximally effective concentration of bradykinin (1 μM) evoked a change in $[Ca^{2+}]_i$ of 137±37 nM (5). At low $[Ca^{2+}]_e$ this was reduced to 86±21 nM (5) representing a numerical but not significant reduction of 37% (see Figure 6 for example traces).

In the continued presence of a maximal carbachol challenge, the readdition of extracellular Ca^{2+} (2 mM) to cells initially challenged at low $[Ca^{2+}]$ provoked a sustained increase in $[Ca^{2+}]_i$ (Figure 4) of 168±10 nM (3). This compared to an increase of only 18±1 nM (3) (Figures 4 and 6) following the readdition of extracellular Ca^{2+} to unstimulated cells and 57±7 nM (6) upon readdition to cells challenged with bradykinin (Figure 6).

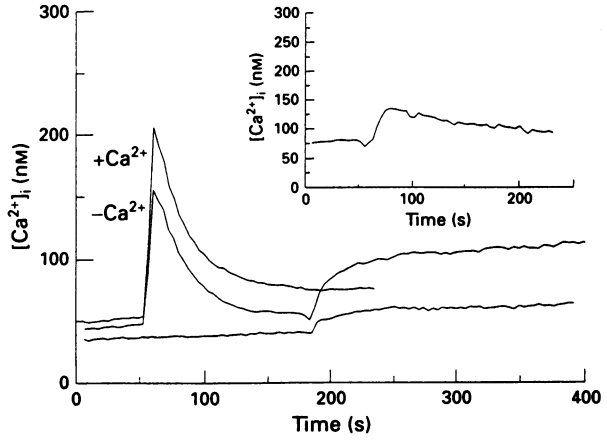

Figure 6 Representative traces of the time course of $[Ca^{2+}]_i$ elevation in populations of adherent SH-SY5Y cells in response to 1 μM bradykinin in the presence or absence of extracellular Ca^{2+}. At 180 s Ca^{2+} was added back to cells stimulated in its absence. The lower trace demonstrates the effect of Ca^{2+} readdition to cells incubated, but not stimulated, in the absence of extracellular Ca^{2+}. Inset is shown the time course of the response to 10 nM bradykinin in the presence of extracellular Ca^{2+}.

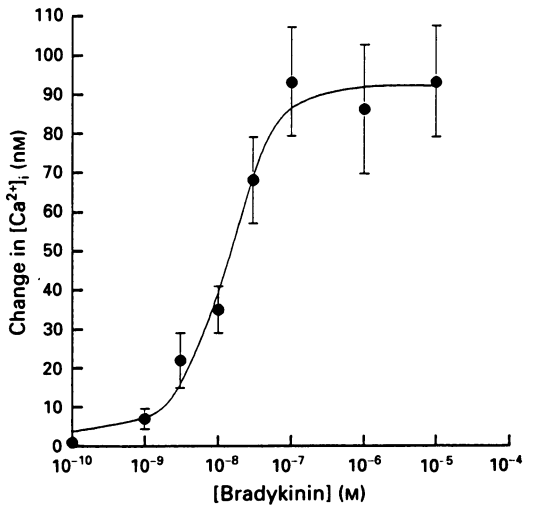

Figure 7 Dose-response relationship for bradykinin-mediated peak elevations of $[Ca^{2+}]_i$ in populations of adherent SH-SY5Y cells. Data are mean ± s.e.mean, $n = 3-18$. EC_{50} ($\log_{10}$M, mean ± s.e.mean) −7.80 ± 0.11 (16 nM).

Comparison of agonist potencies for elevation of Ins(1,4,5)P_3 and $[Ca^{2+}]_i$

The potency of carbachol, as judged from EC_{50} values, was significantly greater for elevation of $[Ca^{2+}]_i$ than Ins(1,4,5)P_3 at both peak (−6.26±0.16 (0.55 μM) versus −4.63±0.07 (11) (24 μM) respectively, $P<0.01$) and sustained (−6.64±0.22 (0.23 μM) versus −5.37±0.23 (6) (4.3 μM) respectively, $P<0.05$) phases (Figure 8). Similarly bradykinin elevated $[Ca^{2+}]_i$ at peak more potently than Ins(1,4,5)P_3 (EC_{50} values of −7.80±0.11 (16 nM) versus −6.58±0.13 (9) (264 nM) respectively, $P<0.01$) (Figure 8). This potency difference was maintained when peak $[Ca^{2+}]_i$ and Ins(1,4,5)P_3 responses

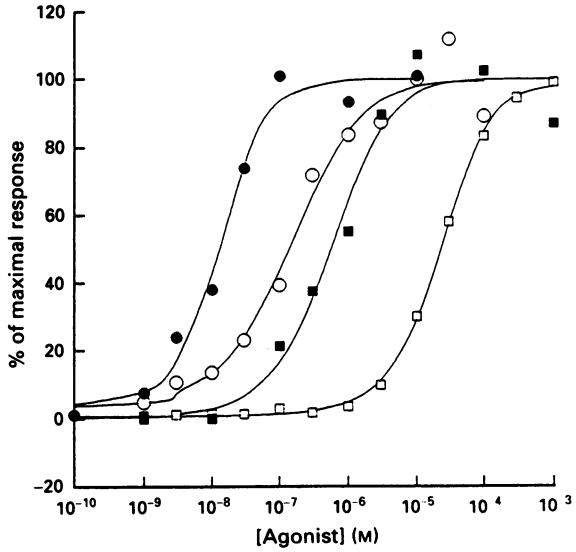

Figure 8 Comparison of normalized dose-response curves for bradykinin-mediated peak elevation of $[Ca^{2+}]_i$ (●) and inositol 1,4,5-trisphosphate (Ins(1,4,5)P_3) (○) and carbachol-mediated peak elevation of $[Ca^{2+}]_i$ (■) and Ins(1,4,5)P_3 (□). This figure was constructed with data collected from cells stimulated in the presence of extracellular Ca^{2+} (see Figures 2, 5 and 7). The EC_{50} value ($\log_{10}$M, mean ± s.e.mean) for elevation of $[Ca^{2+}]_i$ was significantly ($P<0.01$) less than that for elevation of Ins(1,4,5)P_3 for both bradykinin (−7.80 ± 0.11 (16 nM) and −6.58 ± 0.13 (9) (264 nM) respectively) and carbachol (−6.26 ± 0.16 (0.55 μM) and −4.63 ± 0.07 (11) (24 μM) respectively).

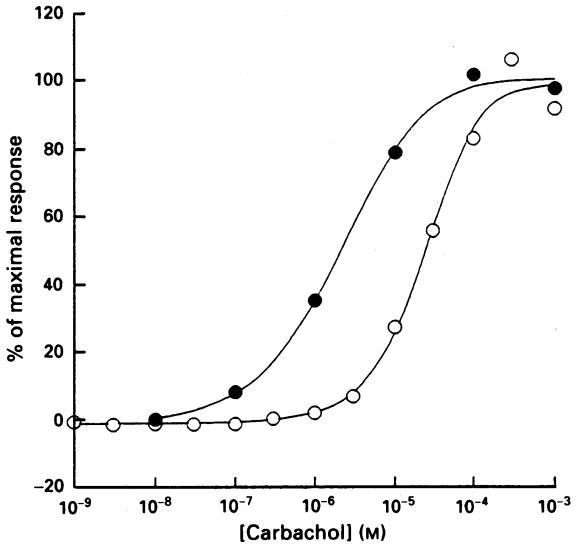

Figure 9 Comparison of normalized dose-response curves for carbachol-mediated elevation of $[Ca^{2+}]_i$ (●) and inositol 1,4,5-trisphosphate (Ins(1,4,5)P_3) (○) in the absence of extracellular Ca^{2+}. Data were taken from Figures 2 and 5. The EC_{50} value (log_{10} M, mean ± s.e.mean) for elevation of $[Ca^{2+}]_i$ (-5.68 ± 0.10 (2.1 μM)) was significantly ($P<0.01$) less than that for elevation of Ins(1,4,5)P_3 (-4.59 ± 0.23 (3) (26 μM)).

were determined for carbachol at low $[Ca^{2+}]_e$ (EC_{50} values of -5.68 ± 0.10 (2.1 μM) versus -4.59 ± 0.23 (3) (26 μM) respectively, $P<0.05$) (Figure 9).

Discussion

The current work provides new information on the quantitative relationships between Ins(1,4,5)P_3 and Ca^{2+} signalling in a human neuroblastoma possessing muscarinic and bradykinin receptors. It is now accepted that these relationships are complex, with important regulatory features displayed by the signalling pathway and with Ca^{2+} playing a potentially crucial role at several levels (Wojcikiewicz *et al.*, 1993).

Carbachol- and bradykinin-mediated elevation of Ins(1,4,5)P_3 and $[Ca^{2+}]_i$

Stimulation of muscarinic receptors with carbachol confirmed that elevations of Ins(1,4,5)P_3 in SH-SY5Y cells are biphasic, consisting of a rapid peak followed by a lower but sustained phase (Lambert & Nahorski, 1990b; Lambert *et al.*, 1991). These changes are matched both in time and pattern by atropine-blockable elevations of $[Ca^{2+}]_i$, as previously reported in these cells (Akerman, 1989; Lambert & Nahorski, 1990b; Murphy *et al.*, 1991), the parental SK-N-SH cell line (Fisher *et al.*, 1989) and indeed consistent with the pattern of response in many other receptor systems (Putney & Bird, 1993). There is now substantial evidence that peak $[Ca^{2+}]_i$ responses are driven predominantly by the actions of Ins(1,4,5)P_3 on ligand-gated Ca^{2+} channels located on specialised components of the endoplasmic reticulum (Berridge, 1993) while sustained phases result from Ca^{2+} influx, by mechanisms still incompletely understood but almost certainly involving a capacitative entry following store depletion (Putney & Bird, 1993).

The current study also revealed a bradykinin-mediated PLC activation in these cells, in agreement with a preliminary report of $[Ca^{2+}]_i$ elevation by this peptide (Vaughan *et al.*, 1993). Measurement of $[Ca^{2+}]_i$ in fura-2 loaded single cells demonstrated that in many instances both bradykinin and carbachol were able to elevate $[Ca^{2+}]_i$ in the same cell, indicating co-expression of bradykinin and muscarinic receptors (data not shown). In contrast to the maximal elevations of Ins(1,4,5)P_3 and $[Ca^{2+}]_i$ induced by carbachol, bradykinin produced relatively small peak elevations with little evidence of sustained phases. With the possible exception of NIH3T3 cells (Fu *et al.*, 1988), there is little evidence elsewhere of sustained PLC activation by bradykinin in neuronal or neuronal-like cells, although the decline of some responses may be slower (Fu *et al.*, 1988; Imaizumi *et al.*, 1989; Burgess *et al.*, 1989; Donie & Reiser, 1991; Iredale *et al.*, 1992). It is unknown whether this may be related, for example, to differences in the level of receptor expression. Although the significance and mechanism of the slight pertussis toxin sensitivity of peak Ins(1,4,5)P_3 responses to carbachol are unclear, the pertussis toxin insensitivity of the Ins(1,4,5)P_3 response to bradykinin in the present study is consistent with that in NG108-15 cells (Fu *et al.*, 1988). This suggests a possible shared pool of $G_{q/11}$ between muscarinic M_3 and bradykinin receptors in SH-SY5Y cells which may have consequences for their simultaneous stimulation. The B_2 bradykinin receptor is likely to mediate PLC activation in SH-SY5Y cells given that neuronal bradykinin receptors are predominantly B_2 (see Wolsing & Rosenbaum, 1991), its established linkage to PLC activation (Derian & Moskowitz, 1986; Eggerickx *et al.*, 1992) and the inhibition of $[Ca^{2+}]_i$ responses by B_2 antagonists in this and a previous study (Vaughan *et al.*, 1993).

Sensitivity of carbachol- and bradykinin-mediated elevation of Ins(1,4,5)P_3 and $[Ca^{2+}]_i$ to reduction of $[Ca^{2+}]_e$

Accumulating evidence strongly suggests that the activity of many PLC isoforms may be regulated by the prevailing $[Ca^{2+}]$ (Rhee & Choi, 1992). In the current study, while both phases of Ins(1,4,5)P_3 accumulation displayed some sensitivity to reductions in $[Ca^{2+}]_e$, that of the sustained phase was clearly greater than that of the peak as previously demonstrated for maximal muscarinic receptor stimulation of these cells (Lambert & Nahorski, 1990b). We also demonstrate here a reduction in basal levels of Ins(1,4,5)P_3 at low $[Ca^{2+}]_e$ and a reduction in peak elevations of similar absolute size, approximately equivalent to the basal reduction, over the entire carbachol dose-response curve. Despite the clear dependence of sustained Ins(1,4,5)P_3 generation on extracellular Ca^{2+}, this was not absolute as demonstrated by the dose-related elevation at low $[Ca^{2+}]_e$. This sustained elevation to maximal carbachol stimulation was not reduced further when $[Ca^{2+}]_e$ was buffered to approximately 100 nM with EGTA (data not shown) and is consistent with continued accumulation of [^{3}H]-InsPs during a 5 min maximal carbachol stimulation of SH-SY5Y cells at 100 nM $[Ca^{2+}]_e$ (Wojcikiewicz *et al.*, 1994). Peak bradykinin-mediated Ins(1,4,5)P_3 accumulation was proportionately more sensitive to low $[Ca^{2+}]_e$ than that of carbachol. This marked sensitivity is similar to that reported for bradykinin stimulation in NIH3T3 and NG108-5 cells (Fu *et al.*, 1988) although that effect required EGTA buffering of Ca^{2+}. In the current study, the absolute reductions in Ins(1,4,5)P_3 accumulations were, however, similar for both agonists, suggesting a consistent amount of PLC activity sensitive to reductions in $[Ca^{2+}]_e$ independent of the extent of agonist stimulation.

These data argue very strongly for a role of changes in $[Ca^{2+}]_i$ regulating both basal and agonist stimulated PLC activity. The greater sensitivity of the sustained compared to the peak response to carbachol to low $[Ca^{2+}]_e$ suggests either that Ca^{2+} regulation of PLCβ becomes greater during prolonged activation or that a different PLC isoform is involved. Alternatively the replenishment of substrate required to maintain the response may be Ca^{2+}-sensitive or the rapid mobilization of Ca^{2+} from intracellular stores may, through a feed-forward activation of PLC (Wojcikiewicz *et al.*, 1994) be

sufficient to mask any requirement for extracellular Ca^{2+} during the peak of Ins(1,4,5)P_3 generation. Such differences may account for the greater potency of the sustained phase compared to peak carbachol-mediated Ins(1,4,5)P_3 generation demonstrated here and reported recently for these cells and CHO cells expressing the cloned human muscarinic m3 receptor (Wojcikiewicz *et al.*, 1994).

Interestingly, in the present study, the addition of buffer alone containing 2 mM Ca^{2+} provoked a small increase in Ins(1,4,5)P_3 which appeared to be totally dependent upon extracellular Ca^{2+}. Whether this truly reflects Ca^{2+} activation of PLC and whether it is a consequence of, for example, shear stress or damage to the cells is unclear.

Peak and sustained $[Ca^{2+}]_i$ elevations following muscarinic receptor activation, while displaying similar agonist potencies, also displayed a differential sensitivity to reductions in $[Ca^{2+}]_e$ with the sustained phase being more greatly affected. Although peak elevations of $[Ca^{2+}]_i$ to both carbachol and bradykinin were not significantly affected by low $[Ca^{2+}]_e$, it should be noted that the estimates of difference are based upon peak heights only and differences in areas under the $[Ca^{2+}]_i$ versus time plots are more pronounced. This might suggest that either a proportion of intracellular Ca^{2+} stores display marked sensitivity to reduced $[Ca^{2+}]_e$ or alternatively that Ca^{2+} entry, initiated either directly or in response to Ca^{2+}-store depletion (Putney & Bird, 1993) may contribute to the initial elevation of $[Ca^{2+}]_i$ by both agonists. Indeed early Ca^{2+} entry in response to carbachol in SH-SY5Y cells is consistent with an immediate quench of intracellular fura-2 fluorescence by Mn^{2+} when used to replace external Ca^{2+} (Lambert & Nahorski, 1990b).

Receptor desensitization and utility of measurement of [^{3}H]-InsPs accumulation for determination of agonist-mediated PLC activation

The transient nature of $[Ca^{2+}]_i$ and particularly Ins(1,4,5)P_3 peak elevations following both carbachol and bradykinin imply desensitization of receptor/G-protein/PLC coupling. Given the biphasic nature of responses to carbachol compared with monophasic responses to bradykinin, desensitization of the muscarinic receptor must be partial while that of the bradykinin receptor may be complete or near complete. Interestingly the readdition of extracellular Ca^{2+} to cells challenged with bradykinin produced a sustained elevation of $[Ca^{2+}]_i$ apparently greater than that when added to cells incubated at low $[Ca^{2+}]$ but not challenged with agonist. Given the rapid return of $[Ca^{2+}]_i$ to approximately basal levels after bradykinin addition in the presence of extracellular Ca^{2+}, the reason for this is unclear. Whether it is a consequence of bradykinin stimulation under non-physiological conditions which may, for example, reset the Ca^{2+} homeostatic mechanism or whether this truly reflects a persistent bradykinin-mediated Ca^{2+} entry via the same receptor that mediates PLC activation requires further study.

Mechanisms underlying rapid desensitization phenomena are not established but have the potential to include phosphorylation of the receptor (Wojcikiewicz *et al.*, 1993). This is analogous to the β-adrenoceptor kinase (β-ARK) mediating phosphorylation and desensitization of the β-adrenoceptor (Hausdorff *et al.*, 1990). Indeed, phosphorylation of a number of PLC-linked receptors has been reported (Klueppelberg *et al.*, 1992; Kwatra *et al.*, 1993) including that of the m3 receptor by PKC and an additional kinase distinct from either protein kinase A (PKA), Ca^{2+}-calmodulin-dependent kinase or β-ARK (Tobin & Nahorski, 1993; Tobin *et al.*, 1993).

That desensitization of the bradykinin response in SH-SY5Y was not due to enhanced metabolism of Ins(1,4,5)P_3 was demonstrated by the lack of continued accumulation of [^{3}H]-InsPs following the initial rapid but small increase in cells where inositol monophosphatase was uncompetitively blocked by lithium. Thus, when there is no sustained Ins(1,4,5)P_3 generation and particularly when the peak response is small, measurement of accumulation of [^{3}H]-InsPs may lack the required sensitivity for demonstration of PLC activation. Indeed this may account for previous reports of no bradykinin mediated PLC activation in either the parental SK-N-SH (Yu & Sadee, 1986) or SH-SY5Y cell lines (Ogino & Costa, 1993). The biphasic nature of the [^{3}H]-InsPs responses in the present study are consistent with the pattern in AR4-2J pancreatoma cells stimulated with either bombesin or cholecystokinin (Menniti *et al.*, 1991) and our previous study of SH-SY5Y cells stimulated with carbachol (Wojcikiewicz *et al.*, 1994) where there were falls in the rates of accumulation following 20–30 s of exposure. Many studies have used the measurement of accumulation of [^{3}H]-InsPs in lithium-blocked cells generally employing relatively long periods of agonist exposure and assumed linearity of accumulation over tens of minutes to reflect a lack of desensitization (Wojcikiewicz *et al.*, 1993). However, more detailed analysis may reveal biphasic accumulations where the change in rate may reflect the biphasic nature of the Ins(1,4,5)P_3 response. We have argued (Wojcikiewicz *et al.*, 1993) that this reflects a rapid desensitization of receptor-G_q-PLC coupling. Thus, although measurement of accumulation of [^{3}H]-InsPs at extremely short time points (<30 s) may reflect initial levels of PLC activity, most studies will measure predominantly PLC activity during the sustained phase of Ins(1,4,5)P_3 generation. This is emphasized by the similarity of the EC_{50} values for sustained carbachol-mediated Ins(1,4,5)P_3 generation and accumulation of [^{3}H]-InsPs and their greater potency relative to peak Ins(1,4,5)P_3 generation shown here. Thus, early desensitization events may be missed and either different PLC isoforms may be active or there could be a differing inositol lipid substrate profile during prolonged activation. In addition to these pitfalls, measurement of [^{3}H]-InsPs will also reflect the Ca^{2+} sensitivity of the sustained but not the peak phase of Ins(1,4,5)P_3 generation, which may differ. Thus, although several studies have determined muscarinic receptor activation of PLC by this method in SK-N-SH (Yu & Sadee, 1986; Fisher & Heacock, 1988; Fisher *et al.*, 1989; Baird *et al.*, 1989) and SH-SY5Y cells (Lambert & Nahorski, 1990b; Lambert *et al.*, 1991) the substantial sensitivity to reductions in $[Ca^{2+}]_e$ reported in SK-N-SH cells (Fisher *et al.*, 1989) is likely to reflect the sensitivity of a partially desensitized receptor.

Comparison of agonist potencies for elevation of Ins(1,4,5)P_3 and $[Ca^{2+}]_i$

The present study has also revealed that the potencies of both carbachol and bradykinin for the peak elevation of $[Ca^{2+}]_i$ were substantially greater than those for peak Ins(1,4,5)P_3 elevation. This is unlikely to result from an enhanced PLC activation due to Ca^{2+} entry as the difference existed when responses to carbachol were determined at low $[Ca^{2+}]_e$ when little or no Ca^{2+} influx would occur. One potential difficulty in the interpretation of these data is that the magnitude of both Ins(1,4,5)P_3 and $[Ca^{2+}]_i$ elevations are a consequence of mechanisms designed to both elevate and decrease these variables. Thus, Ins(1,4,5)P_3 elevation will be limited by metabolism to both higher and lower inositol phosphates, while $[Ca^{2+}]_i$ elevation may be limited by buffering, uptake and extrusion systems. However, such differences in agonist potency are in accord with the amplification within PLC-linked systems such that dose-response curves for agonist-mediated PLC activation, as assessed by accumulation of [^{3}H]-InsPs in lithium-blocked cells, generally lie to the left of receptor occupation curves and to the right of downstream events such as smooth muscle contraction (Kenakin, 1987). The present study and a previous demonstration of a 33 fold greater potency for fMet-Leu-Phe stimulation of Ca^{2+} mobilization compared to Ins(1,4,5)P_3 accumulation in neutrophils at low $[Ca^{2+}]_e$ (Thompson *et al.*, 1991) suggests that a potency difference

does exist during acute stimulation of fully sensitized receptors. This is likely, therefore, to reflect a true amplification step in the phosphoinositide pathway. Thus, the observed difference in agonist potency for Ins(1,4,5)P_3 and $[Ca^{2+}]_i$ elevation is an expected phenomenon, defining a site of amplification and allowing consideration of the mechanisms involved.

Mechanism for amplification within the phosphoinositide signal transduction pathway

There is evidence from single cells that agonist-mediated elevation of $[Ca^{2+}]_i$ is an 'all-or-none' response (Bootman *et al.*, 1992; Shao & McCarthy, 1993). The amplitude of agonist-mediated $[Ca^{2+}]_i$ elevation within a single cell may not, therefore, be proportionately related to the concentration of agonist. Thus $[Ca^{2+}]_i$ elevation will or will not occur at a given agonist concentration and this concentration may differ between cells of the same population. A consequence of this is that concentration-effect curves for agonist-mediated elevation of $[Ca^{2+}]_i$ in cell populations would represent cell recruitment profiles with more cells responding at higher agonist concentrations. Generation of Ins(1,4,5)P_3 above that required to trigger the $[Ca^{2+}]_i$ response of a single cell may therefore play no part in Ca^{2+} signalling and represent a spare capacity within the system. This is supported by the observation of the full Ca^{2+} mobilization at sub-maximal Ins(1,4,5)P_3 levels in populations of cells in the current study. The precise mechanisms underlying potential all-or-none $[Ca^{2+}]_i$ responses in single cells are unclear. Such responses may be a simple reflection of a threshold level of Ins(1,4,5)P_3 being attained with subsequent emptying of all of the Ca^{2+} from the rapidly releasable pool. If, however, heterogeneity of Ins(1,4,5)P_3 receptor sensitivity exists within a cell (see Oldershaw *et al.*, 1991; Bootman *et al.*, 1992), this would suggest cooperativity of the Ca^{2+} release process, such that the release of a small amount of Ca^{2+} causes the release of all available Ca^{2+}. This may be via Ca^{2+}-induced Ca^{2+} release whereby the release of a small amount of Ca^{2+} initiates the release of further Ca^{2+} from ryanodine-sensitive stores (see Putney & Bird, 1993). Alternatively the release of a small amount of Ca^{2+} may sensitize Ins(1,4,5)P_3 receptors such that release escalates at the same Ins(1,4,5)P_3 concentration until the elevated $[Ca^{2+}]_i$ inhibits further Ins(1,4,5)P_3 receptor activation (Bezprozvanny *et al.*, 1991).

Thus, the greater agonist potency for elevation of $[Ca^{2+}]_i$ relative to that of Ins(1,4,5)P_3 could occur as a consequence of all-or-none $[Ca^{2+}]_i$ responses in single cells mediated either by threshold levels of Ins(1,4,5)P_3 or the feed-forward interactions described. These feed-forward interactions could also account for the observed potency difference if agonist-mediated $[Ca^{2+}]_i$ elevation were graded as opposed to an all-or-none phenomenon. Whatever the mechanism, the potency difference defines a step which features as an important amplification stage within the signal transduction pathway.

Summary

In summary, this study has provided a detailed evaluation of the time- and concentration-dependent aspects of polyphosphoinositide and Ca^{2+} signalling by muscarinic and bradykinin receptor stimulation of the human SH-SY5Y neuroblastoma cell line. Clear differences in the ability of agonists to activate PLC and mobilize intracellular Ca^{2+} are revealed and the complexities of Ca^{2+} entry in these responses are highlighted. Finally, rapid regulatory features of this signalling pathway indicate that the experimental approaches for determining agonist-stimulated PLC activity require careful evaluation.

This study has been supported by a Programme Grant from the Wellcome Trust and an equipment grant from the Mental Health Foundation.

References

AKERMAN, K.E.O. (1989). Depolarization of human neuroblastoma cells as a result of muscarinic receptor-induced rise in cytosolic Ca^{2+}. *FEBS Lett.*, **242**, 337–340.

BAIRD, J.G., LAMBERT, D.G., MCBAIN, J. & NAHORSKI, S.R. (1989). Muscarinic receptors coupled to phosphoinositide hydrolysis and elevated cytosolic calcium in a human neuroblastoma cell line SK-N-SH. *Br. J. Pharmacol.*, **98**, 1328–1334.

BERRIDGE, M.J. (1993). Inositol trisphosphate and calcium signalling. *Nature*, **361**, 315–325.

BEZPROZVANNY, I., WATRAS, J. & EHRLICH, B.E. (1991). Bell-shaped calcium response curves of Ins(1,4,5)P_3- and calcium-gated channels from endoplasmic reticulum of cerebellum. *Nature*, **351**, 751–754.

BOOTMAN, M.D., BERRIDGE, M.J. & TAYLOR, C.W. (1992). All-or-nothing Ca^{2+} mobilization from the intracellular stores of single histamine-stimulated HeLa cells. *J. Physiol.*, **450**, 163–178.

BURGESS, G.M., MULLANEY, I., MCNEILL, M., DUNN, P.M. & RANG, H.P. (1989). Second messengers involved in the mechanism of action of bradykinin in sensory neurons in culture. *J. Neurosci.*, **9**, 3314–3325.

CHALLIS, R.A.J., CHILVERS, E.R., WILLCOCKS, A.L. & NAHORSKI, S.R. (1990). Heterogeneity of [^{3}H]inositol 1,4,5-trisphosphate binding sites in adrenal-cortical membranes. Characterization and validation of a radioreceptor assay. *Biochem. J.*, **265**, 421–427.

DERIAN, C.K. & MOSKOWITZ, M.A. (1986). Polyphosphoinositide hydrolysis in endothelial cells and carotid artery segments. Bradykinin-2 receptor stimulation is calcium-independent. *J. Biol. Chem.*, **261**, 3831–3837.

DONIE, F. & REISER, G. (1991). Mass measurements of inositol 1,4,5-trisphosphate and inositol 1,3,4,5-tetrakisphosphate in a neuronal cell line stimulated with bradykinin: inositolphosphate response shows desensitization. *Biochem. Biophys. Res. Commun.*, **181**, 997–1003.

EGGERICKX, D., RASPE, E., BERTRAND, D., VASSART, G. & PARMENTIER, M. (1992). Molecular cloning, functional expression and pharmacological characterization of a human bradykinin B2 receptor gene. *Biochem. Biophys. Res. Commun.*, **187**, 1306–1313.

FISHER, S.K., DOMASK, L.M. & ROLAND, R.M. (1989). Muscarinic receptor regulation of cytoplasmic Ca^{2+} concentrations in human SK-N-SH neuroblastoma cells: Ca^{2+} requirements for phospholipase C activation. *Mol. Pharmacol.*, **35**, 195–204.

FISHER, S.K. & HEACOCK, A.M. (1988). A putative M_3 muscarinic cholinergic receptor of high molecular weight couples to phosphoinositide hydrolysis in human SK-N-SH neuroblastoma cells. *J. Neurochem.*, **50**, 984–987.

FU, T., OKANO, Y. & NOZAWA, Y. (1988). Bradykinin-induced generation of inositol 1,4,5-trisphosphate in fibroblasts and neuroblastoma cells: effect of pertussis toxin, extracellular calcium, and down-regulation of protein kinase C. *Biochem. Biophys. Res. Commun.*, **157**, 1429–1435.

GRYNKIEWICZ, G., POENIE, M. & TSIEN, R.Y. (1985). A new generation of Ca^{2+} indicators with greatly improved fluorescence properties. *J. Biol. Chem.*, **260**, 3440–3450.

HAUSDORFF, W.P., CARON, M.G. & LEFKOWITZ, R.J. (1990). Turning off the signal: desensitization of β-adrenergic receptor function. *FASEB J.*, **4**, 2881–2889.

IMAIZUMI, T., OSIGI, T., MISAKI, N., UCHIDA, S. & YOSHIDA, H. (1989). Heterologous desensitization of bradykinin-induced phosphatidylinositol response and Ca^{2+} mobilization by neurotensin in NG108-15 cells. *Eur. J. Pharmacol.*, **161**, 203–208.

IREDALE, P.A., MARTIN, K.F., HILL, S.J. & KENDALL, D.A. (1992). Agonist-induced changes in $[Ca^{2+}]_i$ in NE–115 cells: differential effects of bradykinin and carbachol. *Eur. J. Pharmacol.*, **226**, 163–168.

KENAKIN, T.P. (1987). *Pharmacological Analysis of Drug-Receptor Interaction*. New York: Raven Press.

KLUEPPELBERG, U.G., GATES, L.K., GORELICK, F.S. & MILLER, L.J. (1991). Agonist-regulated phosphorylation of the pancreatic cholecystokinin receptor. *J. Biol. Chem.*, **266**, 2403–2408.

KWATRA, M.M., SCHWINN, D.A., SCHREURS, J., BLANK, J.L., KIM, C.M., BENOVIC, J.L., KRAUSE, J.E. CARON, M.G. & LEFKOWITZ, R.J. (1993). The substance P receptor, which couples to $G_{q/11}$, is a substrate of β-adrenergic receptor kinase 1 and 2. *J. Biol. Chem.*, **268**, 9161–9164.

LAMBERT, D.G., CHALLIS, R.A.J. & NAHORKSI, S.R. (1991). Accumulation and metabolism of Ins(1,4,5)P_3 and Ins(1,3,4,5)P_4 in muscarinic-receptor-stimulated SH-SY5Y neuroblastoma cells. *Biochem. J.*, **273**, 791–794.

LAMBERT, D.G., GHATAORRE, A.S. & NAHORSKI, S.R. (1989). Muscarinic receptor binding characteristics of a human neuroblastoma SK-N-SH and its clones SH-SY5Y and SH-EP1. *Eur. J. Pharmacol.*, **165**, 71–77.

LAMBERT, D.G. & NAHORSKI, S.R. (1990a). Pertussis toxin inhibits α_2-adrenoceptor-mediated inhibition of adenylate cyclase without affecting muscarinic regulation of $[Ca^{2+}]_i$ or inositol phosphate generation in SH-SY5Y neuroblastoma cells. *Biochem. Pharmacol.*, **40**, 2291–2295.

LAMBERT, D.G. & NAHORSKI, S.R. (1990b). Muscarinic-receptor-mediated changes in intracellular Ca^{2+} and inositol 1,4,5,trisphosphate mass in a human neuroblastoma cell line, SH-SY5Y. *Biochem. J.*, **265**, 555–562.

MENNITI, F.S., TAKEMURA, H., OLIVER, K.G. & PUTNEY J.W. Jr. (1991). Different modes of regulation for receptors activating phospholipase C in the rat pancreatoma cell line AR4-2J. *Mol. Pharmacol.*, **40**, 727–733.

MURPHY, N.P., VAUGHAN, P.F.T., BALL, S.G. & MCCORMACK, J.G. (1991). The cholinergic regulation of intracellular calcium in the human neuroblastoma, SH-SY5Y. *J. Neurochem.*, **57**, 2116–2123.

OGINO, Y. & COSTA, T. (1992). The epithelial phenotype of human neuroblastoma cells express bradykinin, endothelin, and angiotensin II receptors that stimulate phosphoinositide hydrolysis. *J. Neurochem.*, **58**, 46–56.

OLDERSHAW, K.A., NUNN, D.L. & TAYLOR, C.W. (1991). Quantal Ca^{2+} mobilization stimulated by inositol 1,4,5-trisphosphate in permeabilized hepatocytes. *Biochem. J.*, **278**, 705–708.

PUTNEY, J.W. & BIRD, G.St.J. (1993). The inositol phosphate-calcium signalling system in nonexcitable cells. *Endoc. Rev.*, **14**, 610–631.

RHEE, S.G. & CHOI, K.D. (1992). Regulation of inositol phospholipid-specific phospholipase C isozymes. *J. Biol. Chem.*, **267**, 12393–12396.

ROSS, R.A., SPENGLER, B.A. & BIEDLER, J.L. (1983). Coordinate morphological and biochemical interconversion of human neuroblastoma cells. *J. Nat. Canc. Inst.*, **371**, 741–745.

SHAO, Y. & MCCARTHY, K.D. (1993). Quantitative relationship between α_1-adrenergic receptor density and the receptor-mediated calcium response in individual astroglial cells. *Mol. Pharmacol.*, **44**, 247–254.

THOMPSON, N.T., BONSER, R.W., TATESON, J.E., SPACEY, G.D. RANDALL, R.W., HODSON, H.F. & GARLAND, L.G. (1991). A quantitative investigation into the dependence of Ca^{2+} mobilization on changes in inositol 1,4,5-trisphosphate levels in the stimulated neutrophil. *Br. J. Pharmacol.*, **103**, 1592–1596.

TOBIN, A.B., KEYS, B. & NAHORSKI, S.R. (1993). Phosphorylation of a phosphoinositide C-linked muscarinic receptor by a novel kinase distinct from β-adrenergic receptor kinase. *FEBS Lett.*, **335**, 353–357.

TOBIN, A.B. & NAHORSKI, S.R. (1993). Rapid agonist-mediated phosphorylation of m3-muscarinic receptors revealed by immunoprecipitation. *J. Biol. Chem.*, **268**, 9817–9823.

VAUGHAN, P.F.T., KAYE, D.F., MCDONALD, R., REEVE, H.L., BALL, S.G. & PEERS, C. (1993). Bradykinin-evoked release of [^{3}H]noradrenaline from the human neuroblastoma SH-SY5Y. *Biochem. Soc. Trans.*, **21**, 42OS.

WALL, S.J., YASUDA, R.P. & WOLFE, B.B. (1991). Development of an antiserum against m3 muscarinic receptors: distribution of m3 receptors in rat tissues and clonal cell lines. *Mol. Pharmacol.*, **40**, 783–789.

WOJCIKIEWICZ, R.J.H., TOBIN, A.B. & NAHORSKI, S.R. (1993). Desensitization of cell signalling mediated by phosphoinositide C. *Trends Pharmacol. Sci.*, **14**, 279–285.

WOJCIKIEWICZ, R.J.H., TOBIN, A.B. & NAHORSKI, S.R. (1994). Muscarinic receptor-mediated inositol 1,4,5-trisphosphate formation in SH-SY5Y neuroblastoma cells is regulated acutely by cytosolic Ca^{2+} and by rapid desensitization. *J. Neurochem.*, **63**, 177–185.

WOLSING, D.H. & ROSENBAUM, J.S. (1991). Bradykinin-stimulated inositol phosphate production in NG108-15 cells is mediated by a small population of binding sites which rapidly desensitize. *J. Pharmacol. Exp. Ther.*, **257**, 621–633.

YU, V.C. & SADEE, W. (1986). Phosphatidylinositol turnover in neuroblastoma cells: regulation by bradykinin, acetylcholine, but not μ- and δ-opioid receptors. *Neurosci. Lett.*, **71**, 219–223.

(Received July 22, 1994
Revised November 14, 1994
Accepted November 16, 1994).

British Journal of Pharmacology (1995) 114, 1143-1148

Rapid, agonist-induced desensitization of α_2-autoreceptors modulating transmitter release

[1]Stefan Boehm, Sigismund Huck, Karin Schwarz, *Ernst Agneter, *Helmut Drobny & *Ernst A. Singer

Institutes of Neuropharmacology and *Pharmacology, University of Vienna, Waehringerstrasse 13a, A-1090 Vienna, Austria

1 The release of previously incorporated [^{3}H]-noradrenaline was investigated in cultures of dissociated chick or rat sympathetic neurones and in cerebrocortical slices from neonatal or adult rats. Noradrenaline, in the presence of 10 μmol l^{-1} of the uptake inhibitor, cocaine, or the selective α_2-adrenoceptor agonist, 5-bromo-*N*-(4,5-dihydro-1*H*-imidazol-2-yl)-6-quinoxalinamine (UK 14,304), was applied for different periods of time in order to detect a possible time-dependence of the α_2-adrenoceptor-mediated inhibition of electrically evoked tritium outflow.

2 In chick sympathetic neurones, stimulation-evoked overflow was reduced to 30%, 42%, or 56% of control when noradrenaline (1 μmol l^{-1}) was present for 2, 8, or 16 min, respectively. Likewise, UK 14,304 (1 μmol l^{-1}) present for these periods of time reduced ^{3}H overflow to 35%, 51%, and 53% of control, respectively. Addition of 1 nmol l^{-1} to 10 μmol l^{-1} UK 14,304 for either 2 or 16 min did not produce significantly different IC_{50} values, but the inhibitory effects were smaller with 16 min as compared to 2 min exposure at concentrations $\geqslant$ 10 nmol l^{-1}.

3 In rat sympathetic neurones, noradrenaline (100 nmol l^{-1}) reduced stimulation-evoked overflow to 33%, 56%, or 57% of control, when present for 2, 8, or 16 min, respectively. Addition of UK 14,304 (1 μmol l^{-1}) for these periods of time caused inhibition to 11%, 41%, and 46% of control. Applying UK 14,304 for either 2 or 16 min did not result in significantly different IC_{50} values, but the inhibition induced by 16 min as compared to 2 min exposure was smaller at concentrations $\geqslant$ 10 nmol l^{-1}.

4 In cerebrocortical slices from either neonatal or adult rats, exposure to 0.1 to 1.0 μmol l^{-1} UK 14,304 for 16 min never caused a smaller inhibition than a corresponding 3 min exposure, although various experimental conditions were investigated.

5 The results demonstrate that α_2-adrenoceptors which regulate noradrenaline release from sympathetic neurones undergo agonist-induced desensitization within minutes. Such rapid desensitization of α_2-autoreceptors was not detected in brain slice preparations.

Keywords: Desensitization; α_2-adrenoceptor; noradrenaline release; sympathetic neurones; brain slices

Introduction

α_2-Adrenoceptors control transmitter release from central and peripheral noradrenergic neurones (for review, see Starke, 1987). Effects of transmitters in many instances show desensitization which is most commonly caused by protein phosphorylation (see Huganir & Greengard, 1990). However, in the case of the α_2-adrenoceptors, receptor desensitization has remained a controversial issue (see e.g. the discussion in Liggett *et al.*, 1992). After 10 min of agonist exposure, phosphorylation by β-adrenoceptor kinase and sequestration of α_2-adrenoceptors have been demonstrated, paralleled in this time course by desensitization of the α_2-adrenoceptor-induced inhibition of adenylyl cyclase activity (Liggett *et al.*, 1992). However, it has not yet been shown whether such short term desensitization occurs during α_2-autoreceptor-mediated inhibition of transmitter release. Hence, the present study aimed at demonstrating a possible rapid, agonist-induced desensitization of α_2-adrenoceptors which modulate noradrenaline release.

Electrically evoked tritium overflow from primary cultures of rat (Schwartz & Malik, 1993) or chick sympathetic neurones (Boehm *et al.*, 1991) labelled with [^{3}H]-noradrenaline is markedly reduced by the activation of α_2-adrenoceptors. In addition, these monolayer cultures virtually lack autoinhibitory feedback (e.g. Boehm *et al.*, 1991) and thus are useful preparations to study various properties of α_2-autoreceptors. However, tissue slice preparations containing noradrenergic axon terminals of central or peripheral origin are utilized more frequently to investigate the α_2-adrenoceptor-mediated inhibition of transmitter release (see review by Starke, 1987). The present paper examines the inhibition of electrically evoked [^{3}H]-noradrenaline release by α_2-adrenoceptor agonists in both types of preparations, i.e. cultures of sympathetic neurones and cerebrocortical slices. The experiments were designed to detect a possible attenuation of this inhibition induced by the time of agonist exposure.

[1] Author for correspondence.

Methods

Preparation of cell cultures and brain slices

Neurones derived either from lumbosacral paravertebral sympathetic ganglia of 12 day old chick embryos (Boehm *et al.*, 1991) or from superior cervical ganglia of 2 to 6 day old Sprague Dawley rat pups (Boehm, 1994) were dissociated and cultured as described previously. Cultures of rat neurones were used for transmitter release experiments after 3 to 4 days *in vitro*, those of chick neurones after 5 days.

The parieto-occipital cortex was removed from the brains of either the rat pups which were used for the dissection of superior cervical ganglia or adult rats (weight $\geqslant$ 250 g), and 0.35 mm thick slices were prepared with a McIlwain tissue chopper.

Uptake and superfusion

After incubation in [^{3}H]-noradrenaline (0.03 μmol l^{-1} for neuronal cell cultures, 0.07 μmol l^{-1} for brain slices) the cultures or slices were superfused with a modified Krebs Ringer bicarbonate buffer, as described previously (see Boehm *et al.*, 1994). Cultures were superfused at 25°C, slices at 37°C or 25°C. Collection of 4 min superfusate fractions was started after a 60 min washout period, and electrical field stimulations were performed after 68 min (S_1) and 96 min (S_2) of superfusion (cultures: 36 monophasic rectangular pulses, 3 Hz, 0.5 ms, 60 mA, 40 V cm^{-1}; slices: 54 monophasic rectangular pulses, 3 Hz, 2.0 ms, 18 mA, 14 V cm^{-1}). Noradrenaline or 5-bromo-*N*-(4,5-dihydro-1*H*-imidazol-2-yl)-6-quinoxalinamine (UK 14,304) was added to the superfusion medium at different times before S_2 (cultures: 2, 8, or 16 min; slices: 3 or 16 min) and maintained at constant concentrations until the end of experiments. Cocaine (10 μmol l^{-1}) was included in the medium for the entire superfusion period when noradrenaline was used as an agonist in order to prevent uptake of the unlabelled amine. In some experiments with brain slices yohimbine (10 nmol l^{-1}) was added to the buffer for uptake and superfusion. At the end of experiments, the radioactivity remaining in cultures or tissue slices was extracted by immersion of discs or slices in 1.2 ml 2% (v/v) perchloric acid followed by sonication. Radioactivity in extracts and collected fractions was determined by liquid scintillation counting (Beckmann LS 6500).

Calculations

The fractional rate of ^{3}H outflow was obtained by dividing the radioactivity of a 4 min sample by the total radioactivity of cultures at the beginning of the corresponding 4 min collection period. The rate of outflow per minute was obtained by a subsequent division by 4. Stimulation-evoked overflow was calculated as the difference between the total tritium outflow during and after the stimulation and the estimated basal outflow, which was assumed to decline linearly from the sample preceding stimulation, to the sample 8–12 min after the beginning of the stimulus. This difference was expressed as a percentage of the total radioactivity in the cultures at the beginning of the respective stimulation (S_1%, S_2%). Effects of α_2-adrenoceptor agonists were evaluated by calculating ratios of the overflow evoked by S_2 and S_1 (S_2/S_1). Ratios between the arithmetic mean of S_2/S_1 values obtained with identical concentrations of UK 14,304 present for either 16 or 2 min ([16']/[2']) were taken as a measure of desensitization. Effects on basal ^{3}H outflow were estimated by the ratio of the fractional rate of outflow during the 4 min period preceding S_2 and during the 4 min period preceding S_1 (L_2/L_1).

All data are given as arithmetic means ± s.e.mean; n = number of cell culture discs or brain slices. Significance of differences between various groups was determined by the Mann-Whitney test. Concentration-response curves were fitted to the experimentally obtained data points by using the ALLFIT programme (DeLean *et al.*, 1978) which estimates the IC_{50}, the slope, and the maximal effect as well as corresponding standard errors. Moreover, the programme indicates significant differences between concentration-response curves by simultaneous fitting with shared parameters and subsequent calculation of the *F*-statistic on the resulting 'extra sum of squares' (DeLean *et al.*, 1978).

Drugs

Drugs were obtained from the following sources: (-)-[ring-2,5,6-^{3}H]-noradrenaline (71.7 Ci $mmol^{-1}$; NEN, Dreieich, Germany); 5-bromo-*N*-(4,5-dihydro-1*H*-imidazol-2-yl)-6-quinoxalinamine (UK 14,304; Research Biochemicals, Natick, MA, U.S.A.); (−)-noradrenaline HCl, cocaine HCl (Sigma, München, Germany); yohimbine HCl (Merck, Darmstadt, Germany).

UK 14,304 was initially dissolved at 1 mmol l^{-1} in 0.1 mol l^{-1} HCl; all other drugs were dissolved in distilled water. All drugs were diluted to the final concentrations in superfusion medium.

Results

Cultures of chick sympathetic neurones

Values of spontaneous and stimulation-evoked tritium outflow from cultures of chick sympathetic neurones are shown in Table 1. Inclusion of 10 μmol l^{-1} cocaine in the medium significantly enhanced electrically induced overflow, but failed to alter fractional basal outflow (Table 1). These results corroborate the previously described enhancement by cocaine of stimulation-evoked noradrenaline overflow from chick sympathetic neurones (Boehm *et al.*, 1991). Noradrenaline (in the presence of 10 μmol l^{-1} cocaine) or the selective α_2-adrenoceptor agonist, UK 14,304 (Cambridge, 1981), both at 1 μmol l^{-1}, significantly reduced stimulation-evoked overflow from chick sympathetic neurones ($P \leq 0.001$ vs. corresponding controls). The inhibition caused by each of the two was significantly smaller with 16 min than with 2 min exposure. However, effects did not significantly differ if agonists were present for 8 min as compared to 16 min before S_2 (Figure 1a).

Addition of 1 nmol l^{-1} to 10 μmol l^{-1} UK 14,304 either 2 or 16 min before S_2 yielded concentration-response curves for the inhibition of stimulation-evoked tritium overflow (Figure 1b) not differing ($P > 0.05$) with respect to IC_{50} values which were 16.6 ± 9.3 nmol l^{-1} for 16 min and 6.5 ± 2.3 nmol l^{-1} for 2 min agonist exposure. However, the extent of inhibition by UK 14,304 at concentrations of 10 nmol l^{-1} and above was significantly smaller with 16 min as compared to 2 min exposure. The ratio of mean S_2/S_1 values obtained with 16 and 2 min exposures to UK 14,304 ([16']/[2']), taken as a measure of desensitization, displayed a concentration-dependent increase which was half maximal at around 10 nmol l^{-1} (Figure 1b). Thus, UK 14,304 induced desensitization and inhibition of stimulation-evoked overflow in the same range of concentrations.

Neither noradrenaline in the presence of cocaine nor UK 14,304, at any of the above concentrations or periods of

Table 1 Fractional basal tritium outflow per minute and electrically evoked overflow (S_1%) from superfused cultures of chick or rat sympathetic neurones labelled with [^{3}H]-noradrenaline

Species	*Cocaine* (μmol l^{-1})	*Basal outflow* (min^{-1})	*Stimulated overflow* (S_1%)	n
Chick	0	0.0016 ± 0.0001	1.58 ± 0.17	119
	10	0.0019 ± 0.0002	1.89 ± 0.14*	24
Rat	0	0.0017 ± 0.0001	0.41 ± 0.02	90
	10	0.0015 ± 0.0001	0.80 ± 0.04***	23

After labelling, neurones were superfused, 4 min fractions of superfusate were collected, and electrical field stimulation (36 pulses at 3 Hz, 0.5 ms, 60 mA) was performed after 68 (S_1) and 96 min (S_2) of superfusion. Data were obtained either under control conditions or in the presence of cocaine (10 μmol l^{-1}) which was included in the medium for the entire superfusion period. The basal ^{3}H efflux under control conditions corresponded to 0.027 ± 0.001 nCi min^{-1} in chick and to 0.076 ± 0.004 nCi min^{-1} in rat neurones. Stimulation-evoked overflow equalled 0.263 ± 0.014 nCi per stimulation period in chick and 0.204 ± 0.012 nCi per stimulation period in rat sympathetic neurones, respectively. *$P \leq 0.05$; ***$P \leq 0.001$ vs. corresponding controls, respectively.

exposure, caused significant alterations of spontaneous tritium efflux from chick sympathetic neurones (not shown).

Cultures of rat sympathetic neurones

Fractional basal efflux from rat sympathetic neurones was similar to spontaneous tritium outflow from chick neurones. However, electrically induced overflow was much smaller in rat than in chick sympathetic neurones (Table 1). In accordance with the results obtained with chick neurones, stimulation-evoked overflow was markedly enhanced in the presence of cocaine (10 μmol l^{-1}) without changes in spontaneous outflow (Table 1). Noradrenaline (0.1 μmol l^{-1}) in the presence of cocaine (10 μmol l^{-1}) as well as UK 14,304 (1 μmol l^{-1}) reduced stimulation-evoked overflow ($P \leq 0.001$ vs. controls) to a higher degree when added 2 min before S_2 than when added 16 or 8 min before S_2 (Figure 2a).

The concentration-response curves for the reduction of stimulation-evoked overflow by either 16 or 2 min exposure to UK 14,304 (Figure 2b) displayed IC_{50} values that were not significantly different (2 min: 6.1 ± 1.7 nmol l^{-1}; 16 min: 17.9 ± 7.5 nmol l^{-1}; $P > 0.05$), although the effects of 16 min exposure were significantly smaller at concentrations ⩾ 10 nmol l^{-1} (Figure 2b). Similar to the results obtained with chick neurones, the ratio of mean S_2/S_1 values after 16 and 2 min exposures to UK 14,304 ([16']/[2']) showed a concentration-dependent increase that was half maximal at around 10 nmol l^{-1} (Figure 2b). Thus, in rat sympathetic neurones, the potency of UK 14,304 was about the same for the induction of desensitization as for the reduction of electrically evoked overflow.

Spontaneous ^3H outflow from rat sympathetic neurones was not affected by 0.1 μmol l^{-1} noradrenaline at any period of exposure, but slightly altered in the presence of some concentrations of UK 14,304 added 2, 8, or 16 min before S_2 (not shown).

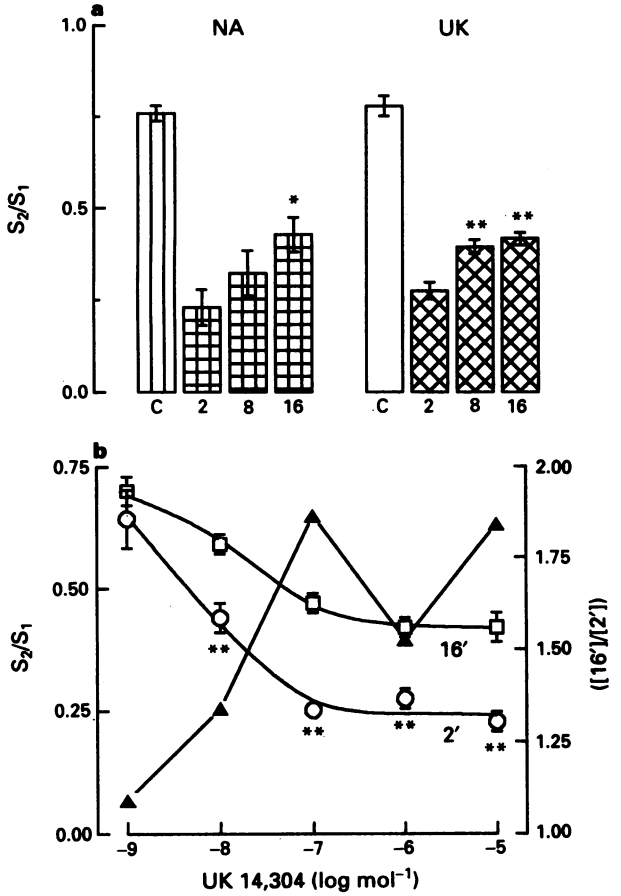

Figure 1 Effects of noradrenaline and UK 14,304 on electrically evoked tritium overflow from cultures of chick sympathetic neurones labelled with [^{3}H]-noradrenaline after various periods of agonist exposure. After labelling, neurones were superfused, and tritium overflow was triggered by electrical field stimulation (36 pulses at 3 Hz) after 68 min (S_1) and 96 min (S_2) of superfusion. (a) The indicated S_2/S_1 ratios were obtained under control conditions (*C*) or after addition of either 1 μmol l^{-1} noradrenaline (NA) or 1 μmol l^{-1} UK 14,304 (UK) to the superfusion medium 2, 8, or 16 min before S_2. The data with noradrenaline as agonist and corresponding controls were obtained with cocaine (10 μmol l^{-1}) in the superfusion medium. The columns show arithmetic means ± s.e.mean of 6 to 9 observations. All S_2/S_1 ratios determined in the presence of α_2-adrenoceptor agonists were significantly different from corresponding controls at $P \leq 0.001$. Significantly different from the value obtained after a 2 min exposure to the same agonist at $^*P \leq 0.05$ and $^{**}P \leq 0.01$, respectively. (b) The indicated concentrations of UK 14,304 were added to the superfusion medium 2 (○) or 16 min (□) before S_2, and effects of UK 14,304 were evaluated by calculating S_2/S_1 ratios. Values shown are arithmetic means ± s.e.mean of 6 to 9 observations. $^{**}P \leq 0.01$ vs. the S_2/S_1 ratio obtained with a 16 min application of the same concentration of UK 14,304. As a measure of desensitization, the ratio between mean S_2/S_1 values obtained with 16 and 2 min exposures ([16']/[2']) to the indicated concentrations of UK 14,304 is shown by (▲).

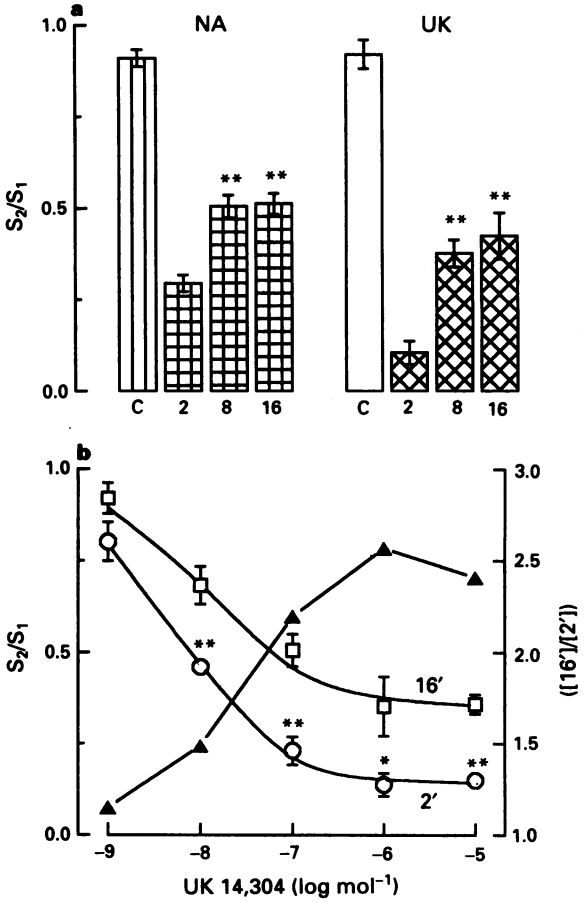

Figure 2 Effects of noradrenaline and UK 14,304 on electrically evoked tritium overflow from cultures of rat sympathetic neurones labelled with [^{3}H]-noradrenaline after various periods of agonist exposure. (a) Noradrenaline (NA) 0.1 μmol l^{-1} or UK 14,304 (UK) 1 μmol l^{-1} were added to the superfusion medium 2, 8, or 16 min before S_2. All S_2/S_1 ratios determined in the presence of α_2-adrenoceptor agonists were significantly different from corresponding controls (*C*) at $P \leq 0.001$. (b) UK 14,304 was added to the superfusion medium 2 (○) or 16 min (□) before S_2. Values shown are arithmetic means ± s.e.mean of 6 observations. $^*P \leq 0.05$, $^{**}P \leq 0.01$ vs. the S_2/S_1 ratio obtained with a 16 min exposure to the same concentration of UK 14,304. See legend to Figure 1 for further details.

Brain slices

Values of basal tritium outflow and of stimulation-evoked overflow from cerebrocortical slices from neonatal rats are given in Table 2. Addition of 0.3 μmol l^{-1} UK 14,304 either 3 or 16 min before S_2 caused significant reductions in electrically induced overflow from neonatal rat brain slices ($P \leq 0.001$ vs control). In contrast to the data obtained with dissociated neurones, however, there was no difference between the effects of these two periods of exposure (Table 3). Assuming that the desensitization caused by addition of an agonist to the superfusion medium might be occluded by effects of the biophase concentration of endogenous noradrenaline, experiments were repeated in presence of 10 nmol l^{-1} of the α_2-adrenoceptor antagonist, yohimbine: as expected, yohimbine significantly enhanced stimulation-evoked overflow leaving the basal rate of ^3H outflow unaltered (Table 2). However, instead of revealing a decreased effect, yohimbine rather increased the inhibitory effect of 16 min (compared to 3 min) exposure to UK 14,304 (Table 3).

One major difference between the experiments on cell cultures and brain slices was the temperature which was 37°C for brain slices and 25°C for neuronal cell cultures. In order to exclude the possibility that this was the reason for the lack of desensitization in cerebrocortical slices, experiments on cortex slices from neonatal rats were repeated at 25°C. This decrease in temperature reduced spontaneous and stimulation-evoked outflow (Table 2) and increased the inhibitory effect of UK 14,304 (Table 3). However, even at 25°C no desensitization was seen in cortex slices from neonatal rats. On the contrary, at this temperature 0.3 μmol l^{-1} UK 14,304 was much more effective when present for 16 instead of 3 min (Table 3).

Cerebrocortical slices derived from adult rats showed a similar outflow of tritium as slices obtained from neonatal rats. Stimulation-evoked overflow, however, was markedly smaller in brain slices from adult rats (Table 2). As in cortex slices from neonatal rats, 0.1 or 1.0 μmol l^{-1} UK 14,304 significantly reduced electrically induced tritium outflow ($P \leq 0.05$ vs. control). There was no difference between the inhibition caused by 3 and 16 min exposure to UK 14,304 (Table 3). Lowering the temperature from 37°C to 25°C, apart from reducing basal outflow (Table 2), resulted again in a smaller inhibitory effect of the agonist added 3 min before S_2 compared to the 16 min period of exposure (Table 3).

Spontaneous ^3H outflow from either neonatal or adult rat cortex slices was not affected by UK 14,304, whether added 3 or 16 min before S_2 ($P > 0.05$ vs. corresponding controls; data not shown).

Table 2 Fractional basal tritium outflow per minute and electrically evoked overflow (S_1%) from superfused cerebrocortical slices obtained either from neonatal ($\leq$ 6 d) or from adult rats and labelled with [^3H]-noradrenaline

Preparation	*Condition*	*Basal outflow* (min^{-1})	*Stimulated overflow* (S_1%)	n
Neonatal rat Cortex	37°C	0.0037 ± 0.0001	8.16 ± 0.28	36
	37°C/Yoh	0.0037 ± 0.00004	9.95 ± 0.4***	24
	25°C	0.0016 ± 0.0001***	4.34 ± 0.28***	22
Adult rat Cortex	37°C	0.0034 ± 0.0001	1.64 ± 0.19	21
	25°C	0.0017 ± 0.0001***	1.32 ± 0.03	12

After labelling, cortex slices were superfused at the indicated temperatures (25°C or 37°C), 4 min fractions of superfusate were collected, and electrical field stimulation (54 pulses at 3 Hz, 2.0 ms, 18 mA) was performed after 68 (S_1) and 96 min (S_2) of superfusion. Data were obtained either under control conditions or in the presence of 10 nmol l^{-1} yohimbine (37°C/Yoh) which was included in the medium for uptake and superfusion. The basal ^3H efflux under control conditions at 37°C equalled 0.152 ± 0.006 nCi min^{-1} in neonatal rat cortex and 0.229 ± 0.011 nCi min^{-1} in adult rat cortex. Stimulation-evoked overflow corresponded to 3.483 ± 0.232 nCi per stimulation period in neonatal and to 1.152 ± 0.157 nCi per stimulation period in adult rat cortex, respectively. ***$P \leq 0.001$ vs. corresponding controls.

Discussion

Conclusive evidence for agonist-induced desensitization of α_2-adrenoceptors involved in the modulation of transmitter release has been lacking. A recent study (Fuder & Schwarz, 1993) indicated a decrease in the α_2-adrenoceptor-mediated inhibition of stimulation-evoked noradrenaline release after 30 min pre-exposure to supramaximal agonist concentrations followed by extended ($\geq$ 50 min) washout periods. However, whether the application of α_2-adrenoceptor agonists could cause desensitization within only a few minutes was not investigated.

Hence, the present results show for the first time that α_2-autoreceptors involved in the feedback inhibition of transmitter release may undergo agonist-induced desensitization within minutes. This desensitization was obvious in superfused cultures of sympathetic neurones. We observed inhibition of transmitter release after 2 min exposure to maximal concentrations of UK 14,304 down to about 15% of control in rat and to approximately 30% of control in chick sympathetic neurones. Previous experiments with these cell cultures indicated considerably smaller maximal effects of UK 14,304 (50% of control in rat, Schwartz & Malik, 1993; 55% of control in chick, Boehm *et al.*, 1994), most likely because extended exposure ($\geq$ 10 min) to the α_2-adrenoceptor agonist had been used in these studies.

Table 3 Effects of 3 or 16 min exposure to UK 14,304 on electrically evoked tritium overflow from superfused cerebrocortical slices obtained either from neonatal ($\leq$ 6 d) or from adult rats and labelled with [^3H]-noradrenaline

Preparation	*Condition*	*UK 14,304* (μmol l^{-1})	*S_2/S_1* 3 min	16 min	n
Neonatal rat Cortex	37°C	0.3	0.33 ± 0.03	0.27 ± 0.02	14
	37°C/Yoh	0.3	0.38 ± 0.03	0.21 ± 0.03**	7
	25°C	0.3	0.22 ± 0.02	0.08 ± 0.01***	11
Adult rat Cortex	37°C	0.1	0.31 ± 0.03	0.18 ± 0.02	3
	37°C	1.0	0.17 ± 0.03	0.11 ± 0.01	4
	25°C	1.0	0.31 ± 0.02	0.24 ± 0.02*	4

The indicated concentrations of UK 14,304 were added to the superfusion medium 3 or 16 min before S_2. The data were obtained either under control conditions (37°C), in presence of 10 nmol l^{-1} yohimbine (37°C/Yoh), or at 25°C. S_2/S_1 values obtained under control conditions were 0.99 ± 0.01 ($n = 8$) in neonatal rat cortex and 0.78 ± 0.05 ($n = 5$) in adult rat cortex. All data obtained in the presence of UK 14,304 were significantly different from these control values at $P \leq 0.001$ for neonatal and at $P \leq 0.05$ for adult rat cerebrocortical slices. *$P \leq 0.05$; **$P \leq 0.01$, ***$P \leq 0.001$ vs. the corresponding 3 min exposure, respectively.

Although peripheral noradrenergic neurones of neonatal rats showed a marked agonist-induced desensitization of α_2-autoreceptors, parieto-occipital cortex slices derived from the same rats did not display this phenomenon under conventional experimental conditions. One reason for this obvious lack of rapid, agonist-induced desensitization could have been previous desensitization caused by the accumulation of endogenously released noradrenaline. Hence, prevention of this effect of endogenous noradrenaline by an α_2-adrenoceptor antagonist should uncover agonist-induced desensitization also in brain slices. However, in the presence of 10 nmol l^{-1} yohimbine, the inhibition of electrically evoked transmitter release after 16 min exposure to UK 14,304 was significantly larger (instead of being smaller) than the inhibition after 3 min exposure. Likewise, reduction of the temperature used for the cell culture experiments from 37°C to the 25°C did not promote desensitization, but rather increased the effect of long term (16 min) agonist exposure. These results obtained with brain tissue of neonatal rats were corroborated by results obtained in experiments with cerebrocortical slices derived from mature animals. In this tissue, the inhibitory effects of 3 or 16 min exposure to UK 14,304 did not differ significantly when assessed in experiments performed at 37°C. Lowering the temperature to 25°C resulted again in an increased effect of the long term agonist exposure, just as described for the brain tissue of neonatal rats.

It should be borne in mind, however, that both manipulations, inclusion of yohimbine (10 nmol l^{-1}) in the superfusion medium as well as lowering the temperature, which aimed at optimizing the conditions for the detection of autoreceptor desensitization, may have selectively impeded the effects of short (versus long) term agonist exposure: (a) in cerebrocortical slice preparations, blockade of α_2-adrenoceptors by yohimbine has previously been shown to facilitate stimulation-evoked transmitter release even if yohimbine was applied for only 10 min followed by more than 2 h of washout (see Figure 5 in Hölting & Starke, 1986). Hence, removal of yohimbine from the sites of action in superfused brain slice preparations apparently proceeds very slowly. This feature of yohimbine may have retarded the occupancy of receptors by agonists in the present study. (b) In superfusion experiments on rat brain slices, reduction of the temperature from 37°C to 23°C caused marked alterations in synaptic morphology, with the higher temperature yielding a greater number of freely accessible presynaptic nerve terminals (Cichini *et al.*, 1986). Hence, α_2-adrenoceptor agonists added to the superfusion medium presumably reach their sites of action more slowly at 25°C than at 37°C. Taken together, the detection of rapid agonist-induced events in brain slices may be limited by the fact that a time period in the range of several minutes is required to achieve homogeneous drug concentrations throughout tissue samples. Thus, the present failure to demonstrate an agonist-induced desensitization within the time course of a few minutes in rat brain slices does not necessarily indicate that central α_2-adrenoceptors involved in the modulation of transmitter release do not undergo desensitization. Postsynaptically located α_2-adrenoceptors of the rat central nervous system have previously been shown to be subject to desensitization in response to long term (14 days) agonist exposure *in vivo* (Finberg & Kopin, 1987). However, in slices of the rabbit hypothalamus, the inhibition of [^{3}H]-noradrenaline release induced by exogenous noradrenaline added for either 8 or 20 min did not differ, whereas the dopamine-induced inhibition completely desensitized within this time course (Galzin & Langer, 1985).

α_2-Adrenoceptors which regulate adenylyl cyclase activity desensitize with a similar time course (Liggett *et al.*, 1992) to the autoreceptors of sympathetic neurones which inhibited transmitter release in the present study. However, adenylyl cyclase is not involved in the inhibition of transmitter release in any of the preparations used in this study, at least when α_2-adrenoceptor agonists were applied for 6 min or more (rat occipital cortex: Ong *et al.*, 1991; rat sympathetic neurones: Schwartz & Malik, 1993; chick sympathetic neurones: Boehm *et al.*, 1994). Hence, the α_2-adrenoceptors of sympathetic neurones probably operate and desensitize independently of adenylyl cyclase. Alternatively, there may be two mechanisms of inhibition, one involving, the other not involving adenylyl cyclase. Only the mechanism involving adenylyl cyclase may then desensitize rapidly, making the neurones less sensitive to α_2-adrenoceptor activation after a few minutes.

The detection of short term agonist-induced desensitization of the α_2-adrenoceptor-mediated inhibition of noradrenaline release in sympathetic neurones derived from two species, points to the general importance of this phenomenon at least in postganglionic sympathetic neurotransmission. The present study failed to detect a similar mechanism in rat cerebrocortical slices. It therefore remains open whether rapid agonist-induced desensitization is a universal characteristic of α_2-autoreceptors involved in the regulation of transmitter release or whether it can be assigned to discrete nervous structures or to certain receptor subtypes.

The perfect technical assistance of G. Koth and A. Motejlek is gratefully acknowledged.

References

BOEHM, S. (1994). Noradrenaline release from rat sympathetic neurones evoked by P_2-purinoceptor activation. *Naunyn-Schmied. Arch. Pharmacol.*, **350**, 454–458.

BOEHM, S., HUCK, S., DROBNY, H. & SINGER, E.A. (1991). Electrically evoked noradrenaline release from cultured chick sympathetic neurones: modulation via presynaptic α_2-adrenoceptors and lack of autoinhibition. *Naunyn-Schmied. Arch. Pharmacol.*, **344**, 130–132.

BOEHM, S., HUCK, S., KOTH, G., DROBNY, H., AGNETER, E. & SINGER, E.A. (1994). α_2-Adrenoceptor-mediated inhibition of electrically evoked [^{3}H]noradrenaline release from chick sympathetic neurones: role of cyclic AMP. *J. Neurochem.*, **63**, 146–154.

CAMBRIDGE, D. (1981). UK-14,304, a potent and selective α_2-agonist for the characterization of α-adrenoceptor subtypes. *Eur. J. Pharmacol.*, **72**, 413–415.

CICHINI, G., LASSMANN, H., PLACHETA, P. & SINGER, E.A. (1986). Effects of clonidine on the stimulation-evoked release of ^{3}H-noradrenaline from superfused brain slices as a function of the biophase concentration -Temperature dependent widening of extracellular space. *Naunyn-Schmied. Arch. Pharmacol.*, **333**, 36–42.

DELEAN, A., MUNSON, P.J. & RODBARD, D. (1978). Simultaneous analysis of families of sigmoidal curves: Application to bioassay, radioligand assay, and physiological dose-response curves. *Am. J. Physiol.*, **235**, E97–E102.

FINBERG, J.P.M. & KOPIN, I.J. (1987). Chronic clonidine treatment produces desensitisation of post- but not presynaptic α_2-adrenoceptors. *Eur. J. Pharmacol.*, **138**, 95–100.

FUDER, H. & SCHWARZ, P. (1993). Desensitization of inhibitory prejunctional α_2-adrenoceptors and putative imidazoline receptors on rabbit heart sympathetic nerves. *Naunyn-Schmied. Arch. Pharmacol.*, **348**, 127–133.

GALZIN, A.M. & LANGER, S.Z. (1985). Inhibition by 5,6-dihydroxy-2-dimethylaminotetralin (M7) of noradrenergic neurotransmission in the rabbit hypothalamus: role of alpha-2 adrenoceptors and of dopamine receptors. *J. Pharmacol. Exp. Ther.*, **233**, 459–465.

HÖLTING, T. & STARKE, K. (1986). Receptor protection experiments confirm the identity of presynaptic α_2-autoreceptors. *Naunyn-Schmied. Arch. Pharmacol.*, **333**, 262–270.

HUGANIR, R.L. & GREENGARD, P. (1990). Regulation of neurotransmitter receptor desensitization by protein phosphorylation. *Neuron*, **5**, 555–567.

LIGGETT, S.B., OSTROWSKI, J., CHESTNUT, L.C., KUROSE, H., RAYMOND, J.R., CARON, M.G. & LEFKOWITZ, R.J. (1992). Sites in the third intracellular loop of the α_{2A}-adrenergic receptor confer short term agonist-promoted desensitization – evidence for a receptor kinase-mediated mechanism. *J. Biol. Chem.*, **267**, 4740–4746.

ONG, M.L., BALL, S.G. & VAUGHAN, P.F.T. (1991). Regulation of noradrenaline release from rat occipital cortex tissue chops by α_2-adrenergic agonists. *J. Neurochem.*, **56**, 1387–1393.

SCHWARTZ, D.D. & MALIK, K.U. (1993). Cyclic AMP modulates but does not mediate the inhibition of [^{3}H]norepinephrine release by activation of alpha-2 adrenergic receptors in cultured rat ganglion cells. *Neuroscience*, **52**, 107.

STARKE, K. (1987). Presynaptic α-Autoreceptors. *Rev. Physiol. Biochem. Pharmacol.*, **107**, 73–146.

(Received October 24, 1994
Revised November 10, 1994
Accepted November 16, 1994).

British Journal of Pharmacology (1995) 114, 1149–1158

Modulation by stereoselective inhibition of cyclo-oxygenase of electromechanical coupling in the guinea-pig isolated renal pelvis

[1]Paolo Santicioli, *Germano Carganico, Stefania Meini, Sandro Giuliani, Antonio Giachetti & Carlo Alberto Maggi

Pharmacology Department, A. Menarini Pharmaceuticals, Florence Italy and *R & D Department, Laboratories Menarini SA, Badalona, Spain

1 The effects of the (S)- and (R)-enantiomers of the cyclo-oxygenase (COX) inhibitor, ketoprofen, have been investigated on the spontaneous activity of the guinea-pig isolated renal pelvis and on electrical field stimulation-(EFS) induced contractions of the guinea-pig ureter in comparison with the effects of the achiral COX inhibitor, indomethacin.

2 (S)-ketoprofen (0.1–100 μM) produced a concentration- and time-dependent inhibition of the spontaneous myogenic activity of the renal pelvis. The maximal inhibitory effect (% inhibition of motility index) averaged 29, 42, 47 and 56% inhibition of control values at 0.1, 1, 10 and 100 μM. The (R)-enantiomer was ineffective up to 10 μM.

3 Indomethacin (0.1–100 μM) likewise produced a concentration- and time-dependent inhibition of spontaneous motility of the isolated renal pelvis: its maximal inhibitory effect was larger than that produced by (S)-ketoprofen and averaged 21, 40, 69 and 95% inhibition of motility index at 0.1, 1, 10 and 100 μM respectively. In the presence of a maximally effective (100 μM) concentration of (S)-ketoprofen, 100 μM indomethacin produced >90% inhibition of residual motility.

4 In the guinea-pig isolated ureter, phasic contractions were induced by EFS (5 ms pulse width, 60 V): (S)-ketoprofen (100–500 μM) had no effect on the EFS-evoked contractions. Indomethacin (100–500 μM) produced a concentration-dependent inhibition and/or suppression of the EFS-evoked contractions. When contraction of the ureter was evoked by 80 mM KCl, indomethacin produced about 30 and 80% inhibition at 100 and 300 μM, respectively, while (S)-ketoprofen (300 μM) was ineffective.

5 The effect of (S)-ketoprofen or indomethacin (10 μM each) on the propagation of myogenic impulses along the ureter was determined by use of a three chamber organ bath. The renal end of the ureter was electrically stimulated while recording the mechanical activity of the renal and bladder ends of the ureter: addition of either (S)-ketoprofen or indomethacin (10 μM) did not effect propagation of impulses from the renal to the bladder end of the ureter, while nifedipine (10 μM) promptly blocked the propagated contractions.

6 In sucrose gap experiments, (S)-ketoprofen (10-100 μM) produced a time-dependent shortening of spontaneous action potentials of the guinea-pig renal pelvis and reduced the amplitude and duration of the accompanying phasic contractions. Indomethacin (10 μM) produced comparable effects on the same parameters and significantly reduced the maximal amplitude of depolarization of the pacemaker potential. In the presence of 100 μM (S)-ketoprofen, 100 μM indomethacin promptly suppressed the residual pacemaker potential and contraction.

7 Neither (S)-ketoprofen nor indomethacin (10 μM each for 60 min) affected the parameters of action potential and contraction of the guinea-pig ureter evoked by EFS. Both drugs produced a sustained membrane depolarization.

8 The present findings demonstrate that stereoselective COX inhibition affects pacemaker potentials and contractility (electromechanical coupling) in the guinea-pig renal pelvis. The modulatory role of endogenous prostanoids involves an amplification of electromechanical coupling in the renal pelvis while excitability, contractility or propagation of impulses along the ureter appear almost independent of prostanoid generation. Previous reports of a total suppression of pyeloureteral motility by indomethacin may reflect a combination of COX inhibition and nonspecific effect on electromechanical coupling.

Keywords: Guinea-pig ureter; guinea-pig renal pelvis; cyclo-oxygenase; ketoprofen; indomethacin; stereoselective

Introduction

Metabolites of arachidonic acid produced along the cyclo-oxygenase (COX) pathway (prostanoids) act as modulators/mediators of smooth muscle activity in the urinary tract. In the urinary bladder, prostanoids are produced during bladder distension at cystometry and exert both a direct myotropic action on detrusor muscle and a sensitizing activity on bladder afferents which set the gain for the activation of the micturition reflex (Maggi, 1992, for review). A role of prostanoids in the local regulation of motility has also been postulated in the upper urinary tract but the picture emerging from the available data is far from clear (see below). The tissue is of clinical relevance because of the increasing evidence that COX inhibitors produce pain relief during renal colic (Holmlund & Sjodin, 1978; Lundstrom *et al.*, 1982; Oosterlink *et al.*, 1990).

Conflicting results have been reported with regard to the effect of prostaglandins on pyeloureteral motility. Prostaglan-

[1] Author for correspondence at: Pharmacology Department, A. Menarini Pharmaceuticals, Via Sette Santi 3, 50131, Florence, Italy.

dins of the E or F series produce excitatory effects on the motility of the ureter or renal pelvis (Thulesius & Angelo-Khatter, 1985; Lundstam *et al.*, 1985; Thulesius *et al.*, 1986; 1987; Cole *et al.*, 1988), but smooth muscle hyperpolarization, relaxation and adenosine 3': 5'-cyclic monophosphate (cyclic AMP) accumulation in response to added prostaglandins have been reported in some studies (Johns & Wooster, 1975; Vermue & Den Hertog, 1987). Since different prostanoids could be produced from the same tissue in a species- and stimulus-dependent manner, the results obtained with exogenously added prostaglandins do not necessarily reflect the physiological role of endogenous prostanoids, while the effects produced by COX inhibitors would be more informative in this respect.

Several groups have shown that COX inhibitors, for e.g. indomethacin, produce a profound inhibitory effect on spontaneous or evoked motility of isolated pyeloureteral smooth muscle from various species (Thulesius & Angelo-Khattar 1985; Lundstam *et al.*, 1985; Thulesius *et al.*, 1986; 1987; Cole *et al.*, 1988; Kimoto & Constantinou, 1991): the general conclusion emerging from these studies is that prostanoid generation is an important step for the local regulation of pyeloureteral motility. In some studies, a complete suppression of pyeloureteral motility by COX inhibitors has been reported (Lundstam *et al.*, 1984; Thulesius & Angelo-Khattar 1985; Thulesius *et al.*, 1987; Cole *et al.*, 1988): this may suggest that prostanoid generation is mandatory for the maintenance/activation of ureteral peristalsis. The evidence from this approach is, however, strictly limited by the selectivity and specificity of the pharmacological tools employed. Whenever high concentrations of COX inhibitors have been used for producing inhibition/total suppression of pyeloureteral motility (e.g. 10–100 μM indomethacin), the possibility cannot be completely ruled out that nonspecific drug effects on excitation/contraction coupling may have been produced. Indomethacin and other COX inhibitors have been reported to affect transmembrane ion movements in various cell types, including smooth muscle cells (Northover, 1971; 1973; Whittle, 1976).

A powerful tool to discriminate between specific and nonspecific effects of drugs is stereoselectivity. In this study, we have employed the enantiomers of ketoprofen, a well known COX inhibitor, to assess the importance of endogenous prostanoids in regulating the spontaneous (renal pelvis) and evoked (ureter) motility of the guinea-pig isolated pyeloureteral tract. The action of the (S)-enantiomer of ketoprofen (active in blocking COX) and of the (R)-enantiomer (inactive in blocking COX) (Hayball *et al.*, 1992; Suesa *et al.*, 1993) were compared with that of indomethacin.

Methods

General

All experiments were performed on the renal pelvis or ureter excised from male albino guinea-pigs (250–300 g body wt) which were stunned and bled. The renal pelvis and ureter (from the inferior renal pole to its entry into the bladder) were excised, cleaned of adhering fat and connective tissue and placed in oxygenated and warmed Krebs solution (95% O_2 and 5% CO_2, pH 7.4 at 37°C), as described previously (Maggi & Giuliani 1991; Maggi *et al.*, 1994a,b). The Krebs solution had the following composition ($mmol^{-1}$): NaCl 119, $NaHCO_3$ 25, KH_2PO_4 1.2, $MgSO_4$ 1.5, KCl 4.7, $CaCl_2$ 2.5 and glucose 11.

Organ bath experiments

In a first series of experiments we investigated the effect of (S)- or (R)-ketoprofen and indomethacin on the spontaneous activity of the guinea-pig isolated renal pelvis: the renal pelvis was opened, connected to silk threads and mounted in a 5 ml organ bath for isotonic recording (load 2 mN) of mechanical activity along its circular axis, as described previously (Maggi & Giuliani, 1992; Maggi *et al.*, 1994a). After setup, all preparations developed a spontaneous activity which reached steady state values of amplitude and frequency within 60 min. At this stage, the stated concentration of the drug under study was added to the bath and its effects were observed for 60 min. The inhibitory effects of COX inhibitors on the motility of the renal pelvis were evident either as a progressive reduction in the amplitude of contractions with a minor effect on their frequency or as a mixed inhibitory effect on both frequency and amplitude of contraction. As described previously (Maggi *et al.*, 1994a) a motility index (in arbitrary units) was calculated in each preparation by multiplying the frequency of spontaneous contractions (contraction min^{-1}) and their amplitude (in mm of chart); the inhibitory effect of drugs was expressed as % inhibition of the basal motility index.

In each preparation, only one concentration of test drug was investigated, except in experiments in which the additivity of the effect of (S)-ketoprofen and indomethacin were determined. (S)-ketoprofen and indomethacin were investigated at concentrations ranging between 0.1 and 100 μM. For (R)-ketoprofen, concentrations greater than 10 μM were not investigated: since the threshold concentration of (S)-ketoprofen is 0.1 μM (see Results) and the purity of the sample of (R)-ketoprofen used is 99.4%, the (R)-enantiomer if tested at concentrations > 10 μM would contain a fraction of (S)-enantiomer capable of exerting biological activity in the renal pelvis.

In a second series of experiments, we studied the effect of (R)- or (S)-ketoprofen toward electrically- or KCl-evoked contractions of the guinea-pig ureter. A segment of ureter about 2 cm long was excised from its middle portion and the specimen was mounted in a 5 ml organ bath for isotonic recording (load 3 mN) of mechanical activity along the longitudinal axis, as described previously (Maggi & Giuliani, 1991). The ureters were exposed to capsaicin 10 μM for 15 min to prevent the release of sensory neuropeptides produced by application of depolarizing stimuli, as described previously (Maggi *et al.*, 1994a,b). Electrical pulses of long width (5 ms, 60 V) were automatically delivered every 60 s by means of two platinum wire electrodes placed at the top and the bottom of the organ bath (field stimulation) by means of a GRASS S88 stimulator and in the presence of the calcium channel agonist, Bay K 8644 (1 μM). In separate experiments (Bay K 8644 was not added in this case) contractions of the ureter were elicited at 30 min intervals by application of KCl (80 mM, added to the bath for 10 min) and the effect of drugs determined after 25 min contact time.

Propagation of activity in the ureter

The following experiments were performed to assess whether COX inhibitors may affect propagation of impulses along the ureter: a method developed for this purpose was used. Briefly, male albino guinea-pigs weighing 250–300 g body wt. were stunned and bled. The whole kidney and ureter were excised and placed in a Petri dish containing oxygenated Krebs solution. A segment (4–5 cm in length) of ureter was dissected from the inferior renal pole and placed in a 3 chamber organ bath which enabled a separate superfusion of different parts of the organ. Two perspex partitions were used to separate the renal-, middle- and bladder sites (henceforth referred to as the R-, M- and B-site, respectively) which included a window covered with condom rubber: a small hole was made in the rubber to enable the passage of the ureter. Proximally to each partition, the renal and bladder ends of the ureter were pinned onto a Sylgard support. The renal and bladder ends of the ureter were connected via pulleys to isotonic transducers (Basile 7006) (load 2 mN) for recording of mechanical activity on a two-channel polygraph

(Basile 7080). Each compartment was perfused by means of a peristaltic pump at a rate of 1 ml min^{-1} with oxygenated (95% O_2 and 5% CO_2, pH 7.4) Krebs solution at 34°C. All experiments were performed in ureters pre-exposed to capsaicin (10 μM for 15 min).

Electrical field stimulation (EFS) was applied to the renal (R-site) compartment by means of two wire platinum electrodes positioned in parallel at the two sides of the ureter. Square wave pulses (5–25 ms pulse width, 20 V) were automatically delivered every 100 s by means of a GRASS S88 stimulator.

The method is based on the assumption that contractions recorded at the bladder end of the ureter (B-site) following application of depolarizing stimuli at the R-site depend upon propagation of action potentials throughout the ureter and that restricted drug application to the middle region (M-site) will affect propagation of impulses: the assumption was verified by experiments involving section of the ureter at the M-site, by comparing the effect of applying the stimulus at the R-, M- and B-sites and by studying the effect of nifedipine at each of the three compartments.

Sucrose gap experiments

Male albino guinea-pigs (250–300 g) were stunned and bled. The renal pelvis was excised and placed in oxygenated (95% O_2 and 5% CO_2) Krebs solution. A single sucrose-gap, modified as described in detail by Artemenko *et al.* (1982) and Hoyle (1987) was used to investigate changes in membrane potential and mechanical activity. The renal pelvis was superfused with oxygenated Krebs solution at a rate of 1 ml min^{-1}. The temperature of the solution was kept constant at 35 ± 0.5°C. Under these conditions all preparations tested developed spontaneous electrical and mechanical activity within 10–20 min from setup. When the spontaneous activity had reached a steady state either (S)-ketoprofen (10–100 μM) or indomethacin (10–100 μM) was added to the superfusion medium and their effects were assessed over a 60 min observation period.

The duration of spontaneous (pacemaker) action potential and contraction were measured at 50% of repolarization and relaxation, respectively. The duration of repolarization was calculated from the peak of depolarization to 50% of repolarization.

In other experiments, the effects of (S)-ketoprofen or indomethacin (10 μM for 60 min) were investigated on the action potential and contraction produced by direct EFS in the guinea-pig ureter (Shuba, 1977; Brading *et al.*, 1983). The experiments were performed in capsaicin-pretreated ureters (10 μM for 15 min) and in the presence of Bay K 8644 (1 μM), as described previously (Maggi *et al.*, 1994a,b). Square wave pulses (1–2 ms pulse width, 10–20 V) were automatically delivered every 2.5 min by means of a GRASS S88 stimulator.

Statistical analysis

Each value is mean ± s.e.mean. Statistical analysis was performed by means of Student's *t* test or analysis of variance, when appropriate. Linear regression was performed by the least squares method: EC_{50} values and 95% confidence limits were calculated accordingly.

Drugs

Drugs used were: nifedipine, capsaicin and indomethacin (Sigma), Bay K 8644 (methyl 1,4-dihydro-2,6-dimethyl-3-nitro-4-(2-trifluoromethylphenyl)-pyridine-5-carboxylate) (Calbiochem). The (S)- and (R)-enantiomers of ketoprofen were synthesized in the Chemistry Department of Laboratories Menarini by enzymatic resolution of the racemic trifluoroethylester (Palomer *et al.*, 1993). The optical purity was determined by a direct enantiospecific h.p.l.c. method, using a Chiralcel OJ column (Daicel, Japan), as described previously (Palomer *et al.*, 1993). The measured enantiomeric excess values were 99.4 and 99.7% for the (R)- and (S)-enantiomers, respectively.

Results

Organ bath

Effect on spontaneous activity of the renal pelvis The guinea-pig isolated renal pelvis shows spontaneous mechanical activity at a frequency of 4–7 contractions min^{-1} and an amplitude ranging between 40–65% of the maximal contractile response to added KCl. At steady state (about 60 min from setup), both frequency and amplitude of spontaneous contractions are stable for >60 min. The spontaneous activity of the renal pelvis was abolished within 90 min from the addition of 1 μM nifedipine ($n = 6$), indicating its close dependency from the activation of L-type voltage-sensitive calcium channels.

The addition of indomethacin or (S)-ketoprofen (0.1–100 μM) produced a concentration- and time-dependent inhibition of the spontaneous activity of the renal pelvis. The inhibitory effect was evident either as a reduction in the amplitude of contractions with only a minor effect on their frequency (as in the examples shown in Figure 1) or as a mixed inhibitory effect on both the amplitude and frequency of spontaneous contractions. To account for both effects, a motility index was calculated by multiplying the frequency and amplitude values before addition of drugs: the time-dependent changes of motility index produced by various concentrations of COX inhibitors are shown in Figure 2. At 0.1 and 1.0 μM, the maximal inhibitory effects of (S)-ketoprofen and indomethachin were comparable. At 10 and 100 μM the inhibitory effect of (S)-ketoprofen showed a plateau, whereby a substantial fraction (40–50% of control values) of motility index was preserved at 60 min from the addition of 100 μM (S)-ketoprofen.

On the other hand, 10–100 μM indomethacin produced a further marked and concentration-dependent inhibition of the motility index and in about 30% of cases tested, completely suppressed the spontaneous motility of the renal pelvis within 60 min of addition to the bath. On average, 10 and 100 μM indomethacin produced 68 ± 7 and 95 ± 3% inhibition of motility index at 60 min from its addition to the bath (Figure 2, $n = 6$ for each group). At both concentrations, the effect of indomethacin was significantly larger ($P < 0.05$) than that produced by (S)-ketoprofen (Figure 2).

Up to 10 μM, the (R)-enantiomer of ketoprofen did not significantly affect the motility index of the renal pelvis (Figures 1 and 3).

Since a substantial fraction of the spontaneous motility of the renal pelvis was unaffected by 100 μM (S)-ketoprofen, whilst indomethacin produced a much larger inhibitory effect, the effect of 100 μM indomethacin was also investigated on the (S)-ketoprofen-resistant (100 μM, 60 min before) activity of the renal pelvis. In these experiments, (S)-ketoprofen produced a 52 ± 9% inhibition of motility index ($n = 4$); the addition of 100 μM indomethacin produced a further marked inhibition or suppression (90 ± 2% inhibition) of the residual activity.

Effect on stimulated contractions of the ureter Electrical field stimulation (EFS, 5 ms pulse width, 60 V every 60 s) produced phasic contractions of the guinea-pig ureter which, in the presence of Bay K 8644, were steady for several hours. Nifedipine produced 67 ± 8 and 100% inhibition of EFS-evoked contractions at 10 and 30 μM, respectively ($n = 6$). At 10 μM, neither (S)-ketoprofen nor indomethacin ($n = 4$ each) significantly affected the amplitude of EFS-evoked contractions of the ureter (Figure 3).

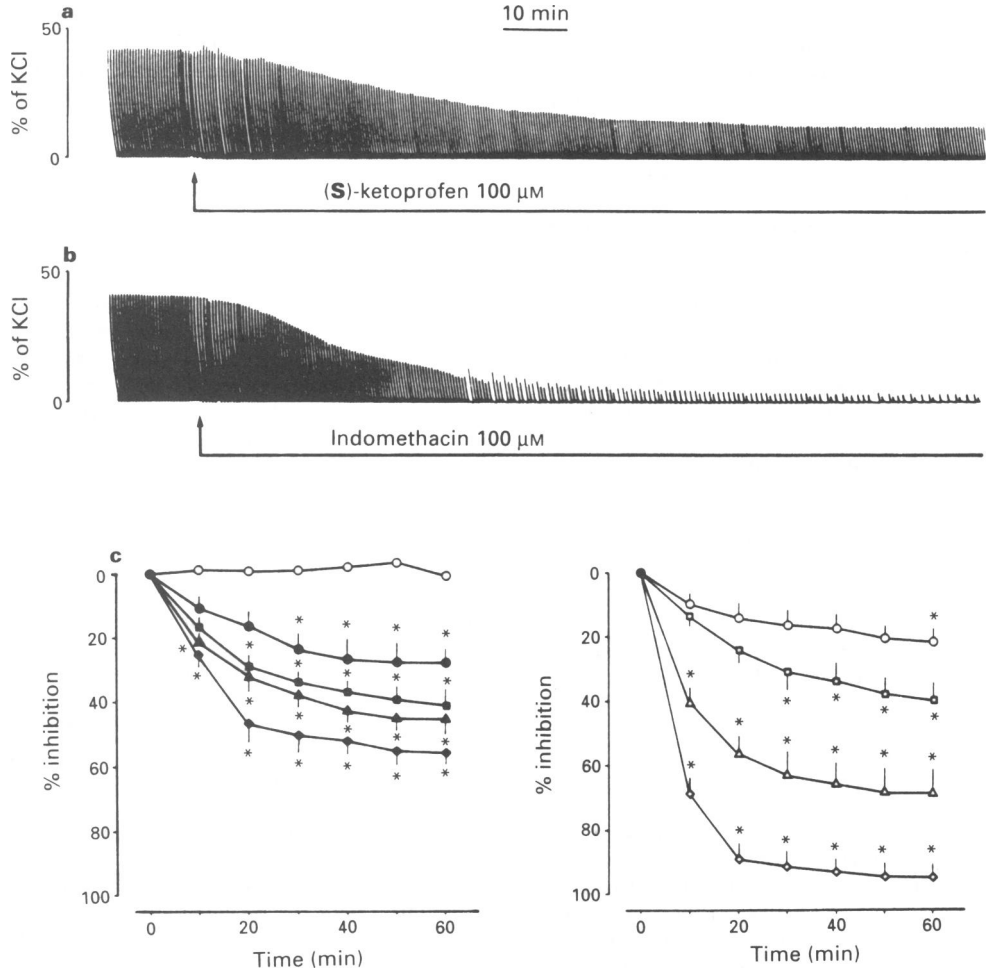

Figure 1 (a and b) Tracings showing the time dependent inhibitory effect produced by 100 μM (S)-ketoprofen and indomethacin on the spontaneous activity of the guinea-pig isolated renal pelvis. Note the much larger inhibitory effect produced by indomethacin as compared to (S)-ketoprofen. Vertical scales represent % of the maximal contractile response to KCl 80 mM. (c) Concentration and time-dependent inhibitory effect produced by cyclo-oxygenase (COX) inhibitors on motility of the guinea-pig isolated renal pelvis. In each preparation a motility index was calculated (in arbitrary units) by multiplying frequency and amplitude values of spontaneous contractions. The % inhibition of basal motility index produced by COX inhibitors is shown for (S)- and (R)-ketoprofen (left panel) or indomethacin (right panel) at various times after their addition to the bath. Concentrations tested are as follows: in left panel, (R)-ketoprofen 10 μM (○); (S)-ketoprofen 0.1 μM (●), 1 μM (■), 10 μM (▲) and 100 μM (◆); in right panel, indomethacin 0.1 μM (○), 1 μM (□), 10 μM (△) and 100 μM (◇). Each value is mean ± s.e.mean of 6–9 experiments. *Significantly different from control values, $P<0.05$.

At 100–500 μM, indomethacin produced a concentration-dependent inhibition of the EFS-evoked contractions: the inhibitory effect developed quickly, each concentration producing steady state inhibition in 4–8 min; the effect averaged 13 ± 2, 40 ± 5 and 82 ± 6% inhibition at 100, 300 and 500 μM, respectively ($n = 4$ for each concentration) and was rapidly reversed upon washout (Figure 3). (S)-ketoprofen was without significant inhibitory effect up to 500 μM ($n = 4$).

Application of KCl (80 mM for 5 min) produced a biphasic contraction of the guinea-pig ureter; both components of response are inhibited by >90% by 1 μM nifedipine after 120 min contact time ($n = 4$). Indomethacin produced 27 ± 9 and 72 ± 6% inhibition of the phasic response to KCl at 100 and 300 μM, respectively ($n = 4$–6). The corresponding values for the tonic component of the response to KCl were 29 ± 12 and 80 ± 5% inhibition, respectively. (S)-ketoprofen (100–300 μM, $n = 4$) had no effect on the responses to KCl.

Effect on propagation of impulses along the ureter Electrical field stimulation (EFS, 5 ms pulse width, 20 V) applied at the renal end (R-site) of the ureter produced a phasic contraction at both the R- and bladder (B-site) ends of the ureter: both responses ranged between 40–60% of the response to KCl (80 mM) applied at the respective compartment and will be referred to hereafter as the direct and propagated responses to EFS, respectively. (S)-ketoprofen or indomethacin (10 μM each, $n = 4$) applied via superfusion at the M-site for 60 min did not affect either the direct or the propagated responses to EFS (Figure 4). In contrast, application of nifedipine (10 μM, n = 4) at the M-site promptly suppressed the propagated response without affecting the direct response to EFS (Figure 4).

Sucrose gap

Pacemaker potentials in the renal pelvis The guinea-pig renal pelvis showed a spontaneous electrical and mechanical activity at a mean frequency of 1.62 ± 0.11 cycles min^{-1} ($n = 54$) and an average amplitude of maximal depolarization and amplitude of contractions of 9.95 ± 0.47 mV and 4.84 ± 0.1 mN, respectively. Nifedipine (10 μM) produced a rapid suppression of spontaneous action potential and contractions of the guinea-pig renal pelvis (Figure 5).

The electrical activity of the guinea-pig isolated renal pelvis

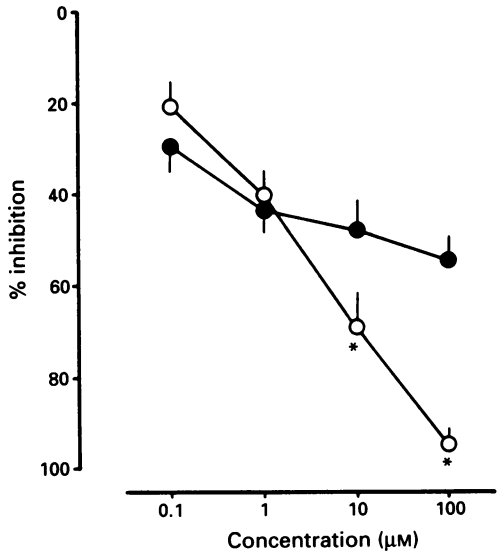

Figure 2 Concentration-dependency of the inhibitory effect of (S)-ketoprofen (●) and indomethacin (○) on motility index of the guinea-pig isolated renal pelvis, measured as the maximal inhibitory effect observed within 60 min of drug addition to the bath. Note that the maximal effect of (S)-ketoprofen plateaued at about 50–60% inhibition while indomethacin produced an almost full blockade of spontaneous activity. Each value is mean ± s.e.mean of 6–9 experiments. *Significantly different from the inhibitory effect of (S)-ketoprofen, $P<0.05$.

was characterized by a slow 'diastolic' depolarization or prepotential to a threshold value when a spontaneous (pacemaker) action potential was observed, followed by a phasic contraction. The shape of the action potential was quite heterogeneous from one preparation to another (see below), especially for the presence and duration of a plateau. In most instances (43 out of 54 cases tested) a series of small amplitude rapid fluctuations of membrane potential superimposed onto the ascending limb of the action potential and/or its peak (Figure 5 and 7). We noted that those preparations showing a pronounced plateau in the action potential also showed a relatively fast rate of depolarization.

Combining the two criteria, 2 groups of preparations were subjected to further analysis: group A was defined by a slower rate of depolarization ($<15\ mV\ s^{-1}$) and absence of a pronounced plateau (Figure 5a); group B by a faster rate of depolarization ($>15\ mV\ s^{-1}$) and presence of a plateau (Figure 5b). In the population of 54 preparations investigated, 9 cases were not classified because of their failure to meet one of the 2 above criteria, 22 cases were classified as group A and 23 cases as group B. The characteristics of the excitation-contraction cycle in Groups A and B are further analysed in Table 1. As can be seen, group A was characterized by a higher frequency of pacemaker potentials, lower values of maximal amplitude of depolarization, longer time to peak of depolarization and lower depolarization rate as compared to group B (Table 1). Furthermore, the time from peak depolarization to 50% repolarization was significantly shorter in group A than in group B, reflecting the absence of a pronounced plateau in the action potential in group A (Table 1). The amplitude of afterhyperpolarization was not significantly different in the two groups. The parameters of the contraction-relaxation cycle were likewise not different between group A and group B (Table 1).

The frequency of pacemaker potentials did not show significant changes over the 60 min observation period in either controls ($n=13$, 5 from group A and 5 from group B), (S)-ketoprofen ($n=11$, 4 from group A, 5 from group B) or indomethacin- ($n=13$, 4 from group A and 4 from group B) treated groups. On average, there was a slight tendency to a

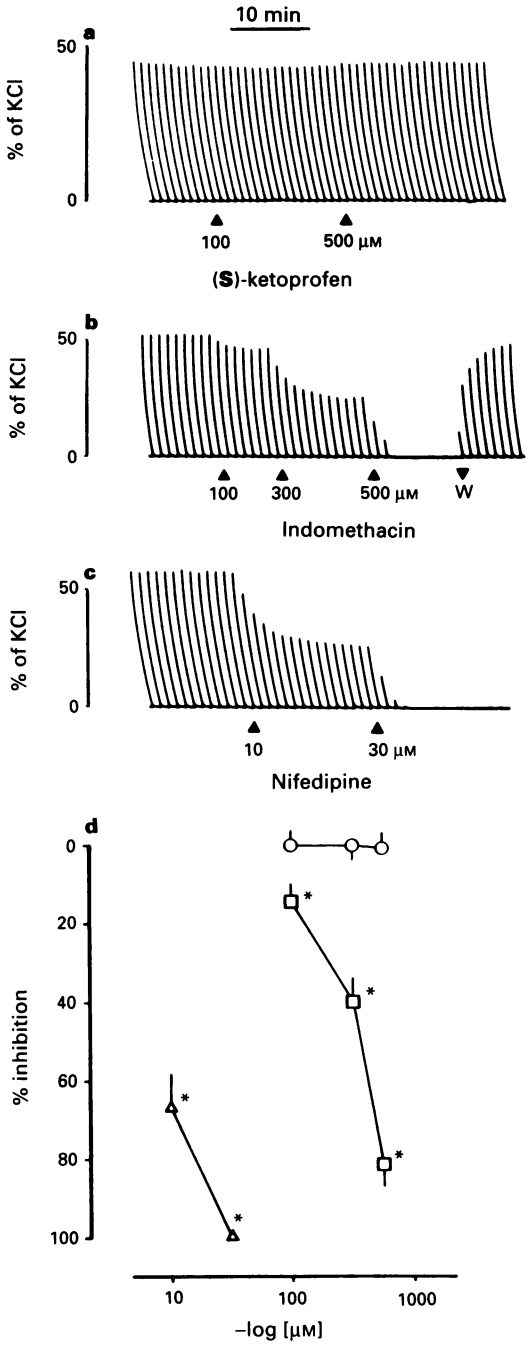

Figure 3 Tracings (a, b, c) and mean values (d) showing the effect of (S)-ketoprofen (○), indomethacin (□) and nifedipine (△) on EFS-induced contractions of the guinea-pig isolated ureter. In (d), each value is mean ± s.e.mean of 4–6 experiments. *Significantly different from control values $P<0.05$. W = washout.

reduced frequency of pacemaker potentials in the control group (1.54 ± 0.24 and 1.39 ± 0.2 cycles min^{-1} before and after 60 min superfusion with drug-free Krebs solution, $n=13$) and a slight tendency to an increased frequency in the indomethacin group (from 1.65 ± 0.29 to 1.89 ± 0.35 cycles min^{-1}, $n=13$), while no change was evident in the (S)-ketoprofen-treated group (from 1.33 ± 0.13 to 1.38 ± 0.15 cycles min^{-1}, $n=11$). In control preparations ($n=13$) a slight decline in the maximal amplitude of depolarization was observed throughout the 60 min observation period (Figure 6): this small effect (16% reduction) was statistically significant at 50 and 60 min. Other parameters of the action potential and accompanying contraction did not show any significant time-related modification during a 60 min superfusion with drug-free Krebs solution (Figure 6).

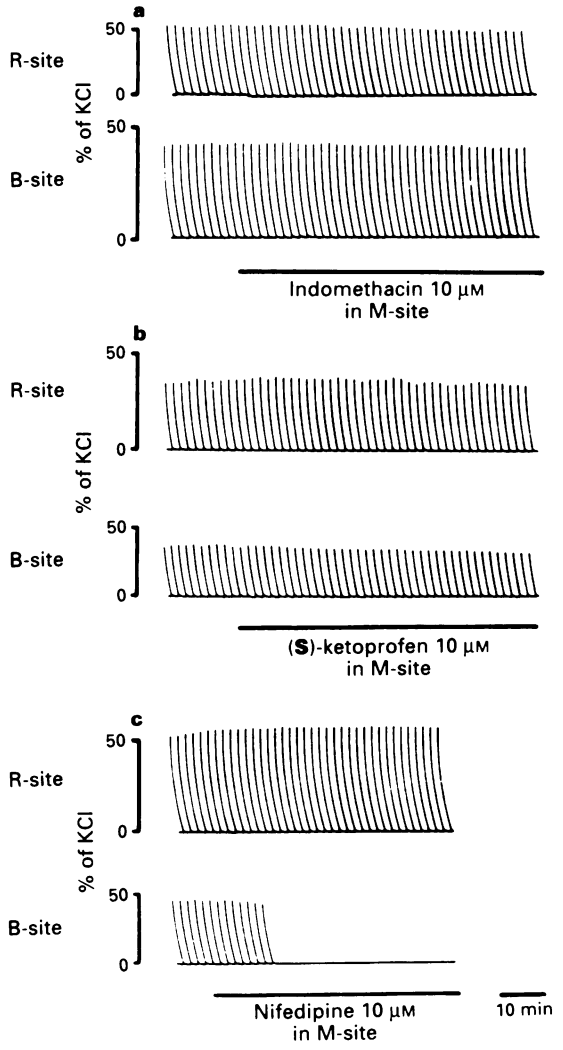

Figure 4 Effect of indomethacin (a), (S)-ketoprofen (b) and nifedipine (c) on propagation of impulses along the guinea-pig ureter. The ureter was placed in a three-compartment organ bath and electrical stimuli were applied at its renal end while simultaneously recording mechanical activity at both renal and bladder ends (R- and B-sites, respectively). The response observed at the B-site is due to propagation of myogenic impulses along the ureter. Nifedipine applied at the middle compartment (M-site) suppressed the propagation of impulses while leaving the response recorded at the R-site unaffected. (S)-ketoprofen and indomethacin had no effect on the propagation of impulses along the guinea-pig ureter.

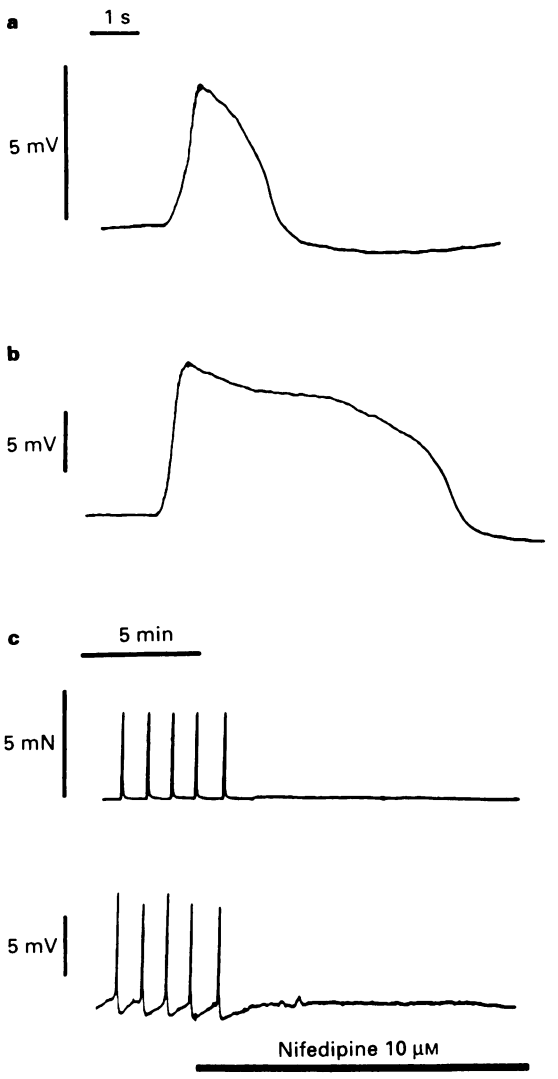

Figure 5 Examples (panels a and b) of the pacemaker potential recorded by sucrose gap from the guinea-pig renal pelvis smooth muscle. Preparations described in the text as group A (panel a, see also Table 1) are characterized by a relatively slow rate of depolarization and by the absence of a pronounced plateau; those described in the text as group B (panel b) are characterized by a relatively fast rate of depolarization and by a pronounced plateau in the action potential, similar to that recorded in the ureter. In both cases, small rapid oscillations of membrane potential were observed on the ascending limb of depolarization and/or on the peak of the action potential. (c) Nifedipine (10 μM) suppresses pacemaker potential (lower tracing) and spontaneous contractions (upper tracing) of the renal pelvis.

(S)-ketoprofen (10 μM, $n = 11$) and indomethacin (10 μM, $n = 13$) both produced a progressive, time-dependent modification of various parameters of the excitation contraction coupling of the guinea-pig renal pelvis (Figures 6 and 7a): these effects include a shortening of action potential duration (45 and 56% reduction by (S)-ketoprofen and indomethacin, respectively), a reduced amplitude of contraction (37 and 43% inhibition, respectively) and a shortening of contraction duration (36 and 47% inhibition, respectively). Indomethacin (10 μM) also produced a significant time-dependent reduction of the maximal amplitude of depolarization (32% inhibition at 60 min) which was significantly larger than the small spontaneous decline observed in controls (Figure 6). This effect of indomethacin was not shared by (S)-ketoprofen which produced a 9% reduction at 60 min (n.s. vs. time-matched controls, Figure 6).

Considering the differences in resting values of some parameters between groups A and B, a further analysis was made of possible differential effects of (S)-ketoprofen or indomethacin in the two groups. The only difference found was related to the effect of (S)-ketoprofen (10 μM) on the maximal amplitude of depolarization which was more pronounced in group A (29 ± 8% inhibition, $n = 4$) than in group B (6 ± 3% inhibition, $n = 4$). Such a difference was not observed for indomethacin (10 μM) which produced a comparable inhibitory effect in the two groups (34 ± 8 and 36 ± 6% inhibition, $n = 4$ each).

A tenfold greater concentration of (S)-ketoprofen (100 μM, $n = 4$, 3 from group A) produced a time-dependent shortening of action potential duration (49% reduction), a reduced amplitude of contraction (46% inhibition) and a shortening of contraction duration (50% inhibition), not significantly different from the effect produced at 10 μM. At 100 μM (S)-ketoprofen also produced a significant reduction of the maximal amplitude of depolarization (23 ± 6% inhibition, $P < 0.05$).

When 100 μM indomethacin was added to the superfusion medium 60 min after superfusion with 100 μM (S)-ketoprofen, it produced a prompt suppression of the residual action potential and contraction (Figure 7b).

Evoked action potentials in the ureter

As described in previous studies (Maggi *et al.*, 1994a,b), the capsaicin-pretreated guinea-pig ureter in the presence of Bay K 8644 (1 μM) responds with regular action potentials and phasic contractions following repetitive cycles of direct electrical stimulation (1–2 ms pulse width, 10–20 V). (S)-ketoprofen and indomethacin (10 μM for 60 min, $n = 5$ for each drug) did not significantly affect the action potential and contraction of the guinea-pig ureter as compared to control preparations superfused for 60 min with drug-free Krebs solution ($n = 5$). The only effect produced by COX inhibitors was depolarization of the membrane: this effect ensued at 10–20 min and reached a steady state at 40–60 min from start of superfusion with (S)-ketoprofen or indomethacin. At 60 min from the start of superfusion, the effect of (S)-ketoprofen and indomethacin averaged 3.21 ± 0.78 and 2.03 ± 0.34 mV ($n = 5$), while no significant changes were observed in controls.

Table 1 Parameters of spontaneous (pacemaker) potentials and accompanying phasic contractions of the guinea-pig renal pelvis (sucrose gap)

Action potential	*Group A* ($n = 22$)	*Group B* ($n = 23$)
Action potential		
Frequency (cycles min^{-1})	2.01 ± 0.18	1.25 ± 0.08*
Amplitude of depolarization (mV)	7.85 ± 0.54	11.95 ± 0.47*
Time to peak (ms)	962 ± 81	543 ± 36*
Rate of depolarization (mV s^{-1})	8.9 ± 0.67	24.1 ± 1.94*
Duration (ms)	2683 ± 139	3156 ± 314
Repolarization (ms)	1722 ± 137	2613 ± 321*
After hyperpolarization (mV)	1.25 ± 0.22	1.55 ± 0.20
Mechanical activity		
Amplitude (mN)	4.70 ± 0.33	4.98 ± 0.39
Time to peak (ms)	1789 ± 88	1933 ± 140
Duration (ms)	3946 ± 142	4022 ± 348
Relaxation time (ms)	1707 ± 80	2088 ± 217

Each value is mean ± s.e.mean. The preparations were subgrouped to meet two criteria: (a) rate of depolarization < or > than 15 mV; (b) absence or presence of a plateau in the action potential. Nine out of 54 preparations studied failed to meet both criteria of inclusion: of the remainders, 22 were classified as group A and 23 as group B. *Significantly different from group A ($P < 0.05$).

Discussion

Electromechanical coupling in the upper urinary tract

The smooth muscle of the upper urinary tract (renal pelvis and ureter) relies on electromechanical coupling to accomplish its physiological function of transport of urine. Action potentials are spontaneously generated by pacemaker cells in the renal pelvis while the ureter smooth muscle is normally quiescent unless invaded by action potentials travelling through the ureter to produce a peristaltic wave. Phasic contractions are invariably preceded by action potentials in both the renal pelvis and ureter and L-type calcium channel blockers suppress the generation of action potentials and contractility (Weiss 1992 for review; Shuba 1977; Brading *et al.*, 1983). This concept is further strengthened here by the fact that nifedipine was found to eliminate totally action potentials and contractility in the renal pelvis, evoked contractility of the ureter and propagation of impulses through the ureter.

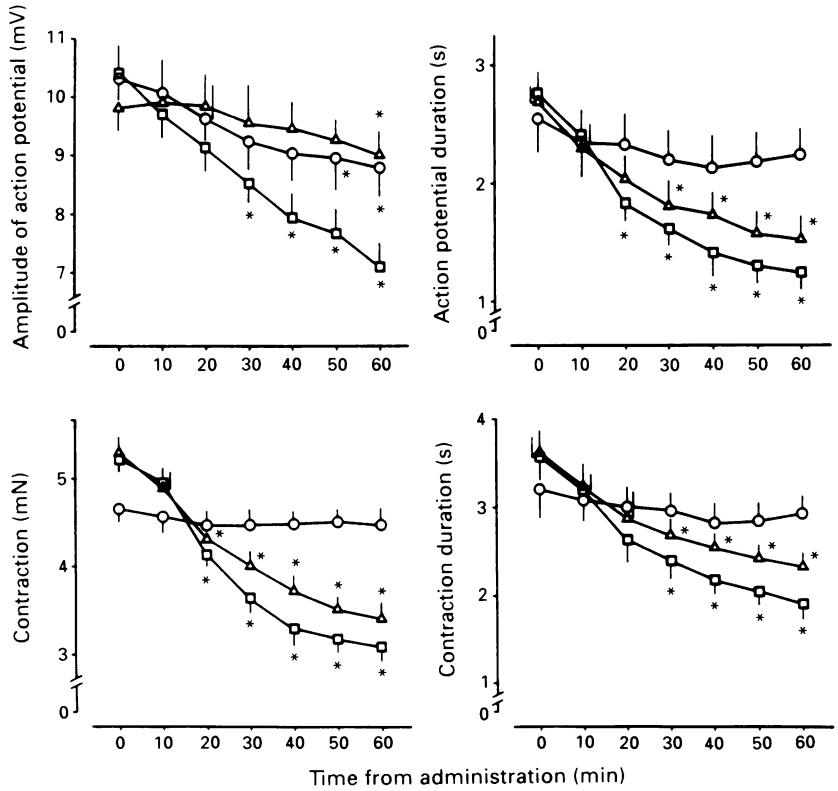

Figure 6 Time-dependent changes in amplitude and duration (at 50% of repolarization) of the action potential and amplitude and duration of contraction (at 50% of relaxation) observed in preparations superfused for 60 min with drug-free Krebs solution (controls, ○), 10 μM (S)-ketoprofen (□) or 10 μM indomethacin (△). Each value is mean ± s.e.mean of 11–13 experiments. *Significantly different from baseline values, $P < 0.05$.

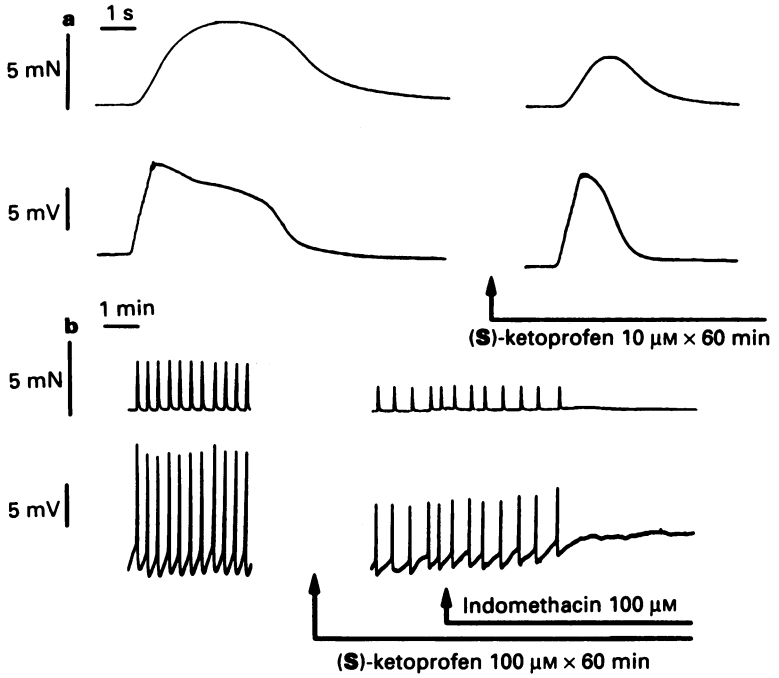

Figure 7 (a) Effect of (S)-ketoprofen on pacemaker potential and contraction of the guinea-pig renal pelvis. (b) The (S)-ketoprofen-resistant pacemaker potentials of the guinea-pig renal pelvis are promptly suppressed by 100 μM indomethacin. In both panels, the lower tracing shows changes in membrane potential and the upper tracing tracing shows tension.

It is currently held that prostanoids play a local autocrine and paracrine role regulating excitation-contraction coupling in the upper urinary tract (see Introduction for references). Crucial for this interpretation is the notion that blockers of prostanoid generation inhibit or suppress excitation-contraction coupling at this level: several COX inhibitors have been used in experiments on the isolated renal pelvis and ureter smooth muscle from different species yet, as outlined in the Introduction, the exact importance of locally generated prostanoids in setting excitation-contraction coupling in the upper urinary tract is unclear, especially from a quantitative point of view. We have re-addressed this issue by investigating the action of the two enantiomers of ketoprofen, a well known COX inhibitor. We speculated that the qualitative and quantitative differences observed between the action of (S)- and (R)-ketoprofen would provide an exact estimate of the true importance of COX products in modulating excitation-contraction coupling at this level. A direct comparison with indomethacin also appeared of interest for re-interpretation of previous findings on this topic.

The estimate of the potency of COX inhibitors in blocking prostanoids production greatly varies with the assay employed: for instance, racemic ketoprofen is either less potent (about ten fold) or slightly more potent (about three fold) than indomethacin in inhibiting prostaglandin production from cultured macrophages and sheep seminal vesicle microsomes, respectively (Brune *et al.*, 1981); yet IC_{50} values in the low μM range have been reported in various assays for inhibition of prostaglandin/thromboxane synthesis for both compounds (Rainsford, 1988 for review). Following the separation of the two enantiomers, COX inhibition by racemic ketoprofen was found to reside almost entirely in the (S)-enantiomer which, in different cellular models, is 33–3,000 fold more potent than the (R)-enantiomer (Suesa *et al.*, 1993). Indeed, contamination by small amounts of (S)-ketoprofen (about 0.5%) may well account for COX inhibition observed when using high concentrations of the (R)-enantiomer. The present findings demonstrate that, up to 10 μM, the effects of (S)-ketoprofen and indomethacin on motility of the guinea-pig isolated renal pelvis are essentially superimposable. At concentrations equal or greater than 100 μM, indomethacin produces a general suppressant effect on spontaneous and evoked motility of the pyeloureteral system. These effects are not shared by (S)-ketoprofen and are likely to involve a nonspecific action of indomethacin (Northover, 1971; 1973; Whittle, 1976) on membrane channels, excitability and contractility.

Stereoselective COX inhibition and renal pelvis motility

The present findings indicate that endogenous prostanoids play a modulatory and amplifying role in spontaneous excitation-contraction coupling of the guinea-pig renal pelvis, yet also indicate that the generation of endogenous prostanoids is nonessential for this process: pacemaker potentials modified in their shape/duration were observed after 60 min superfusion with 10 or 100 μM (S)-ketoprofen and each of them was able to produce contraction. Although the possibility that species-related differences exist in this respect, the total suppression of spontaneous contractions of the sheep and rabbit renal pelvis observed with 10–100 μM indomethacin (Lundstam *et al.*, 1985; Thulesius *et al.*, 1986) is likely to arise from a mixed effect on COX and nonspecific effects on excitation-contraction coupling.

The interpretation of the physiological relevance of the present findings is somewhat complicated by the notion that mechanical trauma increases the production of prostanoids: therefore the basal prostanoids production (and consequently the intensity of the effects produced by inhibiting COX) may have been artificially increased by the dissection procedure. In this respect, it is worth noting that the frequency of spontaneous contractions of the isolated renal pelvis in organ bath experiments (4–7 cycles min^{-1}) is higher than the frequency of pacemaker potentials measured during continuous superfusion in sucrose gap (1–2 cycles min^{-1} in groups A and B).

At least two factors could be important in determining this difference. On the one hand, there is evidence that in species with unicalyceal kidney (e.g. guinea-pig and rabbit) specialized muscle cells with putative pacemaker function are distributed in the whole renal pelvis (Gosling & Dixon,

1971), yet the basic frequency of pacemaker potentials shows a distinct proximal-to-distal gradient. Each small region of the renal pelvis behaves as an oscillator and the integrated function is best described as a hierarchically organized multiple-coupled pacemaker system (Constantinou & Tamaguchi, 1981; Kimoto & Constantinou, 1991). In sucrose gap, the multicellular recording of electrical activity originates from a small region of the sample: it appears conceivable that, in preparations having the lower frequencies of pacemaker activity (group B) the area of recording was closer to the ureter. This is further suggested by the presence of a pronounced plateau in the action potential in group B, since this is a well characterized feature of the action potential of the guinea-pig ureter (Shuba, 1977; Brading *et al.*, 1983). By contrast recordings made from preparations in group A are likely to involve more proximal regions of the renal pelvis where pacemaker cells with higher intrinsic frequencies are located. On the other hand, in organ bath experiments, the activity of the whole renal pelvis is recorded, which is anyway driven by the pacemaker cell(s) with the highest intrinsic frequency of discharge.

A second factor may be linked to the continuous superfusion performed in sucrose-gap, enabling the removal of locally released mediators (such as prostanoids). We observed that the renewal of bathing solution by washout slows down the frequency of contractions of the renal pelvis in organ bath experiments, and some minutes are needed for recovery to the original values of frequency and amplitude. Thus, endogenous prostanoids may accumulate in the organ bath fluid to provide an optimal reinforcement of the activity of pacemaker cells. Either one of these factors may explain the higher values of spontaneous activity observed in organ bath vs. sucrose gap experiments.

The mean values of frequencies (and other parameters) were not significantly different from each other in the experimental groups aimed to analyse the effect of (S)-ketoprofen and indomethacin (10 μM each) vs. spontaneous time-related changes in sucrose gap experiments. This reflects a balanced distribution of preparations from groups A and B in the three experimental groups (controls, (S)-ketoprofen and indomethacin). When the effects of (S)-ketoprofen and indomethacin were analysed for possible differential effects in groups A and B, the only difference was found about the inhibitory effect of (S)-ketoprofen on the amplitude of depolarization which, at 10 μM, was apparently larger in group A than in group B. Overall, the present findings do not support the possibility of a differential effect of prostanoids on excitation-contraction coupling in different regions of the guinea-pig renal pelvis, yet the limitation of the technique (multicellular recording) leaves this point open to further investigation. Considering the effect of 10 μM (S)-ketoprofen as a pure consequence of full COX inhibition, it would follow that modulation of action potential duration is the main mechanism through which endogenous prostanoids regulate pacemaker potentials of the guinea-pig renal pelvis. These findings suggest an amplifying or facilitatory effect of endogenous prostanoids in L-type calcium current which sustains the pacemaker of the renal pelvis.

Stereoselective COX inhibition and ureter motility

Previous studies have suggested a facilitatory influence of endogenous prostanoids on excitation-contraction coupling of the human and ovine isolated ureter. Contrary to the guinea-pig, the isolated ureter of the sheep is spontaneously active, although the frequency of spontaneous contraction is irregular and anyway lower than in the renal pelvis (Thulesius & Angelo-Khattar, 1985; Thulesius *et al.*, 1986). Indomethacin (10 nM–100 μM) was shown to produce a complete blockade of this spontaneous activity, the time required for full blockade being inversely proportional to the concentration tested (Thulesius & Angelo-Khattar, 1985). The human isolated ureter was reported to be either spontaneously active and blocked by indomethacin (Angelo-Khattar *et al.*, 1985) or quiescent (Cole *et al.*, 1988): in the latter study, 100 μM indomethacin blocked contractions evoked by direct stimulation of smooth muscle. Prostaglandins of the E and F series were found to be excitatory in both species (Thulesius & Angelo Khattar, 1985; Cole *et al.*, 1988).

The guinea-pig ureter is electrically and mechanically quiescent: prostaglandins of the F series are inactive while prostaglandins of the E series produce muscle relaxation and membrane hyperpolarization, both effects being possibly linked to adenylate cyclase stimulation and elevation of cyclic AMP (Johns & Wooster, 1975; Vermue & Den Hertog, 1987). It appears conceivable that the slowly developing and sustained depolarization of the ureter observed in this study is ascribable to the removal of endogenous prostanoids by COX inhibition. However, this modulatory influence had no apparent major influence on the action potential and contractility of the ureter nor on the propagation of impulses along the ureter. High concentrations of indomethacin suppressed the evoked motility of the guinea-pig ureter: the involvement of COX inhibition appears highly debatable since (S)-ketoprofen was ineffective when tested at similarly high concentrations.

In all, our findings do not lend support to the idea that endogenous prostanoids play a major role in regulating electromechanical coupling and propagation of impulses along the guinea-pig ureter. Previous studies have suggested that the pyeloureteral junction may be a crucial target for action of endogenous prostanoids in regulating propagation of impulses to the ureter (Kimoto & Constantinou, 1991). Our data do not allow speculation on this matter because of the technical problem in isolating and studying such a small region of the guinea-pig pyeloureteral system.

Pathophysiological implications

The reinforcement of pacemaker activity of the renal pelvis by endogenous prostanoids demonstrated here could be of importance for the effect of COX inhibitors on renal colic. In addition to a possible central analgesic effect, a reduction of renal blood flow and urine production is held as a major mechanism through which COX inhibitors produce pain relief in renal colic (e.g. Perlmutter *et al.*, 1993). Assuming that endogenous prostanoids reinforce spontaneous excitation-contraction coupling in the renal pelvis, blockade of this effect by COX inhibitors may contribute to the overall pain relief produced by these drugs in renal colic, by reducing intraureteral pressure.

References

ANGELO-KHATTAR, M., THULESIUS, O., NILSSON, T., CHERIAN, T. & JOSEPH, L. (1985). Motility of the human ureter with special reference to the effects of indomethacin. *Scand. J. Urol. Nephrol.*, **19**, 261–265.

ARTEMENKO, D.P., BURY, V.A., VLADIMIROVA, I.A. & SHUBA, M.F. (1982). Modification of the single sucrose-gap method. *Physiol. Zhurn.*, **28**, 374–380.

BRADING, A.F., BURDYGA, T.H.V. & SCRIPNYUK, Z.D. (1983). The effects of papaverine on the electrical and mechanical activity of the guinea-pig ureter. *J. Physiol.*, **334**, 79–89.

BRUNE, K., RAINSFORD, K.D., WAGNER, K. & PESKAR, B.A. (1981). Inhibition by antinflammatory drugs of prostaglandin production in culture macrophages. Factors influencing the apparent drug effects. *Naunyn-Schmied. Arch. Pharmacol.*, **315**, 269–276.

COLE, R.S., FRY, C.H. & SHUTTLEWORTH, K.E.D. (1988). The action of prostaglandins on isolated human ureteric smooth muscle. *Br. J. Urology*, **61**, 19–26.

CONSTANTINOU, C.E. & YAMAGUCHI, O. (1981). Multiple-coupled pacemaker system in renal pelvis of the unicalyceal kidney. *Am. J. Physiol.*, **241**, R412–R418.

GOSLING, J.A. & DIXON, J.S. (1971). Morphologic evidence that the renal calyx and pelvis control ureteric activity in the rabbit. *Am. J. Anatomy*, **130**, 393–408.

HAYBALL, P.J., NATION, R.L. & BOCHNER, F. (1992). Enantioselective pharmacodynamics of nonsteroidal antinflammatory drug ketoprofen: *in vitro* inhibition of human platelet cyclo-oxygenase activity. *Chirality*, **4**, 484–487.

HOLMLUND, D. & SJODIN, J.G. (1978). Treatment of ureteral colic with intravenous indomethacin. *J. Urology*, **120**, 676–677.

HOYLE, C.H.V. (1987). A modified single sucrose gap -junction potentials and electrotonic potentials in gastrointestinal smooth muscle. *J. Pharmacol. Methods.*, **18**, 219–226.

JOHNS, A. & WOOSTER, M.J., (1975). The inhibitory effects of PGE1 on guinea-pig ureter. *Can. J. Physiol. Pharmacol.*, **53**, 239–247.

KIMOTO, Y. & CONSTANTINOU, C.E. (1991). Regional effects of indomethacin, acetylsalicylic acid and SC-19-220 on the contractility of rabbit renal pelvis (pacemaker regions and pelviureteric junction). *J. Urology*, **146**, 433–438.

LUNDSTAM, S., JONSSON, O., KIHL, B. & PETTERSSON, S. (1985). Prostaglandin synthetase inhibition of renal pelvis smooth muscle in the rabbit. *Br. J. Urology*, **57**, 390–393.

LUNDSTROM, S., LEISSNER, K.H., HAHLANDER, L.A. & KRAL, J.G. (1982). Prostaglandin synthetase inhibition with diclofenac sodium in treatment of renal colic: comparison with use of narcotic analgesis. *Lancet*, **i**, 1096–1097.

MAGGI, C.A. (1992). Prostanoids as local modulators of reflex micturition. *Pharmacol. Res.*, **25**, 13–20.

MAGGI, C.A. & GIULIANI, S. (1991). The neurotransmitter role of CGRP in the rat and guinea-pig ureter: effect of a CGRP antagonist and species-related differences in the action of omega conotoxin on CGRP release from primary afferents. *Neuroscience*, **43**, 261–271.

MAGGI, C.A. & GIULIANI, S. (1992). Nonadrenergic noncholinergic excitatory innervation of the guinea-pig isolated renal pelvis: involvement of capsaicin-sensitive primary afferent neurons. *J. Urology*, **147**, 1394–1397.

MAGGI, C.A., GIULIANI, S. & SANTICIOLI, P. (1994a). Effect of cromakalim and glibenclamide on spontaneous and evoked motility of the guinea-pig isolated renal pelvis and ureter. *Br. J. Pharmacol.*, **111**, 687–694.

MAGGI, C.A., GIULIANI, S. & SANTICIOLI, P. (1994a). Effect of Bay K 8644 and ryanodine on the refractory period, action potential and mechanical response of the guinea-pig ureter to electrical stimulation. *Naunyn-Schmied. Arch. Pharmacol.*, **349**, 510–522.

NORTHOVER, B.J. (1971). Mechanism of the inhibitory action of indomethacin on smooth muscle. *Br. J. Pharmacol.*, **41**, 540–551.

NORTHOVER, B.J. (1973). Effect of antinflammatory drugs on the binding of calcium to cellular membranes in various human and guinea-pig tissues. *Br. J. Pharmacol.*, **48**, 496–504.

OOSTERLINK, W., PHILIP, N.H., CHARIG, C., GILLIES, G., HETHERINGTON, J.W. & LLOYD, J. (1990). A double blind single dose comparison of intramuscular ketorolac tromethamine and pethidine in the treatment of renal colic. *J. Clin. Pharmacol.*, **30**, 336–342.

PALOMER, A., CABRE, M., GINESTA, J., MAULEON, D. & CARGANICO, G. (1993). Resolution of rac-ketoprofen esters by enzymatic reactions in organic media. *Chirality*, **5**, 320–328.

PERLMUTTER, A., MILLER, L., TRIMBLE, L.A., MARION, D.N., VAUGHAN, E.D. & FELSEN, D. (1993). Toradol, an NSAID used for renal colic, decreases renal perfusion and ureteral pressure in a canine model of unilateral ureteral obstruction. *J. Urology*, **149**, 926–930.

RAINSFORD, K.D. (1988). Inhibitors of eicosanoids metabolism. In *Biology and Chemistry of Prostaglandins and Related Eicosanoids*. ed. P.B. Curtis-Prior, pp. 52–68. Edinburgh: Churchill Livingstone.

SHUBA, M.F. (1977). The effect of sodium-free and potassium-free solutions ionic current inhibitors and ouabain on electrophysiological properties of smooth muscle of guinea-pig ureter. *J. Physiol.*, **264**, 837–851.

SUESA, N., FERNANDEZ, M.F., GUTIERREZ, M., RUFAT, M.J., ROTLLAN, E., CALVO, L., MAULEON, D. & CARGANICO, G. (1993). Stereoselective cyclo-oxygenase inhibition in cellular models by the enantiomers of ketoprofen. *Chirality*, **5**, 589–595.

THULESIUS, O. & ANGELO-KHATTAR, M. (1985). The effect of indomethacin on the motility of isolated sheep ureters. *Acta Pharmacol. Toxicol.*, **56**, 298–301.

THULESIUS, O., ANGELO-KHATTAR, M. & ALI, M. (1987). The effect of prostaglandin synthesis inhibition on motility of the sheep ureter. *Acta Physiol. Scand.*, **131**, 51–54.

THULESIUS, O., UGAILY-THULESIUS, L. & ANGELO-KHATTAR, M. (1986). Generation and transmission of ovine ureteral contractions with special reference to prostaglandins. *Acta Physiol. Scand.*, **127**, 485–490.

VERMUE, N.A. & DEN HERTOG, A. (1987). The action of prostaglandins on ureter smooth muscle of guinea-pig. *Eur. J. Pharmacol.*, **142**, 163–167.

WEISS, R.M. (1992). Physiology and pharmacology of renal pelvis and ureter. In *Campbell's Urology*, ed. Walsh, P.C., Retik, A.B., Stamey, T.A. & Vaughan, E.D. Volume I, pp. 113–144. Philadelphia PA: W.B. Saunders Co.

WHITTLE, B.J.R. (1976). Calcium and the inhibition of histamine release from rat peritoneal mast cells by nonsteroid antinflammatory agents. *Br. J. Pharmacol.*, **58**, 446P.

(Received July 26, 1994
Revised November 14, 1994
Accepted November 16, 1994)

British Journal of Pharmacology (1995) 114, 1159-1164

Characterization of [^{3}H]-imidazenil binding to rat brain membranes

Maria Lipartiti, Roberto Arban, Emanuela Fadda, *Adriano Zanotti & [1]Pietro Giusti

Department of Pharmacology, Largo E. Meneghetti, 2, University of Padua, 35131 Padua, Italy and *Fidia Research Laboratories, Abano Terme, Italy

1 The binding of [^{3}H]-imidazenil, an imidazobenzodiazepine carboxamide, to rat cerebellar membranes was characterized at different temperatures.

2 Specific binding was linear with tissue concentrations and reached maximum after 90, 30 and 5 min incubation at 0, 21 and 37°C, respectively. The binding was of high affinity, specific and saturable; non linear regression and Scatchard analysis of the data was compatible with the presence of a single population of receptor sites with B_{max} of 0.74 ± 0.020, 0.90 ± 0.011 and 1.0 ± 0.036 pmol mg^{-1} protein at 0, 21 and 27°C, respectively. Binding affinity decreased with increasing temperature: K_d were 0.29 ± 0.051 nM (0°C), 1.0 ± 0.080 nM (21°C) and 2.4 ± 0.38 nM (37°C).

3 At all tested temperatures, [^{3}H]-imidazenil binding was reversible and the K_d calculated from the dissociation and association rate constants approximated the equilibrium K_d.

4 In the presence of γ-aminobutyric acid (GABA), K_d increased 4 fold at 0°C, whereas B_{max} increased, albeit slightly, at all temperatures.

5 Benzodiazepines (BZDs), imidazopyridines and methyl-β-carboline-3-carboxylate (βCCM) were effective inhibitors of [^{3}H]-imidazenil binding. Conversely, $GABA_A$ antagonists, barbiturates, picrotoxin and peripheral BZD receptor ligands were devoid of any activity.

6 Comparing [^{3}H]-imidazenil to [^{3}H]-flumazenil binding in various brain areas, similar densities of recognition sites as well as like regional differences in the distribution of binding sites for both radioligands were observed (cortex = striatum > cerebellum > spinal cord).

7 The present results indicate that [^{3}H]-imidazenil specifically binds to the BZD sites of $GABA_A$ receptors. Furthermore, the effects of GABA and temperature differentiate imidazenil from classical BZDs. It is suggested that the characteristics of imidazenil binding may be relevant to the *in vivo* pharmacology of the drug.

Keywords: $GABA_A$ receptor complex; benzodiazepine; partial agonist; [^{3}H]-imidazenil binding; thermodynamic analysis; kinetic analysis

Introduction

Benzodiazepines (BZDs) are in widespread use as anxiolytics, anticonvulsants, hypnotics and myorelaxants (Greenblatt *et al.*, 1983). These neuropharmacological actions are presumably mediated by an enhancement of GABAergic synaptic transmission at $GABA_A$ receptors (Costa *et al.*, 1975; Haefely *et al.*, 1975). Specific binding sites for BZDs have been reported on brain membranes, in close association with $GABA_A$ receptors (Olsen, 1982). GABA and BZD binding sites are reciprocally regulated, since GABA or muscimol stimulate binding of [^{3}H]-flunitrazepam to brain membranes (Olsen, 1982) and BZDs increase binding of GABA at $GABA_A$ receptors (Matsumoto & Fukuta, 1982). Furthermore, the clinical potency of BZDs is positively correlated with their affinity for these [^{3}H]-flunitrazepam binding sites. Therefore, it is assumed that the pharmacological and clinical effects of BZDs are exerted via a positive allosteric modulation of GABA action following a specific interaction with these binding sites named central BZD receptors (Haefely *et al.*, 1985). Conversely, unrelated to $GABA_A$ receptor-associated BZD binding sites are peripheral BZD receptors, which are localized on the outer mitochondrial membranes of many tissues including the brain (Verma & Snyder, 1989).

A whole family of $GABA_A$ receptor subtypes is now known following the successful cloning and expression of the receptor subunits (Seeburg *et al.*, 1990). The exact interplay of BZD with these receptor subtypes is currently being investigated. Recently, based on their distinctive actions at different recombinant $GABA_A$ receptors, a classification of BZDs into three categories has been proposed: (i) full allosteric modulators (FAMs) that act with high potency and efficacy at many $GABA_A$ receptors; (ii) selective allosteric modulators (SAMs) that act with high potency and high efficacy at selective $GABA_A$ receptors; and (iii) partial allosteric modulators (PAMs) that act with high potency but low efficacy at many $GABA_A$ receptors (Puia *et al.*, 1991; Ducic *et al.*, 1993). The *in vivo* pharmacological activity of PAMs appears different from that of high efficacy allosteric modulators (i.e. SAMs and FAMs). In particular, the separation of the desirable (i.e. anxiolytic) and undesirable (i.e. sedation and ataxia) effects of some BZD receptor ligands has been attributed to their partial allosteric modulation and explained in terms of different receptor reserves of neural systems involved in the various effects of BZDs (Haefely *et al.*, 1990).

Imidazenil (6-(2-bromophenyl)-8-fluoro-4H-imidazo [1,5-a]-benzodiazepine-3-carboxamide), an imidazobenzodiazepine carboxamide has been recently characterized as a representative of the PAM class (Giusti *et al.*, 1993). In *in vivo* tests, imidazenil showed anticonflict and anticonvulsant properties. Furthermore, it was virtually devoid of side effects such as ataxia, sedation, potentiation of ethanol and barbiturates at doses considerably higher than those producing the anticonflict and anticonvulsant effects. In binding experiments, imidazenil displaced [^{3}H]-flumazenil binding both *in vivo* and in crude synaptic membranes. On the other hand, it failed to displace a number of other radioligands from their binding sites, thus indicating no interaction with peripheral BZD,

[1] Author for correspondence.

$GABA_B$, dopamine, 5-hydroxytryptamine (5-HT_1 and 5-HT_2), glutamate, opiate, cholecystokinin (CCK) and β-adrenoceptors.

To investigate further the binding properties of imidazenil, [³H]-imidazenil with high specific activity was synthesized and its interactions with BZD receptor sites on washed rat cerebellar membranes were studied. Moreover, the effects of GABA and temperature on [³H]-imidazenil binding were evaluated, since the affinity of many ³H-BZDs for their receptors is strongly affected by both factors (Speth *et al.*, 1978; Quast *et al.*, 1982; Earle *et al.*, 1987). Finally, binding parameters were measured in different rat brain areas and compared with those obtained from the binding of [³H]-flumazenil, which is a selective, high affinity and competitive ligand at central BZD receptors (Hunkeler *et al.*, 1981). We are now reporting that the high affinity, saturable and specific binding of [³H]-imidazenil to rat cerebellar membranes is associated with the BZD receptor site on the $GABA_A$ receptor macromolecular complex at which it exhibits a peculiar profile with respect to known positive allosteric modulators.

Methods

Membrane preparation

Male SD/Rij rats (FRAR, S. Pietro al Natisone, UD, Italy) weighing 200–250 g were used. Different brain areas were rapidly dissected on ice and homogenized in 20 ml of ice-cold 0.32 M sucrose, pH 7.4, in a glass homogenizer with a Teflon pestle (10 up and down strokes).

The homogenate was centrifuged at 1,000 *g* at 4°C for 10 min, the P_1 pellet was discarded and the supernatant was collected and recentrifuged at 20,000 *g* at 4°C for 20 min. The resulting crude mitochondrial pellet (P_2) was resuspended in 20 ml of ice-cold distilled water and homogenized. The homogenate was centrifuged at 8,000 *g* at 4°C for 20 min, the supernatant was collected and recentrifuged at 48,000 *g* at 4°C for 20 min and the final crude microsomal pellet (P_3) was frozen for at least 24 h.

The pellet was resuspended in 10 ml of 50 mM Tris-HCl pH 7.4, centrifuged at 48,000 *g* at 4°C for 20 min and then resuspended in 10 volumes of Tris-HCl, pH 7.4 + NaCl 120 mM + KCl 5 mM (incubation medium) for standard binding assay.

Radioligand binding assay

Aliquots of membrane suspensions (100 µl, or 0.15 mg of protein) were added to incubation medium containing different concentrations of [³H]-imidazenil (specific activity 20.65 Ci $mmol^{-1}$) or [³H]-flumazenil (specific activity 72.4 Ci $mmol^{-1}$) in a final volume of 1 ml.

Incubations were carried out in triplicate and non specific binding measured in the presence of 1 µM flumazenil, dissolved in 1% dimethylsulphoxide (DMSO). In saturation experiments, reactions were carried out for 90 min at 0°C, 30 min at 21°C and 5 min at 37°C for [³H]-imidazenil and for 60 min at 21°C for [³H]-flumazenil. Reactions were stopped by the addition of 5 ml ice-cold Tris-HCl followed by rapid filtration through Whatman GF/C glass fibre filters (Whatman Inc., Clifton, NJ) and two additional washes.

The radioactivity trapped on the filters was counted after the addition of 8 ml of Filter Count (Packard), by liquid scintillation spectrometry. Saturation binding isotherm were analysed either according to Scatchard (1949) or by a non linear regression computer programme (Sacchi-Landriani *et al.*, 1983).

Kinetic experiments

Kinetic studies of [³H]-imidazenil were performed at 0, 21 and 37°C. In association studies, membranes were incubated with [³H]-imidazenil (1 nM) in the presence or absence of 1 µM flumazenil to define specific binding. Samples were filtered at different times as described above. Because less than 10% of the radioligand added was bound to the tissue homogenate, pseudo-first-order kinetics could be assumed. The association rate constants K_1 were determined from the slope of the pseudo-first-order plot, $\ln B_o/(B_o-B_t)$, where B_o is the equilibrium binding in association experiments and B_t, is the amount of specific binding at time t (Weiland & Molinoff, 1981). The slope of the plot is the observed rate constant (K_{obs}) for the pseudo-first-order reaction. The association rate constant K_1 was calculated from $K_1 = (K_{obs}-K_{-1})/$ [[³H]-imidazenil]. K_{-1} is the dissociation rate constant and [³H]-imidazenil is the used concentration of radioligand. Dissociation studies were performed by incubating membranes with [³H]-imidazenil (1 nM) to equilibrium and then adding excess cold flumazenil (10 µM) to prevent rebinding of dissociated [³H]-imidazenil. The remaining binding of [³H]-imidazenil was measured at different time intervals. Dissociation rate constant (K_{-1}) followed first-order kinetics and was calculated from the slope of the first order plot, $\ln B_t/B_o$ where B_o and B_t are binding at equilibrium and time t, respectively and t is the time after the addition of flumazenil. The slope of the first-order plot is the dissociation constant $-K_{-1}$ (Weiland & Molinoff, 1981). The K_d for the kinetic binding experiments was determined from the quotient of K_{-1}/K_1.

Effect of ATP on association kinetics

The association of [³H]-imidazenil (1 nM) was measured as a function of time at 21°C in the absence or presence of 5 mM ATP. The rate constant K_{obs} was calculated as described above.

Thermodynamics

Thermodynamic analysis was performed according to Weiland & Molinoff (1981). The K_d values were plotted on a semilogarithmic scale versus T^{-1} (Van't Hoff plot). The change in enthalpy (ΔH) can be calculated from the slope of the plot, -ΔH/R, where R is the gas constant (1.987 cal $degree^{-1}$ mol^{-1}). The free energy of binding (ΔG), is related to the equilibrium dissociation constant K_d by the following formula: $\Delta G = -RT\ln K_A$, where R is the gas constant, T is the absolute temperature and K_A is $1/K_d$. The variations in free energy and enthalpy are connected to the changes in entropy (ΔS) by the Gibbs equation: $\Delta G = DH-T\Delta S$.

Effect of GABA on the specific binding of [³H]-imidazenil

GABA (100 µM) was added to washed, frozen-thawed membranes in the presence of different concentrations of [³H]-imidazenil (0.1–90 nM) at 0, 21 and 37°C. Incubations were carried out as described above. Specific binding was defined in the presence of 1 µM flumazenil.

Inhibition of [³H]-imidazenil binding by various drugs

Increasing concentrations (0.01 nM–10 µM) of drugs were dissolved in DMSO (1%) and added to 1 nM [³H]-imidazenil. All subsequent steps were performed as above. IC_{50} was defined as the concentration of drug that elicited half-maximal inhibition of specific binding. The inhibition constant (K_i) was calculated with the Cheng and Prusoff equation, $K_i = IC_{50}/(1 + L/K_d)$ where L is the concentration of free labelled ligand and K_d the equilibrium dissociation constant of the labelled ligand (Cheng & Prusoff, 1973).

Drugs

Imidazenil and [³H]-imidazenil were synthesized at Hoffmann-La Roche (Nutley, NJ, U.S.A.). The radiochemical

purity of [³H]-imidazenil was initially found to be 99% when determined by high pressure liquid chromatography on a ODS-10 column (250 by 4 mm) (Bio-Rad Laboratories, Richmond, CA, U.S.A.) using the following mobile phase: 60% acetonitrile-0.1% trifluoroacetic acid. [³H]-flumazenil was obtained from New England Nuclear (Boston, MA, U.S.A.).

Diazepam, bretazenil, flumazenil, ethyl-8-azido-5,6-dihydro-5-methyl-6-oxo-4H-imidazo-[1,5a][1,4]benzodiazepine-3-carboxylate (Ro 15-4513) and clonazepam were a gift from Hoffman-La Roche (Nutley, NJ, U.S.A.). Zolpidem and alpidem were generously supplied from Synthélabo (Paris, France). Triazolam was obtained from Upjohn Co. (Kalamazoo, MI, U.S.A.). Thiopentone, bicuculline, pentylenetetrazole (PTZ), GABA and ATP were purchased from Sigma (St. Louis, MO, U.S.A.). 1-(2-Chlorophenyl)-*N*-methyl-*N*-(1-methyl-propyl)-3-isoquinaline carboxamide (PK 11195) and methyl-β-carboline-3-carboxylate (βCCM) were obtained from RBI (Natick, MA, U.S.A.).

Results

Radioligand binding assay

The specific binding of [³H]-imidazenil increased linearly with the concentration of rat cerebellar membranes up to 0.25 mg ml^{-1} (data not shown). A tissue concentration of 0.15 mg ml^{-1} was subsequently used for routine binding studies. The binding of [³H]-imidazenil to rat cerebellar membranes, evaluated as a function of radioactive ligand concentration, indicated the occurrence of high-affinity, specific and saturable binding sites at 0, 21 and 37°C (Figure 1). Non linear regression and Scatchard analysis of the data were compatible with the presence of a single population of receptor sites at all tested temperatures. The maximal density of binding sites (B_{max}) was 0.74 ± 0.02, 0.90 ± 0.01 and 1.01 ± 0.04 pmol mg^{-1} protein at 0, 21 and 37°C, respectively. The equilibrium dissociation constants (K_d) were 0.29 ± 0.052 nM (0°C), 1.0 ± 0.084 nM (21°C) and 2.4 ± 0.38 nM (37°C).

Kinetic experiments

Kinetics of [³H]-imidazenil binding was performed at the same temperatures and indicated that binding was rapid and fully reversible. In association studies, the reaction reached equilibrium after 90 min at 0°C, 25 min at 21°C and less than 5 min at 37°C. No further binding was observed up to 24 h (0°C) (data not shown), 4 h (21°C) and 1 h (37°C) (Figure 2). At 37°C, the maximum specific binding attained with 1 nM [³H]-imidazenil was 0.45 ± 0.0073 pmol mg^{-1} protein, whereas it was 0.77 ± 0.083 and 0.77 ± 0.0051 at 0 and 21°C, respectively (Figure 2). The association rate constants (K_1) were calculated, as described in Methods, at all temperatures with the exception of 37°C, where the equilibrium state was reached too fast to allow the calculation of a reliable value of K_1 (Table 1). The addition of 5 mM ATP to the incubation medium did not modify the association rate constant at 21°C. In fact, K_{obs} values were 0.097 ± 0.015 and 0.098 ± 0.017 min^{-1} in the absence or presence of ATP, respectively. Maximum specific binding was 0.77 ± 0.021 (− ATP) and 0.72 ± 0.023 (+ ATP) pmol mg^{-1} protein. In dissociation studies, [³H]-imidazenil binding appeared fully reversible at all tested temperatures (Figure 3). The reaction was very slow at 0°C, but it proceeded faster with increasing temperatures. For instance, at 37°C, [³H]-imidazenil was completely displaced from its binding sites in less than 5 min (Figure 3). The calculated dissociation rate constants (K_{-1}) are shown in Table 1. The K_d values calculated according to the formula ($K_d = K_{-1}/K_1$) approximated the dissociation constants measured in equilibrium binding studies, when determined (Table 1).

Thermodynamics

Thermodynamic analysis of receptor-ligand interaction showed that binding of [³H]-imidazenil to its recognition sites was associated with a decrease in enthalpy and only a slight decrease in entropy. ΔH was −9.12 kcal mol^{-1} at all the temperatures; ΔG were −11.91, −12.08 and −12.23 kcal mol^{-1} at 0, 21 and 37°C, respectively; ΔS were +10.22,

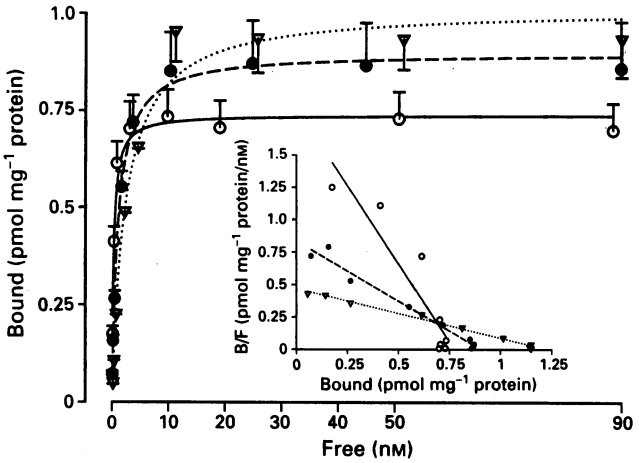

Figure 1 Binding of [³H]-imidazenil (0.1–90 nM) to rat cerebellar membranes was performed under standard conditions at 0 (○), 21 (●) and 37°C (▽), as described in Methods. Results are presented as the mean values ± s.e.mean from at least three observations. Inset shows Scatchard plot for specific [³H]-imidazenil binding at the same temperatures. The mean values ± s.e.mean of the K_d and B_{max} are given in the text.

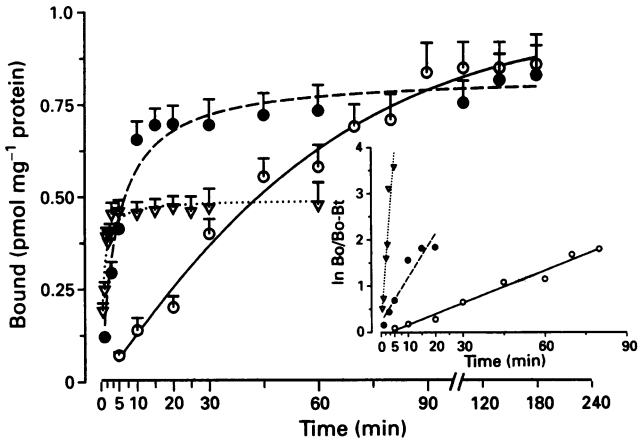

Figure 2 Association kinetics of [³H]-imidazenil (1.0 nM) binding were measured as a function of time at 0 (○), 21 (●) and 37°C (▽). Specific binding was determined in the presence of 1 μM flumazenil. Inset shows pseudo-first-order kinetic plot of specific [³H]-imidazenil binding at all tested temperatures. Association rate constants are shown in Table 1.

Table 1 [³H]-imidazenil kinetic parameters on rat cerebellar membranes

Temperature (°C)	K_1 (min^{-1} nM^{-1})	K_{-1} (min^{-1})	K_d (nM)
0	0.023 ± 0.0011	0.0041 ± 0.0030	0.18 ± 0.0020
21	0.032 ± 0.015	0.063 ± 0.0056	1.99 ± 0.012
37	ND[a]	0.70 ± 0.047	ND

Assays of [³H]-imidazenil binding were performed as described in Methods. Each kinetic value is the mean ± s.e.mean from three independent determinations. [a]ND, not determined.

+10.07 and +10.03 kcal mol^{-1} T^{-1} at 0, 21 and 37°C, respectively. In addition, when the dependence upon temperature of the K_d of [³H]-imidazenil binding was studied using a Van't Hoff plot, the plotted data were fitted by a straight line ($r = 0.984$). K_d were: 0.29 ± 0.051 nM (0°C); 0.83 ± 0.10 nM (12°C); 1.0 ± 0.080 nM (21°C); 1.9 ± 0.25 (30°C); and 2.4 ± 0.38 (37°C).

Effect of GABA on the specific binding of [³H]-imidazenil

The addition of GABA (100 μM) to the incubation medium slightly increased the B_{max} values of [³H]-imidazenil binding to washed cerebellar membranes. Similar values of K_d were obtained at 21° and 37°C, in the absence or presence of GABA. In contrast, at 0°C, a fourfold increase in K_d could be observed (Table 2).

Inhibition of [³H]-imidazenil binding by various drugs

Specificity of imidazenil binding to central BZD receptors was studied in displacement experiments by use of several substances interacting with distinct sites on the $GABA_A$ receptor complex. [³H]-imidazenil binding to rat cerebellar membranes was effectively inhibited by BZDs (bretazenil, clonazepam, diazepam, flumazenil, imidazenil, Ro 15-4513 and triazolam), imidazopyridines (alipidem and zolpidem) and a β-carboline (βCCM). Among these drugs, bretazenil, imidazenil and βCCM were the most effective displacers (Table 3). Triazolam and flumazenil were effective inhibitors at nanomolar concentrations, followed by Ro 15-4513 and clonazepam. Diazepam, alpidem and zolpidem were less effective as displacing agents, whereas bicuculline, thiopentone, PTZ and PK 11195 were completely inactive (Table 3).

Regional distribution of [³H]-imidazenil binding sites

Marked regional variations in [³H]-imidazenil binding parameters were measured in different rat brain areas. The greatest density of binding sites was found in rat cerebral cortex and striatum; the cerebellum exhibited a smaller number of binding sites and the spinal cord displayed the least amount of binding (Table 4). A similar number as well as regional distribution of [³H]-flumazenil binding sites was observed (Table 4).

Discussion

Our data showed that the binding of [³H]-imidazenil to rat cerebellar membranes met most conventional criteria defining a specific receptor-ligand interaction. It was of high affinity, saturable, reversible and specific between 0 and 37°C. Moreover, binding analysis indicated the presence of a single population of receptor sites. We measured a temperature-dependent change in the binding affinity whereas the maximal number of recognition sites was unchanged. The same pattern of K_d changes was observed using a kinetic analysis of [³H]-imidazenil binding. These results are consistent with previous findings, that indicate a temperature dependence for *in vitro* ³H-BZD binding (Speth *et al.*, 1978; Quast *et al.*, 1982; Möhler *et al.*, 1981).

In association studies, the [³H]-imidazenil maximum

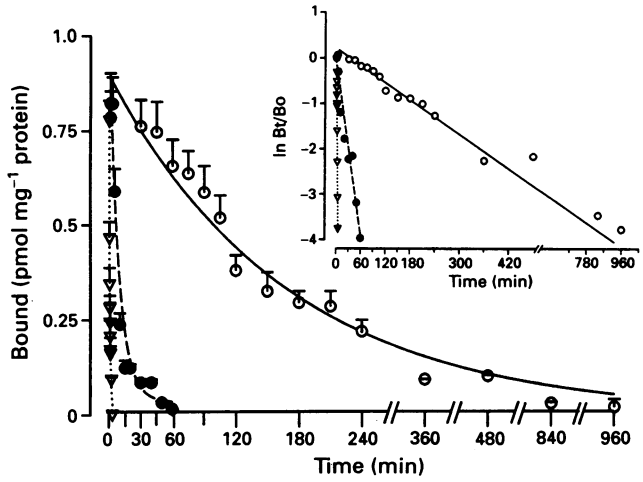

Figure 3 Dissociation kinetics of [³H]-imidazenil binding. [³H]-imidazenil was allowed to equilibrate for 90 min at 0°C (○), 30 min at 21°C (●) and 5 min at 37°C (▽). After equilibrium binding, excess cold flumazenil (10 μM) was added for the indicated time and residual binding was measured. Inset shows a semilogarithmic plot of B_t/B_o as a function of time. Dissociation rate constants are shown in Table 1.

Table 3 Inhibition of [³H]-imidazenil binding on rat cerebellar membranes

Displacers	K_i (nM)
Bretazenil	0.03 ± 0.0051
Imidazenil	0.24 ± 0.032
βCCM	0.45 ± 0.042
Triazolam	0.98 ± 0.14
Flumazenil	1.40 ± 0.23
Ro 15-4513	3.6 ± 0.42
Clonazepam	4.5 ± 0.43
Diazepam	20 ± 1.8
Zolpidem	33 ± 2.9
Alpidem	39 ± 2.7
Bicuculline	>30,000
Thiopentone	>30,000
PTZ	>30,000
PK 11195	>30,000

Displacement of [³H]-imidazenil (1 nM) was performed as described in Methods at 21°C. Data are presented as mean values ± s.e.mean from three observations. Each curve consisted of at least nine concentrations, each performed in triplicate.

Table 2 Effect of GABA on [³H]-imidazenil binding to rat cerebellar membranes

	−GABA		*+GABA*	
Temperature (°C)	B_{max} (pmol mg^{-1} protein)	K_d (nM)	B_{max} (pmol mg^{-1} protein)	K_d (nM)
0	0.74 ± 0.020	0.29 ± 0.051	0.9 ± 0.026	1.2 ± 0.15
21	0.90 ± 0.011	1.0 ± 0.080	1.2 ± 0.055	1.4 ± 0.15
37	1.0 ± 0.036	2.4 ± 0.38	1.2 ± 0.035	2.3 ± 0.13

Binding of [³H]-imidazenil (0.1–90 nM) was performed under standard conditions, at the indicated temperatures, in the presence or absence of GABA (100 μM). Results are presented as mean values ± s.e.mean from three independent experiments, each performed in triplicate.

Table 4 Regional distribution of specific [³H]-imidazenil and [³H]-flumazenil binding in rat CNS

	[³H]-imidazenil		[³H]-flumazenil	
	B_{max} (pmol mg^{-1} protein)	K_d (nM)	B_{max} (pmol mg^{-1} protein)	K_d (nM)
Cerebellum	0.90 ± 0.01	1.04 ± 0.08	0.88 ± 0.12	1.3 ± 0.18
Cortex	1.4 ± 0.14	0.89 ± 0.012	1.2 ± 0.014	1.3 ± 0.023
Striatum	1.2 ± 0.0012	1.5 ± 0.056	0.98 ± 0.052	1.6 ± 0.13
Spinal cord	0.24 ± 0.011	0.90 ± 0.014	0.22 ± 0.023	3.8 ± 0.12

Washed brain membranes from various CNS regions were prepared as described in Methods and incubated with different concentrations of [³H]-imidazenil for 90 min at 21°C or [³H]-flumazenil for 60 min at 21°C. Results are presented as mean values ± s.e.mean from three independent experiments.

specific binding at 37°C was nearly a half of that measured both at 0 and 21°C. This observation is apparently in contrast with the results of saturation experiments. An explanation for this discrepancy could be that a conformational rearrangement of the $GABA_A$ receptor complex takes place at high temperature. The β-subunits of the $GABA_A$ receptors contain sites for intracellular phosphorylation and this process may be crucial in the regulation of $GABA_A$ receptors (Zorumski *et al.*, 1991). Therefore, a temperature-dependent high level of $GABA_A$ receptor phosphorylation could account for the reduced number of [³H]-imidazenil binding sites measured at 37°C. Should this be the case, the addition of ATP, at 21°C, to stimulate a receptor kinase that phosphorylates ligand-receptor complexes (Sibley *et al.*, 1987), would have reduced the amount of [³H]-imidazenil binding to the same value observed at 37°C. The number of binding sites, however, was not decreased in the presence of ATP. It is possible that at 37°C, when incubation is protracted beyond equilibrium, some proteolysis of receptors occurs. Because of the inadequacy of the binding approach, an answer to this question can be obtained only by using transfected cells containing cDNA encoding for the different $GABA_A$ receptor subunits.

Thermodynamic studies showed that [³H]-imidazenil binding was enthalpy and entropy driven. K_d and temperature were related by a linear Van't Hoff plot. Similar results have been reported for [³H]-flumazenil binding (Möhler *et al.*, 1981; Kopp *et al.*, 1990). Conversely, a break in linearity at about 16°C has been observed for [³H]-flunitrazepam (Speth *et al.*, 1978), [³H]-clonazepam (Möhler *et al.*, 1981) and [³H]-diazepam (Braestrup *et al.*, 1977) binding. This phenomenon has been described in the context of a two-step interaction model of receptor binding (Weiland *et al.*, 1979; Möhler *et al.*, 1981). Accordingly, all BZD ligands bind to their receptors with similar thermodynamic components at low temperature, but only BZD ligands provided with intrinsic activity are able to induce a conformational change of the receptors above 16°C.

The interaction of BZDs with their recognition site at the $GABA_A$ receptor is allosterically modulated by the presence of GABA (GABA shift) (Möhler *et al.*, 1981; Braestrup *et al.*, 1982; Earle *et al.*, 1987). The binding of SAMs and FAMs is markedly enhanced by GABA, whereas that of PAMs or ligands with no intrinsic activity is largely unaffected (Giusti *et al.*, 1993). Unlike positive allosteric modulators, the potency of βCCM (a negative allosteric modulator) in displacing [³H]-flumazenil is decreased in the presence of GABA (Möhler *et al.*, 1981). A negative (at 0°C) or no shift (21 and 37°C) in the K_d of [³H]-imidazenil binding was measured in the presence of GABA. On the contrary, in a previous paper (Giusti *et al.*, 1993) we showed that GABA increased 1.7 fold the potency of imidazenil in displacing [³H]-flumazenil binding and the effect was less than that obtained with diazepam. Differences in temperature and binding methodology could explain such discrepancies. It should be considered, however, that only few partial agonists have been studied so far to infer a general behaviour for this class of drugs in the GABA shift.

In displacement experiments, only BZD ligands (BZDs, imidazopyridines and βCCM) were shown to be active inhibitors of [³H]-imidazenil binding. Compounds acting at other sites on the $GABA_A$ receptor complex showed no significant inhibition of [³H]-imidazenil binding. The experiments were performed at 21°C. Then, similar to what has been reported in saturation studies, a leftward shift in K_i could be expected if binding is measured at lower temperatures. However, the rank order of potency of the various compounds should be maintained (Speth *et al.*, 1978).

In regional studies [³H]-imidazenil marked the same number of binding sites as [³H]-flumazenil, in agreement with data reported for positive allosteric modulators such as clonazepam (Möhler *et al.*, 1981) and zolpidem (Arbilla *et al.*, 1986), which selectively bind to the central type of the BZD receptors.

Altogether, the present results show that imidazenil selectively binds to the BZD site located on the supramolecular $GABA_A$ receptor complex. Moreover, GABA- and temperature-induced effects on K_d indicate that imidazenil interacts with this receptor in a manner similar to flumazenil. Imidazenil, therefore, should be classified as a BZD ligand with no intrinsic activity. Findings that this agent failed to modify [³⁵S]-TBPS binding and muscimol-stimulated $^{36}Cl^-$ uptake (Serra *et al.*, 1994) seem consistent with this suggestion. However, a clear PAM profile for imidazenil has emerged from both *in vitro* and *in vivo* tests (Giusti *et al.*, 1993). In these studies imidazenil was compared to several BZDs, including clonazepam. Clonazepam is the only commercially available BZD ligand showing features of a PAM; in fact, its intrinsic efficacy is lower than that of diazepam (Bonetti *et al.*, 1987). Nevertheless, imidazenil and clonazepam exhibit different pharmacological profiles in rats. Imidazenil is more potent but less effective than clonazepam against bicuculline- and PTZ-induced seizures (Giusti *et al.*, 1993). Clonazepam, but not imidazenil, was found to potentiate the action of ethanol and thiopentone and to produce sedation and ataxia at anxiolytic doses (Giusti *et al.*, 1993). Moreover, tolerance to the anticonvulsant effects of clonazepam has been reported (Gent *et al.*, 1985; Young *et al.*, 1987), while preliminary evidence indicates low tolerance liability for imidazenil (Auta *et al.*, 1994). Furthermore, binding studies showed that, unlike imidazenil, clonazepam interacts with BZD receptors in a manner that is closer to that of FAMs and SAMs (Möhler *et al.*, 1981). It is suggested that the peculiar nature of imidazenil interaction with the BZD-$GABA_A$ supramolecular receptor complex could account for the production of beneficial effects (i.e. anxiolytic and anticonvulsant) with less unwanted outcomes (i.e. sedation, ataxia and tolerance) after imidazenil administration. The study of the thermodynamic interactions at BZD-$GABA_A$ receptors may then allow the identification of active BZD ligands with minimal side effects.

References

ARBILLA, S., ALLEN, J., WICK, A. & LANGER, S.S. (1986). High affinity [^{3}H]-zolpidem binding in the rat brain: an imidazopyridine with agonist properties at central benzodiazepine receptors. *Eur. J. Pharmacol.*, **130**, 257–263.

AUTA, J., GIUSTI, P., GUIDOTTI, A. & COSTA, E. (1994). Imidazenil, a partial positive allosteric modulator of $GABA_A$ receptors, exhibits low tolerance and dependence liability in the rat. *J. Pharmacol. Exp. Ther.*, **270**, 1262–1269.

BONETTI, E.P., POLC, P., LAURENT, J.-P., SCHOCH, P. & HAEFELY, W. (1987). Clonazepam is a partial agonist at benzodiazepine receptor. *Neuroscience*, **22** (Suppl.), S82.

BRAESTRUP, C & SQUIRES, R.F. (1977). Specific benzodiazepine receptors in rat brain characterized by high affinity [^{3}H]-binding. *Proc. Natl. Acad. Sci. U.S.A.*, **74**, 3805–3809.

BRAESTRUP, C., SCHMIECHEN, R., NEFF, G., NIELSEN, M. & PETERSEN, E.N. (1982). Interaction of convulsive ligands with benzodiazepines receptors. *Science*, **216**, 1241–1243.

CHENG, Y.L. & PRUSOFF, W.H. (1973). Relationship between the inhibition constant (K_i) and the concentration of inhibitor which causes 50 per cent inhibition (IC_{50}) of an enzymatic reaction. *Biochem. Pharmacol.*, **22**, 3099–3108.

COSTA, E., GUIDOTTI, A., MAO, C.C. & SURIA, A. (1975). New concepts on the mechanism of action of benzodiazepines. *Life Sci.*, **17**, 167–186.

DUCIC, I., PUIA, G., VICINI, S. & COSTA, E. (1993). Triazolam is more efficacious than diazepam in a broad spectrum of recombinant $GABA_A$ receptors. *Eur. J. Pharmacol.*, **244**, 29–35.

EARLE, M.E., CONCAS, A., WAMSLEY, J.K. & YAMAMURA, H.I. (1987). Temperature dependence and GABA modulation of [^{3}H]-triazolam binding in the rat brain. *Life Sci.*, **41**, 397–403.

GENT, J.P., FEELY, M.P. & HAIGH, J.R.M. (1985). Differences between the tolerance characteristics of two anticonvulsant benzodiazepines. *Life Sci.*, **37**, 849–856.

GIUSTI, P., DUCIC, I., PUIA, G., ARBAN, R., WALSER, A., GUIDOTTI, A. & COSTA, E. (1993). Imidazenil: a new partial positive allosteric modulator of GABA action at $GABA_A$ receptors. *J. Pharmacol. Exp. Ther.*, **266**, 1018–1028.

GREENBLATT, D.J., ABERNATHY, M.D., DIVOLL, R., HARMATZ, J.S. & SHADER, R.I. (1983). Pharmacokinetic properties of benzodiazepine hypnotics. *J. Clin. Psychopharmacol.*, **3**, 129–136.

HAEFELY, W., KULCSAR, A., MÖHLER, H., PIERI, L., POLC, P. & SCHAFFNER, R. (1975). The involvement of GABA in the central actions of benzodiazepines. In *Mechanism of Action of Benzodiazepines*. ed. Costa, E. & Greengard, P. p. 131 New York: Raven Press.

HAEFELY, W., KYBURTZ, E., GERECKE, M. & MÖHLER, H. (1985). Recent advances in the molecular pharmacology of benzodiazepine receptors and in the structure activity relationship of their agonist and antagonist. *Adv. Drug Res.*, **14**, 167–322.

HAEFELY, W., MARTIN, J.R. & SCHOCH, P. (1990). Novel anxiolytics that act as partial agonists at benzodiazepine receptors. *Trends Pharmacol. Sci.*, **11**, 452–456.

HUNKELER, W., MÖHLER, H., PIERI, L., POLC, P., BONETTI, E.P., CUMIN, R., SHAFFNER, R. & HAEFELY, W. (1981). Selective antagonists of benzodiazepine. *Nature*, **290**, 514–516.

KOPP, J., HALL, H., PERSSON, A. & SEDVALL, G. (1990). Temperature dependence of [^{3}H]-Ro 15-1788 binding to benzodiazepine receptors in human postmortem brain homogenates. *J. Neurochem.*, **55**, 1310–1315.

MATSUMOTO, K. & FUKUTA, H. (1982). Stimulatory and protective effects of benzodiazepine on GABA receptors labelled with [^{3}H]-muscimol. *Life Sci.*, **30**, 935–943.

MÖHLER, H. & RICHARDS, J.G. (1981). Agonist and antagonist benzodiazepine receptor interaction *in vitro*. *Nature*, **294**, 763–765.

OLSEN, R.W. (1982). Drug interactions at the GABA receptor-ionophore complex. *Annu. Rev. Pharmacol. Toxicol.*, **22**, 245–277.

PUIA, G., VICINI, S., SEEBURG, P.H. & COSTA, E. (1991). Influence of recombinant γ-aminobutyric $acid_A$-receptor subunit composition on the action of allosteric modulators of gamma-aminobutyric acid-gated Cl^- channels. *Mol. Pharmacol.*, **39**, 691–696.

QUAST, U., MÄHLMANN, H. & VOLLMER, K.-O. (1982). Temperature dependence of the benzodiazepine-receptor interaction. *Mol. Pharmacol.*, **22**, 20–25.

SACCHI-LANDRIANI, G., GUARDABASSO, V. & ROCCHETTI, M. (1983). A microcomputer program for non-linear fitting. *Comp. Programs Biomed.*, **16**, 35–42.

SCATCHARD, G. (1949). The attractions of proteins for small molecules and ions. *Ann. N.Y. Acad. Sci.*, **51**, 660–672.

SEEBURG, P.H., WISDEN, W., VERDOORN, T.A., PRITCHETT, D.B., WERNER, P., HERB, A., LUEDDENS, H., SPRENGEL, R. & SACKMANN, B. (1990). The $GABA_A$ receptor family molecular and functional diversity. *Cold Spring Harbour Symp. Quant. Biol.*, **55**, 29–40.

SERRA, M., GHIANI, C.A., MOTZO, C., CUCCHEDDU, T., FLORIS, S., GIUSTI, P. & BIGGIO, G. (1994). Imidazenil, a new partial agonist of benzodiazepine receptors, reverses the inhibitory action of isoniazid and stress on γ-aminobutyric $acid_A$ receptor function. *J. Pharmacol. Exp. Ther.*, **269**, 32–38.

SIBLEY, D.R., BENOVIC, J.L., CARON, M.G. & LEFKOWITZ, R.J. (1987). Regulation of transmembrane signalling by receptor phosphorylation. *Cell*, **48**, 913–922.

SPETH, R.C., WASTEK, G.J. & YAMAMURA, H. (1978). Benzodiazepine receptors: temperature dependence of [^{3}H]-flunitrazepam binding. *Life. Sci.*, **24**, 351–358.

VERMA, A. & SNYDER, S.H. (1989). Peripheral type benzodiazepine receptors. *Annu. Rev. Pharm. Toxicol.*, **29**, 307–322.

WEILAND, G.A., MINNEMAN, K.P. & MOLINOFF, P.B. (1979). Fundamental difference between the molecular interactions of agonists and antagonists with the β-adrenergic receptor. *Nature*, **281**, 114–117.

WEILAND, G.A. & MOLINOFF, P.B. (1981). Quantitative analysis of drug-receptor interaction: I. Determination of kinetic and equilibrium properties. *Life Sci.*, **29**, 313–330.

YOUNG, N.A., LEWIS, S.J., HARRIS, Q.L.G., JARROT, B. & VAJDA, F.J.E. (1987). The development of tolerance to the anticonvulsant effects of clonazepam, but not sodium valproate, in the amygdaloid kindled rats. *Neuropharmacol.*, **26**, 1611–1614.

ZORUMSKI, C.F. & ISEMBERG, K.E. (1991). Insights into the structure and functions of GABA-benzodiazepine receptors: ion channels and psychiatry. *Am. J. Psychiatry*, **148**, 162–173.

(Received May 24, 1994
Revised October 13, 1994
Accepted November 17, 1994)

British Journal of Pharmacology (1995) 114, 1165–1170

Ca^{2+} entry activated by emptying of intracellular Ca^{2+} stores in ileal smooth muscle of the rat

[1]Toshio Ohta, Kazue Kawai, Shigeo Ito & Yoshikazu Nakazato

Department of Pharmacology, Faculty of Veterinary Medicine, Hokkaido University, Sapporo 060, Japan

1 The effects of depletion of intracellular Ca^{2+} stores on muscle tension and the intracellular Ca^{2+} concentration ($[Ca^{2+}]_i$) were studied in fura-2 loaded longitudinal smooth muscle cells of the rat ileum.

2 After exposure to a Ca^{2+}-free solution, application of Ca^{2+} caused a small contraction and a rise in $[Ca^{2+}]_i$, both of which were potentiated when the muscle was challenged with carbachol or caffeine before the addition of Ca^{2+}.

3 Cyclopiazonic acid (CPA), a specific inhibitor of sarcoplasmic reticulum Ca^{2+}-ATPase, dose-dependently decreased tension development and the rises in $[Ca^{2+}]_i$ induced by carbachol and caffeine in the Ca^{2+}-free solution, but conversely increased the Ca^{2+}-induced responses even in the presence of the voltage-dependent Ca^{2+} channel blockers, methoxyverapamil and nifedipine.

4 The contraction and rise in $[Ca^{2+}]_i$ evoked by Ca^{2+} gradually declined with time after removal of CPA, while the reverse was the case for the responses to carbachol and caffeine.

5 The Ca^{2+}-induced contraction and rise in $[Ca^{2+}]_i$ in the presence of CPA were inhibited by the replacement of Na^+ with K^+ or Cs^+, and by the addition of Cd^{2+}, Ba^{2+}, Ni^{2+} or La^{3+}.

6 The influx of Mn^{2+} was much greater in extent in the presence of CPA than in its absence.

7 These results suggest that the emptying of intracellular Ca^{2+} stores may activate Ca^{2+} influx not associated with voltage-dependent Ca^{2+} channels in the rat ileal smooth muscle.

Keywords: Ca^{2+} influx; cyclopiazonic acid; intestinal smooth muscle; intracellular Ca^{2+} stores; Mn^{2+}-quenching

Introduction

A rise in the concentration of intracellular Ca^{2+} ($[Ca^{2+}]_i$) is essential for evoking contractile responses in smooth muscle. This activator Ca^{2+} is either released from intracellular Ca^{2+} stores that possess Ca^{2+}-release channels activated by inositol 1,4,5-trisphosphate (IP_3) (Somlyo *et al.*, 1985; Hashimoto *et al.*, 1986) and Ca^{2+} itself (Iino, 1989), or enters into the cells through voltage-dependent Ca^{2+} channels and receptor-operated ones (Bolton, 1979). Recently, the 'capacitative Ca^{2+} entry' hypothesis, postulating that a decrease in the Ca^{2+} content of the intracellular Ca^{2+} stores is sufficient to trigger the Ca^{2+} influx in non-excitable cells, has been proposed (Putney, 1986; 1990). A similar phenomenon has also been observed in vascular (Missiaen *et al.*, 1990; Xuan *et al.*, 1992; Noguera & D'Ocon, 1993; Pacaud *et al.*, 1993) and urinary smooth muscle (Munro & Wendt, 1994). In the rat intestinal smooth muscle, we found that Ca^{2+} caused a large increase in muscle tension, when added after depletion of intracellular Ca^{2+} stores by Ca^{2+}-releasing agents under Ca^{2+}-free conditions. Therefore, it is possible that the 'capacitive Ca^{2+} entry' mechanism is present in this tissue. Nevertheless, in visceral smooth muscle, there is little information about the presence of such a regulatory mechanism for intracellular Ca^{2+} stores.

Cyclopiazonic acid (CPA) has been shown to inhibit the sarcoplasmic reticulum (SR) Ca^{2+}-ATPase pump selectively (Seidler *et al.*, 1989), thereby preventing the uptake of Ca^{2+} into SR. It has also been reported in smooth muscle that CPA promotes depletion of Ca^{2+} from the stores by functionally inhibiting refilling (Bourreau *et al.*, 1991; Shima & Blaustein, 1992; Uyama *et al.*, 1992; Kasai *et al.*, 1994; Munro & Wendt, 1994). CPA, therefore, has been used as a pharmacological tool to study the functional role of Ca^{2+} stores (Darby *et al.*, 1993).

The aim of the present experiments is to determine whether Ca^{2+} stores regulate Ca^{2+} entry, dependent on their filling state in intestinal smooth muscle of the rat. For this purpose, we measured isometric tension and $[Ca^{2+}]_i$ simultaneously in fura-2 loaded tissues. The effects of depletion of store Ca^{2+} induced by CPA on Ca^{2+}-induced contractile responses and $[Ca^{2+}]_i$ responses were also examined. We have already reported that this muscle has both IP_3- and caffeine sensitive Ca^{2+} stores that are functionally important in mediating contractile and membrane current responses (Ito *et al.*, 1993; Ohta *et al*, 1993; 1994). In the present study, we have demonstrated that the emptying of the Ca^{2+} stores induced by CPA initiated a considerable rise in $[Ca^{2+}]_i$ and the contractile response, dependent on the presence of extracellular Ca^{2+}.

Methods

Male Wistar rats (200–300 g) were stunned and bled to death. The ileum was excised and luminal contents were removed by washing with normal physiological salt solution (PSS). The longitudinal muscle layer was peeled from the underlying circular muscle layer and thin muscle strips (1 mm in width, 8 mm in length) were dissected. Then they were incubated with 20 μM fura-2 acetoxymethyl ester (fura-2/AM) and 0.02% cremophore EL, a noncytotoxic detergent, for more than 3 h at room temperature for simultaneous measurement of the contractile activity and intracellular Ca^{2+} concentration ($[Ca^{2+}]_i$). Experiments were carried out with a fluorimeter (CAF-110, Japan Spectroscopic) at room temperature (22–25°C). The muscle strip was held horizontal to the experimental chamber (volume about 0.2 ml) : one end of the muscle strip was fixed with pins to the silicon rubber at the edge of the bottom of the chamber, and the other end was connected to a strain gauge transducer to measure the isometric tension. The bathing solutions were changed by rapidly injecting 5 ml of solution and removing the overflow

[1] Author for correspondence.

by suction. The muscle strips were alternately illuminated by 340 nm and 380 nm light (128 Hz) and the intensity of fluorescence at 500 nm was measured. The ratio of the fluorescence due to excitation at 340 nm to that at 380 nm (F340/F380) was calculated from successive illumination periods and was considered to be an index of $[Ca^{2+}]_i$.

Normal PSS contained (mM): NaCl 144, KCl 5.8, $MgCl_2$ 1.2, $CaCl_2$ 2.5, glucose 11.1, HEPES 5 (pH 7.4 with NaOH). Ca^{2+}-free solution was made by omitting $CaCl_2$ and adding 2 mM EGTA. To determine the effects of Na^+ removal, NaCl was isosmotically replaced by KCl, LiCl or CsCl.

The following chemicals were used: caffeine and methoxyverapamil (Wako Pure. Chem.), carbachol, cremophore EL and cyclopiazonic acid (Sigma), EGTA, Fura-2/AM and HEPES (Dojindo), and nifedipine (Bayer).

Results of the experiments are expressed as the mean ± s.e.mean. Student's t test was used for statistical analysis of the results and $P<0.05$ was considered to indicate a significant difference.

Results

Effects of Ca^{2+}-store release on contraction and $[Ca^{2+}]_i$ induced by application of Ca^{2+}

In the rat ileal longitudinal smooth muscle loaded with fura-2, the contraction and rise in $[Ca^{2+}]_i$ induced by application of Ca^{2+} were observed before and after stimulation with carbachol or caffeine in the Ca^{2+}-free solution. Representative results are shown in Figure 1. After tissues had been incubated with Ca^{2+}-free solution for 7 min, the reintroduction of Ca^{2+} (2.5 mM) produced a small contraction associated with a rise in $[Ca^{2+}]_i$. Two minutes after removal of the external Ca^{2+}, the administration of carbachol (0.1 mM) or caffeine (30 mM) to Ca^{2+}-free solution resulted in a transient contraction and a rise in $[Ca^{2+}]_i$ mediated by Ca^{2+} released from the intracellular Ca^{2+} stores. After washout with fresh Ca^{2+}-free solution, no response was evoked by either carbachol or caffeine applied subsequently, indicating that the intracellular Ca^{2+} stores had been depleted. In such tissues with depleted Ca^{2+} stores, both contractile and $[Ca^{2+}]_i$ responses to the application of Ca^{2+} were markedly enhanced. The contraction and rise in $[Ca^{2+}]_i$ induced by Ca^{2+}-application were enhanced 2.6 ± 0.8 and 1.4 ± 0.3 fold (n = 8), respectively, by the preceding stimulation with caffeine, and 2.2 ± 0.4 and 1.6 ± 0.3 fold (n = 8) with carbachol.

Effects of cyclopiazonic acid on the content of stored Ca^{2+} and on the response to Ca^{2+}-application

To determine the relationship between the filling state of the Ca^{2+} stores and the magnitude of Ca^{2+}-induced responses, the effect of cyclopiazonic acid (CPA) on the responses to Ca^{2+}-application and subsequent carbachol or caffeine was observed. After the control responses were obtained, tissues were treated with various concentrations of CPA for 26 min. At 20 min after the start of CPA treatment, the tissues were exposed to 2.5 mM Ca^{2+} for 3 min to load Ca^{2+} into intracellular stores and were then washed for 2 min with Ca^{2+}-free solution containing 2 mM EGTA. Subsequently, carbachol or caffeine was applied for 1 min under Ca^{2+}-free conditions. The Ca^{2+} content in the stores was estimated by measuring the amplitude of the response to carbachol or caffeine. As shown in Figure 2, 0.3 μM CPA had almost no effect on the contractile and $[Ca^{2+}]_i$ responses to either carbachol or Ca^{2+}-application. CPA over 1 μM caused a decrease in the responses to carbachol and an increase in responses to Ca^{2+} in a concentration-dependent manner. These effects of CPA gradually recovered after washout of the drug as mentioned below. A typical experimental result on the effect of CPA (10 μM) is depicted in Figure 3. In the presence of CPA, the responses to Ca^{2+} were sustained during its application and quickly returned to the original level after its removal. The relationships between the responses to Ca^{2+} and those to carbachol were inverse; that is, the smaller the responses to carbachol, the larger the responses to Ca^{2+}-application. Qualitatively the same result was obtained when caffeine was used instead of carbachol. All these experiments were carried out in the presence of methoxyverapamil (10 μM) or nifedipine (1 μM) to eliminate the possible involvement of voltage-dependent Ca^{2+} channels.

When CPA was withdrawn from the bathing solution, the contraction and rise in $[Ca^{2+}]_i$ evoked by the application of Ca^{2+} gradually declined, dependent on the time after removal of CPA, while the reverse was the case for the responses to

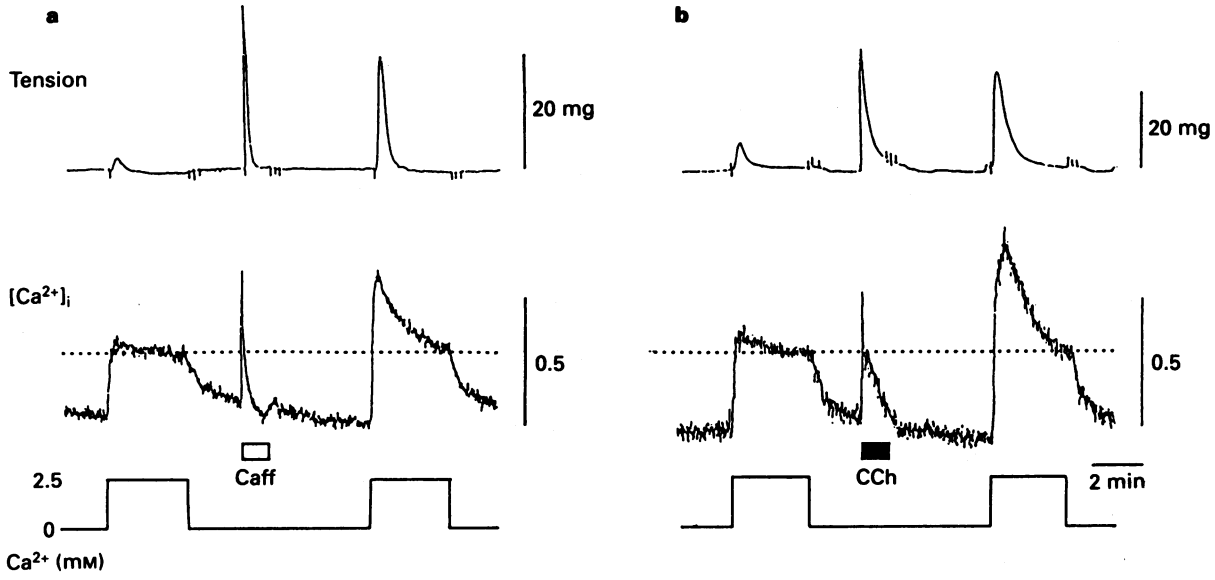

Figure 1 Effects of the preceding application of caffeine (a) and carbachol (b) on the contraction and rise in $[Ca^{2+}]_i$ induced by application of Ca^{2+}. Traces from top to bottom: tension, $[Ca^{2+}]_i$ and the concentration of external Ca^{2+}. The tissues were incubated with Ca^{2+}-free solution for 7 min before the first reintroduction of Ca^{2+} (2.5 mM) for 3 min. Then the tissues were washed for 2 min with Ca^{2+}-free solution containing 2 mM EGTA and were stimulated by caffeine (Caff, □ ; 30 mM) or carbachol (CCh, ■ ; 0.1 mM) for 1 min from 5 min before the second application of Ca^{2+}. Dotted lines indicate the resting $[Ca^{2+}]_i$ level in the normal PSS.

carbachol (Figure 3). The same results were obtained in 3 other experiments and when caffeine was used instead of carbachol. These results indicate that CPA promotes depletion of Ca^{2+} from the stores and potentiates Ca^{2+}-induced responses, suggesting that the Ca^{2+} content in the stores may regulate Ca^{2+} entry into rat intestinal smooth muscle cells.

Effects of CPA on Mn^{2+} influx

It has been shown that Mn^{2+} is a good substitute for Ca^{2+} in defining Ca^{2+} entry pathways, because it can pass through almost all the Ca^{2+} permeable channels but cannot be a substrate for the sarcoplasmic reticulum pump (Gomes De Costa & Madeira, 1986; Missiaen *et al.*, 1990). Therefore, to obtain more direct evidence that Ca^{2+} depletion in the stores promotes Ca^{2+} entry into the cell, Mn^{2+} influx was monitored by Mn^{2+} quenching of fura-2 fluorescence. These experiments were carried out in the presence of methoxyverapamil (10 μM). After tissues were incubated with nominal Ca^{2+}-free solution with or without CPA (10 μM) for 20 min, the external solution was replaced with solution containing Mn^{2+} (0.1 mM). The time courses of Mn^{2+}-induced fura-2 quenching in the presence and absence of CPA are shown in Figure 4. Although the quenching of fura-2 was initiated even in the absence of CPA, the rate of quenching was much greater in the presence of CPA than in its absence. These results suggest that Ca^{2+} permeability of the plasma membrane may be increased by CPA.

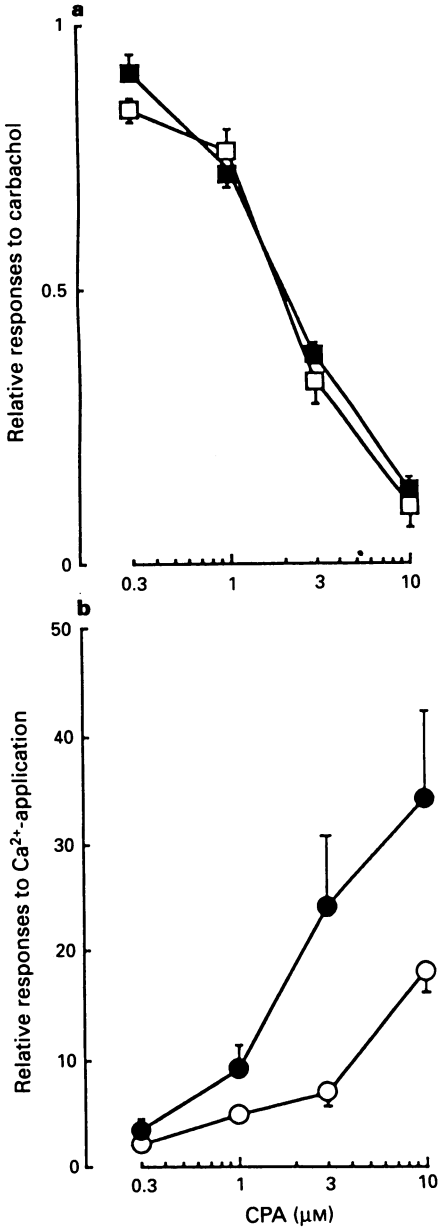

Figure 2 The cyclopiazonic acid (CPA)-evoked concentration-dependent decreases in the responses to carbachol (0.1 mM, a) and increases in responses to Ca^{2+} (2.5 mM, b). The tissues were incubated with each given concentration of CPA for 26 min. The amplitudes (a) and area (b) of the contractile (open symbols) and $[Ca^{2+}]_i$ (filled symbols) responses are plotted against a given concentration of CPA as a percentage of those obtained in the absence of CPA (mean ± s.e. mean, $n = 4$). In the case of the rise of $[Ca^{2+}]_i$ induced by Ca^{2+}, the area above the resting level in normal PSS (2.5 mM Ca^{2+}) was measured. Methoxyverapamil (10 μM) was present throughout the experiments.

Effects of metal ions and replacement of Na^+ with other monovalent cations on $[Ca^{2+}]_i$ and contractile responses in the presence of CPA

Tissues were pretreated with CPA (10 μM) for 20 min and experiments were carried out in its presence. After a sustained rise in $[Ca^{2+}]_i$ and contraction had been evoked by Ca^{2+} (2.5 mM), metal ions were cumulatively added to the bathing solution. Figure 5a is the original traces showing the concentration-dependent inhibitory action of La^{3+}. With this experimental protocol, the concentration-inhibition curves for Cd^{2+}, Ba^{2+}, Ni^{2+} and La^{3+} were constructed and are shown in Figure 5b. All these metal ions dose-dependently inhibited the rise in $[Ca^{2+}]_i$ and contraction induced by Ca^{2+}-application. La^{3+} was the most potent ion and was effective at less than 1 μM. The potency order was $La^{3+} > Ni^{2+} = Ba^{2+} > Cd^{2+}$.

Figure 5c shows the effects of isosmotic replacement of external Na^+ with K^+, Cs^+ or Li^+. Complete substitution of Li^+ for Na^+ slightly increased $[Ca^{2+}]_i$ and contractile responses to Ca^{2+}-application, but that with Cs^{2+} decreased both responses. Replacement of Na^+ with K^+ showed a much greater effect on these responses: increases of K^+ concentrations dose-dependently decreased the rise in $[Ca^{2+}]_i$ and contraction induced by Ca^{2+}-application.

Discussion

The present experiments showed that transient contractions and rises in $[Ca^{2+}]_i$ induced by carbachol and caffeine in Ca^{2+}-free solution were inhibited by a specific sarcoplasmic reticulum Ca^{2+}-ATPase inhibitor, CPA (Seidler *et al.*, 1989) in the longitudinal smooth muscle of the rat ileum, suggesting that Ca^{2+} uptake into the stores is mediated by Ca^{2+}-ATPase pump protein as reported in other smooth muscles (Bourreau *et al.*, 1991; Shima & Blaustein, 1992; Uyama *et al.*, 1992; Kasai *et al.*, 1994; Muro & Wendt, 1994). On the other hand, CPA markedly augmented the rise in $[Ca^{2+}]_i$ and contraction in response to Ca^{2+}-application even in the presence of voltage-dependent Ca^{2+} channel blockers. Both in different concentrations of CPA and during recovery from CPA action there was an inverse correlation between the inhibitory effects on the responses mediated by Ca^{2+} released from the stores, and the potentiating effects on those induced by Ca^{2+}-application.

Since the potentiating effect of CPA on responses to Ca^{2+}-application was still observed in solutions containing Li^+ instead of external Na^+, it is unlikely that depression of the Na^+/Ca^{2+} exchange mechanism contributes to the potentiating effects of CPA. Replacement of Na^+ by Cs^+ or K^+ decreased the CPA-induced potentiation of responses and this inhibitory effect was greater when Na^+ was replaced by K^+. It is well-known that an increase in the external K^+ concentration initiates membrane depolarization (Bolton, 1979) and the same is true for Cs^+ (Sjodin, 1959). Therefore, the inhibitory effect of external K^+ on the responses induced

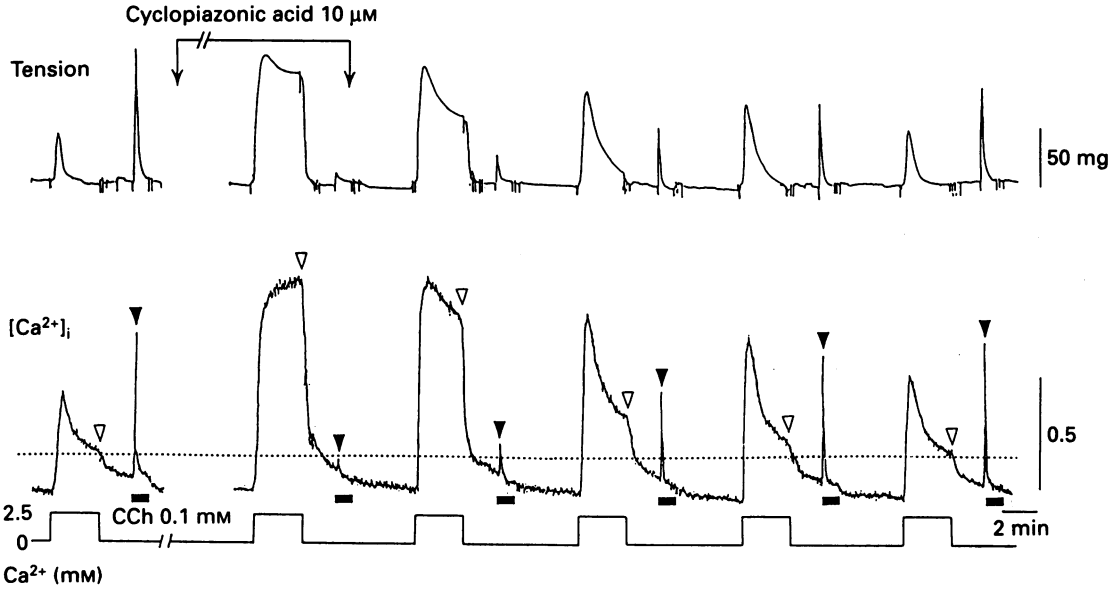

Figure 3 Representative responses to carbachol and Ca^{2+}-application before, during and after the addition of cyclopiazonic acid (CPA). Tissues were treated with CPA (10 μM) for 26 min during the period indicated at the top of the trace. At 20 min after the start of CPA treatment, the tissues were exposed to 2.5 mM Ca^{2+} for 3 min and were then washed for 2 min with Ca^{2+}-free solution containing 2 mM EGTA. Subsequently carbachol (0.1 mM, ■ , 1 min) was applied under Ca^{2+}-free condition. Methoxyverapamil (10 μM) was present throughout the experiments. The dotted line indicates the resting $[Ca^{2+}]_i$ level in normal PSS. ▽ : $[Ca^{2+}]_i$ at 3 min after the application of Ca^{2+}; ▼: peak $[Ca^{2+}]_i$ induced by carbachol in Ca^{2+}-free solution.

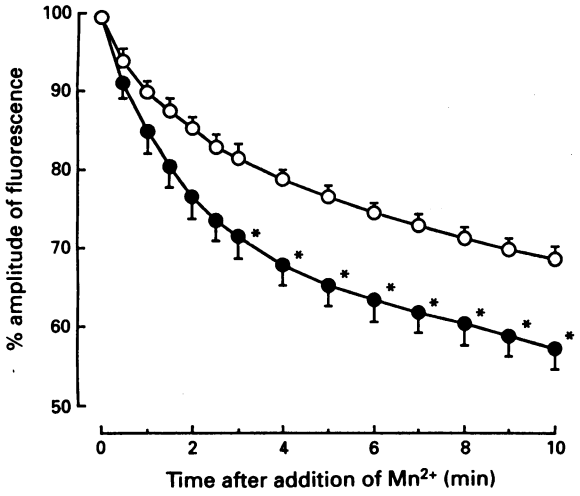

Figure 4 Effects of cyclopiazonic acid (CPA) on Mn^{2+} influx. The time course of quenching of fura-2 fluorescence due to Mn^{2+} influx was monitored in the presence (●, $n = 5$) and absence (○, n = 5) of CPA (10 μM). The amplitude of the fluorescent signal excited at 360 nm (isosbestic point of fura-2) after the addition of Mn^{2+} (0.1 mM) to the nominal Ca^{2+}-free solution is expressed as a percentage of that before the addition of Mn^{2+}. *Significantly different from the control value at $P<0.05$.

by depletion of the Ca^{2+} stores might be due to the reduction of the electrochemial gradient for Ca^{2+} across the cell membrane. A similar phenomenon has been reported in voltage-clamped smooth muscle cells (Pacaud & Bolton, 1991; Pacaud *et al.*, 1993). Furthermore, some metal ions that are known to affect Ca^{2+} flux through the plasma membrane blocked the CPA-induced rise in $[Ca^{2+}]_i$ and contraction in a concentration-dependent manner. These results suggest that the content of Ca^{2+} in the stores may regulate Ca^{2+} entry in rat intestinal smooth muscle.

Most reports concerning Ca^{2+} entry into vascular smooth muscle cells show that Mn^{2+} influx is potentiated by emptying of Ca^{2+} stores (Jacob, 1990; Missiaen *et al.*, 1990; Xuan *et al.*, 1992). Similarly, in the present experiments, acceleration of Mn^{2+} influx was observed in tissues treated with CPA. However, it has been reported that treatments leading to the depletion of Ca^{2+} stores fail to increase Mn^{2+} influx in the rabbit inferior vena cava, suggesting that the rise in $[Ca^{2+}]_i$ resulting from the depletion of the Ca^{2+} stores is due to a disturbance of the superficial buffer barrier system rather than to the activation of Ca^{2+} entry (Chen & van Breeman, 1993). Although we cannot exclude the existence of such a system in the rat ileal smooth muscle, the potentiating effects of store depletion on the responses to Ca^{2+}-application were observed even in tissues with functionally intact Ca^{2+} stores. Since the Ca^{2+} content in the stores must be much less in tissues challenged with Ca^{2+}-releasing agents, the buffering-action capacity of the stores in these tissues should be stronger than in those without Ca^{2+}-releasing stimulation. If so, the rise in $[Ca^{2+}]_i$ should have been small in the tissues stimulated by Ca^{2+}-releasing drugs. Since this was not the case, the contribution of Ca^{2+} buffering, if any, must be small in the rat ileal smooth muscle. The extent of its contribution may be dependent on the different preparations and tissues, because in some smooth muscles a procedure leading to the emptying of Ca^{2+} stores failed to increase $[Ca^{2+}]_i$ (Shima & Blaustein, 1992; Kasai *et al.*, 1994).

Although the precise mechanism of Ca^{2+} entry induced by the depletion of Ca^{2+} stores remains unsolved, several substances have recently been reported to be mediators for this mechanism such as the 'Ca^{2+}-influx factor' found in lymphocyte cell lines (Randriamampita & Tsien, 1993), a phosphatase-related diffusible messenger in *Xenopus* oocytes (Parekh *et al.*, 1993) and a small GTP binding protein in basophilic leukaemia cells (Fasolato *et al.*, 1993) and lacrimal acinar cells (Bird & Putney, 1993). Furthermore, a Ca^{2+}-selective current activated by depletion of intracellular Ca^{2+} stores (I_{CRAC}) has been recorded in mast cells (Hoth & Penner, 1992; Fasolato *et al.*, 1993). Therefore, further biochemical and electrophysiological analyses are necessary to identify the mechanism of Ca^{2+} entry activated by emptying the Ca^{2+} stores in rat intestinal smooth muscle cells.

This work was supported by a Grant-in-Aid for Scientific Research from the Ministry of Education, Science and Culture of Japan. We wish to thank Mr. M. Tabo for his assistance in this research.

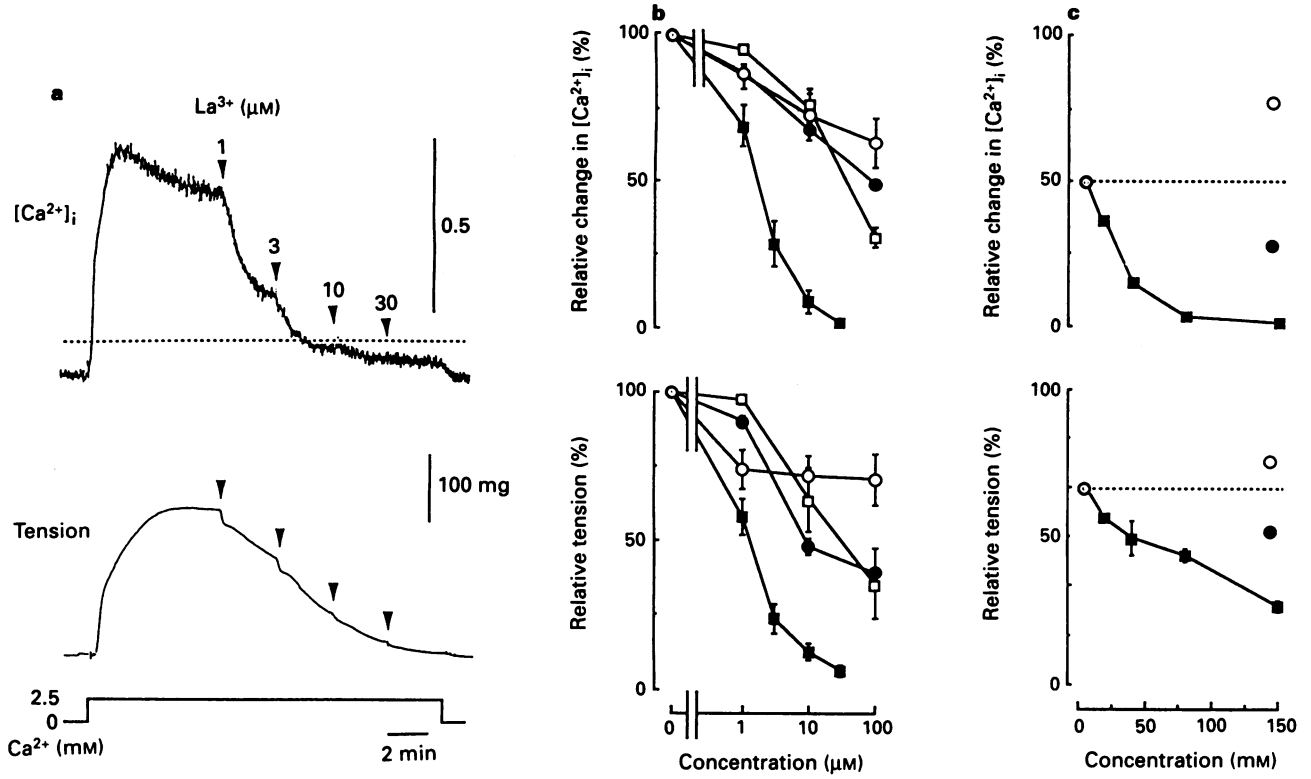

Figure 5 Effects of Cd^{2+}, Ba^{2+}, Ni^{2+} and La^{3+}, and of the replacement of Na^+ with Cs^+, K^+ and Li^+ on the contractile and $[Ca^{2+}]_i$ responses induced by application of Ca^{2+} (2.5 mM) in the presence of cyclopiazonic acid (CPA 10 μM). (a) The original traces showing concentration-dependent inhibitory action of La^{3+}. After the responses to Ca^{2+}-application attained a constant level, La^{3+} was added cumulatively. Traces from top to bottom: tension, $[Ca^{2+}]_i$ and the concentration of external Ca^{2+}. (b) Concentration-response relationships for metal ions: (○) Cd^{2+}; (●) Ba^{2+}; (□) Ni^{2+} and (■) La^{3+}. (c) The effects of Na^+ replacement with other monovalent cations on the contractile and $[Ca^{2+}]_i$ responses induced by application of Ca^{2+}: (○) Li^+; (●) Cs^+ and (■) K^+. Amplitude of the evoked flurorescent signal above the basal level (in the absence of Ca^{2+}) was measured. The amplitude of each response was plotted against the concentration of ions as a percentage of the control (mean ± s.e.mean, $n = 4$). Methoxyverapamil (10 μM) was present throughout the experiments.

References

BIRD, G.St.J. & PUTNEY, J.W. Jr. (1993). Inhibition of thapsigargin-induced calcium entry by microinjected guanine nucleotide analogues. *J. Biol. Chem.*, **268**, 21486–21488.

BOLTON, T.B. (1979). Mechanisms of action of transmitters and other substances on smooth muscle. *Physiol. Rev.*, **59**, 606–718.

BOURREAU, J.P., ABELA, A.P., KWAN, C-Y. & DANIEL, E.E. (1991). Acetylcholine Ca^{2+} stores refilling directly involves a dihydropyridine-sensitive channel in dog trachea. *Am. J. Physiol.*, **261**, C497–C505.

CHEN, Q. & VAN BREEMEN, C. (1993). The superficial buffer barrier in venous smooth muscle: sarcoplasmic reticulum refilling and unloading. *Br. J. Pharmacol.*, **109**, 336–343.

DARBY, P.J., KWAN, C-Y. & DANIEL, E.E. (1993). Use of calcium pump inhibitors in the study of calcium regulation in smooth muscle. *Biol. Signals*, **2**, 293–304.

FASOLATO, C., HOTH, M & PENNER, R. (1993). A GTP-dependent step in the activation mechanism of capacitative calcium influx. *J. Biol. Chem.*, **268**, 20737–20740.

GOMES DE COSTA, A.G. & MADEIRA, V.M.C. (1986). Magnesium and manganese ions modulate Ca^{2+} uptake and its energic coupling in sarcoplasmic reticulum. *Arch. Biochem. Biophys.*, **249**, 199–206.

HASHIMOTO, T., HIRATA, M., ITOH, T., KANMURA, Y. & KURIYAMA, H. (1986). Inositol 1,4,5-trisphosphate activates pharmacomechanical coupling in smooth muscle of the rabbit mesenteric artery. *J. Physiol.*, **370**, 605–618.

HOTH, M. & PENNER, R. (1992). Depletion of intracellular calcium stores activates a calcium current in mast cells. *Nature*, **355**, 353–356.

IINO, M. (1989). Calcium-induced calcium release mechanism in guinea pig taenia caeci. *J. Gen. Physiol.*, **94**, 368–383.

ITO, S., OHTA, T. & NAKAZATO, Y. (1993). Inward current activated by carbachol in rat intestinal smooth muscle cells. *J. Physiol.*, **470**, 395–409.

JACOB, R. (1990). Agonist-stimulated divalent cation entry into single cultured human umbilical vein endothelial cells. *J. Physiol.*, **421**, 55–77.

KASAI, Y., IINO, M., TSUTSUMI, O., TAKETANI, Y. & ENDO, M. (1994). Effects of cyclopiazonic acid on rhythmic contractions in uterine smooth muscle bundles of the rat. *Br. J. Pharmacol.*, **112**, 1132–1136.

MISSIAEN, L., DECLERCK, I., DROOGMANS, G., PLESSERS, L., DE SMEDT, H., RAEYMAEKERS, L. & CASTEELS, R. (1990). Agonist-dependent Ca^{2+} and Mn^{2+} entry dependent on state of filling of Ca^{2+} stores in aortic smooth muscle cells of the rat. *J. Physiol.*, **427**, 171–186.

MUNRO, D.D. & WENDT, I.R. (1994). Effects of cyclopiazonic acid on $[Ca^{2+}]_i$ and contraction in rat urinary bladder smooth muscle. *Cell Calcium*, **15**, 369–380.

NOGUERA, M.A. & D'OCON, M.P. (1993). Evidence that depletion of internal calcium stores sensitive to noradrenaline elicits a contractile response dependent on extracellular calcium in rat aorta. *Br. J. Pharmacol.*, **110**, 861–867.

OHTA, T., ITO, S. & NAKAZATO, Y. (1993). Chloride currents activated by caffeine in rat intestinal smooth muscle cells. *J. Physiol.*, **465**, 149–162.

OHTA, T., ITO, S. & NAKAZATO, Y. (1994). All-or-nothing responses to carbachol in single intestinal smooth muscle cells of rat. *Br. J. Pharmacol.*, **112**, 972–976.

PACAUD, P. & BOLTON, T.B. (1991). Relationship between muscarinic receptor cationic current and internal calcium in guinea-pig jejunal smooth muscle cells. *J. Physiol.*, **441**, 477–499.

PACAUD, P., LOIRAND, G., GRÉGOIRE, G., MIRONNEAU, C. & MIRONNEAU, J. (1993). Noradrenaline-activated heparin-sensitive Ca^{2+} entry after depletion of intracellular Ca^{2+} store in portal vein smooth muscle cells. *J. Biol. Chem.*, **268**, 3866–3872.

PAREKH, A.B., TERLAU, H. & STUHMER, W. (1993). Depletion of $InsP_3$ stores activates a Ca^{2+} and K^+ current by means of a phosphatase and a diffusible messenger. *Nature*, **364**, 814–818.

PUTNEY, J.W. Jr. (1986). A model for receptor-regulated calcium entry. *Cell Calcium*, **7**, 1–12.

PUTNEY, J.W. Jr. (1990). Capacitative calcium entry revisited. *Cell Calcium*, **11**, 611–624.

RANDRIAMAMPITA, C. & TSIEN, R.Y. (1993). Emptying of intracellular Ca^{2+} stores releases a novel small messenger that stimulates Ca^{2+} influx. *Nature*, **364**, 809–814.

SEIDLER N.M., JONA, I., VEGH, M. & MARTONOSI, A. (1989). Cyclopiazonic acid is a specific inhibitor of the Ca^{2+}-ATPase of sarcoplasmic reticulum. *J. Biol. Chem.*, **264**, 17816–17823.

SHIMA, H. & BLAUSTEIN, M.P. (1992). Modulation of evoked contractions in rat arteries by ryanodine, thapsigargin and cyclopiazonic acid. *Circ. Res.*, **70**, 968–977.

SJODIN, R.A. (1959). Rubidium and cesium fluxs in muscle as related to the membrane potential. *J. Gen. Physiol.*, **42**, 983–1003.

SOMLYO, A.V., BOND, M., SOMLYO, A.P. & SCARPA, A. (1985). Inositol trisphosphate-induced calcium release and contraction in vascular smooth muscle. *Proc. Natl. Acad. Sci. USA*, **85**, 5231–5235.

UYAMA, Y., IMAIZUMI, Y. & WATANABA, M. (1992). Effects of cyclopiazonic acid, a novel Ca^{2+}-ATPase inhibitor, on contractile responses in skinned ileal smooth muscle. *Br. J. Pharmacol.*, **106**, 208–214.

XUAN, Y-T., WANG O-L. & WHORTON, A.R. (1992). Thapsigargin stimulates Ca^{2+} entry in vascular smooth muscle cells: nicardipine-sensitive and -insensitive pathways. *Am. J. Physiol.*, **262**, C1258–C1265.

(Received October 17, 1994
Revised November 18, 1994
Accepted November 24, 1994)

British Journal of Pharmacology (1995) 114, 1171-1178

Regulation of prostaglandin production by nitric oxide; an *in vivo* analysis

[1]Daniela Salvemini, Steven. L. Settle, Jaime. L. Masferrer, Karen Seibert, Mark. G. Currie & Philip Needleman

G.D. Searle, Department of Molecular Pharmacology, 800 N. Lindbergh Boulevard, St. Louis, MO 63167, U.S.A.

1 Endotoxin *E. Coli* lipopolysaccharide (LPS)-treatment in conscious, restrained rats increased plasma and urinary prostaglandin (PG) and nitric oxide (NO) production. Inducible cyclo-oxygenase (COX-2) and nitric oxide synthase (iNOS) expression accounted for the LPS-induced PG and NO release since the glucocorticoid, dexamethasone inhibited both effects. Thus, LPS (4 mg kg^{-1}) increased the plasma levels of nitrite/nitrate from 14 ± 1 to 84 ± 7 μM within 3 h and this rise was inhibited to 35 ± 1 μM by dexamethasone. Levels of 6-keto $PGF_{1\alpha}$ in the plasma were below the detection limit of the assay (< 0.2 ng ml^{-1}). However, 3 h after the injection of LPS these levels rose to 2.6 ± 0.2 ng ml^{-1} and to 0.7 ± 0.01 ng ml^{-1} after LPS in rats that received dexamethasone.

2 The induced enzymes were inhibited *in vivo* with selective COX and NOS inhibitors. Furthermore, NOS inhibitors, that did not affect COX activity *in vitro* markedly suppressed PG production in the LPS-treated animals. For instance, the LPS-induced increased in plasma nitrite/nitrate and 6-keto $PGF_{1\alpha}$ at 3 h was decreased to 18 ± 2 μM and 0.5 ± 0.02 ng ml^{-1}, 23 ± 1 μM and 0.7 ± 0.01 ng ml^{-1}, 29 ± 2 μM and 1 ± 0.01 ng ml^{-1} in rats treated with LPS in the presence of the NOS inhibitors N^G- monomethyl-L-arginine, N^G-nitro arginine methyl ester and aminoguanidine, respectively.

3 The intravenous infusion of the NO donors sodium nitroprusside (SNP) or glyceryl trinitrate (GTN) increased prostaglandin production in normal animals (for instance urinary PGE_2 excretion was increased from 96 ± 10 to 576 ± 12 pg min^{-1} and 400 ± 24 pg min^{-1} in the presence of GTN or SNP respectively).

4 Proteinuria was measured in order to evaluate the roles of NO and PG in renal damage associated with the *in vivo* injection of LPS. Interestingly, dexamethasone and the NOS inhibitors attenuated proteinuria in the LPS-treated rats. The COX inhibitors had no effect. It therefore appears that NO and not PG contributes to the LPS-induced renal damage; these findings support the potential use of NOS inhibitors in the treatment of renal inflammation.

5 This study demonstrates the regulatory contribution of NO on the *in vivo* production of prostanoids and suggests that in inflammatory diseases that are driven by both NO and the prostaglandins, NOS inhibitors may act to reduce inflammation by the dual inhibition of cytotoxic NO and pro-inflammatory PG.

Keywords: Nitric oxide synthase inhibitors; cyclo-oxygenase; prostaglandins; *E.coli* lipopolysaccharide; nitric oxide

Introduction

Nitric oxide (NO) is derived from L-arginine (L-Arg) by the enzyme nitric oxide synthase (NOS) whereas cyclo-oxygenase (COX) converts arachidonic acid to prostaglandins (PG). There are two major forms of NOS and COX. The constitutively expressed isoforms of these enzymes are found in numerous cell types in the absence of immunostimulation (see Moncada *et al.*, 1991 and DeWitt 1991 for reviews). Production of NO and prostaglandins from the constitutive isoforms is important for the normal physiological function of various systems. The inducible isoforms (iNOS and COX-2) are not normally expressed, but are induced following appropriate stimulation with pro-inflammatory agents such as *E.coli* lipopolysaccaride (LPS) (Fu *et al.*, 1990; Masferrer *et al.*, 1990; 1992; Moncada *et al.*, 1991). Anti-inflammatory steriods, including dexamethasone, inhibit the induction of iNOS and COX-2 *in vitro* and *in vivo* with no apparent effect on the constitutive forms of the enzymes (Masferrer *et al.*, 1990; 1992; Radomski *et al.*, 1990; Moncada *et al.*, 1991). Inhibition of NO in LPS-induced macrophages *in vitro* results in an attentuation of PG release from these cells (Salvemini *et al.*, 1993). This action of NO on the COX pathway has been confirmed as well in other cell systems including hypothalamic slices (Rettori *et al.*, 1992), smooth muscle cells (Inoue *et al.*, 1993), islet cells (Corbett *et al.*, 1993) and in an intact organ system (Salvemini *et al.*, 1994).

To date, most of the effects of NO on COX activity and hence PG production have been assessed in cells or enzyme preparations. It is not yet known whether the COX pathway is modulated by NO *in vivo*. We have addressed this question in our study in order to unravel the therapeutic implications of our *in vitro* discovery. *In vivo* administration of LPS in rats induces iNOS resulting in increased production of NO_2^-, a breakdown product of NO (see Moncada *et al.*, 1991; Moncada & Higgs, 1993 for reviews). Furthermore, LPS injection in rats has been shown to cause marked *in vivo* stimulation of arachidonic acid metabolism resulting in a profound increase in plasma and urinary prostaglandin (see Flynn, 1985 for review). We have therefore used this *in vivo* model to evaluate the contributions of NO on the exaggerated production of PG evoked by bolus injection of LPS in conscious, restrained rats.

Methods

In vivo *measurements*

Male Sprague Dawley rats (300-350 g) were purchased from Charles River (Wilmington, MA, U.S.A.) and used through-

[1] Author for correspondence.

out these studies. All animal protocols were approved by the Institutional Animal Care and Use Committee. Animals were anaesthetized with methoxyflurane before surgical preparation. Polyethylene catheters (PE50), were inserted into a femoral artery and vein. The urinary bladder was cannulated with a flared PE90 polyethylene catheter. The animals were placed into individual restraining cages and allowed to regain consciousness. Mean arterial blood pressure and heart rate were measured continuously via the femoral artery with a pressure transducer (type 041-500-503, Cobe, Lakewood, CO, U.S.A.) connected to a Grass Model 7E polygraph. Mean arterial pressure and heart rate were recorded at 5 min intervals on a computerized data acquisition system.

Drug administration and protocols

The lowest dose of LPS that promoted a maximal iNOS induction with minimal cardiovascular changes in our conscious rats was found to be 4 mg kg^{-1}. Higher doses were not used since they promoted severe deleterious effects that hindered the collection of blood and urine samples. Upon completion of the surgical procedure, cardiovascular parameters were allowed to stabilise for 30 min. Rats then received a bolus intravenous injection of 4 mg kg^{-1} LPS (serotype 0111:B4) dissolved in saline. Haemodynamic parameters were monitored for a subsequent 5 h. All drug treatments began 30 min prior to the injection of LPS. Urine was collected during this time frame and a blood sample (500 µl) was taken from the femoral artery immediately before and after drug administration. These time points are referred to as T_0; the amount of NOS and COX products obtained at T_0 reflect basal levels. Subsequent blood samples were taken every hour for 5 h after LPS or saline; 60 min urine volumes were collected for the duration of the experiment.

The non-selective cNOS and iNOS inhibitors, N^G-nitro-L-arginine methyl ester (L-NAME, 0.1 mg kg^{-1} min^{-1}) or N^G-monomethyl-L-arginine (L-NMMA, 1 mg kg^{-1} min^{-1}) or the more selective iNOS inhibitor, aminoguanidine (AG, 1 mg kg^{-1} min^{-1}) were infused for the entire duration of the experiment via the femoral vein. Control rats received an infusion of 0.9% sodium chloride via the femoral vein (0.07 ml kg^{-1} min^{-1}) for the entire duration of the study. Indomethacin (or an equivalent volume of the vehicle; phosphate buffered saline, 1% Tween 80, pH 7.4) or dexamethasone were given intraperitoneally at a dose of 3 mg kg^{-1} or 4 mg kg^{-1} respectively. The selective COX-2 inhibitor, NS398 (Futaki *et al.*, 1993; Masferrer *et al.*, 1994b) was given by gavage (10 mg kg^{-1}).

In some experiments, rats were treated with LPS for 4 h and then received an intravenous bolus injection of AG (1 mg kg^{-1}), dexamethasone (3 mg kg^{-1}) or an equivalent volume of saline (0.5 ml). Blood samples were taken immediately before and at 1 h after the injection of saline, AG or dexamethasone for the determination of plasma NO_2^- and 6-keto $PGF_{1\alpha}$.

In order to evaluate the role of exogenous nitric oxide on *in vivo* prostaglandin formation two nitric oxide donors namely sodium nitroprusside (SNP) and glyceryl trinitrate (GTN) were used. The effects of verapamil, a vasodilator which does not release NO was also used. SNP (0.125 mg kg^{-1} min^{-1}), GTN or verapamil (0.25 mg kg^{-1} min^{-1}) were infused for a total period of 1 h; blood samples were taken before and after drug administration and urine was collected throughout the 1 h period of infusion.

Mediators measured to assess the presence of the NOS and COX systems

The production of nitrite/nitrate (NO_2^-/NO_3^-), breakdown products of NO, or PGE_2 and 6-keto $PGF_{1\alpha}$ mediators released after activation of COX, were used, respectively as markers for the presence of the L-arginine to NO pathway and the COX pathway. NO stimulates the soluble guanylate cyclase leading to increased excretion of guanosine 3' : 5'-cyclic monophosphate (cyclic GMP) which can be detected in the urine (Wilkins *et al.*, 1990). Therefore, urinary cyclic GMP levels were also measured as an index of the activation of the L-arginine to nitric oxide pathway. Total excretion of NO_2^-/NO_3^-, cyclic GMP and prostanoids in the urine was calculated, based on the concentration and the urine volume so as to take into account any changes in urinary output.

Nitrite/nitrate determination

Arterial blood was collected in Microtainer tubes containing lithium heparin (Becton Dickinson, Rutherford, NJ, U.S.A.) and centrifuged to collect plasma samples. Plasma samples were passed through an Ultra-MC filter (10,000 MWCO, Millipore, Bedford, MA, U.S.A.). NO reacts with oxygen to yield nitrate and nitrite. Nitrate in plasma aliquots (5 µl) was converted to nitrite by the addition of nitrate reductase (14 mu) and the reduced form of nicotinamide adenine dinucleotide phosphate (NADPH, 1 nmol) with incubation for 10 min at room temperature. The reaction was terminated by dilution with water and addition of the diaminonapthalene reagent (Misko *et al.*, 1993b). Nitrite concentrations in these samples were determined fluorimetrically (Misko *et al.*, 1993b) with sodium nitrite used as a standard. This procedure was also used to determine the levels of NO_2^-/NO_3^- excreted in the urine. All determinations were performed in duplicate. Results are expressed as plasma or urinary NO_2^-/NO_3^- levels.

PGE_2, 6-keto $PGF_{1\alpha}$, cyclic GMP and protein determinations

6-keto $PGF_{1\alpha}$ was measured in the unextracted plasma by ELISA (Cayman Chemicals, Ann Arbor, MI, U.S.A.). (Fletcher *et al.*, 1981). Urinary levels of 6-keto $PGF_{1\alpha}$ and PGE_2 were determined by specific ELISAs. Concentrations of cyclic GMP in urine were measured by radioimmunoassay as described previously (Wilkins *et al.*, 1990). Urinary protein excretion was measured by the Bradford assay (Bio-Rad Laboratories, CA, U.S.A.). Each experiment was performed in duplicate.

Preparation of human recombinant (r) COX enzymes

Insect cells expressing human COX-1 or COX-2 were homogenized as previously described (Masferrer *et al.*, 1994b) and membranes were incubated with arachidonic acid (10 µM) for 15 min. COX activity was determined by measuring PGE_2 by ELISA, expressed as ng PGE_2 μg^{-1} protein min^{-1}. Drugs

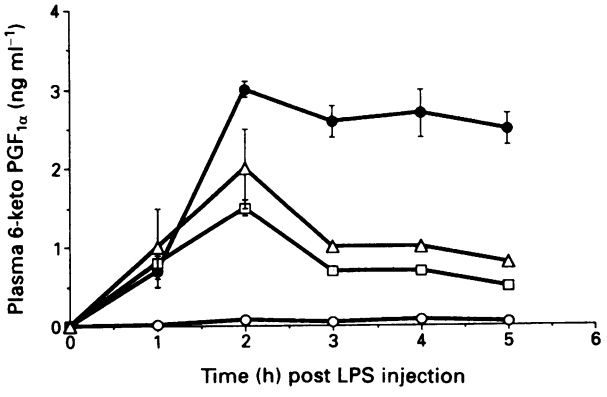

Figure 1 Effects of cyclo-oxygenase inhibitors (indomethacin and NS398) and dexamethasone on LPS-induced increases in plasma 6-keto prostaglandin $F_{1\alpha}$ (6-keto $PGF_{1\alpha}$) levels. *E. coli* lipopolysaccharide (LPS, 4 mg kg^{-1}, i.v, $n = 11$) caused a time-dependent increase in the levels of 6-keto $PGF_{1\alpha}$ (●) and this was attentuated by indomethacin (○, $n = 6$), NS398 (△, $n = 4$) and dexamethasone (□, $n = 6$). Each point is the mean ± s.e.mean for n experiments.

were preincubated with homogenates for 10 min before the addition of arachidonic acid.

Drugs and chemicals

Reagents were obtained from Sigma Chemical Co (St Louis, MO, U.S.A.). NS398 [N-(2-cyclohexexyloxy-4-nitrophenyl)-] methanesulphonamide was synthesized by J. Rogier and J. Talley, Monsanto Corporate Research as previously described (Futaki *et al.*, 1993). Indomethacin and NS398 were dissolved in phosphate-buffered saline, pH 7.4/1% (v/v) Tween-80. All other compounds were dissolved in saline.

Statistical analysis

Statistical significance of difference between groups was determined by a two-way analysis of variance (ANOVA) followed by Student's unpaired *t* test. A probability (*P*) value of 0.05 or less was taken to indicate statistical significance. Results are expressed as mean ± s.e.mean for (*n*) experiments.

Results

Induction of the COX pathway by LPS: effects of COX inhibitors and dexamethasone

An increase in plasma and urinary 6-keto $PGF_{1\alpha}$ (Figures 1 and 2b) and urinary PGE_2 (Figure 2a) was observed 1 h post-LPS injection and reached a peak by 2 h (Figures 1 and 2). The non-selective COX-1/COX-2 inhibitor, indomethacin (3 mg kg^{-1}, i.p, $n = 6$), blocked the rise in these arachidonic acid metabolites at all time points (Figures 1 and 2) whereas the inhibitory effects of dexamethasone (4 mg kg^{-1} i.p, $n = 6$) or of the COX-2 selective inhibitor NS398 (Masferrer *et al.*, 1994b; 10 mg kg^{-1} p.o., $n = 4$) were observed 2 h post-LPS and continued to the end of the experiment (Figures 1 and 2).

Effects of NOS inhibitors on prostanoid production

The basal plasma nitrite, urinary nitrite and cyclic GMP levels were respectively, 14 ± 1 μM, 1.25 ± 0.1 nmol min^{-1} and 51 ± 8 pmol min^{-1} ($n = 11$). L-NMMA or L-NAME slightly but significantly reduced these levels (Table 1). Thereafter, plasma NO_2^-/NO_3^- (Table 1), urinary NO_2^-/NO_3^- and cyclic GMP levels (Table 2A and B) started to increase 2 h post-LPS injection and by 5 h the values attained were, respectively, at least 18, 33 and 47 fold higher than basal ($n = 11$). Intravenous infusion of either L-NMMA (1 mg kg^{-1} min^{-1}, $n = 6$), L-NAME (0.1 mg kg^{-1} min^{-1}, $n = 7$), AG (1 mg kg^{-1} min^{-1}, $n = 8$) or dexamethasone (4 mg kg^{-1} i.p., $n = 6$) blocked the LPS-induced rise in NO_2^-/NO_3^- and cyclic GMP (Tables 1 and 2). Inhibition of NO formation by the NOS inhibitors at these time points, resulted in a marked inhibition of PG in plasma (Figure 3) and urine (Figure 4a and b). In some experiments, rats were treated first with LPS (so as to induce the NOS and COX systems) for 4 h and then received an intravenous bolus injection of AG (1 mg kg^{-1}), dexamethasone (3 mg kg^{-1}) or an equivalent volume of saline (0.5 ml). Blood samples were taken immediately before and at 1 h after the injection of saline, AG or dexamethasone for the determination of plasma NO_2^-/NO_3^- and 6-keto $PGF_{1\alpha}$. Table 3 shows that AG caused a fall in the levels of NO_2^-/NO_3^- (from 150 ± 7 μM before AG to 60 ± 7 μM after AG, $n = 4$, $P < 0.05$) which was associated with a fall in 6-keto $PGF_{1\alpha}$ (from 2.7 ± 0.2 ng ml^{-1} before AG to 0.7 ± 0.01 ng ml^{-1} after AG, $n = 4$, $P < 0.05$). Dexamethasone had no effect (Table 3).

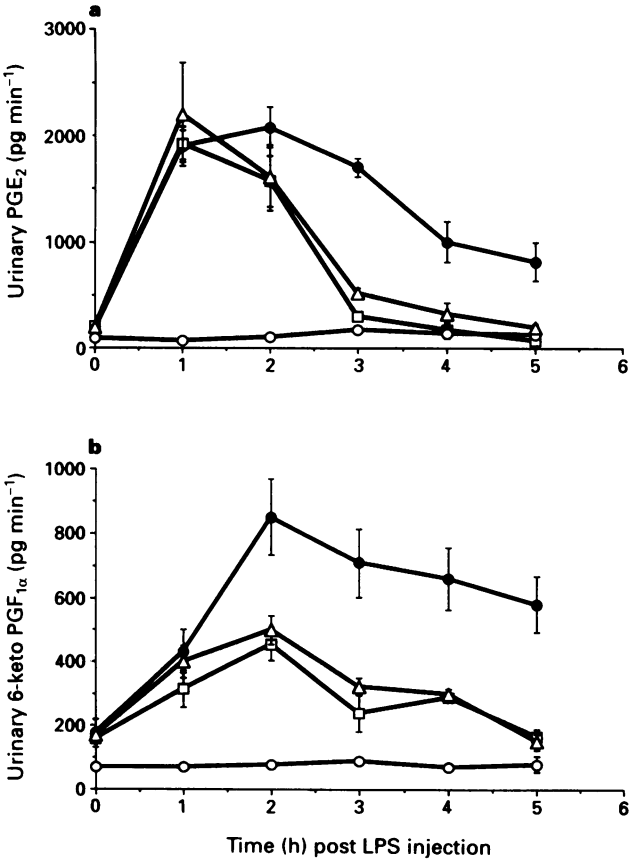

Figure 2 Effects of cyclo-oxygenase inhibitors and dexamethasone on *E. coli* lipopolysaccharide (LPS)-induced increases in urinary prostalandin E_2 (PGE_2) and 6-keto $PGF_{1\alpha}$ levels. LPS (4 mg kg^{-1}, i.v) caused a time-dependent increase (●) in the urinary levels of PGE_2 (a) and 6-keto $PGF_{1\alpha}$ (b) and this was abolished by indomethacin (○, $n = 6$), NS398 (△, $n = 4$) or dexamethasone (□, $n = 6$) (a and b). Each point is the mean ± s.e.mean for *n* experiments.

Table 1 *E. coli* lipopolysaccharide (LPS) increases the plasma levels in nitrite/nitrate: effects of NO synthase (NOS) inhibitors (L-NMMA, L-NAME and AG), cyclo-oxygenase inhibitors (indomethacin, NS398) and dexamethasone

	Time (h) after LPS					
Drugs	0	1	2	3	4	5
None	14 ± 1	13 ± 1	60 ± 5	84 ± 7	160 ± 12	256 ± 9
L-NMMA	7 ± 0.5*	6 ± 1*	15 ± 3*	18 ± 2**	16 ± 4**	22 ± 4**
L-NAME	7 ± 0.3*	7 ± 1*	10 ± 2*	23 ± 1**	36 ± 3**	40 ± 3**
AG	23 ± 4	23 ± 3	20 ± 5*	29 ± 2**	26 ± 3**	24 ± 2**
Indo	12 ± 1	13 ± 1	50 ± 1	75 ± 5	130 ± 7	213 ± 13
NS398	19 ± 1	11 ± 2	59 ± 5	76 ± 6	180 ± 5	215 ± 40
Dex	14 ± 1	12 ± 1	20 ± 1*	35 ± 1**	33 ± 1**	33 ± 2**

The NOS inhibitors or dexamethasone (Dex) prevented the increase in the levels of NO_2^-/NO_3^- (μM). Indomethacin (Indo) or NS398 were in effective. *$P < 0.05$ and **$P < 0.01$ when compared to the values obtained with LPS alone.
AG, aminoguanidine; L-NMMA: N^G-monomethyl-L-arginine; L-NAME: N^G-nitro-L-arginine methyl ester.

Table 2 Effects of nitric oxide synthase inhibitors, cyclo-oxygenase inhibitors and dexamethasone (Dex) on *E. coli* lipopolysaccharide (LPS)-induced increases in urinary nitrite/nitrate (A, nmol min^{-1}) and cyclic GMP (B, pmol min^{-1}) output in rats

	Time (h) after LPS					
A						
Drugs	0	1	2	3	4	5
None	125 ± 0.1	2.27 ± 0.5	13 ± 1.2	55 ± 8	40 ± 5	42 ± 6
L-NMMA	0 ± 0*	0 ± 0*	2 ± 0.1*	7 ± 0.5**	7 ± 1**	6 ± 2**
L-NAME	0.7 ± 0.01*	1 ± 0.1*	3 ± 0.03*	9 ± 0.2**	10 ± 2**	6 ± 1**
AG	2 ± 0.2	2 ± 1	5 ± 1	7 ± 2**	5 ± 1**	4 ± 0.5**
Indo	2 ± 1	3 ± 1	10 ± 1	50 ± 3	33 ± 4	40 ± 5
NS398	2 ± 1	5 ± 2	12 ± 4	60 ± 5	55 ± 3	40 ± 10
Dex	1 ± 0.1	3 ± 1	4 ± 0.5*	6 ± 2**	7 ± 1**	6 ± 0.5**
B						
None	51 ± 8	49 ± 7	669 ± 180	3568 ± 200	2976 ± 93	2407 ± 48
L-NMMA	20 ± 5*	20 ± 7*	70 ± 4**	90 ± 3**	90 ± 10**	70 ± 5**
L-NAME	22 ± 5*	21 ± 1*	80 ± 13**	101 ± 8**	99 ± 12**	74 ± 21**
AG	45 ± 8	59 ± 9	96 ± 10*	96 ± 6**	76 ± 6**	73 ± 25**
Indo	53 ± 6	48 ± 7	492 ± 115	2383 ± 700	2000 ± 230	2426 ± 64
NS398	55 ± 9	50 ± 8	500 ± 100	3900 ± 300	3000 ± 200	2000 ± 200
Dex	51 ± 10	58 ± 10	114 ± 29*	138 ± 31**	136 ± 25**	143 ± 29**

*$P<0.05$ and **$P<0.01$ when compared to values obtained in the absence of drugs. For abbreviations, see Table 1

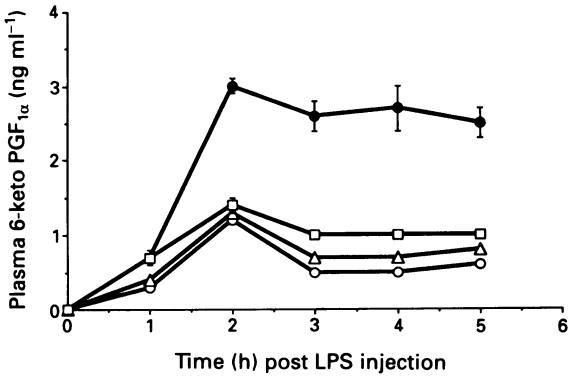

Figure 3 Effects of nitric oxide synthase inhibitors (L-NMMA, L-NAME and AG) on *E. coli* lipopolysaccaride (LPS)-induced increases in plasma 6-keto prostaglandins $F_{1\alpha}$ (6-keto $PGF_{1\alpha}$) levels. Intravenous infusion of N^G-monomethyl-L-arginine (L-NMMA,○,1 mg kg^{-1} min^{-1}, $n=6$), N^G-nitro-L-arginine methyl ester (L-NAME, △, 0.1 mg kg^{-1} min^{-1}, $n=7$) or aminoguanidine (AG,□,1 mg kg^{-1}, $n=8$) attenuated the increase in 6-keto $PGF_{1\alpha}$ following LPS administration (●). Each point is the mean ± s.e.mean for n experiments.

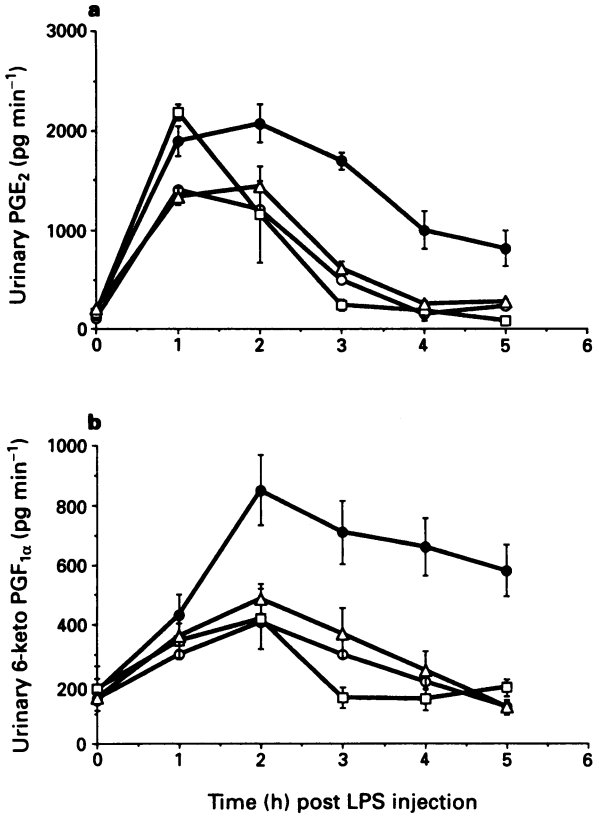

Figure 4 Effects of NO synthase (NOS) inhibitors on *E. coli* lipopolysaccharide (LPS)-induced increases in urinary prostaglandin E_2 (PGE_2) and 6-keto $PGF_{1\alpha}$ levels. Intravenous infusion of N^G monomethyl-L-arginine (○, $n=6$), N^G-nitro-L-arginine methyl ester (△, $n=7$) or aminoguanidine (□, $n=8$) attenuated the rise (●) in urinary output of PGE_2 (a) and 6-keto $PGF_{1\alpha}$ (b). Each point is the mean ± s.e.mean for n experiments.

The NOS inhibitors, L-NMMA, L-NAME or aminoguanidine (1–300 μM, $n=6$) failed to inhibit human recombinant COX-1 and COX-2 activity directly (Figure 5a and b). Similar results were obtained with murine recombinant COX-1 and COX-2 (data not shown). Indomethacin inhibited COX-1 ($IC_{50}=0.058$ μM, $n=10$, Figure 5a) and COX-2 ($IC_{50}=1.1$ μM, $n=10$; Figure 5b), whereas NS398 selectively inhibited COX-2 ($IC_{50}=0.1$ μM, $n=10$; Figure 5b), with no effect on COX-1 (Figure 5a). The observation that the IC_{50} of indomethacin for COX-2 is higher than for COX-1 has been reported by others (Meade *et al.*, 1993; Gierse *et al.*, 1994). The assumption is (although not proven) that this is due to the intrinsic ability of indomethacin to bind differently the active site of COX-1 versus COX-2. In contrast to the effects of the NOS inhibitors, *in vivo* administration of indomethacin or NS398 had no effect on the LPS-induced increase in nitrite or cyclic GMP production (Tables 1 and 2).

Release of 6-keto $PGF_{1\alpha}$ in plasma by the administration of NO-donors in normal rats

The intravenous infusion (for 1 h) of glyceryl trinitrate (0.25 mg kg^{-1} min^{-1}, $n=6$) or sodium nitroprusside (0.125 mg kg^{-1} min^{-1}, $n=6$) caused a 14 fold increase in the plasma levels of NO_2^-/NO_3^- (from 14 ± 1 μM to 200 ± 20 μM and 175 ± 15 μM respectively). Levels of 6-keto $PGF_{1\alpha}$ in the plasma were below the detection limit of the assay (< 0.2 ng ml^{-1}). These increased respectively to 2.5 ± 0.3 ng ml^{-1} and 1.7 ± 0.5 ng ml^{-1} following the 1 h infusion with either GTN or SNP. Urinary PGE_2 excretion was increased from 96 ± 10 to 576 ± 12 pg min^{-1} and to

Table 3 The effects of aminoguanidine (AG) or dexamethasone (Dex) on plasma NO_2^-/NO_3^-(μM) and 6-keto $PGF_{1\alpha}$ (ng ml^{-1}) at 4 h after *E. coli* lipopolysaccharide (LPS) injection

	Before bolus injection of the drug	*1 h after bolus injection of the drug*
None		
NO_2^-	140 ± 12	300 ± 15
6-keto $PGF_{1\alpha}$	2.5 ± 0.1	3 ± 0.2
AG		
NO_2^-	150 ± 7*	60 ± 7*
6-keto $PGF_{1\alpha}$	2.7 ± 0.2*	0.7 ± 0.01*
Dex		
NO_2^-	135 ± 9	285 ± 10
6-keto $PGF_{1\alpha}$	2 ± 0.1	2.2 ± 0.5

Rats were treated with LPS for 4 h and then received an intravenous bolus injection of AG, Dex or an equivalent volume of saline (0.5 ml). Blood samples were taken immediately before and at 1 h after treatment. AG caused an immediate fall in the levels of NO_2^-/NO_3^- and this was associated with an immediate fall in 6-keto $PGF_{1\alpha}$. Dex had no effect. Each point is the mean ± s.e.mean for 4 experiments. *$P<0.05$ when compared to values obtained before the injection of saline, AG or Dex.

400 ± 24 pg min^{-1} in the presence of GTN or SNP respectively ($n=6$). Verapamil when infused for 1 h at a dose (0.25 mg kg^{-1} min^{-1}, $n=8$) that elicited a similar fall in blood pressure to the one evoked by the NO-donors, failed to increase the levels of NO_2^-/NO_3^- or PG (data not shown).

Mean arterial pressure decreased from a basal level of 120 ± 2 mmHg to 93 ± 2 mmHg, 80 ± 4 mmHg and 61 ± 4 mmHg following the 1 h period of infusion with GTN, SNP or verapamil respectively.

Effects of NOS or COX inhibitors and dexamethasone on proteinuria

Urinary protein excretion was observed 2 h post-LPS injection, reached a peak by 3 h and remained constant for the remaining of the experiment (Figure 6). Proteinuria was inhibited by at least 50% by aminoguanidine (Figure 6a) or dexamethasone (Figure 6b) and to a lesser extent by L-NMMA or NO_2Arg (Figure 6a) but was not affected by indomethacin or NS398 (Figure 6b).

Haemodynamic effect

Inhibition of cNOS by non-selective cNOS/iNOS inhibitors such as L-NMMA or L-NAME has been shown to increase blood pressure in a variety of animal species (see Moncada *et al.*, 1991; Moncada & Higgs, 1993 for reviews). This phenomenon is not observed with selective iNOS inhibitors such as aminoguanidine (Misko *et al.*, 1993a; Griffith *et al.*, 1993) or with steriods such as dexamethasone (see Moncada *et al.*, 1991; Moncada & Higgs, 1993 for reviews). Mean arterial blood pressure (MAP) and heart rate in conscious normotensive restrained rats was 113 ± 2 mmHg and 410 ± 2 b.p.m. ($n=16$). In normotensive rats and at the doses used throughout our experiments, L-NMMA or L-NAME increased MAP by 35 mmHg within 30 min post infusion; the increase in MAP elicited by these agents remained at that level for the duration of the experiment (6 h). Aminoguanidine or dexamethasone did not increase MAP in normotensive animals ($n=6$, data not shown), consistent with their selectivity for iNOS.

LPS injection caused a slight fall in mean arterial pressure within approximately 90 min which returned to basal levels by 2 h (Table 4). In contrast to their lack of effect on MAP in normotensive rats, aminoguanidine or dexamethasone increased MAP in the LPS-treated rats; this effect was observed within 2 h after the injection of LPS and for the remainder of the experiment (Table 4). Indomethacin or NS398 did not increase BP in normotensive rats or rats treated with LPS (Table 4).

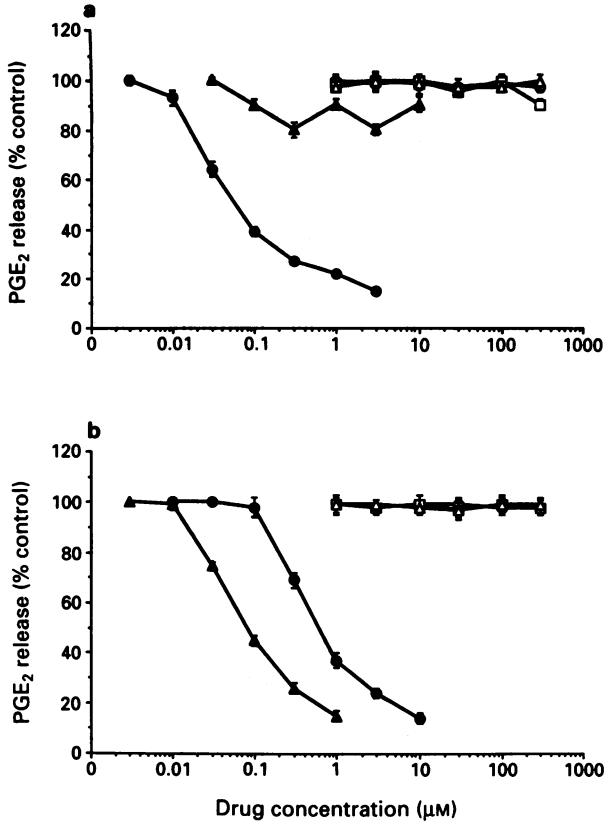

Figure 5 Effects of cyclo-oxygenase (COX) inhibitors and NO synthase (NOS) inhibitors on human recombinant COX-1 and COX-2 (hrec COX-1 and hrec COX-2) activity. The non-selective COX-1 and COX-2 inhibitor, indomethacin, blocked the activity of both hrec COX-1 and hrec COX-2 (●, $n=10$) whereas the selective COX-2 inhibitor NS398 affected only hrec COX-2 activity (▲, $n=10$) (a and b). The NOS inhibitors, N^G-monomethyl-L-arginine (○, $n=6$), N^G-nitro-L-arginine methyl ester (△, $n=6$) or aminoguanidine (□, $n=6$) had no effect (a and b). Results are expressed as prostaglandin E_2 (PGE_2) release (% of control).

Discussion

We recently demonstrated *in vitro* that NO can activate COX resulting in an increase in the production of prostaglandins. In this study we demonstrate a similar relationship between NO and COX *in vivo*.

LPS caused an increase in plasma 6-keto $PGF_{1\alpha}$ and urinary excretion of 6-keto $PGF_{1\alpha}$ and PGE_2 over time although the peak urinary excretion of PGE_2 occurred before (1 h post LPS) the one obtained for 6-keto $PGF_{1\alpha}$ (2 h post LPS). Different cell types which respond differently to LPS or a difference in the kinetics of their isomerases may account for this observation. For purposes of clarity we will refer to the release of prostanoids (6-keto $PGF_{1\alpha}$ and PGE_2) that occurred within 1 h post LPS as 'acute release' and the one that occurred within 2 h post LPS as 'delayed release'. Acute release of PG was inhibited by indomethacin, but not by NS398 a selective COX-2 inhibitor (Masferrer at al., 1994b) or dexamethasone suggesting that constitutive COX-1 is responsible for the acute release of PG elicited by LPS; constitutive COX-1 activation may result from the LPS-promoted

release of vasoactive substances such as kinins (Parratt, 1983; Wilson *et al.*, 1989). NS398 or dexamethasone inhibited the delayed release of prostanoid indicating that induced COX-2 is responsible for the delayed release of PG. This is substantiated by the findings that within 2 h after LPS injection in rats and mice COX-2 mRNA and protein was expressed in various organs (Seibert *et al.*, 1994) and inflammatory cells (Masferrer *et al.*, 1990; 1994a).

Besides activating the COX pathway, LPS activated the NOS system within a similar time frame. Release of NO (as assessed by measurements of NO_2^-/NO_3^- and cyclic GMP) observed at 1 h post-LPS injection was aminoguanidine and dexamethasone-insensitive, but inhibitable by the non-selective cNOS/iNOS inhibitors L-NMMA and L-NAME. This indicates that cNOS accounts for NO release during the acute phase and iNOS accounts for NO release during the later phase of endotoxin administration. This is supported by the demonstration that LPS releases NO from cNOS within minutes *in vitro* and *in vivo* (Salvemini *et al.*, 1990; Thiermermann & Vane, 1990; Fleming *et al.*, 1992) and that within 2 h post injection it induces iNOS mRNA and protein in various organs (Salter *et al.*, 1991; Liu *et al.*, 1993).

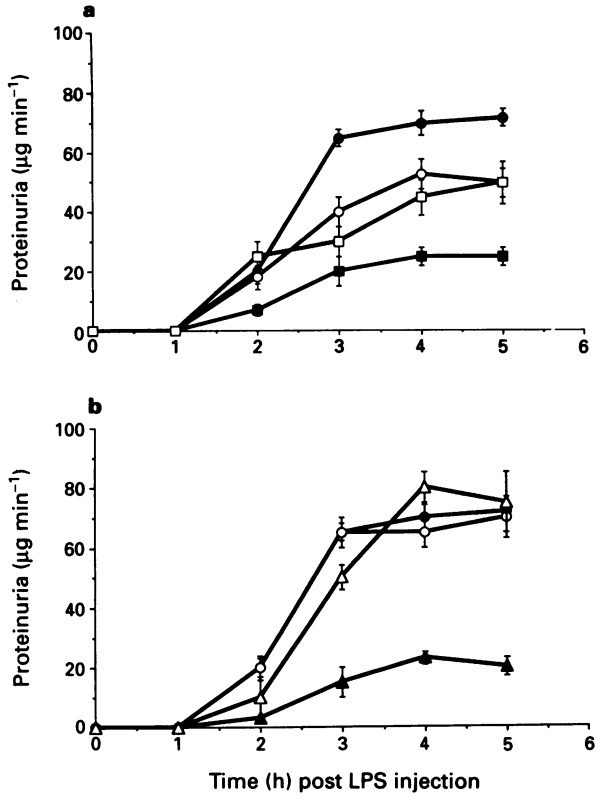

Figure 6 Effects of drugs on the proteinuria elicited by *E. coli* lipopolysaccharide (LPS). The increase in urinary excretion of protein elicited by LPS (●, $n = 11$) was attenuated by N^G-monomethyl-L-arginine (□, $n = 6$), N^G-nitro-L-arginine methyl ester (○, $n = 7$) or aminoguanidine (■, $n = 8$) (a) and dexamethasone ($n = 6$) (b) but not by indomethacin (○, $n = 6$) or NS398 (△, $n = 4$) (b). Results are expressed as μg protein min^{-1} for n experiments.

LPS stimulates the release of a variety of mediators (noradrenaline, angiotensin II, 5-hydroxytryptamine, thromboxane) with vasoconstrictor capacities that would oppose the vasodilator effects of NO (see Moncada *et al.*, 1991, for review). Therefore, a balance between vasoconstrictor/vasodilator mediators is involved in the maintenance of the blood pressure level. This may exlain why LPS at the dose used in our study did not (as intended) cause measurable changes in blood pressure yet induced NOS. Nevertheless, the effects of NO on the modulation of blood vessel tone was detected when iNOS activity (by AG) or iNOS induction (by dexamethasone) were inhibited. Thus, AG or Dex increased blood pressure 2/3 h post LPS injection whereas they had no effect in saline-treated animals.

What is the consequence of NO inhibition *in vivo* on the production of PG? Using *in vitro* systems, we and others have reported that inhibition of NO has inhibitory effects on PG release, whereas addition of exogenous NO augments PG release (Rettori *et al.*, 1992; Salvemini *et al.*, 1993; Corbett *et al.*, 1993; Inoue *et al.*, 1993; Salvemini *et al.*, 1994). Here we have shown that when the increased endogenous production of NO was blocked by the NOS inhibitors at the time point of iNOS induction (2 h), the increase in plasma and urinary production of prostanoids was inhibited by at least 50%. This suggests that induction of iNOS release enough NO to modulate the COX pathway. This was demonstrated further by showing that removal of NO by bolus injection of AG 4 h after LPS (a time point when iNOS was induced) resulted in a concomitant decrease in PG production. Under the same experimental conditions, dexamethasone failed to alter NO_2^-/NO_3^- and PG formation consistent with the fact that once iNOS is induced, NO release cannot be affected by this steriod (Wright *et al.*, 1992; Paya *et al.*, 1993). The ability of the NOS inhibitors to inhibit PG production was not due to direct inhibition of COX enzymes for they failed to affect the activity of human recombinant COX-1 or COX-2.

The effects of endogenously produced NO on prostaglandin formation were mimicked by the exogenous *in vivo* administration of NO. Thus, in normal rats, release of NO_2^-/NO_3^- by glyceryl trinitrate or sodium nitroprusside was accompanied by an increase in the plasma levels of 6-keto $PGF_{1\alpha}$. PG release elicited by the NO-donor must be reflecting COX-1 activation because COX-1 and not COX-2 mRNA and protein is found in organs from normal animals

Table 4 Blood pressure (mmHg) determinations in conscious, restrained Sprague Dawley rats treated with *E. coli* lipopolysaccharide (LPS, 4 mg kg^{-1}, i.v.) in the absence or presence of various drugs

	Drugs						
Time (min)	*None*	*L-NAME*	*L-NMMA*	*AG*	*Dex*	*Indo*	*NS398*
−30	113 ± 2	112 ± 2	113 ± 3	112 ± 3	113 ± 3	112 ± 2	112 ± 1
0	116 ± 2	127 ± 7*	127 ± 7*	116 ± 3	116 ± 3	111 ± 2	110 ± 2
30	114 ± 2	152 ± 4*	152 ± 4*	115 ± 2	112 ± 2	113 ± 4	110 ± 2
60	113 ± 1	146 ± 4*	146 ± 4*	113 ± 3	112 ± 3	115 ± 5	117 ± 1
90	106 ± 2	145 ± 3*	145 ± 3*	129 ± 2*	126 ± 3*	102 ± 5	103 ± 2
120	117 ± 2	144 ± 4*	144 ± 4*	140 ± 1*	136 ± 3*	121 ± 4	120 ± 2
150	120 ± 2	144 ± 4*	144 ± 4*	141 ± 2*	138 ± 2*	121 ± 5	121 ± 2
180	120 ± 2	148 ± 4*	148 ± 4*	140 ± 2*	133 ± 4*	124 ± 4	121 ± 2
210	119 ± 2	146 ± 4*	146 ± 4*	145 ± 1*	130 ± 2*	118 ± 5	119 ± 3
240	115 ± 3	146 ± 6*	146 ± 6*	140 ± 2*	138 ± 2*	112 ± 3	118 ± 2

Drugs were administered 30 min before LPS injection (−30). *$P < 0.05$ when compared to values obtained at the corresponding time point for the none group. Each point is the mean ± s.e.mean for 7–11 experiments. See Table 1 for abbreviations.

(Seibert et al., 1994). In addition, PG release by the NO-donors was not a consequence of changes in blood pressure for verapamil (a non NO-donor) when used at a dose which caused a fall in blood pressure similar to the one obtained with GTN or SNP, did not increase plasma PG.

Appearance of protein in the urine following LPS injection is an index of renal damage elicited by endotoxin (see Schlag & Redl, 1987, for review). Figure 6 shows that the time course for proteinuria was similar to the one obtained for NO and PG. Aminoguanidine or dexamethasone, but not the COX inhibitors abrogated the development of proteinuria indicating that NO release from iNOS is responsible at least in part for renal damage. These findings will allow us to evaluate the potential use of iNOS inhibitors in the management of renal damage. A role for iNOS in mediating glomerular damage in models of renal inflammation has also been reported (Cattell et al., 1990; Cook & Sullivan, 1991; Jansen et al., 1992). A weaker protective effect was observed with the non-selective cNOS/iNOS inhibitor L-NMMA or L-NAME. Since the release of NO from cNOS is important for maintaining adequate perfusion to a variety of vital organs including the kidney (see Luscher & Bock, 1991; King & Brenner, 1991, for reviews) it is possible that inhibition of cNOS in an already compromised organ (kidney inflammation elicited by LPS) may counteract the beneficial effects that would result if only iNOS were inhibited. The recent discovery that the COX pathway is modulated by NO, indicates that inhibition of NOS activity may remove the drive that NO has on COX, thereby lowering the amounts of pro-inflammatory PG; dual inhibition of the release of pro-inflammatory NO and PG could therefore contribute to the anti-inflammatory properties of NOS inhibitors. Possible mechanisms by which NO augments PG release include, but is not restricted to, direct activation of the COX enzymes (Salvemini et al., 1993; Hajjar et al., 1994) and inhibition of the autoinactivation of the COX enzymes, a phenomenon associated with the production of free radicals (Egan et al., 1976).

The effects of the iNOS inhibitors may provide a therapeutic advantage over steriods in that they may provide anti-inflammatory effects without the mechanism-based side effects described with chronic use of steriods.

We thank Dr Allen Nickols for the review of this manuscript and Carol Koboldt for her help with the recombinant COX experiments.

References

CATTELL, V., COOK, T. & MONCADA, S. (1990). Glomeruli synthesize nitrite in experimental nephrotoxic nephritis. *Kidney. Int.*, **38**, 1056–1060.

CORBETT, J.A., KWON, G., TURK, J. & MCDANIEL, M.L. (1993). IL-1b induces the coexpression of both nitric oxide synthase and cyclooxygenase by islets of langerhans: activation of cyclooxygenase by nitric oxide. *Biochem.*, **32**, 13767–13770.

COOK, H.Y. & SULLIVAN, R. (1991). Glomerular nitrite synthesis in in situ immune complex glomerulonephritis in the rat. *Am. J. Pathol.*, **139**, 1047–1052.

DEWITT, D.L. (1991). Prostaglandin endoperoxide synthase: regulation of enzyme expression. *Biochim. Biophys. Acta*, **1083**, 121–134.

EGAN, R.W., PAXTON, J. & KUEHL, F.A.Jr. (1976). Mechanisms for irreversible self-deactivation of prostaglandin synthase. *J. Biol. Chem.*, **251**, 7329–7335.

FLEMING, I., DAMBACHER, T. & BUSSE, R. (1992). Endothelium-derived kinins account for the immediate response of endothelial cells to bacterial lipopolysaccharide. *J. Cardiovasc. Pharmacol.*, **20**, S135–S138.

FLETCHER, J.R., RAMWELL., P.W. & HARRIS, R.H. (1981). Thromboxane, prostacyclin, and hemodynamic events in primate endotoxin shock. *Adv. Shock Res.*, **5**, 143–148.

FLYNN, J.T. (1985). The role of arachidonic acid metabolites in endotoxin shock II: involvement of prostanoids and thromboxanes. In *Handbook of Endotoxin*, Vol 2: *Pathophysiology of Endotoxin*, ed. Hinshaw, L.B. pp. 237–279. Amsterdam:Elsevier Science Publishers.

FU, J.Y., MASFERRER, J.L., SEIBERT, K., RAZ, A. & NEEDLEMAN, P. (1990). The induction and suppression of prostaglandin H_2 synthase (cyclooxygenase) in human monocytes. *J. Biol. Chem.*, **265**, 16737–16740.

FUTAKI, N., ARAI, I., KAMASARA, Y., TAKAHASHI, S., HIGUCHI, S. & OKANO, S. (1993). Selective inhibition of NS398 on prostanoid production in inflamed tissue in carrageenan-air-pouch inflammation. *J. Pharm. Pharmacol.*, **45**, 753–755.

GIERSE, J., HAUSER, S., CREELY, D., KOBOLT, C., RANGWALA, S., ISAKSON, P. & SEIBERT, K. (1994). Expression and selective inhibition of the constitutive and inducible forms of human cyclooxygenase. *Biochem. J.*, (in press).

GRIFFITH, M.J.D., MESSENT, M., MACALLISTER, R.J. & EVANS, T.W. (1993). Aminoguanidine selectively inhibits inducible nitric oxide synthase. *Br. J. Pharmacol.*, **110**, 963–968

HAJJAR, D.O., LANDER, H.M., PEARCE, S.A.F. & POMERANTZ, K.B. (1994). Evidence for nitric oxide induction of cyclooxygenase-1 activity by heme-independent mechanisms. *FASEB. J.*, **A1**, 432.

INOUE, T., FUJUO, K., MORIMOTO, S., KOH, E. & OGIHARA, T. (1993). Nitric oxide mediates interleukin-1-induced prostaglandin E_2 production by vascular smooth muscle cells. *Biochem. Biophys. Res. Commun.*, **194**, 420–424.

JANSEN, A., LEWIS, S., CATTELL, V. & COOK, H.T. (1992). Arginase is a major pathway of L-arginine metabolism in nephritic glomeruli. *Kidney. Inter.*, **42**, 1107–1112.

KING, A.J. & BRENNER, B.M. (1991). Endothelium-derived vasoactive factors and the renal vasculature. *Am. J. Physiol.*, **260**, R653–R662.

LIU, S., ADCOCK, I.M., OLD, R.W., BARNES, P.J. & EVANS, T.W. (1993). Lipopolysaccharide treatment in vivo induces widespread tissue expression of inducible nitric oxide synthase mRNA. *Biochem. Biophys. Res. Commun.*, **196**, 1208–1213.

LUSCHER, T.F. & BOCK, H.A. (1991). The endothelial L-arginine/nitric oxide pathway and the renal circulation. *Klin. Wochenschr.*, **69**, 603–609.

MASFERRER, J.L., REDDY, S.T., ZWEIFEL, B.S., SEIBERT, K., NEEDLEMAN, P., GILBERT, R.S. & HERSCHMAN, H.R. (1994a). In vivo glucocorticoids regulate cyclooxygenase-2 but not cyclooxygenase-1 in peritoneal macrophages. *J. Pharmacol. Exp. Ther.*, **270**, 1340–1344.

MASFERRER, J.L., SEIBERT, K., ZWEIFEL, B. & NEEDLEMAN, P. (1992). Endogenous glucocorticoids regulate an inducible cyclooxygenase enzyme. *Proc. Natl. Acad. Sci. U.S.A.*, **89**, 3917–3921.

MASFERRER, J.L., ZWEIFEL, B.S., MANNING, P.T., HAUSER, S.D., LEAHY, K.M., SMOTH, W.G., ISAKSON, P.C. & SEIBERT, K. (1994b). Selective inhibition of inducible cyclooxygenase 2 in vivo is antiinflammatory and nonulcerogenic. *Proc. Natl. Acad. Sci. U.S.A.*, **91**, 3228–3232.

MASFERRER, J.L., ZWEIFEL, B.S., SEIBERT, K. & NEEDLEMAN, P. (1990). Selective regulation of cellular cyclooxygenase by dexamethasone and endotoxin in mice. *J. Clin. Invest.*, **86**, 1375–1379.

MEADE, E.A., SMITH, W.L. & DEWITT, D.L. (1993). Differential inhibition of prostaglandin endoperoxide synthase (cyclooxygenase) isozymes by aspirin and other non-steroidal anti-inflammatory drugs. *J. Biol. Chem.*, **268**, 6610–6614.

MISKO, T.P., MOORE, W.M., KASTEN, T.P., NICKOLS, G.A., CORBETT, J.A., TILTON, R.G., MCDANIEL, M.L., WILLIAMSON, J.R. & CURRIE, M.G. (1993a). Selective inhibition of the inducible nitric oxide synthase by aminoguanidine. *Eur. J. Pharmacol.*, **233**, 119–225.

MISKO, T.P., SCHILLING, R.J., SALVEMINI, D., MOORE, W.M. & CURRIE, M.G. (1993b). A flurimetric assay for the measurements of nitrite in biological samples. *Anal. Biochem.*, **214**, 11–16.

MONCADA, S. & HIGGS, A. (1993). The L-arginine-nitric oxide pathway. *N. Engl. J. Med.*, **329**, 2002–2012.

MONCADA, S., PALMER, R.M.J. & HIGGS, E.A. (1991). Nitric oxide: physiology, pathophysiology and pharmacology. *Pharmacol. Rev.*, **43**, 109–141.

PARRATT, J.R. (1983). Neurohumoral agents and their release in shock. In *Handbook of Shock and Trauma*, Vol 1: *Basic Science*. ed. Altura, B.M., Lefer, A.M. & Schumar, W. pp. 331–336. New York: Raven Press.

PAYA, D., GRAY, G.A., FLEMING, I. & STOCLET, J.C. (1993). Effect of dexamethasone on the onset and persistance of vascular hyporeactivity induced by E. coli lipopolysaccharide in rats. *Circ. Shock.*, **41**, 103–112.

RADOMSKI, M.W., PALMER, R.M.J. & MONCADA, S. (1990). Glucocorticoids inhibit the expression of an inducible but not the constitutive nitric oxide synthase in vascular endothelial cells. *Proc. Natl. Acad. Sci. U.S.A.*, **87**, 10043–10047.

RETTORI, V., GIMENO, M., LYSON, K. & MCCANN, S.M. (1992). Nitric oxide mediates norepinephrine-induced prostaglandin E_2 release from the hypothalamus. *Proc. Natl. Acad. Sci. U.S.A.*, **89**, 11543–11546.

SALTER, M., KNOWLES, R.G. & MONCADA, S. (1991). Widespread tissue distribution, species distribution and changes in activity of Ca^{2+}-dependent and Ca^{2+}-independent nitric oxide synthase. *FEBS Lett.*, **291**, 145–149.

SALVEMINI, D., KORBUT, R., ANGGARD, E. & VANE, J.R. (1990). Immediate release of a nitric oxide-like factor from bovine aortic endothelial cells by E. coli lipopolysaccharide. *Proc. Natl. Acad. Sci. U.S.A.*, **87**, 2593–2597.

SALVEMINI, D., MISKO, T.P., SEIBERT, K., MASFERRER, J.L., CURRIE, M.G. & NEEDLEMAN, P. (1993). Nitric oxide activates cyclooxygenase enzymes. *Proc. Natl. Acad. Sci. U.S.A.*, **90**, 7240–7244.

SALVEMINI, D., SEIBERT, K., MASFERRER, J.L.,MISKO, T.P., CURRIE, M.G. & NEEDLEMAN, P. (1994). Endogenous nitric oxide enhances prostaglandin production in a model of renal inflammation. *J. Clin. Invest.*, **93**, 1940–1947.

SCHLAG, G. & REDL, H. (1987). Mediators of sepsis. In *Update in Intensive Care and Emergency Medicine*, Vol 4. ed. Vincent, J.L. & Thijs, L.G. pp. 51–73. Berlin:Springer-Verlag.

SEIBERT, K., MASFERRER, J.L. ZHANG, Y., GREGORY, S., OLSON, G., HAUSER, S., LEAHY, K., PERKINS, W. & ISAKSON, P. (1994). Mediation of inflammation by cyclooxygenase 2. In *Proceedings of the 9th International Conference of Prostaglandins and Related Compounds*. New York:Raven Press (in press).

THIEMERMANN, C. & VANE, J. (1990). Inhibition of nitric oxide synthesis reduces the hypotension induced by bacterial lipopolysaccharides in the rat in vivo. *Eur. J. Pharmacol.*, **182**, 591–595.

WILKINS, M.R., SETTLE, S. & NEEDLEMAN, P. (1990). Augmentation of the natriuretic activity of exogenous and endogenous atriopeptin in rats by inhibition of guanosine 3′,5′-cyclic monophosphate degradation. *J. Clin. Invest.*, **85**, 1274–1279.

WILSON, D.D., DEGARAVILLA, L., KIHN, W., TOGO, J., BURCH, R.M. & STERANKA, L.R. (1989). D-Arg-[Hyp^3-D-Phe^7]bradykinin, a bradykinin antagonist, reduces mortality in a rat model of endotoxic shock. *Circ. Shock.*, **27**, 93–101.

WRIGHT, C.E., REES, D.D. & MONCADA, S. (1992). Protective and pathological roles of nitric oxide in endotoxin shock. *Cardiovasc. Res.*, **26**, 48–57.

(Received October 31, 1994
Revised November 14, 1994
Accepted November 29, 1994)

British Journal of Pharmacology (1995) 114, 1179-1184

Comparison of the pharmacological profile of S-nitrosothiols, nitric oxide and the nitrergic neurotransmitter in the canine ileocolonic junction

Joris G. De Man, Guy E. Boeckxstaens, Benedicte Y. De Winter, Tom G. Moreels, Menno E. Misset, Arnold G. Herman & [1]Paul A. Pelckmans

Divisions of Gastroenterology and Pharmacology, Faculty of Medicine, University of Antwerp (UIA), B-2610 Antwerpen-Wilrijk, Belgium

1 In organ bath experiments, hydroquinone (30-100 μM) and hydroxocobalamin (30-100 μM) concentration-dependently inhibited the relaxations induced by NO (0.3-30 μM) but not those by nitroglycerin (GTN, 1 μM) in the canine ileocolonic junction (ICJ). Hydroxocobalamin reduced the relaxation to low frequency (2 Hz) stimulation of the non-adrenergic, non-cholinergic (NANC) nerves, whereas hydroquinone only reduced the NANC nerve-mediated relaxations to electrical stimulation at 16 Hz, 0.5 ms.

2 Relaxations to S-nitroso-L-cysteine (CysNO, 1-30 μM), or S-nitroso-N-acetyl-D,L-penicillamine (SNAP, 1-30 μM) were not inhibited by hydroquinone (30-100 μM), hydroxocobalamin (30-100 μM), pyrogallol (30-100 μM) or L-cysteine (1-3 μM). Hydroquinone (100 μM) only reduced the relaxation to 10 μM CysNO. Hydroxocobalamin, but not hydroquinone, pyrogallol or L-cysteine, potentiated the relaxations to the lowest concentration (1 μM) of S-nitrosoglutathione (GSNO, 1-30 μM).

3 In the superfusion bioassay, hydroquinone (100 μM) and hydroxocobalamin (1 μM) concentration-dependently inhibited the biological activity of authentic NO (1-4 pmol) to the same extent as that of the transferable nitrergic factor, released from the canine ICJ in response to NANC nerve stimulation (8-16 Hz, 2 ms). Responses to GTN (10 pmol) or adenosine 5'-triphosphate (10 nmol) were not affected.

4 In conclusion, the nitrosothiols CysNO, SNAP and GSNO relax the canine ileocolonic junction, but these relaxations, pharmacologically, behave differently from the NANC nerve-mediated relaxations. From the bioassay experiments, we conclude that the nitrergic factor, released in response to NANC nerve stimulation of the canine ICJ, behaves pharmacologically like NO but not like a nitrosothiol. Therefore, we suggest NO, and not CysNO, SNAP or GSNO as the inhibitory NANC neurotransmitter in the canine ICJ.

Keywords: Bioassay; canine ileocolonic junction; nitrergic neurotransmission; nitric oxide; S-nitrosothiols; non adrenergic non cholinergic transmission

Introduction

Since nitric oxide (NO) was proposed as a non-adrenergic non-cholinergic (NANC) neurotransmitter in the alimentary tract (Bult *et al.*, 1990; Boeckxstaens *et al.*, 1990), the so-called nitrergic transmission has been demonstrated throughout the whole gastrointestinal tract (for reviews see: Sanders & Ward, 1992; Stark & Szurszewski, 1992). At present the role of NO in NANC neurotransmission has been well-established, but the exact chemical identity of the nitrergic neurotransmitter remains controversial. It was reported that drugs like hydroquinone, pyrogallol and LY 83583, which act as free radical scavengers or superoxide anion generators, had a differential effect on relaxations induced by authentic NO compared to those induced by NANC nerve stimulation in the bovine retractor penis muscle (Gillespie & Sheng, 1990), the rat gastric fundus and mouse anococcygeus (Barbier & Lefebvre, 1994; Hobbs *et al.*, 1991). Furthermore, in the rat anococcygeus muscle, hydroxocobalamin, which is thought to act as a NO scavenger, clearly inhibited relaxations to NO but only those to low frequency stimulation of the NANC nerves (Rajanayagam *et al.*, 1993). It was therefore hypothesized that the inhibitory nitrergic NANC neurotransmitter is not free NO but rather a superoxide-resistant, NO-releasing molecule, such as a S-nitrosothiol. S-nitrosothiols have indeed been shown to relax vascular (Ignarro *et al.*, 1981; Myers *et al.*, 1990) and non-vascular, including gastrointestinal, smooth muscle (Gibson *et al.*, 1992; Kerr *et al.*, 1992; Knudsen *et al.*, 1992; Rand & Li, 1993; Liu *et al.*, 1994; Barbier & Lefebvre, 1994) and to mimic NANC hyperpolarizations in canine colon (Thornbury *et al.*, 1991) and rat gastric fundus (Kitamura *et al.*, 1993).

In order to investigate whether the inhibitory NANC neurotransmitter is NO or an S-nitrosothiol, we recently studied the effect of L-cysteine, shown to discriminate between NO and S-nitrosothiols (Feelisch *et al.*, 1994), and the effect of pyrogallol on the nitrergic neurotransmitter in the canine ileocolonic junction (ICJ), both in organ baths and in a bioassay set-up (Boeckxstaens *et al.*, 1994). In organ baths, pyrogallol and L-cysteine inhibited the NO-induced but not the NANC nerve-induced relaxations. It was hypothesized that this differential effect was due to their pharmacological inactivity at the neuromuscular junction, since in bioassay superfusion experiments, both agents inhibited the biological activity of the nitrergic neurotransmitter released in response to NANC nerve stimulation to the same extent as the biological activity of authentic NO (Boeckxstaens *et al.*, 1994). In contrast, responses to S-nitrosothiols were not affected, indicating that the inhibitory nitrergic NANC neurotransmitter is free NO rather than a S-nitrosothiol.

To investigate further whether the nitrergic neurotransmit-

[1] Author for correspondence.

ter is NO or a S-nitrosothiol, we studied the effect of the nitrosothiols S-nitroso-L-cysteine (CysNO), S-nitroso-glutathione (GSNO) and S-nitroso-N-acetyl-D,L-penicillamine (SNAP) in the canine ICJ. In addition, we compared the effect of hydroquinone, hydroxocobalamin, pyrogallol and L-cysteine on the relaxations to S-nitrosothiols, authentic NO and the endogenous nitrergic NANC neurotransmitter. Finally, using a superfusion bioassay, we investigated the effect of hydroquinone and hydroxocobalamin on the biological activity of authentic NO and the transferable nitrergic factor.

Methods

Organ bath experiments

Tissue preparation Mongrel dogs of either sex (body weight 10–30 kg) were anaesthetized with sodium pentobarbitone (30 mg kg^{-1}, i.v.) and a laparotomy was performed. The ileum and colon were resected 10 cm above and 3 cm below the ICJ. After the resected specimen was cleaned and rinsed, the mucosa was removed from the ileum and ICJ by means of sharp dissection. Circular muscle strips of the ICJ were cut, approximately 1.5 cm long and 0.3 cm wide, and mounted in organ baths (25 ml) (Pelckmans *et al.*, 1989) filled with a modified Krebs-Ringer solution (mM: NaCl 118.3, KCl 4.7, $MgSO_4$ 1.2, KH_2PO_4 1.2, $CaCl_2$ 2.5, $NaHCO_3$ 25, CaEDTA 0.026 and glucose 11.1). The solution was maintained at 37°C and aerated with a mixture of 95% O_2 and 5% CO_2.

Isometric tension recording One end of each muscle strip was connected to a metal rod while the other end was attached to a strain gauge transducer (Statham UC2) for continuous recording of isometric tension. After the muscle strips were brought to the optimal point of their length-tension relationship (Pelckmans *et al.*, 1989), they were washed three times and then allowed to equilibrate for at least 45 min before experimentation.

Experimental protocols All experiments were performed on 0.1 μM substance P-contracted muscle strips and in the presence of 0.3 μM atropine. After each contraction, the muscle strips were washed four times with an interval of at least 5 min.

The effects of hydroquinone (30–100 μM) and hydroxocobalamin (30–100 μM) were investigated on the frequency-response curve to electrical stimulation (2–16 Hz, 0.5–2 ms), on the relaxations to nitroglycerin (GTN, 1 μM) and on the concentration-response curves to NO (0.3–30 μM), CysNO (1–30 μM), GSNO (1–30 μM) and SNAP (1–30 μM). Possible changes with time were evaluated in parallel muscle strips serving as time control. Electrical pulses (rectangular waves, 100 mA, 9 V) were delivered by a Grass stimulator and a direct current amplifier in trains of stimuli of 10 s.

Superfusion bioassay cascade

Preparation of the donor tissue After resection, cleaning and rinsing of the ICJ, the mucosa and submucosa was peeled off and a circular muscle strip was prepared and mounted in a perfusion chamber, as described previously (Boeckxstaens *et al.*, 1991). The tissue was perfused (3 ml min^{-1}) with a modified Krebs-Ringer solution maintained at 37°C. This solution contained L-arginine (50 μM), guanethidine (3 μM) and superoxide dismutase (20 u ml^{-1}) and was aerated with a mixture of 80% N_2, 15% O_2 and 5% CO_2. As hydroquinone acts as a superoxide- and/or radical scavenger, the experiments with hydroquinone were performed in the absence of exogenous superoxide dismutase. The perfusion chamber contained two platinum ring electrodes, through which the muscle strip was pulled. Electrical impulses (rectangular waves, 25 mA, 9 V) were delivered by a Grass stimulator and a direct current amplifier in trains of stimuli of 20 s and with an interval of at least 15 min, resulting in reproducible responses.

Preparation of the detector tissue New Zealand white rabbits (2000–2500 g) were killed by an overdose of sodium pentobarbitone. After a laparotomy, the abdominal aorta was removed and placed in modified Krebs-Ringer solution. Rings of abdominal aorta (3 mm wide) were cut, denuded of their endothelium by gentle rubbing and arranged in parallel under 8 g resting tension for isometric tension recording. The aortic rings were contracted by an infusion of noradrenaline (0.1 μM) and then superfused with the effluent of the superfusion tube that contained the muscle strip of the canine ileocolonic junction. A bolus of acetylcholine (3 nmol) was injected directly onto the aortic rings to verify the absence of endothelium. Subsequently, atropine (0.3 μM) was introduced into the perfusate and the sensitivity of the bioassay tissues was standardized by a bolus injection of nitroglycerin (GTN, 10 pmol).

Experimental protocols The effects of hydroquinone (100 μM) and hydroxocobalamin (1 μM) were investigated on the relaxations of the rabbit aortic ring in response to the nitrergic factor released in response to electrical stimulation (8–16 Hz, 2 ms) of the NANC nerves of the canine ICJ and on relaxations induced by bolus injections of authentic NO (1–4 pmol), GTN (10 pmol) and ATP (10 nmol).

Drugs

The following drugs were used: adenosine 5'-triphosphate, glutathione, hydroquinone, hydroxocobalamin, L-arginine, L-cysteine, N-acetyl-D,L-penicillamine, pyrogallol, substance P (Sigma Chemical Co., St. Louis, MO., U.S.A.), atropine sulphate (Federa, Brussels, Belgium), guanethidine monosulphate (Ciba-Geigy, Switzerland), nitroglycerin (Merck, Darmstadt, Germany), noradrenaline hydrogentartrate (Fluka AG, Buchs SG, Switzerland). Solutions of NO were prepared as described previously (Kelm *et al.*, 1988). Solutions of CysNO, GSNO and SNAP were prepared as described by Barbier & Lefebvre (1994).

Presentation of results and statistical analysis

Results are expressed as percentage decrease of the substance P- or noradrenaline-induced contraction and shown as mean ± s.e.mean for the number of dogs indicated. Differences were considered statistically significant for $P<0.05$, using Student's t test for paired observations.

Results

Organ bath experiments

Responses to NANC nerve stimulation Electrical stimulation of the canine ICJ (2–16 Hz, 0.5–2 ms) induced frequency-dependent NANC relaxations, previously shown to be mediated by NO or a NO-releasing substance (Boeckxstaens *et al.*, 1990). Hydroquinone (30–100 μM) only reduced the NANC nerve-induced relaxations to electrical stimulation at 16 Hz, 0.5 ms (Figure 1). Hydroxocobalamin (30–100 μM) did not affect the nitrergic NANC relaxations, except those to low frequency stimulation (2 Hz, 0.5 ms) which were inhibited by 100 μM hydroxocobalamin (Figure 1). None of these drugs affected the basal tension or the substance P-induced contraction of the canine ICJ.

Concentration-response curves to NO NO (0.3–30 μM) concentration-dependently relaxed the muscle strips of the canine ICJ. Hydroquinone (30–100 μM) and hydroxocobal-

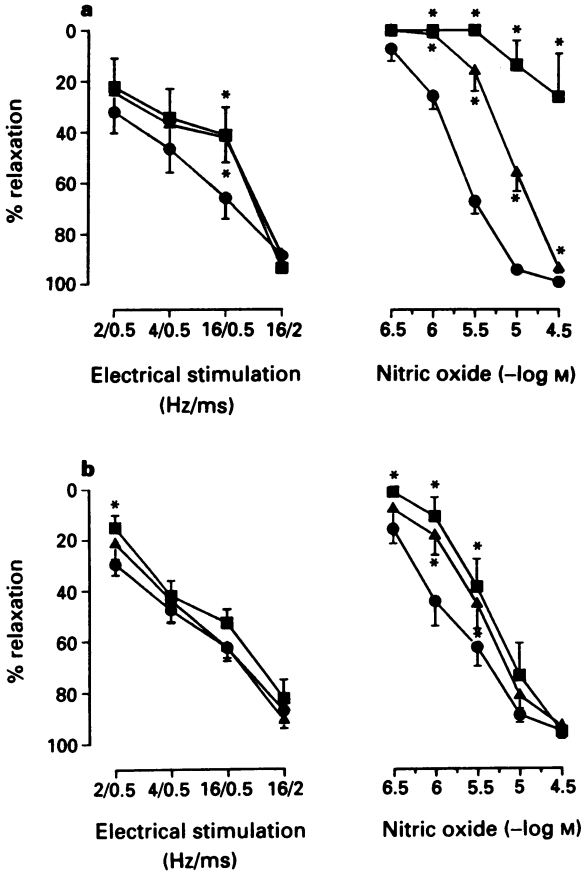

Figure 1 Effect of (a) hydroquinone (▲, 30 μM; ■, 100 μM) and (b) hydroxocobalamin (▲, 30 μM; ■, 100 μM) on the NANC relaxations induced by electrical stimulation (●, 2–16 Hz, 0.5–2 ms) and on the concentration-response curve to NO (●, 0.3–30 μM) in the canine ileocolonic junction. Results are expressed as percentage decrease of the substance P (0.1 μM)-induced contraction and shown as mean ± s.e.mean for $n = 7-8$ experiments. $^*P < 0.05$ is considered as significantly different from control; Student's t test for paired observations.

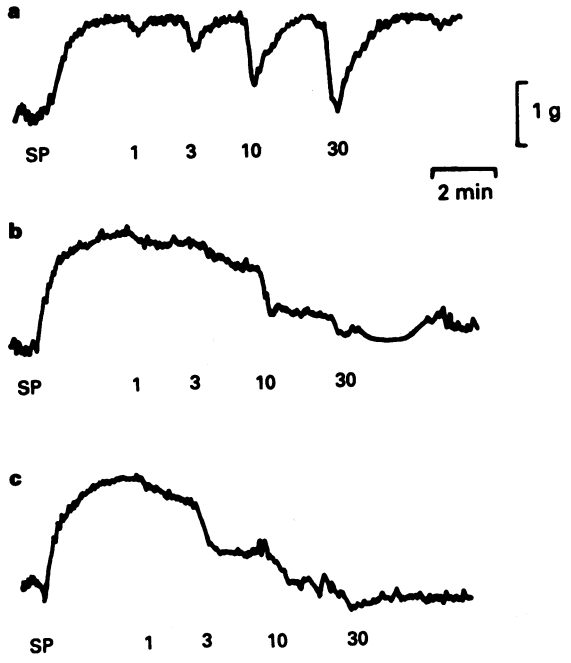

Figure 2 Typical tracings showing the concentration-dependent effect of (a) S-nitroso-L-cysteine (1–30 μM), (b) S-nitrosoglutathione (1–30 μM) and (c) S-nitroso-N-acetyl-D,L-penicillamine (1–30 μM) on the canine ICJ during a substance P (SP, 0.1 μM)-induced contraction.

amin (30–100 μM) significantly shifted the concentration-response curve to NO to the right (Figure 1). In addition, hydroquinone (100 μM) significantly reduced the maximal relaxation to NO from 100% to 26 ± 17% ($n = 6$) of the substance P-induced contraction. In contrast, hydroxocobalamin had no effect on the maximal response to NO.

Concentration-response curves to S-nitrosothiols CysNO, GSNO and SNAP (all 1–30 μM) relaxed the muscle strips of the canine ICJ. Relaxations to CysNO were transient and resembled those to NO and NANC nerve stimulation (Figure 2), but they were not affected by hydroquinone (30–100 μM), hydroxocobalamin (30–100 μM), pyrogallol (30–100 μM) or L-cysteine (1–3 μM) (Figure 3). However, the highest concentration of hydroquinone (100 μM) inhibited the relaxation to 10 μM CysNO. In contrast to NO and CysNO, relaxations to GSNO were sustained (Figure 2). They were not inhibited by pyrogallol (30–100 μM), hydroquinone (30–100 μM) or L-cysteine (1–3 μM). Hydroxocobalamin (30–100 μM) on the other hand potentiated the relaxations to the lower concentrations of GSNO (Figure 4). Relaxations to SNAP were also sustained (Figure 2) and were not significantly affected by hydroquinone (30–100 μM), hydroxocobalamin (30–100 μM), pyrogallol (30–100 μM) or L-cysteine (1–3 μM) (Figure 5).

Bioassay experiments

Responses to NANC nerve stimulation Electrical stimulation (8–16 Hz, 2 ms) of the canine ICJ induced the release of a

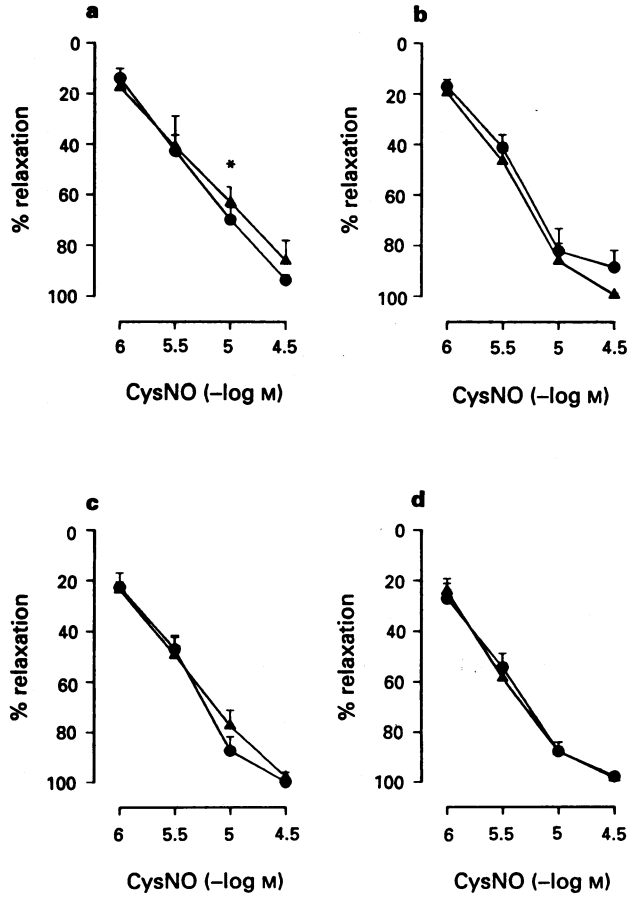

Figure 3 Effect of (a) hydroquinone (▲, 100 μM), (b) hydroxocobalamin (▲, 100 μM), (c) pyrogallol (▲, 100 μM) and (d) L-cysteine (▲, 3 μM) on the concentration-response curve to S-nitroso-L-cysteine (●, CysNO, 1–30 μM) in the canine ileocolonic junction. Results are expressed as percentage decrease of the substance P (0.1 μM)-induced contraction and shown as mean ± s.e.mean for $n = 5$ experiments. $^*P < 0.05$ is considered as significantly different from control; Student's t test for paired observations.

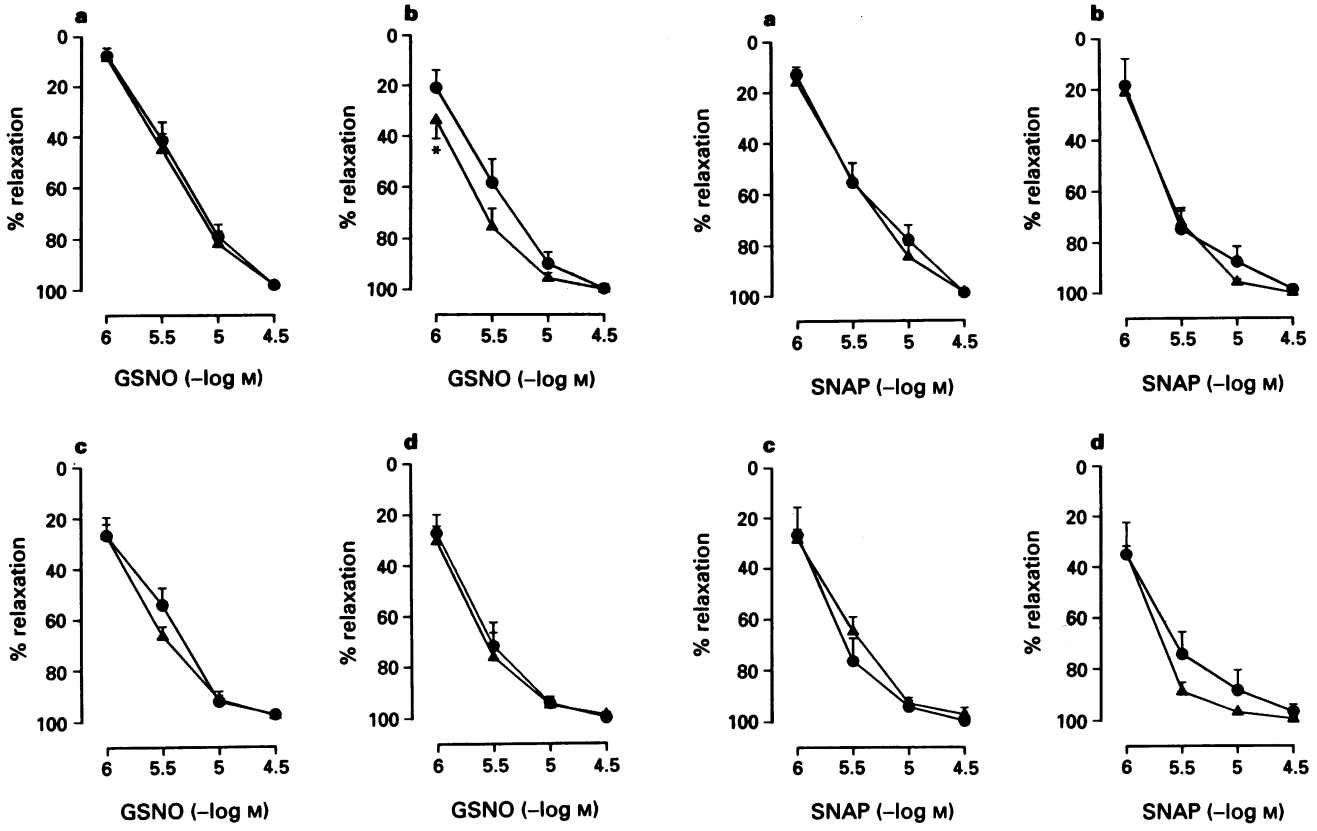

Figure 4 Effect of (a) hydroquinone (▲, 100 μM), (b) hydroxocobalamin (▲, 100 μM), (c) pyrogallol (▲, 100 μM) and (d) L-cysteine (▲, 3 μM) on the concentration-response curve to S-nitrosogluthathione (●, GSNO, 1–30 μM) in the canine ileocolonic junction. Results are expressed as percentage decrease of the substance P (0.1 μM)-induced contraction and shown as mean ± s.e.mean for $n = 5$ experiments. $*P < 0.05$ is considered as significantly different from control; Student's t test for paired observations.

Figure 5 Effect of (a) hydroquinone (▲, 100 μM), (b) hydroxocobalamin (▲, 100 μM), (c) pyrogallol (▲, 100 μM) and (d) L-cysteine (▲, 3 μM) on the concentration-response curve to S-nitroso-D,L-penicillamine (●, SNAP, 1–30 μM) in the canine ileocolonic junction. Results are expressed as percentage decrease of the substance P (0.1 μM)-induced contraction and shown as mean ± s.e.mean for $n = 5$ experiments. $*P < 0.05$ is considered as significantly different from control; Student's t test for paired observations.

vasorelaxant factor, previously characterized as NO or a NO-related substance (Boeckxstaens *et al.*, 1991). The biological activity of the transferable nitrergic vasorelaxant factor was significantly and concentration-dependently inhibited by hydroquinone (10–100 μM) or hydroxocobalamin (0.1–1 μM) (Figure 6). Hydroquinone or hydroxocobalamin did not affect the noradrenaline-induced contraction of the rabbit aorta or the relaxation to nitroglycerin (10 pmol) (Figure 6) and ATP (10 nmol) (results not shown).

Concentration-response curves to NO NO (1–4 pmol), injected into the effluent of the superfusion tube, induced concentration-dependent relaxations of the rabbit aorta which were significantly inhibited by hydroquinone (100 μM) and hydroxocobalamin (1 μM) (Figure 7). In Figure 7, the data obtained with the transferable factor under control conditions were plotted on the corresponding concentration-response curve to NO according to their value on the Y-axis. This figure shows that hydroquinone and hydroxocobalamin inhibit the relaxations to the nitrergic factor to the same extent as those to NO.

Discussion

Since substances like pyrogallol, hydroquinone, LY 83583 and hydroxocobalamin had different effects on NO as compared to NANC nerve-induced responses, it has been suggested that a NO releasing substance, such as a nitrosothiol, acts as NANC neurotransmitter rather than authentic NO.

To date, a number of S-nitrosothiols have been investigated (Thornbury *et al.*, 1991; Gibson *et al.*, 1992; Kerr *et al.*, 1992; Knudsen *et al.*, 1992; Kitamura *et al.*, 1993; Rand & Li, 1993; Barbier & Lefebvre, 1994; Liu *et al.*, 1994) as possible nitrergic NANC neurotransmitters. In the present study CysNO, GSNO and SNAP all concentration-dependently relaxed the canine ICJ. However, only the relaxations to CysNO were transient and resembled those to NANC nerve stimulation while the relaxations to GSNO and SNAP were sustained. None of the nitrosothiols had a pharmacological profile similar to that of nerve stimulation: hydroxocobalamin reduced the electrically-induced relaxations with lower amplitude, whereas it failed to reduce the relaxations induced by the nitrosothiols under study. Hydroxocobalamin even enhanced the relaxations to the lowest concentration of GSNO. Furthermore, hydroquinone failed to reduce the relaxations to SNAP and GSNO, whereas it reduced those to nerve stimulation at 16 Hz, 0.5 ms. Hydroquinone also inhibited the relaxation to 10 μM CysNO, however not to the same extent as the nerve-mediated relaxation at 16 Hz, 0.5 ms. Like the nerve-mediated relaxations (Boeckxstaens *et al.*, 1994), those induced by CysNO, SNAP or GSNO were not affected by L-cysteine and pyrogallol. However, based on the finding that hydroxocobalamin and hydroquinone affect the nerve-mediated responses differently from the responses to CysNO, SNAP and GSNO, these nitrosothiols can be excluded as possible neurotransmitters in the canine ileocolonic junction. Furthermore, S-nitrosothiols, which are

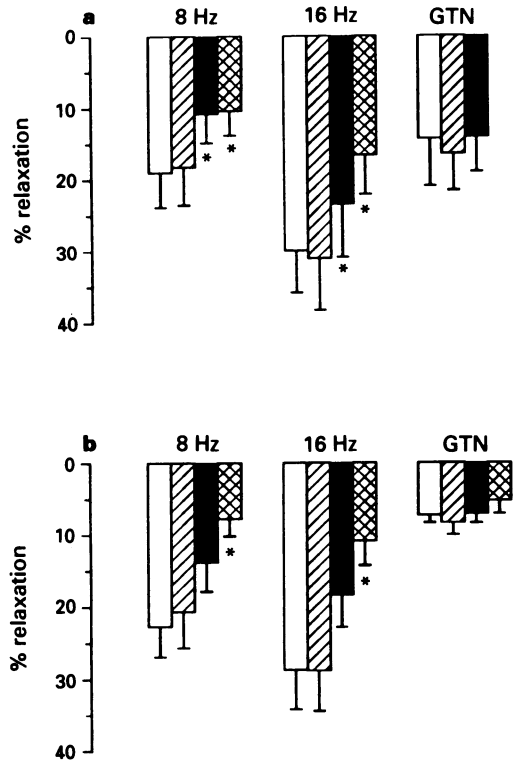

Figure 6 Concentration-dependent effect of (a) hydroquinone (hatched columns, 10 μM; solid columns, 30 μM; cross hatched columns, 100 μM) and (b) hydroxocobalamin (hatched columns 0.3 μM; solid columns, 1 μM; cross hatched columns, 3 μM) on the biological activity of the vasorelaxant nitrergic factor, released in response to NANC nerve stimulation (8–16 Hz, 2 ms) of the canine ICJ, and on the activity of nitroglycerin (GTN, 10 pmol). Results are expressed as percentage decrease of the noradrenaline (0.1 μM)-induced contraction and shown as mean ± s.e.mean for $n = 4-7$ experiments. $^*P < 0.05$ is considered as significantly different from control; Student's t test for paired observations.

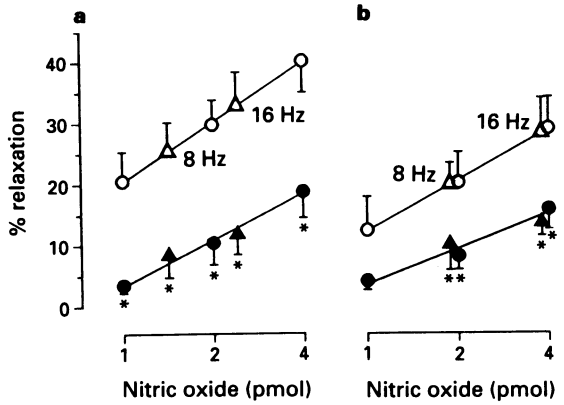

Figure 7 Effect of (a) hydroquinone (100 μM, filled symbols) and (b) hydroxocobalamin (1 μM, filled symbols) on the biological activity of NO (○, 1–4 pmol), injected in the effluent of the superfusion tube and on the activity of the vasorelaxant nitrergic factor, released in response to NANC nerve stimulation (△, 8–16 Hz, 2 ms) of the canine ICJ. Results are expressed as percentage decrease of the noradrenaline (0.1 μM)-induced contraction and shown as mean ± s.e.mean for $n = 6$ experiments. $^*P < 0.05$ is considered as significantly different from control; Student's t test for paired observations.

generally polarized substances (Kowaluk & Fung, 1990), are unlikely to permeate cell membranes whereas free NO is a highly permeable gas which can diffuse rapidly across cell membranes.

Although in the organ baths the pharmacological profile of exogenous NO is not identical to that of the endogenous nitrergic neurotransmitter, we do believe that the neurotransmitter released by the inhibitory NANC nerves is free NO. As reported earlier (Boeckxstaens *et al.*, 1994), the differential effect of pyrogallol and L-cysteine on NO- and NANC nerve-induced relaxations studied in organ baths, can be explained by inactivity of these substances at the site of the neuromuscular junction. Although these superoxide anion generators had no effect on NANC nerve-mediated relaxations in organ baths, in the bioassay set-up they inhibited the biological activity of NO and the nitrergic transferable factor, released in response to NANC nerve stimulation, with equal potency. Also in the present study, the data obtained from the organ bath experiments revealed a differential effect of hydroquinone and hydroxocobalamin on the responses to NO and to NANC nerve stimulation. However, in the bioassay experiments, the biological activity of the transferable factor and NO were affected to the same extent, suggesting that NO is released in response to NANC nerve stimulation. However, it has to be considered that the NANC nerves might actually release a nitrosothiol, from which NO is liberated either spontaneously or after contact with the effector cell (Kowaluk & Fung, 1990; Mathews & Kerr, 1993) and subsequently detected by the bioassay tissue. However, the biological activity of CysNO, SNAP or GSNO, even after they superfused the ileocolonic junction, was not affected by pyrogallol or L-cysteine (Boeckxstaens *et al.*, 1994) providing evidence against this possibility. Furthermore, it has to be emphasized that in the organ bath, exogenous NO is directly injected into the bathing fluid that contains the inhibitor under study, whereas this inhibitor has to move into the neuromuscular junction to block the biological activity of the endogenous neurotransmitter. This difference is not present in the bioassay, resulting in an identical pharmacological profile for NO and the nitrergic neurotransmitter, illustrating that the differential effect of pyrogallol, L-cysteine, hydroquinone and hydroxocobalamin in the organ baths results from their reduced activity at the neuromuscular junction. Such a reduced activity may be due to high tissue activity of superoxide dismutase, which was recently shown to protect effectively the nitrergic neurotransmitter in the rat anococcygeus against the action of pyrogallol (Liu & Szurszewski, 1994).

In conclusion, we have illustrated that the pharmacological profile of CysNO, SNAP and GSNO differs from that of the nitrergic neurotransmitter in the canine ileocolonic junction. Although NO and the nitrergic neurotransmitter were differently affected by hydroquinone and hydroxocobalamin in the organ bath experiments, they had an identical pharmacological profile in the superfusion bioassay. From these results, we suggest that the differential effect in the organ baths results from reduced activity of these inhibitors at the neuromuscular junction and conclude that the nitrergic NANC neurotransmitter of the canine ICJ is NO, and not CysNO, SNAP or GSNO.

The authors wish to thank Mrs L. Van de Noort for typing the manuscript and F. Jordaens for technical assistance.

References

BARBIER, A.J.M. & LEFEBVRE, R.A. (1994). Influence of S-nitrosothiols and nitrate tolerance in the rat gastric fundus. *Br. J. Pharmacol.*, **111**, 1280–1286.

BOECKXSTAENS, G.E., DE MAN, J.G., DE WINTER, B.Y., HERMAN, A.G. & PELCKMANS, P.A. (1994). Pharmacological similarity between nitric oxide and the nitrergic neurotransmitter in the canine ileocolonic junction. *Eur. J. Pharmacol.*, **264**, 85–89.

BOECKXSTAENS, G.E., PELCKMANS, P.A., BULT, H., DE MAN, J.G., HERMAN, A.G. & VAN MAERCKE, Y.M. (1990). Non-adrenergic non-cholinergic relaxation mediated by nitric oxide in the canine ileocolonic junction. *Eur. J. Pharmacol.*, **190**, 239–246.

BOECKXSTAENS, G.E., PELCKMANS, P.A., RUYTJENS, I.F., BULT, H., DE MAN, J.G., HERMAN, A.G. & VAN MAERCKE, Y.M. (1991). Bioassay of nitric oxide released upon stimulation of non-adrenergic non-cholinergic nerves in the canine ileocolonic junction. *Br. J. Pharmacol.*, **103**, 1085–1091.

BULT, H., BOECKXSTAENS, G.E., PELCKMANS, P.A., JORDAENS, F.H., VAN MAERCKE, Y.M. & HERMAN, A.G. (1990). Nitric oxide as an inhibitory non-adrenergic non-cholinergic neurotransmitter. *Nature*, **345**, 346–347.

FEELISCH, M., TE POEL, M., ZAMORA, R., DEUSSEN, A. & MONCADA, S. (1994). Understanding the controversy over the identity of EDRF. *Nature*, **368**, 62–65.

GIBSON, A., BABBEDGE, R., BRAVE, S.R., HART, S.L., HOBBS, A.J., TUCKER, J.F., WALLACE, P. & MOORE, P.K. (1992). An investigation of some S-nitrosothiols, and of hydroxy-arginine on the mouse anococcygeus. *Br. J. Pharmacol.*, **107**, 715–721.

GILLESPIE, J.S. & SHENG, H. (1990). The effects of pyrogallol and hydroquinone on the response to NANC nerve stimulation in the rat anococcygeus and the bovine retractor penis muscles. *Br. J. Pharmacol.*, **99**, 194–196.

HOBBS, A.J., TUCKER, J.F. & GIBSON, A. (1991). Differentiation by hydroquinone of relaxations induced by exogenous and endogenous nitrates in non-vascular smooth muscle: role of superoxide anions. *Br. J. Pharmacol.*, **104**, 645–650.

IGNARRO, L.J., LIPPTON, H., EDWARDS, J.C., BARICOS, W.H., HYMAN, A.L. KADOWITZ, P.J. & GRUETTER, C.A. (1981). Mechanism of vascular smooth muscle relaxation by organic nitrates, nitrites, nitroprusside and nitric oxide: evidence for the involvement of S-nitrosothiols as active intermediates. *J. Pharmacol. Exp. Ther.*, **218**, 739–749.

KELM, M., FEELISCH, M., SPAHR, R., PIPER, H.M., HOACK, E. & SCHRADER, J. (1988). Quantitative and kinetic characterization of nitric oxide and EDRF released from cultured endothelial cells. *Biochem. Biophys. Res. Commun.*, **154**, 236–244.

KERR, S.W., BUCHANAN, L.V., BUNTING, S. & MATHEWS, W.R. (1992). Evidence that S-nitrosothiols are responsible for the smooth muscle relaxing activity of the bovine retractor penis inhibitory factor. *J. Pharmacol. Exp. Ther.*, **263**, 285–292.

KITAMURA, K., LIAN, Q., CARL, A. & KURIYAMA, H. (1993). S-nitrosocysteine, but not sodium nitroprusside, produces apamin-sensitive hyperpolarization in rat gastric fundus. *Br. J. Pharmacol.*, **109**, 415–423.

KNUDSEN, M.A. SVANE, D. & TØTTRUP, A. (1992). Action profiles of nitric oxide, S-nitro-L-cysteine, SNP, and NANC responses in opossum lower esophageal sphincter. *Am. J. Physiol.*, **262**, G840–G846.

KOWALUK, E.A. & FUNG, H.L. (1990). Spontaneous liberation of nitric oxide cannot account for *in vitro* vascular relaxation by S-nitrosothiols. *J. Pharmacol. Exp. Ther.*, **255**, 1256–1264.

LIU, X., GILLESPIE, J.S. & MARTIN, W. (1994). Non-adrenergic non-cholinergic relaxation of the bovine retractor penis muscle: role of S-nitrosothiols. *Br. J. Pharmacol.*, **111**, 1287–1295.

LIU, X. & SZURSZEWSKI, J.H. (1994). The nitrergic neurotransmitter in the rat anococcygeus muscle is protected by endogenous superoxide dismutase. *Gastroenterology*, **107**, 1230.

MATHEWS, W.R. & KERR, S.W. (1993). Biological activity of S-nitrosothiols: the role of nitric oxide. *J. Pharmacol. Exp. Ther.*, **267**, 1529–1537.

MYERS, P.R., MINOR, R.L., GUERRA, R., BATES, J.N. & HARRISON, D.G. (1990). Vasorelaxant properties of the endothelium-derived relaxing factor more closely resemble S-nitrosocysteine than nitric oxide. *Nature*, **345**, 161–163.

PELCKMANS, P.A., BOECKXSTAENS, G.E., VAN MAERCKE, Y.M., HERMAN, A.G. & VERBEUREN, T.J. (1989). Acetylcholine is an indirect inhibitory transmitter in the canine ileocolonic junction. *Eur. J. Pharmacol.*, **170**, 235–242.

RAJANAYAGAM, M.A.S., LI, C.G. & RAND, M.J. (1993). Differential effects of hydroxocobalamin on NO-mediated relaxations in rat aorta and anococcygeus muscle. *Br. J. Pharmacol.*, **108**, 3–5.

RAND, M.J. & LI, C.G. (1993). Differential effects of hydroxocobalamin on relaxations induced by nitrosothiols in rat aorta and anococcygeus muscle. *Eur. J. Pharmacol.*, **241**, 249–254.

SANDERS, K.M. & WARD, S.M. (1992). Nitric oxide as a mediator of nonadrenergic noncholinergic neurotransmission. *Am. J. Physiol.*, **262**, G379–G392.

STARK, M.E. & SZURSZEWSKI, J.H. (1992). Role of nitric oxide in gastrointestinal function and disease. *Gastroenterology*, **103**, 1928–1949.

THORNBURY, K.D., WARD, S.M., DALZIEL, H.H., CARL, A., WESTFALL, D.P. & SANDERS, K.M. (1991). Nitric oxide and nitrosocysteine mimic nonadrenergic noncholinergic hyperpolarization in canine proximal colon. *Am. J. Physiol.*, **261**, G553–G557.

(Received October 31, 1994
Revised November 21, 1994
Accepted November 29, 1994)

British Journal of Pharmacology (1995) 114, 1185-1192

Role of angiotensin converting enzyme in the vascular effects of an endopeptidase 24.15 inhibitor

Sarah E. Telford, A. Ian Smith, Rebecca A. Lew, *Rose B. Perich, Anna C. Madden & [1]Roger G. Evans

Baker Medical Research Institute, Prahran, Victoria, Australia and *University of Melbourne Department of Medicine, Austin Hospital, Heidelberg, Victoria, Australia

1 We investigated the role of angiotensin converting enzyme (ACE) in the cardiovascular effects of N-[1-(**R**,**S**)-carboxy-3-phenylpropyl]-Ala-Ala-Tyr-*p*-aminobenzoate (cFP), a peptidase inhibitor selective for metalloendopeptidase (EP) E.C. 3.4.24.15.

2 In conscious rabbits, cFP (5 mg kg^{-1}, i.v.) markedly slowed the degradation of [^{3}H]-bradykinin, potentiated the depressor response to right atrial administration of bradykinin (10–1000 ng kg^{-1}), and inhibited the pressor response to right atrial angiotensin I (10–100 ng kg^{-1}). In each of these respects, the effects of cFP were indistinguishable from those of the ACE inhibitor, captopril (0.5 mg plus 10 mg kg^{-1}h^{-1} i.v.). Furthermore, the effects of combined administration of cFP and captopril were indistinguishable from those of captopril alone.

3 In experimentally naive anaesthetized rats, cFP administration (9.3 mg kg^{-1}, i.v.) was followed by a moderate but sustained fall in arterial pressure of 13 mmHg. However, in rats pretreated with bradykinin (50 μg kg^{-1}) a more pronounced fall of 30 mmHg was observed. Captopril (5 mg kg^{-1}) had similar hypotensive effects to those of cFP, and cFP had no effect when it was administered after captopril.

4 CFP displaced the binding of [^{125}I]-351A (the *p*-hydroxybenzamidine derivative of lisinopril) from preparations of rat plasma ACE and solubilized lung membrane ACE (K_D = 1.2 and 0.14 μM respectively), and inhibited rat plasma ACE activity (K_I = 2.4 μM). Addition of phosphoramidon (10 μM), an inhibitor of a range of metalloendopeptidases, including neutral endopeptidase (E.C.3.4.24.11), markedly reduced the potency of cFP in these systems.

5 Taken together these findings suggest that the actions of cFP *in vivo* are attributable to inhibition of ACE rather than EP 24.15. Given that cFP is a poor inhibitor of ACE in the presence of phosphoramidon *in vitro*, it is likely that cFP is cleaved by a phosphoramidon-sensitive metallopeptidase *in vivo* to liberate N-[1-(**R**,**S**)-carboxy-3-phenylpropyl]-Ala-Ala, a potent ACE inhibitor.

Keywords: Angiotensin converting enzyme; blood-pressure-physiology; bradykinin; metalloendopeptidase 24.15

Introduction

Recently there has been renewed interest in the role that metalloendopeptidases play in blood pressure control, and thus their potential as therapeutic agents (Carretero & Scicli, 1991). Much of this interest has focussed on endopeptidase E.C.3.4.24:15 (EP 24.15), first identified in soluble fractions of brain homogenates by Orlowski *et al.* (1983). Although this enzyme is widely distributed in animal tissue, it is found predominantly in the brain, pituitary and testis, with lower levels in other tissues, such as liver, kidney, lung and spleen (Chu & Orlowski, 1985). In the brain, endopeptidase 24.15 exists in two forms, the predominant soluble form constituting about 80% of the total activity and a membrane-bound form accounting for the remainder of activity (Acker *et al.*, 1987). Both the soluble and membrane-bound forms of the enzyme convert larger opioid peptides, such as dynorphin$^{1-8}$, α-and β-neoendorphin and Met-enkephalin-Arg-Gly-Leu into bioactive pentapeptides (Acker *et al.*, 1987; Orlowski *et al.*, 1988; 1989). The enzyme also has high affinity for several other peptides such as bradykinin, neurotensin and angiotensin II, which it converts to inactive forms (Orlowski *et al.*, 1983; Chu & Orlowski, 1985).

The design and synthesis of selective EP 24.15 inhibitors has allowed investigation of the possible involvement of EP 24.15 in the regulation of physiological processes. Orlowski *et al.* (1988) demonstrated that peptides containing a free N-(carboxymethyl) group, capable of interacting with the active site zinc ion of EP 24.15, act as transition state inhibitors of this enzyme. The most potent and selective of these EP 24.15 inhibitors is N-[1-(**R**,**S**)-carboxy-3-phenylpropyl]-Ala-Ala-Tyr-*p*-aminobenzoate (cFP), with a reported inhibitory constant (K_I) of 16 nM (Chu & Orlowski, 1984; Orlowski *et al.*, 1988).

The impetus for the present study results from a report showing that in anaesthetized rats a closely related analogue of cFP (N-[1-(**R**,**S**)-carboxy-3-phenylpropyl]-Ala-Ala-Phe-*p*-aminobenzoate (cFP[Phe])) both potentiated the effects of exogenous bradykinin, and had a hypotensive effect that could be blocked by a bradykinin antagonist (Genden & Molineaux, 1991). The authors of this paper inferred from these findings that cFP[Phe] lowered blood pressure by inhibiting EP 24.15-mediated bradykinin breakdown, and that EP 24.15 is therefore involved in the breakdown of endogenous bradykinin *in vivo*. However, the authors provided no direct evidence that the effects observed were mediated by inhibition of EP 24.15 and not other peptidases, such as angiotensin converting enzyme (ACE), which is known to be the principal mediator of bradykinin degradation (Yang *et al.*, 1970). Indeed, recent studies have shown that this compound can be degraded *in vitro* to form an ACE-inhibiting metabolite (Chappell *et al.*, 1992; Cardozo *et al.*, 1993; Williams *et al.*, 1993).

In the present study we have re-evaluated the hypothesis that cFP inhibits bradykinin breakdown through an interac-

[1] Author for correspondence at: Emily E.E. Stewart Renal Laboratory, Baker Medical Research Institute, P.O. Box 348, Prahran, Victoria, 3181, Australia.

tion with EP 24.15. Specifically, we have compared the effects of cFP with those of the angiotensin converting enzyme inhibitor captopril, in both conscious rabbits, and in a preparation similar to that employed by Genden & Molineaux (1991), the pentobarbitone anaesthetized rat. In addition, we have tested the interaction of cFP with both crude and purified ACE *in vitro*, using both enzymatic and binding assays. We conclude that cFP inhibits bradykinin breakdown, and lowers blood pressure, by interacting with ACE. These data do not support the notion that EP 24.15 plays a major role in systemic bradykinin metabolism and blood pressure control.

Methods

Twelve male rabbits of a cross-bred English strain and 27 male Sprague-Dawley rats were used. The experiments were conducted in accordance with the Australian Code of Practice for the Care and Use of Animals for Scientific Purposes (1990), and were approved in advance by the Alfred Hospital/Baker Medical Research Institute Animal Experimentation Committee.

Experiments on conscious rabbits

These were designed in a within-subject fashion, so that in each of the three experiments, each rabbit (1.50–2.80 kg (mean 2.25)) was studied on four separate occasions at 7–14 day intervals. The order of these studies was randomised using a 4×4 Latin square design.

Placement of catheters These were inserted on the morning of each study day, and removed at the end of the day. The rabbit was placed in a 15×40×18 cm box fitted with a wire mesh lid and intravascular catheters were inserted under local analgesia (1% lignocaine; Xylocaine, Astra Pharmaceuticals, North Ryde, NSW, Australia). A catheter (Insyte; Deseret Medical, Sandy, Utah, U.S.A.) was inserted into the central ear artery, to measure arterial pressure and to take blood samples when required. A nylon catheter (i.d 0.50 mm; o.d 0.63 mm) with a dead space of 40 µl was inserted into the marginal ear vein and advanced 11–15 cm so that the tip was near the right atrium for bolus drug administration. A catheter (Insyte) was also placed in the marginal vein of the other ear for drug infusion. Each rabbit was then allowed 30 min to adapt to its new environment before the experimental procedures began.

Experimental protocols

(1) Effects of cFP (1–25 mg kg^{-1}) on hypotensive responses to exogenous bradykinin and acetylcholine The dose-response relationships were determined for the haemodynamic effects of bradykinin (10, 30, 100, 300 and 1000 ng kg^{-1}) and acetylcholine (30, 300 and 3000 ng kg^{-1}). Both drugs were administered via the right atrial catheter in ascending doses at 4 min intervals, in a volume of 0.1 ml kg^{-1} of 154 mM NaCl. The two agents were administered alternately except the final two doses of bradykinin, which were in sequence. Five minutes after the last dose of bradykinin, either cFP (1, 5, or 25 mg kg^{-1}) or its vehicle (1.0 ml kg^{-1} 10% w/v 2-hydroxypropyl-β-cyclodextrin) was administered i.v. After a further 5 min period, dose-response curves to bradykinin and acetylcholine were repeated as above. The effects of a single dose of bradykinin (300 ng kg^{-1}) were also tested 60 and 90 min after cFP or vehicle administration.

(2) Comparisons of the effects of cFP and captopril on haemodynamic responses to angiotensin I and bradykinin On each of the four study days the rabbits received either captopril (0.5 mg plus 10 mg kg^{-1}h^{-1}, i.v.) or its vehicle (1 ml plus 10 ml kg^{-1}h^{-1} 154 mM NaCl, i.v.). Thirty minutes later, 5 mg kg^{-1} cFP or its vehicle was administered i.v., and after a 5 min equilibration period, dose-response curves to angiotensin I and bradykinin (10, 30 and 100 ng kg^{-1}) were constructed. Angiotensin I and bradykinin were administered via the right atrial catheter in ascending doses, alternating between the two drugs at 4 min intervals.

(3) Comparison of the effects of cFP and captopril on [^{3}H]-bradykinin metabolism In this experiment the effects of cFP and captopril on the breakdown of [^{3}H]-bradykinin were examined. The aim was to use exogenously administered [^{3}H]-bradykinin as a marker for endogenous bradykinin metabolism. As in Experiment 2, on each of the four study days the rabbits received either captopril (0.5 mg plus 10 mg kg^{-1} h^{-1}) or its vehicle i.v. Thirty minutes later, 5 mg kg^{-1} cFP or its vehicle was administered i.v. and a control (background) blood sample was taken. One minute after cFP or vehicle administration a bolus of [^{3}H]-bradykinin (1 µCi in 1 ml of 154 mM NaCl) was administered via the right atrial catheter, and 1 ml arterial blood samples were taken 5 and 15 s and 1, 5, 15 and 30 min later. These were collected into chilled syringes containing a cocktail of enzyme inhibitors (see Drugs) over 1–3 s, and analysed by high performance liquid chromatography (h.p.l.c.) as described below.

Rat experiment

The aim was to compare the effects of cFP and captopril on blood pressure and hindlimb vascular resistance, and to test the effect of bradykinin pretreatment on these responses. Rats ($n = 21$; 300–450 g, mean 394 g) were anaesthetized with sodium pentobarbitone (60–120 mg kg^{-1}, i.p.). A tracheal cannula was inserted and catheters were inserted into a femoral artery (for measurement of blood pressure) and a jugular vein (for drug administration). An ultrasonic (transit time) flow probe (type 2S, Transonic Systems, Ithaca, NY, U.S.A.) was placed around the abdominal aorta, below the level of the renal arteries and above the level of the inferior mesenteric artery. A 30 min equilibration period was then allowed before the experimental procedures began.

The effects on blood pressure, heart rate and hindlimb blood flow of bolus injections of cFP (1.5 µmol kg^{-1} (9.3 mg kg^{-1}), in 1.5 ml kg^{-1} 10% w/v 2-hydroxypropyl-β-cyclodextrin) and captopril (5 mg kg^{-1}; in 1.0 ml kg^{-1} 154 mM NaCl) were tested. In some rats these treatments were administered 5 min after pretreatment with bradykinin (50 µg kg^{-1} in 1 ml kg^{-1} 154 mM NaCl).

Collection of in vivo *data*

Recording of haemodynamic variables Arterial pressure was measured continuously throughout the experiments by connecting the arterial catheter to a Statham P23Dc strain gauge, set to zero at the level of the animal's heart. Hindlimb blood flow was measured by connecting the flow probe to an ultrasonic volume flow meter (Model T108; Transonic Systems, Ithaca, NY). The signals were amplified and recorded on a Grass Model 7 polygraph, and sent to an Olivetti M24 computer equipped with an A-D converter which provided mean values for mean arterial pressure (mmHg) and hindlimb blood flow (ml min^{-1}).

Preparation of blood samples for h.p.l.c. Blood samples (1 ml) were collected via an ear artery catheter into chilled syringes, containing a cocktail of enzyme inhibitors (see *Drug* section), and immediately transferred into chilled 5 ml tubes containing ethylenediaminetetraacetic acid (Sequestrene tube, Johns Disposable Products, South Oakleigh, Australia). Each sample was centrifuged at 3000 r.p.m. for 10 min at 4°C (Minifuge G.L, Heraeus, Germany). The plasma supernatant was aspirated and added to 2 ml methanol (BDH-Chemicals, Australia; analytical grade) to precipitate protein, and cent-

rifuged at 3000 r.p.m. for a further 10 min at 4°C. The supernatant was collected into 5 ml tubes and partially evaporated (to remove the organic component) in a Speedvac concentrator (Savant Instruments, U.S.A). The remaining aqueous phase (~0.5 ml) was then transferred to Eppendorf tubes. Prior to analytical h.p.l.c., each sample was centrifuged (Eppendorf microcentrifuge Model 5415C, Germany) for 5 min to remove any remaining particulate material. Preliminary studies demonstrated that bradykinin breakdown during the collection and sample preparation process was about 20%. The data presented in Results were not corrected for this systematic error.

H.p.l.c. analysis Plasma extracts were analysed in a Millipore Waters 510 liquid chromatograph system (Milford, MA, U.S.A), comprising two 510 pumps, a Model 680 gradient controller, a U6K injector and a Model 411 absorbance detector connected to a fraction collector (Pharmacia Fine Chemicals, Australia). The column effluent was monitored at 214 nM. Each 500 µl sample was injected onto a radially compressed C_{18} Nova Pak reversed-phase column (8 mm × 10 cm) (Waters Associates, U.S.A). Solvent A was 11 mM trifluoroacetic acid (TFA) and solvent B was 70% acetonitrile containing 11 mM TFA. The separations were achieved using a linear gradient of 3-55% of solvent B over 25 min at a flow rate of 1 ml min^{-1}. Fractions (0.5 ml) were collected into 6 ml glass vials to which 5 ml scintillation fluid (Insta-Gel; Packard, U.S.A) was added. The vials were then counted for 5 min on a Tri-Carb Model 1900CA liquid scintillation analyser. Synthetic bradykinin (1-9), bradykinin (1-7) and bradykinin (1-5) were used as standards to verify the elution times of the tritiated peptides.

Analysis of in vivo *results*

The recovery of [^{3}H]-bradykinin, [^{3}H]-bradykinin 1-7 and 1-5, and of non-retained [^{3}H]-bradykinin metabolites over time was quantified graphically. The analysis was complicated by the fact that the time at which blood samples were taken was not always exactly the same. To overcome this problem, we fitted spline curves to the relationships between percentage recovery of ^{3}H (in the form of bradykinin, bradykinin 1-7 and 1-5, and non-retained metabolites) against time in each individual experiment. This was done with the graphical computer software package SIGMAPLOT (Norby *et al.*, 1992). The percentage recoveries at the set time points of 5 and 15 s and at 1, 5, 15 and 30 min, were interpolated (and in a few cases extrapolated) from these curves.

The statistical computer software package SYSTAT (Wilkinson, 1990) was used for statistical analyses. P values ≤ 0.05 were considered to be significant. When repeated measures analysis of variance was used P values were conservatively adjusted by the Greenhouse-Geisser correction (Ludbrook, 1994). Conventional analysis of variance followed by specific multiple comparisons was also performed in some cases. When more than one P value was used from a particular analysis, the Dunn-Sidak correction was applied to protect against the increased risk of type I error (Ludbrook, 1991). All data are expressed as the mean ± s.e.mean.

Enzyme kinetic assay for angiotensin converting enzyme

Rat plasma angiotensin converting enzyme activity was quantified using the synthetic substrate hippuryl-histidyl-leucine (Cushman & Cheung, 1971). Increasing concentrations of cFP or enalaprilat were incubated with 10 µl of plasma and 250 µl of substrate (5 mM in 0.1 M K_2HPO_4 buffer at pH 8.3 containing 300 mM NaCl) for 15 min at 37°C. To a parallel set of assay tubes 10 µM phosphoramidon was also added. Degradation of substrate was terminated by placing tubes in an ice cold bath followed by rapid addition of 1.5 ml of 0.28 M NaOH. Liberated histidyl-leucine was quantified by fluorometric detection of its product with *o*-phthalaldehyde (Friedland & Silverstein, 1976). Results for plasma samples were read from a standard curve of known concentrations of histidyl-leucine.

Angiotensin converting enzyme radioligand binding studies

Radioiodination of 351A Preparation, purification and stability of radioiodinated 351A have been previously detailed (Jackson *et al.*, 1986). Purified [^{125}I]-351A (the *p*-hydroxybenzamidine derivative of lisinopril) was pH adjusted with 10 M NaOH (100 µl per ml of tracer) for subsequent binding experiments at pH 7.0. [^{125}I]-351A was stored at −20°C and each batch was used for no longer than 2 months.

Preparation of plasma and solubilized lung membranes Six rats (200–250 g) were killed by decapitation. Trunk blood was collected into chilled tubes containing heparin (500 iu ml^{-1}) and the lungs were removed. Blood was centrifuged at 1,800 *g* for 15 min at 4°C. Plasma was pooled and lungs were stored at −20°C until required. Membranes were prepared from thawed lungs by a modification of the method of Florentin *et al.* (1984) as described by Perich *et al.* (1992). Lung membranes were solubilized by adding 0.1% v/v Triton X-100, and then mixing on a rotating wheel for 2 h at 4°C. The preparation was centrifuged at 60,000 *g* at 4°C and the supernatant fraction containing solubilized lung membranes stored at −20°C until assay.

Purification of rat lung ACE The ACE inhibitor, lisinopril, was used to prepare an affinity column and pure ACE was prepared as described by Perich *et al.* (1992). Aliquots were stored at −80°C until required.

Binding studies Binding of [^{125}I]-351A to rat plasma and tissue ACE has previously been validated and optimized (Jackson *et al.*, 1986). Plasma and solubilized lung membranes were studied over a range of dilutions to establish the dilution required for approximately 10 to 20% binding of [^{125}I]-351A, at which concentration subsequent binding experiments were performed. All assay components were prepared in binding buffer (Jackson *et al.*, 1986). The diluted ACE source (250 µl) was incubated with 50 µl of [^{125}I]-351A (10 pg per tube, 40,000 c.p.m. when fresh) and 10 µl of cFP (10 pM to 6 µM final concentration). In a parallel set of assay tubes 10 µM phosphoramidon was also added. All tubes were mixed and equilibrated for 16 h at room temperature. Absolute ethanol (1 ml) was then added and the tubes mixed and then centrifuged at 1,800 *g* for 5 min at 4°C. The supernatant fraction was discarded and the pellet containing ACE-bound radioligand quantified by gamma-counter (LKB-Wallac Multigamma 1260, Turku, Finland). Displacement of [^{125}I]-351A from ACE was analysed by the LIGAND computer programme to derive equilibrium dissociation constants (K_D) (Munson & Rodbard, 1980).

Drugs

Drugs used in this study were: phosphoramidon, acetylcholine, angiotensin I (Sigma Chemical Company, U.S.A.); bradykinin (1-9), bradykinin (1-7), bradykinin (1-5) (Auspep, Australia); captopril (Squibb Institute for Medical Research, U.S.A); 2-hydroxypropyl-β-cyclodextrin (Research Biochemicals Incorporated, U.S.A); [^{3}H]-bradykinin (25–70 Ci $mmol^{-1}$; Du Pont Ltd, Australia); 351A, lisinopril, enalaprilat (gifts from Merck Sharpe and Dohme, Rahway, NJ, U.S.A); hippuryl-histidyl-leucine (Peptide Institute Inc., Osaka, Japan); and N-[1(**R**,**S**)-carboxy-3-phenylpropyl]-Ala-Ala-Tyr-*p*-aminobenzoate (cFP) which was synthesized by the method of Chu & Orlowski (1984).

Blood samples were collected into chilled syringes contain-

ing 110 μl of a cocktail of enzyme inhibitors comprising: 100 mM ethylenediaminetetra-acetic acid di-sodium salt (Ajax Chemicals, Australia); 10 mM N-ethylmaleimide (Calbiochem, U.S.A); 1 mg ml^{-1} bacitracin, 2.31 tiu ml^{-1} traysolol, 10 mM phenylmethylsulphonyl fluoride (Sigma Chemical Company, U.S.A); 100 μM lisinopril and 500 μM amastatin (Auspep, Australia).

Results

Experiments on rabbits

Experiment 1: Effects of cFP (1-25 mg kg^{-1}) on haemodynamic responses to bradykinin and acetylcholine Intravenous administration of bradykinin (10–1000 ng kg^{-1}) was followed by transient falls in arterial pressure (Figures 1–2). Both the magnitude and the duration of these effects increased with dose (P always ≤ 0.003). Intravenous administration of cFP dose-dependently increased both the magnitude and duration of the bradykinin responses (P always ≤ 0.04). A dose of bradykinin which had no effect under control conditions (30 ng kg^{-1}) produced a marked decrease in arterial pressure following cFP treatment (Figures 1–2). Similarly, the hypotensive effects of higher doses of bradykinin (300–1000 ng kg^{-1}) were potentiated and also prolonged after cFP administration (Figures 1–2). A near maximum effect on the response to bradykinin was produced by a dose of 5 mg kg^{-1} cFP, so this dose was used in subsequent experiments.

The duration of action of cFP was dose-dependent, and was not maximal at a dose of 5 mg kg^{-1}. The hypotensive response to 300 ng kg^{-1} bradykinin was still potentiated at 60 min, but not 90 min after 5 mg kg^{-1} cFP. After a dose of 25 mg kg^{-1} cFP the response to bradykinin was potentiated for at least 90 min (data not shown).

Intravenous administration of acetylcholine was also followed by transient falls in arterial pressure (Figure 1). The response increased both in duration and maximum effect with increasing doses (P always ≤ 0.003). The response to acetylcholine was not influenced by cFP at any of the doses tested (see Figure 1).

Experiment 2: Comparison of the effects of cFP and captopril on blood pressure responses to bradykinin and angiotensin I Depressor responses to bradykinin (30–3000 ng kg^{-1}) were potentiated by cFP (5 mg kg^{-1}) (P always ≤ 0.003) (Figure 3). The effect of captopril was both qualitatively and quantitatively similar to cFP. Responses to bradykinin following combined treatment with captopril and cFP, were indistinguishable from those following treatment with captopril alone (Figure 3).

Intravenous administration of angiotensin I (30–3000 ng kg^{-1}) was followed by dose-dependent rises in arterial pressure ($P = 0.003$). The pressor response at each dose of angiotensin I was reduced after cFP treatment ($P \leq 0.001$). The response to angiotensin I was abolished both following captopril administration, and when cFP and captopril were co-administered (Figure 3).

Experiment 3: Comparison of the effects of cFP and captopril on [^{3}H]-bradykinin metabolism In rabbits receiving vehicle, bradykinin was rapidly broken down. Five seconds after administration 81 ± 5% of the injected [^{3}H]-bradykinin had already been metabolised. Of this, 60 ± 9% was in the form of the intermediate metabolites, bradykinin 1-7 and 1-5, while 13 ± 5% was not retained on the h.p.l.c. column, and thus comprised free proline and/or tritium containing proline metabolites (hereafter referred to as proline). The two peptide fragments (1–7 and 1–5), which eluted together, were then more slowly metabolized to proline. Thus by 30 min

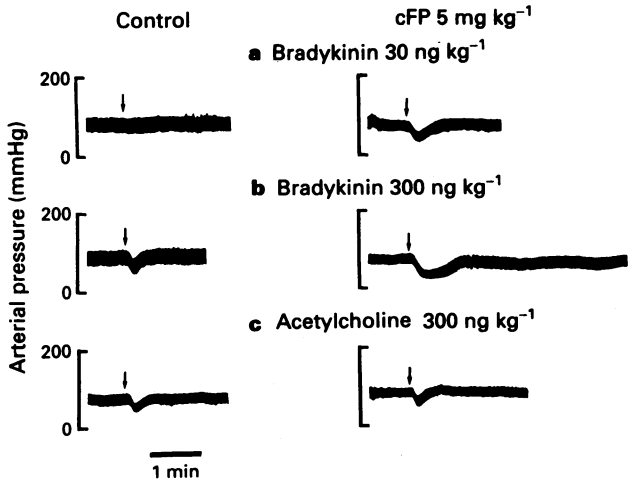

Figure 1 Representative experimental record showing the effects of right atrial administration of (a,b) bradykinin (30 and 300 ng kg^{-1}) and (c) acetylcholine (300 ng kg^{-1}), on arterial pressure before and after right atrial administration of cFP (5 mg kg^{-1}) in a conscious rabbit. ↓ Denotes time of bradykinin or acetylcholine administration.

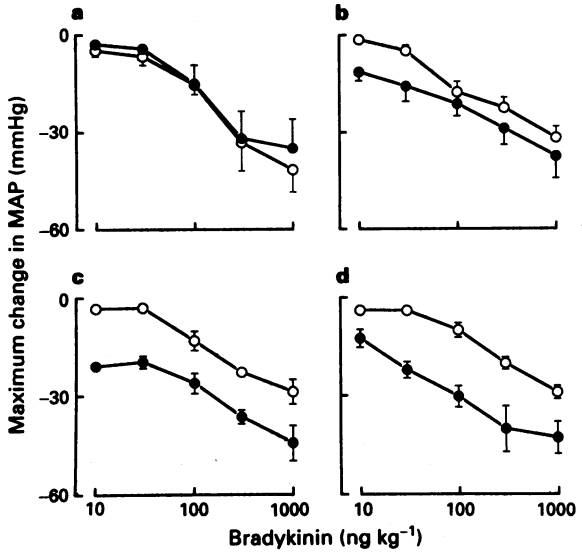

Figure 2 Maximum changes in mean arterial pressure (MAP) following right atrial administration of bradykinin (10–1000 ng kg^{-1}) in conscious rabbits. (○) Control period; (●) after vehicle (a) or cFP 1 mg kg^{-1} (b), 5 mg kg^{-1} (c) or 25 mg kg^{-1} (d) administration. The symbols represent mean ± s.e.mean values for 4 rabbits.

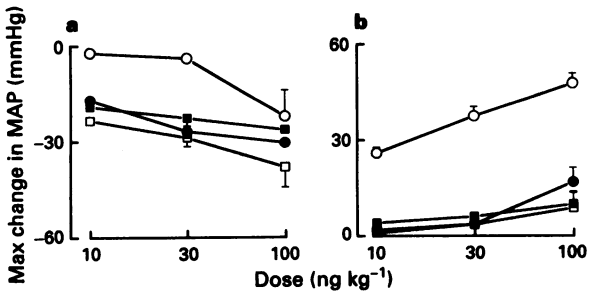

Figure 3 Maximum changes in mean arterial pressure (MAP) following right atrial administration of bradykinin (10–100 ng kg^{-1}) (a) or angiotensin I (10–100 ng kg^{-1}) (b) in conscious rabbits. Rabbits were pretreated with either: vehicle (○); cFP (5 mg kg^{-1}) (●); captopril (0.5 mg + 10 mg kg^{-1}h^{-1}) (□); or cFP + captopril (■). The symbols represent mean ± s.e.mean values for 4 rabbits.

after [^{3}H]-bradykinin administration, proline comprised 54 ± 15% of the recovered tritium; whilst intact bradykinin and fragments (1-7 and 1-5) comprised only a small proportion of the recovered tritium (3 ± 3 and 14 ± 8% respectively) (Figure 4). The metabolism of bradykinin was markedly slowed by cFP treatment. At the 5 s time point, native bradykinin recovery was 69 ± 7% after cFP treatment. The significant effect of cFP on native bradykinin recovery was indicated by both an increase in the amount of bradykinin recovered, averaged over each time point ($P = 0.02$) and an altered slope of the relationship between bradykinin recovery and time (rate of bradykinin breakdown) ($P = 0.003$). In addition, cFP treatment slowed the rate of formation of bradykinin 1-7 and 1-5 ($P = 0.003$). The rate of formation of free proline was not affected by cFP ($P = 0.2$) (Figure 4).

Captopril had almost identical effects to those of cFP. The profile of bradykinin metabolism, following concurrent treatment with cFP and captopril, was not different from that seen when either agent was administered alone. Thus, when compared to captopril alone, cFP plus captopril had no effect on the levels of native bradykinin, bradykinin 1-7 and 1-5, or of free proline averaged across all time points ($P \geqslant 0.9$). Moreover, the relationships between the recovery of these moieties and elapsed time from [^{3}H]-bradykinin administration were parallel ($P \geqslant 0.6$) (Figure 4).

Effects of cFP on resting blood pressure in conscious rabbits The effects of cFP on resting arterial blood pressure were tested in two separate experiments. In Experiment 1, cFP (5 mg kg^{-1}) was administered approximately 10 min after the completion of dose-response curves to bradykinin and acetylcholine. Under these circumstances, there was a small (−4.1 ± 2.3 mmHg) fall in arterial pressure which was absent when the vehicle was administered alone (+0.5 ± 1.0 mmHg) ($P = 0.05$). In Experiment 2, cFP (5 mg kg^{-1}) or its vehicle was administered to rabbits that had received no previous drug treatment. Under these circumstances, arterial pressure did not fall following either cFP (+0.5 ± 1.0 mmHg) or its vehicle (+1.5 ± 1.0 mmHg).

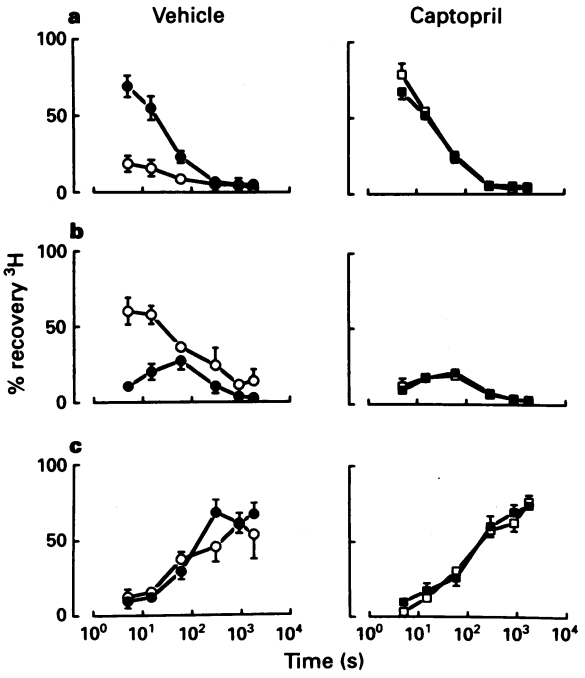

Figure 4 Effects of cFP and captopril on percentage of recovered ^{3}H in the form of native bradykinin (a), bradykinin 1-7 and 1-5 (b), and free proline (c) in conscious rabbits. The treatments were: vehicle (○), cFP (5 mg kg^{-1}) (●), captopril (0.5 mg + 10 mg kg^{-1}h^{-1}) (□), and cFP + captopril (■). The left and right hand panels show responses in rabbits receiving vehicle and captopril respectively. The symbols represent mean ± s.e.mean for 4 rabbits.

Experiments on rats

Effects of cFP and captopril on blood pressure and hindlimb vascular resistance in anaesthetized rats Intravenous administration of cFP (9.3 mg kg^{-1}, $n = 5$) was followed by a sustained fall in mean arterial pressure. The maximum fall averaged 12.6 ± 3.3 mmHg (Figure 5). Captopril (5 mg kg^{-1}, $n = 5$) administration was followed by a maximum fall of mean arterial pressure of 23.0 ± 6.2 mmHg (Figure 5). The depressor effects of cFP and captopril were accompanied by decreases in hindlimb vascular resistance of 25 ± 6 and 23 ± 9% of their baseline levels respectively (data not shown).

Intravenous administration of bradykinin (50 μg kg^{-1}, $n = 11$) was followed by transient falls in arterial pressure (39.0 ± 4.7 mmHg) and hindlimb vascular resistance (51 ± 4% of its baseline level). Four minutes later, arterial pressure had returned to its pretreatment level, and hindlimb vascular resistance was 22 ± 4% higher than its pretreatment level. When cFP ($n = 5$) or captopril ($n = 6$) was administered 5 min after bradykinin, arterial pressure fell by 30.2 ± 4.4 and 37.8 ± 8.8 mmHg respectively, and hindlimb vascular resistance fell by 41 ± 6 and 44 ± 8% respectively, significantly more than was the case when they were administered to naive rats ($P \leqslant 0.005$). When cFP was administered after both bradykinin and captopril ($n = 5$), no depressor effect was observed (data not shown).

Inhibition of ACE by cFP in vitro CFP displaced [^{125}I]-351A from both solubilized rat lung membrane ACE and rat plasma ACE ($pK_D = 6.85 \pm 0.05$, 5.93 ± 0.16), although its apparent affinity was much lower than that of the ACE inhibitor enalaprilat ($pK_D = 9.97 \pm 0.09$ in plasma). Co-incubation with the EP 24.11 inhibitor phosphoramidon (10 μM) reduced the apparent affinity of cFP for [^{125}I]-351A-labelled sites in rat lung ($pK_D = 5.28 \pm 0.41$) (Figure 6) and to a lesser extent in rat plasma ($pK_D = 5.18 \pm 0.43$). When purified rat lung ACE was tested, only 30% displacement

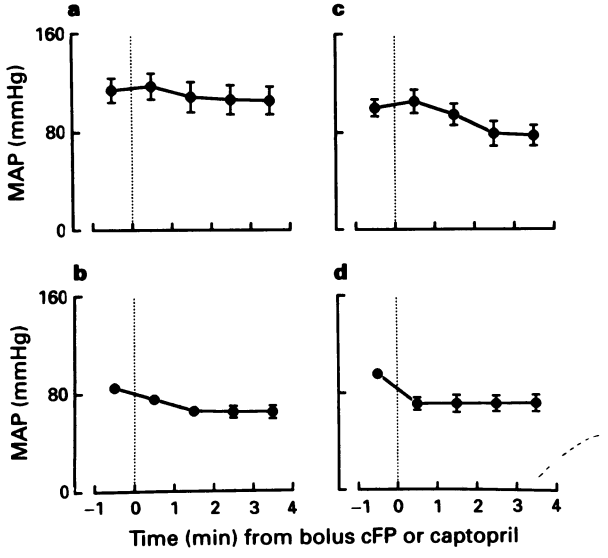

Figure 5 Levels of arterial pressure in anaesthetized rats before and after intravenous administration of cFP (9.3 mg kg^{-1}) or captopril (5 mg kg^{-1}). The left panels show the effects of cFP (a) and captopril (b) in experimentally naive rats. The right panels show the effects of cFP (c) and captopril (d) in rats treated 5 min previously with bradykinin (50 μg kg^{-1}). Symbols represent the mean ± s.e.mean levels for 5-6 rats, of arterial pressure averaged over 60 s periods.

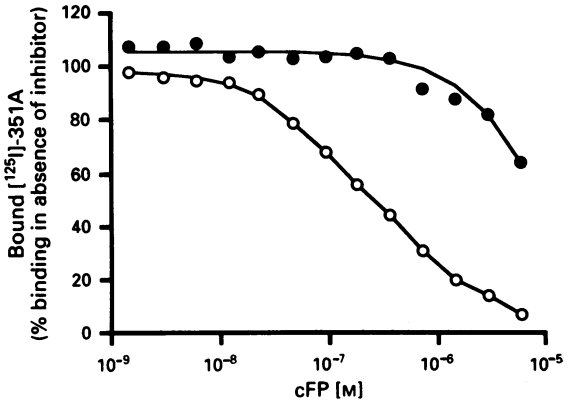

Figure 6 Displacement of [^{125}I]-351A from rat lung ACE by cFP. Solubilized rat lung membranes were incubated with 10 pg [^{125}I]-351A and cFP (10 fM–6 μM) in the absence (○) or presence (●) of 10 μM phosphoramidon. Phosphoramidon reduced the potency of cFP in displacing [^{125}I]-351A by nearly 40 fold.

was observed at the highest concentration of cFP used (2.5 μM). The enzymatic activity of plasma ACE was inhibited by cFP ($pK_I = 5.61 \pm 0.13$), although its potency was again much lower than that of enalaprilat ($pK_I = 8.34 \pm 0.09$). Addition of phosphoramidon (10 μM) to the incubate reduced the potency of cFP at least 4 fold ($pK_I > 5$).

Discussion

The results of the present study confirm and extend those of Yang *et al.* (1994), who recently found that in anaesthetized rats, the phenylalanine substituted analogue of cFP (N-[1-(R,S)-carboxy-3-phenylpropyl]-Ala-Ala-Phe-*p*-aminobenzoate (cFP[Phe])) had similar effects to the ACE inhibitor, enalaprilat. They found that cFP[Phe] potentiated the hypotensive action of bradykinin and inhibited the pressor effect of angiotensin I, but had no further action when administered after enalaprilat. We have shown not only that the specific EP 24.15 inhibitor cFP potentiates the depressor effect of bradykinin, but have also provided direct evidence that it inhibits bradykinin breakdown in the conscious rabbit. It also appears to inhibit conversion of angiotensin I to its bioactive metabolite angiotensin II, since it markedly attenuates the haemodynamic response to angiotensin I. In both respects, its effects are quantitatively and qualitatively similar to those of the angiotensin converting enzyme inhibitor, captopril, and the effects of cFP and captopril are not additive. Given that captopril has no inhibitory effects on EP 24.15 (Acker *et al.*, 1987), it seems reasonable to conclude that the actions of cFP *in vivo* are not mediated by EP 24.15 inhibition, but rather by inhibition of ACE. Furthermore, we have shown in a series of *in vitro* experiments, that cFP does bind to and inhibit ACE. The apparent increased affinity of cFP for ACE in the absence of phosphoramidon suggests that this interaction is at least partly dependent on the conversion of cFP by a phosphoramidon-sensitive metalloendopeptidase to an ACE inhibiting product. We also conclude that the blood-pressure lowering effects of cFP in conscious rabbits and anaesthetized rats are entirely attributable to ACE inhibition, since they are similar to those of captopril and at least in the rat, cFP has no further blood pressure lowering effect when it is administered after captopril.

Following intravascular administration, exogenous bradykinin is rapidly degraded. Pesquero *et al.* (1992) found in conscious rats that exogenous bradykinin was at least 50 fold more potent when injected intra-arterially than when injected intravenously. They inferred from this that 98% of bradykinin inactivation occurred in the pulmonary circulation. This breakdown process involved rapid conversion of intact bradykinin to bradykinin 1-7 and 1-5. The present study confirms and extends these observations, using a dose of [^{3}H]-bradykinin (~8 ng kg^{-1}) that would not alter arterial pressure in intact rabbits, and which can therefore be used as a marker for the metabolic fate of endogenous bradykinin. Basal plasma levels of bradykinin have not been determined in rabbits, but in rats they have been found to range from 2–35 pg ml^{-1} (Salgado *et al.*, 1986; Nakagawa & Nasjliti, 1989; Campbell *et al.*, 1993). Based on an estimated blood volume in the rabbit of 65 ml kg^{-1} (Schalm, 1965), the peak plasma level of [^{3}H]-bradykinin in the present experiment would have been in the order of 100 pg ml^{-1}.

In vehicle-treated rabbits, 81 ± 5% of right atrially administered [^{3}H]-bradykinin was degraded 5 s after its injection. Most of this was in the form of bradykinin 1–7 or 1–5 (the chromatographic separation procedure only poorly resolves these two peptides). CFP administration dramatically increased bradykinin recovery (to 69 ± 7% at 5 s) and significantly slowed the formation of bradykinin metabolites (1–7 and 1–5).

In conscious rabbits, administration of cFP (1–25 mg kg^{-1}) dose-dependently potentiated the hypotensive response to bradykinin. The effects of cFP were specific for bradykinin and not attributable to a general increase in sensitivity to vasodilator agents, since cFP had no effect on the hypotensive response to acetylcholine. However, we also found that cFP markedly attenuated the pressor response to angiotensin I, indicating that it inhibited the conversion of angiotensin I to its active metabolite angiotensin II.

The effects of cFP on the haemodynamic responses to bradykinin and angiotensin I, and on the metabolism of a bolus dose of [^{3}H]-bradykinin, were qualitatively and quantitatively similar to those of the angiotensin converting enzyme inhibitor captopril. Moreover, the effects of combined treatment with both agents were not greater than treatment with either agent alone. Given that captopril has negligible activity as an inhibitor of EP 24.15 (Acker *et al.*, 1987), if cFP were having an action on bradykinin metabolism in addition to inhibition of ACE, the effects of combined treatment with cFP and captopril should be greater than those of either agent alone. Thus, these data provide strong evidence that cFP and captopril act at the same level to inhibit both bradykinin breakdown and conversion of angiotensin I to angiotensin II in the rabbit; that is, inhibition of angiotensin converting enzyme.

This conclusion seems at odds with the observation that cFP has negligible ACE-inhibiting activity when tested with purified or recombinant ACE preparations (Prof. Pierre Corvol, personal communication). However, two recent reports have provided evidence that cFP[Phe], which also has negligible ACE-inhibiting activity when tested with purified ACE preparations (Williams *et al.*, 1993), can be converted to a potent inhibitor of angiotensin converting enzyme through the actions of endopeptidase 24.11 (Cardozo & Orlowski, 1993; Williams *et al.*, 1993). The ACE inhibiting product of cFP[Phe], N-[1(R,S)-carboxy-3-phenylpropyl]-Ala-Ala, is structurally similar to enalaprilat, inhibiting ACE with a K_i of about 40 nM (Cardozo & Orlowski, 1993; Williams *et al.*, 1993). Our experiments using crude and purified ACE preparations suggest that cFP itself is similarly susceptible to degradation *in vitro* to form N-[1(R,S)-carboxy-3-phenylpropyl]-Ala-Ala. We found that cFP displaced [^{125}I]-351A from ACE binding sites in preparations of rat lung membrane and rat plasma with apparent micromolar affinity but had negligible affinity for purified rat lung ACE. CFP also inhibited rat plasma ACE activity at micromolar concentrations. The affinity and activity of cFP at these sites was dramatically reduced by the addition of phosphoramidon. Phosphoramidon potently inhibits the activity of a wide range of metalloendopeptidases including endopeptidase 24.11 (Williams *et al.*, 1993), endothelin converting enzyme

(Ohnaka *et al.*, 1993) and endothelin 1 inactivating enzyme (Janas *et al.*, 1994). Therefore, the precise nature of the product(s) of cFP metabolism *in vivo*, and the enzyme(s) involved, remain to be determined.

Our conclusion that cFP acts as an ACE inhibitor *in vivo* also seems at odds with the observation by Genden & Molineaux (1991) of a transient yet profound fall in arterial pressure following intravenous administration of cFP[Phe] to anaesthetized rats. In the present study we found that administration of cFP to conscious, experimentally naive rabbits did not lower their arterial pressure. We did find, however, that cFP had a small yet statistically significant depressor effect in rabbits that had been administered bradykinin and acetylcholine. These observations in rabbits led us to compare the effects of cFP and captopril in anaesthetized rats, under conditions similar to those used in the study by Genden & Molineaux (1991). We observed modest yet sustained falls in arterial pressure after administration of either cFP (13 mmHg) or captopril (23 mmHg), consistent with the results of other studies in which ACE inhibitors have been shown to reduce moderately arterial pressure in anaesthetized normotensive rats (Mattson & Roman, 1991). We also found that the hypotensive effects of both cFP and captopril were markedly potentiated by pretreatment with a single dose of bradykinin. Indeed, the magnitudes (30–40 mmHg) of these depressor responses were similar to the magnitude of the depressor effect observed by Genden & Molineaux (1991). Ours is not a particularly novel finding, since bradykinin pretreatment has been previously shown to potentiate the hypotensive effects of ACE inhibition in conscious rats (Van Den Buuse & Kerkhoff, 1991). It does, however, reinforce the point that the response to ACE inhibition is dependent upon the prevailing haemodynamic circumstances, not the least of which is probably the level of plasma renin activity. Our observation that cFP produced no further fall in arterial pressure following captopril administration provides strong evidence that the hypotensive effect of cFP is mediated through inhibition of ACE.

In conclusion, these results show that the effects of cFP on systemic bradykinin metabolism and arterial pressure can be attributed to inhibition of angiotensin converting enzyme rather than EP 24.15. The possibility that EP 24.15 plays some role in systemic bradykinin metabolism and blood pressure control can therefore neither be confirmed nor denied until more stable inhibitors become available that do not have metabolites with angiotensin converting enzyme inhibiting activity. A recent report, however, demonstrated a natriuretic effect of cFP[Phe] which though blunted, was not abolished by pretreatment with the ACE inhibitor enalaprilat (Yang *et al.*, 1994). Whether or not this observation reflects a specific role of EP 24.15 in the kidney also awaits the development of more stable inhibitors of EP 24.15.

This study was supported by grants from the National Health and Medical Research Council of Australia, the Clive and Vera Ramaciotti Foundations, and the Alfred Group of Hospitals. We are most grateful to Dr Jaroslav Boublik and Mr Louis Lakat for the synthesis of cFP. We are also grateful for the gifts of drugs from pharmaceutical companies, and to Professor P. Corvol for allowing us to cite his unpublished data. Our thanks go to Professor John Funder and Dr Maarten Van Den Buuse for their advice during the preparation of this manuscript.

References

ACKER, G.R., MOLINEAUX, C. & ORLOWSKI, M. (1987). Synaptosomal membrane-bound form of endopeptidase-24.15 generates Leu-enkephalin from dynorphin$_{1-8}$, α-and β-neoendorphin, and Met-enkephalin from Met-enkephalin-Arg^6-Gly^7-Leu^8. *J. Neurochem.*, **48**, 284–292.

AUSTRALIAN CODE OF PRACTICE FOR THE CARE AND USE OF ANIMALS FOR SCIENTIFIC PURPOSES (1990). Canberra, Australia: Australian Government Publishing Service.

CAMPBELL, D.J., KLADIS, A. & DUNCAN A.-M. (1993). Bradykinin peptides in kidney, blood, and other tissues of the rat. *Hypertension*, **21**, 155–165.

CARDOZO, C. & ORLOWSKI, M. (1993). Evidence that enzymatic conversion of N-[1(R,S)-carboxy-3-phenylpropyl]-Ala-Ala-Phe-p-aminobenzoate, a specific inhibitor of endopeptidase 24.15, to N-[1(R,S)-carboxy-3-phenylpropyl]-Ala-Ala is necessary for inhibition of angiotensin converting enzyme. *Peptides*, **14**, 1259–1262.

CARRETERO, O.A. & SCICLI, A.G. (1991). Zinc metallopeptidase inhibitors. A novel antihypertensive treatment. *Hypertension*, **18**, 366–371.

CHAPPELL, M.C., WELCHES, W.R., BROSNIHAN, K.B. & FERRARIO, C.M. (1992). Inhibition of angiotensin converting enzyme by metalloendopeptidase 3.4.24.15 inhibitor c-phenylpropyl-alanyl-alanyl-phenylalanyl-p-aminobenzoate. *Peptides*, **13**, 943–946.

CHU, T.G. & ORLOWSKI, M. (1984). Active site directed N-carboxymethyl peptide inhibitors of a soluble metalloendopeptidase from rat brain. *Biochemistry*, **23**, 3598–3603.

CHU, T.G. & ORLOWSKI, M. (1985). Soluble metalloendopeptidase from rat brain: action on enkephalin-containing peptides and other bioactive peptides. *Endocrinology*, **116**, 1418–1425.

CUSHMAN, D.W. & CHEUNG, H.S. (1971). Spectrophotometric assay and properties of the angiotensin converting enzyme of rabbit lung. *Biochem. Pharmacol.*, **20**, 1637–1648.

FLORENTIN, D., SASSI, A. & ROQUES, B.P. (1984). A highly sensitive fluorometric assay for 'enkephalinase', a neutral metalloendopeptidase that releases tyrosine-glycine-glycine from enkephalins. *Anal. Biochem.*, **141**, 62–69.

FRIEDLAND, J. & SILVERSTEIN, E. (1976). A sensitive fluorometric assay for serum angiotensin converting enzyme. *Am. J. Clin. Pathol.*, **66**, 416–424.

GENDEN, E.M. & MOLINEAUX, C.J. (1991). Inhibition of endopeptidase-24.15 decreases blood pressure in normotensive rats. *Hypertension*, **18**, 360–365.

JACKSON, B., CUBELA, R. & JOHNSON, C.I. (1986). Angiotensin converting enzyme (ACE), characterization by ^{125}I-MK351A binding studies of plasma and tissue ACE during variation of salt status in the rat. *J. Hypertension*, **4**, 759–765.

JANAS, J., SITKIEWICZ, D., WARNAWIN, K. & JANAS, R.M. (1994). Characterization of a novel, high molecular weight, acidic, endothelin-1 inactivating metalloendopeptidase from the rat kidney. *J. Hypertension*, **12**, 1155–1162.

LUDBROOK, J. (1991). On making multiple comparisons in clinical and experimental pharmacology and physiology. *Clin. Exp. Pharmacol. Physiol.*, **18**, 379–392.

LUDBROOK, J. (1994). Repeated measurements and multiple comparisons in cardiovascular research. *Cardiovasc. Res.*, **28**, 303–311.

MATTSON, D.L. & ROMAN, R.J. (1991). Role of kinins and angiotensin II in the renal hemodynamic response to captopril. *Am. J. Physiol.*, **260**, F670–F679.

MUNSON, P.J. & RODBARD, D. (1980). LIGAND: a versatile computerized approach for characterization of ligand-binding systems. *Anal. Biochem.*, **107**, 220–239.

NAKAGAWA, M. & NASJLITI, A. (1989). Plasma kinin levels in experimental hypertension in rats. *Adv. Exp. Med. Biol.*, **247B**, 115–119.

NORBY, J., RUBENSTEIN, S., TUERKE, T., SCHWALLIE-FARMER, C., FOROOD, R. & BENNINGTON, J. (1992). *Sigmaplot Scientific Graph System*. San Rafael, U.S.A: Jandel Scientific.

OHNAKA, K., TAKAYANAGI, R., NISHIKAWA, M., HAJI, M. & NAWATA, H. (1993). Purification and characterization of a phosphoramidon-sensitive endothelin-converting enzyme in porcine aortic endothelium. *J. Biol. Chem.*, **268**, 26759–26766.

ORLOWSKI, M., MICHAUD, C. & CHU, T.G. (1983). A soluble metalloendopeptidase from rat brain. Purification of the enzyme and determination of specificity with synthetic and natural peptides. *Eur. J. Biochem.*, **135**, 81–88.

ORLOWSKI, M., MICHAUD, C. & MOLINEAUX, C.J. (1988). Substrate-related potent inhibitors of brain metalloendopeptidase. *Biochemistry*, **27**, 597–602.

ORLOWSKI, M., REZNIK, S., AYALA, J. & PIEROTTI, A.R. (1989). Endopeptidase 24.15 from rat testes. Isolation of the enzyme and its specificity toward synthetic and natural peptides, including enkephalin-containing peptides. *Biochem. J.*, **261**, 951–958.

PERICH, R.B., JACKSON, B., ROGERSON, F., MENDELSOHN, F.A., PAXTON, D. & JOHNSON, C.I. (1992). Two binding sites on angiotensin-converting enzyme: evidence from radioligand binding studies. *Mol. Pharmacol.*, **42**, 286–293.

PESQUERO, J.B., JUBILUT, G.N., LINDSEY,C.J. & PAVIA, A.C.M. (1992). Bradykinin metabolism pathway in the rat pulmonary circulation. *J. Hypertension*, **10**, 1471–1478.

SALGADO, M.C.O., RABITO, S.F. & CARRETERO, O.A. (1986). Blood kinin in one kidney, one clip hypertensive rats. *Hypertension*, **8** (suppl I), I–110–I–113.

SCHALM, O.W. (1965). *Veterinary Hematology*. 2nd ed. Philadelphia, USA: Lea and Febiger.

WILLIAMS, C.H., YAMAMOTO, T., WALSH, D.M. & ALLSOP, D. (1993). Endopeptidase 3.4.24.11 converts N-1-(R,S)carboxy-3-phenylpropyl-Ala-Ala-Phe-p-carboxyanilide to a potent inhibitor of angiotensin-converting enzyme. *Biochem. J.*, **294**, 681–684.

VAN DEN BUUSE, M. & KERKHOFF, J. (1991). Interaction of bradykinin and angiotensin in the regulation of blood pressure in conscious rats. *Gen. Pharmacol.*, **22**, 759–762.

WILKINSON, L. (1990). *Systat: The System for Statistics*. Evanston, USA: SYSTAT Inc.

YANG, H.Y.T., ERDÖS, E.G. & LEVIN, Y. (1970). A dipeptidyl carboxypeptidase that converts angiontensin I and inactivates bradykinin. *Biochem. Biophys. Acta*, **214**, 374–376.

YANG, X.-P., SAITOH, S., SCICLI, A.G., MASCHA, E., ORLOWSKI, M. & CARRETERO, O.A. (1994). Effects of a metalloendopeptidase-24.15 inhibitor on renal hemodynamics and function in rats. *Hypertension*, **23**, (suppl 1), I–235–I–239.

(Received July 4, 1994
Revised November 23, 1994
Accepted December 6, 1994)

British Journal of Pharmacology (1995) 114, 1193–1205

Participation of NMDA and non-NMDA excitatory amino acid receptors in the mediation of spinal reflex potentials in rats: an *in vivo* study

[1]S. Farkas & *[2]H. Ono

Department of Electrophysiology, Pharmacological Research Centre, Chemical Works of Gedeon Richter Ltd. H-1475, Budapest, 10, POB.: 27, Hungary and *Department of Toxicology and Pharmacology, Faculty of Pharmaceutical Sciences, University of Tokyo, Bunkyo-ku, Tokyo 113, Japan

1 The effect of various intravenously administered excitatory amino acid (EAA) antagonists on the dorsal root stimulation-evoked, short latency (up to 10 ms) spinal root reflex potentials of chloralose-urethane anaesthetized C_1 spinal rats was studied, in order to gain information on the involvement of non-NMDA (AMPA/kainate; AMPA = α-amino-3-hydroxy-5-methyl-isoxazole-4-propionate) and NMDA (N-methyl-D-aspartate) receptors in their mediation. The competitive non-NMDA antagonist, 2,3-dihydroxy-6-nitro-7-sulphamoyl-benzo(F)quinoxaline (NBQX; 1–32 mg kg^{-1}), the non-competitive non-NMDA antagonist, 1-(amino)phenyl-4-methyl-7,8-methylendioxy-5H-2,3-benzodiazepine (GYKI 52466; 0.5–8 mg kg^{-1}), the competitive NMDA antagonist 3-((±)-2-carboxypiperazin-4-yl)-propyl-1-phosphonic acid (CPP, 2–8 mg kg^{-1}) and two non-competitive NMDA antagonists: MK-801 (0.5–2 mg kg^{-1}) and ketamine (2–32 mg kg^{-1}) were used as pharmacological tools.

2 Validating the applied pharmacological tools regarding selectivity at the applied doses, their effects were tested on direct (electrical) as well as on synaptic excitability of motoneurones evoked by intraspinal stimulation. Furthermore, their effect was investigated on the responses elicited by microiontophoretic application of EAA agonists (AMPA, kainate and NMDA) into the motoneurone pool, where the extracellular field potential evoked by antidromic stimulation of the ventral root was recorded to detect the effects of EAA agonists.

3 NBQX and GYKI 52466 were able to abolish completely the mono-, di- and polysynaptic ventral root reflexes (MSR, DSR, PSR) and the synaptic excitability of motoneurones, while hardly influencing direct excitability of motoneurones. They markedly attenuated AMPA and kainate responses whilst having little or no effect on NMDA responses.

4 Apparently 'supramaximal' doses of CPP and MK-801 slightly inhibited MSR (by about 10%) moderately reduced DSR and PSR (by about 20–30%) and did not influence excitability of motoneurones. They selectively blocked responses to NMDA.

5 Ketamine dose-dependently inhibited MSR, DSR and PSR. Nevertheless, diminution of none of the responses exceeded 50%. It reduced both direct and synaptic excitability of motoneurones, thus displaying a local anaesthetic-like effect, which may contribute to its reflex inhibitory action. It depressed responses to NMDA whilst having negligible effects on responses to AMPA and kainate.

6 We conclude that non-NMDA receptors play a substantial role in the mediation of MSR, DSR and PSR, while NMDA receptors contribute little to this. Neither MSR nor PSR is mediated exclusively by non-NMDA or NMDA receptors, respectively.

7 The drugs investigated in this study, with the exception of ketamine, proved to be useful tools for elucidation of the involvement of EAA receptors in various processes *in vivo*

Keywords: Glutamate receptors; AMPA; kainate; NMDA; NBQX; GYKI 52466; CPP; MK-801; spinal reflex; spinal cord

Introduction

There is abundant evidence that endogenous L-glutamate is released in the spinal cord by dorsal root stimulation (Kawagoe *et al.*, 1986) and glutamate receptors (excitatory amino acid, EAA, receptors) are involved in mediating synaptic transmission in the spinal cord (for review see: Mayer & Westbrook, 1987; Evans, 1989).

Ionotropic EAA receptors have been classified into three groups based on their agonist selectivity: N-methyl-D-aspartate-(NMDA), kainate- and α-amino-3-hydroxy-5-methyl-isoxazole-4-propionate- (AMPA) receptors (Collingridge & Lester, 1989; Watkins *et al.*, 1990). Pharmacological and electrophysiological distinction between AMPA and kainate receptors, however, is a matter of controversy (see e.g. Zeman & Lodge, 1992), and molecular biological studies have also failed to demonstrate clear selectivity of these agonists (Sommer & Seeburg, 1992). Consequently the terms non-NMDA or AMPA/kainate receptors are also in use.

Along with the development of EAA antagonists numerous studies have been performed to reveal the involvment of EAA receptors in the mediation of reflex transmission in the mammalian spinal cord. Since at first only selective NMDA antagonists (e.g. D-amino-5-phosphonovalerate, AP5; D-2-amino-7-phosphonoheptanoate, AP7) were available, early studies had to draw conclusions from the effect of NMDA antagonists alone or from a comparison with the effect of non-selective antagonists (such as *cis*-2,3-piperidine dicarboxylate, PDA, or kynurenate). The conclusion of Evans *et al.* (1981), using PDA and AP5 in immature rat spinal cord, that NMDA receptors mediate polysynaptic, while non-NMDA receptors mediate mono-

[1] Author for correspondence.
[2] Present address: Department of Pharmacy, Faculty of Medicine, Branch Hospital, University of Tokyo, Meijirodai 3-28-6, Bunkyo-ku, Tokyo 112, Japan.

synaptic excitation, was further supported by Ganong *et al.* (1983), by intracellular investigations of Jahr & Yoshioka (1986) using kynurenate in the same *in vitro* preparation or by iontophoretic application of antagonists on dorsal horn neurones of cats *in vivo* (Davies & Watkins, 1983). Similar conclusions were drawn by Polc (1985) studying the effect of AP7 and of the apparent kainate antagonist nuciferine, an apomorphine related alkaloid (Polc & Haefely, 1977) on feline spinal ventral root reflex potentials *in vivo*.

Nevertheless, it is practically impossible to draw clear and reliable conclusions especially on the involvement of non-NMDA receptors in polysynaptic excitation with non-selective antagonists. Therefore, the discovery of more potent and selective non-NMDA antagonist, quinoxalinediones (Honoré *et al.*, 1988) had a great impact on further development. Turski *et al.* (1990) comparing the effect of the potent NMDA antagonist 3-((±)-2-carboxypiperazin-4-yl)-propyl-1-phosphonic acid (CPP) and that of 6-cyano-7-nitroquinoxaline (CNQX, administered intrathecally) on the monosynaptic Hoffmann (H)-reflex and on the polysynaptic flexor reflex also came to the above conclusion. On the other hand, Long *et al.* (1990) comparing the effect of CNQX and AP5 on the ventral root reflex in mature rat spinal cord *in vitro* have shown considerable depression of the polysynaptic reflex response by 3 μM CNQX, a concentration which did not inhibit the NMDA response.

Recently new selective non-NMDA antagonists have been reported which are also active by systemic administration *in vivo*: the competitive antagonist 2,3-dihydroxy-6-nitro-7-sulphamoyl-benzo(F)quinoxaline (NBQX; Sheardown *et al.*, 1990) and the non-competitive antagonist, 1-(amino)phenyl-4-methyl-7,8-methylendioxy-5*H*-2,3-benzodiazepine (GYKI 52466; Tarnawa *et al.*, 1990; Donevan & Rogawski, 1993). Penetration of these antagonists through the blood brain barrier allows reliable antagonist studies to be performed *in vivo*.

Spinal root reflexes in the rat and cat spinal cord *in vivo* have often been used in studies of the modulatory effects of catecholamine-, 5-hydroxytryptamine-, GABA-related and centrally acting muscle relaxant drugs (e.g Barasi & Roberts, 1974; Ono, 1982; Ryan & Boisse, 1984; Kaneko *et al.*, 1987; Yamazaki *et al*, 1992). However, the participation of EAA receptors, especially that of non-NMDA receptors in the mediation of these reflex potentials has not yet been systematically studied.

In order to draw conclusions on the EAA receptor involvement in the mediation of spinal reflexes, we have investigated the effects of EAA antagonists, which are active by systemic administration, on ventral and dorsal root potentials of the rat spinal cord evoked by dorsal root stimulation *in vivo*. To obtain clear results we intended to use the antagonists in a wide dose-range and/or to apply a 'supramaximal' dose as far as possible. To avoid misinterpretation due to non-selectivity of the pharmacological tools used, several antagonists of different types were employed: the competitive non-NMDA antagonist NBQX, the non-competitive non-NMDA antagonist GYKI 52466, the competitive NMDA antagonist, CPP (Davies *et al.*, 1986) and the non-competitive NMDA antagonists, MK-801 (Wong *et al.*, 1986) and ketamine (Anis *et al.*, 1983). The effects of these drugs were also investigated on the motoneurone excitability to exclude a possible non-specific 'membrane stabilizing' action which may influence spinal reflexes (Ono *et al.*, 1984). Furthermore, we investigated the effects of these drugs against responses of AMPA, kainate and NMDA applied iontophoretically on the motoneurones, in order to gain information on their selectivity and reliability at the given site *in vivo*.

Methods

In all experiments male Wistar rats weighing 270–400 g were anaesthetized with chloralose (25 mg kg^{-1}, i.p.) and urethane (1 g kg^{-1}, i.p.). The vagus nerves were severed and the common carotid arteries ligated bilaterally at the cervical region. Blood pressure was monitored via a cannula in the carotid artery. The femoral vein was also cannulated to allow intravenous injections. A tracheal cannula was inserted and the animals were artificially ventilated throughout the experiment. The spinal cord was infiltrated with lignocaine (1%, 50 μl) and transected at the C_1 level. Animals were fixed in a spinal stereotaxic frame and a dorsal laminectomy was performed on vertebrae L_1–L_6. Ventral and dorsal roots below L_4 were cut bilaterally, dorsal and ventral roots of the segments L_4 and L_5 were isolated. A pool was formed from the skin of the back and filled with warm paraffin oil. Dorsal and ventral roots used for stimulation and recording were placed on bipolar silver wire electrodes. Rectal and oil pool temperatures were maintained at 36 ± 0.6°C with a heating pad and a heating lamp, respectively. In the majority of the experiments a 1:1 mixture of Ringer solution and glucose solution (6%) was infused (10–20 ml kg^{-1} h^{-1}) in order to keep the mean arterial blood pressure of spinal animals above 60 mmHg. This was essential for the recording of stable reflexes (particularly of the sensitive polysynaptic reflex) over a long period and for avoiding secondary effects to drug administration.

Spinal reflex study

The L_5 dorsal root was stimulated by single impulses (stimulus strength: supramaximal voltage; pulse width: 0.05 ms; frequency: 10 min^{-1}). The ventral root reflexes (VRR) from the L_5 ventral root and dorsal root potential (DRP) from the L_4 dorsal root were recorded ipsilaterally using differential preamplifiers. For perfect monophasic recording of VRR the nerve was crushed between the two poles of the electrode. For recording of the DRP one pole of the recording electrode was placed as close as possible to the entry of the dorsal root without touching the spinal cord. The other pole was in contact with the distal end of the same dorsal root. Responses were band-pass filtered (0.5 Hz–5 kHz), averaged (averager: Nihonkohden DAT-1100) and displayed on a digital storage oscilloscope (Nihonkohden VC-10). An average of 8 responses was plotted every minute on a two channel oscillographic thermorecorder. Moreover, different components of the ventral root reflex response were separated based on their post-stimulus latency and duration using a time-window signal selector, and electronically integrated (see Figure 1a) after appropriate amplification. Five integrated responses were summed and the integrator reset every 30 s. Integrated responses were recorded on a multi-pen ink-writing recorder (Nihonkohden RM-45). Pen deflection was exactly proportional to the area under the curve of the selected response. (For more details on this signal processing see: Farkas *et al.*, 1989.) Quantitative evaluation of VRR components was based on the integrated records, while the amplitude of DRP was evaluated from records of the averaged responses.

Excitability test

Excitability of the motoneurone soma and of the primary afferent fibres were measured according to the technique described earlier (Ono *et al.*, 1979). Anaesthetized animals were paralyzed with (+)-tubocurarine (1 mg kg^{-1} starting dose plus 1 mg kg^{-1} h^{-1} in infusion). A tungsten microelectrode, insulated except its tip, was inserted into the motoneurone pool, which was stimulated by negative pulses (stimulus strength: 0.2–0.5 mA; pulse width: 0.05 ms; frequency: 10 min^{-1}). The compound action potential evoked by direct stimulation of motoneurones (MN, first peak), and the one caused by (mono)synaptic activation of motoneurones (MS, second peak), were recorded from the L_5 ventral root. The antidromic action potential which reflects excitability of the primary afferent fibres (PAF) was recorded

from the L_5 dorsal root. Exact tip position and stimulus strength were adjusted to yield similar amplitude of MN and MS. The signal processing and recording system were the same as that described above for the spinal reflex study.

Microiontophoretic study

Anaesthetized animals were paralyzed with (+)-tubocurarine. The L_5 ventral root was stimulated (stimulus strength: 2–5 V; pulse width: 0.5 ms; interval: 500 or 600 ms). The field potential evoked by antidromic stimulation (antidromic field potential, AFP) was recorded via a seven barrelled glass microelectrode, having a tip diameter of 5–7 μm, inserted into the motoneurone pool. Outer barrels were filled with solutions of AMPA (0.01 M, pH 7.5), NMDA (0.15 M, pH 8), kainate (0.02 M, pH 8) and 3 M NaCl (compensating current barrel) solutions. The central recording barrel was also filled with 3 M NaCl yielding a tip resistance of 3–8 MΩ *in situ*. Excitatory amino acid agonists were regularly (intervals: 3–6 min) applied microiontophoretically into the motoneurone pool, ejection current being 15–45 nA. Usually it was necessary to use a retaining current of 1–5 nA to avoid leakage.

In some iontophoretic experiments the above described analog signal processing and recording system was used. In the majority of the iontophoretic experiments, however, the amplified responses (band-pass filtering: 50 Hz–5 kHz) were fed into an IBM PC AT compatible computer via an analog-to-digital converter (Scientific Solutions, Lab Master TM-100; conversion rate: 20 kHz). Every AFP response was again integrated. The integrated responses and their amplitudes were recorded on-line via a digital-to-analog converter and a chart recorder (Graphtec, Mark VII). The averaged shape of each ten AFP responses from 15 s before to 1 min after the iontophoretic ejection was automatically stored. The average values of every ten integrated responses and of every ten amplitude values arising throughout the experiment were also stored for later evaluation. Stimulations, recordings and iontophoretic applications were all controlled by the computer programme: 'Stimulat 1.0' (by P. Molnár). The integrated value represented the area bounded by the negative wave of AFP and the zero line. Amplitude was defined as the difference between the negative peak and the zero line. Zero line was determined from the pretrigger segment.

Drugs

The anaesthetic solution contained 0.25% α-chloralose (TCI) and 10% urethane (Aldrich) dissolved in distilled water. The cannula for blood pressure monitoring was filled with saline containing 200 iu ml^{-1} heparin. NBQX (gift from Novo Nordisk) 2 mg ml^{-1} was freshly dissolved in 6% glucose solution containing 0.01 N NaOH. GYKI 52466 (gift from I. Tarnawa) 2 mg ml^{-1} was freshly dissolved in 6% glucose solution. ± MK-801 (dizocilpine maleate) 0.5 mg ml^{-1} (synthesized at Richter), ± CPP (RBI) 2 mg ml^{-1} and ketamine HCl (Ketalar-50, Parke Davis) 2 or 8 mg ml^{-1}, were dissolved in saline. Lignocaine (Xylocaine, 1%, Fujisawa), (+)-tubocurarine chloride (TCI), NMDA (RBI), AMPA (RBI) and kainate (kainic acid, Sigma) were also used.

Results

Spinal reflex study

The ventral root reflex (VRR) potential evoked by dorsal root stimulation typically consists of three components (see Figure 1a, Figure 2f, Figure 3d; sell also e.g. figures of Barasi & Roberts, 1974; or Ono, 1982). A first spike (monosynaptic reflex, MSR) is followed by a second smaller spike, apparently reflecting still rather synchronized discharge which, based on its latency, may be regarded to represent a disynaptic reflex (DSR; Fukuda *et al.*, 1977). The time from stimulation to the peak of MSR was about 1.8–2 ms, while the time between the first and second peak was 0.8–1.2 ms (cf. 'disynaptic excitatory path from group Ib afferents' in Eccles, 1957). The second spike (which in other studies has often been termed polysynaptic reflex) is followed by a smaller gradually declining potential (termed polysynaptic reflex, PSR in the present study) lasting for about 10 ms from the stimulation. It has usually been ignored in other studies of the rat spinal reflex, since it has a magnitude of 0.1–0.2 mV and is less synchronized than the MSR of 1–2 mV. It is clearly observed, however in perfect monophasic recording (see also Methods) by increasing the amplification. During the stabilisation period of experiments the three components (MSR, DSR, PSR) seemed to alter independently, i.e. both concurrent and opposite spontaneous changes could be observed. PSR seemed to be the most labile and sensitive to experimental conditions, injections of placebo (Figure 1d) and changes in the blood pressure. Therefore, it seemed reasonable to differentiate between these three components. These components were separated for integration based on their different post-stimulus time of appearance as shown in Figure 1a. This separation is acceptable if latencies of various components do not undergo changes during the experiment. Latencies of components proved to be surprisingly stable. The only error in this separation was occasional partial shifting of the late MSR part into the window of DSR when MSR was almost completely blocked by NBQX or GYKI 52466. This error in either integrated response can be estimated to be less than 5% in those experiments where it occurred, and hence it may be disregarded. A typical time-window setting was: 1.25–2.5 ms for MSR, 2.6–3.4 ms for DSR and 3.4–10 ms for PSR. Although time-windows were individually adjusted from experiment to experiment only minor deviations (0.1–0.2 ms), if any, from the above values had to be set.

All drug effects referred in this section were obtained from previously drug-free animals except for the initial dose of anaesthetic, for cumulative administrations of the same drug or for repeated administrations of increasing doses of GYKI 52466 after appropriate time for recovery.

The effect of NBQX was investigated in 4 rats. The cumulative dosing protocol, records from an experiment and average data are presented in Figure 1. NBQX (1–32 mg kg^{-1}, i.v.) dose-dependently attenuated MSR, DSR and PSR. The sensitivity order was DSR > MSR > PSR. While 1 mg kg^{-1} NBQX considerably depressed the DSR, appreciable decrease in PSR was only achieved with 4 mg kg^{-1}. MSR and DSR but not PSR were completely abolished by 32 mg kg^{-1} NBQX. However, if it was attempted (2 cases) additional doses (16 or 32 mg kg^{-1}) completely abolished PSR as well. Dorsal root potential (DRP) and reflex (DRR) were much more resistant to NBQX but high doses also caused significant (24%) inhibition. Because of the poor water solubility of NBQX, a large amount of NaOH solution had to be injected. Therefore, solvent control experiments ($n = 6$) were performed with the solvent for NBQX (Figure 1d), most of them before investigation of the effect of NBQX. The solvent caused no statistically significant change except for a transient 5% increase in PSR which proved to be statistically significant only at 5 min ($P < 0.05$, paired t test). This effect may be a secondary one via marked elevation of the blood pressure or via the effect of the high pH.

The effects of various single doses of GYKI 52466 (0.5–8 mg kg^{-1}, i.v.) were investigated (each dose in 4–5 experiments; see Figure 2). This compound also dose-dependently inhibited all the three VRR components. The highest dose could also produce complete inhibition. The sensitivity order, as for NBQX, was DSR > MSR > PSR, and DRP was considerably (by 27%) inhibited only by the high doses causing complete inhibition of VRR components. The dose-response relationship for GYKI 52466 was steeper and

this compound was about 4 fold more potent but had a much shorter duration of action than NBQX. It is noteworthy that relative depressions of various spinal root potentials (MSR, PSR and DRP) in rats by GYKI 52466 found in this study were surprisingly similar to those described in our previous study in cats (Tarnawa *et al.*, 1989).

The effect of CPP (2 mg kg^{-1}, i.v.) was studied in 5 rats (see Figure 3a, b and d). The onset of the effect was very slow, the maximum effect being achieved in 30–60 min. CPP caused moderate inhibition of DSR and PSR (34 and 33% in average, respectively), and slight (10%) but statistically significant depression of MSR ($P<0.01$ at 30 min; paired t test). The inhibition of MSR was distinct, since the MSR records were very stable and a clear-cut breakpoint on the integrated record (as in Figure 3a) could always be observed after administration of the drug. Administration of an additional 2 mg kg^{-1} ($n=3$) or even later of an additional 4 mg kg ($n=1$) apparently did not cause any further inhibi-

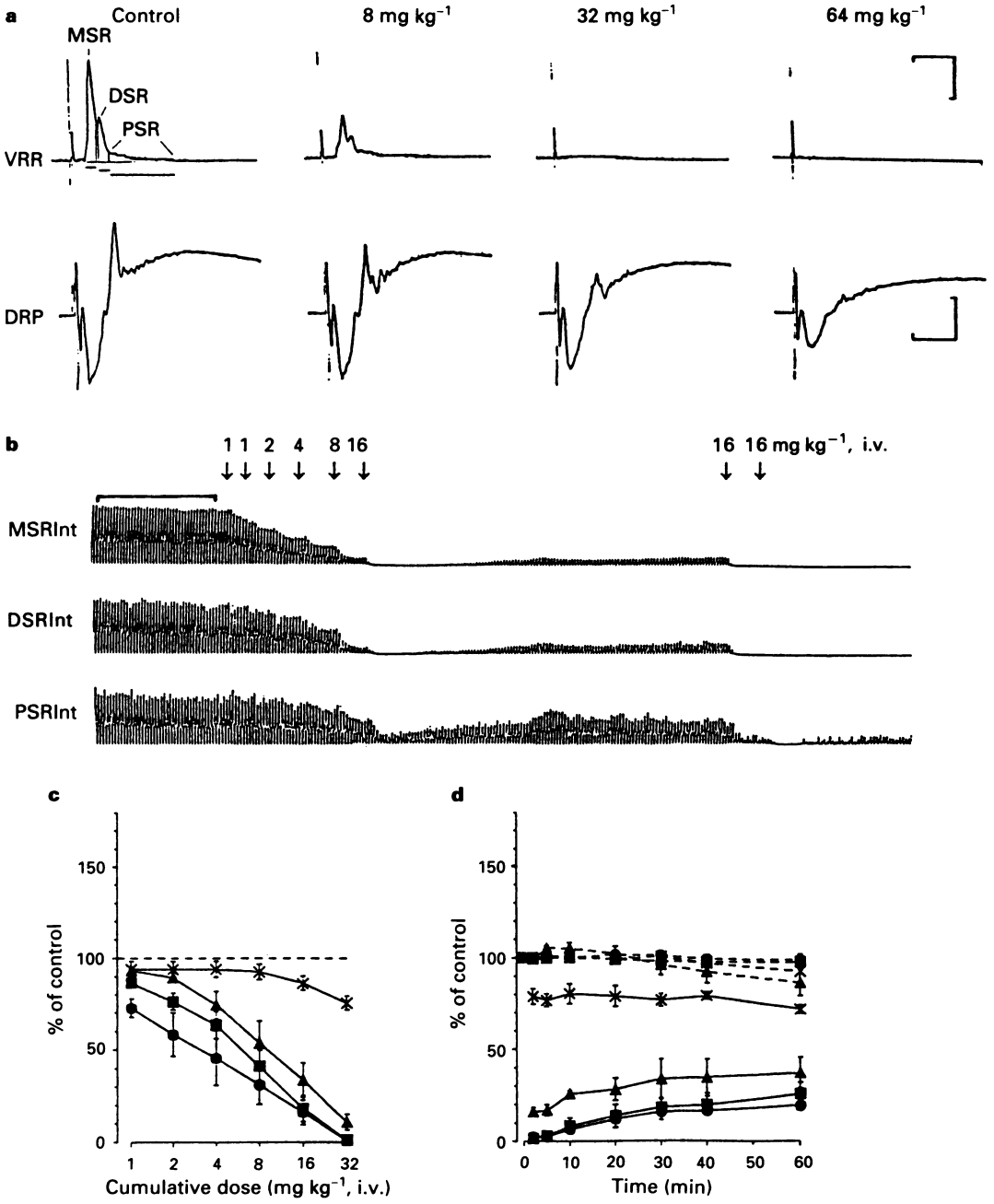

Figure 1 Effect of NBQX on the spinal root potentials evoked by dorsal root (L_5) stimulation studied by cumulative i.v. administration of doses 1–32 mg kg^{-1}. (a)–(b) Records from an experiment where 1 h after the last administration, additional 16 mg kg^{-1} was administered twice. (a) Averaged reflex potentials (average of 8) from an experiment. Upper trace: ventral root reflex (VRR, calibration: 0.5 mV, 4 ms); lower trace: ascending part of the dorsal root potential (DRP) with the dorsal root reflex superimposed (calibration: 0.2 mV, 4 ms), from left to right: control; after 8 mg kg^{-1} after 32 mg kg^{-1}; after 64 mg kg^{-1} (cumulative doses), respectively. Note that all components of the ventral root reflex could be abolished completely. Horizontal bars under the control ventral root reflex show the time-segments selected for integration of the corresponding response. Vertical lines and zero line close the areas under the curve which are represented by the integrated records. (b) Integrated reflex (Int) records of the monosynaptic- (MSR), disynaptic- (DSR), and polysynaptic reflex (PSR); (calibration: 20 min). (c) Dose-response relationship for the different potentials ($n=4$): (■) MSR Int; (●) DSR Int; (▲) PSR Int; (×) DRP Ampl. (d) Time-course of the effect after cumulative administration of 32 mg kg^{-1} ($n=3$). Abscissa scale: time from the last administration. (■——■) MSR Int; (●——●) DSR Int; (◀——▶) PSR Int; (X——X) DRP Ampl. Data obtained with the solvent for NBQX (4 ml kg^{-1}) (the same symbols but with broken line). Data are presented as mean ± s.e.mean.

tion of either reflex response suggesting that the effect of 2 mg kg^{-1} was supramaximal. Amplitude of DRP was unaffected by CPP.

The effect of MK-801 (0.5 mg kg^{-1}, i.v.) was studied in 4 animals (see Figure 3c). The onset of the effect was also rather slow, maximum effect being usually attained 20–30 min after the administration. DSR, PSR and MSR (in order of sensitivity) were decreased slightly (by 20, 15 and 9%, respectively), the latter two changes were not statistically significant. Despite the lack of statistical significance the clear-cut effect of MK-801 was apparent in most experiments. Moreover, repetition of the dose of 0.5 mg kg^{-1} yielded further significant depression of DSR and PSR in 2 out of 3 trials. Calculated average maximum depressions in these 3 experiments were: MSR: 15%, PSR: 21% and DSR: 31%. A further dose of 1 mg kg^{-1}, however, did not cause any further inhibition (3 trials). The amplitude of DRP was unaffected by MK-801.

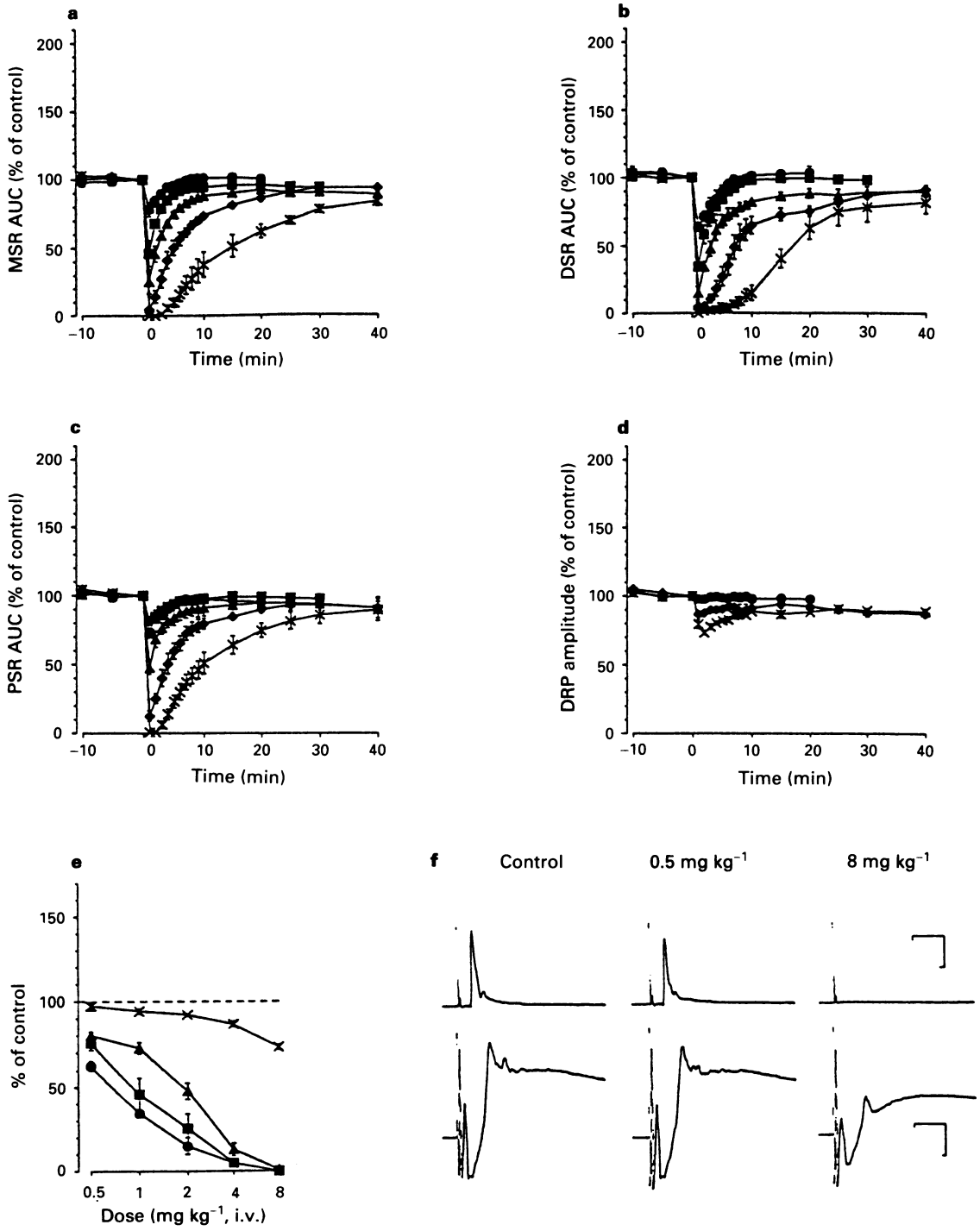

Figure 2 Effect of various i.v. doses of GYKI 52466 on the spinal root potentials. (a)–(c) Time-effect curves of integrated ventral root responses: (a) MSR, (b) DSR, (c) PSR. AUC = area under curve. (d) Time-effect curve of the amplitude of DRP. In (a), (b), (c) and (d) doses are (●) 0.5 mg kg^{-1}; (■) 1 mg kg^{-1}; (▲) 2 mg kg^{-1}; (◆) 4 mg kg^{-1}; (×) 8 mg kg^{-1}. (e) Dose-response relationship for the different potentials. (■) MSR Int; (●) DSR Int; (▲) PSR Int; (×) DRP Ampl. Data are presented as mean ± s.e.mean in 4–5 experiments. (f) Averaged reflex potentials from an experiment. Upper trace: ventral root reflex (VRR, calibration: 1 mV, 4 ms); lower trace: ascending part of the dorsal root potential (DRP) with the dorsal root reflex superimposed (calibration: 0.2 mV, 4 ms). From left to right: control, 2 min after injection of 0.5 mg kg^{-1}, 2 min after injection of 8 mg kg^{-1}. Note that all components of the ventral root reflex were abolished completely.

Ketamine, which had a rapid onset of action, was investigated in 4 animals according to a cumulative dosing protocol similar to that for NBQX. Results are presented in Figure 3e. Unlike CPP and MK-801, ketamine did not reach a plateau on the dose-response curve and at the highest applied dose produced more marked inhibition (32%, 48% and 30% for MSR, DSR and PSR, respectively) of the first two VRR components than did the other two NMDA antagonists. At a dose of 32 mg kg^{-1} its effect proved to be rather durable (Figure 3f). The amplitude of the DRP was not influenced by ketamine.

Excitability test

Neither success rate nor long-term stability of these experiments were as good as those of the reflex study. Therefore, in these experiments, if the administered drug had no effect or apparent recovery was achieved, further drug

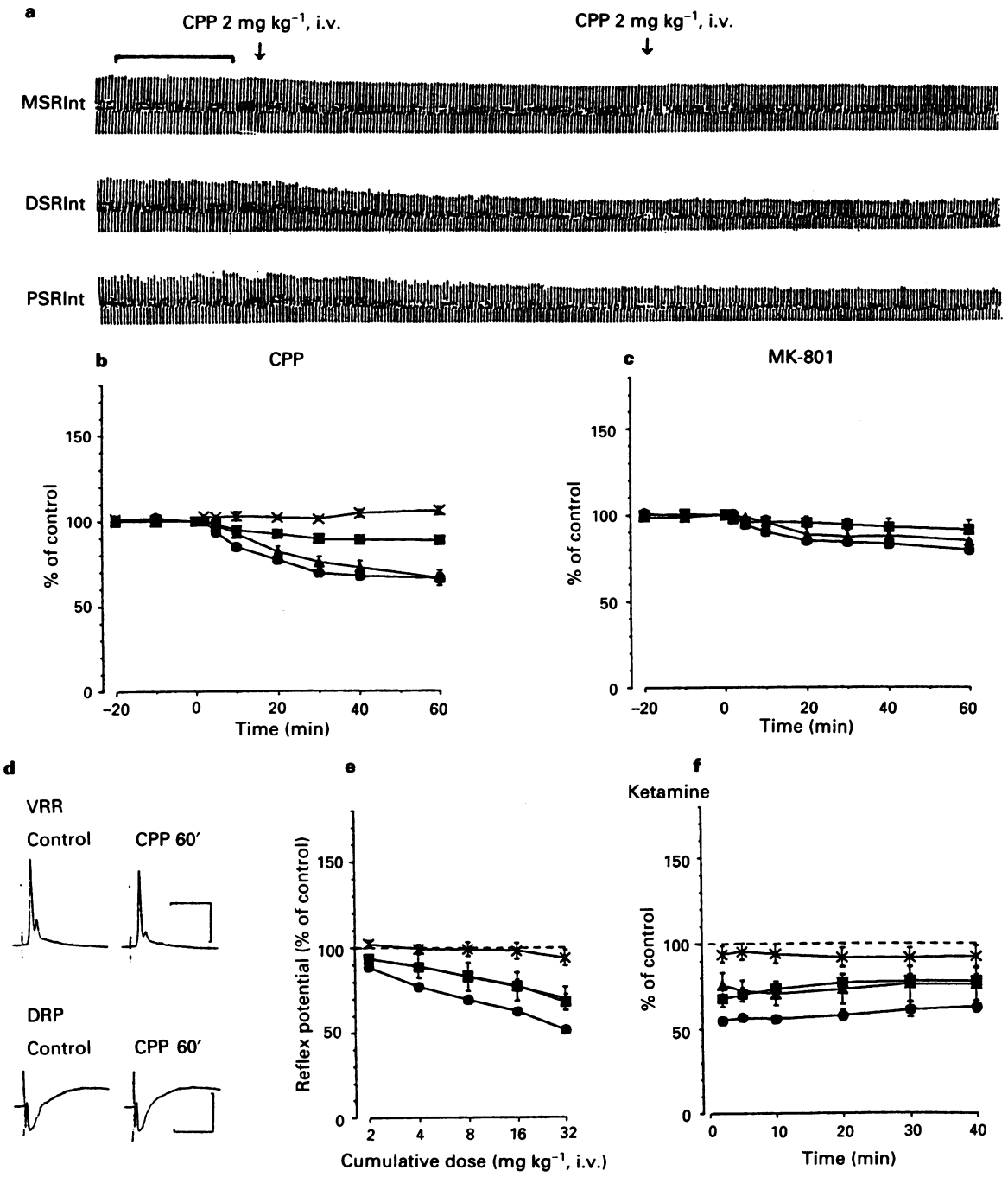

Figure 3 Effect of i.v. administered NMDA antagonists on the spinal root potentials. (a) Records from an experiment where 1 h after the administration of 2 mg kg^{-1} of CPP, additional 2 mg kg^{-1} was administered (calibration: 20 min). Note that no remarkable further reflex depression could be achieved. (b) Effect of CPP (2 mg kg^{-1}, i.v. at time: 0 min) on the time-course of integrated ventral root responses (MSR, DSR, PSR) and of amplitude of DRP ($n = 5$). (c) Effect of MK-801 (0.5 mg kg^{-1}, i.v., at time: 0 min) on the time-course of integrated ventral root responses (MSR, DSR, PSR). For the purpose of clarity the curve indicating no change in amplitude of DRP, was omitted from this figure ($n = 4$). (d) Averaged reflex potentials from the experiment shown in (a). Upper trace: ventral root reflex (calibration: 1 mV, 8 ms); lower trace: ascending phase of DRP (calibration: 0.4 mV, 8 ms) left: control; right: 60 min after administration of CPP (first dose). (e) Cumulative dose-response curves for ketamine ($n = 4$). (f) Time-course of the effect of ketamine after cumulative administration of 32 mg kg^{-1} ($n = 4$). In (b), (c), (e) and (f) (■) MSR Int; (●) DSR Int; (▲) PSR Int and (×) DRP Ampl. Abscissa scale: time from the last administration. In all graphs data are presented as mean ± s.e.mean but symbols often mask error bars.

effects were studied. Nevertheless, all drugs were investigated in 'drug-free' (except for the anaesthetic) animals as well, to confirm the findings. Representative records for each drug involved are presented in Figure 4. Ventral horn stimulation elicited two peaks of compound action potentials (MN and MS; see Methods) with different latencies recorded from the ventral root. Sometimes further activity of lower amplitude could be recorded following the monosynaptic (MS) component, which presumably reflected polysynaptic excitement of motoneurones (see for example Figure 4a and e).

GYKI 52466 (doses ranging 2–8 mg kg^{-1}, studied in 7 animals) reliably and selectively blocked all synaptic components of the ventral root response (see Figure 4a). Apart from a small (less than 10%) reduction observed in some experiments, GYKI 52466 exerted no effect on the MN component. Such a slight reduction seemed to appear if the drug was administered relatively long after the spinal transection. In Figure 4a, 8 mg kg^{-1} GYKI 52466 had no effect on MN. In a later phase of the same experiment, 2 mg kg^{-1} GYKI 52466 (not shown) and 8–32 mg kg^{-1} NBQX (see Figure 4b) had an apparent slight depressant effect. Excitability of primary afferents was not influenced by GYKI 52466.

Very similar results, i.e. selective abolition of MS, very slight or no inhibition of MN and no effect on PAF (see Figure 4b), were obtained with NBQX (studied in 4 animals). The time course of the effect of the two drugs was different and conform with that detected in the reflex study.

CPP and MK-801 ($n = 4$ and 3, respectively) apparently did not have any effect on either response. No inhibition of MS, like that of MSR in the reflex study, could be detected but taking into consideration the insufficient long-term stability, detection of an effect of 10% with such a slow onset may not be expected with this method.

On the contrary, ketamine (doses ranging 8–32 mg kg^{-1}, $n = 5$) considerably depressed MN and MS to a comparable

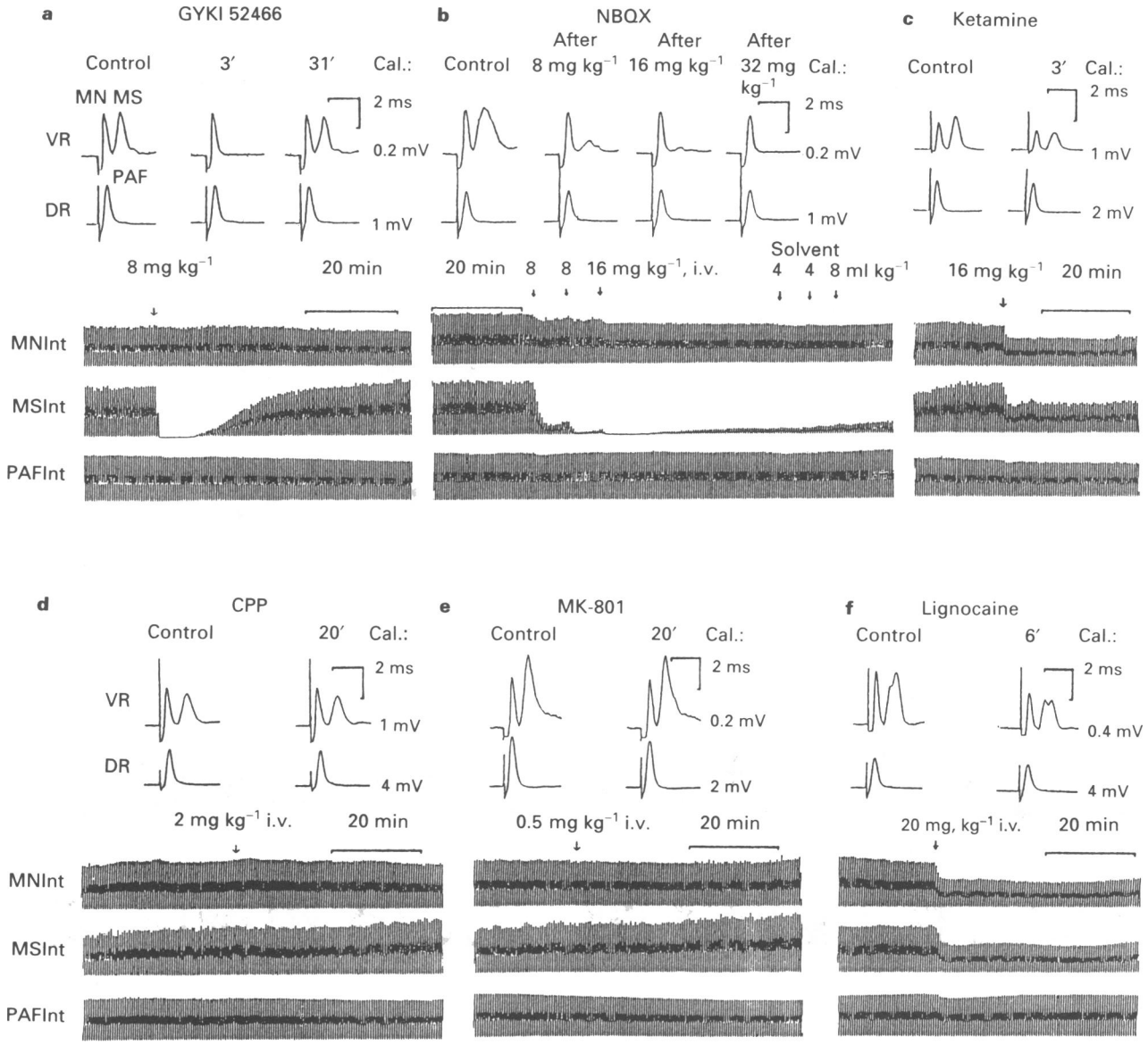

Figure 4 Effect of various excitatory amino acid antagonists and lignocaine administered i.v. in the excitability test. Panels (a) and (b) present records from the same experiment. GYKI 52466 (first drug in the experiment) was injected 4 h 33 min, while NBQX 8h 9 min after spinal transection. Tip position of the stimulating tungsten microelectrode was moved 40 μm more ventral between the two drugs. All other panels (c)–(f) show first drug administrations and records from different experiments. In each panel VR: averaged potential from the L_5 ventral root; DR: averaged potential recorded from the L_5 dorsal root; MN: potential representing direct stimulation of motoneurones; MS: potential representing monosynaptic activation of motoneurones; PAF: antidromically conducted compound action potential generated by direct stimulation of primary afferents; MNInt, MSInt, PAFInt: integrated records of the corresponding potentials. Treatments and calibrations are presented in the figure.

extent (Figure 4c). The excitability of primary afferents was also slightly decreased. The profile of ketamine was similar to that of the local anaesthetic, lignocaine (Figure 4f).

Microiontophoretic study

Iontophoretic administration of EAA agonists produced characteristic alterations in the antidromic field potential (AFP) of the motoneurone pool. Typical AFP, and its reliable response to agonists in the L_5 segment could be recorded from electrode tip positions of 0.7–1.1 mm lateral from the midline (lateral from the dorsal root entry zone) and 1.7–2.2 mm depth (ventral) from the dorsal spinal cord surface. Figure 5 shows records from an experiment in which almost all characteristic phenomena could be observed. The AFP starts with a positive wave followed by a negative one (P_1 and N_1, respectively, terms used by Engberg *et al.*, 1979).

Iontophoretic application of increasing 'doses' (i.e. ejection currents) of AMPA yielded the following alterations. First, some increase in the amplitude accompanied by shortening of the duration of the N_1 wave appeared; however, the enhancement of the amplitude often failed to appear. This was followed by appearance of a second positive wave (P_2). Then the N_1 wave decreased, disappeared and usually a large positive wave appeared. Altogether these phenomena caused dual changes in the amplitude i.e. both increase and decrease. However, the integrated record mostly showed a net decrease. The 'resting' AFP recovered usually within 2 min after cessation of the iontophoresis.

The effects of kainate were quite similar to those of AMPA, except that after cessation of the iontophoretic application, a gradual enhancement of AFP ('afterfacilitation') developed and lasted for several minutes. Even if the inhibitory response, which usually appeared promptly, was missing, the 'afterfacilitation' developed slowly starting with some delay, suggesting that it may be the result of diffusion of kainate to a relatively large area.

In contrast, NMDA always increased both the amplitude and the integrated response. Depression of the N_1 wave or appearance of a positive wave could only be observed after using very large ejection currents exceeding 50 nA. However, when we tried to apply NMDA with such high currents repeatedly, it led to apparent destruction of the otherwise very stable AFP response. In the recovery from the enhancing effects of either kainate or NMDA stepwise changes or units behaving in an 'all-or-nothing' manner could often be observed.

In some cases following iontophoretic application of the EAA agonists we could observe, on a free running oscilloscope, neurones (probably motoneurones) firing with extracellular action potentials of 1–2 mV. After administration of AMPA or kainate, parallel with the above described change in the AFP, the negative action potentials became

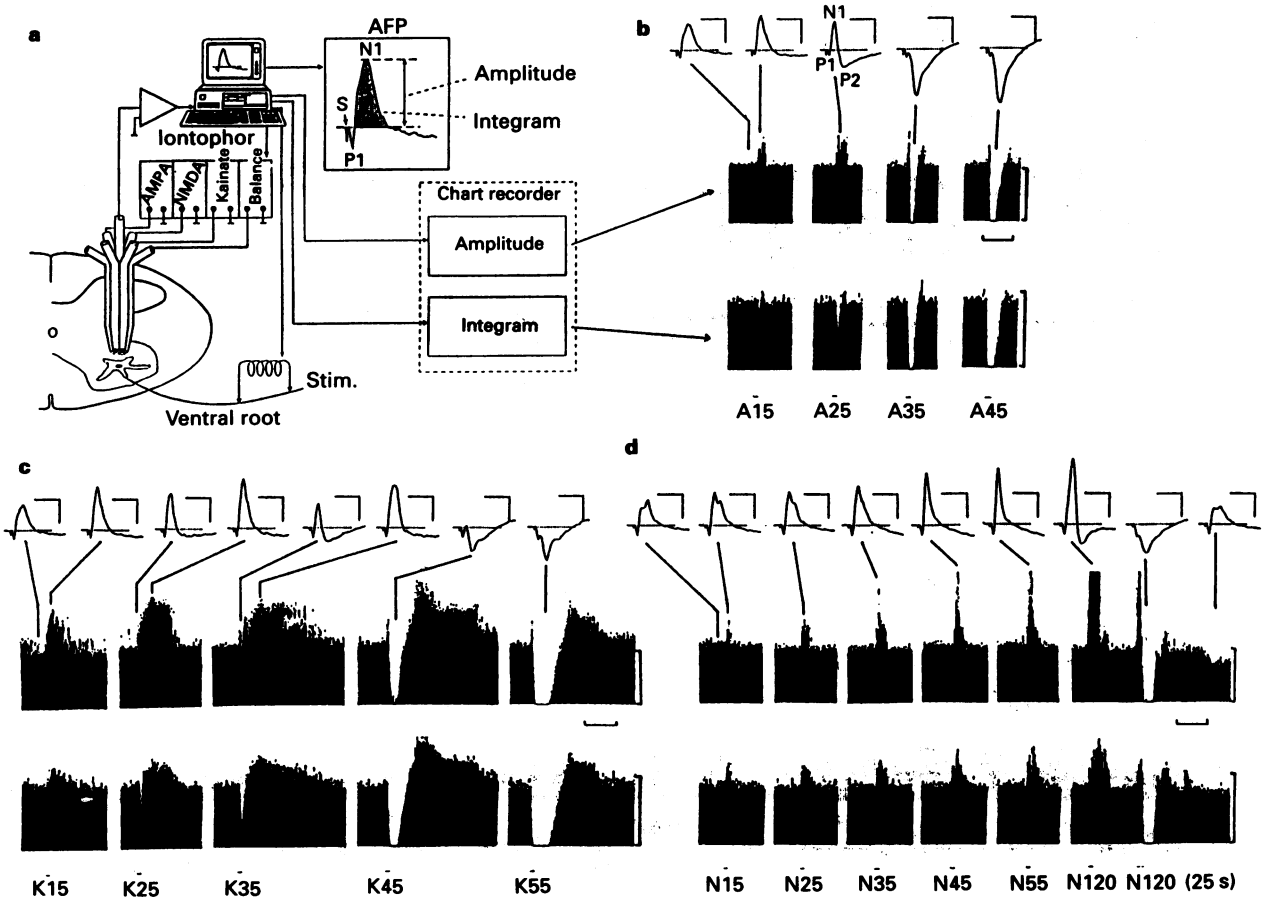

Figure 5 Schematic drawing of the experimental arrangement in the iontophoretic study and a typical antidromic field potential (AFP) recorded from the motoneurone pool, consisting of a positive wave (P_1) followed by a negative one (N_1) with the stimulus artefact (S) (a); and records from an experiment showing typical alterations in the AFP, induced by iontophoretic application of EAA agonists AMPA (A), kainate (K) and NMDA (N) by different ejection currents (in nA, numbers following the letters) (b–d). In each panel: averaged AFP of 10 responses (upper row; negativity is upwards; calibration: 1 mV, 2 ms); chart record segments of the amplitude record (middle row), each response is represented by a pen deflection every 500 ms (calibration: 1 mV, 2 min); simultaneous chart record segments of the integrated response record (bottom row), each response is represented by a pen deflection proportional to the area under the N_1 wave (calibration: 1 μVs, 2 min). Horizontal bars below the integrated records show iontophoretic applications lasting for 15 s (except the last application of 25 s). Lines connect the averaged potentials with corresponding parts of the amplitude record. Amplitude records at last four NMDA applications were truncated by the recorder.

biphasic (negative-positive), then often reversed to be only positive before they disappeared (depolarization blockade). A transient firing could also be observed in the recovery phase judged from the integrated AFP record. Ejection of NMDA also elicited firing; however, reversal of the extracellular action potentials or depolarization blockade did not occur.

Based on the above findings, the depressant effects of AMPA and kainate (between 50–100%) as well as the enhancing effects of NMDA on the integrated response

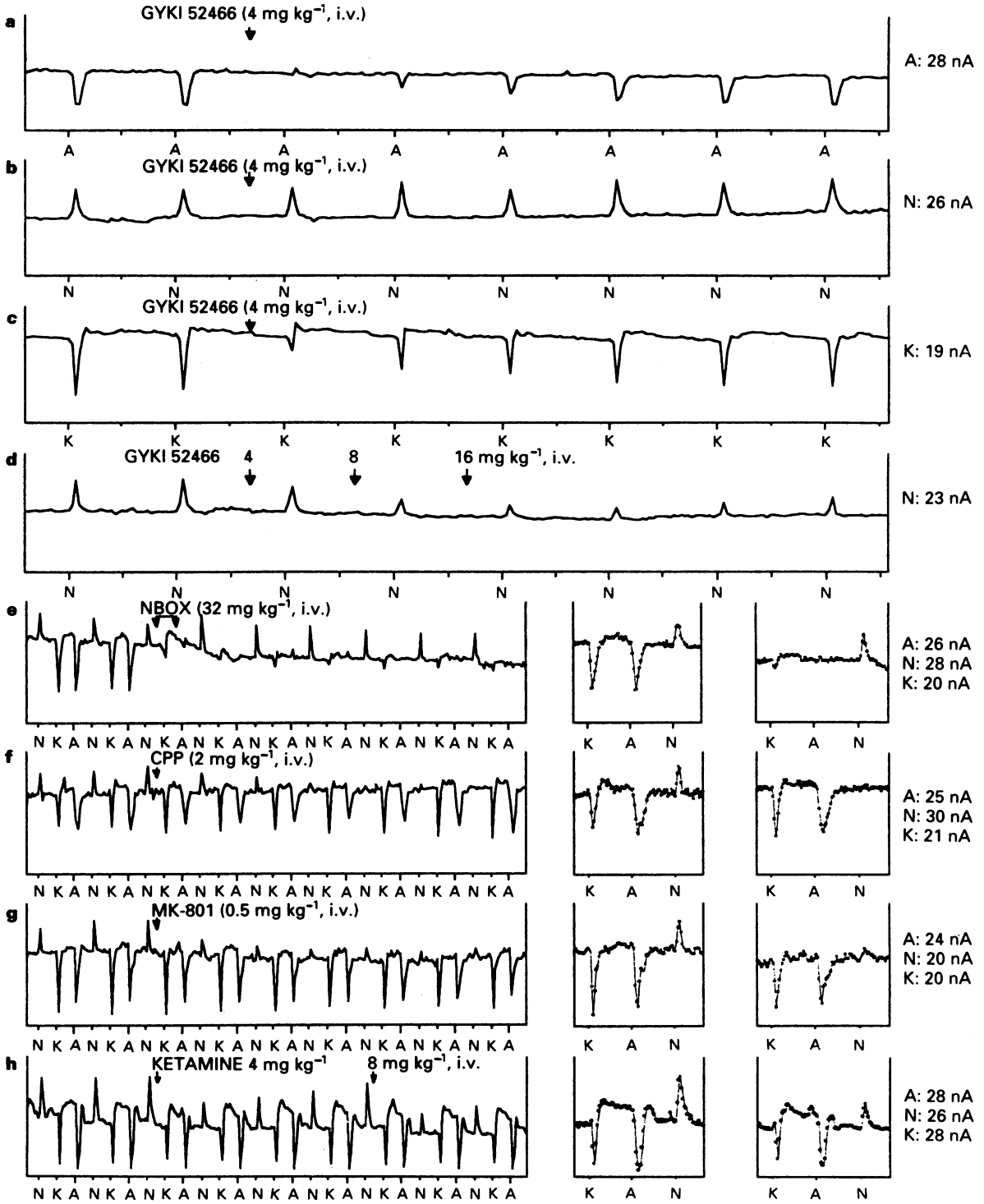

Figure 6 Effect of various excitatory amino acid antagonists on the alteration induced in the antidromic field potential of the motoneurone pool by regular alternating iontophoretic application of AMPA (A), NMDA (N) and kainate (K). Tickmarks above letters in each chart indicate start of the iontophoretic ejection current lasting for 15 s. Ordinates: integrated field potential (uncalibrated). Abscissae: time. Distance between two tickmarks represents 3 min. Each line-graph connects points (10 or 12 points min^{-1}) representing the average integrated value of 10 responses. (a)–(c) Successive records from the same experiment. The gap in the time between these graphs was that used for the determination of the appropriate ejection current and for the stabilization of responses to the next agonist. (d) Record from another experiment, in which the effects of high doses of GYKI 52466 on the NMDA responses were studied. (e–h) The rows present records from different animals obtained with administrations of various antagonists. Left graph: compressed time-scale, continuous record. Right two graphs: segments from the same record with a more extended time-scale. Left panel: control responses; right panel starts 46 min (e–g) or immediately (h) after the (first) drug administration. Applied iontophoretic currents are presented at the right side.

seemed to be the best methods for detection of the effects of EAA antagonists.

The effect of GYKI 52466 on EAA agonist-induced responses was investigated in 11 rats. Four of these experiments were performed according to the same protocol as that shown in Figure 6a–c. After stabilization of responses to an EAA agonist, 4 mg kg^{-1} GYKI 52466 was injected 2 min before the iontophoresis. Following the recovery from the effect of GYKI 52466, recurrent ejection of the next agonist was started and in this manner the effect of GYKI 52466 against all the three agonists was tested. In the other 7 experiments effects of higher doses or effects against only one or two agonists were tested similarly. GYKI 52466 typically abolished the responses to AMPA or caused reversal of the apparently 'depressant' responses to a very slight facilitation (Figure 6a). Responses to NMDA were typically not affected by 4 mg kg^{-1} GYKI 52466 (see Figure 6b); however, 8 mg kg^{-1} clearly reduced NMDA responses in 2 out of 3 trials. Administration of higher doses (semicumulative administration up to 28 mg kg^{-1}, Figure 6d) yielded marked depression but did not cause complete abolition of NMDA responses. Repeated ejection of kainate every 6 min usually resulted in some long-term 'enhancement' in the 'resting' AFP, i.e. the interval between two ejections was not sufficient for complete recovery. The 'depressant' response to kainate was markedly reduced but never abolished completely (see Figure 6c). The 'afterfacilitation' was inconsistently affected: slightly enhanced or reduced or not affected by GYKI 52466. In some cases the 'resting' AFP was also slightly diminished.

The antagonists having longer action were tested against alternating ejection of all the three agonists (Figure 6e–h). It must be noted that some maintained potentiating effect of kainate due to an insufficient recovery was often present in these experiments. NBQX (32 mg kg^{-1}, $n = 4$) markedly reduced or abolished responses to AMPA, or caused reversal to a slight facilitation. Responses to NMDA were apparently not affected, while those to kainate were markedly reduced but not completely abolished (see Figure 6e). NBQX consistently reduced 'resting' AFP but the 'afterfacilitation' was inconsistently affected like that described at GYKI 52466.

CPP (2 mg kg^{-1}) completely (in 2 out of 4 trials) or almost completely abolished the effect of NMDA, while responses to AMPA or kainate were practically unaffected (see Figure 6f). The maximum effect was achieved in 45–60 min.

MK-801 (0.5 mg kg^{-1}, $n = 4$) markedly reduced the NMDA response but complete abolition was achieved only in one case. It also exerted practically no effect on AMPA or kainate-induced alterations. The very slight gradual decrease in the 'resting' AFP and in the effect of kainate seen in Figure 6g were not consistent findings and the latter one may probably be attributed to a spontaneous drifting. The effect of MK-801 reached a maximum in about 30 min.

The effect of ketamine (4 mg kg^{-1}) was investigated in 6 rats, 3 of them according to the protocol used for GYKI 52466, and the others (e.g. Figure 6h) according to that for NBQX, CPP and MK-801. Ketamine markedly reduced or in 2 cases transiently abolished the effect of NMDA. Effects of AMPA or kainate were minimally reduced or unaffected. In most cases, some reduction in the 'resting' AFP was observed.

Discussion

Before drawing conclusions from the reflex studies on the involvement of EAA receptors in the reflex transmission, the adequacy of the methods and suitability of the antagonists used should be considered.

As far as we know, our data have for the first time demonstrated a complete and selective blockade of the MS response in the excitability test by some pharmacological agents (i.e. GYKI 52466 and NBQX). Selective abolition of MS by antagonists of the supposed transmitter of excitatory synapses on motoneurones gives further support to the view that the MS spike clearly represents synaptic excitation, while MN may represent direct electrical excitability of motoneurones (Ono *et al.*, 1979). The inconsistent very slight depressant effect of the two non-NMDA antagonists on the MN may indicate that a slight tonic facilitatory influence modulating electrical excitability of motoneurones may have been present in our spinal rats, perhaps depending on the time allowed for recovery from the 'spinal shock'. Of course, a very slight local-anaesthetic like effect (not comparable to their reflex inhibitory action) cannot be fully excluded. The local anaesthetic-like effect of ketamine, clearly seen in the higher dose-range (e.g. at 8 mg kg^{-1}) may explain its relatively greater effect on MSR (in comparison with the other two NMDA antagonists) and the lack of reaching a plateau on the dose-response curves in the reflex study. This finding suggests ketamine is not a valuable tool for answering the basic questions of the present study.

Interpretation of iontophoretically applied drug-induced changes in the AFP is difficult (for more details see Engberg *et al.*, 1979). Enhancing effects (Barasi & Roberts, 1977; Roberts *et al.*, 1988; in rats) as well as depressant effects by depolarizing agents (Barasi & Roberts, 1974; Engberg *et al.*, 1979) have already been described. Based on the above studies and on our experience possible conflicting factors influencing the AFP can be summarized as follows: (a) Antidromically evoked action potentials often fail to invade the motoneurone soma or dendritic regions (see also Renshaw, 1942; Coombs *et al.*, 1955). Slight depolarization or enhanced membrane resistance can increase the number of motoneurones invaded, leading to an increase in the AFP. (b) Depolarization may decrease the amplitude of the action potential in those motoneurones which have already been invaded, resulting in a decrease in the extracellularly recorded AFP. (c) Profound depolarization can lead to depolarization blockade. This can easily be achieved with kainate but hardly with NMDA (Engberg *et al.*, 1978). Although both compounds depolarize motoneurones, kainate increases, while NMDA gives an apparent decrease in the membrane conductance (Engberg *et al.*, 1978). (d) Compensatory outward currents for the action potential (inward current) generated at remote membrane parts of the motoneurones act as current 'source' at the electrode tip yielding a positive wave superimposed on the negative wave caused by the action potential of close segments. A marked increase in the membrane conductance in the vicinity of the electrode tip can enhance the current density of this 'source', yielding biphasic or inverted (positive) extracellular action potential recording, narrow N_1 wave, appearance of a P_2 wave (perhaps representing invasion of remote dendritic regions), or of a large positive wave on the AFP, phenomena typically observed after ejection of AMPA or kainate.

In summary, AFP does not simply reflect depolarization of motoneurones but also conductance mechanisms activated by the depolarizing agent. While NMDA presumably acted via the first and possibly only insignificantly via the second mechanism, in the action of kainate and AMPA third and fourth items of the above mechanisms may have dominated in determining the net effect on the AFP leading to an opposite alteration.

Whatever the underlying mechanism, the described iontophoretic method seemed to be suitable for testing interactions between agonists and antagonists on motoneurones *in vivo*. All the EAA antagonists (NMDA or non-NMDA) used in this study proved to be selective in attenuating responses of the corresponding agonists at the same doses as those applied in the reflex study. Although both NBQX and GYKI 52466 had apparently somewhat greater effect on AMPA- than on kainate-induced changes, responses to both agonists were markedly reduced; thus we could not demonstrate clear-cut selectivity of either GYKI 52466 or NBQX towards AMPA vs. kainate responses on spinal motoneurones. This is

in agreement with results obtained with GYKI 52466 on cat spinal motoneurones (Engberg *et al.*, 1993), but in contrast with results of Ouardouz & Durand (1991), who reported GYKI 52466 to antagonize glutamate but not kainate responses on rat abducens motoneurones.

In summary, according to the results of the excitability test and of the iontophoretic study, both CPP and MK-801 but not ketamine proved to be suitable tools for investigating involvement of NMDA receptors, while NBQX and GYKI proved to be suitable for testing that of non-NMDA receptors in the reflex transmission.

The effect of 2 mg kg^{-1} CPP seemed to be 'supramaximal' in depressing the spinal reflex, while 0.5 mg kg^{-1} MK-801 (in contrast with our preliminary finding on which this selection was based) proved 'submaximal'. Therefore, data obtained with 2 mg kg^{-1} CPP (see Figure 3) demonstrate most clearly the contribution of NMDA receptors (about 10% to MSR and 20–30% to PSR and DSR). The fact that both non-NMDA antagonists could completely abolish not only MSR but also DSR and PSR, indicates that non-NMDA receptors play a substantial role in the mediation of all short latency reflexes (up to 10 ms). The lack of a non-NMDA antagonist resistant part, despite the indication of contribution of NMDA receptors to PSR, is consistent with the view that NMDA receptors *in vivo* are under a considerable voltage-sensitive Mg^{2+} blockade (Nowak *et al.*, 1984) and the synaptically released transmitter is unable to depolarize motoneurones to a suprathreshold level via NMDA receptors alone.

Our results conflict with the general view that non-NMDA and NMDA receptors mediate MSR and PSR, respectively. Not even MSR was fully resistant to NMDA antagonists. This is in good agreement with the slight depression of MSR and of the peak of monosynaptic excitatory postsynaptic potential (e.p.s.p.) of motoneurones by AP5 in rat spinal cord *in vitro* reported recently by King *et al.* (1992). The term 'monosynaptic' or 'polysynaptic' in the field of electrophysiology has been based on the estimation of synaptic delay(s) and on the assumption of a single transmitter substance acting on a single receptor. However, data are accumulating for long lasting effects mediated via receptors activated by a presumably monosynaptically released transmitter. A significant depression of the descending phase and a slight depression of the peak of clearly monosynaptic e.p.s.ps by NMDA antagonists have been demonstrated (for review see Headley & Grillner, 1990). In the case of dorsal root stimulation (not functionally separated input) disynaptic and polysynaptic e.p.s.ps are presumably summed with the descending phase of the monosynaptic one. The higher but not exclusive effect of NMDA antagonists on DSR and PSR vs. MSR may result from the NMDA receptor-mediated 'late' effect of the monosynaptically released transmitter, too. Since in complex systems, such as the mammalian spinal cord, the differentiation is difficult even with intracellular recording, the terms 'monosynaptic' or 'polysynaptic' (which for simplicity we have also been using) may be misleading regarding the underlying mechanisms, and the use of 'early-' or 'late-' or given latency components would be more correct.

The fact that MS (i.e. the synaptically evoked) peak was fully antagonized in the excitability test by non-NMDA antagonists does not support the hypothesis that, in contrast with primary afferents, interneuronal 'secondary afferents' may use an NMDA-like transmitter (see Davies & Watkins, 1983), since 'secondary afferents' may also have been excited by the intraspinal stimulation in our experiments.

It must be emphasized that the present study extended only for short latency (up to 10 ms) polysynaptic components that are evoked by *single* shock stimulation and are dependent on activation of A fibres only (concluded from input-output curve, i.e. responses reached a maximum below 5T). Turski *et al.* (1992) using EMG recording reported no effect of NBQX on the 'polysynaptic' flexor reflex (time window: $\approx$10–100 ms) evoked by high intensity *train* stimulation in mice. On the contrary, apart from the present data, we have found GYKI 52466 to abolish the flexor reflex (time window: 10–50 ms) in cats also recorded by EMG but evoked by high intensity *single* shocks (Farkas *et al.*, 1992). The difference in the latency is not likely to be sufficient to explain fully this discrepancy. Marked depression of long lasting (up to 800 ms) PSR components (Long *et al.*, 1990) and of late e.p.s.p. components (King *et al.*, 1992) by CNQX has been reported using single shock stimulation of the dorsal root in *in vitro* rat spinal cord preparations. AMPA receptors become desensitized very quickly (time const.: <10 ms; Mayer *et al.*, 1991) and complete recovery from desensitization after short pulse ejection of glutamate onto motoneurones, comparable to the synaptic release, takes more than 1 s. (Onodera & Takeuchi, 1991). On the other hand, the onset (Onodera & Takeuchi, 1991) and the desensitization kinetics of NMDA receptors is slower and lesser in degree (time const.: $\approx$300 ms, Mayer *et al.*, 1991). These features may predestine *AMPA receptors* for preferential mediation of *single volleys*, while participation of *NMDA receptors* may become dominant in mediation of *impulse trains*, which may liberate larger amounts of the transmitter being present in (or around) the synaptic cleft for a much longer period. In the generation of long latency components, even if they were evoked by a single afferent volley, presumably train like firing of interneurones is involved giving more importance to the NMDA receptors than that demonstrated in the present study for short latency PSR components. Moreover, it must be noted that the use of a competitive antagonist (e.g. CNQX or NBQX) may yield underestimation of the involvement of non-NMDA receptors if train like firing liberates excess amounts of the transmitter resulting in insufficient antagonism. The glycine receptor mediated NMDA antagonist feature of CNQX at 10 μM (Long *et al.*, 1990) limits usefulness of this compound due to the inability to produce a 'supramaximal' but still selective effect.

DRP which represents depolarization of primary afferents evoked by a GABA-ergic interneurone is thought to be associated with the presynaptic inhibition (for review see Levy, 1980). Since the first synapse of this pathway is that formed by primary afferents, involvement of some EAA receptors may be assumed. Our results do not indicate contribution of NMDA receptors to the mediation of DRP (but only its early part was studied). From the partial (about 25%) inhibition of DRP by both non-NMDA antagonists it cannot be decided whether non-NMDA receptors are only partly involved, or the high safety factor in this pathway and thus the lack of a supramaximal effect is responsible for the only partial inhibition. The fact that the dose-response curves of both non-NMDA antagonist started to get steeper suggests the latter conclusion. Higher doses should have been used to gain a clear conclusion but this was limited by poor solubility of NBQX, while GYKI 52466 above the dose of 4 mg kg^{-1} seemed to lose its selectivity towards AMPA/kainate vs. NMDA responses in this complex *in vivo* system. Whether this apparent non-selectivity is due to the relative re-establishment of the voltage-sensitive Mg-blockade of NMDA receptors by removal of all excitatory influences via selective blockade of non-NMDA receptors or whether other mechanisms are involved (true non-selectivity) remains open.

In conclusion, our results demonstrate that non-NMDA EAA receptors play a substantial role in the mediation of short latency mono-, di- and polysynaptic spinal reflexes, while NMDA receptors contribute to a smaller extent. We suggest that differential function of non-NMDA and NMDA receptors is not specifically distributed between mono- and polysynaptic pathways but rather determined by the firing patterns involved. To get a clear picture of the specific involvement of non-NMDA receptors in the mediation of longer latency reflex components and train- or physiological stimulus evoked reflexes further studies are necessary with

supramaximal doses of highly selective antagonists. GYKI 52466 and NBQX may be suitable tools for such investigations *in vivo* and probably *in vitro* as well; however, as was pointed out in the discussion of DRP, they also have their limitations.

This work was supported by a scholarship from the Ministry of Education, Science and Culture of Japan (Monbusho) to S.F. We are grateful to Dr I. Tarnawa for a sample of GYKI 52466, to Novo Nordisk company for a sample of NBQX, to P. Molnár for providing the excellent data acquisition programme: Stimulat 1.0 and to I. Engberg for critical reading of the manuscript.

References

ANIS, N.A., BERRY, S.C., BURTON, N.R. & LODGE, D. (1983). The dissociative anaesthetics, ketamine and phencyclidine, selectively reduce excitation of central mammalian neurones by N-methyl-aspartate. *Br. J. Pharmacol.*, **79**, 565–575.

BARASI, S. & ROBERTS, M.H.T. (1974). The modification of lumbar motoneurone excitability by stimulation of a putative 5-hydroxytryptamine pathway. *Br. J. Pharmacol.*, **52**, 339–348.

BARASI, S. & ROBERTS, M.H.T. (1977). Responses of motoneurones to electrophoretically applied dopamine. *Br. J. Pharmacol.*, **60**, 29–34.

COLLINGRIDGE, G.L. & LESTER, R.A. (1989). Excitatory amino acid receptors in the vertebrate central nervous system. *Pharmacol. Rev.*, **40**, 143–210.

COOMBS, J.S., ECCLES, J.C. & FATT, P. (1955). The electrical properties of the motoneurone membrane. *J. Physiol.*, **130**, 291–325.

DAVIES, J., EVANS, R.H., HERRLING, P.L., JONES, A.W., OLVERMAN, H.J., POOK, P. & WATKINS, J.C. (1986). CPP, a new potent and selective NMDA antagonist. Depression of central neuron responses, affinity for [^{3}H]D-AP5 binding sites on brain membranes and anticonvulsant activity. *Brain Res.*, **382**, 169–173.

DAVIES, J. & WATKINS J.C. (1983). Role of excitatory amino acid receptors in mono- and polysynaptic excitation in the cat spinal cord. *Exp. Brain Res.*, **49**, 280–290.

DONEVAN, S.D. & ROGAWSKI, M.A. (1993). GYKI 52466, a 2,3-benzodiazepine, is a highly selective, noncompetitive antagonist of AMPA/Kainate receptor responses. *Neuron*, **10**, 51–59.

ECCLES, J.C. (1957). *The Physiology of Nerve Cells*. Baltimore: John Hopkins Press.

ENGBERG, I., FLATMAN, J.A. & LAMBERT, J.D.C. (1978). The action of N-methyl-D-aspartic and kainic acids on motoneurones with emphasis on conductance changes. *Br. J. Pharmacol.*, **64**, 384–385P.

ENGBERG, I., FLATMAN, J.A. & LAMBERT, J.D.C. (1979). A comparison of extracellular and intracellular recording during extracellular microiontophoresis. *J. Neurosci. Methods*, **1**, 219–233.

ENGBERG, I., TARNAWA, I., DURAND, J. & OUARDOUZ, M. (1993). An analysis of synaptic transmission to motoneurones in the cat spinal cord using a new selective receptor blocker. *Acta Physiol. Scand.*, **148**, 97–100.

EVANS, R.H. (1989). The pharmacology of segmental transmission in the spinal cord. *Progr. Neurobiol.*, **33**, 255–279.

EVANS, R.H., SMITH, D.A.S. & WATKINS, J.C. (1981). Differential role of excitant amino acid receptors in spinal transmission. *J. Physiol.*, **320**, 55P.

FARKAS, S., TARNAWA, I. & BERZSENYI, P. (1989). Effects of some centrally acting muscle relaxants on spinal root potentials: a comparative study. *Neuropharmacology*, **28**, 161–173.

FARKAS, S., TARNAWA, I., BERZSENYI, P., PÁTFALUSI, M., ANDRÁSI, F. & ONO, H. (1992). The role of non-NMDA excitatory amino acid receptors in the mediation of spinal reflexes. In *Frontiers and New Horizons in Amino Acid Research*, ed. Takai, K., pp. 471–475. Amsterdam: Elsevier Science Publishers.

FUKUDA, H., KUDO, Y. & ONO, H. (1977). Effects of β-(p-chlorophenyl)-GABA(baclofen) on spinal synaptic activity. *Eur. J. Pharmacol.*, **44**, 17–24.

GANONG, A.H., LANTHORN, T.H. & COTMAN, C.W. (1983). Kynurenic acid inhibits synaptic and acidic amino acid-induced responses in the rat hippocampus and spinal cord. *Brain Res.*, **273**, 170–174.

HEADLEY, P.M. & GRILLNER, S. (1990). Excitatory amino acids and synaptic transmission: the evidence for a physiological function. *Trends Pharmacol. Sci.*, **11**, 205–211.

HONORE, T., DAVIES, S.N., DREJER, J., FLETCHER, E.J., JACOBSEN, P., LODGE, D. & NIELSEN, F.E. (1988). Quinoxalinedions: potent competitive non-NMDA glutamate receptor antagonists. *Science*, **241**, 701–703.

JAHR, C.E. & YOSHIOKA, K. (1986). Ia afferent excitation of motoneurones in the in vitro new-born rat spinal cord is selectively antagonized by kynurenate. *J. Physiol.*, **370**, 515–530.

KANEKO, T., ONO, H. & FUKUDA, H. (1987). Simultaneous evaluation of drug effects on both the spinal cord and the descending pathways in rats. *Arch. Int. Pharmacodyn.*, **287**, 203–210.

KAWAGOE, R., ONODERA, K. & TAKEUCHI, A. (1986). The release of endogenous glutamate from the newborn rat spinal cord induced by dorsal root stimulation and substance P. *Biomed. Res.*, **7**, 253–259.

KING, A.E., LOPEZ-GARCIA, J.A. & CUMBERBATCH, M. (1992). Antagonism of synaptic potentials in ventral horn neurones by 6-cyano-7-nitroquinoxaline-2,3-dione: a study in the rat spinal cord *in vitro*. *Br. J. Pharmacol.*, **107**, 375–381.

LEVY, R.A. (1980). Presynaptic control of input to the central nervous system. *Can. J. Physiol. Pharmacol.*, **58**, 751–766.

LONG, S.K., SMITH, D.A.S., SIAREY, R.J. & EVANS, R.H. (1990). Effect of 6-cyano-2,3-dihydroxy-7-nitro-quinoxaline (CNQX) on dorsal root-, NMDA-, kainate- and quisqualate-mediated depolarization of rat motoneurones *in vitro*. *Br. J. Pharmacol.*, **100**, 850–854.

MAYER, M.L., VYKLICKY, L., BENVENISTE, M. & WILLIAMSON, L. (1991). Desensitization at NMDA and AMPA-kainate receptors. In *Excitatory Amino Acids and Synaptic Function*. ed. Wheal, H. & Thomson, A., pp. 123–139. New York: Academic Press.

MAYER, M.L. & WESTBROOK, G.L. (1987). The physiology of excitatory amino acids in the vertebrate central nervous system. *Progr. Neurobiol.*, **28**, 197–276.

NOWAK, L., BREGESTOVSKI, P., ASCHER, P., HERBET, A. & PROCHIANTZ, A. (1984). Magnesium gates glutamate-activated channels in mouse central neurones. *Nature*, **307**, 462–465.

ONO, H. (1982). Animal techniques for evaluating muscle relaxants. In *Kyoto Symposia*, ed. Buser, P.A., Cobb, W.A. & Okuma, T. pp. 199–208. Amsterdam: Elsevier Biomedical Press.

ONO, H., FUKUDA, H. & KUDO, Y. (1984). Mechanisms of depressant action of muscle relaxants on spinal reflexes: participation of membrane stabilizing action. *J. Pharm. Dyn.*, **7**, 171–176.

ONO, H., FUKUDA, H. & KUDO, Y. (1979). Mechanisms of depressant action of baclofen on the spinal reflex in the rat. *Neuropharmacology*, **18**, 647–653.

ONODERA, K. & TAKEUCHI, A. (1991). Uneven distribution of excitatory amino acid receptors on ventral horn neurones of newborn rat spinal cord. *J. Physiol.*, **439**, 257–276.

OUARDOUZ, M. & DURAND, J. (1991). GYKI 52466 antagonizes glutamate responses but not NMDA and kainate responses in rat abducens motoneurones. *Neurosci. Lett.*, **125**, 5–8.

POLC, P. (1985). 2-Amino-7-phosphonoheptanoic acid depresses γ-motoneurons and polysynaptic reflexes in the cat spinal cord. *Eur. J. Pharmacol.*, **117**, 387–389.

POLC, P. & HAEFELY, W. (1977). Effects of intravenous kainic acid, N-methyl-D-aspartate, and (−)-nuciferine on the cat spinal cord. *Naunyn-Schmied. Arch. Pharmacol.*, **300**, 199–203.

RENSHAW, B. (1942). Effects of presynaptic volleys on spread of impulses over the soma of the motoneurones. *J. Neurophysiol.*, **5**, 235–243.

ROBERTS, M.H.T., DAVIES, M., GIRDLESTONE, D. & FOSTER, G.A. (1988). Effects of 5-hydroxytryptamine agonists and antagonists on the responses of rat spinal motoneurones to raphe obscurus stimulation. *Br. J. Pharmacol.*, **95**, 437–448.

RYAN, G.P. & BOISSE, N.R. (1984). Benzodiazepine tolerance, physical dependence and withdrawal: electrophysiological study of spinal reflex function. *J. Pharmacol. Exp. Ther.*, **231**, 464–471.

SHEARDOWN, M.J., NIELSEN, E.O., HANSEN, A.J., JACOBSEN, P. & HONORE, T. (1990). 2,3-Dihydroxy-6-nitro-7-sulfamoyl-benzo(F) quinoxaline: A neuroprotectant for cerebral ischemia. *Science*, **247**, 571–574.

SOMMER, B. & SEEBURG, P.H. (1992). Glutamate receptor channels: novel properties and new clones. *Trends Pharmacol. Sci.*, **13**, 291–296.

TARNAWA, I., ENGBERG, I. & FLATMAN, J.A. (1990). GYKI 52466, an inhibitor of spinal reflexes is a potent quisqualate antagonist. In *Amino Acids: Chemistry, Biology and Medicine*. ed. Lubec, G. & Rosenthal, G.A., pp. 538–546. Leiden: Escom.

TARNAWA, I., FARKAS, S., BERZSENYI, P., PATAKI, Á. & ANDRÁSI, F. (1989). Electrophysiological studies with a 2,3-benzodiazepine muscle relaxant: GYKI 52466. *Eur. J. Pharmacol.*, **167**, 193–199.

TURSKI, L., BRESSLER, K., KLOCKGETHER, T. & STEPHENS, D.N. (1990). Differential effects of the excitatory amino acid antagonists, 6-cyano-7-nitroquinoxaline-2,3-dione (CNQX) and 3-((+)-2-carboxypiperazin-4-yl)-propyl-1-phosphonic acid (CPP), on spinal reflex activity in mice. *Neurosci. Lett.*, **113**, 66–71.

TURSKI, L., JACOBSEN, P., HONORE, T. & STEPHENS, D.N. (1992). Relief of experimental spasticity and anxiolytic/anticonvulsant actions of the alpha-amino-3-hydroxy-5-methyl-4-isoxazolepropionate antagonist 2,3-dihydroxy-6-nitro-7-sulfamoyl-benzo(F) quinoxaline. *J. Pharmacol. Exp. Ther.*, **260**, 742–747.

WATKINS, J.F., KROGSGAARD-LARSEN, P. & HONORE, T. (1990). Structure-activity relationships in the development of excitatory amino acid receptor agonists and competitive antagonists. *Trends Pharmacol. Sci.*, **11**, 25–33.

WONG, E.H.F., KEMP, J.A., PRIESTLEY, T., KNIGHT, A.R., WOODRUFF, G.N. & IVERSEN, L.L. (1986). The anticonvulsant MK-801 is a potent N-methyl-D-aspartate antagonist. *Proc. Natl. Acad. Sci. U.S.A.*, **83**, 7104–7108.

YAMAZAKI, J., ONO, H. & NAGAO, T. (1992). Stimulatory and inhibitory effects of serotonergic hallucinogens on spinal mono- and polysynaptic reflex pathways in the rat. *Neuropharmacology*, **31**, 635–642.

ZEMAN, S. & LODGE, D. (1992). Pharmacological characterization of non-NMDA subtypes of glutamate receptor in the neonatal rat hemisected spinal cord *in vitro*. *Br. J. Pharmacol.*, **106**, 367–372.

(Received May 31, 1994
Revised October 21, 1994
Accepted November 22, 1994)

British Journal of Pharmacology (1995) 114, 1206–1210

Acute withdrawal after bremazocine and the interaction between μ- and κ-opioid receptors in isolated gut tissues

[1]P. Valeri, L.A. Morrone, L. Romanelli & M.C. Amico

Institute of Pharmacology and Pharmacognosy, University of Rome 'La Sapienza', P.le A. Moro, 5 00185 Rome, Italy

1 This study was undertaken to investigate whether, after a brief exposure of guinea-pig isolated ileum and rabbit jejunum to bremazocine, a κ-opioid agonist also possessing antagonist activity at μ-opioid receptors, the addition of opioid antagonists produced withdrawal contractures. Our aim was to verify in these tissues the existence of an interaction between the μ- and κ-opioid systems.

2 In guinea-pig ileum preparations previously exposed for 5 min to bremazocine at 5.7×10^{-7} M and 5.7×10^{-8} M, naloxone (5×10^{-7} M) elicited no response whereas in tissues exposed to a lower bremazocine concentration (5.7×10^{-9} M), naloxone (5×10^{-7} M) and the selective κ-opioid antagonist, nor-binaltorphimine (3.4×10^{-8} M) both produced a strong contracture.

3 Bremazocine (5.7×10^{-7} M) administered to guinea-pig isolated ileum, previously exposed for 5 min to morphine (10^{-7} M), induced a withdrawal contracture. In contrast, lower bremazocine concentrations (1.4 and 7.1×10^{-8} M) did not elicit a withdrawal contracture.

4 Naloxone (5×10^{-7} M), added to the bath after a 5 min exposure of guinea-pig ileum to morphine (10^{-7} M), elicited the characteristic withdrawal contracture. Bremazocine ($1.4–7.1 \times 10^{-8}$ M) added 1 min before naloxone (5×10^{-7} M) inhibited the naloxone withdrawal contracture in a dose-related way whereas naloxone 5×10^{-8} M added 1 min before naloxone 5×10^{-7} M, did not affect the withdrawal response.

5 In the rabbit jejunum, bremazocine ($1.4–7.1 \times 10^{-8}$ M) caused a decrease in amplitude in the spontaneous tissue activity. In tissues exposed to these bremazocine concentrations, naloxone (5×10^{-7} M) elicited a marked contracture. A similar contracture occurred when nor-binaltorphimine (3.4×10^{-8} M) was added in place of naloxone. These effects were dose-related to the bremazocine concentration. The specific κ-agonist, U-50,488H (5×10^{-8} M), elicited the same effects as bremazocine.

6 These findings show that stimulation of κ-opioid receptors induces a state of dependence that is not prevented by blocking the μ-opioid system. The observation that low bremazocine concentrations inhibit the morphine-induced withdrawal contractures, indicates an interaction between the μ- and κ-opioid system in guinea-pig isolated ileum, similar to that observed in the whole animal.

Keywords: Bremazocine; κ-opioid agonists; μ-antagonist; κ-induced dependence; withdrawal inhibition; gut isolated tissues

Introduction

Although opiate dependence appears to be mediated primarily by μ-opioid receptors, recent studies have shown that chronic administration of κ-opioid agonists causes physical dependence to develop in monkeys and rats (Young & Khazan, 1985; Gmerek *et al.*, 1987; Jaw *et al.*, 1993). The withdrawal signs developing in animals chronically exposed to κ-agonists differ from those occurring in animals exposed to μ-agonists. μ-Agonist administration does not reverse withdrawal signs in the κ-dependent animal and *vice versa* (Gmerek *et al.*, 1987; Fukagawa *et al.*, 1989; Brent *et al.*, 1993).

Hence, the processes of adaptation leading to dependence appear to be determined by the distinct activation of either μ- or κ-opioid receptors. Accordingly, in our previous study in guinea-pig ileum and rabbit jejunum we showed that the selective κ-opioid antagonist, nor-binaltorphimine, induced a sustained contraction in isolated preparations previously exposed to the selective κ-opioid agonist, U-50,488H. The addition of nor-binaltorphimine, before opioid agonists, also prevented the naloxone-induced contracture in tissues previously exposed to U-50,488H but not in those previously exposed to morphine (Valeri *et al.*, 1990b; 1992; Morrone *et al.*, 1993).

On the other hand, some reports have indicated the existence in the development and expression of opiate dependence of interactions between the various opioid receptor subtypes. In mice, the development of morphine dependence is prevented by the selective blockade of δ-opioid receptors (Abdelhamid *et al.*, 1991; Miyamoto *et al.*, 1993) and is potentiated by the selective blockade of the κ-opioid system (Suzuki *et al.*, 1992). In the guinea-pig ileum made dependent to μ-receptor agonists, κ-agonists suppress the withdrawal contracture to naloxone (Schulz *et al.*, 1985; Chahl, 1990).

When challenged with naloxone or with selective antagonists, gut isolated preparations briefly exposed to opiates display a withdrawal contracture, the expression of acute dependence (Chahl 1986; Valeri *et al.*, 1990a,b; 1992; Morrone *et al.*, 1993).

We undertook this work to investigate whether the brief activation of κ-opioid receptors in isolated gut preparations, by a drug also having antagonistic activity at μ-opioid receptors, would induce dependence, as does the selective κ-agonist, U-50,488H (Morrone *et al.*, 1993). We also studied the effects of κ-receptor activation on the naloxone-induced contracture after exposure of the gut isolated tissues to morphine, to observe the possible interaction between κ- and μ-receptors under experimental conditions unlike those of previous studies (Schulz *et al.*, 1985; Chahl, 1990). For these purposes, we used bremazocine, a drug known to be a potent κ-agonist and a μ-antagonist (Romer *et al.*, 1980; Petrillo *et al.*, 1984; Corbett & Kosterlitz, 1986). The study was carried out in guinea-pig isolated ileum, which contains μ- and κ-opioid receptors and rabbit jejunum, which possesses κ- and δ-opioid receptors (Hutchinson *et al.*, 1975; Valeri *et al.*, 1992). These tissues are currently used to study the homeostatic mechanism involved in the dependence phenomena.

[1] Author for correspondence.

Methods

The experimental procedures were essentially those used previously (Valeri *et al.*, 1990a; 1992). Adult male guinea-pigs weighing 300–350 g and New Zealand White rabbits weighing 2–2.5 kg were killed by a blow on the neck and bled. Three to five segments of guinea-pig ileum or rabbit jejunum, 2–3 cm long, were removed from the same animal, suspended under 1 g tension in a 10 ml tissue organ bath containing Tyrode solution at 37°C and gassed with 95% O_2 and 5% CO_2. The tissues were connected to an isotonic force transducer connected to a pen recorder (Ugo Basile, 7006 and 7050 Italy) and allowed to equilibrate for 30–45 min.

At the start of each experiment a maximum response to acetylcholine (ACh, 10^{-6} M) was obtained in each tissue in order to check its suitability and to express the responses to opioid antagonists as percentages of the ACh maximum. Each experiment was repeated on at least four separate preparations obtained from different animals.

Naloxone- and nor-binaltorphimine-induced withdrawal contractures after bremazocine exposure of guinea-pig ileum and rabbit jejunum

Because previous studies with the κ-agonist, U-50,488H, had shown that the state of dependence of the tissue could not be revealed if the agonist concentration was too high (Morrone *et al.*, 1993), we tested decreasing doses of bremazocine, starting from 6.3×10^{-7} M. The effects of naloxone (5×10^{-7} M) and nor-binaltorphimine (5×10^{-8} M), a selective κ-opioid antagonist, were tested after leaving the tissues for 5 min in contact with bremazocine or U-50,488H. Regardless of whether a contractile response occurred, after the addition to the bath of the opioid antagonists the preparations were washed out. The antagonists were therefore in contact with the tissues for no more than 2–3 min. In experiments with guinea-pig ileum, after washout and a resting period of 20–30 min the same tissue sample was used for further tests. Because the antagonist activity of nor-binaltorphimine faded out very slowly, after contact with this antagonist the preparations were washed out again three or four times during the resting interval. Rabbit jejunum tissues were always discarded after the first exposure to nor-binaltorphimine, because preliminary observations had shown that they no longer yielded reproducible responses. In experiments using naloxone as the antagonist, after washout and a 25–30 min resting period the same tissue preparation continued to provide reproducible responses.

Bremazocine-induced withdrawal contractures after exposure of guinea-pig ileum to morphine

The tissues were exposed to morphine (10^{-7} M) for 5 min before the addition of naloxone (5×10^{-7} M) or bremazocine ($1.4–63 \times 10^{-8}$ M). The same tissue sample was used for several tests, after washout and a resting period of 20–30 min. Between tests with bremazocine control tests were performed with morphine and naloxone.

Bremazocine inhibition of naloxone-induced withdrawal contractures in guinea-pig ileum after morphine exposure

The tissues were exposed to morphine (10^{-7} M) for 5 min before the injection of naloxone (5×10^{-7} M). Bremazocine ($1.4–7.1 \times 10^{-8}$ M) and naloxone 5×10^{-8} M were injected into the bath 1 min before naloxone 5×10^{-7} M.

Drugs

Morphine hydrochloride and naloxone hydrochloride were purchased from SIFAC (Milan, Italy), nor-binaltorphimine dihydrochloride from Research Biochemical Inc. (Natick, MA, U.S.A.), U-50,488H (trans-(±)-3,4-dichloro-N-methyl-N-[2-(1-pyrrolidinyl)-cyclohexyl]-benzenacetamide metane sulphonate salt) from Upjohn Co. (Kalamazoo, MI, U.S.A.) and bremazocine from Sandoz Ltd (Basel, Switzerland).

Results

Withdrawal responses after exposure of guinea-pig ileum to decreasing concentrations of bremazocine

In tissues exposed for 5 min to U-50,488H (5.4×10^{-8} M), naloxone (5×10^{-7} M) elicited a strong contractile response (Figure 1a). When the same preparation was washed out, left to rest for 25 min and exposed to bremazocine at 5.7×10^{-7} M or 5.7×10^{-8} M, naloxone did not elicit a contracture (Figure 1b and c). In the control tests performed after every dose of bremazocine, naloxone injected after exposure to U-50,488H caused in most tissues a contractile response similar in intensity to the first response. In some tissues, however, particularly those exposed to the highest concentrations of bremazocine, naloxone elicited only a very low-intensity contracture or even no response at all (not shown). These preparations were discarded.

When the bremazocine concentration was reduced to 5.7×10^{-9} M, naloxone caused a sustained contractile response (Figure 1d). In tissues treated with this bremazocine concentration, washed out and left to rest for 20–30 min, naloxone elicited reproducible responses.

The ileum preparations exposed for 5 min to the lowest dose of bremazocine contracted also when challenged with the specific κ-opioid antagonist, nor-binaltorphimine (3.4×10^{-8} M); after washout and a 20–30 min interval between tests, a further exposure to the same concentration of bremazocine followed by nor-binaltorphimine continued to elicit responses of the same intensity as before (Figure 2a). These responses appeared to be maximal, because after a 20 min contact with bremazocine the antagonist still determined a contractile response of the same height (81 ± 12.5% of the maximum to ACh in 10 preparations from 5 individual animals) as that obtained after 5 min of contact (Figure 2b).

Withdrawal responses after exposure of rabbit jejunum to bremazocine

Addition of bremazocine (5.5×10^{-8} M) to rabbit jejunum caused a decrease in the amplitude of the spontaneous tissue

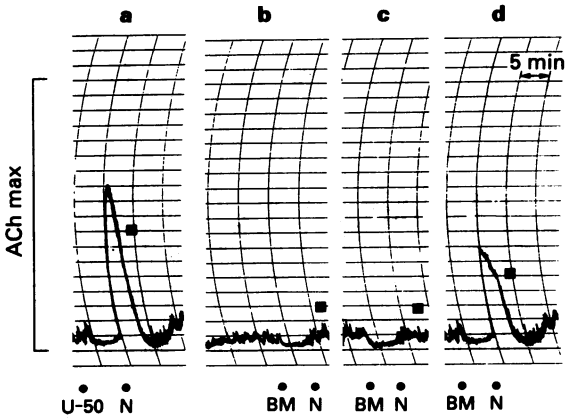

Figure 1 Guinea-pig ileum contractile responses to naloxone (N) after a 5 min exposure of the tissue to U-50,488H (U-50) or bremazocine (BM). A contractile response is elicited by N (5×10^{-7} M) after exposure to U-50 (5.4×10^{-8} M) (a). After exposure to BM concentrations of 5.7×10^{-7} (b) and 5.7×10^{-8} M. (c), N elicited no response. An N-induced contracture was obtained after exposure to BM 5.7×10^{-9} M (d). Tracings (a) and (b) were recorded from the same preparation, tracings (c) and (d) from another. Interval between tests: 25–30 min. ACh max: acetylcholine (10^{-6} M); (■) washout.

activity, sometimes accompanied by a relaxation of the muscle, as did U-50,488H (5×10^{-8} M). After a 5 min contact with bremazocine or with U-50,488H (same concentrations) the addition of naloxone (5×10^{-7} M) caused a marked contracture of the tissue (Figure 3a and b). After washout and a 25–30 min interval, and a further 5 min exposure to bremazocine, naloxone (5×10^{-7} M) caused responses of almost identical intensity in many preparations, so that the same tissue could be used for several tests. The decreases in spontaneous activity and in the height of the contractile responses to naloxone were dose-related to the bremazocine concentrations studied ($1.4–7.1 \times 10^{-8}$ M).

After exposure of the tissue to bremazocine or U-50,488H (same concentrations as above), nor-binaltorphimine (3.4×10^{-8} M) added in place of naloxone caused a similar contractile response (Figure 3c and d). The tissues completely lost their responsiveness to the κ-opioid agonist and antagonist after contact with nor-binaltorphimine, but retained their responsiveness after contact with naloxone. Only few preparations recovered their responsiveness after contact with norbinaltorphimine and did only after a prolonged interval, with several washouts (not shown).

Bremazocine-induced withdrawal responses in guinea-pig ileum after exposure to morphine

In guinea-pig ileum exposed to morphine (10^{-7} M) for 5 min, naloxone (5×10^{-7} M) induced a contractile response (Figure 4a). In experiments designed to study the μ-antagonist activity of bremazocine in the guinea-pig isolated ileum, after a 5 min exposure of the tissue to morphine (10^{-7} M) bremazocine was added to the bath in place of naloxone. Whereas bremazocine concentrations of 1.4×10^{-8} M and 7.1×10^{-8} M failed to contract the morphine-exposed tissues (Figure 4a and b) a higher bremazocine concentration, 5.7×10^{-7} M, close to that of naloxone, yielded a strong contracture as intense as that elicited by naloxone (Figure 4c).

After every dose of bremazocine and before a further bremazocine test, the suitability of the preparation was checked by challenging the tissue with morphine and naloxone. These control tests showed that about 50% of the isolated preparations lost their ability to contract to naloxone, sometimes even after the first exposure to bremazocine.

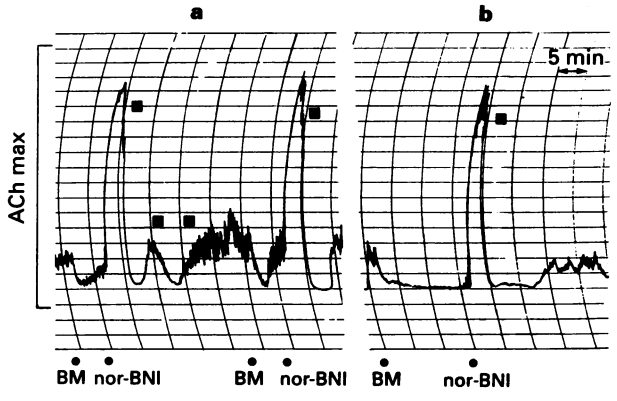

Figure 2 Reproducible contractile responses of guinea-pig ileum to nor-binaltorphimine (nor-BNI) after 5 and 20 min exposure of the tissue to bremazocine (BM). After a 5 min exposure to BM (5.7×10^{-9} M), nor-BNI (3.4×10^{-8} M) elicited a contractile response; after a 25–30 min interval, including 3–4 washouts, and a further 5 min exposure to BM (5.7×10^{-9} M), nor-BNI (3.4×10^{-8} M) induced a contracture of the same amplitude as the first (a). After a 20 min exposure to BM (5.7×10^{-9} M) nor-BNI (3.4×10^{-8} M) still elicited a contracture of the same amplitude (b). All tracings shown in figure were obtained from the same tissue preparation, with a 25–30 min interval and 3–4 washouts between tests. ACh max: acetylcholine (10^{-6} M); (■) washout.

Antagonist activity of bremazocine on naloxone-induced contractures after morphine

As described above, naloxone (5×10^{-7} M) induced a contracture in guinea-pig ileum that had been exposed to morphine (10^{-7} M) for 5 min (Figure 5a). The addition, 1 min before the antagonist, of bremazocine 1.4×10^{-8} M reduced the naloxone-induced contracture (Figure 5b); this response was completely inhibited by bremazocine at 7.1×10^{-8} M (Figure 5c), i.e., a concentration 10 fold lower than that causing a contractile response in the morphine-exposed tissue.

To verify that this inhibitory effect was not due to antagonist activity at μ-receptors, a low dose of naloxone (5×10^{-8} M) was administered 1 min before the naloxone concentration known to elicit a withdrawal response (5×10^{-7} M). In most preparations, when this low concentration of naloxone was administered 4 or 5 min after morphine, it did not elicit contractures, as previously observed (Valeri *et al.*, 1990). Administration of naloxone (5×10^{-8} M) 1 min before naloxone (5×10^{-7} M) left the withdrawal response to the higher dose unchanged (Figure 5d).

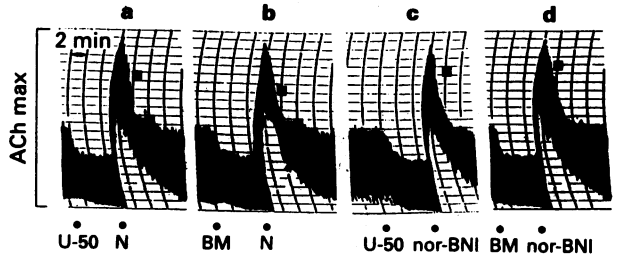

Figure 3 Typical tracings showing the effect of U-50,488H (U-50) and bremazocine (BM) on the rabbit jejunum spontaneous activity and the contractile response of the tissue to naloxone (N) and nor-binaltorphimine (nor-BNI) after a 5 min exposure of the tissue to U-50 or BM. Both U-50 (5.4×10^{-8} M; a and c) and BM (5.5×10^{-8} M; b and d) caused a decrease in the spontaneous tissue activity. N (5×10^{-7} M) elicited a strong contracture after a 5 min exposure of the tissue to U-50 (a) or BM (b). Nor-BNI (3.4×10^{-8} M) also elicited a contractile response, after a 5 min exposure to U-50 (c) or BM (d). Tracings (a), (b) and (c) were recorded from the same tissue preparation with a 25–30 min interval between tests; tracing (d) was from another preparation. ACh max: acetylcholine (10^{-6} M); (■) washout.

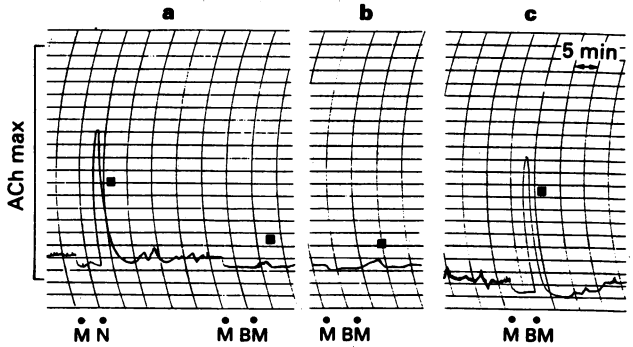

Figure 4 Guinea-pig ileum contractile responses to naloxone (N) and bremazocine (BM) after exposure of the tissue to morphine (M). N (5×10^{-7} M) elicited a contractile response after a 5 min exposure to M (10^{-7} M) (a). Neither BM 1.4×10^{-8} (a) nor 7.1×10^{-8} M (b) elicited a contracture after exposure to M 10^{-7} M. In contrast, BM 5.7×10^{-7} M elicited a contractile response, after the usual 5 min exposure to M 10^{-7} M. ACh max: acetylcholine (10^{-6} M); (■) washout.

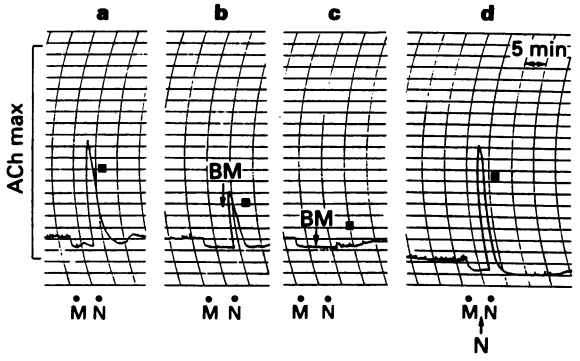

Figure 5 Bremazocine (BM) inhibition of guinea-pig ileum contractile response to naloxone (N) after exposure of the tissue to morphine (M). N (5×10^{-7} M) elicited the characteristic contractile response after a 5 min exposure to M (10^{-7} M) (a). At a concentration of 1.4×10^{-8} M BM added 1 min before N (5×10^{-7} M) reduced (b) and at a concentration of 7.1×10^{-8} M completely inhibited (c) the contractile response to N. N 5×10^{-8} M, added 1 min before N 5×10^{-7} M, failed to affect the contractile response to the higher dose of N. Tracings (a) and (b) were recorded from the same tissue preparation, tracings (c) and (d) from two other preparations. ACh max: acetylcholine (10^{-6} M); (■) washout.

Discussion

This study shows that after a brief exposure to bremazocine, isolated preparations of guinea-pig ileum and rabbit jejunum respond to the addition of both the non-selective opioid antagonist, naloxone and the selective κ-opioid antagonist, nor-binaltorphimine, with a withdrawal contracture resembling that induced by exposure to U-50,488H. These observations confirm that acute activation of κ-opioid receptors induces homeostatic changes that lead to the development of dependence (Valeri *et al.*, 1992; Morrone *et al.*, 1993). Our *in vitro* results agree with those obtained in the whole animal. *In vivo* experiments, however, reveal a difference between withdrawal behaviours induced by κ-opioid agonists and those induced by morphine (Gmerek *et al.*, 1987; Fukagawa *et al.*, 1989; Brent *et al.*, 1993). This distinction cannot be revealed in guinea-pig isolated ileum and rabbit jejunum, because in these tissues the acute activation of μ-, κ- or δ-opioid receptors induces the same withdrawal symptom, i.e., the contractile response to opioid antagonists (Valeri *et al.*, 1992; Morrone *et al.*, 1993; Brent *et al.*, 1993). In the myenteric plexus, the development of dependence to μ-, κ- and δ-opioid receptors is due to multistep homeostatic changes that converge to depress the cholinergic neurone and the expression of dependence is revealed mainly by excitation of this neurone. In the central nervous system, opioid-induced homeostatic changes of action and reaction involve many integrated circuits working with characteristic neurotransmitters and neuromodulators, thus leading to a variety of withdrawal signs. The differences between withdrawal responses in gut isolated preparations and in the whole animal therefore reflect the different complexity of the neuronal circuits involved, but the two models probably share the same basic mechanisms.

Our results also suggest that μ-opioid receptor blockade does not prevent the development of dependence to κ-antagonists, since κ-opioid antagonists induce a withdrawal contracture in tissues exposed to bremazocine despite the intrinsic μ-antagonist activity of the drug. The failure of naloxone to evoke contractures in tissues exposed to bremazocine concentrations higher than 5.7×10^{-9} M depends not on the concentration-related increase of μ-antagonist activity but on the inability of naloxone to displace these high doses of bremazocine, as previously observed with the κ-antagonist U-50,488H (Morrone *et al.*, 1993). This conclusion is confirmed by the observation that the addition of cyprodime (10^{-6} M), a recently available selective μ-opioid antagonist, 1 min before exposure to bremazocine (5.7×10^{-9} M) does not reduce the height of the contracture to nor-binaltorphimine (unpublished observation by the authors). The findings of this and previous (Morrone *et al.*, 1993) studies thus indicate that in the guinea-pig ileum, blocking μ-opioid receptors does not prevent the development of dependence to κ-opioid agonists and *vice versa*. In rabbit jejunum, which appears to have few μ-opioid receptors (Valeri *et al.*, 1992), this conclusion cannot be drawn. In addition, these two isolated preparations differ in their interaction with opioid agonists and antagonists. In particular, we observed that nor-binaltorphimine is harder to wash out from rabbit jejunum than from guinea-pig ileum and naloxone displaces bremazocine more effectively in the jejunum than in the ileum.

Even though the blockade of μ-receptors does not suppress the development of dependence to κ-opioid receptors, this finding does not exclude an interaction between μ- and κ-receptors, as shown by the dose-dependent inhibition of bremazocine on naloxone-induced contracture in the guinea-pig ileum, previously exposed to morphine. This inhibition presumably arises from the activation of κ-opioid receptors rather than from the antagonist activity of bremazocine at μ-receptors, since the naloxone-induced contracture is not affected by the addition, 1 min before the higher dose, of a naloxone concentration ten fold lower than that producing a contracture (see Figure 5). This lower naloxone concentration (5×10^{-8} M) is in the range of the bremazocine concentrations inhibiting the naloxone-induced contracture (1.4–7.1×10^{-8} M) and naloxone has an antagonist potency at μ-receptors equal to that of bremazocine (see Figure 4). The observed inhibition of the naloxone-induced withdrawal response after morphine exposure, elicited by the activation of κ-opioid receptors agrees with previous results obtained *in vitro*, although under different experimental conditions (Schultz *et al.*, 1985; Chahl, 1990), and in the whole animal (Green & Lee, 1988). The finding that a κ-opioid system blockade may aggravate naloxone-precipitated symptoms in morphine-dependent mice and rats (Suzuki *et al.*, 1992) provides further evidence of an interaction between μ- and κ-receptors. Under our experimental conditions it was not possible to verify whether μ-receptors blockade could increase the κ-induced withdrawal response, because we used agonist and antagonist concentrations that yielded a withdrawal contractile response that was already maximal. The biochemical mechanisms that underlie and the physiological meaning of this interaction between μ- and κ-receptors need more detailed studies.

The observation that low concentrations of bremazocine determine a state of dependence in isolated preparations supports studies reporting the high potency and binding affinity of this drug to κ-opioid receptors (Romer *et al.*, 1980; Corbett & Kosterliz, 1986; Dissanayake *et al.*, 1990). As with morphine and U-50,488H (Valeri *et al.*, 1990a; Morrone *et al.*, 1993) the use of low bremazocine concentrations makes it possible to obtain reproducible responses. The reported inability to reveal the development of dependence or to obtain reproducible responses from isolated preparations after exposure to opioid agonists with high receptor affinity (Chahl, 1986; 1990; Brent *et al.*, 1993) probably depends on the fact that the antagonists tested cannot adequately displace the high agonist concentrations used. Reproducible responses are very useful not only for practical but also for theoretical reasons. The loss of reproducibility implies the occurrence of biochemical events that have changed the responsiveness of the tissue. Detailed examination of these changes may help to explain some of the mechanisms involved in development or expression of dependence. Thus, the observation that several guinea-pig ileum preparations previously tested with morphine and bremazocine did not give reproducible responses to naloxone when further tested with morphine and naloxone, suggested that bremazocine

inhibited the expression of morphine dependence, as we subsequently showed.

Bremazocine precipitates an abstinence syndrome in morphine-dependent rats and mice (Vonvoigtlander *et al.*, 1983; Petrillo *et al.*, 1984). As our results show, this antagonist activity at μ-opioid receptors can be easily revealed even *in vitro*, by the contracture that bremazocine elicits in tissues briefly exposed to morphine, without recourse to the complex experimental procedures previously used (Corbett & Kosterliz, 1985).

Bremazocine has been shown to act as a partial agonist in some electrically-stimulated isolated tissues (Miller *et al.*, 1986; Hunter *et al.*, 1990). Yet, guinea-pig ileum has been shown to have a high κ-receptor reserve (Miller *et al.*, 1986) and the features of rabbit jejunum responses to κ-agonists and antagonists suggest that also this tissue has a high number of spare κ-receptors. It is known that in tissues with a high receptor reserve, partial agonists behave like full agonists. In addition, it must be remembered that in field-stimulated tissues the activity of opioids may depend also on the stimulus intensity (Smith, 1984). Hence, some observations made using electric stimulation may not apply to unstimulated models. Thus, under our experimental procedure, i.e., in unstimulated tissues which possess a high κ-receptor reserve, it was not possible to reveal the κ-antagonist activity of the drug.

In conclusion, in this study we have shown that, as we found for the selective κ-agonist U-50,488H (Morrone *et al.*, 1993), a withdrawal contractile response can be obtained in guinea-pig ileum and rabbit jejunum briefly exposed to bremazocine, despite the intrinsic μ-antagonist activity of bremazocine. These findings confirm that the acute activation of κ-opioid receptors induces biochemical changes leading to dependence. In addition, they indicate that a μ-opioid system blockade does not prevent the development of the dependence induced by κ-opioid agonists. Yet, our observation that the bremazocine-induced activation of κ-opioid receptors prevents the naloxone-precipitated contracture in tissues briefly exposed to morphine shows that interactions between μ- and κ-opioid systems operate in the guinea-pig ileum, as reported in whole animal. The possibility of studying the interactions between the opioid systems, in isolated preparations, gives us a simple tool for characterizing the complex homeostatic biochemical events leading to the development and expression of dependence.

References

ABDELHAMID, E.E., SULTANA, M., PORTOGHESE, P.S. & TAKEMORI, A.E. (1991). Selective blockage of delta receptors prevents the development of morphine tolerance and dependence in mice. *J. Pharmacol. Exp. Ther.*, **258**, 299–303.

BRENT, P.J., CHAHL, L.A., CANTARELLA, P.A. & KAVANAGH, C. (1993). The κ-opioid receptor agonist U50,488H induces acute physical dependence in guinea-pigs. *Eur. J. Pharmacol.*, **241**, 149–156.

CHAHL, L.A. (1986). Withdrawal responses of guinea-pig isolated ileum following brief exposure to opiates and opioid peptides. *Naunyn-Schmied. Arch. Pharmacol.*, **333**, 387–392.

CHAHL, L.A. (1990). Effects of putative neurotransmitters and related drugs on withdrawal contractures of guinea-pig isolated ileum following brief contact with Met5 enkephalin. *Br. J. Pharmacol.*, **101**, 908–912.

CORBETT, A.D. & KOSTERLIZ, H.W. (1986). Bremazocine is an agonist at κ-opioid receptors and an antagonist at μ-opioid receptors in guinea-pig myenteric plexus. *Br. J. Pharmacol.*, **89**, 245–249.

DISSANAYAKE, V.U.K., HUNTER, J.C., HILL, R.G. & HUGHES, J. (1990). Characterization of κ-opioid receptors in guinea pig ileum. *Eur. J. Pharmacol.*, **182**, 73–82.

FUKAGAWA, Y., KATZ, J.L. & SUZUKI, T. (1989). Effects of a selective κ-opioid agonist, U-50,488H, on morphine dependence in rats. *Eur. J. Pharmacol.*, **170**, 47–51.

GMEREK, D.E., DYKSTRA, L.A. & WOOD, J.H. (1987). Kappa opioids in rhesus monkeys. III. Dependence associated with chronic administration. *J. Pharmacol. Exp. Ther.*, **242**, 428–436.

GREEN, P.G. & LEE, N.M. (1988). Dynorphin A (1–13) attenuates withdrawal in morphine-dependent rats: effect of route of administration. *Eur. J. Pharmacol.*, **145**, 267–272.

HUNTER, J.C., LEIGHTON, G.E., MEECHAM, K.G., BOYLE, S.J., HORWELL, D.C., REES, D.C. & HUGHES, J. (1990). CI-977, a novel and selective agonist for the κ-opioid receptor. *Br. J. Pharmacol.*, **101**, 183–189.

HUTCHINSON, M., KOSTERLIZ, H.W., LESLIE, F.M. & WATERFIELD, A.A. (1975). Assessment in the guinea-pig ileum and mouse vas deferens of benzomorphans which have strong antinociceptive activity but do not substitute for morphine in the dependent monkey. *Br. J. Pharmacol.*, **55**, 541–546.

JAW, S.P., MAKIMURA, M., HOSKINS, B. & HO, I.K. (1993). Effects of nor-binaltorphimine on butorphanol dependence. *Eur. J. Pharmacol.*, **239**, 133–140.

MILLER, L., SHAW, J.S. & WHITING, E.M. (1986). The contribution of intrinsic activity to the action of opioids *in vitro*. *Br. J. Pharmacol.*, **87**, 595–601.

MIYAMOTO, Y., PORTOGHESE, P.S. & TAKEMORI, E. (1993). Involvement of $Delta_2$ opioid receptors in the development of morphine dependence in mice. *J. Pharmacol. Exp. Ther.*, **264**, 1141–1145.

MORRONE, L.A., ROMANELLI, L., AMICO, M.C. & VALERI, P. (1993). Withdrawal contractures of guinea-pig isolated ileum after activation of κ-opioid receptors. *Br. J. Pharmacol.*, **106**, 48–52.

PETRILLO, P., GAMBINO, M.C. & TAVIANI, A. (1984). Bremazocine induces antinociception, but prevents opioid-induced constipation and catatonia in rats and precipitates withdrawal in morphine-dependent rats. *Life Sci.*, **35**, 917–927.

ROMER, D., BUSCHER, H., HILL, R.C., MAURER, R., PETCHER, T.J., WELLE, H.B.A., BAKEL, H.C.C.K. & AKKERMAN, A.M. (1980). Bremazocine: a potent, long-lasting opiate kappa-agonist. *Life Sci.*, **27**, 971–978.

SCHULZ, R., SEIDEL, E. & HERZ, A. (1985). Opioid dependence in the guinea-pig myenteric plexus is controlled by non-tolerant and tolerant opioid receptors. *Eur. J. Pharmacol.*, **110**, 335–341.

SMITH, C.F.C. (1984). Morphine, but no diacetyl morphine (heroin) possesses opiate antagonist activity in the mouse vas deferens. *Neuropeptides*, **5**, 173–176.

SUZUKI, T., NARITA, M., TAKAHASHI, Y., MISAWA, M. & NAGASE, H. (1992). Effects of nor-binaltorphimine on the development of analgesic tolerance to and physical dependence on morphine. *Eur. J. Pharmacol.*, **213**, 91–97.

VALERI, P., MARTINELLI, B., MORRONE, L.A. & SEVERINI, C. (1990a). Reproducible withdrawal contractions of isolated guinea-pig ileum after brief morphine exposure. Effect of clonidine and nifedipine. *J. Pharm. Pharmacol.*, **42**, 115–120.

VALERI, P., MORRONE, L.A. & ROMANELLI, L. (1990b). Acute dependence to κ-opioid agonist, U-50,488H, in guinea-pig ileum. *Pharmacol. Res.*, **22**, Suppl. 2, 448.

VALERI, P., MORRONE, L.A. & ROMANELLI, L. (1992). Manifestations of acute opiate withdrawal contracture in rabbit jejunum after μ-, κ- and δ-opioid receptor agonist exposure. *Br. J. Pharmacol.*, **106**, 39–44.

VONVOIGTLANDER, P.F., LAHTI, R.A. & LUDENS, J.H. (1983). U-50,488H: a selective and structurally novel non-mu (kappa) opioid agonist. *J. Pharmacol. Exp. Ther.*, **224**, 7–12.

YUOUNG, G.A. & KHAZAN, N. (1985). Comparison of abstinence syndromes following chronic administration of mu and kappa opioid agonists in the rat. *Pharmacol. Biochem. Behav.*, **23**, 457–460.

(Received April 5, 1994
Revised September 15, 1994
Accepted November 11, 1994)

British Journal of Pharmacology (1995) 114, 1211-1221

An electrophysiological investigation of the properties of a murine recombinant 5-HT_3 receptor stably expressed in HEK 293 cells

Catherine H. Gill, [1]John A. Peters & Jeremy J. Lambert

Neuroscience Research Group, Department of Pharmacology and Clinical Pharmacology, Ninewells Hospital and Medical School, University of Dundee, Dundee, DD1 9SY

1 The pharmacological and biophysical properties of a recombinant 5-HT_3 receptor have been studied by use of patch-clamp techniques applied to HEK 293 cells stably transfected with the murine 5-HT_3 R-A cDNA.

2 At a holding potential of −60 mV, 77% of cells investigated responded to ionophoretically applied 5-HT with an inward current. Such currents were unaffected by methysergide (1 μM), or ketanserin (1 μM), but were antagonized in a concentration-dependent and reversible manner by the selective 5-HT_3 receptor antagonist, ondansetron (IC_{50} = 440 pM) and the non-selective antagonists (+)-tubocurarine (IC_{50} = 1.8 nM) and metoclopramide (IC_{50} 50 nM).

3 The 5-HT-induced current reversed in sign ($E_{5\text{-}HT}$) at approximately −2 mV and exhibited inward rectification. The influence of extra- and intracellular ion substitutions upon $E_{5\text{-}HT}$ indicates the 5-HT-evoked current to be mainly mediated by a mixed monovalent cation conductance.

4 Calcium and magnesium (0.1-10 nM) produced a concentration-dependent, voltage-independent, inhibition of the 5-HT-induced response. Zinc (0.3-300 μM) exerted a biphasic effect with low concentrations enhancing, and high concentrations depressing, the 5-HT-evoked current.

5 Fluctuation analysis of inward currents evoked by a low (1 μM) concentration of 5-HT suggests the current to be mediated by the opening of channels with a conductance of 420 fS.

6 The pharmacological and biophysical properties of the 5-HT_3 R-A are similar to those previously described for 5-HT_3 receptors native to murine neuroblastoma cell lines, with the exception that the function of the recombinant receptor was enhanced by low concentrations of zinc. This observation suggests that the properties of the native receptor are not completely represented by the 5-HT_3 R-A subunit alone.

Keywords: 5-HT_3 receptor; recombinant 5-HT_3 receptor; 5-HT_3 receptor antagonists; 5-HT_3 single channels; 5-HT_3 receptor-evoked currents

Introduction

Electrophysiological studies have firmly established that, in contrast to other 5-HT receptors which mediate their effects through G-proteins, the 5-HT_3 subtype is a member of a ligand-gated ion channel family that includes nicotinic, $GABA_A$ and glycine receptors (Derkach *et al.*, 1989; Lambert *et al.*, 1989; Boess & Martin, 1994). Recently, a cDNA encoding a 5-HT_3 receptor subunit, termed 5-HT_3 R-A, was isolated from the murine hybridoma cell line NCB 20 (Maricq *et al.*, 1991). The predicted 5-HT_3 R-A protein shares many structural elements of the nicotinic acetylcholine receptor (Maricq *et al.*, 1991). Furthermore, the mouse 5-HT_3 R-A gene intron exon organisation is very similar to that of the neuronal α_7 nicotinic subunit of the chick (Uetz *et al.*, 1994). Expression of the 5-HT_3 R-A in *Xenopus laevis* oocytes results in the formation of functional, presumably homo-oligomeric, receptors which exhibit many of the physiological and pharmacological properties (Maricq *et al.*, 1991; Downie *et al.*, 1994) determined for the 5-HT_3 receptor native to NCB 20 cells (Lambert *et al.*, 1989).

The pharmacological properties of the 5-HT_3 receptor are species-dependent although, in contrast to other ligand-gated ion channels, there is no compelling evidence of pharmacological diversity within a species (Peters *et al.*, 1992). However, differences in biophysical properties have been noted. In particular, the 5-HT_3 receptor single channel conductance may vary within a species (Yang *et al.*, 1992; Hussy & Jones, 1993) which may suggest the presence of additional subunits. In common with other ligand-gated channels, the 5-HT_3 receptor is predicted to exist as a pentamer (Boess & Martin, 1994). Heterogeneity of these ligand-gated ion channels occurs through distinct subunit combinations, RNA editing and alternative splicing of receptor subunits (Wafford *et al.*, 1991; Sieghart, 1992; Seeburg, 1993). In mouse neuroblastoma cell lines and mouse brain, two forms of the 5-HT_3 R-A occur through the alternative use of two splice acceptor signals (Maricq *et al.*, 1991; Hope *et al.*, 1993; Uetz *et al.*, 1994) which delete six consecutive amino acid residues from the putative large intracellular loop between transmembrane regions M3 and M4. A comparison of the pharmacological profile of the homo-oligomeric receptors assembled in *Xenopus* oocytes from either 5-HT_3 R-A, or 5-HT_3 R-A_s subunits (the subscript 's' denotes the short form with the six amino acid deletion) revealed the maximal response elicited by the agonist 2-methyl-5-HT to be greatly reduced for the latter (Downie *et al.*, 1994). However, in all other aspects of pharmacology examined, the receptors were similar, both to each other, and to 5-HT_3 receptors native to murine neuronal cell lines.

Analysis of the biophysical properties of the 5-HT_3 R-A expressed in *Xenopus* oocytes has yielded variable results. In two studies, current responses to 5-HT were suppressed, in a voltage-dependent manner, by the presence of extracellular calcium and magnesium at physiological concentrations (Maricq *et al.*, 1991; Eiselé *et al.*, 1993). Such effects were not observed in a third study (Yakel *et al.*, 1993). Furthermore,

[1] Author for correspondence.

although 5-HT$_3$ receptor-mediated currents recorded from murine cell lines (Peters *et al.*, 1988; Yang, 1990) are blocked by calcium and magnesium, this effect appears to be voltage-independent. It is unclear as to whether the oocyte expression system itself has any bearing on such differences. One potential limitation regarding the use of oocytes in the characterization of the 5-HT$_3$ R-A is the extremely low single channel conductance (0.3–0.6 pS) of the 5-HT$_3$ receptor native to cell lines that express this subunit (Lambert *et al.*, 1989; Yang, 1990; van Hooft *et al.*, 1994). If the recombinant homo-oligomer were to possess a comparable conductance, fluctuation analysis of whole-cell currents in oocytes would be problematic and the direct detection of current responses representing the simultaneous activation of 5-HT$_3$ R-A populations on excised outside-out membrane patches would require levels of expression far higher than those reported in the literature (Maricq *et al.*, 1991; Hope *et al.*, 1993; Yakel *et al.*, 1993; Downie *et al.*, 1994). Hence, in the present study, we have utilized the whole-cell recording mode of the patch-clamp technique to investigate the properties of the 5-HT$_3$ R-A (Maricq *et al.*, 1991) stably transfected into HEK 293 cells, which are more amenable to such studies. We report the pharmacological and biophysical properties of the 5-HT$_3$ R-A to be similar to those of the receptor native to murine neuronal cell lines, with the exception that 5-HT-mediated currents are enhanced by low concentrations of zinc (*cf.* Lovinger, 1991). Hence the 5-HT$_3$ R-A may not be completely representative of the 5-HT$_3$ receptor native to neuronal cell lines. A preliminary account of a part of this work has appeared in abstract form (Gill *et al.*, 1993).

Methods

Culture of HEK 293 cells

HEK 293 cells were stably transfected in the laboratory of Dr D. Julius (University of California, San Francisco) with the 5-HT$_3$ R-A cDNA contained within the expression vector pLNCX. Stable transformants were selected by the use of media supplemented with geneticin to which the expression vector confers resistance. Cells were grown to confluency in Dulbecco's Modified Eagle Medium (DMEM), supplemented with foetal calf serum (10% v/v), penicillin (1×10^3 iu ml^{-1}), streptomycin (100 μg ml^{-1}) and geneticin (200 μg ml^{-1}) in 25 cm^2 tissue culture flasks. The cells were harvested enzymatically with trypsin (0.5 mg ml^{-1}) and EDTA (0.2 mg ml^{-1}). Enzyme action was terminated by the addition of 10 ml of growth medium and the cells were dissociated further by gentle trituration, prior to centrifugation at 100 *g* for 2 min. For electrophysiological recordings, the cells were resuspended in growth medium and replated onto 35 mm Petri dishes at a density of 1×10^4 cells per dish. The culture medium was refreshed every three days and the cells were maintained at 37°C in an atmosphere of 90% air, 10% CO_2 at 100% relative humidity. Experiments were conducted 2 to 7 days after replating upon cells of passage numbers 5 to 35 inclusive.

Electrical recordings

Whole-cell recordings of agonist-evoked membrane currents were performed at room temperature (18–22°C) under voltage-clamp conditions with either a List Electronics L/M EPC-7 converter headstage and amplifier, or an Axopatch 1D amplifier, using standard patch-clamp techniques (Hamill *et al.*, 1981). Agonist-evoked currents were recorded at a holding potential of −60 mV, unless specified otherwise. Currents were low pass-filtered at a cut-off frequency of 3 KHz (two pole Bessel characteristic) and recorded onto video tape using a PCM-2 VCR adaptor (Medical Systems Corporation, Greenvale, NY, U.S.A.), or onto magnetic tape using a Racal Store 4DS F.M. tape recorder. The cells were continually superfused at a rate of 3–5 ml min^{-1} with an extracellular solution (E1) comprising (in mM): NaCl 140, KCl 2.8, $CaCl_2$ 1.0, $MgCl_2$ 2.0 and HEPES 10. Patch electrodes were fabricated from glass capillary tubing (Corning type 7052, Garner Glass Company, Claremont, CA, U.S.A.) and filled with a solution (I1) containing (in mM): CsCl 140, $MgCl_2$ 2.0, $CaCl_2$ 0.1, EGTA 1.1 and HEPES 10 (free $[Ca^{2+}] = 10^{-8}$ M at pH 7.2). Caesium was used as the predominant intracellular cation to reduce membrane potassium conductances. With the above solutions, electrode resistances were typically within the range 2 to 5 MΩ.

In experiments designed to investigate the ionic dependence of the agonist-evoked current, modified intracellular and extracellular salines were employed. To evaluate the potential contribution of chloride ions to the 5-HT-evoked response, NaCl in the extracellular medium was completely replaced by 140 mM sodium isethionate. The influence of sodium ions was assessed by reducing the extracellular concentration of this ion to either 75 or 20 mM by partial replacement with N-methyl-D-glucamine (NMDG). Additionally, the concentrations of $MgCl_2$ and $CaCl_2$ within the extracellular medium were reduced from 2 mM and 1 mM, respectively, to 0.1 mM each and KCl was totally replaced by NaCl. This simplified solution (E2) was also used in experiments where the internal solution was modified. In such experiments, the concentration of caesium ions was reduced to 20 mM by the partial replacement of CsCl with tetraethylammonium chloride (TEA; solution I2). With the exception of NMDG-containing extracellular solutions which were titrated to pH 7.2 with HCl, the pH of all external and internal solutions was adjusted to 7.2 with NaOH. Sodium ions so introduced were included in the calculation of external and internal sodium ion concentrations. During ion substitution experiments, changes in reference electrode potential due to the perfusion of modified external salines were minimized by using a salt bridge containing 3 M KCl in 4% (w/v) agar which coupled the recording chamber to an Ag/AgCl electrode. Liquid junction potentials at the tip of the patch pipette prior to gigaseal formation were estimated as previously described (Peters *et al.*, 1989) and the holding potential was corrected appropriately.

In the majority of experiments, 5-HT was applied focally to the cells by ionophoresis with an Intra 767 electrometer (World Precision Instruments). Ionophoretic electrodes had resistances > 30 MΩ when filled with a solution containing 20 mM 5-HT in twice distilled deionized water. Ejection currents of 30–120 nA and of 40–100 ms duration were superimposed upon a constant retaining current of approximately 4.0 nA. All antagonist compounds were applied by their inclusion within the superfusate. In experiments where the conductance of the 5-HT$_3$ R-A was assessed by fluctuation analysis of whole-cell currents, 5-HT (1 μM) was applied to cells by diffusion from a coarse-tipped (approximately 10 μm diameter) micropipette which was positioned to achieve a relatively slowly developing response to 5-HT. All quantitative data are expressed as the arithmetic mean ± the standard error of the mean (s.e. mean).

Fluctuation analysis of 5-HT-induced whole-cell currents

Random fluctuations in 5-HT-induced whole-cell currents were used to estimate the single channel conductance of the 5-HT$_3$ R-A. Signals were stored on magnetic tape for subsequent off-line analysis using the programme SPAN V3.0 (Dempster, 1993). For the analysis of whole-cell current noise, current fluctuations were a.c. coupled (high-pass filter, 1.0 Hz cut-off, Butterworth characteristic; Fylde Electronics, Preston, U.K.) and amplified. Anti-aliasing filtration of the current fluctuation signal was performed with a Fylde Electronics 8-pole Butterworth low-pass filter set to half the sampling frequency. Continuous records of mean d.c. current and current fluctuations in the presence and absence of 5-HT were replayed from video tape and digitized at a rate of

1 KHz using a Data Translation DT2801A laboratory interface and stored on a personal computer (Dell 'pentium' Dimension XPSP60). The digitized record was composed of blocks with a duration of $1/f_{res}$s, where f_{res} (Hz) was the desired resolution of the recording (usually 1 Hz). Blocks of data were edited visually and those containing obvious artifacts were excluded from further analysis. The variance method (Cull-Candy *et al.*, 1988; Lambert *et al.*, 1989; Dempster, 1993) was used to estimate the current, i, flowing through a single channel using the equation (Dempster, 1993):

$$\sigma^2 = \frac{1}{N-1} \sum_{j=1}^{N} (I_j - I_m)^2 \quad (1)$$

where σ^2 is the variance; I_m the mean current; I_j current sample j and N is the number A/D samples in the block. The relationship between σ^2 and I_m is parabolic rising from zero to a maximum (at an open channel probability, P, of 0.5) and falling to zero again as P is varied from 0 to 1, i.e.:

$$\sigma^2 = iI_m - \frac{I_m^2}{n} \quad (2)$$

where n is the number of channels within the cell. When P is small, (< 0.1) equation (2) simplifies to the linear function:

$$\sigma^2 = iI_m \quad (3)$$

σ^2 *vs.* I_m plots were obtained from blocks recorded during the development and desensitization of the inward current response to microperfused 5-HT (1 μM). Single channel current was estimated from parabolic or linear functions fitted to such plots by least-squares regression analysis. Background variance, attributable to sources other than 5-HT-activated

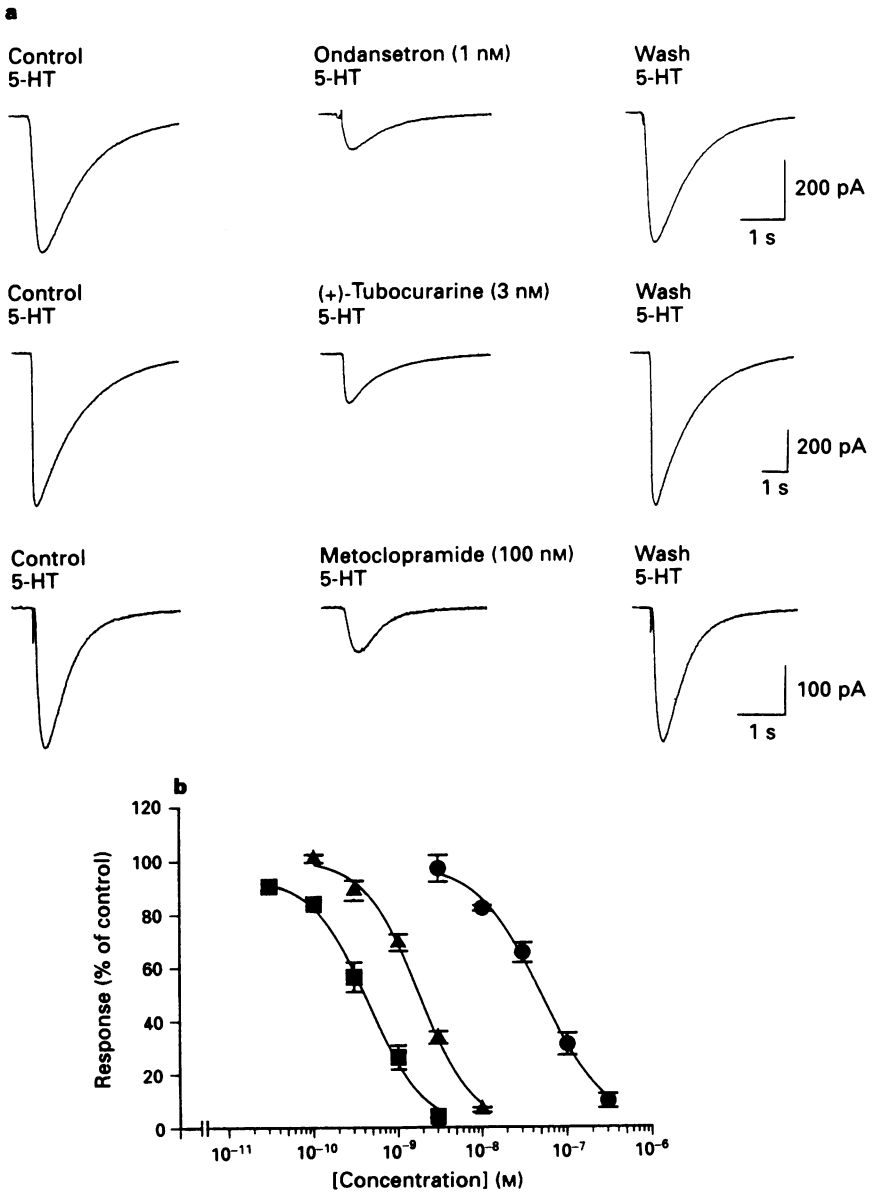

Figure 1 Inhibition of 5-hydroxytryptamine (5-HT)-induced currents by selective and non-selective 5-HT$_3$ receptor antagonists. (a) Inward current responses to ionophoretically applied 5-HT were reversibly inhibited by bath applied ondansetron (1 nM; top panel), (+)-tubocurarine (3 nM; middle panel) and metoclopramide (100 nM; bottom panel). All records are the computer generated average of four responses to 5-HT recorded at a holding potential of −60 mV. Each antagonist was tested on a different cell. (b) Graph depicting the concentration-dependent inhibition of 5-HT-induced currents by ondansetron (■), (+)-tubocurarine (▲) and metoclopramide (●). The amplitude of the 5-HT-induced inward current (expressed as a percentage of control; y axis) is plotted against the concentration of antagonist in the extracellular medium (log scale; x axis). Each point is the mean ± s.e.mean (vertical lines) of a minimum of four observations performed on separate cells. Curves were fitted to the data points by eye.

ion channels, was removed by subtracting the mean value of 16–32 blocks recorded prior to the application of the agonist.

Reagents

With the exception of geneticin (Sigma), all cell culture reagents were obtained from Gibco (UK). The experimental drugs used were: 5-hydroxytryptamine creatinine sulphate complex (5-HT), (+)-tubocurarine chloride, metoclopramide hydrochloride (all Sigma), ondansetron hydrochloride (Glaxo), methysergide hydrogen maleate (Sandoz) and ketanserin tartrate (Janssen). Compounds were freshly dissolved as concentrated stock solutions in either twice distilled deionised water, or extracellular saline.

Results

Pharmacological characterization

The ionophoretic application of 5-HT (20 mM) to solitary HEK 293 cells, voltage-clamped at −60 mV, induced an inward current on 77% (69 of 90) cells tested (range = 225–1080 pA, $n = 30$). Such responses were not observed in untransfected cells. The 5-HT-induced current was antagonised, in a concentration-dependent manner, by the selective 5-HT$_3$ receptor antagonist, ondansetron ($IC_{50} = 440 \pm 66$ pM; $n = 4$) and the non-selective antagonists (+)-tubocurarine ($IC_{50} = 1.8 \pm 0.2$ nM; $n = 4–5$) and metoclopramide (IC_{50} 50 ± 7 nM, $n = 4$). In all cases, the antagonism was readily reversed upon washout (Figure 1). The 5-HT$_2$ receptor

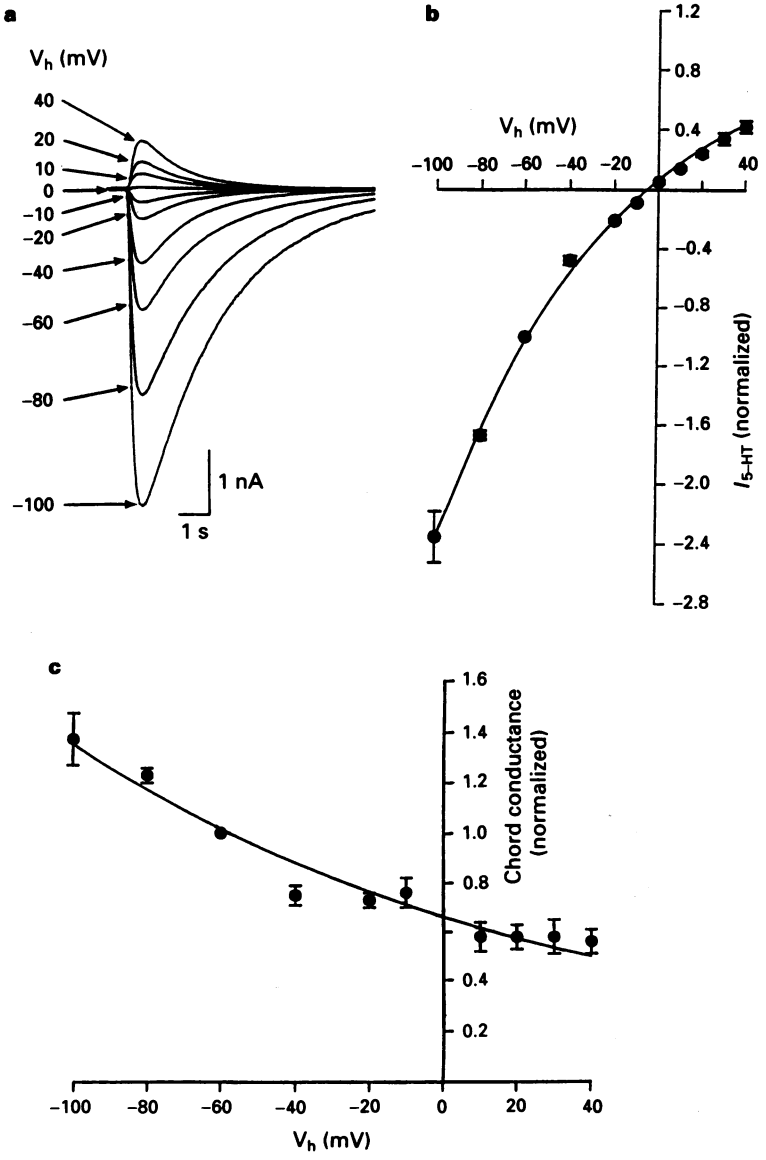

Figure 2 The current-voltage relationship for the 5-HT$_3$ R-A mediated electrical response in HEK 293 cells. (a) Current responses elicited by 5-HT applied ionophoretically to an HEK 293 cell voltage-clamped at the holding potentials (V_h) indicated adjacent to each trace. Each trace is the computer-generated average of 4 responses to 5-HT and leakage currents have been subtracted. (b) Graphical depiction of the 5-HT current-voltage relationship. In order to combine data obtained from several cells, the amplitude of the 5-HT induced current ($I_{5\text{-HT}}$) has been normalized by assigning a value of one to the response recorded at −60 mV and expressing current amplitudes at holding potentials (V_h) in the range −100 to 40 mV relative to that value. The current-voltage relationship demonstrates inward rectification and yields a reversal potential ($E_{5\text{-HT}}$) of −3 mV for the 5-HT$_3$ receptor-mediated response. Each data point is the mean ± s.e.mean of 7 to 10 observations performed on separate cells. The curve is fitted to the data points by eye. (c) The chord conductance of the 5-HT$_3$ R-A-mediated response (i.e. $I_{5\text{-HT}}/(V_h - E_{5\text{-HT}})$) calculated from the data illustrated in (b). The chord conductance increases e-fold for a membrane hyperpolarization of 151 mV. Data points are the mean ± s.e.mean of observations made from 7–10 cells.

antagonist, ketanserin and the mixed '5-HT$_1$-like' and 5-HT$_2$ receptor antagonist methysergide, each applied at a concentration of 1 μM had no effect upon the 5-HT-induced inward current ($n = 4$ for both compounds).

The ionic basis of the 5-HT-evoked response

Using the standard CsCl based pipette solution (I1) and the NaCl based bath saline (E1) described in the Methods, the amplitude of the 5-HT-evoked inward current decreased with membrane depolarization and reversed in sign at a potential ($E_{5\text{-HT}}$) of -2.2 ± 0.6 mV ($n = 15$). This value is similar to that previously found for the 5-HT$_3$ R-A expressed in *Xenopus* oocytes (Maricq *et al.*, 1991) and for 5-HT$_3$ receptor-mediated current responses of NCB-20 and N1E-115 cells (Lambert *et al.*, 1989). Inspection of the current-voltage relationship (Figure 2) reveals the 5-HT current to rectify inwardly. The rectification was quantified by calculating the chord conductance at a range of holding potentials (−100 to +40 mV). This analysis revealed that the 5-HT-induced chord conductance increases e-fold for a 151 mV hyperpolarization (Figure 2).

The total replacement of NaCl by sodium isethionate, to produce a solution in which the extracellular concentration of chloride ions was reduced from 148 mM to 8 mM had little influence upon $E_{5\text{-HT}}$. In the chloride ion deficient solution, $E_{5\text{-HT}}$ was estimated to be -1.0 ± 1.2 mV ($n = 5$), a value similar to that obtained with the standard extracellular medium. Thus as in other systems, the 5-HT$_3$ receptor-mediated current arises from the opening of channels that principally conduct cations. In some systems, permeability to Ca^{2+} and Mg^{2+} has also been clearly demonstrated (Yang, 1990; Yang *et al.*, 1992). In the present study, the contribution of extra- and intracellular monovalent cations to the 5-HT-induced current was examined by use of extracellular salines in which the concentration of both Ca^{2+} and Mg^{2+} was reduced to 0.1 mM to minimize their potential contribution to the response. Additionally, KCl was replaced by NaCl, so that Na was the sole monovalent cation present in the extracellular solution (E2). Under these conditions

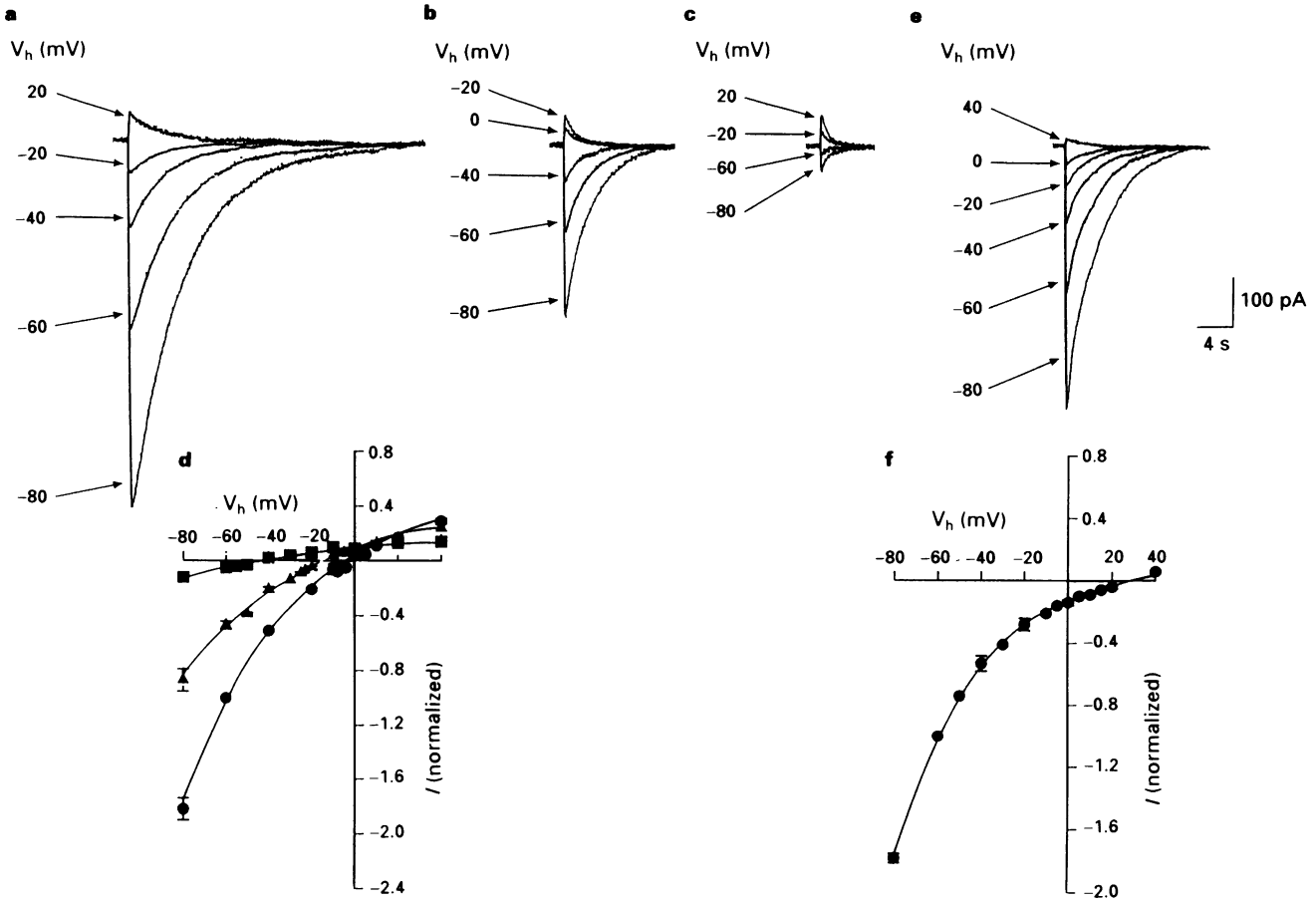

Figure 3 5-Hydroxytryptamine (5-HT)-induced currents are associated with an increase in membrane conductance to monovalent cations. (a-c) Traces illustrating transmembrane currents in response to ionophoretically applied 5-HT recorded at holding potentials (V_h) ranging between +20 and −80 mV. The currents were recorded in extracellular solutions containing 143 mM Na^+ (a), 75 mM Na^+ (b) and 20 mM Na^+ (c). The extracellular concentration of Na^+ ($[Na^+]_o$) was reduced by the partial replacement of NaCl with N-methyl-D-glucamine (see Methods). The records illustrated in (a), (b) and (c) were obtained from the same representative cell. (d) Current-voltage relationships for the 5-HT-evoked electrical response with $[Na^+]_o$ equal to 143 (●), 75 (▲) or 20 (■) mM. The amplitude of the 5-HT- induced current ($I_{5\text{-HT}}$), normalised as described in the legend to Figure 1, is plotted against the holding potential (V_h). The reversal potential ($E_{5\text{-HT}}$) was estimated to be −2.0, −14.5 and −43.0 mV in media containing 143, 75 and 20 mM Na^+ respectively. Data points are the means of 6 (▲) or 4 (●, ■) observations obtained from different cells. Curves were fitted to the data points by eye. Vertical lines, where they exceed the size of the symbol, indicate the standard error of the mean. (e) A family of 5-HT-evoked currents obtained from a representative cell bathed in an extracellular solution (E2) containing 143 mM Na^+ and dialysed with a pipette solution (I2) in which the concentration of Cs^+ was reduced from a standard value of 140 mM to one of 20 mM by partial replacement with the poorly permeant cation, tetraethylammonium chloride (TEA). (f) The amplitude of the normalised 5-HT-induced current ($I_{5\text{-HT}}$) as a function of holding potential (V_h) under the recording conditions described in (e). $E_{5\text{-HT}}$ was estimated to be +25 mV. Data points represent the mean of 3 observations obtained from different cells; the curve was fitted by eye. Vertical lines indicate s.e.mean. The traces illustrated in (a), (b), (c) and (e) are computer-generated average of four responses to 5-HT with leakage currents subtracted.

(Figure 3), $E_{5\text{-HT}}$ was found to be -2.0 ± 0.4 mV ($n = 4$), a value similar to that of -2.2 mV determined in the standard extracellular medium (E1). Reduction of the external concentration of NaCl to 75 and 20 mM by the iso-osmotic replacement of Na^+ with the poorly permeant monovalent cation N-methyl-D-glucamine (Yang, 1990; Malone *et al.*, 1994) produced a negative shift of $E_{5\text{-HT}}$ to values of -14.5 ± 0.4 mV ($n = 6$) and -43 ± 1 mV ($n = 4$) respectively (Figure 3). Reducing the internal concentration of Cs^+ from 140 to 20 mM, by partial substitution of CsCl with tetraethylammonium chloride (solution I2), produced a positive shift in $E_{5\text{-HT}}$ to $+25 \pm 0.8$ mV ($n = 3$; Figure 3). These observations suggest that under these ionic conditions the 5-HT-mediated current is carried mainly by Na^+ and Cs^+. Assuming the response to be mediated exclusively by a mixed Na^+ and Cs^+ cation conductance and utilizing the $E_{5\text{-HT}}$ value of -2 mV for salines I1 and E2, the ratio of Na and Cs permeabilities (P_{Na}/P_{Cs}) may be calculated from the Goldman-Hodgkin-Katz voltage equation (see Discussion) to be 0.94. It should be noted, however, that the computed P_{Na}/P_{Cs} ratio does not adequately account for the shifts in $E_{5\text{-HT}}$ observed with modified extra- and intra-cellular solutions. Possible reasons for this discrepancy are explored in the Discussion.

Modulation of the 5-HT-induced current by calcium, magnesium and zinc

The inhibitory effect of the divalent cations magnesium and calcium upon 5-HT$_3$ receptor-mediated currents is well documented (eg. Peters *et al.*, 1988; 1993; Yang, 1990). In the present study, reducing the extracellular concentrations of Ca^{2+} ($[Ca^{2+}]_o$) and Mg^{2+} ($[Mg^{2+}]_o$) to 0.1 mM, from their standard values of 1 mM and 2 mM respectively, enhanced the amplitude of the 5-HT-induced current, recorded at -60 mV, to $166 \pm 8\%$ of control ($n = 14$; Figure 4). In subsequent experiments, this divalent cation deficient solution was used as a control and the amplitude of the current evoked by 5-HT was expressed as a percentage of that obtained in this

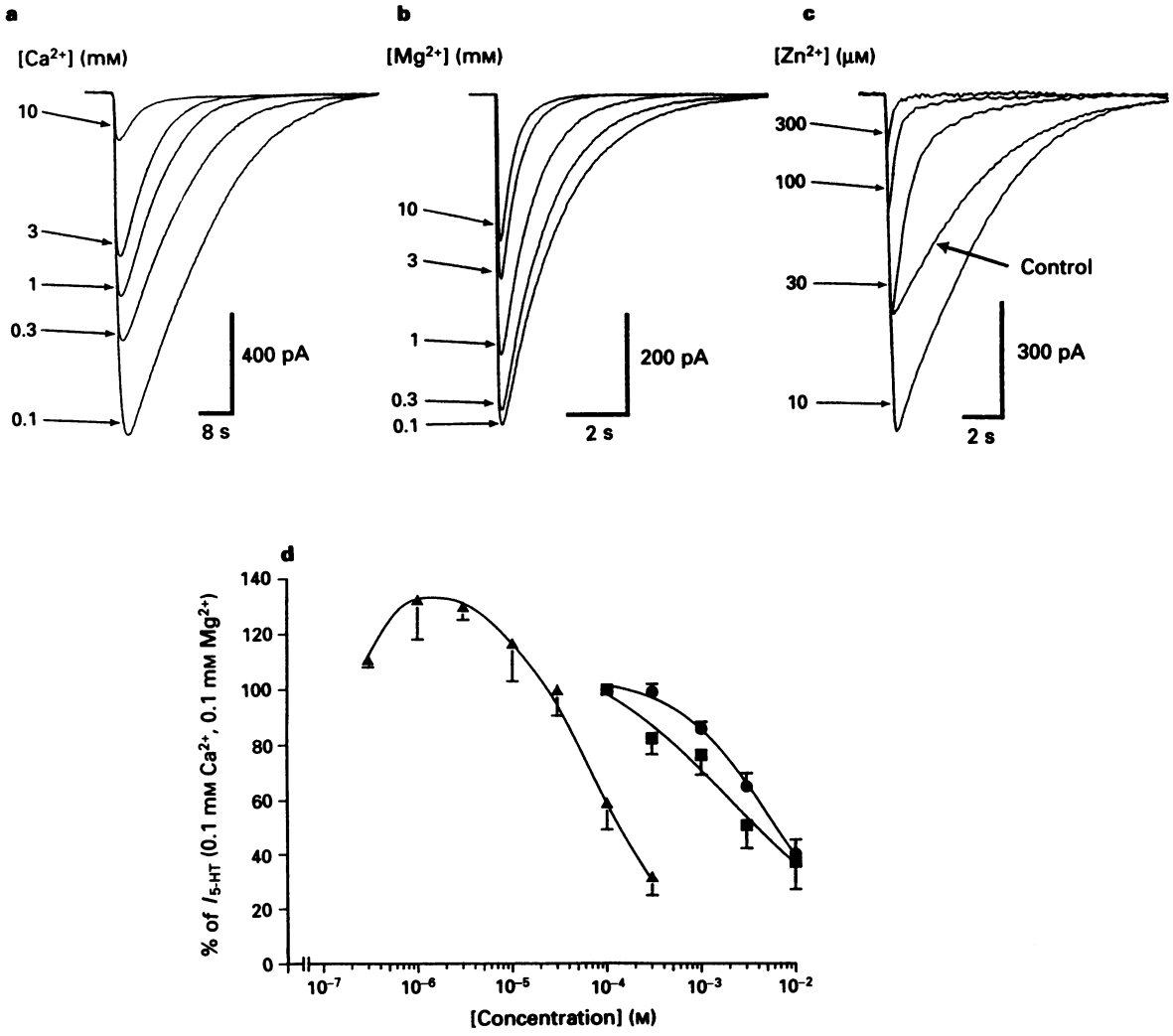

Figure 4 Divalent cations modulate the 5-HT$_3$ R-A-mediated current-response in HEK 293 cells. Superimposed responses to ionophoretically applied 5-HT recorded from 3 different cells illustrating the influence of extracellular Ca^{2+} (a), Mg^{2+} (b) and Zn^{2+} (c) upon current amplitude and duration. (a) Concentration-dependent reduction in current amplitude and duration by Ca^{2+} (0.1–10.0 mM). The concentration of Mg^{2+} was held constant at 0.1 mM. (b) Mg^{2+} exerts a depressant effect that is qualitatively similar to that observed with Ca^{2+}. The extracellular concentration of Ca^{2+} was maintained at 0.1 mM. (c) A low concentration (10 μM) of Zn^{2+} augments 5-HT-evoked currents, whereas higher concentrations (30–300 μM) depress both the amplitude and duration of the response. The effects of Zn^{2+} were examined in the presence of Ca^{2+} and Mg^{2+}, each at a concentration of 0.1 mM. All currents were recorded at a holding potential of -60 mV and each trace represents the computer generated average of 4 responses. (d) Graphical depiction of the concentration-dependent effects of Ca^{2+} (■), Mg^{2+} (●) and Zn^{2+} (▲) upon the amplitude of the response to 5-HT. Responses are expressed as a percentage of the control response amplitude observed in the presence of 0.1 mM Ca^{2+} and 0.1 mM Mg^{2+}. For Ca^{2+} and Mg^{2+}, each point represents the mean of 4 observations performed on separate cells. Data points for Zn^{2+} were obtained from 4 to 7 cells. Error bars indicate s.e.mean.

solution. With $[Mg^{2+}]_o$ fixed at 0.1 mM, increasing $[Ca^{2+}]_o$ from 0.1 mM to 1 mM and 10 mM reduced the amplitude of the 5-HT-induced response to 76.4 ± 7% of control ($n = 4$) and 32.6 ± 11.8% of control ($n = 4$) respectively (Figure 4). Similarly, a blocking action of Mg^{2+} was observed with $[Ca^{2+}]_o$ held constant at 0.1 mM, the response to 5-HT being reduced to 86 ± 3% of control, ($n = 4$) and 40 ± 5% of control ($n = 5$) by 1 and 10 mM Mg^{2+} respectively (Figure 4). The inhibitory effect of Mg^{2+} and Ca^{2+} was voltage-independent and occurred in the absence of a discernible shift in $E_{5\text{-HT}}$ (Figure 5).

In a previous study (Lovinger, 1991), the divalent cation zinc was shown to be a potent antagonist of the 5-HT$_3$ receptor mediated current recorded from NCB-20 cells. However, in this investigation, Zn^{2+} (0.3–300 μM) exerted a biphasic effect upon the amplitude of 5-HT-evoked currents recorded from HEK 293 cells, with low concentrations potentiating, and higher concentrations depressing, the response (Figure 4). For example, in the presence of 3 μM Zn^{2+}, the current amplitude was enhanced to 135 ± 5% of control ($n = 4$), whereas with 300 μM Zn^{2+}, the response was reduced to 29 ± 9% of control ($n = 3$; Figure 4).

Fluctuation analysis of the 5-HT-evoked response

The conductance of the ion channel integral to the 5-HT$_3$ receptor varies markedly between preparations (Peters *et al.*, 1992). In undifferentiated cells of the neuroblastoma cell lines N1E-115 and N18, extremely small single channel conductances of less than 1 pS have been reported. In such cases, single channel currents cannot be directly discerned by the patch clamp technique, but some of their properties may be determined indirectly by fluctuation analysis of 5-HT-induced whole-cell noise (Lambert *et al.*, 1989; Yang, 1990). In the present study, relatively slowly rising and desensitizing inward current responses, suited to fluctuation analysis, were elicited by a low concentration of 5-HT (1 μM) applied by microperfusion. Figure 6 illustrates low gain d.c.- and high

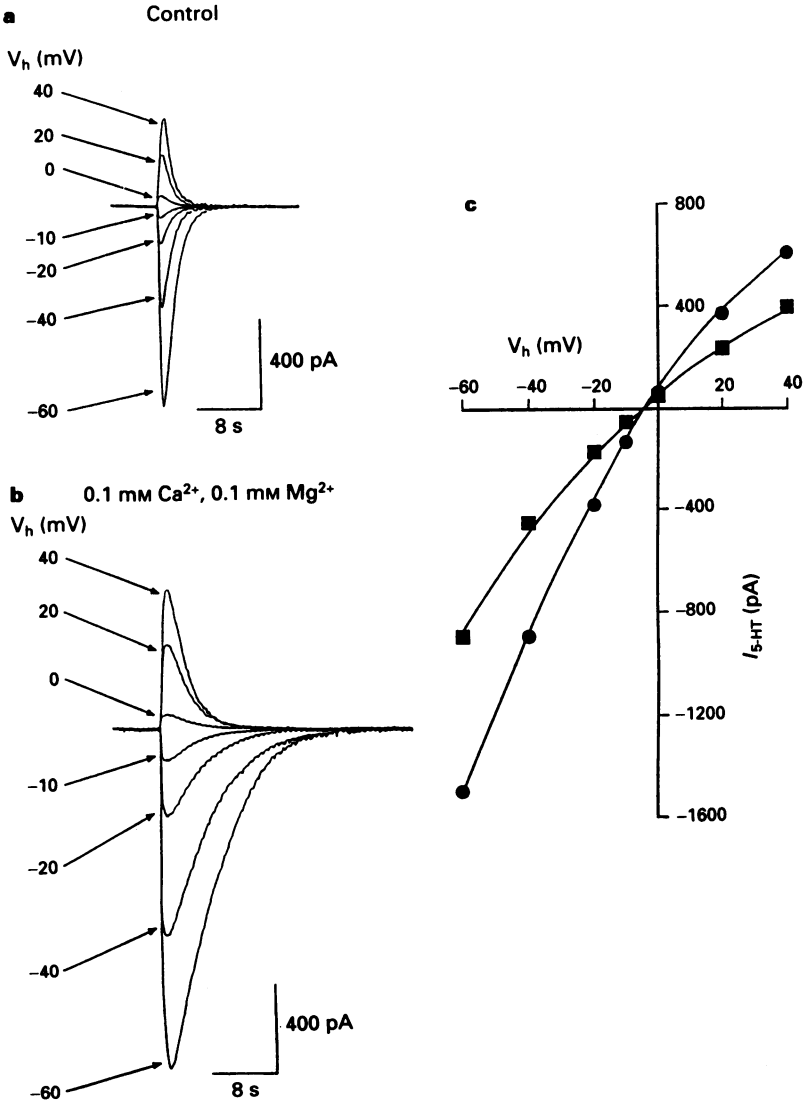

Figure 5 The effect of calcium and magnesium on the current-voltage relationship for the 5-HT$_3$ R-A-mediated electrical response in HEK 293 cells. (a) Current responses to ionophoretically applied 5-HT recorded at holding potentials (V_h) ranging between −60 and +40 mV. Currents were recorded in the standard extracellular saline (E1) containing 1 mM Ca^{2+} and 2 mM Mg^{2+}. (b) Current responses recorded from the same cell as in (a) but in the presence of a solution containing 0.1 mM Ca^{2+} and 0.1 mM Mg^{2+}. Note that the 5-HT-induced currents at all holding potentials are enhanced in amplitude and duration in the divalent cation deficient solution. In both (a) and (b), each current is the average of four responses to 5-HT and leakage currents have been subtracted. (c) Graphical representation of the data shown in (a) and (b) in the form of a current-voltage relationship. Note that in both the control (■) and divalent cation-deficient solutions (●) inward rectification is apparent. The reversal potential of the response to 5-HT is unaffected by the reduction in the extracellular concentration of divalent cations.

gain a.c.-coupled records associated with such a response. The inward current was accompanied by a small increase of current noise that is apparent in the high gain a.c.-coupled record (Figure 6). Fluctuation analysis of this response yielded a linear relationship between the noise variance (σ^2) and mean amplitude (I_m) of the inward current response to 5-HT. By fitting equation (3) to this data, the current i flowing through a single 5-HT activated ion channel was estimated to be 16.9 fA for the exemplar cell. From the holding potential (V_h) at which the recording was made (i.e. −60 mV) and the reversal potential ($E_{5\text{-HT}}$) of the response to 5-HT determined under the appropriate ionic conditions (ie. approximately -2 mV), the single channel conductance can be estimated from the relationship:

$$i = \gamma(V_h - E_{5\text{-HT}}) \quad (4)$$

For the example illustrated in Figure 6, the single channel conductance approximated to 290 fS. The mean single channel conductance derived by fitting either equations (2) or (3) to the data obtained from two and four additional cells respectively was estimated to be 420 ± 74 fS ($n = 7$).

Discussion

The cDNAs encoding the murine 5-HT$_3$ R-A and an alternatively spliced form of the subunit (5-HT$_3$ R-A$_s$) produce functional, presumably homomeric, receptor channel complexes when expressed in *Xenopus laevis* oocytes (Maricq *et al.*, 1991; Eiselé *et al.*, 1993; Hope *et al.*, 1993; Yakel *et al.*, 1993; Downie *et al.*, 1994; Uetz *et al.*, 1994). 5-HT-induced currents recorded from such oocytes exhibit many of the pharmacological and biophysical properties attributed to the 5-HT$_3$ receptor native to the murine N1E-115 and NCB-20 cell lines from which these cDNAs were first isolated. Similarly, the results reported here demonstrate that the 5-HT$_3$ R-A cDNA, when stably transfected into HEK 293 cells, directs the formation of functional 5-HT-activated ion channels.

A number of studies (see Peters *et al.*, 1992) have established that the pharmacological properties of 5-HT$_3$ receptors vary markedly across species. Consistent with previous studies utilizing *Xenopus* oocytes (Maricq *et al.*, 1991; Hope *et al.*, 1993; Downie *et al.*, 1994; Uetz *et al.*, 1994), the murine 5-HT$_3$ R-A expressed in HEK 293 cells was blocked by the selective 5-HT$_3$ receptor antagonist, ondansetron and the non-selective antagonists, metoclopramide and (+)-tubocurarine, at concentrations similar to those reported for murine neuronal cell lines (Lambert *et al.*, 1989; Peters *et al.*, 1990), mouse hippocampal (Yakel & Jackson 1988) and mouse nodose ganglion neurones (Malone *et al.*, 1991; Peters *et al.*, 1992). In particular, (+)-tubocurarine exhibits the characteristically high affinity established for the mouse 5-HT$_3$ receptor. The mechanism of action of (+)-tubocurarine is not known, but in murine N1E-115 neuroblastoma cells the antagonism is both use- and voltage-independent, making the associated ion channel an unlikely locus of action (Peters *et al.*, 1990). Consistent with these findings, functional experiments performed on a chimaeric construct of the N-terminal region of the chick nicotinic α_7 subunit and the C-terminal and the putative transmembrane domains of the 5-HT$_3$ R-A, reveals a receptor that is activated by acetylcholine which demonstrates the relatively low affinity for (+)-tubocurarine characteristic of the α_7 nicotinic subunit (Eiselé *et al.*, 1993). The isolation and sequencing of homologues of the 5-HT$_3$ R-A subunit from species in which the native receptor is known to exhibit divergent pharmacological properties may be instructive in defining ligand binding sites. In this respect, the recently identified rat 5-HT$_3$ R-A$_s$, which differs from the murine 5-HT$_3$ R-A$_s$ at least 100 fold in its sensitivity to (+)-tubocurarine, is of interest (Johnson & Heinemann, 1992; Isenberg *et al.*, 1993). The rat

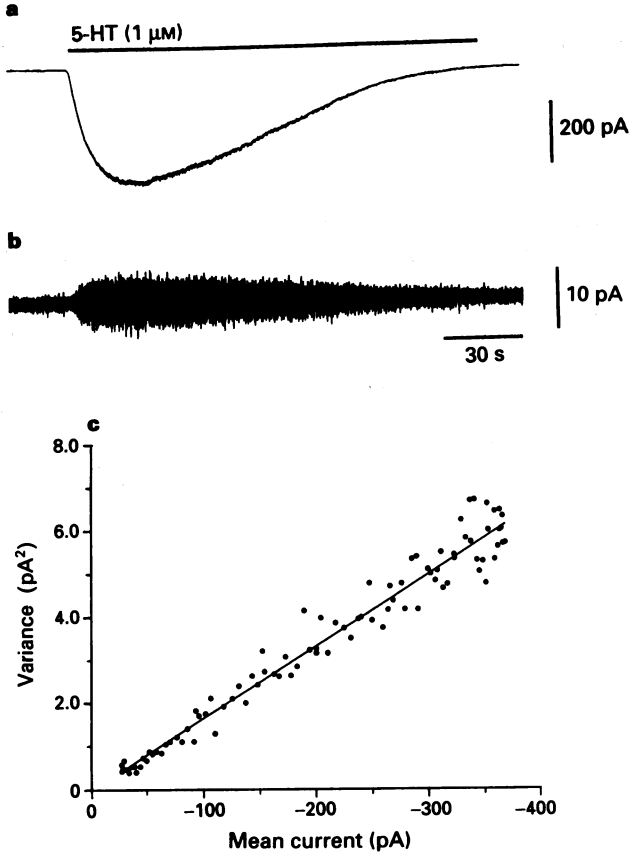

Figure 6 Fluctuation analysis of 5-HT-evoked whole cell currents mediated by the 5-HT$_3$ R-A expressed in HEK 293 cells. (a) Low gain d.c.-coupled record (500 Hz low-pass filtering) of an inward current response elicited by 1 μM 5-HT applied by microperfusion for the period indicated by the solid bar above the trace. (b) High-gain a.c.-coupled record (1 Hz–500 Hz band-pass) of the response illustrated in (a). Note that the changes in the amplitude of the current fluctuation (noise) parallel the development and desensitization of the response depicted in (a). (c). A plot illustrating the relationship between the variance of the a.c.-coupled current and the mean (d.c.) current elicited by 5-HT. Current variance in the absence of 5-HT has been subtracted. The slope of the line, fitted to the data points by least-squares linear regression analysis, indicates the elementary current flowing through a single 5-HT$_3$ R-A complex to be approximately 17 fA. From the holding potential of −60 mV and an $E_{5\text{-HT}}$ of −2 mV, the single channel conductance in this example is estimated to be 290 fS.

subunit exhibits only sixteen differences in primary amino acid sequence within the N-terminal domain (Isenberg *et al.*, 1993). Intriguingly, three of those are in a region corresponding to the C loop of nicotinic α subunits, a domain known to be involved in the binding of (+)-tubocurarine to nicotinic receptors (see Lambert *et al.*, 1995).

The reversal potential (~0 mV) of the 5-HT-induced current recorded from *Xenopus* oocytes expressing the murine 5-HT$_3$ R-A subunit is shifted to more negative potentials by the total replacement of extracellular Na^+ by the poorly permeant cation Tris, suggesting the homo-oligomeric complex to retain selectivity toward monovalent cations (Maricq *et al.*, 1991). The results described here confirm this suggestion, since Na^+ and Cs^+ were found to be approximately equipermeant and the partial replacement of either extracellular Na^+ by NMDG or intracellular Cs^+ by TEA produced large negative and positive shifts in $E_{5\text{-HT}}$ respectively. However, the magnitude of the shift in $E_{5\text{-HT}}$ occurring in response to these ionic substitutions was consistently less than that predicted from the Goldman-Hodgkin-Katz voltage equation (Hille, 1992). As chloride ions appear to be impermeant, and noting that the reduction in the extracellular concentrations

of Ca^{2+} and Mg^{2+} had a negligible effect upon $E_{5\text{-}HT}$, the latter may be expressed as:

$$E_{5\text{-}HT} = \frac{RT}{zF} ln \frac{P_{Na}/P_{Cs}[Na]_0}{P_{Na}/P_{Cs}[Na]_i + [Cs]_i} \quad (5)$$

where R, T, z and F have their usual meaning. From the above, and the value of $E_{5\text{-}HT}$ (−2 mV) determined with solutions E2 and I1, the permeability of Na relative to Cs (i.e. P_{Na}/P_{Cs}) is calculated to be 0.94. However, this ratio fails to predict accurately the observed shifts in $E_{5\text{-}HT}$. For example, reducing $[Na]_o$ to 75 mM and 20 mM would be expected to shift $E_{5\text{-}HT}$ to −18.7 and −52.0 mV respectively, rather than the observed values of −14.5 and −42.9 mV. Similarly, partial replacement of intracellular Cs^+ by TEA resulted in an $E_{5\text{-}HT}$ of +25.9 mV, a value considerably less than that predicted (i.e. +40.3 mV). The most likely explanation of these discrepancies is that, in common with 5-HT$_3$ receptors native to rabbit nodose ganglion neurones (Malone, 1992; Malone *et al.*, 1994) and N1E-115 neuroblastoma cells (Kooyman *et al.*, 1993), the 5-HT$_3$ R-A possesses a finite permeabilty to both NMDG and TEA. Indeed, if equation (5) above is extended to include terms for either P_{NMDG}/P_{Cs} or P_{TEA}/P_{Cs}, and the permeability ratios of 0.047 and 0.131, respectively, determined for nodose ganglion neurones (Malone, 1992; Malone *et al.*, 1994) are employed as estimates of their ability to permeate the 5-HT$_3$ R-A, then the predicted and measured reversal potentials agree in all cases to within 3 mV.

5-HT$_3$ receptors endogenous to murine neuronal cell lines and rabbit nodose ganglion neurones are blocked by the divalent cations calcium and magnesium in a concentration-dependent, voltage-independent manner (Peters *et al.*, 1988, 1993; Yang, 1990; Lovinger, 1991). Such observations are consistent with the results of the present study. Furthermore, inspection of the 5-HT$_3$ current-voltage relationship (Figures 2 and 3) reveals the response to exhibit the inward rectification that is characteristic of murine 5-HT$_3$ receptors (Lambert *et al.*, 1989; Yang 1990; Lovinger, 1991; Yang *et al.*, 1992). The mouse or rat homologues of the 5-HT$_3$ R-A, when expressed in *Xenopus* oocytes, are also blocked by magnesium and calcium, but the antagonism is reported to be voltage-dependent (Maricq *et al.*, 1991; Johnson & Heinemann 1992; Eiselé *et al.*, 1993). This difference is not readily explained by the expression system employed, as in one study performed with *Xenopus* oocytes (Yakel *et al.*, 1993), modest inward rectification of the 5-HT-evoked current in the presence of Mg^{2+} and Ca^{2+} was observed. However, in that study, Ca^{2+} was reported to enhance 5-HT$_3$ receptor desensitization in a voltage-dependent manner and an intracellular site of action was implicated (Yakel *et al.*, 1993). At present, there is no obvious explanation for the divergent observations regarding Ca^{2+}- and Mg^{2+}-induced blockade of recombinant 5-HT$_3$ receptors. Further studies designed to clarify the site(s) of action of these divalent cations are required, particularly in view of a recent report which demonstrated blockade of 5-HT$_3$ receptor mediated currents in rat dentate gyrus basket cells by Ca^{2+} and Mg^{2+} to be voltage-dependent (Kawa, 1994). In this respect, the results of experiments performed upon chimaeric α_7 nicotinic-5-HT$_3$ receptors, which suggest the ion channel as a locus of action, are of interest (Eiselé *et al.*, 1993).

The divalent cation zinc is known to interact with a variety of ligand-gated ion channels (Harrison & Gibbons, 1994; Smart *et al.*, 1994). Micromolar concentrations of Zn^{2+} cause inhibition of NMDA (Mayer *et al.*, 1989; Rassendren *et al.*, 1990) and $GABA_A$ receptor-evoked currents (Draguhn *et al.*, 1990; Smart *et al.*, 1994), but enhancement of ATP, AMPA and kainate-evoked currents (Rassendren *et al.*, 1990; Li *et al.*, 1993). At somewhat higher concentrations, Zn^{2+} antagonizes AMPA and kainate-evoked currents (Mayer *et al.*, 1989; Rassendren *et al.*, 1990). Flux assays suggest that Zn^{2+} also interacts with 5-HT$_3$ receptors, since the receptor-mediated influx of [^{14}C]-guanidinium in NG 108-15 cells is inhibited by Zn^{2+} (Emerit *et al.*, 1993). Under voltage-clamp conditions, Zn^{2+} produces a voltage-dependent inhibition of the 5-HT$_3$ receptor-mediated currents recorded from murine NCB-20 cells (Lovinger, 1991), with an IC_{50} of approximately 20 μM. The 5-HT$_3$ R-A subunit investigated here was isolated from this cell line (Maricq *et al.*, 1991) and it is of interest that low concentrations of Zn^{2+} (0.3–10 μM) enhanced the receptor mediated current with blockade being evident only with higher concentrations (30–300 μM) of Zn^{2+}. In preliminary experiments, a similar biphasic effect of Zn^{2+} was observed with *Xenopus* oocytes expressing the 5-HT$_3$ R-A subunit (D. Belelli, C.H. Gill, J.J. Lambert & J.A. Peters, unpublished observations). By analogy to the influence of subunit composition upon the sensitivity of $GABA_A$ receptors to blockade by Zn^{2+} (Smart *et al.*, 1994), it is conceivable that additional subunits are present within the 5-HT$_3$ receptor expressed by NCB-20 cells. The only additional subunit thus far identified in these cell lines is an alternatively spliced form of the 5-HT$_3$ R-A, termed the 5-HT$_3$ R-A$_s$ (Hope *et al.*, 1993; Hussy & Jones 1993). Whether the 5-HT$_3$ R-A$_s$ expressed alone, or in combination with the 5-HT$_3$ R-A, exhibits a similar biphasic response to Zn^{2+} remains to be determined. However, it is known that alternatively spliced forms of the NMDAR-1 subunit are differentially modulated by this divalent cation (Hollman *et al.*, 1993; Zheng *et al.*, 1994). We are at present investigating the mechanism of Zn^{2+} action on the 5-HT$_3$ R-A in more detail. Furthermore, in view of the species-dependent pharmacological properties of this receptor, studies upon the 5-HT$_3$ receptors of rabbit, mouse and guinea-pig nodose ganglion neurones would be of interest (Peters *et al.*, 1992).

Fluctuation analysis of whole-cell currents mediated by the 5-HT$_3$ R-A suggests the homo-oligomeric complex to possess a single channel conductance of approximately 0.42 pS. It is unlikely that this extremely low value is a result of the exclusion of frequency components that would contribute significantly to the signal variance. Fluctuation analysis conducted over an extended frequency range (i.e. 0.5 Hz to 1 kHz) upon suitably slowly changing signals (see below) yielded estimates of single channel conductance similar to those obtained with the routinely employed bandwidth of 1 Hz–500 Hz. Nonetheless, several limitations to the analysis remain. The estimates of channel conductance were made by stationary analysis applied to a changing current signal in response to microperfused 5-HT (1 μM). For this approach to be valid, the current should not change appreciably within the period of a single variance calculation. Fluctuation analysis was routinely restricted to frequencies $\geq$1 Hz in an effort to avoid possible *overestimation* of the variance from trends that could be introduced by the lengthy data blocks that would be necessary to incorporate lower frequency components. In interpreting the results, we have assumed that neither desensitization nor agonist concentration are likely to affect single channel conductance. The conductance estimate obtained from fluctuation analysis is in fact a weighted mean that is influenced by the relative frequency of all conducting states. Although for simplicity, we have interpreted our data in terms of a 5-HT activated channel of unitary conductance, this need not necessarily be the case. Indeed, a comparison of the conductance of 5-HT$_3$ receptors of rat superior cervical ganglion neurones determined by direct observation of single channel currents and fluctuation analysis reveals a large discrepancy that probably reflects the existence of multiple conductance states (Yang *et al.*, 1992). Similarly, recordings made on membrane patches excised from rodent hippocampal neurones suggest the existence of two populations of channel: one with a conductance of approximately 10 pS, and a second which cannot be directly resolved, but which produces an inward current that is blocked by 5-HT$_3$ receptor antagonists (Jones & Surprenant, 1994). Multiple conductances have also been reported for 5-HT$_3$ receptors expressed by neurones of the guinea-pig submucous plexus (Derkach *et*

al., 1989) and mouse superior cervical ganglion (Hussey & Jones, 1993).

The conductance of the 5-HT$_3$ R-A described here is similar to that estimated for 5-HT$_3$ receptors native to NCB-20, N1E-115 and N18 cells (Lambert *et al.*, 1989; Yang, 1990; van Hooft *et al.*, 1994). It remains unclear as to why the single channel conductance in these systems is so low. The minimal diameter of the ion channel associated with the 5-HT$_3$ receptor, as assessed by studies employing permeant cations of differing sizes (Yang, 1990; Malone *et al.*, 1994), is similar to that established for nicotinic acetylcholine receptors which typically demonstrate conductances of 40–50 pS (Karlin, 1993). Previous suggestions that the 5-HT$_3$ ion channel may be longer, or less polarizable, than that of nicotinic receptors (Yakel *et al.*, 1990) are not supported by the structural information that has been derived from cloned 5-HT$_3$ receptor subunits. Indeed, over the M2 region that is proposed to line the ion channel, subunits of 5-HT$_3$ and nicotinic receptors exhibit a high degree of sequence homology (Maricq *et al.*, 1991). In particular, acidic amino acid residues which are thought to produce rings of negative charge with extracellular, intermediate and cytoplasmic locations, and which are known to influence the conductance of the nicotinic receptor complex, are common to both receptor types (Maricq *et al.*, 1991; Karin, 1993). However, the presence of a basic lysine residue located within the putative M2 domain of the 5-HT$_3$ R-A represents one obvious structural feature that is not shared with nicotinic receptor subunits. Mutation of this residue to glycine (the homologous amino acid found in the chick α_7 nicotinic subunit) dramatically slows the kinetics of desensitization of the 5-HT$_3$ R-A, expressed in *Xenopus* oocytes (A. Hope, D. Belelli, J.J. Lambert & J.A. Peters, unpublished observations). The effect of this mutation upon single channel conductance is currently under evaluation. A potential influence of a post translational modification upon the channel conductance is suggested by a preliminary report demonstrating the conductance of the 5-HT$_3$ receptor endogenous to N1E-115 neuroblastoma cells to be modified by an unidentified intracellular factor(s) (van Hooft & Vijverberg, 1994).

The small conductance associated with the 5-HT$_3$ receptor expressed by murine neuronal cell lines is probably not unique, because there are indications of a similar conductance state in neurones of the rat superior cervical (Yang *et al.*, 1992) and dorsal root (Robertson & Bevan, 1991) ganglia. Furthermore, 5-HT$_3$ receptor single channel mainstate conductances of 12 pS and 10 pS have recently been determined for mouse superior cervical ganglion neurones and hippocampal neurones, respectively, suggesting heterogeneity within this species (Hussy & Jones, 1993; Jones & Surprenant, 1994). The future isolation of cDNAs encoding 5-HT$_3$ receptor channels with divergent conductances should clarify the molecular determinants of ion transport through this channel.

We gratefully acknowledge the gift of the stably transfected HEK 293 cell line from Dr David Julius, University of California. We also thank Drs Anthony Hope, Helen Rogers and Gavin Kilpatrick for helpful discussions and Dr John Dempster, University of Strathclyde, for computer software. CHG is a Glaxo Scholar. This work was supported by grants from the Wellcome Trust, Glaxo Group Research and Tenovus (Tayside).

References

BOESS, F.G. & MARTIN, I.L. (1994). Molecular biology of 5-HT receptors. *Neuropharmacology*, **33**, 275–317.

CULL-CANDY, S.G., HOWE, J.R. & OGDEN, D.C. (1988). Noise and single channels activated by excitatory amino acids in rat cerebellar granule neurones. *J. Physiol.*, **400**, 189–222.

DEMPSTER, J. (1993). *Computer Analysis of Electrophysiological Signals*. London: Academic Press.

DERKACH, V., SURPRENANT, A. & NORTH, R.A. (1989). 5-HT$_3$ receptors are membrane ion channels. *Nature*, **339**, 706–709.

DOWNIE, D.L., HOPE, A.G., LAMBERT, J.J., PETERS, J.A., BLACKBURN, T.P. & JONES, B.J. (1994). Pharmacolological characterization of the apparent splice variants of the murine 5-HT$_3$ R-A subunit expressed in *Xenopus laevis* oocytes. *Neuropharmacology*, **33**, 473–482.

DRAGUHN, A., VERDOORN, T.A., EWERT, M., SEEBURG, P.H. & SAKMANN, B. (1990). Functional and molecular distinction between recombinant rat GABA$_A$ receptor subtypes by Zn^{2+}. *Neuron*, **5**, 781–788.

EISELÉ, J.-L., BERTRAND, S., GALZI, J.-L., DEVILLERS-THIÉRY, A., CHANGEUX, J.-P. & BERTRAND, D. (1993). Chimaeric nicotinic-serotonergic receptor combines distinct ligand binding and channel specificities. *Nature*, **366**, 479–483.

EMERIT, M.B., RIAD, M., FATTACINI, C.M. & HAMON, M. (1993). Characteristics of [^{14}C]guanidinium accumulation in NG 108-15 cells exposed to serotonin 5-HT$_3$ receptor ligands and substance P. *J. Neurochem.*, **60**, 2059–2067.

GILL, C., PETERS, J.A., LAMBERT, J.J., HOPE, A.G. & JULIUS, D. (1993). Modulation by divalent cations of current responses mediated by a cloned murine 5-HT$_3$ receptor (5-HT$_3$ R-A) expressed in HEK 293 cells. *Br. J. Pharmacol.*, **109**, 98P.

HAMILL, O.P., MARTY, A., NEHER, E., SAKMANN, B. & SIGWORTH, F. (1981). Improved patch-clamp techniques for high resolution current recordings from cells and cell-free membrane patches. *Pflügers Arch.*, **391**, 85–100.

HARRISON, N.L. & GIBBONS, S.J. (1994). Zn^{2+}: an endogenous modulator of ligand-and voltage-gated ion channels. *Neuropharmacology*, **33**, 935–952.

HILLE, B. (1992). *Ionic Channels of Excitable Membranes (2nd. Edition)*. Sunderland, MS: Sinaeur Associates.

HOLLMAN, M., BOULTER, J., MARON, C., BEASLEY, L., SULLIVAN, J., PECHT, G. & HEINEMANN, S. (1993). Zinc potentiates agonist-induced currents at certain splice variants of the NMDA receptor. *Neuron*, **10**, 943–954.

HOPE, A.G., DOWNIE, D.L., SUTHERLAND, L., LAMBERT, J.J. PETERS, J.A. & BURCHELL, B. (1993). Cloning and functional expression of an apparent splice variant of the murine 5-HT$_3$ receptor A subunit. *Eur. J. Pharmacol. (Mol. Pharmacol. Sect.)*, **245**, 187–192.

HUSSY, N. & JONES, K. (1993). Differences in single channel conductances of mouse 5-HT$_3$ receptors may indicate the presence of receptor subtypes. *Soc. Neurosci. Abstr.*, **19**, 282.

ISENBERG, K.E., UKHUN, I.A., HOLSTAD, S.G., JAFRI, S., UCHIDA, U., ZORUMSKI, C.F. & YANG, J. (1993). Partial cDNA cloning and NGF regulation of a rat 5-HT$_3$ receptor subunit. *Neuroreport*, **5**, 121–124.

JOHNSON, D.A. & HEINEMANN, S.F. (1992). Cloning and expression of the rat 5-HT$_3$ receptor reveals species-specific sensitivity to curare antagonism. *Soc. Neurosci. Abst.*, **18**, 249.

JONES, K.A. & SURPRENANT, A. (1994). Single channel properties of the 5-HT$_3$ subtype of serotonin receptor in primary cultures of rodent hippocampus. *Neurosci. Lett.*, **174**, 133–136.

KARLIN, A. (1993). Structure of nicotinic acetylcholine receptors. *Current Op. Neurobiol.*, **3**, 299–309.

KAWA, K. (1994). Distribution and functional properties of 5-HT$_3$ receptors in the rat hippocampal dentate gyrus: A patch-clamp study. *J. Neurophysiol.*, **71**, 1935–1947.

KOOYMAN, A.R., ZWART, R. & VIJVERBERG, H.P.M. (1993). Tetraethylammonium ions block 5-HT$_3$ receptor-mediated ion current at the agonist recognition site and prevent desensitization in cultured mouse neuroblastoma cells. *Eur. J. Pharmacol. (Mol. Pharmacol. Sect.)*, **246**, 247–254.

LAMBERT, J.J., PETERS, J.A., HALES, T.G. & DEMPSTER, J. (1989). The properties of 5-HT$_3$ receptors in clonal cell lines studied by patch-clamp techniques. *Br. J. Pharmacol.*, **97**, 27–40.

LAMBERT, J.J., PETERS, J.A. & HOPE, A.G. (1995). 5-HT$_3$ receptors. In *CRC Handbook of Ion Channels*. ed. North, R.A. pp. 177–221. Boca Raton: CRC Press Inc.

LI, C., PEOPLES, R.W., LI, Z. & WEIGHT, F.F. (1993). Zn^{2+} potentiates excitatory action of ATP on mammalian neurons. *Proc. Natl. Acad. Sci. U.S.A.*, **90**, 8264–8269.

LOVINGER, D.M. (1991). Inhibition of 5-HT$_3$ receptor-mediated ion current by divalent metal cations in NCB-20 neuroblastoma cells. *J. Neurophysiol.*, **66**, 1329–1337.

MALONE, H.M. (1992). Physiological and Pharmacological Properties of 5-HT$_3$ Receptors. *Ph.D. Thesis, The University of Dundee.*

MALONE, H.M., PETERS, J.A. & LAMBERT, J.J. (1991). Physiological and pharmacological properties of 5-HT$_3$ receptors – a patch-clamp study. *Neuropeptides*, **19**, (Suppl), 25–30.

MALONE, H.M., PETERS, J.A. & LAMBERT, J.J. (1994). The permeability of 5-HT$_3$ receptors of rabbit nodose ganglion neurones to metallic and organic monovalent cations. *J. Physiol.*, **475**, 151P.

MARICQ, A.V., PETERSON, A.S., BRAKE, A.J., MYERS, R.M. & JULIUS, D. (1991). Primary structure and functional expression of the 5-HT$_3$ receptor, a serotonin-gated ion channel. *Science*, **254**, 432–437.

MAYER, M.L., VYKLICKY, L. JR., & WESTBROOK, G.L. (1989). Modulation of excitatory amino acid receptors by group IIb metal cations in cultured mouse hippocampal neurones. *J. Physiol.*, **429**, 429–449.

PETERS, J.A., HALES, T.G. & LAMBERT, J.J. (1988). Divalent cations modulate 5-HT$_3$ receptor-induced currents in N1E-115 neuroblastoma cells. *Eur. J. Pharmacol.*, **151**, 491–495.

PETERS, J.A., LAMBERT, J.J. & COTTRELL, G.A. (1989). An electrophysiological investigation of the characteristics and function of $GABA_A$ receptors on bovine adrenomedullary chromaffin cells in culture. *Pflügers Arch.*, **415**, 95–103.

PETERS, J.A., MALONE, H.M. & LAMBERT, J.J. (1990). Antagonism of 5-HT$_3$ receptor mediated currents in a clonal cell line by (+)-tubocurarine. *Neurosci. Lett.*, **110**, 107–112.

PETERS, J.A., MALONE, H.M. & LAMBERT, J.J. (1992) Recent advances in the electrophysiological characterization of 5-HT$_3$ receptors. *Trends Pharmacol. Sci.*, **13**, 391–397.

PETERS, J.A., MALONE, H.M. & LAMBERT, J.J. (1993). An electrophysiological investigation of the properties of 5-HT$_3$ receptors of rabbit nodose ganglion neurones in culture. *Br. J. Pharmacol.*, **110**, 665–676.

RASSENDREN, F.-A., LORY, P., PIN, J.-P. & NARGEOT, J. (1990). Zinc has opposite effects on NMDA and non-NMDA receptors expressed in *Xenopus* oocytes. *Neuron*, **4**, 733–740.

ROBERTSON, B. & BEVAN, S. (1991). Properties of 5-hydroxytryptamine$_3$, receptor-gated currents in adult rat dorsal root ganglion neurones. *Br. J. Pharmacol.*, **102**, 272–276.

SEEBURG, P.H. (1993). The molecular biology of mammalian glutamate receptor channels. *Trends Pharmacol. Sci.*, **14**, 297–303.

SIEGART, W. (1992). $GABA_A$ receptors: ligand-gated Cl^- ion channels modulated by multiple drug-binding sites. *Trends Pharmacol. Sci.*, **13**, 446–450.

SMART, T., XIE, X. & KRISHEK, B.J. (1994). Modulation of inhibitory and excitatory amino acid receptor channels by zinc. *Prog. Neurobiol.*, **42**, 393–441.

UETZ, P., ABDELATTY, F., VILLAROEL, A., RAPPOLD, G., WEISS, B. & KOENEN, M. (1994). Organisation of the murine 5-HT$_3$ receptor gene and assignment to human chromosome 11. *FEBS Lett.*, **339**, 302–306.

VAN HOOFT, J.A., KOOYMAN, A.R., VERKERK, A., VAN KLEEF, R.G.D.M. & VIJVERBERG, H.P.M. (1994). Single 5-HT$_3$ receptor-gated ion channel events resolved in N1E-115 mouse neuroblastoma cells. *Biochem. Biophys. Res. Commun.*, **199**, 227–233.

VAN HOOFT, J.A. & VIJVERBERG, H.P.M. (1994). 5-HT$_3$ receptor-gated single channels in excised and cell-attached patches of N1E-115 neuroblastoma cells. *J. Physiol.*, **479**, 113P.

WAFFORD. K.A., BURNETT, D.M., LEIDENHEIMER, N.J., BURT, D.R., WANG, J.B., KOFUJI, P., DUNWIDDIE, T.V., HARRIS, R.A. & SIKELA, J.M. (1991). Ethanol sensitivity of the $GABA_A$ receptor expressed in *Xenopus* oocytes requires 8 amino acids contained in the γ2L subunit. *Neuron*, **7**, 27–33.

YAKEL, J.L. & JACKSON, M.B. (1988). 5-HT$_3$ receptors mediate rapid responses in cultured hippocampus and a clonal cell line. *Neuron*, **1**, 615–621.

YAKEL, J.L., LAGRUTTA, A., ADELMAN, J.P. & NORTH, R.A. (1993). Single amino acid substitution affects desensitization of the 5-hydroxytryptamine type 3 receptor expressed in *Xenopus* oocytes. *Proc. Natl. Sci. U.S.A.*, **90**, 5030–5033.

YAKEL, J.L., SHAO, X.M. & JACKSON, M.B. (1990). The selectivity of the channel coupled to the 5-HT$_3$ receptor. *Brain Res.*, **533**, 46–52.

YANG, J. (1990). Ion permeation through 5-hydroxytryptamine-gated channels in neuroblastoma N18 cells. *J. Gen. Physiol.*, **96**, 1177–1198.

YANG, J., MATHIE, A. & HILLE, B. (1992). 5-HT$_3$ receptor channels in dissociated rat superior cervical ganglion neurones. *J. Physiol.*, **448**, 237–256.

ZHENG, X., ZHANG, L., DURAND, G.M., BENNETT, M.V.L. & ZUKIN, R.S. (1994). Mutagenesis rescues spermine and Zn^{2+} potentiation of recombinant NMDA receptors. *Neuron*, **12**, 811–818.

(Received October 21, 1994
Revised November 28, 1994
Accepted December 1, 1994)

British Journal of Pharmacology (1995) 114, 1222–1226

A novel enhancing effect of clofilium on transient outward-type cloned cardiac K^+ channel currents

[1]Tsutomu Kobayashi, Gabor Mikala & Atsuko Yatani

Department of Pharmacology and Cell Biophysics, University of Cincinnati College of Medicine, Cincinnati, OH 45267-0575, U.S.A.

1 The antiarrythmic drug, clofilium, has been shown to block several types of K^+ channel currents. To investigate the effects of clofilium on the transient outward K^+ current (I_{to}), a cloned I_{to}-type cardiac K^+ channel (RHK1) was expressed in *Xenopus* oocytes and the drug effects were examined on whole cell currents.

2 Extracellular application of clofilium slightly inhibited the current at + 60 mV from a holding potential of − 80 mV. However, it unexpectedly enhanced the current from a holding potential of − 60 mV in a dose-dependent manner (219 ± 39% of control at 100 μM).

3 This enhancement is probably due to an increase in the ratio of channels in the resting state during steady depolarization, since clofilium shifted the inactivation curve in the depolarizing direction.

4 LY97119, a tertiary ammonium analogue of clofilium, did not exhibit this enhancing effect but only inhibited the current.

5 Clofilium may be useful for the study of channel inactivation because this type of phenomenon has not been reported for any other drug.

Keywords: K^+ channel; transient outward; inactivation; antiarrythmic drug; clofilium

Introduction

Clofilium (Figure 1) is one of the class III antiarrythmic agents, which block K^+ channels in cardiac myocytes, prolong the action potential duration and exhibit antiarrythmic effects. This compound blocks the delayed rectifier (I_K) (Arena & Kass, 1988; Reeve & Peers, 1992), the ATP-sensitive K^+ channels (Sakuta *et al.*, 1993) and I_{sk} (Folander *et al.*, 1990). The drug has also been reported to block the transient outward current (I_{to}) in isolated ventricular myocytes, but a long exposure time was required for its action (Castle, 1991).

I_{to} is assumed to be very important in the function of cardiac cells, since it determines the membrane potential of the plateau phase during the action potential that modulates other following voltage-dependent ion channels (Ten Eick *et al.*, 1992). However, the presence of multiple overlapping ion channels in native cardiac cells complicates the study of drug-channel interactions (Colansky *et al.*, 1990).

In an attempt to overcome some of these difficulties, we have examined the inhibitory effects of clofilium on a cloned I_{to}-type cardiac K^+ channel (a *Shaker* type, RHK1) (Tseng-Crank *et al.*, 1990) expressed in *Xenopus* oocytes. During the course of this study, we found that clofilium unexpectedly and dramatically enhanced the current when the resting membrane potential was slightly depolarized and the channels were partially inactivated. This phenomenon is interesting because this type of effect has not been reported for clofilium or any other drugs. This paper describes the enhancing effect on a cloned I_{to} current RHK1 by clofilium that has been known as a K^+ channel blocker.

Methods

The cDNA encoding RHK1 was previously isolated from a rat heart cDNA library (Tseng-Crank *et al.*, 1990). Runoff transcripts of the cRNA were prepared and microinjected into *Xenopus* oocytes in portions of 50 nl per oocyte (50–100 ng μl^{-1}). After injection, the oocytes were maintained at 15–20°C in modified Barth's medium (in mM: NaCl 96, KCl 2, $CaCl_2$ 1.8, $MgCl_2$ 1, sodium pyruvate 2.5, theophylline 0.5, pH 7.3 with Tris base) in the presence of penicillin (100 units ml^{-1}), streptomycin (100 μg ml^{-1}) and gentamicin (50 μg ml^{-1}). These cells were used for experiments within 1 to 3 days after injection.

A two-microelectrode voltage clamp method was used with 3 M KCl-filled electrodes (1 to 2 MΩ) connected to a voltage clamp amplifier (Axoclamp 2A, Axon Instruments Inc, Burlingame, CA, U.S.A.) to measure the whole cell K^+ current. The pCLAMP software (Axon Instruments) was used for data acquisition and analysis. Currents were digitized at 5 kHz after being filtered at 1 kHz. To remove whole cell leak and capacitative currents, pulse protocols contained four hyperpolarizing pulses of one-quarter the test pulse amplitude before a test pulse, unless otherwise indicated. The current responses to all five of these pulses were summed by the pCLAMP system (the P/4 procedure). Recovery from inactivation of RHK1 required longer than 10 s, and voltage-clamp pulses were applied every 15 or 20 s.

A low Cl external solution was used to minimize Ca-activated Cl currents (in mM: N-methyl-D-glucamine 120, methanesulphonic acid 120, KOH 2.5, $MgCl_2$ 2 and HEPES

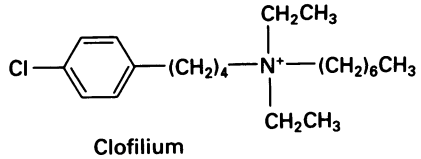

Clofilium

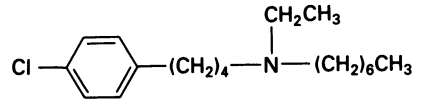

LY97119

Figure 1 Chemical structures of clofilium and LY97119.

[1] Author for correspondence at present address: Pharmacological Research Laboratory, Tanabe Seiyaku Co. Ltd., 2-2-50 Kawagishi, Toda, Saitama 335, Japan.

10, pH 7.4 with Tris base). The experimental chamber (0.3 ml in volume) was perfused continuously with gravity flow at a rate of 2 ml min^{-1}. The solution in the chamber was replaced within 30 s. All experiments were performed at room temperature (20–22°C).

Clofilium tosylate obtained from Research Biochemicals Inc. (Natick, Mass, U.S.A.) and LY97119 (Figure 1) donated by E. Lilly (Indianapolis, U.S.A.) were dissolved in ethanol at 10 and 100 mM and diluted to a final concentration with the external solution. Ethanol did not show any effect on currents even at the highest concentration (0.3%).

The experimental values were expressed as means ± s.e. mean. Statistical significance was tested by Student's paired, two-tailed t test, unless otherwise indicated.

Results

Effects of clofilium on I_{to} from a holding potential of − 80 mV

The oocytes injected with the cRNA encoding RHK1 exhibited K^+ currents that showed rapid activation and inactivation in response to depolarizing voltage clamp pulses. Because these currents are inactivated easily at a positive holding potential, we first tested the effects of clofilium at a holding potential of − 80 mV. Figure 2 shows the effects of clofilium (10, 100 μM) on RHK1 currents elicited by successive depolarizing pulses to + 40 mV from a holding potential of − 80 mV. Application of clofilium did not influence the peak amplitude nor the activation rate. However, it accelerated the inactivation of currents in a concentration-dependent manner. Under the control conditions, the time course of inactivation could be fitted to a single exponential function with time constants of 33.5 ± 1.8 and 34.3 ± 1.9 ms ($n = 5$) at + 20 and + 60 mV, respectively. Four minutes after perfusion with 100 μM clofilium, the time course was also well-fitted to a single exponential function. However, the time constants decreased significantly to 27.4 ± 0.8 ms ($n = 5$, $P<0.02$) and 25.3 ± 1.0 ms ($n = 5$, $P<0.01$) at + 20 and + 60 mV, respectively.

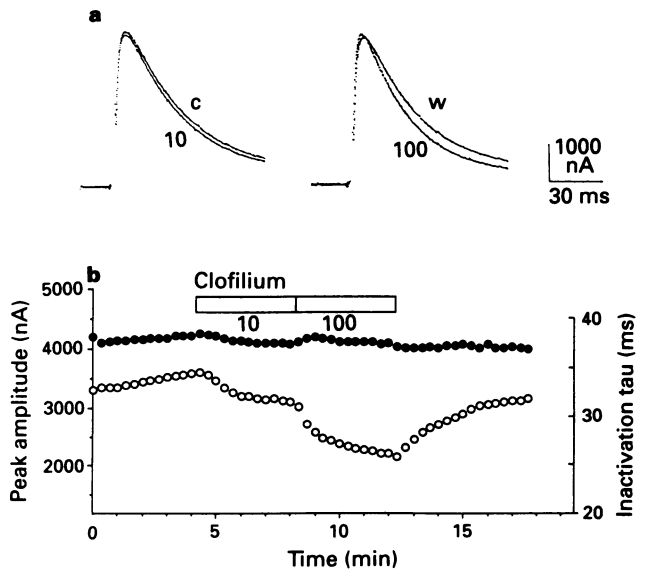

Figure 2 Effects of clofilium (10, 100 μM) on the current of cloned transient outward-type K^+ channel (RHK1) in oocytes injected with RHK1 cRNA. Currents were elicited by 250 ms depolarizing pulses (+ 40 mV) from a holding potential of − 80 mV at intervals of 20 s. (a) Original current tracings before (C) and during superfusion with 10 and 100 μM clofilium (10,100) and after washout (W). (b) Time course of the effects on the I_{to} amplitude (●) and the rate of current inactivation (○).

Effects of clofilium on I_{to} from a holding potential of − 60 mV

The capability of many compounds to block voltage-dependent ion channels is strongly affected by the holding potential in voltage-clamp experiments. For example, dihydropyridines block Ca^{2+} channels more strongly in depolarized cells (Bean, 1984). Therefore, oocytes were maintained at a holding potential of − 60 mV, and the effects of clofilium were tested by successive depolarizing pulses at an interval of 20 s. Figure 3 shows the time courses of the onset of and the recovery from the effects of clofilium. Clofilium dramatically enhanced the currents in a dose-dependent manner. In view of the speed of solution replacement in the experimental chamber, the current amplitude increased and reached a new steady state by the time we measured currents after exposure to clofilium. Recovery from the elevated amplitude occurred with almost the same speed as the onset of enhancement. At the holding potential of − 60 mV, the acceleration of current inactivation by clofilium was observed as was seen at a holding potential of − 80 mV. The time courses of the onset of and recovery from this effect were slower than those of the enhancement effect on the current amplitude.

The enhancement of current amplitude by clofilium was observed at a wide range of depolarizing pulse potentials from − 20 to 60 mV, but was not at the pulse potential of − 40 mV (Figure 4). The peak amplitudes were 268 ± 54 and 1478 ± 276 nA ($n = 5$) at depolarizing pulse potentials of − 20 and + 60 mV, respectively, before application of clofilium, but they increased significantly to 530 ± 99 ($n = 5$, $P<0.02$) and 3096 ± 584 nA ($n = 5$, $P<0.05$) at − 20 and + 60 mV, respectively, after application of 100 μM clofilium.

Steady-state inactivation

Steady-state inactivation was studied by use of a standard double-pulse protocol. Measurements were made before and

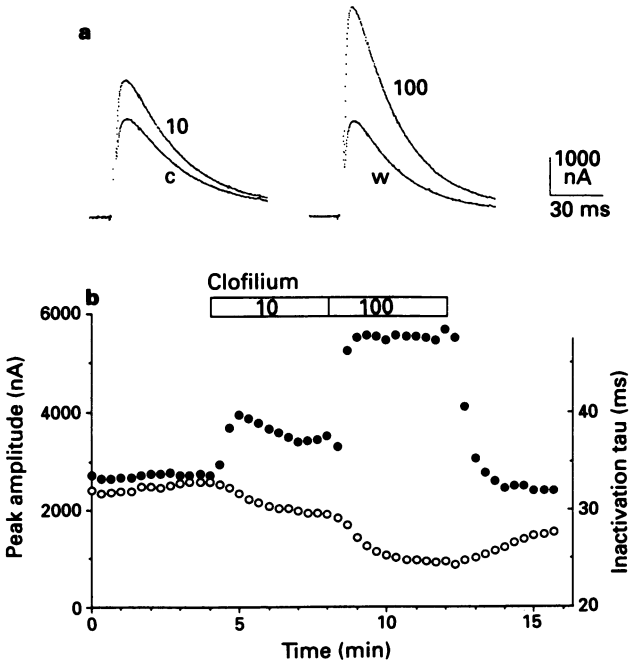

Figure 3 Effects of clofilium (10, 100 μM) on the current of cloned transient outward-type K^+ channels (RHK1) elicited from a holding potential of − 60 mV. Depolarizing pulses of 250 ms in duration (+ 40 mV) were given at intervals of 20 s. (a) Original current tracings before (C) and during superfusion with 10 and 100 μM clofilium (10,100) and after washout (W). (b) Time courses of the effects on the I_{to} amplitude (●) and the rate of current inactivation (○).

4 min after superfusion with clofilium for each oocyte. In the presence of clofilium (100 μM), when the depolarizing conditioning pulse was at − 70 mV, the current amplitude during the second pulse did not change. However, the current was markedly enhanced when the conditioning pulse was at − 55 mV (Figure 5a). Finally, we found that clofilium shifted the inactivation curve in the direction of depolarization (Figure 5b). In order to quantify the steady-state inactivation, the current amplitude of each second pulse was normalized to the control amplitude (no conditioning pulse and no drug) to give relative I, and plotted against the membrane potential of the conditioning pulse. For each individual cell, the equation of Boltzmann distribution was well fitted to the points and those parameters are shown in Table 1. I_{max} (relative) was 0.92–0.96 in the presence of 10–300 μM clofilium. This indicates that clofilium does not change the amplitude of the maximum current obtained at large negative conditioning potentials (− 70 to − 80 mV). The slope factor, s, was 3.88 mV for control and did not change significantly after application of clofilium (Table 1). The mid-potential, Vh, was − 61.13 ± 0.70 for the control conditions and it was shifted by clofilium in the direction of more positive potentials: − 57.62 ± 0.82 and − 50.87 ± 0.75 at 10 and 100 μM, respectively. The effect of 300 μM clofilium was similar to that of 100 μM.

Effects of LY97119

LY97119(LY) is a desethyl tertiary ammonium derivative of clofilium, although clofilium is a quaternary ammonium, positively-charged compound. Figure 6 shows the effects of

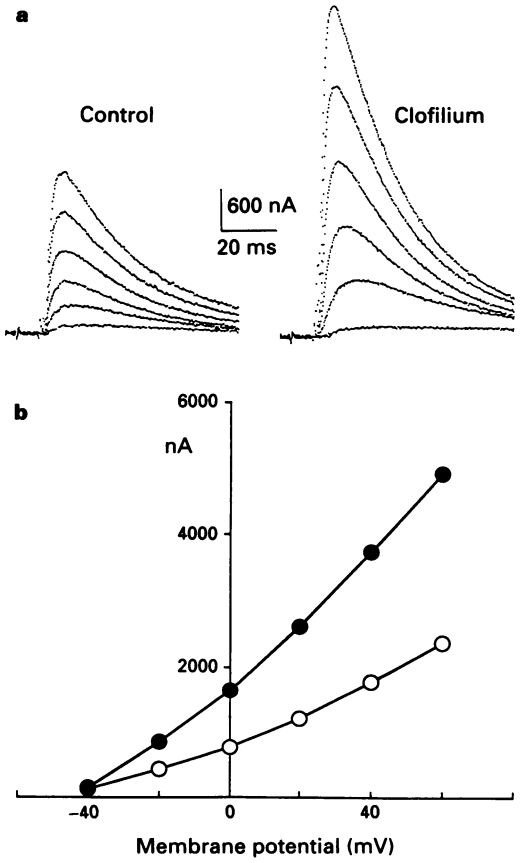

Figure 4 (a) Original current tracings before (left) and after superfusion with 100 μM clofilium (right). Currents were elicited by 250 ms depolarizing pulses from a holding potential of − 60 mV to test potentials between − 40 and + 60 mV with 20 mV increments. (b) The peak amplitude of RHK1 current in the absence (○) and the presence of 100 μM clofilium (●) in the above experiment was plotted against the depolarizing step potentials.

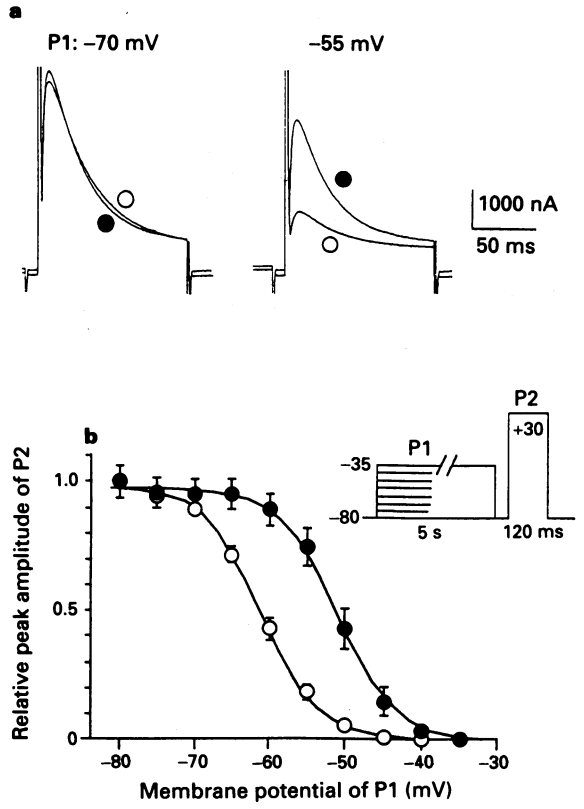

Figure 5 Effects of clofilium on the voltage-dependent inactivation of the cloned transient outward-type K^+ channel (RHK1) current. (a) Current tracings during pulse 2 (P2, see the inset in (b) for pulse protocol) in the absence and presence of 100 μM clofilium. The oocyte was held at − 80 mV and stepped to − 70 (left) or − 55 mV (right) for 5 s and then stepped to + 30 mV to activate the RHK1 current. The interpulse interval was 10 ms, and a double pulse was applied every 20 s. Leak and capacitative currents were not subtracted. (b) Graph indicating voltage-dependence of inactivation. The current amplitudes during P2 pulse plotted against membrane potentials of P1 are expressed as relative values to that during P2 pulse following P1 pulse at − 80 mV in the absence of drug. Solid lines are drawn according to Boltzman distribution: $I_{max} = 1/\{1 + \exp[(V\text{-}Vh)/3.8]\}$, where I is the relative current of P2 and V is the membrane potential of P1. The midpotential, Vh, and the maximum current, I_{max}, were − 61.1 mV and 0.98, respectively, for the control conditions (○, $n = 9$) and − 51.0 mV and 0.97 in the presence of 100 μM clofilium (●, $n = 4$). Each point represents the mean ± s.e.mean.

Table 1 Inactivation parameters for RHK1 channels before and after application of clofilium and LY97119

	I_{max}	Vh (mV)	s (mV)	n
Control	0.99 ± 0.01	− 61.13 ± 0.70	3.88 ± 0.12	9
Clofilium				
10 μM	0.96 ± 0.07	− 57.62 ± 0.82*	3.89 ± 0.18	4
30 μM	0.92 ± 0.04	− 56.53 ± 0.84**	3.81 ± 0.15	4
100 μM	0.97 ± 0.06	− 50.87 ± 0.75**	3.32 ± 0.18	4
300 μM	0.93 ± 0.04	− 51.07 ± 1.89**	3.65 ± 0.49	4
LY97119				
100 μM	0.72 ± 0.05**	− 61.90 ± 0.32	3.89 ± 0.23	5

The figures are parameters for the best fit curves of the equation: $I/I_{max} = 1/\{1 + \exp[(V\text{-}Vh)/s]\}$, where I is the peak amplitude of currents during P2, I_{max} is the maximum current, Vh is the midpotential and s is the slope factor. Before curve fitting, the currents were normalized by taking the maximum current (P1 = − 80 mV) in the absence of drug as 1.0 for each oocyte. *$P < 0.02$. **$P < 0.01$, unpaired t test.

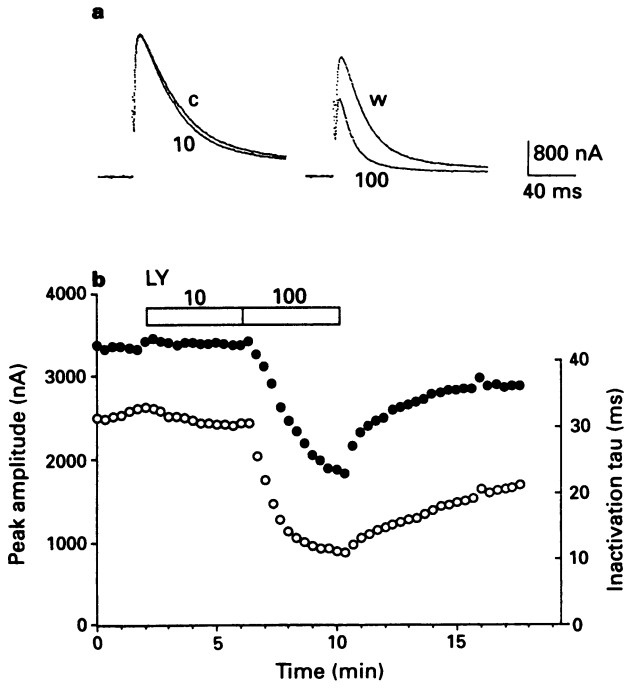

Figure 6 Effects of LY97119 (LY) (10, 100 μM) on the current of cloned transient outward-type K^+ channels (RHK1) in oocytes injected with RHK1 cRNA. Currents were elicited by 250 ms depolarizing pulses (+ 40 mV) from a holding potential of − 60 mV at intervals of 20 s. (a) Original current tracings before (C) and during superfusion with 10 and 100 μM LY (10,100) and after washout (W). (b) Time courses of effects on the I_{to} amplitude (●) and on the rate of current inactivation (○).

LY on the same system under the same conditions as those in the experiment shown in Figure 3 for clofilium. At a concentration of 10 μM, LY accelerated inactivation of the current without having an effect on the current amplitude. Increasing the concentration to 100 μM did not enhance the current amplitude unlike clofilium, but decreased it: 2630 ± 399 and 1110 ± 164 nA ($n = 6$, $P<0.01$) before and after application of LY, respectively.

A large acceleration of current inactivation was observed as was seen with clofilium. The time courses of the onset and recovery were similar to those of the decrease in peak amplitude of currents. The time constant of current inactivation during + 40 mV depolarizing pulses was 30.0 ± 0.9 ms ($n = 5$) before application of LY. After perfusion of LY (100 μM), it decreased significantly to 18.0 ± 3.1 ms ($n = 5$, $P<0.01$).

The effects of LY (100 μM) on steady state inactivation are shown in Table 1. I_{max} was 0.72 for LY, indicating that LY suppressed the current amplitude also at a holding potential of − 80 mV as well as at − 60 mV. The slope factor, s, did not change upon application of LY, and there was no significant difference between the Vh values before and after perfusion with LY.

Discussion

Site of action of clofilium

Clofilium exhibited two distinct effects on I_{to}. One was an acceleration of current inactivation, and the other an augmentation of current amplitude when channels were maintained at a depolarizing holding potential.

The former effect is similar to its inhibitory effect on I_{to} of isolated cardiac cells (Castle, 1991) or on I_K of NG 108-15 cells (Reeve & Peers, 1992). Since this effect is not accompanied by modulation of the activation rate, clofilium acts on the activated state of channels and blocks the channel, or it accelerates conversion to the inactivated state from the open state. They reported that the onset of this effect was very slow and irreversible. In our oocyte experiments, where the environment surrounding the channels was different from that of cardiac cells, a partial and slow recovery from the effect was observed, but the onset of effect was also slow. On the other hand, LY, the analogue without a permanent positive charge, showed a faster onset and a stronger effect than clofilium. Therefore, the site of action is likely to be an intramembrane or intracellular site of the channel, as speculated by Castle (1991). Although clofilium has a permanent charge, it has a lipophilic nature as a whole. With a long exposure time, clofilium may be able to reach the binding site.

The second effect, an enhancement of the current, is considered to be elicited by clofilium bound to another site. Evidence supporting this second binding site is twofold: the time course of the onset of and recovery from the enhancement effect is different from that of the former effect, and the analogue LY showed only the former, inhibitory effect without the latter, enhancing effect. This binding site is probably extracellular, because the onset and washout of the clofilium effect was very fast in spite of the permanent charge carried by the clofilium molecule. Since the nitrogen of LY is mostly protonated in an aqueous environment ($pK_a = 9.3$), LY also has a positive charge in extracellular solution like clofilium. The difference between LY and clofilium is the presence of an ethyl group linked to the nitrogen in clofilium. Therefore, the extracellular site may recognize and accommodate the hydrophobic and bulky ethyl group.

Clofilium and channel inactivation

The clofilium-induced enhancement of the current occurs by a shift of the inactivation curve in the direction of more positive potentials. This is a parallel shift since clofilium does not shift the curve vertically. Therefore, at a holding potential of − 80 mV, where no inactivation occurs, clofilium does not show the enhancement effect. However, under depolarized conditions, where the channels are partially inactivated, clofilium increases the current amplitude.

The inactivation curve of Figure 5, expressed by

$$I/I_{max} = 1/\{1 + \exp((V - Vh)/s)\}$$

is originally the equation of Boltzman's distribution, the ratio of the number of resting channels ([R]) in the total number of channels ([R] + [I]) in a steady state:

$$[R]/([R] + [I]) = 1/\{1 + \exp[-(E_I - E_R)/RT)]\}$$

where E_R and E_I are the energy levels of the resting and inactivated states, respectively. Therefore, the difference in energy level between the two states ΔE at a membrane potential V is

$$\Delta E = E_I - E_R = -RT(V - Vh)/s.$$

Under the control conditions, s = 3.88 mV, Vh = −61.13 mV, and RT = 2.44 kJ mol^{-1} (21°C), the difference is − 0.71 kJ mol^{-1} at − 60 mV, which means the channel favours the inactivated state a little more than the resting state. However, in the presence of 100 μM clofilium, where most channels carry the bound clofilium because the effect was maximal at 100 μM, ΔE increases to 5.75 kJ mol^{-1} (Vh = − 50.87 mV). This means that the binding of clofilium changes the stability of the respective conformations of the channel protein and makes the resting state more stable by 5.75 kJ mol^{-1} than the inactivated state at − 60 mV. Therefore, the number of channels in the resting state is much greater than that in the inactivated state. This would result in an increase in current when the depolarizing pulse is applied.

The increase in ΔE by clofilium is independent of the membrane potential:

$$\Delta E_{drug} - \Delta E_{control} = -RT\ (Vh_{control} - Vh_{drug})/s$$

Calculation yields 6.46 kJ mol^{-1} at 100 μM at all potentials. Therefore, even at a holding potential of − 80 mV, clofilium modulates ΔE to the same extent as at − 60 mV. However, at a holding potential of − 80 mV, most of channels are in resting state even without drug, and therefore the same effect of clofilium on the channel protein does not result in the increase in measurable currents. The value 6.46 kJ mol^{-1} is not so large, compared to 19 kJ mol^{-} of the stabilizing energy by one hydrogen bond (Lehninger, 1975).

This effect is unique and there is no other compound known to act in a similar manner. Bay K8644 also increases the current of Ca^{2+} channels, but it is not due to the shift of inactivation curve in the depolarizing direction. Bay K8644, as well as other dihydropyridines, shifts the curve in the hyperpolarizing direction (Sanguinetti *et al.*, 1986).

Physiological implications

Clofilium has two effects, an inhibitory one and an enhancement of I_{to}. Under depolarized conditions, because the enhancing effect is larger than the inhibitory one, the overall amount of current at a holding potential of − 60 mV becomes larger in the presence of clofilium than in its absence (Figure 7). This means that the effects of clofilium on cells depends on the conditions.

Clofilium is well known as an antiarrythmic drug. The mechanism has been explained by its inhibitory effect on I_K (Arena & Kass, 1988) and the following prolongation of the action potential duration. Compared to I_K, the role of I_{to} on the action potential has been poorly understood. Beuckelmann *et al.* (1993) showed that 4-aminopyridine inhibited I_{to} and increased action potential duration. However, the prolonged action potential duration may not be due to I_{to} inhibition because 4-aminopyridine is well known to inhibit I_K. On the other hand, Zhang *et al.* (1991) reported that 4-aminopyridine blocked I_{to} but shortened the action potential duration.

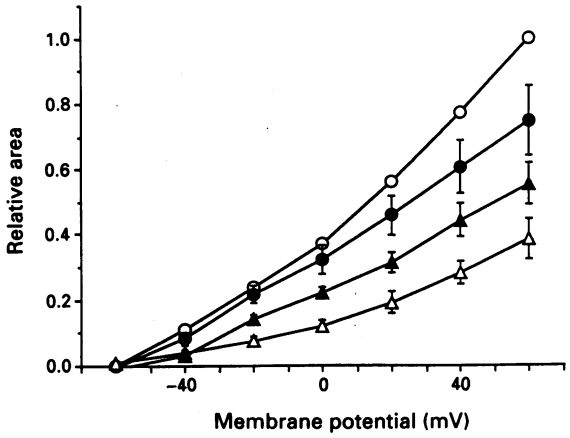

Figure 7 Total amount of RHK1 currents, which are the area under current tracings during 250 ms and expressed as relative values to the maximum current (+ 60 mV depolarization from a − 80 mV holding potential in the absence of drug) for each oocyte. Control conditions from a holding potential of − 80 (○) or − 60 mV (△) and in the presence of 100 μM clofilium from a holding potential of − 80 (●) or − 60 mV (▲). Each point represents the mean ± s.e.mean of 5 experiments.

I_{to} determines the membrane potential of the plateau phase that has a profound influence on both Ca^{2+} currents and I_K during the action potential, and has a major role in the activity of cardiac cells. Therefore, it is of interest whether the effect of clofilium on a cloned I_{to} channel RHK1 is also observed in native cardiac I_{to}.

We would like to thank Prof. A. Schwartz for his support and encouragement. We also thank Drs S. Eager and S. Takeyama for critical review of the manuscript and E. Lilly Co. for supplying us with LY97119.

References

ARENA, J.P. & KASS, R.S. (1988). Block of heart potassium channels by clofilium and its tertiary analogs; Relationship between drug structure and type of channel blocked. *Mol. Pharmacol.*, **34**, 60–66.

BEAN, B.P. (1984). Nitrendipine block of cardiac Ca channels: High-affinity binding to the inactivated state. *Proc. Natl. Acad. Sci. U.S.A.*, **81**, 6388–6392.

BEUCKELMANN, D.J., NABAUER, M. & ERDMANN, E. (1993). Alterations of K currents in isolated human ventricular myocytes from patients with terminal heart failure. *Circ. Res.*, **73**, 379–385.

CASTLE, N.A. (1991). Selective inhibition of potassium currents in rat ventricle by clofilium and its tertiary homolog. *J. Pharmacol. Exp. Ther.*, **257**, 342–350.

COLANSKY, T.J., FOLLMER, C.H. & STARMER, C.F. (1990). Channel Specificity in antiarrythmic drug action. *Circulation*, **82**, 2235–2242.

FOLANDER, K., SMITH, J.S., ANTANAVAGE, J., BENNETT, C., STEIN, R.B. & SWANSON, R. (1990). Cloning and expression of the delayed-rectifier I_{sk} channel from neonatal rat heart and diethylstilbestrol-primed rat uterus. *Proc. Natl. Acad. Sci. U.S.A.*, **87**, 2975–2979.

LEHNINGER, A.L. (1975). In *Biochemistry*, p.69. New York: Worth Publishers.

REEVE, H.L. & PEERS, C. (1992). Blockade of delayed rectifier K currents in neuroblastoma x glioma hybrid (NG 108-15) cells by clofilium, a class III antidysrhythmic agent. *Br. J. Pharmacol.*, **105**, 458–462.

SAKUTA, H., OKAMOTO, K. & WATANABE, Y. (1993). Antiarrythmic drugs, clofilium and cibenzoline are potent inhibitors of glibenclamide-sensitive K currents in *Xenopus* oocytes. *Br. J. Pharmacol.*, **109**, 866–872.

SANGUINETTI, M.C., KRATTE, D.S. & KASS, R.S. (1986). Voltage-dependent modulation of Ca channel current in heart cells by BayK8644. *J. Gen. Physiol.*, **88**, 369–392.

TEN EICK, R.E., WHALLEY, D.W. & RASMUSSEN, H.H. (1992). Connections: heart disease, cellular electrophysiology, and ion channels. *FASEB J.*, **6**, 2568–2580.

TSENG-CRANK, J.C.L., TSENG, G.N., SCHWARTZ, A. & TANOUYE, M.A. (1990). Molecular cloning and functional expression of a potassium channel cDNA isolated from a rat cardiac library. *FEBS Lett.*, **268**, 63–68.

ZHANG, K., HARVEY, R.D., BARRINGTON, P.L., SCHACKOW, T.E., BASSETT, A.L. & TEN EICK, R.E. (1991). Transient outward current in normal and hypertrophied cat right ventricular myocytes. *Biophys. J.*, **59**, 559.

(Received September 1, 1994
Revised November 11, 1994
Accepted November 17, 1994)

British Journal of Pharmacology (1995) 114, 1227-1235

Antiproliferative effects of A02011-1, an adenylyl cyclase activator, in cultured vascular smooth muscle cells of rat

[1]Sheu-Meei Yu, Zhi-Jiao Cheng & *Sheng-Chu Kuo

Department of Pharmacology, Chang Gung Medical College, 259 Wen-Hwa 1st Road, Kwei-San, Tao-Yuan and *Institute of Pharmaceutical Chemistry, China Medical College, Taichung, Taiwan

1 The effects of A02011-1, a pyrazole derivative, on the proliferation of rat vascular smooth muscle cells (VSMCs) were examined.

2 A02011-1 (1-100 μM) concentration-dependently inhibited [^{3}H]-thymidine incorporation into DNA in rat VSMCs that were synchronized by 48 h serum depletion and then re-stimulated by addition of foetal calf serum (FCS, 10%), platelet-derived growth factor (PDGF, 10 ng ml^{-1}), 5-hydroxytryptamine (10 μM) or ADP (10 μM). The inhibitory effect of A02011-1 was fully reversible. However, FCS-induced [^{3}H]-thymidine incorporation into rat endothelial cells was unaffected by A02011-1.

3 The concentration of A02011-1 necessary for inhibition of the FCS-induced proliferation was similar to that necessary for adenosine 3':5'-cyclic monophosphate (cyclic AMP) formation. Adenylyl cyclase activity was increased in A02011-1-treated VSMCs, whereas cyclic AMP-specific phosphodiesterase activity was unchanged.

4 A02011-1 was equipotent with forskolin but was more potent than 8-bromo-cyclic AMP against FCS (10%)-induced proliferation.

5 The antiproliferative action of A02011-1 was mimicked by 8-bromo-cyclic AMP, a membrane-permeable cyclic AMP analogue and was antagonized by 2',5'-dideoxyadenosine, an adenylyl cyclase inhibitor and by Rp-cyclic AMPS, a competitive inhibitor of cyclic AMP-dependent protein kinase (PKA) type I and II. 3-Isobutyl-1-methylxanthine (IBMX) caused significant potentiation of the antiproliferative activity of A02011-1. However, Rp-8-bromo-cyclic GMPS and staurosporine did not affect the antiproliferative activity of A02011-1.

6 A02011-1 still inhibited the FCS-induced DNA synthesis even when added 10-18 h after re-stimulation of the serum-starved VSMCs with 10% FCS. Flow cytometry in synchronized cells revealed an acute blockade of FCS-inducible cell cycle progression at a point in the G_1/S phase in A02011-1-treated cells. The inhibition of proliferation by A02011-1 was shown to be independent of cell damage, as documented by several criteria of cell viability.

7 These results indicate that A02011-1 inhibition of VSMC proliferation was mediated by cyclic AMP and was due to a delay in the progression from the G_1 into S phase of the cell cycle. A02011-1 did not cause cell toxicity and may thus hold promising potential for the prevention of atherosclerosis or vascular diseases.

Keywords: A02011-1; adenylyl cyclase activator; cyclic AMP; antiproliferation; vascular smooth muscle cells

Introduction

Cardiovascular disease remains the chief cause of death in the United States and Western Europe, and atherosclerosis, the principal cause of myocardial and cerebral infarction, accounts for the majority of these deaths (Ross, 1986). Vascular smooth muscle cell (VSMC) proliferation is the key event in the development of the advanced lesions of atherosclerosis. Abnormal proliferation of VSMCs is also a major component of vascular disease, including vascular rejection and re-stenosis following angioplasty (Ross & Glomset, 1973; Ross, 1986). Therefore, modulation of VSMC proliferation has critical therapeutic implications for atherosclerosis and vascular disease.

Extracellular signals such as hormones, neurotransmitters and growth factors control the proliferation of their target cells by binding to specific membrane receptors and thus activating a signalling cascade within the cell. Two stimulating pathways have been partly characterized: the phosphatidylinositol-Ca^{2+} cascade and the receptor protein tyrosine kinase pathway (Dumont *et al.*, 1989). Another pathway is the adenylyl cyclase/adenosine 3':5'-cyclic monophosphate (cyclic AMP) system. The role of cyclic in the regulation of mammalian cell proliferation has been the subject of controversy (Pastan *et al.*, 1975; Dumont *et al.*, 1989). In the yeast *Saccharomyces cerevisiae*, cyclic AMP is the positive signal for growth elicited in response to a sufficient nutrient supply (Dumont *et al.*, 1989). However, cyclic AMP functions as a negative regulator of proliferation in a variety of cell types including VSMCs (Loesberg *et al.*, 1985; Andersson *et al.*, 1994; Bennett *et al.*, 1994). Intracellular concentrations of cyclic AMP are determined by its relative rate of formation, via stimulating adenylyl cyclase, and rate of hydrolysis by phosphodiesterase (PDE) enzymes. Intracellular elevation of cyclic AMP with a subsequent activation of cyclic AMP-dependent protein kinase (PKA) plays a key role in the regulation of DNA replication in a number of cells (Skalhegg *et al.*, 1992).

A02011-1 (3-(5'-hydroxymethyl-2'-furyl)-1-benzyl thieno[3,-2-c]pyrazole) (Figure 1), a novel adenylyl cyclase activator, was chemically synthesized as described by Yoshina & Kuo (1978). We found previously that A02011-1 possessed vaso-relaxant effects in rat aorta as well as antiaggregatory effects in human platelet via increasing cyclic AMP concentration, both of which protect the vascular wall against arteriosclerotic changes. In this study, A02011-1 is found to inhibit proliferation of rat VSMCs, and an attempt is made to characterize its modes of action.

[1] Author for correspondence.

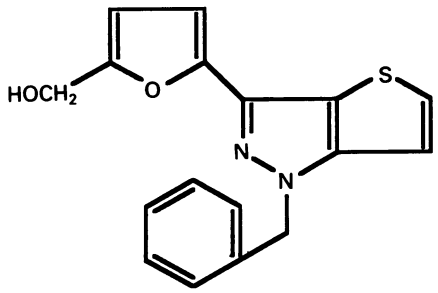

Figure 1 Chemical structure of A02011-1.

Methods

Cell culture

Vascular smooth muscle cells (VSMCs) were harvested from enzymatically dissociated rat thoracic aorta according to the method of Beasley *et al.* (1991) with some minor modifications. The thoracic aorta was excised, under sterile conditions, from male Wistar rats (300–350 g) and placed in ice cold Dulbecco's phosphate buffered saline (PBS, Ca^{2+} and Mg^{2+}-free) with penicillin (100 unit ml^{-1}), streptomycin (200 $\mu g\ ml^{-1}$) and amphotericin B (25 $\mu g\ ml^{-1}$). The aorta was washed and transferred to a Petri dish containing Hanks Balanced Salt Solution (HBSS). Fat, connective tissue, and adventitia were removed by blunt dissection. The cleaned aortae were opened and the endothelium carefully scraped off. Fine pieces of aorta were transferred to a 15 ml plastic centrifuge tube and incubated for 90 min at 37°C in HBSS containing $CaCl_2$ (0.2 mM), HEPES (15 mM), collagenase (type II, 1 $mg\ ml^{-1}$), elastase (type III, 0.125 $mg\ ml^{-1}$), and bovine serum albumin (2 $mg\ ml^{-1}$). The digested tissue was triturated 10 times through an 18-gauge needle, sieved through nylon mesh, and the resulting cell suspension centrifuged at 200 *g* for 5 min. The cells were resuspended in Dulbecco's modified Eagle's medium (DMEM) containing 10% foetal calf serum (FCS), L-glutamine (2 mM), penicillin (100 unit ml^{-1}), streptomycin (200 $\mu g\ ml^{-1}$) and amphotericin B (2.5 $\mu g\ ml^{-1}$) and seeded into 75 cm^2 flasks. After reaching confluence, cells were passaged by harvesting with 0.1% trypsin-4 mM EDTA, placed in an equal volume of medium, and centrifuged at 600 *g* for 5 min. The cells were characterized as smooth muscle cells by morphology and immunostaining with antibodies to smooth muscle α-actin.

[^{3}H]-thymidine incorporation

VSMCs were finally grown in 24 well plates (2.5×10^4 cells/well), washed twice with 1 ml Krebs-Henseleit solution (KHS) which contained (mM): NaCl 117.5, KCl 5.6, $MgSO_4$ 1.18, NaH_2PO_4 1.2, $NaHCO_3$ 25.0., glucose 5.5, HEPES 25.0 and $CaCl_2$ 2.5, then incubated in 0.5 ml DMEM/FCS-free for 48 h to induce quiescence (cell cycle stopped at G_0 phase) at 37°C. To investigate the effect of A02011-1 on proliferation, quiescent cells were cultured for 20 h in medium supplemented with or without 10% FCS, containing or lacking experimental agents. Finally, cells were incubated for 2 h in freshly prepared medium that was additionally supplemented with [^{3}H]-thymidine (1 $\mu Ci\ ml^{-1}$) to measure DNA synthesis by thymidine incorporation (Grainger *et al.*, 1991; Morinelli *et al.*, 1994). The experiments were terminated by washing cells with 1 ml KHS, precipitation of acid-insoluble material with 10% trichloroacetic acid (TCA) and extraction of the DNA with 0.1 N NaOH. The precipitates were collected on Whatman GF/B filters, and filters were washed twice with 5 ml of ice-cold KHS. Filters were cut into pieces and shaken with 3.5 ml scintillation fluid for 24 h before liquid scintillation counting.

Measurement of cyclic AMP and cyclic GMP

Cyclic AMP and cyclic GMP concentrations in rat VSMCs were assayed as previously described (Karniguian *et al.*, 1982; Kariya *et al.*, 1989). VSMCs were finally grown in 35 mm dishes. At confluence, monolayer cells were washed twice with KHS and incubated with forskolin, sodium nitroprusside or A02011-1 for 5 min at 37°C. Incubation was terminated by 0.1 N HCl and then centrifuged at 10,000 *g* for 5 min. Following extraction with ether (1 ml repeated four times), the supernatant was assayed with cyclic AMP or cyclic GMP ELISA kits (Amersham, England).

Adenylyl cyclase assay of rat VSMCs

VSMCs were finally grown in 35 mm dishes. At confluence, monolayer cells were washed with KHS, treated with 0.1% trypsin/4 mM EDTA, and centrifuged at 600 *g* for 5 min. Cells were then resuspended in ice-cold 50 mM Tris-HCl buffer (pH 7.4) and sonicated at 4°C for 10 s bursts (Sonicator W-220F). Homogenates were used for adenylyl cyclase determinations. Adenylyl cyclase activity was determined as previously described by Insel *et al.* (1982). The incubation mixture (100 µl total volume) contained 0.5 mM ATP, 1×10^6 c.p.m. of [α-^{32}P]-ATP, 13 mM $MgCl_2$, 1.0 mM cyclic AMP, 10 mM dithiothreitol, 25 mM creatine phosphate, 1.0 $mg\ ml^{-1}$ of creatine phosphokinase, with or without A02011-1 in a 50 mM Tris-HCl buffer, pH 7.4. Incubations were carried out at 37°C for 10 min with 50 µl (1 $mg\ ml^{-1}$) of enzyme preparation. Incubation was terminated by adding 200 µl of 0.5 N HCl and 200 µl of 1 mM imidazole. The tubes were then heated to 100°C for 3 min in an electric heating block and cooled in an ice bath. To each tube was added 1 ml of 50 mM Tris-HCl buffer, pH 7.4. The contents were stirred and centrifuged at 1000 *g* for 10 min. The supernatant was applied to a neutral alumina column to isolate cyclic AMP for radioassay of ^{32}P and ^{3}H. Recovery of cyclic AMP was estimated by inclusion of [^{3}H]-AMP in the reaction mixture. Protein was determined by using Bradford reagent (Bradford, 1976) (Bio-Rad, Germany), with BSA as standard.

Cyclic AMP-specific phosphodiesterase assay

The suspension of VSMCs, prepared as described above, was sonicated at 4°C for 10 s bursts. The VSMC lysate was centrifuged at 30,000 *g* for 20 min. The supernatant fraction was used for cyclic AMP-specific phosphodiesterase determinations. The phosphodiesterase activity was determined as described previously (Moore *et al.*, 1985). The crude cytosolic enzyme (100 µl, 1.0 $mg\ ml^{-1}$) was incubated with cyclic AMP (10 µM, containing 0.1 µCi [^{3}H]-cyclic AMP) and test compound in a final volume of 0.4 ml (buffer was 50 mM Tris-HCl, 5 mM $MgCl_2$, pH 7.4). After 30 min at 25°C, the samples were heated to 100°C for 1 min before cooling. Snake venom (0.1 ml, 1 $mg\ ml^{-1}$) (from *Ophiophagus hannah* venom) was then added for 30 min to convert the 5'AMP (the product of the phosphodiesterase enzyme) to the uncharged nucleoside, adenosine; 1 ml of anion-exchange resin (Dowex-1) was added to bind all of the unconverted cyclic AMP. This procedure allows for the separation of excess substrate (negatively charged cyclic AMP, bound to the particulate resin) from the noncomplexed product (now, after snake venom degradation, uncharged adenosine). After centrifugation, an aliquot (0.5 ml) of the supernatant was removed for quantitation in a liquid scintillation counter.

Cell cycle analysis

To estimate the proportions of cells in different phases of the cell cycle, cellular DNA contents were measured by flow cytometry as described by March *et al.* (1993). Briefly, cells (2×10^6 cells ml^{-1}) were fixed by 70% ethanol (in PBS) in ice

for 30 min and then resuspended in PBS containing 40 μg ml^{-1} propidium iodide (PI) and 0.1 mg ml^{-1} RNAse (Boehringer, Germany). After 30 min at 37°C, 2 × 10^4 cells were analysed on a FACstar cytofluorometer (Becton-Dickinson; San Jose, USA), exciting at 488 nm and sensing at 585 nm.

Cell growth

To determine the effect of A02011-1 on cell growth, cells were seeded on 12 well plates (density was 2.5 × 10^3/well) and cultured for 48 h in DMEM supplemented with 10% FCS. Cells were then cultured for 48 h in FCS-free medium to induce quiescence. This procedure was followed by culturing for 6 days in medium supplemented with 10% FCS, containing or lacking A02011-1. Culture medium was changed daily and cell numbers were determined by dissociation of adherent cells with trypsin and counting with a haemocytometer.

Data analysis

The results are expressed as the mean ± s.e. mean and accompanied by the number of observations. A one-way analysis of variance (ANOVA) was used for multiple comparison, and if there was significant variation between treatment groups, then the mean values for inhibitors were compared with those for control by Student's t test, and P values of less than 0.05 were considered to be statistically significant.

Drugs

A02011-1 (3-(5'-hydroxymethyl-2'-furyl)-1-benzyl thieno[3,2-c] pyrazole) (Figure 1) was chemically synthesized as described by Yoshina & Kuo (1978). Dulbecco's modified Eagle's medium (DMEM), foetal calf serum (FCS), penicillin G, streptomycin sulphate and all other tissue culture reagents were obtained from Grand Island Biological Co. (GIBCO).

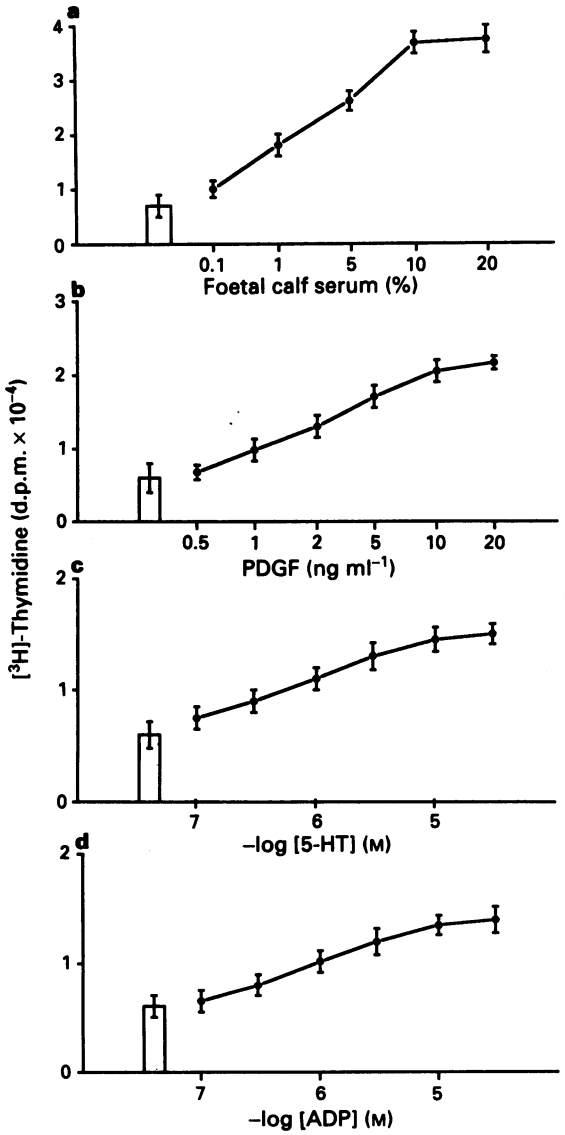

Figure 2 Increase in [^{3}H]-thymidine incorporation in rat vascular smooth muscle cells (VSMCs) stimulated with foetal calf serum (FCS) (a); platelet-derived growth factor (PDGF) (b); 5-hydroxytryptamine (5-HT) (c) and ADP (d). [^{3}H]-thymidine was added 20 h after the quiescent cells had been exposed to mitogens and then incubations were continued for 2 h. Columns represent [^{3}H]-thymidine incorporation in unstimulated cells. Data are expressed as the mean ± s.e. mean (n = 6, each in quadruplicate).

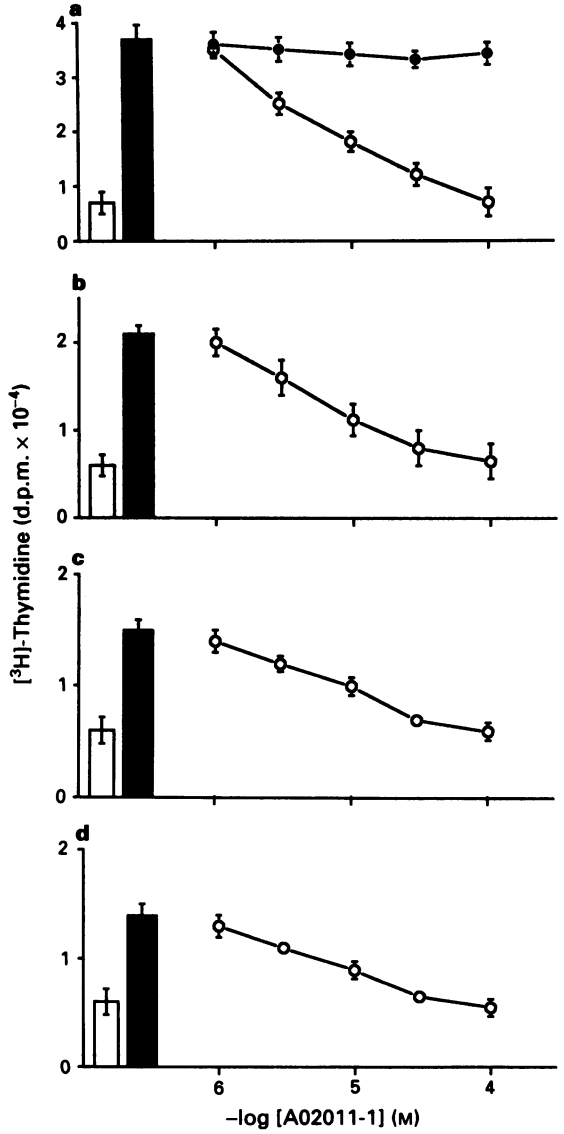

Figure 3 Inhibition by A02011-1 of [^{3}H]-thymidine incorporation in rat VSMCs (○) or endothelial cells (●) stimulated with foetal calf serum (10%) (a); rat VSMCs (○) stimulated with platelet-derived growth factor (PDGF, 10 ng ml^{-1}) (b); 5-hydroxytryptamine (10 μM) (c) or ADP (10 μM) (d). Histograms represent [^{3}H]-thymidine incorporation in unstimulated cells (open columns) and cells stimulated with mitogens (solid column). Data are presented as the mean ± s.e. mean (n = 6, each in quadruplicate).

[^{3}H]-thymidine, [^{3}H]-cyclic AMP, [α-^{32}P]-ATP and cyclic AMP, cyclic GMP ELISA kit were from Amersham (Buckinghamshire, UK). Purified human platelet-derived growth factor (PDGF/BB) from Biomedical Technologies Inc. 2',5'-Dideoxyadenosine from Biomol. Protein dye reagent was from Bio-Rad. Forskolin, 3-isobutyl-1-methylxanthine (IBMX), 8-bromo-cyclic AMP, trypan blue and other chemical reagents were from Sigma Chemical Co. (St. Louis, Mo, U.S.A.). 8-(Aminohexyl)aminoadenosine-3',5'-cyclic monophosphate (8-AHA-cyclic AMP), 8-piperidinoadenosine-3',5'-cyclic monophosphorothioate (Rp-8-PIP-cyclic AMPS), N^6-benzoyladenosine-3',5'-cyclic monophosphate (6-Bnz-cyclic AMP), 8-(chlorophenylthio)-adenosine-3',5'-cyclic monophosphorothioate (Rp-8-CPT-cyclic AMPS) and Rp-8-bromo-cyclic GMPS were obtained from Biolog (Bremen, Germany). The antibody used for immunostaining was anti-smooth muscle α-actin (mouse monoclonal, Dako M851).

Results

Inhibition of mitogen-stimulated [^{3}H]-thymidine incorporation by A02011-1

Initial studies were designed to characterize the capability of mitogens to stimulate incorporation of [^{3}H]-thymidine into DNA as an indicator of proliferation (Nemecek *et al.*, 1986; March *et al.*, 1993). Foetal calf serum (FCS, 10%) elicited the greatest mitogenic response in rat VSMCs, causing a 5.3 ± 0.6 fold increase in [^{3}H]-thymidine incorporation (Figure 2a). Platelet-derived growth factor (PDGF/BB, 10 ng ml^{-1}), 5-hydroxytryptamine (5-HT, 10 μM) and ADP (10 μM) increased [^{3}H]-thymidine incorporation by 3.6 ± 0.2, 2.4 ± 0.3 and 2.3 ± 0.1 fold, respectively (Figure 2b–d). A02011-1 (1–100 μM) concentration-dependently inhibited [^{3}H]-thymidine incorporation to DNA in rat VSMCs that were synchronized by 48 h serum depletion and then re-stimulated by addition of 10% FCS, 10 ng ml^{-1} PDGF/BB, 10 μM 5-HT or 10 μM ADP, with IC_{50} values of 6.3 μM, 6.6 μM, 6.6 μM and 5.6 μM, respectively (Figure 3a–d). The inhibitory effect of A02011-1 was fully reversible, and [^{3}H]-thymidine incorporation recovered within 24 h after the removal of 100 μM A02011-1 (data not shown). A02011-1 (1–100 μM) did not inhibit [^{3}H]-thymidine incorporation of 10% FCS-stimulated rat aortic endothelial cells (Figure 3a).

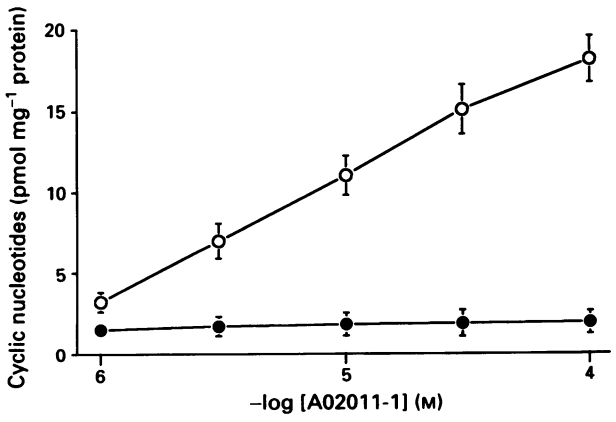

Figure 4 Effects of A02011-1 on cyclic nucleotides formation in rat VSMCs. VSMCs were incubated with various concentrations of A02011-1 for 5 min at 37°C. Cellular cyclic AMP (○) and cyclic GMP (●) were determined by ELISA kit. Basal values of cyclic AMP and cyclic GMP were 3.0 ± 0.2 and 2.0 ± 0.1 pmol mg^{-1} protein, respectively. Data are presented as the mean ± s.e. mean of six experiments.

Effects of A02011-1 on cyclic AMP and cyclic GMP formation

The concentration of A02011-1 necessary for the inhibition of the FCS-induced proliferation was similar to that necessary for cyclic AMP formation, whereas cyclic GMP formation was not significantly changed by A02011-1 (100 μM) (Figure 4). The mechanism of A02011-1-induced cyclic AMP formation was clarified by determining adenylyl cyclase and cyclic AMP-specific phosphodiesterase activity. As shown in Table 1, concentration-dependent increases in adenylyl cyclase activity were observed in A02011-1-treated, or forskolin-treated, VSMCs. The cyclic AMP-specific phosphodiesterase activity was significantly inhibited by 3-isobutyl-1-methylxanthine (IBMX), whereas this enzyme activity remained unchanged by A02011-1 (100 μM) in VSMCs (Table 2).

Inhibition of FCS-stimulated [^{3}H]-thymidine incorporation by 8-bromo-cyclic AMP and forskolin

8-Bromo-cyclic AMP (10–1000 μM) and forskolin (1–100 μM) produced concentration-dependent inhibition of 10% FCS-induced [^{3}H]-thymidine incorporation (Figure 5a); A02011-1 was equipotent with forskolin but was more potent than 8-bromo-cyclic AMP.

Effects of 2',5'-dideoxyadenosine, IBMX, Rp-cyclic AMPS, Rp-8-bromo-cyclic GMPS and staurosporine on A02011-1-induced antiproliferation

2',5'-Dideoxyadenosine (250 μM), an adenylyl cyclase inhibitor, itself had only a slight effect on 10% FCS-induced proliferation. However, the concentration-response curve for A02011-1-induced inhibition of proliferation was shifted to the right (Figure 5b). IBMX (100 μM), a non-selective phosphodiesterase inhibitor, alone caused a 5% decrease of FCS-stimulated [^{3}H]-thymidine incorporation. As shown in Figure 5b, however, it caused significant potentiation of the antiproliferative activity of A02011-1. The antiproliferative action of A02011-1 was also antagonized by Rp-cyclic AMPS (30 μM), a competitive inhibitor of cyclic AMP-dependent protein kinase (PKA) type I and II (Figure 5b). 8-Chloroadenosine-3',5'-cyclic monophosphate (8-Cl-cyclic AMP) (30 μM), an inhibitor of PKA type II, had only a slight effect on the antiproliferative activity of A02011-1 (Figure 5b). Neither Rp-8-bromo-cyclic GMPS (10 μM) nor staurosporine (100 nM) affected the antiproliferative effects of A02011-1 (Figure 5c).

Site-selective cyclic AMP analogues complementing each other in activating either PKA I or PKA II were tested for

Table 1 Effects of A02011-1 and forskolin on adenylyl cyclase activity in rat aortic smooth muscle cells

Treatment	*Adenylyl cyclase activity* (pmol min^{-1} mg^{-1} protein)
None (Basal)	5.8 ± 1.9
Forskolin	
10 μM	39.4 ± 4.9*
30 μM	63.5 ± 7.6*
A02011-1	
3 μM	20.9 ± 3.1*
10 μM	35.7 ± 4.7*
30 μM	56.6 ± 5.9*
100 μM	72.9 ± 5.8*

Cell extracts were incubated with the various concentrations of forskolin or A02011-1 for 10 min and then assayed for adenylyl cyclase activity as described in Methods. Data are expressed as the mean ± s.e.mean ($n = 6$). *$P < 0.001$ as compared with the basal activity.

Table 2 Effects of 3-isobutyl-1-methylxanthine (IBMX) and A02011-1 on cyclic AMP-specific phosphodiesterase activity in rat VSMCs

Treatment	*Phosphodiesterase activity* (c.p.m. mg^{-1} protein)
None (Basal)	10655 ± 599
IBMX 100 μM	8933 ± 413*
500 μM	3888 ± 299*
1000 μM	1000 ± 281*
A02011-1	
30 μM	10600 ± 190
100 μM	10385 ± 100

Cell extracts were incubated with the various concentrations of IBMX or A02011-1 for 10 min and then assayed for enzyme activity as described in Methods. Data are presented as mean ± s.e.mean ($n = 4$). *$P < 0.001$ as compared with the basal activity.

their ability to synergize in the inhibition of VSMC proliferation. Proliferating VSMCs co-treated with 8-aminohexylamino-cyclic AMP (8-AHA-cyclic AMP), at increasing concentrations, and the complementary cyclic AMP analogue, 8-piperidino-cyclic AMPS (Rp-8-PIP-cyclic AMPS) at a constant subinhibitory concentration (90 μM), strongly synergized in the inhibition of VSMC proliferation (Figure 6a). This combination shows strong synergism for activation of PKA type I (Skalhegg *et al.*, 1992). In contrast, addition of 8-chlorophenylthio-cyclic AMP (Rp-8-CPT-cyclic AMP) at increasing concentrations, combined with a constant subinhibitory concentration of N^6-benzoyl-cyclic AMP (6-Bnz-cyclic AMP, 30 μM), showed no such synergism in its inhibitory potency (Figure 6b). This combination shows strong synergism for activation of PKA II (Ogreid *et al.*, 1985).

Effects of A02011-1 on cell cycle in synchronized VSMCs

To ensure that the cells were capable of synchronously re-entering the cell cycle after 48 h serum starvation, the cell stimulation of [^{3}H]-thymidine incorporation was determined. DNA synthesis increased slowly, reached its maximum within 16 h, and declined soon after. The G_1 phase (pre-DNA synthesis) can be confined to the first 8 h, the S phase (DNA synthesis) between 10 to 18 h, and the G_2/M phase (premitosis/mitosis) between 20–26 h. To clarify the mode of antiproliferative action of A02011-1, an examination was made of the relationship between the time of the addition of A02011-1 and its inhibitory action on FCS-induced DNA synthesis. As shown in Figure 7, full inhibition of FCS-induced DNA synthesis still occurred when A02011-1 was present within 10–18 h after the addition of FCS. This result implies that A02011-1 inhibits the FCS-induced proliferation by delaying the progression from the G_1 into S phase of the cell cycle. Furthermore, experimental results in this study have demonstrated that A02011-1 delays the progression from G_1/S phase of cell cycle by using flow cytometry. After a 48 h exposure to a serum-free medium, most of VSMCs stayed at G_0 phase (resting phase)/G_1 phase of the cell cycle (Figure 8a). DNA content in synchronized VSMCs evaluated at 0 h: G_0/G_1, S and G_2/M phase was 48%, 28.6% and 23.4% of the total cells, respectively. After replacement of serum-free medium with DMEM containing 10% FCS, the emergence of cells into and through the S phase was observed by flow cytometry using quantitative DNA staining with propidium iodide (Figure 8b). The majority of cycling cells were found to progress through S phase approximately 18 h after serum repletion ($G_0/G_1 = 20.0\%$, S = 56.6% and G_2/M = 23.7%) (Figure 8b). A02011-1-treated cells showed

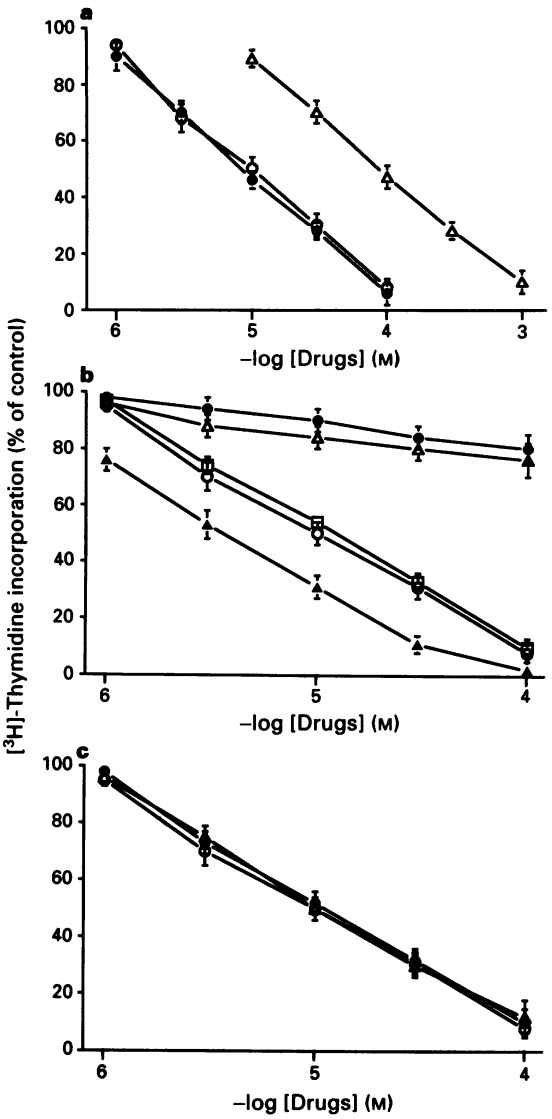

Figure 5 (a) Inhibition by 8-bromo-cyclic AMP (Δ), forskolin (●) or A02011-1 (○) of [^{3}H]-thymidine incorporation in VSMCs stimulated with foetal calf serum (FCS, 10%). (b) Effects of 2',5'-dideoxyadenosine, 3-isobutyl-1-methylxanthine (IBMX), Rp-cyclic AMPS and 8-Cl-cyclic AMP on A02011-1-induced antiproliferation. Quiescent VSMCs were stimulated with FCS (10%) in the presence of various concentrations of A02011-1 (○), or A02011-1 combined with 2',5'-dideoxyadenosine (250 μM) (●), IBMX (100 μM) (▲), Rp-cyclic AMPS (30 μM) (Δ) or 8-Cl-cyclic AMP (30 μM) (□) for 20 h. (c) Effects of Rp-8-bromo-cyclic GMPS and staurosporine on A02011-1-induced antiproliferation. Quiescent VSMCs were stimulated with FCS (10%) in the presence of various concentrations of A02011-1 (○), or A02011-1 combined with Rp-8-bromo-cyclic GMPS (●) or staurosporine (Δ) for 20 h. Measurements of [^{3}H]-thymidine incorporation were then performed as described in the Methods section. Results are expressed as percentage of control, defined as [^{3}H]-thymidine incorporation in the presence of 10% FCS: 3.7 ± 0.2 d.p.m. × 10^{-4}. Data are presented as the mean ± s.e. mean ($n = 6$, each in quadruplicate).

an acute block of cell cycle progression occurring at point G_1/S phase; no increase in DNA content in S phase was observed in cells stimulated by serum in the presence of the A02011-1 (100 μM) (S = 17.2%) (Figure 8c).

Effects of A02011-1 on cell growth

Cell counting was used to evaluate the effects of A02011-1 on cell growth. This revealed growth-inhibition of subconfluent cells by A02011-1 (100 μM) (Figure 9); a lethal effect on the

cell population was discounted as measured by trypan blue exclusion. To examine the possibility that A02011-1 might be toxic to VSMCs the following series of experiments were performed. (a) The number of cells present in the supernatant media was determined daily for 6 days, both in the presence and absence of 100 μM A02011-1. While this concentration of A02011-1 caused significant inhibition of cell growth (>90%), <5% of cells were found to be present in the supernatant during any portion of the culture period. Thus, detachment and loss of cells did not account for inhibition of cell proliferation. (b) Incubation of VSMCs for 24 h with A02011-1 (100 μM) also caused no significant cell loss: the number of cells was $2.8 \pm 0.2 \times 10^3$ in control wells and $3.0 \pm 0.3 \times 10^3$ in A02011-1 (100 μM)-treated wells. Furthermore, no significant release of lactate dehydrogenase was observed in this experiment, again indicating that in short-term incubations, even high concentrations of A02011-1 did not induce cell damage. (c) Less than 1% of the cells treated with A02011-1 (100 μM) for 24 h stained with trypan blue.

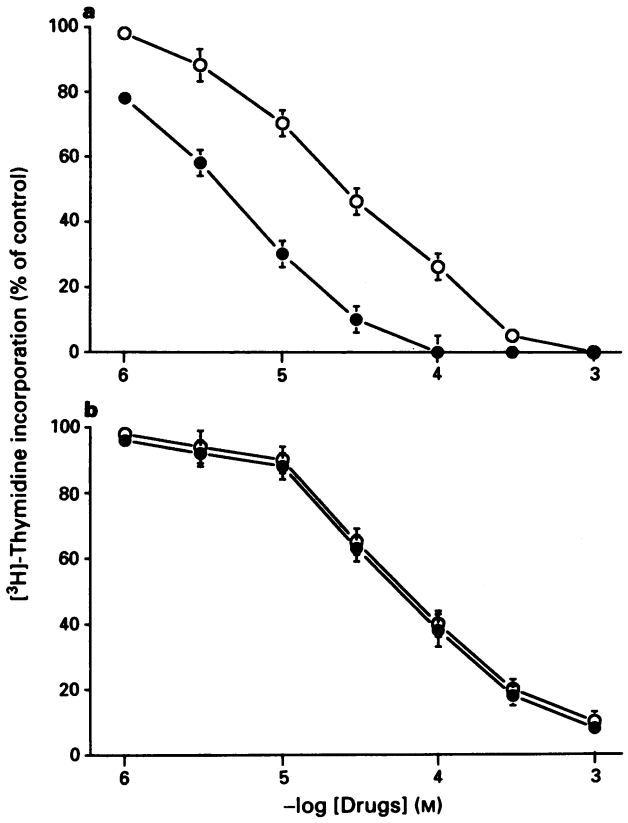

Figure 6 Synergistic activation of cyclic AMP-dependent protein kinase (PKA) I and II using site-selective cyclic AMP analogues in VSMCs. (a) Quiescent VSMCs were stimulated with FCS (10%) in the presence of various concentrations of 8-AHA cyclic AMP (○) or in combination with Rp-8-PIP-cyclic AMPS (90 μM, ●) to activate selectively PKA I. (b) VSMCs were stimulated with FCS (10%) in the presence of Rp-8-CPT-cyclic AMP (○) or in combination with 6-Bnz-cyclic AMP (30 μM, ●) to activate selectively PKA II. Data are presented as the mean ± s.e. mean ($n = 6$, each in quadruplicate). For abbreviations, see text.

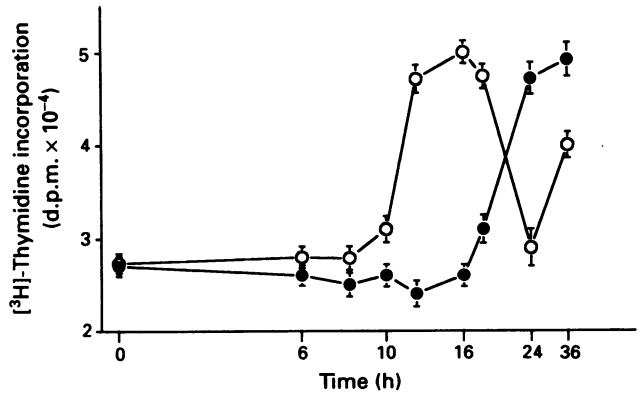

Figure 7 Chronological analysis of effects of A02011-1 on the FCS-induced DNA synthesis. Quiescent VSMCs were stimulated by 10% FCS for 36 h. During this incubation, dimethylsuphoxide (DMSO, 0.05%, control) (○) or A02011-1 (100 μM) (●) was added at the indicated times and incubations were continued for 36 h. [3H]-thymidine was added 2 h before the incubations were terminated. DNA synthesis was assayed by measuring the incorporation of [3H]-thymidine into acid-insoluble materials as described in Methods section. Data are presented as the mean ± s.e. mean ($n = 6$).

Discussion

The present study has demonstrated that A02011-1, a pyrazole derivative, effectively and reversibly inhibits VSMC

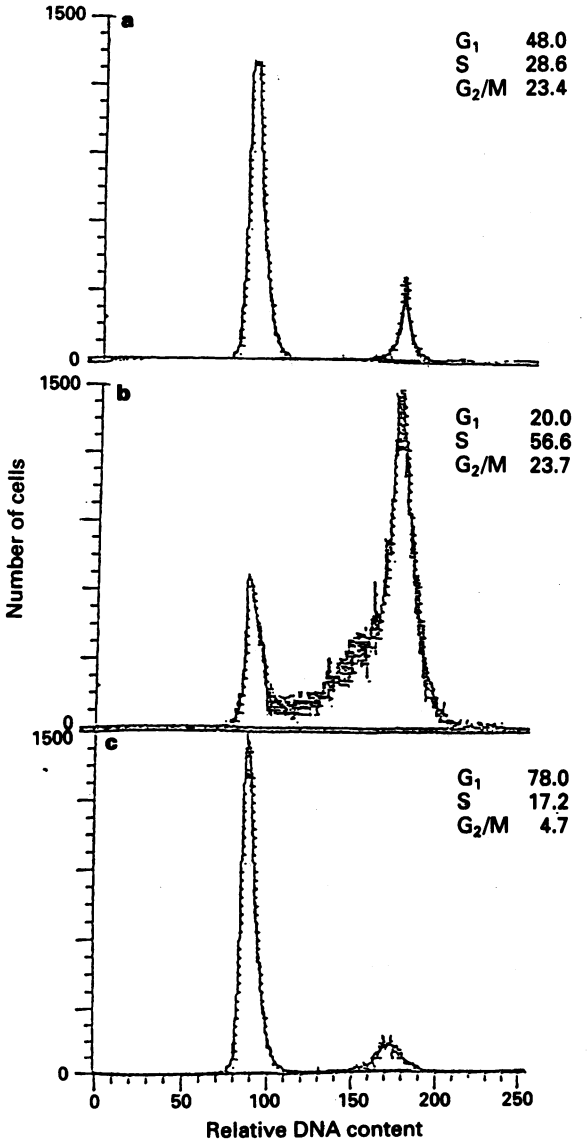

Figure 8 Effect of A02011-1 on cell cycle in synchronized VSMCs. Cell cycle progression was evaluated by flow cytometric determination of DNA content in synchronized subconfluent VSMCs evaluated at 0 h (control) (a) and 18 h after serum repletion in the absence (b) or presence (c) of A02011-1 (100 μM). Individual nuclear DNA content as reflected by fluorescence intensity of incorporated propidium iodide is plotted as a histogram depicting relative cell numbers at each intensity. Each histogram is derived from a data collection of at least 10,000 events.

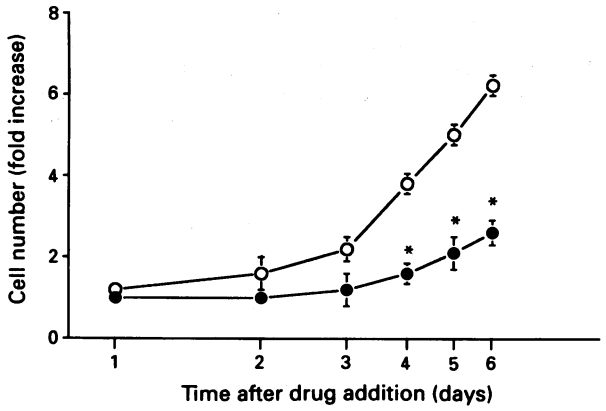

Figure 9 Inhibition of VSMC growth by A02011-1. VSMCs were seeded on 12 well plates (density was 2.5×10^3/well) and counted in trypan blue at subsequent time points. Dimethylsulphoxide (○) or A02011-1 (100 μM) (●) was added and incubated for 6 days in medium supplemented with 10% FCS. Culture media were changed daily and cell numbers were determined. Results are presented as the mean ± s.e. mean of three separate experiments. Each in quadruplicate, and are expressed as the fold increase of cell number, relative to that on day 0 of the experiments. $^*P<0.001$ as compared with control (Cells not treated with A02011-1).

proliferation, which is a prominent feature of vascular response to mechanical injury (Campbell & Campbell, 1985; Ip *et al.*, 1990). Excessive VSMC proliferation is considered to be a hallmark of atherosclerotic disease (Schwartz *et al.*, 1986) and the experimental removal of endothelium has been associated with proliferation of the underlying VSMCs (Clowes *et al*, 1983). It has been postulated that one of the functions of endothelial cells is to maintain the mitogenic quiescence of the underlying medial VSMCs (Garg & Hassid, 1989; Assender *et al.*, 1992). This is despite the fact that modulation of VSMC proliferation has crucial therapeutic implications for vascular disease. A prominent therapeutic aim involves inhibiting VSMC proliferation without interfering with endothelial repair (Grainger *et al.*, 1992). A02011-1, which selectively inhibits VSMC proliferation without affecting endothelial cell repair, might therefore be expected to prevent or inhibit progress of vascular diseases. Furthermore, the inhibition of proliferation by A02011-1 occurred with concentrations (1–100 μM) similar to those causing vasorelaxation and antiplatelet effects (unpublished observation). This property would also contribute towards the vascular protective effect of A02011-1.

Cyclic AMP may be involved in negative, as well as positive, regulation of cellular growth depending on the cell type and culture conditions used (Pastan *et al.*, 1975). In the present study, we demonstrated that cyclic AMP mediated the inhibition of proliferation of rat VSMC. The antiproliferative action of A02011-1 was mimicked by 8-bromo-cyclic AMP, a membrane permeable cyclic AMP analogue, and was antagonized by Rp-cyclic AMPS, a competitive inhibitor of cyclic AMP-dependent protein kinase (PKA) type I and II (Wang *et al.*, 1991). Furthermore, the concentration of A02011-1 necessary for the inhibition of the FCS-induced proliferation was similar to that causing cyclic AMP formation. These experimental results imply that the antiproliferative effect of A02011-1 was likely to be mediated by cyclic AMP as the second messenger. That cyclic AMP formation caused by A02011-1 was likely to be due to activation of adenylyl cyclase was indicated by the decreased potency of A02011-1-induced antiproliferation in the presence of 2',5'-dideoxyadenosine, an adenylyl cyclase inhibitor (Holgate *et al.*, 1980), and by the increased potency of A02011-1 in the presence of IBMX, a phosphodiesterase inhibitor. Moreover, A02011-1 concentration-dependently activated the adenylyl cyclase, but did not affect the phosphodiesterase activity, in rat VSMCs. Although cyclic AMP has been reported to inhibit the proliferation of VSMC (Blomhoff *et al.*, 1987; Skalhegg *et al.*, 1992), the molecular mechanisms remain to be clarified. Until recently, all known actions of cyclic AMP or its derivatives were assumed to operate via activation of PKA (Beebe & Corbin, 1986). Two major types of mammalian PKA (PKA I and PKA II) are described (Skalhegg *et al.*, 1992). Activation of PKA occurs upon binding of four cyclic AMP molecules, two per regulatory (R) monomer, where the binding takes place on two asymmetric sites (designated A and B) (Rannels & Corbin, 1980). It has been shown that cyclic AMP analogues with selectivity for site A and B, respectively, can complement each other in the activation of PKA (Robinson-Steiner *et al.*, 1984) and that analogue pairs, by synergistic action, also can selectivity activate PKA I and II in the intact cell (Lanotte *et al.*, 1991). To what extent PKA I or PKA II mediate cyclic AMP-induced growth-inhibitory effects in VSMC is still unclear. Use of site-selective analogue pairs can to a certain extent distinguish between effects mediated via PKA I and PKA II (Lanotte *et al.*, 1991). Since Rp-8-PIP-cyclic AMPS selects site A of RI and 8-AHA-cyclic AMP selects site B of both RI and RII, they should only synergize in activating PKA I (Skalhegg *et al.*, 1992). Rp-8-CPT-cyclic AMP selects site B of RII and 6-Bnz-cyclic AMP selects sites A of RI and RII, the combination showing strong synergism for activation of PKA II (Ogreid *et al.*, 1985). In the present study, the antiproliferative actions of A02011-1 were antagonized by Rp-cyclic AMPS, a competitive inhibitor of PKA I and II, but not 8-Cl-cyclic AMP, a selective PKA II inhibitor. Furthermore, a cyclic AMP analogue pair directed to activated PKA I (8-AHA-cyclic AMP and Rp-8-PIP-cyclic AMPS) synergized in the inhibition of VSMC proliferation, whereas a PKA II-directed cyclic AMP analogue pair (Rp-8-CPT-cyclic AMPS and 6-Bnz-cyclic AMP) did not. This result indicates that PKA I mediates the inhibitory effects of cyclic AMP in rat VSMCs. At present, the exact mechanism by which the cyclic AMP signal transduction pathway inhibits VSMC proliferation is poorly understood. Several studies have reported that the cyclic AMP reduces the steady-state level of c-myc mRNA in HL60 cells (Schwartz *et al.*, 1991), down-regulates the c-myc mRNA and inhibits PDGF-induced proliferation in fibroblasts and VSMCs (Heldin *et al.*, 1989; Bennett *et al.*, 1994), blocks induction of c-sis mRNA and inhibits the release of PDGF in endothelial cells (Daniel *et al.*, 1987).

To determine whether a protein kinase G (PKG) or protein kinase C (PKC) is involved in the antiproliferative effects of A02011-1, a stable membrane permeant inhibitor of PKG, Rp-8-bromo-cyclic GMPS, and a PKC inhibitor, staurosporine, were used. Neither Rp-8-bromo-cyclic GMPS nor staurosporine had any effect on the antiproliferative effects of A02011-1. This indicated that neither PKG nor PKC is involved in the A02011-1-induced antiproliferative action.

We examined the relationship between the time of the addition of A02011-1 and its inhibitory action on FCS-induced DNA synthesis. Full inhibition of DNA synthesis still occurred when A02011-1 was present within 10–18 h after the re-addition of FCS (Figure 7). A02011-1 is very stable in culture and is not readily degraded. However, A02011-1 had only modest effects in lowering cell number, as assessed over the initial 6 days of the treatment (Figure 9). These results demonstrate that A02011-1 delays rather than prevents the onset of proliferation. Flow cytometry in VSMCs synchronized by serum depletion revealed a delay of FCS-inducible cell cycle progression at the G_1/S phase in A02011-1-treated cells (Figure 8). Cyclic AMP-elevating vasodilators (e.g. forskolin or isoprenaline) also exert their antiproliferative action by delaying the progression from the G_1 into S phase of the cell cycle (Garg & Hassid, 1989; Assender *et al.*, 1992). Our results are also consistent with previous work (Assender *et al.*, 1992) which showed that elevated cyclic AMP concentrations at a latter stage of the G_1 phase of the cell cycle would be necessary to inhibit proliferation.

The antiproliferative effect of A02011-1 was unlikely to be due to cell damage, based on the finding that 100 μM A02011-1 did not cause the release of lactate dehydrogenase or decrease cell number after 24 h of incubation. Moreover, the inhibition of cell proliferation induced by 100 μM A02011-1 in long-term experiments was also unlikely to be the result of toxicity and damage to cells as shown by the lack of lactate dehydrogenase release into the extracellular medium, the lack of staining by trypan blue and the lack of cell detachment.

In conclusion, this study demonstrates that A02011-1 inhibits VSMC proliferation via the adenylyl cyclase/cyclic AMP system, and by delaying the progression from the G_1 into S phase of the cell cycle. Since A02011-1 did not cause cell toxicity, it may hold promising potential for the prevention of vascular diseases.

This work was supported by a research grant of CMRP 377 from Chang Gung Medical Research Foundation and the National Science of the Republic of China (NSC 84-2331-B182-095).

References

ANDERSSON, K.B., TASKEN, K. & BLOMHOFF, H.K. (1994). Cyclic AMP downregulates c-myc expression by inhibition of transcript initiation in human B-precursor Reh cells. *FEBS Lett.*, **337**, 71–76.

ASSENDER, J.W., SOUTHGATE, K.M., HALLETT, M.B. & NEWBY, A.C. (1992). Inhibition of proliferation, but not of Ca^{2+} mobilization, by cyclic AMP and GMP in rabbit aortic smooth-muscle cells. *Biochem. J.*, **288**, 527–532.

BEASLEY, D., SCHWARTZ, J.H. & BRENNER, B.M. (1991). Interleukin 1 induces prolonged L-arginine-dependent cyclic guanosine monophosphate and nitrite production in rat vascular smooth muscle cells. *J. Clin. Invest.*, **87**, 602–608.

BEEBE, S.J. & CORBIN, J.D. (1986). Cyclic nucleotide-dependent protein kinase. In *The Enzymes*, vol. XVII. ed. Boyer, P.D. & Krebs, E.G., pp. 43–111. New York: Academic Press.

BENNETT, M.R., EVAN, G.I. & NEWBY, A.C. (1994). Deregulated expression of the c-myc oncogene abolishes inhibition of proliferation of rat vascular smooth muscle cells by serum reduction, interferon-τ, heparin, and cyclic nucleotide analogues and induces apoptosis. *Circ. Res.*, **74**, 525–536.

BLOMHOFF, H.K., SMELAND, E.B., BEISKE, K., BLOMHOFF, R., RUUD, E., BJORO, T., PFEIFER-OHLSSON, S., WATT, R., WATT, R., FUNDERUD, S., GODAL, T. & OHLSSON, R. (1987). Cyclic AMP-mediated suppression of normal and neoplastic B cell proliferation is associated with regulation of c-myc and Ha-ras protooncogenes. *J. Cell. Physiol.*, **131**, 426–433.

BRADFORD, M.M. (1976). A rapid and sensitive method for the quantitation of microgram quantities of protein utilizing the principle of protein-dye-binding. *Anal. Biochem.*, **72**, 248–254.

CAMPBELL, G.R. & CAMPBELL, J.H. (1985). Recent advances in molecular pathology. *Exp. Mol. Pathol.*, **42**, 139–162.

CLOWES, A.W., REIDY, M.A. & CLOWES, M.M. (1983). Kinetics of cellular proliferation after arterial injury. *Lab. Invest.*, **49**, 327–333.

DANIEL, T.O., GIBBS, V.C., MILFAY, D.F. & WILLIAMS, L.T. (1987). Agents that increase cAMP accumulation block endothelial c-sis induction by thrombin and transforming growth factor-β. *J. Biol. Chem.*, **262**, 11893–11896.

DUMONT, J.E., JAUNIAUX, J.C. & ROGER, P.P. (1989). The cyclic AMP-mediated stimulation of cell proliferation. *Trends Pharmacol. Sci.*, **14**, 67–71.

GARG, U.C. & HASSID, A. (1989). Nitric oxide-generating vasodilators and 8-bromo-cyclic guanosine monophosphate inhibit mitogenesis and proliferation of cultured rat vascular smooth muscle cells. *J. Clin. Invest.*, **83**, 1774–1777.

GRAINGER, D.J., HESKETH, T.R., METCALFE, J.C. & WEISSBERG, P.L. (1991). A large accumulation of non-muscle myosin occurs at first entry into M phase in rat vascular smooth-muscle cells. *Biochem. J.*, **277**, 145–151.

GRAINGER, D.J., HESKETH, T.R., WEISSBERG, P.L. & METCALFE, J.C. (1992). Hexamethylenebisacetamide selectively inhibits the proliferation of human and rat vascular smooth-muscle cells. *Biochem. J.*, **283**, 403–408.

HELDIN, N.-E., PAULSSON, Y., FORSBERG, K., HELDIN, C.-H. & WESTERMARK, B. (1989). Induction of cyclic AMP synthesis by forskolin is followed by a reduction in the expression of c-myc messenger RNA and inhibition of ^{3}H-thymidine incorporation in human fibroblasts. *J. Cell. Physiol.*, **138**, 17–23.

HOLGATE, S.T., LEWIS, R.A. & AUSTEN, K.F. (1980). Role of adenylate cyclase in immunologic release of mediators from rat mast cells: agonist and antagonist effects of purine- and ribose-modifed adenosine analogs. *Proc. Natl. Acad. Sci. U.S.A.*, **77**, 6800–6810.

INSEL, P.A., STENGEL, D., FERRY, N. & HANOUNE, J. (1982). Regulation of adenylate cyclase of human platelet membranes by forskolin. *J. Biol. Chem.*, **257**, 7485–7490.

IP, J.H., FUSTER, V., BADIMON, L., BADIMON, J., TAUBMAN, M.B. & CHESEBRO, J.H. (1990). Syndromes of accelerated atherosclerosis: role of vascular injury and smooth muscle cell proliferation. *J. Am. Coll. Cardiol.*, **15**, 1667–1687.

KARIYA, K.I., KAWAHARA, Y., ARKI, S.I., FUKUZAKI, H. & TAKAI, Y. (1989). Antiproliferative action of cyclic GMP-elevating vasodilators in cultured rabbit aortic smooth muscle cells. *Atherosclerosis*, **80**, 143–147.

KARNIGUIAN, A., LEGRAND, Y.J. & CAEN, J.P. (1982). Prostaglandins: specific inhibition of platelet adhesion to collagen and relationship with cAMP level. *Prostaglandins*, **23**, 437–457.

LANOTTE, M., RIVIERE, J.B., HERMOUET, S., HOUGE, G., VINTERMYR, O.K., GJERTSEN, B.T. & DOSKELAND, S.D. (1991). Programmed cell death (apoptosis) is induced rapidly and with positive cooperativity by activation of cyclic adenosine monophosphate-kinase I in a myeloid leukemia cell line. *J. Cell. Physiol.*, **146**, 73–80.

LOESBERG, C., VAN WIJK, R., ZANBERGEN, J., VAN AKEN, W.G., VAN MOURIK, J.A. & DE GROOT, P.H.G. (1985). Cell cycle-dependent inhibition of human vascular smooth muscle cell proliferation by prostaglandin E_1. *Exp. Cell. Res.*, **160**, 117–121.

MARCH, K.L., WILENSKY, R.L., ROESKE, R.W. & HATHAWAY, D.R. (1993). Effects of thiol protease inhibitors on cell cycle and proliferation of vascular smooth muscle cells in culture. *Circ. Res.*, **72**, 413–423.

MOORE, J.B., FULLER, J.B.L., FALOTICO, R. & TOLMAN, E.L. (1985). Inhibition of rabbit platelet phosphodiesterase activity and aggregation by calcium channel blockers. *Thromb. Res.*, **40**, 401–411.

MORINELLI, T.A., ZHANG, L.M., NEWMAN, W.H. & MEIER, K.E. (1994). Thromboxane A_2/prostaglandin H_2-stimulated mitogenesis of coronary artery smooth muscle cells involves activation of mitogen-activated protein kinase and S6 kinase. *J. Biol. Chem.*, **269**, 5693–5698.

NEMECEK, G.M., COUGHLIN, S.R., HANDLEY, D.A. & MOSKOWITZ, M.A. (1986). Stimulation of aortic smooth muscle cell mitogenesis by serotonin. *Proc. Natl. Acad. Sci. U.S.A.*, **83**, 674–678.

OGREID, D., EKANGER, R., SHUVA, R.H., MILLER, J.P., STURM, P., CORBIN, J.D. & DOSKELAND, S.O. (1985). Activation of protein kinase isozymes by cyclic nucleotide analogs used singly or in combination. *Eur. J. Biochem.*, **150**, 219–227.

PASTAN, I., JOHSON, G.S. & ANDERSON, W.B. (1975). Role of cyclic nucleotides in growth control. *Annu. Rev. Biochem.*, **44**, 491–522.

RANNELS, S.R. & CORBIN, J.D. (1980). Two different intrachain cAMP binding sites of cAMP-dependent protein kinases. *J. Biol. Chem.*, **255**, 7085–7088.

ROBINSON-STEINER, A.M., BEEBE, S., RANNELS, S.R. & CORBIN, J.D. (1984). Microheterogeneity of type II cyclic AMP-dependent protein kinase in various mammalian species and tissues. *J. Biol. Chem.*, **259**, 10596–10605.

ROSS, R. (1986). The pathogenesis of atherosclerosis: an update. *New Engl. J. Med.*, **314**, 488–500.

ROSS, R. & GLOMSET, J.A. (1973). Atherosclerosis and the arterial smooth muscle cell. *Science*, **180**, 1332–1339.

SCHWARTZ, E.L., CHAMBERLAIN, H. & BRECHBIIHL, A.-B. (1991). Regulation of c-myc expression by granulocyte-macrophage colony-stimulating factor in human leukemia cells. *Blood*, **77**, 2716–2723.

SCHWARTZ, S.M., CAMPBELL, G.R. & CAMPBELL, J.H. (1986). Replication of smooth muscle cells in vascular disease. *Circ. Res.*, **58**, 427–444.

SKALHEGG, B.S., LANDMARK, B.F., DOSKELAND, S.O., HANSSON, V., LEA, T. & JAHNSEN, T. (1992). Cyclic AMP-dependent protein kinase type I mediates the inhibitory effects of 3',5'-cyclic adenosine monophosphate on cell replication in human T lymphocytes. *J. Biol. Chem.*, **267**, 15707–15714.

WANG, L.-Y., SALTER, M.W. & MACDONALD, J.F. (1991). Regulation of kainate receptor by cAMP-dependent protein kinase and phosphates. *Science*, **253**, 1132–1135.

YOSHINA, S. & KUO, S.C. (1978). Studies on heterocyclic compounds. XXXV. Synthesis of furo [3,2-c]pyrazole derivatives. (2) Electrophilic substitution of 1,3-diphenyl furo [3,2-c]pyrazole. *Yakugaku Zasshi*, **98**, 204–207.

(Received October 3, 1994
Revised November 11, 1994
Accepted November 15, 1994)

British Journal of Pharmacology (1995) 114, 1236–1240

Potentiation by endothelin-1 of 5-hydroxytryptamine responses in aortae from streptozotocin-diabetic rats: a role for thromboxane A_2

Gail M. James & [1]Wayne C. Hodgson

Department of Pharmacology, Monash University, Clayton, Victoria, Australia 3168

1 We have previously reported maximum responses to 5-hydroxytryptamine (5-HT) are diminished in endothelium-intact and -denuded aortae from rats with streptozotocin-induced diabetes of 2-weeks duration.

2 In the present study, the thromboxane A_2/prostaglandin H_2 (TP) receptor antagonist GR32191B (1 μM) significantly reduced maximum responses to 5-HT in endothelium-intact aortae from both control and diabetic rats. In the presence of GR32191B, maximum responses to 5-HT, in endothelium-intact aortae from diabetic rats, were still significantly reduced compared to those obtained in aortae from controls.

3 GR32191B (1 μM) had no significant effect on maximum responses to 5-HT in endothelium-denuded aortae from either control or diabetic rats.

4 Interaction between 5-HT (0.1 μM–0.1 mM) and threshold concentrations of endothelin-1 (ET-1) or the thromboxane (Tx)A_2-mimetic, U46619, were examined in endothelium-intact and -denuded aortae from control and 2-week streptozotocin-diabetic rats.

5 Maximum responses to 5-HT in the presence of a threshold concentration of ET-1 (3 nM), in endothelium-intact aortae from diabetic rats, were not significantly different from those of control rats.

6 Maximum responses to 5-HT in the combined presence of ET-1 (3 nM) and GR32191B (1 μM), in endothelium-intact aortae from diabetic rats, were significantly reduced compared to those obtained in aortae from controls.

7 Maximum responses to 5-HT in the presence of ET-1 (3 nM) in endothelium-denuded aortae from diabetic rats were significantly reduced compared to those from controls.

8 Maximum responses to 5-HT in the presence of a threshold concentration of U46619 (20 or 30 nM), in endothelium-intact aortae from diabetic rats, were not significantly different from responses of controls.

9 Maximum responses to 5-HT in the presence of a threshold (5–20 nM) concentration of U46619, in endothelium-denuded aortae from diabetic rats, were not significantly different from responses of controls.

10 The results of the present study indicate that endothelial-derived TxA_2 contributes to the contractile response to 5-HT in aortae from control and diabetic rats. Endothelial-derived TxA_2 also appears to play a role in the potentiation of 5-HT responses by ET-1 in aortae from diabetic rats.

Keywords: Endothelin-1; 5-hydroxytryptamine; thromboxane A_2; diabetes; rat aortae

Introduction

It has been previously reported that addition of a threshold concentration of 5-hydroxytryptamine (5-HT) potentiates subsequent contraction induced by endothelin-1 (ET-1). However, a threshold concentration of ET-1 did not potentiate the contractile effect of 5-HT (Yang et al., 1992). We have previously shown that maximum responses to 5-HT were diminished in aortae from streptozotocin (STZ)-diabetic rats of 2- and 6-weeks duration (Sikorski et al., 1993; James *et al.*, 1994). The present study was undertaken to determine whether there was an interaction between 5-HT and ET-1 in aortae from STZ-diabetic rats and whether any interaction observed had an effect on the altered responsiveness previously observed to 5-HT in aortae from diabetic rats.

Methods

Male Wistar rats (270–490 g) were treated with STZ (60 mg kg^{-1}, i.v.) or vehicle (50 mM citrate buffer) under 4% halothane anaesthesia (O_2/N_2O 2:1) as previously described (Fulton *et al.*, 1991; Hodgson & King, 1992). The animals were then housed in treatment pairs, being allowed free access to food and water at all times. Only rats displaying elevated blood glucose levels (>16 mM, Ames Minilab 1) after 2-weeks were considered to be diabetic. Control rats had normal (4–9 mM) blood glucose levels over the 2-week period. After 2 weeks, a STZ-diabetic and a control animal were killed and 5 mm rings cut from each descending thoracic aorta. Where indicated, endothelial cells were removed by gentle rubbing of the intimal surface with a thin wire. Rings were placed under 10 g resting tension in 15 ml organ baths containing Krebs solution of the following composition (mM): NaCl 118.4, KCl 4.7, $CaCl_2$ 2.5, $NaHCO_3$ 25.0, KH_2PO_4 1.2, $MgSO_4.7H_2O$ 1.2, glucose 11.1. Physiological solutions were maintained at 37°C, and bubbled with carbogen (5% CO_2 in O_2). After 1 h equilibration, a submaximal concentration of phenylephrine (0.3 μM) was added to the bath. At the plateau of contraction, acetylcholine (10 μM) was added and the presence of functional endothelial cells was indicated by subsequent relaxation. A threshold concentration of ET-1 (3 nM) or U46619 (20 or 30 nM) was then

[1] Author for correspondence.

added to the organ bath and allowed to equilibrate for 5 min or until the response plateaued. A cumulative concentration-response curve to 5-HT was then obtained. 5-HT was added at intervals of between 3–10 min depending on the time taken for the previous response to reach a plateau. A similar procedure was followed for endothelium-denuded aortae using threshold concentrations of ET-1 (2 nM control; 3 nM diabetic) or U46619 (5–20 nM). Where indicated concentration-response curves to 5-HT were obtained in the presence of the thromboxane A_2/prostaglandin H_2 (TP) receptor antagonist GR32191B, 1 μM, a concentration previously shown to be selective for TP receptors in the rat aorta (Lumley *et al.*, 1989). GR32191B was added after the test for functional endothelium and allowed to equilibrate for 30 min before the start of the concentration-response curve. Only a single concentration-response curve to one agonist was obtained in each tissue. Contractions were recorded on a Grass polygraph (Model 79E).

After each experiment, aortic rings were oven dried (50°C) and then weighed. The order of killing STZ-diabetic and control rats was alternated between days, and the arrangement of tissues in organ baths randomized.

Drugs

The following drugs were used: acetylcholine chloride (Sigma), endothelin-1 (Auspep), GR32191B [1*R*-[1α(Z),2β,3β, 5α]]-(±)-7-[5-[[(1,1'-biphenyl)-4-yl] methoxy]-3-hydroxy-2-(1-piperidinyl)cyclopentyl]-4-heptenoic acid (Glaxo), 5-hydroxytryptamine creatine sulphate (Sigma), phenylephrine HCl (ICN Pharmaceutical), streptozotocin (Sigma) and U46619 ((15S)-hydroxy-11α, 9α-(epoxymethano) prosta-5Z, 13E-dienoic acid) (Upjohn).

Phenylephrine was dissolved in catecholamine diluent (0.312 g NaH_2PO_4 and 0.08 g ascorbic acid per litre of 0.9% (w/v) saline). Acetylcholine, 5-hydroxytryptamine and GR32191B were dissolved in distilled water. Endothelin stock was dissolved in distilled water, divided into aliquots and frozen. On the day of use it was thawed and further diluted in distilled water. U46619 stock was prepared in ethanol, which was evaporated under a stream of N_2 and redissolved in distilled water.

Statistics

Rat body weights and blood glucose levels were analysed for interactions using a two-way analysis of variance (ANOVA), and if significant, by one-way ANOVA and Tukey test (Apple Macintosh, CLR ANOVA package). Aortic ring dry weights were analysed by Student's *t* test. Multiple comparisons with a single control were analysed by a one-way ANOVA, followed by a Dunnett's *t* test (Apple Macintosh, STATVIEW package). pEC_{50} values were determined from the E_{max} of each individual curve and the geometric mean (i.e. mean of the log values) determined. Values shown are ± s.e.mean. In all cases, statistical significance is indicated by $P<0.05$.

Results

As shown in Table 1, control rats displayed significantly increased body weights compared to their pre-injection values. Diabetic rats displayed significantly reduced body weights over the same period ($P<0.05$, ANOVA). Blood glucose levels of diabetic rats were increased significantly, after the 2-weeks ($P<0.05$, ANOVA). Dry weights of aortic rings from diabetic rats were significantly decreased compared to those of controls ($P<0.05$, *t*-test).

Responses in endothelium-intact aortae

Contractile responses to 5-hydroxytryptamine 5-HT (0.1 μM–0.1 mM) produced concentration-dependent contractile responses of endothelium-intact aortae from control and diabetic rats (Figure 1a). Maximum responses to 5-HT of aortae from diabetic rats were significantly less than those of control rats (Figure 1a and Table 2, $P<0.05$, ANOVA, previously published; James *et al.*, 1994). Aortae from diabetic rats were significantly less sensitive to 5-HT than aortae from control rats (indicated by pEC_{50} values, $P<0.05$, ANOVA, Table 2).

Maximum responses to 5-HT in the presence of GR32191B (1 μM) of aortae from diabetic rats were significantly attenuated compared to those from controls (Figure 1a and Table 2, $P<0.05$, ANOVA). Maximum responses to 5-HT in the presence of GR32191B, of aortae from control and diabetic rats, were significantly reduced compared to those obtained in the absence of GR32191B (Figure 1a and Table 2, $P<0.05$, ANOVA).

Contractile responses to 5-hydroxytryptamine in the presence of endothelin-1 ET-1 (3 nM) produced small contractile responses in aortae from control (0.43 ± 0.11 g) and diabetic (0.53 ± 0.16 g) rats. In the presence of ET-1, maximum responses to 5-HT were not significantly different between aortae from control and diabetic rats (Figure 1b and Table 2). However, maximum responses of aortae, in the presence of ET-1, from control and diabetic rats were significantly attenuated and potentiated, respectively, compared to the corresponding responses obtained in the absence of ET-1 (Figure 1b versus 1a; $P<0.05$, ANOVA; Table 2).

Maximum responses to 5-HT, in the combined presence of ET-1 (3 nM) and GR32191B (1 μM), in aortae from diabetic rats were significantly reduced compared to responses of controls (Figure 1c and Table 2, $P<0.05$, ANOVA). Maximum responses to 5-HT in the combined presence of ET-1 (3 nM) and GR32191B (1 μM), in aortae from control rats were significantly reduced compared to responses obtained to 5-HT alone (Figure 1c versus 1a and Table 2, $P<0.05$, ANOVA). Aortae, in the combined presence of ET-1 and GR32191B, from diabetic rats were significantly less sensitive to 5-HT than aortae from control rats (indicated by pEC_{50} values, $P<0.05$, ANOVA, Table 2).

Table 1 Body weights, blood glucose levels and aortic ring dry weights of control and streptozotocin (STZ)-diabetic rats

		Body weight (g)		*Blood glucose* (mM)		*Aortic weight* (mg)	
	(n)	*Initial*	*Final*	*Initial*	*Final*	*With E*	*Without E*
Control	40–48	336 ± 5	384 ± 7#	5.1 ± 0.2	6.6 ± 0.2	1.85 ± 0.04	1.95 ± 0.06
STZ-diabetic	44–50	333 ± 5	300 ± 4*#	5.5 ± 0.2	21.0 ± 0.4*#	1.74 ± 0.03*	1.73 ± 0.06*

Initial measurements were made at the time of STZ or vehicle injection, and final measurements made 2 weeks later. E = endothelial cells.
*$P<0.05$, significantly different from corresponding control group, *t* test or ANOVA
#$P<0.05$, significantly different from initial value in same treatment group, *t* test or ANOVA
Values shown are ± s.e.mean.

Table 2 Maximum and pEC_{50} values for aortae from control (C) and streptozotocin (STZ)-treated rats with (+) and without (−) endothelial cells (E)

		C+E	STZ+E	C−E	STZ−E
5-HT	Maximum (g)	3.06 ± 0.17	1.30 ± 0.07*	4.14 ± 0.24	2.60 ± 0.16*
	pEC_{50} (-log M)	5.52 ± 0.10	5.23 ± 0.05*	5.90 ± 0.20	5.42 ± 0.12
5-HT + ET-1	Maximum (g)	1.97 ± 0.31†	2.04 ± 0.28†	3.30 ± 0.21	2.13 ± 0.09*
	pEC_{50} (-log M)	5.46 ± 0.13	5.29 ± 0.17	6.80 ± 0.33	6.20 ± 0.30
5-HT + ET-1 + GR32191	Maximum (g)	1.88 ± 0.09†	0.89 ± 0.13*	NT	NT
	pEC_{50} (-log M)	5.94 ± 0.06	5.54 ± 0.07*	NT	NT
5-HT + GR32191	Maximum (g)	2.30 ± 0.16†	0.57 ± 0.17*†	3.73 ± 0.20	2.03 ± 0.39*
	pEC_{50} (-log M)	5.57 ± 0.10	5.01 ± 0.24	6.47 ± 0.28	5.52 ± 0.11*
5-HT + U46619	Maximum (g)	3.08 ± 0.39	2.18 ± 0.43	3.23 ± 0.28	3.23 ± 0.14
	pEC_{50} (-log M)	6.51 ± 0.30†	6.01 ± 0.34†	ND	6.42 ± 0.10*†

*$P<0.05$, significantly different from corresponding control group, ANOVA.
†$P<0.05$, significantly different from 5-HT alone from the same treatment group, ANOVA.
NT = not tested; ND = not determined. Values shown are ± s.e.mean.

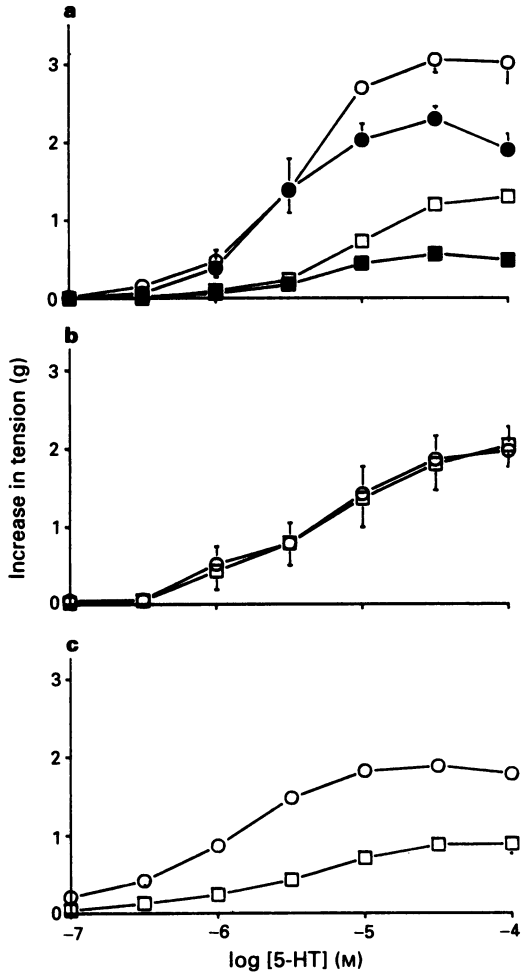

Figure 1 Responses of rat aortic rings, with endothelium, to 5-hydroxytryptamine (5-HT, $n = 5$-6). (a) 5-HT alone (diabetic, □; control, ○) or in the presence of GR32191B (1 μM) (diabetic, ■; control, ●). (b) In the presence of endothelin-1 (ET-1, 3 nM) (diabetic, □; control, ○). (c) In the presence of ET-1 (3 nM) and GR32191B (1 μM) (diabetic, □; control, ○).

Contractile responses to 5-hydroxytryptamine in the presence of U46619 U46619 (20 nM control, 30 nM diabetic) produced small contractile responses in aortae from control (0.60 ± 0.30 g) and diabetic (0.34g ± 0.22g) rats. In the presence of U46619, maximum responses to 5-HT were not significantly different between aortae from control and diabetic rats (Figure 2 and Table 2). There was a significant increase in sensitivity to 5-HT in the presence of U46619 of aortae from control and diabetic rats compared to responses

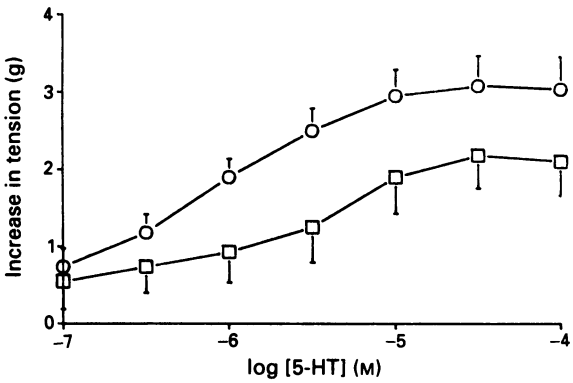

Figure 2 Responses of rat aortic rings, with endothelium, to 5-hydroxytryptamine (5-HT, $n = 5$-6) in the presence of U46619 (20 or 30 nM) (diabetic, □; control, ○).

obtained to 5-HT alone (indicated by pEC_{50} values, $P<0.05$, ANOVA, Table 2).

Responses in endothelium-denuded aortae

5-HT (0.1 μM−0.1 mM) produced concentration-dependent contractile responses in endothelium-denuded aortae from control and diabetic rats (Figure 3a). Maximum responses to 5-HT of aortae from diabetic rats were significantly less than responses from control rats (Figure 3a and Table 2, $P<0.05$, ANOVA; previously published; James *et al.*, 1994). Maximum responses to 5-HT, in the presence of GR32191B (1 μM), of aortae from diabetic rats were still significantly attenuated compared to 5-HT responses, in the presence of GR32191B, from controls (Figure 3a and Table 2, $P<0.05$, ANOVA). In the presence of GR32191B (1 μM), aortae from diabetic rats were significantly less sensitive to 5-HT than aortae from controls (indicated by pEC_{50} values, $P<0.05$, ANOVA, Table 2).

Contractile responses to 5-hydroxytryptamine in the presence of endothelin-1 Threshold concentrations of ET-1 produced small contractile responses in aortae from control (2 nM; 0.24 ± 0.14 g) and diabetic (3 nM; 0.51 ± 0.30 g) rats. In the presence of threshold concentrations of ET-1, maximum responses to 5-HT of aortae from diabetic rats were still significantly less than those obtained in aortae from control rats (Figure 3b and Table 2, $P<0.05$, ANOVA).

Contractile responses to 5-hydroxytryptamine in the presence of U46619 Threshold concentrations of U46619 (5−20 nM) produced small contractile responses in aortae from control (0.08 ± 0.01 g) and diabetic (0.08 ± 0.01 g) rats. In the presence of threshold concentrations of U46619, maximum

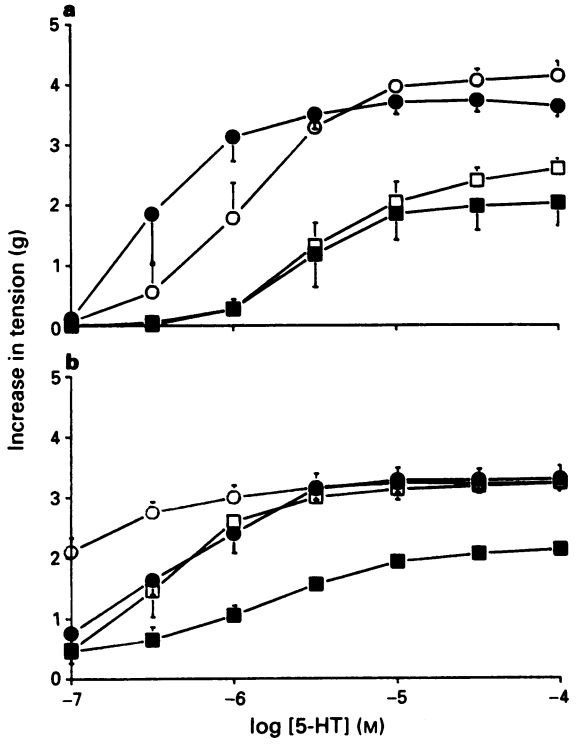

Figure 3 Responses of rat aortic rings, without endothelium, to 5-hydroxytryptamine (5-HT, $n = 4$-6). (a) 5-HT alone (diabetic, □; control, ○) or in the presence of GR32191B (1 μM) (diabetic ■; control, ●). (b) 5-HT in the presence of U46619 (5-20 nM) (diabetic, □; control, ○) or endothelin-1 (ET-1, 2 or 3nM) (diabetic, ■; control, ●).

responses to 5-HT of aortae from diabetic rats were not significantly different from those obtained from control rats (Figure 3b and Table 2). In the presence of U46619, there was an increase in sensitivity to 5-HT in aortae from control and diabetic rats compared to responses obtained to 5-HT alone (indicated by pEC_{50} values, $P<0.05$, ANOVA, Table 2).

Discussion

We have previously reported that maximum contractile responses to 5-HT of aortic rings from 2-week STZ-diabetic rats are attenuated compared to those obtained in control rats (Sikorski *et al.*, 1993; James *et al.*, 1994). It has been widely reported that TxA_2 levels are significantly increased during diabetes and that aortic rings from STZ-diabetic rats synthesize decreased amounts of prostacyclin (for a review see Hodgson *et al.*, 1992). The results of the present study suggest that endothelial-derived TxA_2 contributes to the contractile response to 5-HT in rat aortae. It also appears that TxA_2 is involved in the potentiation of 5-HT responses, by ET-1, in endothelium-intact aortae from diabetic rats.

In the present study, the potent and selective TP receptor antagonist GR32191B (Lumley *et al.*, 1989; Humphrey *et al.*, 1990) attenuated the maximum contractile responses produced by 5-HT in endothelium-intact aortae from both control and diabetic rats suggesting that contraction produced by 5-HT is mediated in part by TxA_2, or possibly its precursor PGH_2, acting at TP receptors. In addition, GR32191B did not affect the maximum contractile responses to 5-HT in endothelium-denuded aortae suggesting that PGH_2/TxA_2 from the endothelium contributes to the contractile response of 5-HT. Indeed, the vasocontrictor effects of 5-HT on placental vessels have been shown to be due, at least in part, to the stimulation of endogenous TxA_2 production (Howarth *et al.*, 1993).

As previously mentioned, it has been reported that threshold concentrations of 5-HT potentiate subsequent contraction induced by submaximal concentrations of ET-1 in rat aorta, but that the opposite does not occur (Yang *et al.*, 1992). This potentiation was inhibited by the addition of either the cyclo-oxygenase inhibitor, indomethacin or the TP receptor antagonist, SQ 29548. However, these workers did notice a reduction (which was not significant) in maximum responses to 5-HT in the presence of ET-1. Nakayama *et al.*, (1991) have shown that although concentration-response curves to 5-HT, in the pig coronary artery, are potentiated by ET-1 (0.1 nM), they were significantly attentuated when the concentration of ET-1 was increased 100-fold (i.e. to 10 nM). The potentiating effect of ET-1 (0.1 nM) occurred without a significant increase in intracellular calcium. This inhibitory effect of higher concentrations of ET-1 (i.e. 3–10 nM) on subsequent responses to 5-HT has also been observed in the endothelium-denuded perfused rabbit ear artery (Wong-Dusting *et al.*, 1991). A similar reduction, in 5-HT responses in the presence of ET-1, was observed in the present study with endothelium-intact aortae from control but not diabetic rats. In fact, ET-1 significantly potentiated contractile responses to 5-HT in endothelium-intact aortae from diabetic rats.

The hypothesis that endothelial-derived eicosanoids may be involved in the altered responses of vascular smooth muscle during diabetes is not new. Tesfamariam *et al.* (1991) have suggested that altered receptor-mediated endothelium-dependent relaxation in diabetes was due to increased production of vasoconstrictor prostanoids by the endothelium as a consequence of protein kinase C (PKC) activation. Larkins & Dunlop (1992) and Ruderman *et al.* (1992) have suggested that the activation of PKC may lead to increased release of vasoconstrictor prostanoids. In the present study the TP receptor antagonist, GR32191B, prevented the potentiating effect of ET-1 in endothelium-intact aortae from diabetic rats suggesting that this potentiation was mediated by a vasoconstrictor cyclo-oxygenase product (i.e. PGH_2 or TxA_2). Importantly, the enhancement of 5-HT responses could be mimicked by the TxA_2-mimetic, U46619, further implicating TxA_2 involvement in the interaction between 5-HT and ET-1. Interestingly, the potentiating effect of ET-1 on 5-HT responses was observed only in endothelium-intact aortae from diabetic rats. However, the addition of exogenous TxA_2 (i.e. U46619) resulted in potentiation of 5-HT responses in both intact- and denuded- aortae, thus providing further support for the role of the endothelium in the interaction between 5-HT and ET-1.

5-HT (Nakaki *et al.*, 1985), ET-1 (Highsmith *et al.*, 1992) and TxA_2 (Dorn & Becker, 1993) produce their contractile effects on rat aorta by similar mechanisms, that is, the stimulation of phospholipase C and a subsequent increase in inositol-1,4,5-trisphosphate (IP_3) and diacylglycerol (DAG) levels. In turn DAG stimulates PKC. Prolonged activation of PKC may lead to the activation of negative feedback pathways which result in the inactivation of cell-surface receptors, the inhibition of hydrolysis of phosphatidyl 4,5 bisphosphate and activation of Ca^{2+} pumps which reduce intracellular Ca^{2+} (Nishizuka, 1984). This negative feedback has been suggested as the mechanism responsible for the ET-1-induced inhibition of 5-HT responses previously observed by other workers (Nakayama *et al.*, 1991; Wong-Dusting *et al.*, 1991). A similar negative feedback pathway, induced by the interaction of exogenous ET-1 and endogenous TxA_2, may explain the inhibition of responses to 5-HT observed in the present study in endothelium-intact aortae from control rats. However, this mechanism does not appear to have been activated in aortae from diabetic rats as potentiation of 5-HT responses was observed rather than inhibition. This indicates that there may be an abnormality in this pathway, in vascular smooth muscle, during diabetes.

The interactions observed in endothelium-denuded aortae displayed an additional component to those observed in endothelium-intact aortae. As well as 'normalizing' maximum responses to 5-HT, the TxA_2-mimetic, U46619, potentiated the responses to lower concentrations of 5-HT, in aortae from both control and diabetic rats. This potentiation could be due to U46619 changing the response threshold for contraction to 5-HT by mobilizing intracellular calcium (Young *et al.*, 1986; Flavahan & Vanhoutte, 1988). This effect may be masked in endothelium-intact aortae by the release of endothelium-derived relaxing factors such as nitric oxide and prostacyclin.

The results of the present study indicate that TxA_2, released from the endothelium, contributes to the contractile response of 5-HT in aortae from control and diabetic rats. Endothelial-derived TxA_2 also appears to play a role in the potentiation of 5-HT responses by ET-1 in aortae from diabetic rats.

We thank Glaxo Group Research (U.K.) and Upjohn Pty Ltd (U.S.A.) for the generous gifts of GR32191B and U46619, respectively.

References

DORN, G.W. & BECKER, M.W. (1993). Thromboxane A_2 stimulated signal transduction in vascular smooth muscle. *J. Pharmacol. Exp. Ther.*, **265**, 447–456.

FLAVAHAN, N.A. & VANHOUTTE, P.M. (1988). Threshold phenomena and interactions between receptors. *J. Cardiovasc. Pharmacol.*, **11**, S67–S72.

FULTON, D.J.R., HODGSON, W.C., SIKORSKI, B.W. & KING, R.G. (1991). Attenuated responses to endothelin-1, KCl and $CaCl_2$, but not noradrenaline, of aortae from rats with streptozotocin-induced diabetes mellitus. *Br. J. Pharmacol.*, **104**, 928–932.

HIGHSMITH, R.F., BLACKBURN, K. & SCHMIDT, D.J. (1992). Endothelin and calcium dynamics in vascular smooth muscle. *Annu. Rev. Physiol.*, **54**, 257–277.

HODGSON, W.C. & KING, R.G. (1992). Effects of glucose, insulin or aldose reductase inhibition on responses to endothelin-1 of aortic rings from streptozotocin-induced diabetic rats. *Br. J. Pharmacol.*, **106**, 644–649.

HODGSON, W.C., SIKORSKI, B.W. & KING, R.G. (1992). Cardiovascular sensitivity changes to eiconsanoids in rats with experimentally induced diabetes mellitus. *Clin. Exp. Pharmacol. Physiol.*, **19**, 9–15.

HOWARTH, S.R., VALLANCE, P. & WILSON, C.A. (1993). The vasoconstricting effect of endothelin and 5-HT on placental vessels is mediated in part by thromboxane A_2. *Br. J. Pharmacol.*, **108**, 137P.

HUMPHREY, P.P.A., HALLET, P., HORNBY, E.J., WALLIS, C.J. COLLINGTON, E.W. & LUMLEY, P. (1990). Pathophysiological actions of thromboxane A_2 and their pharmacological antagonism by thromboxane receptor blockade with GR32191. *Circulation*, **81**, I42–I52.

JAMES, G.M., HODGSON, W.C., DAVIS, E.A. & HAYNES, J.M. (1994). Attenuated 5-hydroxytryptamine receptor-mediated responses in aortae from streptozotocin-induced diabetic rats. *Br. J. Pharmacol.*, **111**, 370–376.

LARKINS, R.G. & DUNLOP, M.E. (1992). The link between hyperglycaemia and diabetic nephropathy. *Diabetologia*, **35**, 499–504.

LUMLEY, P., WHITE, B.P. & HUMPHREY, P.P.A. (1989). GR32191, a highly potent and specific thromboxane A_2 receptor blocking drug on platelets and vascular and airways smooth muscle *in vitro*. *Br. J. Pharmacol.*, **97**, 783–794.

NAKAKI, T., ROTH, B.L., CHUANG, D. & COSTA, E. (1985). Phasic and tonic components in 5-HT_2 receptor-mediated rat aorta contraction: participation of Ca^{++} channels and phospholipase C. *J. Pharmacol. Exp. Ther.*, **234**, 442–446.

NAKAYAMA, K., ISHIGAI, Y., UCHIDA, H. & TANAKA, Y. (1991). Potentiation by endothelin-1 of 5-hydroxytryptamine-induced contraction in coronary artery of the pig. *Br. J. Pharmacol.*, **104**, 978–986.

NISHIZUKA, Y. (1984). The role of protein kinase C in cell surface signal transduction and tumour promotion. *Nature*, **308**, 693–698.

RUDERMAN, N.B., WILLIAMSON, J.R. & BROWNLEE, M. (1992). Glucose and diabetic vascular disease. *FASEB.*, **6**, 2905–2914.

SIKORSKI, B.W., JAMES, G.M., GLANCE, S.D., HODGSON, W.C. & KING, R.G. (1993). Effects of endothelium on diabetes-induced changes in constrictor responses mediated by 5-hydroxytryptamine in rat aorta. *J. Cardiovasc. Pharmacol.*, **22**, 423–430.

TESFAMARIAM, B., BROWN, M.L. & COHEN, R.A. (1991). Elevated glucose impairs endothelium-dependent relaxation by activating protein kinase C. *J. Clin. Invest.*, **87**, 1643–1648.

WONG-DUSTING, H.K., LA, M. & RAND, M.J. (1991). Effect of endothelin-1 on responses of isolated blood vessels to vasoconstrictor agonists. *J. Cardiovasc. Pharmacol.*, **17**, (Suppl. 7), S236–S238.

YANG, B.C., NICHOLS, W.W., LAWSON, D.L. & MEHTA., J.L. (1992). 5-Hydroxytryptamine potentiates vasoconstrictor effect of endothelin-1. *Am. J. Physiol.*, **262**, H931–H936.

YOUNG, M.S., IWANOV, V. & MOULDS, R.F.W. (1986). Interaction between platelet-released serotonin and thromboxane A_2 on human digital arteries. *Clin. Exp. Pharmacol. Physiol.*, **13**, 143–152.

(Received July 22, 1994
Revised November 21, 1994
Accepted November 25, 1994)

British Journal of Pharmacology (1995) 114, 1241-1249

Human muscarinic receptors expressed in A9L and CHO cells: activation by full and partial agonists

[1]Mary H. Richards & Paul L.M. van Giersbergen

Marion Merrell Dow Research Center, 16, rue d'Ankara, 67080 Strasbourg, France

1 A comparative study of receptor activation by ten full and partial muscarinic agonists was undertaken on the five subtypes of human muscarinic receptors expressed at similar receptor densities in Chinese hamster ovary (CHO-K1) cells. In addition, m_1, m_2 and m_3 receptors were expressed in mouse fibroblast A9L cells in order to compare the influences of cell type on agonist activation of these receptors.

2 Receptor-effector coupling efficiencies were greater in CHO than A9L cells and agonists displayed greater potencies and similar or greater intrinsic activities at $CHOm_1$ and $CHOm_3$ than $A9Lm_1$ and $A9Lm_3$ receptors. Although m_2 receptor density was 6 fold higher in A9L than CHO cells, carbachol elicited significantly greater inhibition of adenosine 3':5'-cyclic monophosphate (cyclic AMP) formation in $CHOm_2$ cells. These data suggest that not only receptor density but receptor-effector coupling and/or coupling efficiencies play significant roles in agonist-induced responses.

3 In CHO cells, receptor-effector coupling efficiencies were $m_3 = m_1 > m_5$. Although $CHOm_5$ receptors were the least efficiently coupled, some partial agonists displayed higher intrinsic efficacies at m_5 than m_3 receptors suggesting that, in CHO cells, m_5 and m_3 receptors may activate different G proteins and/or effectors to stimulate inositol monophosphate (IP1) formation.

4 McN-A-343 was a functionally selective m_4 agonist. It had little or no agonist activity at m_3 receptors expressed in either A9L or CHO cells. The slopes of McN-A-343 concentration-response curves in $CHOm_2$ cells were significantly lower than the slopes obtained with this compound in $CHOm_4$ cells suggesting that the mode of activation by McN-A-343 differed between the two muscarinic receptors negatively coupled to adenylyl cyclase.

5 Cloned receptors provide valuable tools for the study of agonist-receptor interaction and agonist-receptor activation but caution should be applied in assuming that the results are valid for all cell types or for tissue-expressed receptors.

Keywords: Recombinant muscarinic receptors; agonist relative efficacy; receptor-effector coupling efficiencies

Introduction

A great deal of effort has been expended in trying to find agonists that selectively activate subtypes of muscarinic receptors. Until recently, only tissues or cultured cells expressing endogenous receptors were available for comparing drug activities. Confounding factors included the necessity of using different tissues or cells as model systems for different receptor subtypes. Thus, differences in species, tissue preparations or cell culture conditions as well as the possible presence of multiple subtypes of receptors and/or effectors could obscure the interpretation of the results. More recently, there is evidence that a given subtype of receptor may activate different responses in different tissues, e.g. in olfactory bulb and striatum, putative m_4 receptors respectively activate (Olianas & Onali, 1991) or inhibit (McKinney *et al.*, 1991; Dokas & Ting, 1993) adenosine 3':5'-cyclic monophosphate (cyclic AMP) formation. In addition, in rat heart, where >92% of muscarinic receptors are of one type (Li *et al.*, 1991), there are multiple responses to muscarinic receptor activation, suggesting that in the same tissue one receptor may activate more than one type of G protein and/or effector (Kenakin & Boselli, 1990). Thus, in tissues, comparison of a series of agonists is confounded not only by the possible occurrence of multiple receptor subtypes but also by differences in receptor densities, the repertoire and relative levels of G proteins and/or isoforms of effectors available for activation by the liganded receptor. The question arises as to whether agonists can truly differentiate among receptor subtypes. This is of more than academic interest since selective muscarinic agonists may be therapeutically useful for the treatment of memory deficits in patients with Alzheimer's disease (see Caulfield, 1993).

It is now known that the amino acid sequences of the five subtypes of muscarinic receptors are highly similar especially in the transmembrane regions that form the ligand binding pocket (reviewed by Hulme *et al.*, 1990). This also suggests that agonists may not differentiate among muscarinic receptor subtypes but that receptor reserve or postreceptor-activation events determine the apparent selectivity observed.

Currently, there are cell lines with few or no endogenous muscarinic receptors that have been transfected with genes for one of the muscarinic receptor subtypes. These cells provide a means to control for differences in receptor densities and repertoires of G proteins and effectors. Chinese hamster ovary (CHO-K1) cells or mouse fibroblast (A9L) cells, transfected with human muscarinic receptor genes, were used in this study. The inhibition constants (K_i or IC_{50} values obtained from radioligand binding studies) of a series of agonists were determined for the five subtypes of receptors in CHO cells and for m_1 and m_3 receptors expressed in A9L cells. This same series of muscarinic agonists was used to compare receptor activation in the seven systems. Receptor-effector coupling efficiencies as well as agonist functional dissociation constants (K_A) and relative efficacies were determined for $CHOm_1$, $CHOm_3$ and $CHOm_5$ receptors. Some of the data have been presented in abstract form (Richards *et al.*, 1993).

[1] Author for correspondence.

Methods

Cell culture

A9L mouse fibroblasts or Chinese hamster ovary cells, transfected with human genes encoding one of the five subtypes of muscarinic receptors, were purchased from Research Genetics, Inc. (Bethesda, MD, U.S.A.). Wild-type A9L (ATCC CCL-1.4) and CHO-K1 (ATCC CCL-61) cells were purchased from American Type Culture Collection (Rockville, MD, U.S.A.). All materials used in cell cultures were obtained from Gibco (Cergy Pontoise, France). Upon arrival, the cell lines were put into culture and the first passages were aliquoted and stored as stock cultures. Passage numbers indicate the number of times the cells were passaged in our institute. A9L cells were maintained in Dulbecco's Modified Eagle Medium (DMEM, Gibco 041-1965), 10% foetal calf serum (FCS), penicillin G (10 u ml^{-1}), streptomycin (10 μg ml^{-1}), 4 mM L-glutamine and 1 mM sodium pyruvate. CHO cells were maintained in DMEM-Nutrient Mixture F-12 (1:1, Gibco 041-1331), 10% FCS, penicillin G (10 u ml^{-1}) and streptomycin (10 μg ml^{-1}), 1% non-essential amino acids, 2 mM L-glutamine, 0.5 mM sodium pyruvate. Both cell lines were grown in humidified incubators at 37°C, 5% CO_2. After 20–22 passages (cyclic AMP assay) or about 30 passages (IP1 formation), the cells were discarded and cells of lower passage number were put into culture. Cell membranes for the binding assays were prepared from confluent cells detached by scraping, washed twice in magnesium- and calcium-free phosphate buffered saline and stored frozen at −80°C.

Binding

Frozen membranes were thawed and homogenized in 10 ml ice-cold 50 mM sodium potassium phosphate buffer (pH 7.4) using a Polytron (setting 6 for 15 s). The homogenate was centrifuged at 40,000 *g* for 10 min at 4°C. The resulting pellet was resuspended in homogenizing buffer to obtain 0.05–0.5 mg protein ml^{-1} (protein content determined by the method of Lowry *et al.*, 1951). The incubation mixtures (0.5 ml final volume) contained buffer, homogenate, test compound and [^{3}H]-N-methylscopolamine ([^{3}H]-NMS) at 0.3 nM final concentration. Non-specific binding was defined by use of 2 μM atropine. In saturation experiments, the radioligand concentration varied between 0.025 and 1 nM. After incubation at room temperature (1 h for m_1-m_4, 1.5 h for m_5), incubation was terminated by rapid filtration through Whatman GF/B glass fibre filters presoaked in water. The filters were rinsed with saline (three times 3 ml using a Brandel cell harvester or for 10 s using a Skatron 96 well cell harvester) and the radioactivity determined by liquid (Beckman 6000 LS) or solid (1205 Betaplate, Wallac) scintillation spectrometry.

Inositol monophosphate (IP1) formation

Cells at >90% confluency were gently rinsed twice with physiological buffer (see below) and then incubated 2–5 min with 5 mM EDTA in 10 mM Na_2HPO_4, 0.25 M sucrose (pH = 7.4). The solution was gently decanted, the cells detached with a rubber 'cell scraper' into buffer and precipitated by low speed centrifugation. The cells were resuspended in a known volume of buffer and aliquots taken immediately to determine the percentage of cells excluding trypan blue. The volume of the cell suspension was then adjusted so as to obtain about 2×10^5 trypan blue-excluding cells per assay tube. The cells were added to tubes containing buffer with 5 mM LiCl and 0.1 μM [^{3}H]-*myo*-inositol and incubated for 30 min in a shaking bath at 37°C before the addition of different concentrations of standard or test agonists (final incubation volume = 300 μl). Twenty-five minutes after adding agonists, the reaction was stopped with 940 μl chloroform:methanol (1:2, v:v) and [^{3}H]-inositol monophosphates were quantified by column chromatography following the procedure of Brown *et al.* (1984), as modified by Richards (1990). Each treatment, i.e. blank (no cells), basal or a given concentration of an agonist, was determined in triplicate. Results are expressed as a percentage of the maximum response above basal obtained with a standard agonist (oxotremorine-M or carbachol) included in each experiment.

Measurement of cyclic AMP levels

We observed that cells near or at confluency tended to have higher basal cyclic AMP levels but the response to forskolin was unchanged, thus giving rise to a smaller stimulation. To avoid confluency, cells were seeded at a low density 20–22 h before the experiment began. The cells were detached, resuspended and counted as described above and the volume adjusted to obtain about 2×10^5 trypan blue-excluding cells per assay tube. Each tube contained physiological buffer and 0.1 mM 3-isobutyl-1-methyl-xanthine (IBMX). After an initial incubation of 10 min in a shaking bath at 37°C, agonists were added, followed 10 min later by forskolin (final concentration = 1 or 3 μM). The final volume was 250 μl. The reactions were stopped 10 min after the addition of forskolin with 250 μl ice-cold 10% perchloric acid (PCA). The protein was precipitated by centrifugation and quantified by the Lowry procedure. An aliquot of each supernatant was extracted with Freon:trioctylamine (1:1, v:v) to remove the PCA and the cyclic AMP content determined using radioimmunoassay (RIA) kits.

Each treatment was assayed in duplicate samples of cells and duplicate samples of each assay tube were subjected to radioimmunoassay (RIA). Blank values (no cells), which varied from 0 to an equivalent of around 200 fmol cyclic AMP, were determined in each experiment. Blank values were subtracted from sample values which were then converted to pmol [mg^{-1} protein (% trypan-blue-excluding cells)]. The percentage inhibition relative to the standard agonist (carbachol or oxotremorine-M included in every experiment) was calculated for each agonist.

Receptor alkylation

The active aziridinium ion of propylbenzilylcholine mustard was obtained by the procedure of Hu & El-Fakahany (1990). Receptor alkylation proceeded for 15 min ($CHOm_4$) or 20 min ($CHOm_1$, $CHOm_3$, $CHOm_5$) at 37°C in a shaking water bath. Excess propylbenzilylcholine mustard was removed by centrifugation and the cells were resuspended in physiological buffer to obtain the desired number of trypan blue-excluding cells per assay tube as described above.

Drugs and chemicals

Radioimmunoassay kits and [^{3}H]-*myo*-inositol (18–20 Ci $mmol^{-1}$) were purchased from DuPont de Nemours S.A., Les Ulis, France and Amersham France, Les Ulis, France. Propylbenzilylcholine mustard and [^{3}H]-N-methylscopolamine ([^{3}H]-NMS, 83 Ci mol^{-1}) were purchased from DuPont de Nemours S.A., Les Ulis, France. RS 86 (2-ethyl-8-methyl-2,8-diazaspiro-[4,5]-decan-1,3-dion hydrobromide) was a gift from Sandoz (Basel, Switzerland). Oxotremorine-M (N,N,N,-trimethyl-4-)2-oxo-1-pyrrolidinyl)-2-butyn-1-ammonium iodide) and McN-A-343 (4-hydroxy-2-butynyl)-1-trimethylammonium-*m*-chlorocarbanilate chloride) were purchased from Research Biochemicals Incorporated (Natick, MA, U.S.A.). The following products were purchased from Sigma Chimie, La Verpillière, France: arecoline hydrobromide, carbamyl-β-methyl choline chloride (bethanechol), carbamylcholine chloride (carbachol), (±)-acetyl-β-methylcholine chloride (methacholine), (±)-muscarine chloride, oxotremorine sesquifumarate, pilocarpine hydrochloride, bovine albumin fraction V, IBMX, N-[2-hydroxyethyl]piperazine-N′-

[2-ethanesulphonic acid] (HEPES), ethylenediaminetetraacetic disodium salt (EDTA), and Freon (1,1,2-trichlorotrifluoroethane). Trioctylamine was from Aldrich-Chimie, Strasbourg, France. Physiological buffer was prepared with analytical grade chemicals and contained (in mM): NaCl 118, KCl 5.0, $CaCl_2$ 1.3, KH_2PO_4 1.0, $MgSO_4$ 1.2, $NaHCO_3$ 25, glucose 10 and HEPES 10, pH 7.4

Calculations

(1) Binding assay Displacement curves were analysed by InPlot GraphPad (GraphPad Software, Inc., San Diego California, U.S.A.) to obtain Hill slopes and inhibition values (IC_{50}). In cases where the slope ≥ 0.8, K_i values were calculated using the Cheng-Prusoff equation (Cheng & Prusoff, 1973). The dissociation constants (K_D) for [^{3}H]-NMS were obtained from saturation experiments performed under the same conditions as the agonist binding assays.

(2) Functional assays A standard logistic equation was fitted to the data obtained from the functional assays (i.e. stimulation of IP1 formation or inhibition of forskolin-stimulated cyclic AMP accumulation relative to the standard agonist) using a curve-fitting programme (GraFit, Erithacus Software Limited, London, UK, or SigmaPlot, Jandel Scientific, Erkrath, Germany) to obtain estimates of the parameters EC_{50}, slope and maximum response.

(3) Dissociation constants, relative efficacy and receptor occupancy The dissociation constants (K_A) of oxotremorine-M for $CHOm_1$, $CHOm_3$ and $CHOm_5$ receptors were determined by the partial receptor occlusion method (Furchgott & Bursztyn, 1967) using propylbenzilylcholine mustard as the alkylating agent. Relative efficacies and dissociation constants of partial agonists were estimated from the slopes and intercepts of plots of $[A]\,[P]^{-1}$ vs [A] for equieffective concentrations of standard [A] and partial agonist [P] (Kenakin, 1987). The averaged values of the standard agonist, oxotremorine-M, and individual experimental results of partial agonists were used. For weak partial agonists, the response elicited by a 1 mM concentration was determined. A plot of log relative efficacy against % maximal response (Kenakin, 1987) for partial agonists in the series provided a rough estimation, by extrapolation (NB), of the relative efficacies of these weak partial agonists at $CHOm_3$ and $CHOm_5$ receptors.

To compare receptor-effector coupling efficiencies among the different receptor subtypes expressed in CHO cells, or of the same receptor subtype expressed in the two cell lines, the ratios of dissociation or inhibition constant (K_A or K_i) to EC_{50} (Kenakin, 1987) were calculated using oxotremorine-M as agonist.

(4) Statistical analysis The data obtained from curve fitting procedures and the relative efficacies were analysed for statistical differences using single factor ANOVA and Dunnett's *t* test. The parameters obtained with oxotremorine-M served as control. EC_{50} values were converted to the negative log values for statistical analysis, the latter being more likely to be normally distributed (Fleming *et al.*, 1972). Student's *t* test was used to compare differences obtained with an agonist at a given receptor expressed in two cell lines. Differences were statistically significant when $P<0.05$.

Results

Binding

The receptor densities and K_D values of [^{3}H]-NMS at the different muscarinic receptor subtypes expressed in A9L or CHO cells are indicated in Table 1. The K_A values of [^{3}H]-NMS were similar to the range of values reported by Buckley *et al.* (1989) in CHO cells and using somewhat different assay conditions. Analysis of competition curves to displace specifically bound [^{3}H]-NMS by agonists was used to calculate IC_{50} values and slopes for these agents (Table 2). For agonists with slopes equal to or greater than 0.8, the IC_{50} was converted to K_i.

The IC_{50}/K_i values obtained with seven muscarinic agonists were similar in A9L and CHO cells expressing m_1 receptors (differences <5 fold) except for oxotremorine (ratio of K_i at $CHOm_1/A9Lm_1 = 6$). Differences of 4 fold or less were observed with m_3 receptors in the two cell lines. In CHO cells, all agonists but McN-A-343 and RS 86 displayed the lowest IC_{50} value for m_2 receptors, higher values were observed at m_4, m_5 and m_3 receptors, and the highest IC_{50} values were for m_1 receptors. With three exceptions, all agonists displayed IC_{50} values that were more than 30 fold lower at m_2 than at m_1 receptors. Pilocarpine, RS 86 and the so-called 'M_1-selective' agonist, McN-A-343, did not distinguish (differences of 3 fold or less) among the five subtypes of muscarinic receptors.

The Hill slopes from the data obtained with these agonists were lowest for m_2 receptors, followed by m_4 receptors, both coupled predominantly to G proteins that inhibit adenylyl cyclase activity. The interactions of the agonists with the three receptor subtypes coupled to phospholipase C(s) gave rise to slopes of 0.80 or greater except carbachol at $A9Lm_1$, $A9Lm_3$ and $CHOm_3$ receptors.

IP1 formation induced by full and partial agonists at m_1, m_3 and m_5 receptors

The current methods used to quantify receptor-activated phosphatidylinositol hydrolysis have been reviewed by Nahorski and coworkers (Nahorski & Challiss, 1991; Wojcikiewicz *et al.*, 1993) and the advantages and disadvantages of each method considered. The continuous labelling method used in this study could give rise to erroneous conclusions if the two cell lines incorporate the label into different inositol pools with different sensitivities to agonists such that the agonist-induced responses are due to differences in specific radioactivity rather than or in addition to receptor-activation. We observed differences in the amount of labelling and in the kinetics of IP1 formation following activation of m_1 receptors expressed in CHO and A9L cells (Richards & van Giersbergen, 1995) but the extent of phospholipid hydrolysis obtained at two different incubation times with 1 mM carbachol were similar for A9Lm1 (times basal) (30 min: 10.6 ± 3.5; 60 min: 16.3 ± 4.6, each $n = 4$), A9Lm3 (12.0 and 10.3 in 2 experiments at 30 min; 60 min: 15.8 ± 5.8, each $n = 3$), CHOm1 (30 min: 11.8 ± 3.1; 60 min:

Table 1 Dissociation constants (K_D in pM) for [^{3}H]-N-methylscopolamine and receptor densities (B_{max} = fmol binding sites mg^{-1} protein) of the different receptor subtypes expressed in A9L or CHO cells

	A9L m_1	*CHO* m_1	*A9L* m_2	*CHO* m_2	*A9L* m_3	*CHO* m_3	*CHO* m_4	*CHO* m_5
K_D	87 ± 9	214 ± 26	207 ± 26	226 ± 9	175 ± 53	112 ± 18	81 ± 11	426 ± 15
B_{max}	369 ± 73	824 ± 59	2625 ± 449	410 ± 42	611 ± 42	651 ± 177	531 ± 29	414 ± 97

$n = 3$

Table 2 Affinity constants (K_i, μM) of agonists determined by the inhibition of the specific binding of [^{3}H]-N-methylscopolamine to human muscarinic receptors expressed in A9L or CHO cells

Agonist	$A9Lm_1$			$CHOm_1$		$CHOm_2$		$A9Lm_3$		$CHOm_3$		$CHOm_4$		$CHOm_5$	
	IC_{50}	K_i	Slope	IC_{50}	K_i	Slope	IC_{50}	Slope	IC_{50}	K_i	Slope	IC_{50}	Slope	IC_{50}	K_i	Slope
Oxo-M	23 ±5	7 ±1	0.83 ±0.03	34 ±9	13 ±3	0.80 ±0.04	0.8 ±0.4	0.53 ±0.05	38 ±8	11 ±2	0.85 ±0.03	54 ±22	25 ±3	0.86 ±0.05	7.2 ±1.4	0.67 ±0.03	1.7 ±0.3	0.9 ±0.04	1.06 ±0.04
Arecoline	34 ±6	10 ±2	0.83 ±0.04	75 ±10	31 ±3	0.93 ±0.03	2.3 ±0.3	0.58 ±0.02	31 ±1	9.3 ±0.3	0.88 ±0.03	36 ±5	12 ±1	0.93 ±0.03	44 ±2	0.76 ±0.01	34 ±5	20 ±3	0.86 ±0.05
Bethanechol	657 ±71	197 ±23	0.85 ±0.06	1837 ±294	771 ±15	0.91 ±0.03	25 ±4	0.59 ±0.04	278 ±25	84 ±7	0.92 ±0.03	631 ±8	214 ±6	0.95 ±0.02	317 ±60	0.93 ±0.16	393 ±51	232 ±36	0.92 ±0.04
Carbachol	500 ±70		0.76 ±0.07	465 ±123	320 ±75	0.82 ±0.07	4.5 ±1.4	0.51 ±0.04	173 ±30		0.76 ±0.01	417 ±19		0.76 ±0.00	49 ±9	0.76 ±0.04	196 ±53	125 ±22	0.83 ±0.06
McN-A-343	21 ±3	6 ±1	0.85 ±0.06	61 ±21	17 ±1	0.88 ±0.03	37 ±7	0.85 ±0.07	16 ±1	5 ±1	0.93 ±0.02	29 ±5	10 ±2	0.98 ±0.04	27 ±3	0.77 ±0.03	21 ±3	13 ±2	0.98 ±0.02
Methacholine	NT			766 ±97	316 ±35	0.88 ±0.02	2.6 ±0.5	0.56 ±0.01	NT			134 ±11	46 ±2	0.92 ±0.03	52 ±14	0.78 ±0.08	62 ±8	36 ±5	0.85 ±0.06
Oxotremorine	1.8 ±0.2	0.55 ±0.07	0.92 ±0.03	7.6 ±0.2	3.2 ±0.04	0.85 ±0.10	0.19 ±0.05	0.61 ±0.04	3.5 ±0.4	1.0 ±0.1	0.97 ±0.07	2.7 ±0.3	0.9 ±0.2	0.89 ±0.08	3.4 ±0.7	0.78 ±0.06	1.4 ±0.2	0.8 ±0.1	0.90 ±0.02
Pilocarpine	13 ±0.6	3.9 ±0.2	0.97 ±0.06	26 ±3	11 ±1	0.92 ±0.04	5.7 ±1.1	0.79 ±0.06	5.6 ±0.7	1.7 ±0.2	0.87 ±0.04	21 ±2	7.1 ±0.4	0.90 ±0.04	20 ±1	0.77 ±0.04	9 ±1	5.1 ±0.9	0.91 ±0.02
RS 86	11 ±3	3.3 ±0.1	0.90 ±0.03	38 ±13	16 ±6	0.93 ±0.03	16 ±4	0.79 ±0.06	7.1 ±1.3	2.1 ±0.4	0.94 ±0.05	11 ±1	3.8 ±0.6	0.87 ±0.03	27 ±4	0.85 ±0.08	13 ±2	7.5 ±1.2	0.96 ±0.05

Values are mean ± s.e.mean; $n = 3$.
Oxo-M = oxotremorine-M.
NT = not tested.

17.7 ± 4.2, each $n = 3$) and CHOm5 (30 min: 9.8 ± 2.6; 60 min: 25.6 ± 4.2, each $n = 9$) whereas significantly smaller stimulations were observed in CHOm3 cells (30 min: 3.6 ± 0.6; 60 min: 4.7 ± 0.5, each $n = 3$). Although the inositol pools were not at isotopic equilibrium, the time course and levels of IP1 accumulation induced by carbachol that we observed in $CHOm_1$ cells using the continuous labelling method were similar to those observed in $CHOm_1$ cells labelled for 48 h with [^{3}H]-*myo*-inositol (Atack *et al.*, 1993; degree of isotopic labelling not indicated). Moreover, results we obtained with the continuous labelling method were largely similar (see Discussion) to those obtained using a pulse-labelling procedure (Wang & El-Fakahany, 1993) or results obtained with agonist-stimulated GTPase activity (Lazareno *et al.*, 1993).

Oxotremorine-M, carbachol and muscarine were full agonists at m_1, m_3 and m_5 receptors expressed in CHO cells (Table 3). Arecoline and oxotremorine were full or strong partial (> 50% maximal response) agonists. Pilocarpine and RS 86 were partial agonists at the three receptor subtypes. Bethanechol was the least potent agonist, displaying similar EC_{50} values at the three receptors where it was a full or strong partial agonist. McN-A-343 was a potent full agonist at $CHOm_1$ receptors, 18 fold less potent and a partial agonist at $CHOm_5$ receptors and almost inactive at $CHOm_3$ receptors.

Comparison of m_1 receptors expressed in A9L and CHO cells

CHO cells expressed 2.2 times more m_1 receptors than did A9L cells and all agonists except RS 86 were more potent in $CHOm_1$ cells (Table 3). Differences in agonist potency in the two cell lines fell into two groups: differences of less than 3 fold (bethanechol, carbachol, McN-A-343, pilocarpine, RS 86) and differences of 6 fold or greater (oxotremorine-M, arecoline, methacholine, muscarine, oxotremorine). As might be expected from a slightly higher receptor density in CHO cells, McN-A-343 and RS 86 displayed greater intrinsic activity in CHO than A9L cells. Oxotremorine and pilocarpine appeared to be strong partial agonists. In six out of seven experiments with $A9Lm_1$ cells, RS 86 was a partial agonist (32% ± 7% of maximum response) but in one experiment it was a full agonist (no change in potency). It thus appears likely that RS 86 is a partial agonist of similar potency in both cell lines. Bethanechol was again the least potent but a full agonist in the two systems.

Comparisons of m_3 receptors expressed in A9L and CHO cells

Although receptor densities for m_3 receptors expressed in CHO and A9L cells were similar, all agonists (except McN-A-343) were significantly more potent at stimulating m_3 receptors in CHO cells (Table 3); differences in agonist potencies at m_3 receptors in the two cell lines were 8 fold or greater except for bethanechol. The agonists displayed a similar order of intrinsic activities at m_3 receptors in the two cell lines except oxotremorine which was a partial agonist in $A9Lm_3$ and a full agonist in $CHOm_3$ cells ($P = 0.0011$). McN-A-343 was inactive or a weak partial agonist at m_3 receptors expressed in either cell line. A striking difference was observed with RS 86 and pilocarpine which were partial agonists, as potent as carbachol at m_3 receptors expressed in CHO cells but only weakly active at m_3 receptors expressed in A9L cells.

Stimulation of cyclic AMP formation with forskolin

A9L and CHO cells (wildtype) were incubated for 10 min in the absence or presence of increasing concentrations (0.1 to 30 μM) of forskolin and the levels of cyclic AMP were determined. Basal activity was significantly lower in the A9L

Table 3 Agonist-induced inositol monophosphate (IP1) accumulation in A9L or CHO cells expressing human muscarinic receptors

	$A9Lm_1$		$CHOm_1$		$A9Lm_3$		$CHOm_3$		$CHOm_5$	
Agonist	EC_{50}	R_{max}	EC_{50}	R_{max}	EC_{50}	R_{max}	EC_{50}	R_{max}	EC_{50}	R_{max}
Oxotrem.-M	0.64	112	0.10	99	3.7	107	0.22	108	0.39	107
(n = 9,14,5,9,8)	±0.12	±7	±0.03	±3	±1.1	±4	±0.07	±7	±0.06	±4
Arecoline	14[abe]	102	1.06[ab]	85	7.2	59*	0.96[acd]	77*	6.5[a]	79*
(n = 8,8,3,6,3)	±5	±12	±0.16	±6	±1.4	±8	±0.12	±8	±4	±6
Bethanechol	72[+]	98	35[+]	98	77[+]	71*	14.5[+]	72*	32[abce]	91
(n = 6,10,8,4,3)	±12	±6	±7	±7	±19	±4	±2.9	±4	±17	±3
Carbachol	5.3[a]	96	1.83[abc]	98	9.4[b]	101	0.90[ac]	100	1.31	100
(n = 17,18,10,13,9)	±0.9	±6	±0.26	±2	±2.1	±2	±0.23	±1	±0.35	±1
McN-A-343	5.0[a]	51*	1.74[ab]	90	(x)	2*	(x)	9*	33[abce]	49*
(n = 5,9,3,6,5)	±1.8	±10	±0.24	±7		±2		±3	±16	±9
Methacholine	8.2[a]	115	0.83[ab]	89	6.0	102	0.33	83	nt	
(n = 8,6,4,5,–)	±2.9	±11	±0.22	±6	±2.5	±12	±0.07	±9		
Muscarine	5.2[a]	127	0.55[a]	93	8.4[b]	92	0.29	94	0.76	108
(n = 7,8,5,6,3)	±2.2	±9	±0.12	±4	±2.3	±6	±0.08	±8	±0.20	±2
Oxotremorine	1.3	91	0.13	78*	2.8	56*	0.33	88	0.55	74*
(n = 4,11,7,4,3)	±0.3	±11	±0.03	±7	±1.2	±5	±0.05	±4	±0.22	±8
Pilocarpine	5.6[a]	86	4.1[abcd]	76*	(x)	11*	2.19[abcd]	43*	(x)	23*
(n = 6,9,6,4,3)	±1.1	±6	±1.7	±5		±7	±0.36	±9		±5
RS-86	4.4[a]	45*	5.8[abcdf]	78	(x)	13*	1.06[a]	50*	(x)	10*
(n = 7,9,6,3,4)	±1.5	±14	±2.8	±9		±4	±0.18	±11		±5

EC_{50} = μM; [a–f] or [+]indicate statistical differences among EC_{50} values: [a]from oxo-M, [b]from oxotremorine, [c]from muscarine,[d]from methacholine, [e]from carbachol, [f] from arecoline, [+]from all other agonists. x = response obtained with 1 mM agonist. R_{max} = % of maximum response (above basal) obtained with a standard agonist; * = R_{max} values significantly different from oxotremorine-M.

(15.6 ± 3.8 pmol cyclic AMP mg^{-1} protein) than in CHO cells (47.0 ± 7.5 pmol cyclic AMP mg^{-1} protein; n = 4 and 5, respectively, P = 0.01). At 30 μM forskolin, the stimulation was significantly greater in CHO than in A9L cells: 27.4 ± 3.1 (n = 5) and 5.9 ± 0.9 (n = 4, P < 0.01) times basal, respectively.

Comparison of m_2 receptors expressed in A9L and CHO cells

Carbachol inhibited cyclic AMP formation at m_2 receptors expressed in these cell lines with similar potencies (P > 0.05): 114 ± 28 nM at $A9Lm_2$ (n = 7), 41 ± 13 nM at $CHOm_2$ (n = 5). However, the intrinsic activity was significantly greater in CHO than A9L cells despite the 6 fold greater receptor density in the latter cell line. The maximum inhibition elicited by carbachol in $A9Lm_2$ cells was 51.3 ± 5.1% (n = 7) compared to 89.1 ± 1.2% (n = 5) in $CHOm_2$ (P < 0.01).

Effect of preincubation with carbachol on forskolin-stimulated cyclic AMP formation

$CHOm_4$ cells (as were $A9Lm_2$ and $CHOm_2$ cells) were preincubated 10 min with the agonists to allow ligand-receptor equilibration before the addition of forskolin. In order to determine if preincubation could desensitize the m_4 receptors. $CHOm_4$ cells were exposed to carbachol for 0 to 30 min before the addition of forskolin. The inhibition of forskolin-stimulated cyclic AMP formation by 0.3 μM carbachol was constant for up to 20 min: inhibition was 75 ± 4% at time 0, 79 ± 1% at 10 min and 78 ± 2% at 20 min incubation (n = 3 at each time). A significantly smaller inhibition by carbachol was observed after 30 min preincubation (51 ± 7%, n = 3; P < 0.05).

Inhibition in $CHOm_4$ and $CHOm_2$ cells of forskolin-stimulated cyclic AMP formation by full and partial agonists (Table 4)

Activation of $CHOm_2$ or $CHOm_4$ receptors by oxotremorine-M inhibited forskolin-stimulated cyclic AMP formation to a similar extent: 85% ± 3% (n = 6) at m_2, 79% ± 1% (n = 16; P = 0.062) at m_4 receptors. In $CHOm_4$ cells, none of the maximum responses differed significantly from that of oxotremorine-M. However, the maximum response elicited by bethanechol was significantly less than the responses elicited by carbachol and oxotremorine, suggesting that bethanechol may be a strong partial agonist at these receptors.

Table 4 Agonist-induced inhibition of forskolin-stimulated cyclic AMP formation in CHO cells transfected with human genes for m_2 or m_4 muscarinic receptors

	$CHOm_2$		$CHOm_4$	
Agonist	EC_{50} (nM)	R_{max} (%)	EC_{50} (nM)	R_{max} (%)
Oxotrem.-M	23	106	1.2	105
(n = 6,18)	±6	±6	±0.3	±2
Arecoline			21[a]	101
(n = –,6)			±7	±3
Bethanechol			787[x]	88[bc]
(n = –,5)			±218	±6
Carbachol	41	102	20[ab]	107
(n = 5,19)	±13	±4	±4	±4
McN-A-343	1659[ac]	72[ac]	50[ab]	109
(n = 4,6)	±632	±5	±12	±5
Methacholine			26[ab]	105
(n = –,6)			±6	±4
Muscarine			154[a]	97
(n = –,7)			±5	±4
Oxotremorine			7[a]	114
(n = –,7)			±4	±7
Pilocarpine			5804[x]	110
(n = –,6)			±1041	±7
RS-86			151[x]	107
(n = –,6)			±39	±5

Values are means ± s.e.means for n experiments.
[a] = significantly different from oxotremorine-M; [b] = significantly different from oxotremorine; [c] = significantly different from carbachol; [x] = significantly different from all other agonists.

Three agonists were also used to inhibit forskolin-stimulated cyclic AMP formation via m_2 receptors, in CHO cells, expressed at a similar density as m_4 receptors. Carbachol, a full agonist, displayed similar potencies (P > 0.05) at the two receptors. Both oxotremorine-M and McN-A-343 were significantly (P < 0.01) more potent at m_4 than m_2 receptors. McN-A-373 displayed greater intrinsic activity at

m_4 than m_2 receptors ($P<0.05$). The slopes of the concentration-response curves for McN-A-343 at m_2 receptors (0.51 ± 0.03, $n = 4$) were significantly less ($P = 0.0493$) than those obtained at m_4 receptors (0.98 ± 0.15, $n = 8$).

Experiments with propylbenzilylcholine mustard

Incubation of $CHOm_4$ cells with 30 nM propylbenzilylcholine mustard shifted the concentration-response curve of oxotremorine-M to the right 15.1 ± 3.1 fold ($n = 3$) with no change in the maximum response. Higher concentrations of propylbenzilylcholine mustard, up to 10 μM, further shifted the concentration-response curves of oxotremorine-M but had no effect on the maximum response.

In $CHOm_1$ and $CHOm_3$ cells, incubation with 10 μM propylbenzilylcholine mustard decreased the maximum responses and increased the EC_{50} values obtained with oxotremorine-M (Figure 1a and b). The shift in the EC_{50} values were similar for $CHOm_1$ and $CHOm_3$: 77 ± 15 fold for m_1 ($n = 5$) and 85 ± 25 fold for m_3 ($n = 6$). Similar decreases in the maximum stimulation of IP1 to $46 \pm 10\%$ for m_1 ($n = 5$) and $42 \pm 7\%$ for m_3 ($n = 6$) were observed. From these data, the dissociation constants (K_A) for oxotremorine-M in $CHOm_1$ and $CHOm_3$ cells were found to be in good agreement (differences $\leqslant 2$) with the corresponding K_i values (Tables 2 and 5).

In $CHOm_5$ cells, incubation with 1 μM propylbenzilylcholine mustard shifted the concentration-response curve of oxotremorine-M to the right 27 ± 13 fold ($n = 4$) and decreased the maximal response to $58 \pm 6\%$ of the response to oxotremorine-M in the absence of propylbenzilylcholine mustard (Figure 1c). From these data, the K_A was found to be 4.8 ± 0.7 μM ($n = 4$), somewhat greater than the K_i of 0.90 ± 0.04 μM ($n = 3$).

The dissociation constants of some partial agonists (Table 5) differed by 5 fold or less from their corresponding K_i values (Table 2). The exception was oxotremorine at $CHOm_1$ receptors (9 fold difference).

Relative efficacies, receptor-effector coupling efficiencies

Receptor-effector coupling efficiencies were similar for m_3 receptors (K_A/EC_{50} for oxotremorine-M = 60) and m_1 receptors ($K_A/EC_{50} = 58$) whereas m_5 receptors were less efficiently coupled ($K_A/EC_{50} = 12$). Comparing ratios of K_i/EC_{50} for oxotremorine-M at m_1 and m_3 receptors expressed in CHO and A9L cells suggest that receptor-effector coupling is more efficient in CHO cells. In A9L cells, m_1 receptors appeared to be coupled somewhat more efficiently than m_3 receptors.

The relative efficacies (compared to oxotremorine-M) of partial agonists at m_1, m_3 and m_5 receptors expressed in CHO cells are presented in Table 5. Relative efficacies of McN-A-343 at $CHOm_3$ and pilocarpine and RS 86 at $CHOm_5$ receptors are estimated by extrapolation from plots of log relative efficacy versus % maximal response of more active partial agonists. Linear regression of the points plotted from data obtained with $CHOm_3$ had a correlation coefficient of 0.97; standard errors of the slope and intercept were 10% and 14% of the corresponding values. Linear regression of the three points obtained with $CHOm_5$ receptors had a correlation coefficient of 1, the standard errors of the slope and intercept were less than 2% of their corresponding variables. Pilocarpine displayed greater intrinsic acitivity at m_1 than at m_3 or m_5 receptors. RS 86 was more efficacious at m_1 and m_3 than m_5 receptors. Although $CHOm_5$ receptors were less efficiently coupled than $CHOm_1$ or $CHOm_3$ receptors, arecoline and oxotremorine were more efficacious at m_5 than m_3 (and, for oxotremorine, m_1) receptors.

The apparent inability of propylbenzilylcholine mustard to block $CHOm_4$ receptors sufficiently prevented an estimation of the K_A value for oxotremorine-M and calculating an inhibition constant, K_i, is of dubious value due to the low Hill slope. However, substituting K_i for K_A would allow a very rough estimate of the efficacy of oxotremorine-M. We have found that GTP analogues such as GppNHp steepen and shift the binding concentration-response curves of oxotremorine-M to the right so using the K_i value would give a *minimal* figure for the receptor reserve for this agonist. In our transfected CHO cells, oxotremorine-M-activated m_4 receptors are coupled with a high degree of efficiency as indicated by an apparent receptor reserve >900.

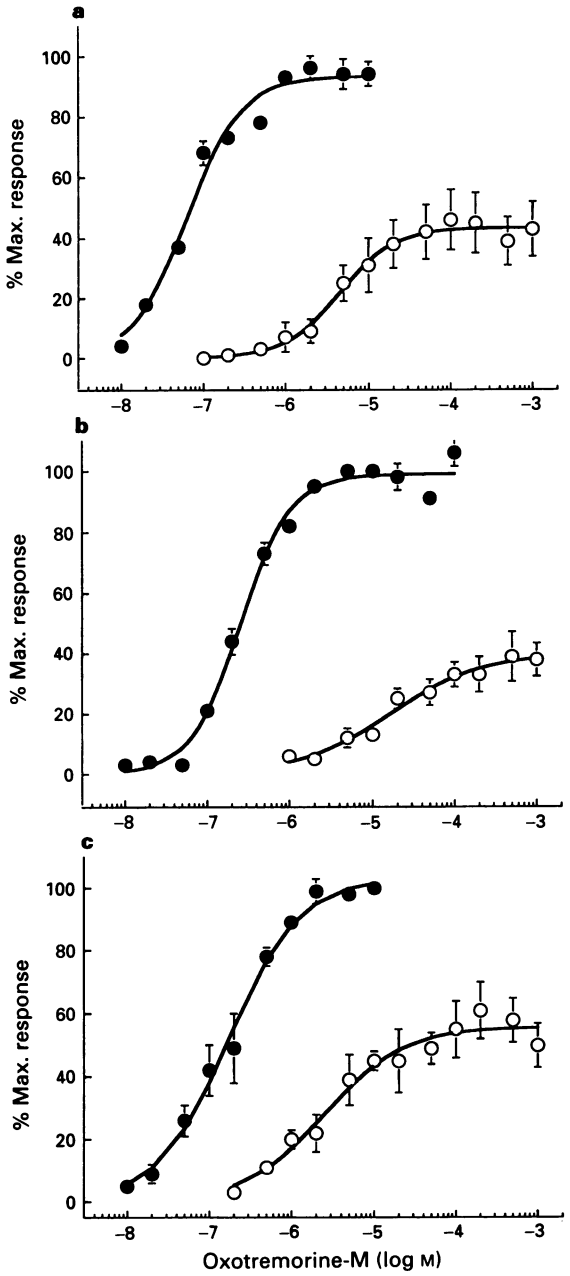

Figure 1 Concentration-response curves of oxotremorine-M in the absence (●) or presence (○) of propylbenzilylcholine mustard (20 min incubation). (a) $CHOm_1$ cells ($n = 5$), 10 μM propylbenzilylcholine mustard; (b) $CHOm_3$ cells ($n = 5$), 10 μM propylbenzilylcholine mustard; (c) $CHOm_5$ cells ($n = 4$), 1 μM propylbenzilylcholine mustard.

Discussion

A series of muscarinic agonists were used to study agonist-receptor interaction and agonist-receptor activation of muscarinic receptor subtypes expressed in mouse fibroblasts (A9L) and Chinese hamster ovary (CHO-K1) cells. The

Table 5 Dissociation constants (K_A) and relative efficacies of partial agonists compared to the standard agonist oxotremorine-M

	$CHOm_1$		$CHOm_3$		$CHOm_5$	
	K_A (μM)	*Rel. Eff.*	K_A (μM)	*Rel. Eff.*	K_A (μM)	*Rel. Eff.*
Oxo-M (5,5,4)	5.82 ± 1.03	1.0	13.20 ± 1.96	1.0	4.80 ± 0.67	1.0
Arecoline (–,5,3)			7.38 ± 1.34	0.058[a] ± 0.020	15.79 ± 4.41	0.198 ± 0.057
Bethanechol (–,4,–)			44.79 ± 5.87	0.028 ± 0.002		
McN-A-343 (–,–,4)				0.0012*	18.53 ± 7.47	0.025[x] ± 0.005
Oxotremorine (9,4,3)	0.35 ± 0.07	0.023[a] ± 0.003	2.10 ± 0.47	0.058[a] ± 0.015	2.31 ± 0.50	0.139 ± 0.029
Pilocarpine (8,4,–)	4.32 ± 1.16	0.022 ± 0.002	4.19 ± 0.79	0.007[b] ± 0.002		0.0041*
RS 86 (8,3,–)	4.40 ± 1.27	0.021 ± 0.003	1.58 ± 0.18	0.010 ± 0.003		0.0017*

Values are means ± s.e.mean, *n* number of experiments is indicated in parentheses. Statistical analysis across receptor subtypes for a given agonist. a = significantly different from m_5; b = significantly different from m_1. Statistical analysis among agonists for a given receptor subtype: [x] = significantly different from arecoline. *relative efficacy values obtained by extrapolation.

parameters examined included agonist inhibition values determined in a binding assay, a comparison of intrinsic activities and potencies of a series of agonists activating a given receptor in the two expression systems, and receptor-effector coupling efficiencies and relative agonist efficacies at homologous receptors expressed in the same cell line at similar receptor densities. We considered differences of 5 fold or less as unlikely to be physiologically relevant even if these differences were statistically significant. This was based, in part, on the observations that atropine, a putatively non-selective antagonist, displayed five fold differences among muscarinic receptor subtypes in both functional (Richards, 1990) and binding studies (Nivelbrant & Sparf, 1986) and that estimates of muscarinic antagonist affinity values at a given receptor subtype may vary by three fold or more (Mitchelson, 1988; Caulfield, 1993).

The conditions used to determine agonist inhibition values were those generally used with antagonists, i.e. non-physiological buffer and membrane preparations devoid of cytosolic factors that influence agonist binding. As far as we are aware, no other study has systematically compared inhibition values for a large series of agonists at all subtypes of cloned muscarinic receptors expressed in the same cell line or of a given receptor expressed in different types of cells. A significant difference in IC_{50} values was observed with carbachol using membranes prepared from recombinant (Results) or endogenous m_3 and m_4 receptors (Baumgold & White, 1989, membranes prepared in physiological buffer) whereas no difference was observed in intact CHO cells (Schwarz *et al.*, 1993). Carbachol did not distinguish between $CHOm_1$ and $CHOm_3$ receptors in membrane preparations (Results) or intact cells (Hu & El-Fakahany, 1990; Schwarz *et al.*, 1993). However, Hu & El-Fakahany (1990) found that the K_i of McN-A-343 was 23 fold greater in intact $CHOm_1$ than $CHOm_3$ cells, in contrast to Schwarz *et al.* (1993), also using intact cells, or in membrane preparations (Results), where no differences were found. Six out of nine agonists clearly distinguished between $CHOm_1$ and $CHOm_2$ receptors with differences in IC_{50} values of 30 fold or greater (Table 2) whereas in intact cells differences among (fewer) agonists were six fold or less (Schwarz *et al.*, 1993). Slopes and affinities of agonists binding to muscarinic receptors that inhibit adenylyl cyclase are more readily modulated by changes in the ionic strength of the buffer and the presence or absence of GTP than are muscarinic receptors linked to phosphatidylinositol turnover (references cited in Richards, 1991). Although both $CHOm_2$ and m_4 receptors inhibited adenylyl cyclase, the slopes determined in the binding assay were consistently lower at m_2 (except that of McN-A-343) than at m_4 receptors suggesting differences in agonist-receptor-G protein interactions but which produce the same end response.

Ligand-receptor equilibrium dissociation constants (K_i) at $CHOm_1$, $CHOm_3$ and $CHOm_5$ receptors were compared with 'functional' dissociation constants (K_A) obtained using the null method (Furchgott & Bursztyn, 1967; Kenakin, 1987). In most cases K_i and K_A values differed by 5 fold or less. The exception was a 9 fold difference for oxotremorine at $CHOm_1$ receptors. It is not known if this difference is due to chance, i.e. arose from scatter in the data, or reflect a particular receptor-interaction mode for this agonist sensitive to the differences in the two assay conditions. The utility of binding constants and functional dissociation constants as indicators of agonist-receptor interactions has been criticized by Colquhoun (1987). Specifically, in both radioligand binding assays and receptor alkylation studies, the constants obtained will depend not only on the affinity but also the efficacy of the agonist, especially for strong agonists. The inability to model quantitatively the various steps between agonist-receptor binding and the subsequent biological response and thus obtain precise information concerning agonist affinity and efficacy means that these terms are not strictly quantitative and their use to compare a series of agonists are indicative of relative rather than absolute differences.

The relative inefficacy of propylbenzilylcholine mustard to inactivate muscarinic receptors in CHO cells was unexpected. Despite high muscarinic receptor densities in rat striatum and rat cerebral cortex (2–3 pmol mg^{-1} protein, Wall *et al.*, 1991; Yasuda *et al.*, 1993), 10 nM propylbenzilylcholine mustard (McKinney *et al.*, 1989) or 10 nM benzilylcholine mustard (Keen & Nahorski, 1988) was sufficient to decrease the maximum responses to carbachol in these tissues. In contrast, cloned m_1 and m_3 receptors were more resistant to propylbenzilylcholine mustard, requiring 200 nM of the alkylating agent to decrease the maximum response to carbachol in CHO cells expressing low receptor densities ($B_{max} < 300$ fmol binding sites mg^{-1} protein; Hu & El-Fakahany, 1990) and 10 μM propylbenzilylcholine mustard in cells expressing moderate (this paper) or high receptor densities ($B_{max} = 2900$ fmol mg^{-1} protein; Schwarz *et al.*, 1993). This suggests that cloned muscarinic receptors, at least in CHO cells, are much more efficiently linked to effectors than are the corresponding muscarinic receptors in rat brain.

Agonist activation of human m_4 receptors in CHO cells was compared with the results of McKinney *et al.* (1991), who used a similar series of agonists at endogenous m_4 receptors in N1E-115 cells and putative m_4 receptors in rat striatum. The m_4 receptor density in rat striatum is around

1 pmol mg^{-1} protein (Yasuda *et al.*, 1993; see Table 1 for density of $CHOm_4$ receptors). All agonists were more potent in inhibiting cyclic AMP formation in $CHOm_4$ cells than in rat striatum. The ratios of EC_{50} values at $CHOm_4$ versus striatal receptors (from McKinney *et al.*, 1991) were 118 for oxotremorine-M, 26–43 for six other agonists and 2 for pilocarpine. In the three systems, identical rank orders of potencies were observed for seven of the eight agonists: oxotremorine-M ≥ oxotremorine > muscarine > carbachol > arecoline > McN-A-343 > bethanechol, providing additional evidence that the muscarinic receptors inhibiting adenylyl cyclase in rat striatum are of the m_4 subtype. The exception was pilocarpine which was less potent than bethanechol in $CHOm_4$ cells, more potent than bethanechol at striatal receptors and more potent than muscarine in N1E-115 cells.

Expressing a given receptor in two cell lines permitted comparison of the influences of different cell systems on receptor activation. We observed differences in the kinetics of IP1 formation in A9L and CHO cells transfected with m_1 (Richards & van Giersbergen, 1995) and m_3 receptors (unpublished observations). We also observed differences in cyclic AMP formation in these two cell lines (Results) suggesting differences in the levels and/or complement of G proteins or adenylyl cyclase(s) in these cells. Differences in receptor-effector coupling and/or coupling efficiency are suggested by the observation that the inhibition of forskolin-stimulated cyclic AMP formation by carbachol was significantly greater at m_2 receptors expressed in CHO cells despite the higher density of m_2 receptors in A9L cells.

Eight of the ten agonists displayed greater intrinsic activities and (except for RS 86) greater potencies in $CHOm_1$ than $A9Lm_1$ cells, consistent with the somewhat greater receptor density and apparently more efficient receptor-effector coupling observed in $CHOm_1$ cells. However, comparison of agonist potencies in the two cell lines suggested that the 10 agonists could be divided into two groups (see Results). The reasons for this are unknown. However, data obtained from point mutations of m_1 receptors (Hibert *et al.*, 1995) and from comparison of agonist potency ratios (Richards & van Giersbergen, 1995) suggest that agonist occupancy and activation of m_1 receptors differ among agonists and that m_1 receptors may complex with different isoform(s) of couplers or effectors depending on agonist structure.

We also compared activation of m_3 receptors expressed in either A9L or CHO cells. Although receptor densities were similar, the greater coupling efficiency in CHO cells was reflected in greater agonist potencies and intrinsic activities in these cells. The exception was bethanechol which had the same intrinsic activity in the two cell lines. Ratios of K_i/EC_{50} close to unity for bethanechol and arecoline in the apparently less efficiently coupled A9L cells suggests that receptor occupancy and response are approximately linearly related. This is compared to ratios of 14 and 12, respectively, in the more efficiently coupled CHO cells. Thus for cloned receptors, as for tissue receptors (Kenakin, 1987), the functions relating receptor occupancy and response may not be linear even for drugs that occupy 100% of the receptors to produce their maximal response.

We compared relative efficacies of partial agonists at m_1, m_3 and m_5 receptors expressed in CHO cells at similar receptor densities. Some agonists were more efficacious at activating the less efficiently coupled $CHOm_5$ receptors. For example, agonists producing about 75% of the maximal response in $CHOm_5$ cells were 14–20% as efficient at oxotremorine-M whereas in $CHOm_1$ and $CHOm_3$ cells, agonists producing about the same maximal response were only 2–6% as efficient as oxotremorine-M. Thus, in CHO cells, m_5 receptors may activate different G proteins and/or different phospholipases C(s) to stimulate IP1 formation.

Lazareno *et al.* (1993) determined agonist potencies and intrinsic activities of a series of agonists stimulating GTPase activity in human m_1, m_2, m_3 and m_4 receptors expressed in CHO cells at high density (1–7 pmol binding sites mg^{-1} protein). Wang & El-Fakahany (1993) also studied agonist activation (second messenger formation) using rat m_1 and m_3 and human m_2, m_4 and m_5 muscarinic receptors expressed in CHO cells at relatively low densities (B_{max} = 165–545 fmol mg^{-1} protein). Comparing data obtained in three independent laboratories using these cloned muscarinic receptors highlighted the many similarities despite differences in receptor densities and techniques. For example, both groups that determined agonist potencies (Lazareno *et al.*, 1993; present study) found that full agonists were at least 10 fold more potent at m_2 and m_4 than m_1 and m_3 receptors. Pilocarpine and McN-A-343 were weak partial agonists at m_5 receptors (Wang & El-Fakahany, 1993; present study). All three groups found McN-A-343 to display functional selectivity for m_4 receptors, to be a partial agonist at m_2 receptors and a weak partial agonist or inactive at m_3 receptors. The low slope of the concentration-response curves we observed with McN-A-343 suggests that m_2 receptor activation by this agonist may differ from the mode of activation observed at m_4 receptors. Non-classical interaction of McN-A-343 with muscarinic binding sites in rat myocardial membranes was observed by Birdsall *et al.* (1983).

There were also some notable differences among the results from these groups. Although the m_4 receptor densities were quite similar in our study and that of Wang & El-Fakahany (1993), we found the intrinsic activities of bethanechol and McN-A-343 to be less or equal, respectively, to that of carbachol whereas Wang & El-Fakahany (1993) found the intrinsic activities of both compounds to be significantly greater than that of carbachol. In addition, Wang & El-Fakahany (1993) reported that, in CHO cells, the order of receptor-effector coupling efficiencies was $m_5 > m_3 > m_1$ whereas we found that m_1 and m_3 receptors were equally and much more efficiently coupled to IP1 formation than were m_5 receptors.

Other contradictory results observed with muscarinic receptors expressed in CHO cells include a report by Schwarz *et al.* (1993) that PI turnover is more sensitive to muscarinic agonists than the cyclic AMP assay, clearly different from the data of Lazareno *et al.* (1993), Wang & El-Fakahany (1993) and the present results. Although the cloned muscarinic receptors used in three of these studies are from the same source, there are differences in receptor gene expression, receptor-effector coupling efficiencies and agonist activation of these receptors. These differences might arise because the insertion of genes into the cellular genome could influence not only receptor expression but perhaps the expression of other proteins that contribute to the cellular response subsequent to receptor activation. In our cultures, one of the transfected lines of CHO cells differ in morphology and growth curves from the other transfected CHO cells (J.-P. Ledig, personal communication). In addition, although the CHO cell line was found to have a relatively stable karyotype (Worton *et al.*, 1977), genetic 'drift' has been observed (Worton, 1978) and could be a factor in changes in gene expression or cell responses that occur with passage number or culture conditions (personal observations; for an example with another cell line, see Varrault *et al.*, 1992), variables that are not often reported in the literature. Cloned receptors are useful tools for the study of potential receptor-coupler-effector activation models in tissues but until the factors determining receptor-activation and response are better understood, it seems premature to extrapolate agonist profiles from cloned to tissue-expressed receptors.

In conclusion, agonist-induced responses depend not only on receptor density but also on a particular mode of receptor-effector coupling and the efficiency of this process.

It is a pleasure to acknowledge the contributions of J.-P. Ledig (cell culture), M. Eck (subcloned $CHOm_2$ cells), M. Schneider (IP1 assay) and N. Edel (binding assay) as well as Dr C.R. Hiley whose comments concerning propylbenzilylcholine mustard were informative.

References

ATACK, J.R., PRIOR, A.M., GRIFFITH, D. & RAGAN, I. (1993). Characterization of the effects of lithium on phosphatidylinositol (PI) cycle activity in human muscarinic m_1 receptor-transfected CHO cells. *Br. J. Pharmacol.*, **110**, 809–815.

BAUMGOLD, J. & WHITE, T. (1989). Pharmacological differences between muscarinic receptors coupled to phosphoinositide turnover and those coupled to adenylate cyclase inhibition. *Biochem. Pharmacol.*, **38**, 1605–1616.

BIRDSALL, N.J.M., BURGEN, A.S.V., HULME, E.C., STOCKTON, J.M. & ZIGMOND, M.J. (1983). The effect of McN-A-343 on muscarinic receptors in cerebral cortex and heart. *Br. J. Pharmacol.*, **78**, 257–289.

BROWN, E., KENDALL, D.A. & NAHORSKI, S.R. (1984). Inositol phospholipid hydrolysis in rat cerebral cortex: I. Receptor classification. *J. Neurochem.*, **42**, 1379–1387.

BUCKLEY, N.J., BONNER, T.I., BUCKLEY, C.M. & BRANN, M.R. (1989). Antagonist binding properties for five cloned muscarinic receptors expressed in CHO-K1 cells. *Mol. Pharmacol.*, **35**, 469–479.

CAULFIELD, M.P. (1993). Muscarinic receptors – characterization, coupling and function. *Pharmacol. Ther.*, **58**, 319–379.

CHENG, Y.-C. & PRUSOFF, W.H. (1973). Relationship between the inhibition constant (K_I) and the concentration of inhibitor which causes 50 percent inhibition (I_{50}) of an enzymatic reaction. *Biochem. Pharmacol.*, **22**, 3099–3108.

COLQUHOUN, D. (1987). Affinity, efficacy, and receptor classification: is the classical theory still useful? In *Perspectives in Receptor Classification*, pp. 103–114. ed. Black, J., *et al.* New York: Alan R. Liss.

DOKAS, L.A. & TING, S.-M. (1993). A comparison of the regulatory properties of striatal and cortical adenylate cyclase. *Neurobiol. Aging*, **14**, 65–72.

FLEMING, N.N., WESTFALL, D.P., DE LA LANDE, I.S. & JELLET, L.B. (1972). Log normal distribution of equi-effective doses of norepinephrine and acetylcholine in several tissues. *J. Pharmacol. Exp. Ther.*, **181**, 339–345.

FURCHGOTT, R.F. & BURSZTYN, P. (1967). Comparison of dissociation constants and of relative efficacies of selected agonists acting on parasympathetic receptors. *Ann. N.Y. Acad. Sci.*, **144**, 882–889.

HIBERT, F.M., HOFLACK, J., TRUMPP-KALLMEYER, S., PAQUET, J.-L. & LEPPIK, R. (1995). 3D Models of hormone receptors: experimental validation. In *Trends in QSAR and Molecular Modelling '94*, Proceedings of the 10th European Symposium on Structure-Activity Relationships, ed. Sanz, F. Barcelona, Spain: J.R. Prouss, S.A. (in press).

HU, J. & EL-FAKAHANY, E.E. (1990). Selectivity of McN-A-343 in stimulating phosphoinositide hydrolysis mediated by M_1 muscarinic receptors. *Mol. Pharmacol.*, **38**, 895–903.

HULME, E.C., BIRDSALL, N.J.M. & BUCKLEY, N.J. (1990). Muscarinic receptor subtypes. *Annu. Rev. Pharmacol. Toxicol.*, **30**, 633–673.

KEEN, M. & NAHORSKI, S.R. (1988). Muscarinic acetylcholine receptors linked to the inhibition of adenylate cyclase activity in membranes from the rat striatum and myocardium can be distinguished on the basis of agonist efficacy. *Mol. Pharmacol.*, **34**, 769–778.

KENAKIN, T.P. (1987). *Pharmacological Analysis of Drug-Receptor Interaction*, pp. 163–204 and 262–273. New York: Raven Press.

KENAKIN, T.P. & BOSELLI, C. (1990). Promiscuous or heterogeneous muscarinic receptors in rat atria? I. Schild analysis with simple competitive analysis. *Eur. J. Pharmacol.*, **191**, 39–48.

LAZARENO, S., FARRIES, T. & BIRDSALL, N.J.M. (1993). Pharmacological characterization of guanine nucleotide exchange reactions in membranes from CHO cells stably transfected with human muscarinic receptors m_1–m_4. *Life Sci.*, **52**, 449–456.

LI, M., YASUDA, R.P., WALL, S.J., WELLSTEIN, A. & WOLFE, B.B. (1991). Distribution of m2 muscarinic receptors in rat brain using antisera selective for m2 receptors. *Mol. Pharmacol.*, **40**, 28–35.

LOWRY, O.H., ROSEBROUGH, N.J., FARR, A.L. & RANDALL, R.J. (1951). Protein measurement with the Folin phenol reagent. *J. Biol. Chem.*, **193**, 265–275.

MCKINNEY, M., ANDERSON, D. & VELLA-ROUNTREE, L. (1989). Different agonist-receptor active conformations for rat brain M1 and M2 muscarinic receptors that are separately coupled to two biochemical effector systems. *Mol. Pharmacol.*, **35**, 39–47.

MCKINNEY, M., MILLER, J.H., GIBSON, V.A., NICKELSON, L. & AKSOY, S. (1991). Interactions of agonists with M2 and M4 muscarinic receptor subtypes mediating cyclic AMP inhibition. *Mol. Pharmacol.*, **40**, 1014–1022.

MITCHELSON, F. (1988). Muscarinic receptor differentiation. *Pharmacol. Ther.*, **37**, 357–423.

NAHORSKI, S.N. & CHALLISS, R.A.J. (1991). Modulation of receptor-mediated inositol phospholipid breakdown in the brain. *Neurochem. Int.*, **19**, 207.

NIVELBRANT, L. & SPARF, B. (1986). Dicyclomine, benzhexol and oxybutynine distinguish between subclasses of muscarinic binding sites. *Eur. J. Pharmacol.*, **123**, 133–143.

OLIANAS, M.C. & ONALI, P. (1991). Muscarinic stimulation of adenylate cyclase activity of rat olfactory bulb. II. Characterization of the antagonist sensitivity and comparison with muscarinic inhibitions of the enzyme in striatum and heart. *J. Pharmacol. Exp. Ther.*, **259**, 680–686.

RICHARDS, M.H. (1990). Rat hippocampal muscarinic autoreceptors are similar to the M2(cardiac) subtype: comparison with hippocampal M1, atrial M2 and ileal M3 receptors. *Br. J. Pharmacol.*, **99**, 753–761.

RICHARDS, M.H. (1991). Pharmacology and second messenger interactions of cloned muscarinic receptors. *Biochem. Pharmacol.*, **42**, 1645–1653.

RICHARDS, M.H. & VAN GIERSBERGEN, P.L.M. (1995). Differences in agonist potency ratios at human m1 muscarinic receptors expressed in A9L and CHO cells. *Life Sci.* (in press).

RICHARDS, M.H., VAN GIERSBERGEN, P.L.M. & JONES, C.R. (1993). Activation by full and partial agonists of m1 to m5 human muscarinic receptors expressed in A9L or CHO cells. *Life Sci.*, **52**, 576.

SCHWARZ, R.D., DAVIS, R.E., JAEN, C.J., SPENCER, C.J., TECLE, H. & THOMAS, A.J. (1993). Characterization of muscarinic agonists in recombinant cell lines. *Life Sci.*, **52**, 465–472.

VARRAULT, A., JOURNOT, L., AUDIGIER, Y. & BOCKAERT, J. (1992). Transfection of human 5-hydroxytryptamine$_{1A}$ receptors in NIH-3T$_3$ fibroblasts: effects of increasing receptor density on the coupling of 5-hydroxytryptamine$_{1A}$ receptors to adenylyl cyclase. *Mol. Pharmacol.*, **41**, 999–1007.

WALL, S.J., YASUDA, R.P., HORY, F., FLAGG, S., MARTIN, B.M., GINNS, E.I. & WOLFE, B.B. (1991). Production of antisera selective for m1 muscarinic receptors using fusion proteins: distribution of m1 receptors in rat brain. *Mol. Pharmacol.*, **39**, 643–649.

WANG, S.Z. & EL-FAKAHANY, E.E. (1993). Application of transfected cell lines in studies of functional receptor subtype selectivity of muscarinic agonists. *J. Pharmacol. Exp. Ther.*, **266**, 237–243.

WOJCIKIEWICZ, R.J., TOBIN, A.B. & NAHORSKI, S.R. (1993). Desensitization of cell signaling mediated by phosphoinositidase C. *Trends Pharmacol. Sci.*, **14**, 279–285.

WORTON, R.G. (1978). Karyotypic heterogeneity in CHO cell lines. *Cytogenet. Cell Genet.*, **21**, 105–110.

WORTON, R.G., HO, C.C. & DUFF, C. (1977). Chromosome stability of CHO cells. *Somatic Cell Genet.*, **3**, 27–45.

YASUDA, R.P., CIESLA, W., FLORES, L.R., WALL, S.J., LI, M., SATKUS, S.A., WEISSTEIN, J.S., SPAGNOLA, B.V. & WOLFE, B.B. (1993). Development of antisera selective for m4 and m5 muscarinic cholinergic receptors: distribution of m4 and m5 receptors in rat brain. *Mol. Pharmacol.*, **43**, 149–157.

(Received July 7, 1994
Revised November 3, 1994
Accepted November 23, 1994)

British Journal of Pharmacology (1995) 114, 1250–1256

Comparative study of endotoxin-induced hypotension in kininogen-deficient rats with that in normal rats

[1]Akinori Ueno, Hideki Ishida & Sachiko Oh-ishi

Department of Pharmacology, School of Pharmaceutical Sciences, Kitasato University, Shirokane, Minato-ku, Tokyo 108, Japan

1 The aim of this study was to clarify the role of endogenous bradykinin (BK) in the hypotensive response induced by lipopolysaccharide (LPS) by comparing the degree of hypotension caused by LPS in a strain of specific pathogen-free (SPF) Brown Norway (B/N), kininogen-deficient mutant Katholiek rats with that of B/N normal Kitasato rats.

2 The dose-dependent hypotensive responses caused by intravenous injection of BK (1–100 nmol kg^{-1}) or platelet-activating factor (PAF, 0.003–1 $\mu g\ kg^{-1}$), were not different in the two strains of rats used. However, there was a strong difference in the hypotensive response induced by LPS in kininogen-deficient and normal rats; in normal rats the hypotensive response was composed of two phases (15 min and 70–80 min after LPS injection), but in kininogen-deficient rats LPS caused a delayed (second phase), but not an acute (first phase) hypotension.

3 We demonstrate that Hoe 140 (1 mg kg^{-1}, i.v.) is a potent, selective, and long-lasting antagonist of the hypotensive effects of BK. Hoe 140 diminished the hypotension caused by LPS in normal rats to the level observed in kininogen-deficient rats, but had no effect on the hypotension caused by LPS in kininogen-deficient rats.

4 TCV309 (0.1 mg kg^{-1}, i.v.) selectively inhibited the hypotension caused by repetitive injection of PAF for up to 180 min. Pretreatment with TCV309 caused a near complete inhibition of the LPS-induced hypotension in kininogen-deficient and normal B/N rats.

5 In the normal rats, dexamethasone (0.5 mg kg^{-1}, i.p.) inhibited the second phase of the hypotension induced by LPS, but not the first phase of the hypotension.

6 A small amount of BK (0.1 nmol kg^{-1}) potentiated the hypotensive action of PAF (0.01 $\mu g\ kg^{-1}$), when they were injected simultaneously.

7 In conclusion, we demonstrate that formation of endogenous BK contributes primarily to the acute, but not to the delayed hypotension afforded by endotoxin in the rat. In contrast, formation of endogenous PAF contributes to both the acute and the delayed hypotension afforded by endotoxin *in vivo*.

Keywords: Endotoxin; kininogen-deficient rats; BK antagonist; PAF antagonist; blood pressure; hypotension

Introduction

Endotoxin (lipopolysaccharide, LPS), present in the outer membrane of gram-negative bacteria, can induce a wide range of systemic or local inflammatory responses, including septic shock (Nishijima *et al.*, 1973). Several animal models have been used to study the pathophysiological mechanisms of septic shock. In these models, the pathochemical alterations comprise of increase in the formation of platelet-activating factor (PAF) (Chang *et al.*, 1987; Dobrowsky *et al.*, 1991), prostaglandins and thromboxane (Kolsterhalfen *et al.*, 1992) as well as a release of cytokines including interleukins and tumour necrosis factor-α (Cannon *et al.*, 1990; Folhe *et al.*, 1991). The involvement of bradykinin (BK) in the pathophysiology of septic shock was indirectly shown by the partial consumption of factors of the kallikrein-kinin system (Nies, *et al.*, 1968; Herman *et al.*, 1974), such as prekallikrein and high-molecular-weight kininogen, and by the detection of BK or breakdown products of BK in the plasma of animals with septic shock (Katori *et al.*, 1989). As some of these mediators including BK (Kontos *et al.*, 1964) and PAF (Sybertz *et al.*, 1984) have potent hypotensive effects, it has been postulated that these mediators contribute to the hypotension caused by endotoxin *in vivo*. However, a rise in plasma BK or PAF following LPS injection to animals does not necessarily mean that these mediators account for the hypotension caused by endotoxin. Furthermore, the interactions of these mediators during the time course of the LPS-induced hypotension are not well understood and need to be investigated.

Brown Norway (B/N) Katholiek rats are the only strain of rats that genetically lack high-molecular-weight kininogen as well as low-molecular-weight kininogen in their plasma, and also have a very low level of plasma prekallikrein (Damas & Adam 1980; Oh-ishi *et al.*, 1982; 1984; Hayashi *et al.*, 1984; 1992). B/N Katholiek rats originated from the Catholic University of Leuven (Belgium) (Damas & Adam, 1980; Danckwardt *et al.*, 1990), and some of their offsprings were obtained by Caesarean sections for two generations to become specific pathogen-free (SPF) animals. These rats are being maintained at Kitasato University, School of Pharmaceutical Sciences, along with SPF B/N Kitasato rats, which have a normal kallikrein-kinin system (Oh-ishi *et al.*, 1982). Furthermore, the inflammatory response to an inflammatory stimulus, such as carrageenin or kaolin, is significantly smaller in kininogen-deficient rats than in normal rats (Oh-ishi *et al.*, 1986; 1987). Thus, the potential involvement of BK in any pathophysiological event can be investigated by comparing the respective responses of kininogen-deficient rats with those of normal rats.

Recently, a new potent and long-lasting antagonist against BK, Hoe 140 (D-Arg-[Hyp^3,Thi^5,D-Tic^7, Oic^8]BK), was reported to attenuate the vasodilator responses elicited by BK when given as a bolus, intravenous injection (Hock *et al.*, 1991; Wirth *et al.*, 1991). Furthermore, a selective antagonist

[1] Author for correspondence.

against PAF, TCV309 (3-bromo-5-[N-phenyl-*N*-[2-[[2-(1,2,3,4-tetrahydro-2-isoquinolylcarbonyl-oxy)ethyl]carbamoyl]ethyl]carbamoyl]1-propylpyridinium nitrate), was also reported to exert beneficial haemodynamic effects in rodent (Terashita *et al.*, 1991) and canine (Yamanaka *et al.*, 1993) models of septic shock.

This study was designed to elucidate the potential role and relative contribution of BK to the hypotension caused by endotoxin *in vivo* by comparing the hypotension afforded by LPS in kininogen-deficient rats with those caused by LPS in normal rats. In addition, we have investigated the differences in the degree of hypotension caused by LPS in the presence or absence of antagonists of BK or PAF in kininogen-deficient rats and normal rats in order to elucidate the relative contribution as well as the potential interaction of BK and PAF in the hypotension elicited by endotoxin in the anaesthetized rat.

Methods

Measurement of systemic blood pressure

In this study, male SPF Sprague-Dawley (SD) rats (300–340 g, Nihon SLC Co., Hamamatsu, Japan) and male SPF B/N rats (300-350 g), genetically kininogen-deficient Katholiek rats and normal kitasato rats, were used for the measurement of systemic blood pressure. These rats were anaesthetized with pentobarbitone sodium (50 mg kg^{-1}, i.p.). Supplementary doses (15 mg kg^{-1}, i.p.) of anaesthetic were given as needed, to maintain a uniform level of anaesthesia. There was no difference between the strains of rats with respect to the amount of supplementary anaesthesia needed. The right femoral artery was cannulated with a polyethylene catheter (Hibiki No. 3) filled with physiological saline containing heparin (100 units ml^{-1}) to measure arterial blood pressure with a transducer (model TP 200T, Nihon Koden, Tokyo, Japan). The right femoral vein was also cannulated to enable the intravenous bolus injection of drugs. The systemic blood pressure was recorded on a polygraph system (model RM6000, Nihon Koden); and the heart rate, calculated from the ECG, was also monitored.

The drugs (in a volume of 0.1 ml per 100 g body weight; followed by 0.3 ml of sterile physiological saline to wash out the cannula) were administered following stabilization of the blood pressure and heart rate, which was achieved within 20–30 min after completion of the surgical intervention. The haemodynamic effects of LPS were expressed as the difference in the systolic, mean, and diastolic systemic blood pressure (SBP, MBP, and DBP, respectively) from the respective values just before the injection of LPS.

Experimental protocol

The first series of experiments was designed to examine the effect, specificity and duration of action of each of the two antagonists used in this study, which were Hoe 140 (1 mg kg^{-1}, i.v.), a potent BK_2 receptor antagonist, and TCV309 (0.1 mg kg^{-1}, i.v.), a selective PAF receptor antagonist. Each antagonist was tested by measuring its effect on the hypotensive responses to BK (3 or 10 nmol kg^{-1}, i.v.) and PAF (0.01 or 0.03 $\mu g\ kg^{-1}$, i.v.). BK or PAF was injected repeatedly 30 min before and every 30 min for 150 min after injection of each antagonist.

The second series of experiments was performed to estimate the interaction of BK and PAF on hypotension. The hypotensive response induced by simultaneous injection of BK (0.1 nmol kg^{-1}) and PAF (0.01 $\mu g\ kg^{-1}$) was compared with that induced by the same dose of BK or PAF alone.

The third series of experiments was performed to elucidate the involvement of BK in the hypotension induced by LPS (10 mg kg^{-1}, i.v.). The hypotensive effect of LPS in the B/N kininogen-deficient Katholiek rats was compared with that in B/N normal Kitasato rats by observing both responses over a 120 min period after injection of LPS.

The fourth series of experiments examined the effects of the antagonists against the hypotensive response induced by LPS (10 mg kg^{-1}, i.v.) in both B/N kininogen-deficient and normal rats. Hoe 140 (1 mg kg^{-1}, i.v.) and TCV309 (0.1 mg kg^{-1}, i.v.) were administered 30 min before injection of LPS.

The fifth series of experiments tested the effect of dexamethasone (0.5 mg kg^{-1}, i.p.) on the hypotension induced by LPS (10 mg kg^{-1}, i.v.) in B/N normal rats. Dexamethasone was administered 2 h before injection of LPS.

Drugs

Nembutal (pentobarbitone sodium, 50 mg ml^{-1}) was purchased from Abott Lab., North-Chicago, IL, U.S.A., LPS (*E. coli* 055:B5) was from Difco Lab., Detroit, MI, U.S.A. and was dissolved in pyrogen-free sterile physiological saline (Otsuka Pharmaceut. Co., Tokushima, Japan) at a concentration of 10 mg ml^{-1} just before use. BK (Peptide Institute Co.; Osaka, Japan) was kept as a stock solution of 100 nmol ml^{-1} in sterile saline at −20°C until used. PAF (Funakoshi Co.; Tokyo, Japan) was dissolved in filtered (0.45 μm) Tyrode solution containing 0.25% bovine serum albumin (BSA, fraction V, Sigma Chemical Co., St. Louis, MO, U.S.A.).

Hoe 140 was made available from Hoechst AG (Frankfurt, Germany). TCV309 was a generous gift from Takeda Pharmaceutical Ind., Osaka, Japan. These antagonists were dissolved in pyrogen-free sterile saline just before use.

Dexamethasone (Sigma Chemical Co., St. Louis, MO, U.S.A.) was suspended in 1% carboxymethylcellulose at a concentration of 0.5 mg ml^{-1}.

Statistical analysis

Values are presented as the means ± s.e.mean of the indicated number of animals. Statistical significance of differences between means was calculated by two-way analysis of variance followed by Student's *t* test or with paired *t* test where indicated. Probability values (*P*) of less than 0.05 were considered significant.

Results

Dose-response curves to BK and PAF in B/N rats

In SD rats, intravenous injections of BK (10 nmol kg^{-1}) or PAF (0.03 $\mu g\ kg^{-1}$) caused a substantial fall in systolic blood pressure of −46 ± 2 mmHg ($n = 3$) and −47 ± 3 mmHg ($n = 3$), respectively. Even when the injections of these two agents were repeated every 30 min, the degree of hypotension induced by either BK or PAF did not change throughout the 3.5 h observation period.

As shown in Figure 1, BK (1–100 nmol kg^{-1}) or PAF (0.003–1 $\mu g\ kg^{-1}$) caused dose-dependent hypotension in both strains of B/N rats, kininogen-deficient Katholiek rats and normal Kitasato rats. There were no significant differences between the hypotensive responses elicited by BK or PAF in either kininogen-deficient and normal rats.

Duration of the actions of antagonists and their specificities

When rats were pretreated with Hoe 140 (1 mg kg^{-1}, i.v.), the hypotension induced by BK (3 or 10 nmol kg^{-1}) when given immediately after injection of Hoe 140 was almost abolished, and this inhibition lasted for 150 min (Figure 2). However, the hypotension afforded by PAF was not influenced by Hoe 140.

The specificity of TCV309 as an inhibitor of the responses of PAF and the duration of this inhibition are also depicted in Figure 2. The hypotensive effects induced by PAF (0.01–0.03 μg kg^{-1}) were abolished for 150 min by treatment of rats with TCV309 (0.1 mg kg^{-1}, i.v.), while the hypotension induced by BK was not affected.

Potentiation of the action of PAF by BK

Injection of a small dose of BK (0.1 nmol kg^{-1}, i.v.) into five rats caused no significant hypotension (−1.8 ± 2.0 mmHg), whereas PAF (0.01 μg kg^{-1}, i.v.) induced a considerable hypotension (−27.0 ± 2.0 mmHg). However, when these doses of BK and PAF were administered simultaneously to the same rat, the hypotensive response was potentiated; i.e., the response to simultaneous injection of BK and PAF (−38.6 ± 1.8 mmHg) was significantly ($P<0.05$, paired t test) larger than the sum of the responses to BK alone and PAF alone (Table 1).

Difference between normal and kininogen-deficient B/N rats in hypotension induced by LPS.

The systolic and diastolic arterial blood pressures and the heart rate of B/N normal rats ($n = 16$) before injection of LPS were 138 ± 8 mmHg (SBP), 95 ± 5 mmHg (DBP) and 363 ± 10 beats min^{-1} (HR), respectively. In B/N kininogen-deficient rats ($n = 7$), the respective control values were 147 ± 9 mmHg (SBP), 101 ± 5 mmHg (DBP), and 359 ± 9 beats min^{-1} (HR). Thus, prior to starting the experiment (baseline), there were no significant differences in any of the haemodynamic parameters measured between the two strains of rats used.

LPS (10 mg kg^{-1}, i.v.) induced a hypotension in both B/N normal and kininogen-deficient rats. However, there was a difference in the time-course of the hypotensive response of kininogen-deficient rats from that of the normal rats. When LPS was injected into B/N normal rats (Figure 3), a severe biphasic hypotension was observed. An initial hypotension (first phase) was maximal at 15 min after LPS injection and was −64 ± 7 mmHg for SBP and −46 ± 5 mmHg for DBP; thereafter the blood pressure partially recovered and subsequently fell again (second phase) to −50 ± 4 mmHg for SBP and to −47 ± 4 mmHg for DBP at 70 min after LPS injection. In contrast, in kininogen-deficient rats, injection of LPS did not cause a substantial, immediate hypotension (first phase). Thus, the fall in blood pressure caused by endotoxin in kininogen-deficient rats within 15 min (acute phase) (at 15 min; −15 ± 4 mmHg for SBP and −10 ± 2 mmHg for DBP) was significantly ($P<0.01$) smaller than the fall in blood pressure caused by LPS in normal rats. In kininogen-deficient rats which had received endotoxin, there was, however, a secondary fall in blood pressure which was maximal after 70 min. This secondary fall in blood pressure elicited by LPS (70 min) was, however, still significantly ($P<0.01$)) smaller in kininogen-deficient rats than in normal rats. How-

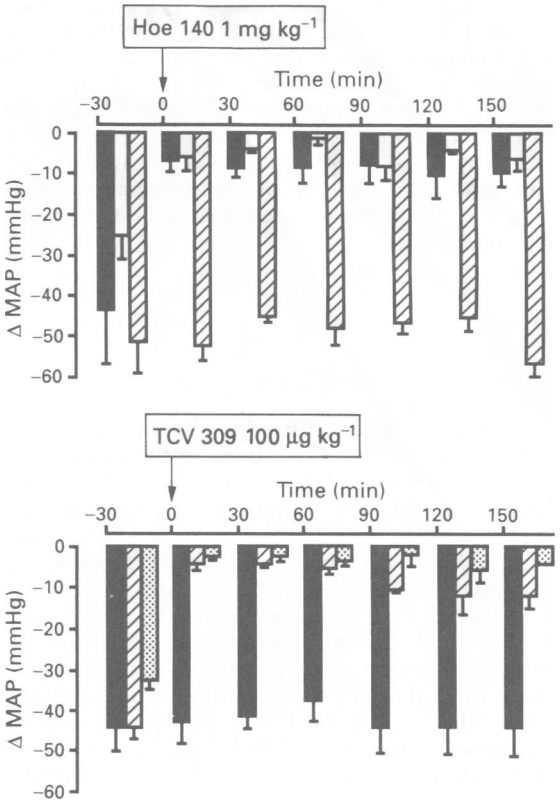

Figure 2 The specificities and duration of action of Hoe 140 and TCV309 in inhibiting the hypotensive responses induced by repeated injections of bradykinin (BK) and platelet activating factor (PAF) into SD rats. Panels (a) and (b) show the effects of Hoe 140 (1 mg kg^{-1}) and TCV309 (0.1 mg kg^{-1}), respectively. These antagonists were injected at 0 min indicated on the abscissa scale, which shows the time course of the experiments. BK (3 nmol kg^{-1}) (open columns) and 10 nmol kg^{-1} (solid columns) and PAF 0.01 μg kg^{-1} (stippled columns) and 0.03 μg kg^{-1} (hatched columns) were injected intravenously 30 min before and every 30 min after the treatment with the antagonist. The ordinate scale indicates the change in mean arterial blood pressure (MAP) induced by injections of BK and PAF. Each column shows the mean value with s.e.mean obtained from 3 rats.

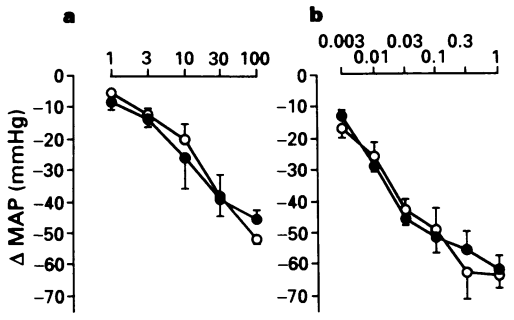

Figure 1 The dose-response curves to bradykinin (BK) (a) and platelet-activating factor (PAF) (b) in kininogen-deficient Katholiek rats (●) and normal Kitasato rats (○) of Brown Norway stain rats. BK (1–100 nmol kg^{-1}) and PAF (0.003–1 μg kg^{-1}) were injected intravenously into the right femoral vein. Each point shows the mean value with s.e.mean ($n = 3$) of the maximal difference from the mean arterial blood pressure (MAP) just before injection of BK or PAF.

Table 1 Interaction of bradykinin (BK) and platelet activating factor (PAF) in the hypotensive response

Rat No.	*BK alone*	*PAF alone*	*BK plus PAF*
1	+4.3	−24.9	−34.4
2	−0.0	−32.0	−43.5
3	−7.0	−21.2	−38.0
4	−5.6	−30.9	−41.6
5	−0.3	−26.2	−35.3
Mean	−1.8	−27.0	−38.6
s.e.mean	2.0	2.0	1.8

The values indicate the change (mmHg) in arterial mean blood pressure in five individual rats induced by injections of BK (0.1 nmol kg^{-1}) alone, of PAF (0.01 μg kg^{-1}) alone and by simultaneous injection of BK and PAF (BK plus PAF), respectively. When calculated with paired t test, the values obtained in the experiment with simultaneous injection of BK and PAF were significantly ($P<0.05$) different from the sum of the values of BK alone and PAF alone.

ever, by 120 min, the fall in blood pressure in kininogen-deficient rats was almost the same as that in normal rats.

Effect of Hoe 140 on the hypotension induced by LPS in B/N rats

In Figure 3, the effect of pretreatment of B/N rats with Hoe 140 (10 mg kg^{-1}, i.v.) at 30 min prior to LPS injection is indicated. In this series of experiments, the values of blood pressure before LPS injection were 136 ± 10 mmHg for SBP and 95 ± 8 mmHg for DBP in normal rats ($n = 4$) and 145 ± 3 mmHg for SBP and 101 ± 8 mmHg for DBP in kininogen-deficient rats ($n = 4$).

In normal rats, the treatment with Hoe 140 abolished the first phase of hypotension induced by LPS ($P < 0.001$, Figure 3a). At 70 min (second phase), the falls in both systolic and diastolic blood pressure were also significantly ($P < 0.05$) diminished. However, the blood pressure values at 120 min in rats with Hoe 140-treatment were identical to those observed in rats without Hoe 140-treatment. Thus, the time course of

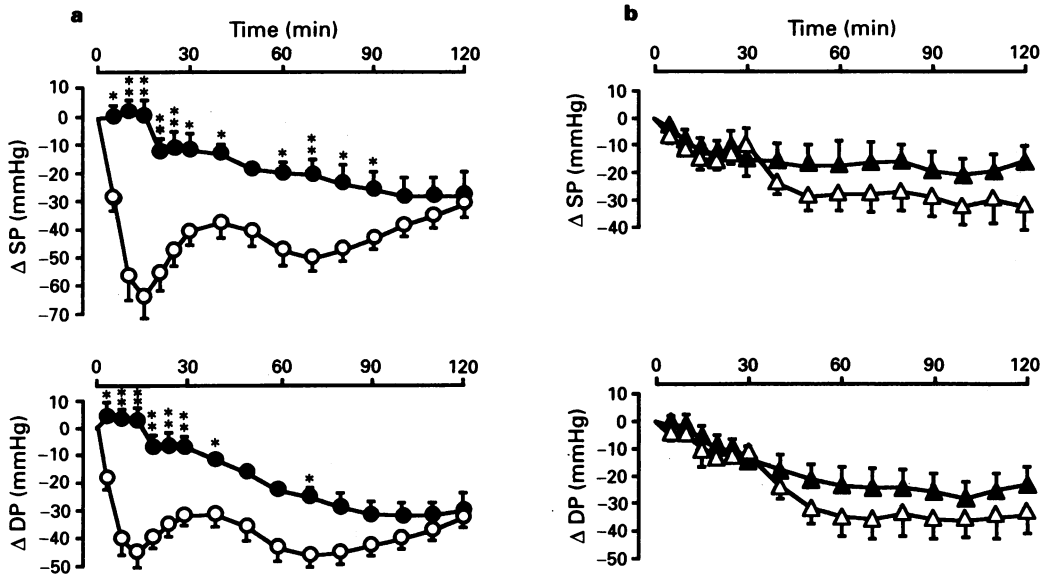

Figure 3 Hypotensive responses induced by lipopolysaccharide (LPS, 10 mg kg^{-1}, i.v.) in Brown Norway normal rats (circles in a) and kininogen-deficient Katholiek rats (triangles in b) and the effects of Hoe 140 (1 mg kg^{-1}, closed symbols). The responses of control experiments in both B/N rats are shown with open symbols. The antagonist was administered intravenously 30 min before injection of LPS. The figures on the abscissa scale indicate the time (min) after injection of LPS. The upper curves of each panel indicate the changes in the systolic blood pressure (ΔSP) and the lower ones show the changes in the diastolic blood pressure (ΔDP). Each point ($n = 4-16$) represents the mean with s.e.mean.

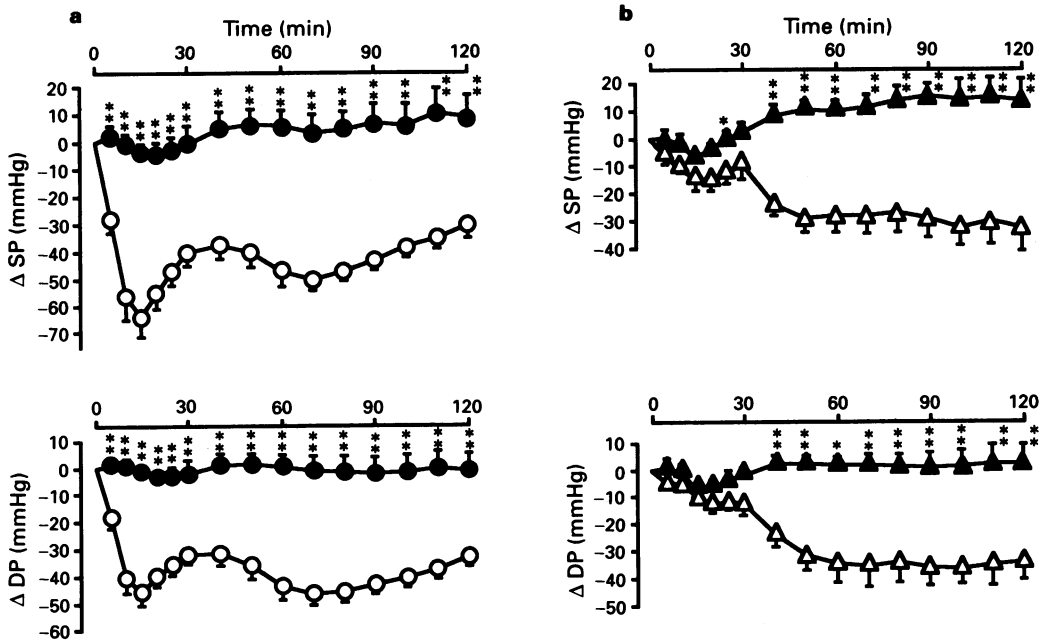

Figure 4 Hypotensive responses induced by lipopolysaccharide (LPS, 10 mg kg^{-1}, i.v.) in Brown Norway normal rats (circles in a) and kininogen-deficient Katholiek rats (triangles in b) and the effects of TCV309 (0.1 mg kg^{-1}, closed symbols). The responses of control experiments in both B/N rats are superimposed with open symbols. The antagonist was administered intravenously 30 min before injection of LPS. The figures on the abscissa scale represent the time (min) after injection of LPS. The upper curves of each panel indicate the changes in the systolic blood pressure (ΔSP) and the lower ones show the changes in the diastolic blood pressure (ΔDP). Each point ($n = 5-16$) represents the mean with s.e.mean.

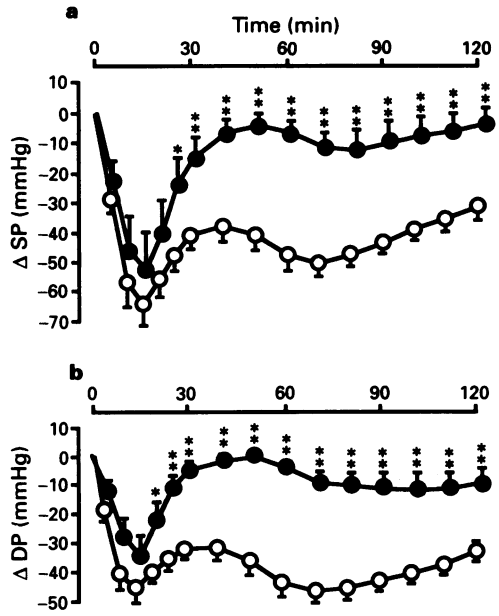

Figure 5 The effect of dexamethasone (0.5 mg kg^{-1}, i.p., ●) on the hypotension induced by lipopolysaccharide (LPS, 10 mg kg^{-1}, i.v.) in Brown Norway normal Kitasato rats. The responses obtained in control experiments with B/N rats are shown (○). Dexamethasone was administered 2 h before injection of LPS. The figures on the abscissa scale represent the time (min) after injection of LPS. The curves in (a) show changes in the systolic blood pressure (ΔSP) and in (b) the changes in the diastolic blood pressure (ΔDP). Each point (n = 5–16) represents the mean with s.e.mean.

the hypotension induced by LPS in normal rats treated with Hoe 140 showed the same pattern as that of kininogen-deficient rats which had not received Hoe 140.

In contrast, Hoe 140 had no significant effect on the hypotension caused by LPS in kininogen-deficient rats (Figure 3b).

Inhibitory effect of TCV309 on the hypotension induced by LPS in B/N rats

The baseline blood pressure values of B/N rats before injection of LPS in this experiment were not significantly different from those observed in the other experiments. Pretreatment with TCV 309 (0.1 mg kg^{-1}, i.v.) inhibited the hypotension induced by LPS in both strains of B/N rats (Figure 4).

The effect of dexamethasone on the hypotension induced by LPS in B/N rats

In Figure 5, the effect of pretreatment of B/N normal rats with dexamethasone (0.5 mg kg^{-1}, i.p.) at 2 h prior to injection of LPS is indicated. Dexamethasone inhibited the second phase, but not the first (acute) phase of hypotension induced by LPS.

Discussion

We demonstrate here that the acute hypotension elicited by endotoxin in kininogen-deficient Katholiek rats was significantly smaller than the hypotension caused by endotoxin in normal Kitasato rats, although the hypotension elicited by BK in these two strains of rats was similar. Thus, an enhanced formation of BK in response to endotoxin contributes to the acute hypotension (at 15 min), but only to a minor extent to the delayed hypotension (second phase) observed between 70 and 120 min after injection of LPS.

The dose of Hoe 140 used in this study (1 mg kg^{-1}, i.v.) was sufficient to prevent the hypotension caused by BK during the 150 min observation period, but was not effective against the hypotension elicited by PAF. Similarly, Hoe 140 attenuates the bronchoconstriction caused by BK, but not by PAF (Sakamoto *et al.*, 1992). However, pretreatment with this dose of Hoe 140 did not affect the hypotension caused by LPS in kininogen-deficient rats. This result supports the notion that (i) the plasma kallikrein-kinin system in this species cannot be activated by LPS due to a lack of kininogens in plasma; and that (ii) BK is not involved in the hypotension caused by LPS in kininogen-deficient rats. On the other hand, the hypotensive response caused by LPS in normal rats was attenuated by Hoe 140 to the level of kininogen-deficient rats. As Hoe 140 is a competitive as well as non-competitive antagonist of BK_2 receptors (Griesbacher & Lembeck, 1992), our results in normal rats support previous work demonstrating that other competitive BK antagonists cause a partial inhibition of the hypotension induced by LPS in rats (Weipert *et al.*, 1988; Wilson *et al.*, 1989). Comparing the hypotension produced by LPS in kininogen-deficient rats with that in normal rats and the effect of Hoe 140 in both rats, our results demonstrate that an enhanced formation of endogenous BK contributes primarily to the acute, but not or to a much lesser degree to the delayed hypotension afforded by LPS in the rat. This conclusion is in line with previous reports demonstrating that enhanced plasma levels of BK can be demonstrated within minutes after injection of endotoxin in the anaesthetized rat (Katori *et al.*, 1989).

TCV309 (0.1 mg kg^{-1}, i.v.) blocked the hypotension induced by PAF, but not that induced by BK. Pretreatment with TCV309 almost completely inhibited the hypotension caused by LPS in both strains of B/N rats for over 120 min from the time just after injection of LPS. Thus, we propose that endogenous PAF makes an important contribution to the biphasic hypotension caused by LPS in the rat.

In addition, we demonstrate that BK and PAF synergise to cause hypotension in the rat, for a small dose of BK (which did not cause a significant fall in blood pressure) potentiated the hypotension caused by PAF. Thus, it is possible that trace amounts of BK released in response to LPS interact with endogenous PAF to cause the observed fall in blood pressure elicited by endotoxin.

We found that dexamethasone inhibited the second phase of the hypotension induced by LPS, but not the first phase. Dexamethasone is known to inhibit the induction of NO synthase (NOS, Knowles *et al.*, 1990; Radomski *et al.*, 1990) and of the inducible isoform of cyclo-oxygenase (DeWitt & Meade, 1993). Inhibition of NOS activity attenuates the hypotension induced by PAF and LPS in dogs (Kilbourn *et al.*, 1990; Takekoshi *et al.*, 1993), and the LPS-induced hypotension in the rat (Thiemermann & Vane, 1990). There is evidence that the enhanced formation of NO elicited by LPS in endothelial cells (Salvemini *et al.*, 1990) as well as the acute hypotension caused by endotoxin in the rat (Thiemermann & Vane, 1990; Szabo *et al.*, 1993a) is secondary to the release of endogenous BK (from endothelial cells) which is known to activate the constitutive NOS present in the vascular endothelium (Fleming *et al.*, 1992). PAF also activates the constitutive NOS in the rat thoratic aorta (Moritoki *et al.*, 1992) and endogenous PAF contributes to the induction of NOS caused by LPS *in vivo* (Szabo *et al.*, 1993b). PAF also activates the inducible prostaglandin synthase gene (Bazan *et al.*, 1994). Thus, the acute hypotension afforded by LPS in the rat is due to the release of BK and PAF, which in turn activate the constitutive NOS. The delayed hypotension (the second phase) elicited by LPS might be explained by the induction by LPS of NO synthase and/or cyclo-oxygenase; which is prevented by dexamethasone.

In conclusion, we demonstrate that an enhanced formation

of endogenous BK contributes primarily to the acute, but not to the delayed hypotension afforded by endotoxin in the rat. In contrast, an enhanced formation of endogenous PAF contributes to both the acute and the delayed hypotension afforded by endotoxin *in vivo*.

This study was partly supported by a Grant-in-Aid from the Ministry of Education, Science and Culture of Japan (No. 04454534). We are grateful to Hoechst AG and Takeda Chemical Ind. for their kind gifts of Hoe 140 and TCV309, respectively.

References

BAZAN, N.G., FLETCHER, B.S., HERSCHMAN, H.R. & MUKHERJEE, P.K. (1994). Platelet-activating factor and retinoic acid synergistically activate the inducible prostaglandin synthase gene. *Proc. Natl. Acad. Sci. U.S.A.*, **91**, 5252–5256.

CANNON, J.G., TOMPKINS, R.G., GELFAND, J.A., MICHIE, H.R., STANFORD, G.G., VAN DER MEER, J.W.M., ENDRED, S., LONNEMANN, G., CORSETTI, J., CHERNOW, B., WILMORE, D.W., WOLFF, S.M., BURKE, J.M. & DINARELLO, C.A. (1990). Circulating interleukin-1 and tumor necrosis factor in septic shock and experimental endotoxin fever. *J. Infect. Dis.*, **61**, 79–84.

CHANG, S.W., FEDDERSEN, C.O., HENSEN, P.M. & VOELKEL, N.F. (1987). Platelet-activating factor mediates hemodynamic changes and lung injury in endotoxin-treated rats. *J. Clin. Invest.*, **79**, 1498–1509.

DAMAS, J. & ADAM, A. (1980). Congenital deficiency in plasma kallikrein and kininogens in the Brown Norway rat. *Experientia*, **36**, 586–587.

DANCKWARDT, L., SHIMIZU, I., BONNER, G., RETTIG, R. & UNGER, T. (1990). Converting enzyme inhibition in kinin-deficient Brown Norway rats. *Hypertension*, **16**, 429–435.

DEWITT, D.L. & MEADE, E.A. (1993). Serum and glucocorticoid regulation of gene transcription and expression of the prostaglandin H synthase-1 and prostaglandin H synthase-2 isozymes. *Arch. Biochem. Biophys.*, **306**, 94–102.

DOBROWSKY, R.T., VOYKSNER, R.D. & OLSON, N.C. (1991). Effect of SRI 63–675 on hemodynamics and blood PAF levels during porcine endotoxemia. *Am. J. Physiol.*, **260**, H1455–1465.

FLEMING, I., DAMBACHER, T. & BUSSE, R. (1992). Endothelium-derived kinins account for the immediate response of endothelial cells to bacterial lipopolysaccharide. *J. Cardiovasc. Pharmacol.*, **20** (Suppl.12), S135–138.

FOLHE', S., HEINRICH, P.C., SCHNEIDER, J., WENDEL, A. & FOLHE', L. (1991). Time course of IL-6 and TNF alpha release during endotoxin-induced endotoxin tolerance in rats. *Biochem. Pharmacol.*, **41**, 1607–1614.

GRIESBACHER, T. & LEMBECK, F. (1992). Analysis of the antagonistic actions of Hoe 140 and other novel bradykinin analogues on the guinea-pig ileum. *Eur. J. Pharmacol.*, **211**, 393–398.

HAYASHI, I., FUJIE, H., MITA, M. & OH-ISHI, S. (1992). Characterization of the heredity of kininogen deficiency in Brown Norway Katholiek strain rats. *Life Sci.*, **51**, 135–142.

HAYASHI, I., INO, T., KATO, H., IWANAGA, S., NAKANO, T. & OH-ISHI, S. (1984). Demonstration of the third kininogen in high and low molecular weight kininogen-deficient Brown Norway Katholiek rat. *Thromb. Res.*, **36**, 509–516.

HERMAN, C.M., OSHIMA, G. & ERDOS, E.G. (1974). The effect of adrenocorticosteroid pretreatment on kinin system and coagulation response to septic shock in the baboon. *J. Lab. Clin. Med.*, **84**, 731–739.

HOCK, F.J., WIRTH, K., ALBUS, U., LINZ, W., GERHARDS, H.J., WIEMER, G., HENKE, S.T., BREIPOHL, G., KONIG, W., KNOLLE, J. & SCHOLKENS, B.A. (1991). Hoe 140, a new potent and long acting bradykinin-antagonist: *in vitro* studies. *Br. J. Pharmacol.*, **102**, 769–773.

KATORI, M., MAJIMA, M., ODOI-ADME, R., SUNAHARA, N. & UCHIDA. Y. (1989). Evidence for the involvement of a plasma kallikrein-kinin system in the immediate hypotension produced by endotoxin in anaesthetized rats. *Br. J. Pharmacol.*, **98**, 1383–1391.

KILBOURN, R.G., JUBRAN, A.J., GROSS, S.S., GRIFFITH, O.W., LEVI, R., ADAMS, J. & LODATO, R.F. (1990). Reversal of endotoxin-mediated shock by N^G-methyl-L-arginine, an inhibitor of nitric oxide synthesis. *Biochem. Biophys. Res. Commun.*, **172**, 1132–1138.

KNOWLES, R.G., SALTER, M., BROOKS, S.L. & MONCADA, S. (1990). Anti-inflammatory glucocorticoids inhibit the reduction by endotoxin of nitric oxide synthase in the lung, liver and aorta of the rat. *Biochem. Biophys. Res. Commun.*, **172**, 1042–1048.

KOLSTERHALFEN, B., HORSTMANN-JUNGEMANN, P., VOGEL, P., FOLHE', S., OFFNER, F., KIRKPATRICK, C.J. & HEINRICH, P.C. (1992). Time course of various inflammatory mediators during recurrent endotoxemia. *Biochem. Pharmacol.*, **43**, 2103–2109.

KONTOS, M.A., MAGEE, J.H. & SHAPIRO, W. (1964). General and regional circulation effects of synthetic bradykinin in man. *Circ. Res.*, **14**, 351–356.

MORITOKI, H., HISAYAMA, T., TAKEUCHI, S., MIYANO, H. & KONDOH, W. (1992). Involvement of nitric oxide pathway in the PAF-induced relaxation of rat thoracic aorta. *Br. J. Pharmacol.*, **107**, 196–201.

NIES, A.S., FORSYTH, R.P., WILLIAMS, H.E. & MELMON, K.L. (1968). Contribution of kinins to endotoxin shock in unanesthetized rhesus monkeys. *Circ. Res.*, **22**, 155–164.

NISHIJIMA, H., WEIL, M.H., SHUBIN, H. & CAVANILES, J. (1973). Hemodynamic and metabolic studies on shock associated with gram negative bacteremia. *Medicine*, **52**, 287–294.

OH-ISHI, S., HAYASHI, I., HAYASHI, M., YAMAKI, K., YAMASU, A., NAKANO, T., UTSUNOMIYA, I. & NAGASHIMA, Y. (1986). Evidence for a role of the plasma kallikrein-kinin system in acute inflammation: reduced exudation during carrageenin- and kaolin-pleurisies in kininogen-deficient rats. *Agents and Actions*, **18**, 450–454.

OH-ISHI, S., HAYASHI, I., SATOH, K. & NAKANO, T. (1984). Prolonged activated partial thromboplastin time and deficiency of high molecular weight kininogen in Brown Norway rat mutant (Katholiek strain). *Thromb. Res.*, **33**, 371–377.

OH-ISHI, S., HAYASHI, I., UTSUNOMIYA, I., HAYASHI, M., YAMAKI, K., YAMASU, A. & NAKANO, T. (1987). Roles of kallikrein-kinin system in acute inflammation: studies on high- and low-molecular weight kininogens-deficient rats (B/N-Katholiek strain). *Agents Actions*, **21**, 384–386.

OH-ISHI, S., SATOH, K., HAYASHI, I., YAMAZAKI, K. & NAKANO, T. (1982). Differences in prekallikrein and high molecular kininogen levels in two strains of Brown Norway rat. *Thromb. Res.*, **28**, 143–147.

RADOMSKI, M.W., PALMER, P.M.J. & MONCADA, S. (1990). Glucocorticoid inhibit the expression of an inducible, but not the constitutive, nitric oxide synthase in vascular endothelial cells. *Proc. Natl. Acad. Sci. U.S.A.*, **87**, 10043–10047.

SAKAMOTO, T., ELWOOD, W., BARNES, P.J. & CHUNG, K.F. (1992). Effect of Hoe 140, a new bradykinin receptor antagonist, on bradykinin- and platelet-activating factor-induced bronchoconstriction and airway microvascular leakage in guinea pig. *Eur. J. Pharmacol.*, **213**, 367–373.

SALVEMINI, D., KORBUT, R., ANGGARD, E. & VANE, J. (1990). Immediate release of a nitric oxide-like factor from bovine aortic endothelial cells by *Escherichia coli* lipopolysaccharide. *Proc. Natl. Acad. Sci. U.S.A.*, **87**, 2593–2597.

SYBERTZ, E.J., WATKINS, R.W., BAUM, T., PULA, K.& RIVELLI, M. (1984). Cardiac, coronary and peripheral vascular effects of acetyl glyceryl either phosphorylcholine in the anaesthetized dogs. *J. Pharmacol. Exp. Ther.*, **232**, 156–162.

SZABO, C., MITCHELL, J.A., THIEMERMANN, C. & VANE, J.R. (1993a). Nitric oxide-mediated hyporeactivity to noradrenaline precedes the induction of nitric oxide synthase in endotoxin shock. *Br. J. Pharmacol.*, **108**, 786–792.

SZABO, C., WU, C.-C., MITCHELL, J.A., GROSS, S.S., THIEMERMANN, C. & VANE, J.R. (1993b). Platelet-activating factor contributes to the induction of nitric oxide synthase by bacterial lipopolysaccharide. *Circ. Res.*, **73**, 991–999.

TAKEKOSHI, K., KASAI, K., SUZUKI, Y., SEKIGUCHI, Y., BANBA, N., NAKAMURA, T. & SHIMODA, S. (1993). Effect of N^G-nitro-L-arginine on shock induced by endotoxin and by platelet activating factor in dogs. *Eur. J. Pharmacol.*, **250**, 465–467.

TERASHITA, Z., KAWAMURA, M., TAKATANI, M., TSUSHIMA, S., IMURA, Y. & NISHIKAWA, K. (1991). Beneficial effects of TCV309, a novel potent and selective platelet activating factor antagonist in endotoxin and anaphylactic shock in rodents. *J. Pharmacol. Exp. Ther.*, **260**, 748–755.

THIEMERMANN, C. & VANE, J.R. (1990). Inhibition of nitric oxide synthesis reduces the hypotension induced by bacterial lipopolysaccharides in the rat *in vivo*. *Eur. J. Pharmacol.*, **182**, 591–595.

WEIPERT, J., HOFFMANN, H., SIEBECK, M. & WHALLEY, E.T. (1988). Attenuation of arterial blood pressure fall in endotoxin shock in the rat using the competitive bradykinin antagonist Lys-Lys-[Hyp^2,Thi^{5,8},D-Phe^7]-BK(B4148). *Br. J. Pharmacol.*, **94,** 282–284.

WILSON, D.D., DE GARAVILLA, L., KUHN, W., TOGO, J., BURCH, R.M. & STERANKA, L.R. (1989). D-Arg-[Hyp^3-D-Phe^7]-bradykinin, a bradykinin antagonist, reduced mortality in a rat model of endotoxic shock. *Circ. Shock.*, **27,** 93–101.

WIRTH, K., HOCK, F.J., ALBUS, U., ALPERMANN, H.G., ANAGNOSTOPOULOS, H., HENKE, ST., BREIPOHL, G., KONIG, W., KNOLLE, J. & SCHOLKENS, B.A. (1991). Hoe 140, a new potent and long acting bradykinin-antagonist: *in vivo* studies. *Br. J. Pharmacol.*, **102,** 774–777.

YAMANAKA, S., IWAO, H., YUKIMURA, T., KIM, S. & MIURA, K. (1993). Effect of the platelet-activating factor antagonist, TCV-309, and the cyclo-oxygenase inhibitor, ibuprofen, on the haemodynamic changes in canine experimental endotoxic shock. *Br. J. Pharmacol.*, **110,** 1501–1507.

(Received September 13, 1994
Revised November 9, 1994
Accepted November 10, 1994)

British Journal of Pharmacology (1995) 114, 1257–1265

Release by ultraviolet B (u.v.B) radiation of nitric oxide (NO) from human keratinocytes: a potential role for nitric oxide in erythema production

[1]George Deliconstantinos, Vassiliki Villiotou & John C. Stravrides

Department of Physiology, University of Athens Medical School, GR.11527 Athens, Greece

1 The mechanism of human sunburn is poorly understood but its characteristic features include the development of erythema. In this study we attempted to determine whether human keratinocytes possess a nitric oxide (NO) synthase (NOS), if this enzyme could be activated to release NO following exposure to ultraviolet B (u.v.B) and to define whether this photo-induced response could be involved in the pathogenesis of sunburn erythema.

2 Treatment of human keratinocytes with various doses of u.v.B (290–320 nm) radiation (up to 100 mJ cm^{-2}) resulted in a dose-dependent release of NO and cyclic GMP production that was reduced by N^G-monomethyl-L-arginine (L-NMMA).

3 u.v.B irradiation of keratinocyte cytosol at varying doses (up to 50 mJ cm^{-2}), resulted in a gradual rise in NO production, with a concomitant increase in soluble guanylate cyclase activity (sGC).

4 NOS isolated from the keratinocyte cytosol was constitutively expressed and was dependent on NADPH, Ca^{2+}/calmodulin, tetrahydrobiopterin and flavins.

5 In reconstitution experiments, when purified NOS was added to purified sGC, both isolated from keratinocyte cytosol, a four fold increase in cyclic GMP was observed. The GMP was increased by NO synthesized following u.v.B radiation (up to 20 mJ cm^{-2}) of NOS.

6 In *in vivo* experiments, guinea-pigs were subjected to u.v.B light. A Protection Factor (PF) of 8.71 ± 2.85 was calculated when an emulsified cream formulation containing L-NMMA (2%) was applied to their skin.

7 The present results indicate that u.v.B radiation acts as a potent stimulator of NOS in keratinocytes. NO is lipophilic and may diffuse out of the keratinocytes, activating sGC in endothelial cells and neighbouring smooth muscle cells. This may be a major part of the integrated response of the skin leading to vasodilatation and erythema.

Keywords: Endothelium-derived relaxing factor, EDRF; nitric oxide; NO synthase; soluble guanylate cyclase; ultraviolet B radiation; keratinocyte; erythema; inflammation; vasodilatation

Introduction

Since the description by Furchgott (1988) of endothelium-derived relaxing factor (EDRF), substantial new investigative efforts have been directed to the characterization and identification of the nature of this biological mediator (Lowenstein *et al.*, 1994). Evidence accumulated in recent years suggests that nitric oxide (NO) (or a closely-related compound) represents at least one type (if not the only type) of EDRF, because both NO and EDRF have similar biological and pharmacological properties (Mayer *et al.*, 1989; Busse & Mulsch, 1990). NO is released in sufficient quantities to explain the biological action of EDRF (Ignarro, 1990; Kiechle & Malinski, 1993). Other investigations have provided data suggesting that NO may not account for all the actions of EDRF and that, depending on the vascular bed, and the activator, there may be more than one type of EDRF (Myers *et al.*, 1990). Recent evidence suggests that sulphydryl species can react with oxides of nitrogen under physiological conditions and thereby stabilize EDRF activity. Serum albumin reacts with oxides of nitrogen to form a stable S-nitrosothiol with properties reminiscent of authentic EDRF, supporting the view that protein-associated thiol may participate in the actions and metabolism of EDRF (Keaney *et al.*, 1993).

In many tissues, including vascular endothelium and brain, the basal activity of constitutive nitric oxide synthase (cNOS) rapidly increases in response to activation of specific G-protein-coupled surface receptors. This cNOS is stimulated by Ca^{2+}/calmodulin and the rapid increase in enzyme activity is not dependent on new protein synthesis. By contrast, activation of NOS in macrophages and other leukocytes occurs over several hours in response to specific cytokines and requires new protein synthesis; the inducible NOS (iNOS) is Ca^{2+}-independent (Deliconstantinos *et al.*, 1994; Lowenstein *et al.*, 1994). These regulatory differences possibly reflect the distinct physiological roles for NO in different cell types; in the macrophage, high local concentrations of secreted NO probably play a role in the cell-dependent killing, whereas the primary role of neuronal or endothelial NO appears to be in intracellular signalling (Palmer *et al.*, 1987; Moncada *et al.*, 1991). Purified cNOS contains tightly bound flavin adenine dinucleotide (FAD) and flavin mononucleotide (FMN). The purified enzyme binds haeme tightly and absorbs at 450 nm following treatment with carbon monoxide, indicating that NOS is a cytochrome P_{450} enzyme (Pufahl & Marletta, 1993). Many of the effects of NO are mediated by guanosine 3′:5′-cyclic monophosphate (cyclic GMP), and it appears that NO represents a prevalent inter- and intracellular signal molecule with soluble guanylate cyclase (sGC) as the effector enzyme (Deliconstantinos *et al.*, 1993; Henry *et al.*, 1993).

It has been proposed that direct photon absorption by dermal blood vessels could explain ultraviolet-induced vasodilatation. Photoexcitation of an epidermal chromophore that absorbs the incident energy and then evokes an injurious response culminating in the release of vasoactive agents that

[1] Author for correspondence.

migrate to the dermal vascular to evoke the vasodilator response has also been reported (Greaves, 1986).

Thus in the present study we decided to investigate whether keratinocytes are directly connected with the skin vasculature, functionally. Here we describe a NOS in human keratinocytes that is constitutively expressed, is Ca^{2+}/calmodulin dependent and when stimulated by u.v.B radiation, causes a concomitant increase in sGC activity. By applying timed and measured doses of u.v.B radiation to a transparent chamber with two compartments separated by a thin teflon membrane, biological samples in one compartment can be stimulated to produce NO which diffuses across the teflon membrane to stimulate other biologically active samples in the opposite compartment. This has proven to be a useful tool in the study of NO-induced interactions between different cell types, which is the subject of much research interest. Our *in vivo* experiments demonstrated, for the first time that u.v.B radiation results in the synthesis of NO by epidermal keratinocytes.

Methods

Cell culture

Human keratinocytes (derived from an epidermal squamous cell carcinoma SCC-13 cell line), were cultured in a medium consisting of Dulbecco's modified Eagle's medium, supplemented with 10% foetal calf serum and essential amino acids, 2 mM L-glutamine, 100 u ml^{-1} penicillin, 100 $\mu g\ ml^{-1}$ streptomycin and 5 $\mu g\ ml^{-1}$ insulin. The cells were grown in a humidified chamber (10% CO_2 and 90% air).

Confluent cells from 10-20 T-75 flasks were harvested by treatment with trypsin 0.25%-Hank's Balanced Salt Solution (HBSS)-EDTA (1 mM) and placed in an incubator until the cells no longer adhered to the flasks (about 5 min). HBSS (pH 7.4) contained (mM): $CaCl_2$ 1.0, KCl 5.3, KH_2PO_4 0.45, $MgSO_4$ 0.5, NaCl 1.25, Na_2HPO_4 0.18, $NaHCO_3$ 4.2 and glucose 5.6. Cells were centrifuged at 5,500 *g* for 10 min and resuspended in HBSS-EDTA (1 mM) medium and then counted. Prior to use, the final concentration was 1×10^8–8×10^8 cells per 4 ml. The cell viability throughout the experiments was >95% as judged by trypan blue exclusion.

The cells suspended in HBSS-EDTA (1 mM) were homogenized on ice by sonication for 30 s (at 5 s intervals) and the resulting cell homogenate was used to obtain the cytosolic fraction. The homogenates were centrifuged at 10,000 *g* for 20 min and the supernatant fractions then centrifuged for 1 h at 100,000 *g* in a Beckman L7 ultracentrifuge. The supernatant fractions of the high-speed spin were employed as cytosolic preparations.

Ultraviolet irradiation

A fluorescence u.v.B lamp (VL-6M 1×6 wavelength 290–320 nm with a peak at 312 nm Tube, Power 12 W, Vilber Lourmat, France) was used. Culture medium was removed and the keratinocytes were washed twice with HBSS. Cells ($10^6\ ml^{-1}$) were resuspended in HBSS. Keratinocytes or their cytosol (200 $\mu g\ ml^{-1}$) or purified NOS (1 $\mu g\ ml^{-1}$) were irradiated with various u.v.B doses delivered within 2 min. Radiation doses were controlled by altering the distance between the radiation source and the samples and were measured with an IL-200 lightmeter. After irradiation of the keratinocytes, HBSS was replaced with fresh HBSS. Cell viability was >90% as judged by trypan blue exclusion.

Chemical determination of NO

The chemical determination of NO is based on the diazotization of sulphanilamide by NO at acidic pH and subsequent oxidation of scopoletin which can be detected fluorophotometrically as previously described (Deliconstantinos *et al.*, 1992). Keratinocytes (10^6 cells per 3 ml of HBSS) were mixed with 100 μl of a reagent consisting of: 20% sulphanilamide in 20% *ortho*-phosphoric acid (H_3PO_4) and 25 μM scopoletin. The NO was monitored as described below. Keratinocyte cytosol (200 $\mu g\ ml^{-1}$) enriched with L-arginine (100 μM), NADPH (100 μM), FAD (5 μM), FMN (5 μM) and tetrahydrobiopterin (5 μM) was incubated at 37°C for 5 min and the reaction was terminated by adding 10 u of L-lactic dehydrogenase and 100 μl of Na^+ pyruvate (10 mM). In some experiments the free Ca^{2+} concentration was adjusted by Ca^{2+}/EDTA buffer (Segal, 1986). N^G-monomethyl-L-arginine monoacetate (L-NMMA) (1 mM) dissolved in HBSS, was added where indicated. A stock solution (10 mM) of the calmodulin antagonist, calmidazolium (compound R24571), was prepared in dimethylsulphoxide. One hundred μl of the sulphanilamide–scopoletin reagent was mixed with the incubates and the NO was monitored at room temperature (22°C) with an excitation wavelength of 350 nm and an emission of 460 nm, in an Aminco SPF-500 Fluorescence Spectrophotometer. The fluorescence was monitored continuously in time until the slope of the line could be measured (approx. 8 min). Slope measurements were then converted to pmol of NO by use of a standard curve constructed with various concentrations of pure NO. Solutions of acidified saline (9 mg ml^{-1} NaCl, 0.1 mM HCl, pH 4.0) were deoxygenated by bubbling with 100% nitrogen for 2 h. NO gas was bubbled into 10 ml of deoxygenated acidified saline at a rate of one bubble s^{-1} for 20 min, while the gas above was flushed away with N_2. The solubility of NO in water is 7.34 cm^3 100 ml^{-1} and, assuming saturation, the maximum concentration of NO in the solution is 3.3 mM (Shikano *et al.*, 1987). Stock solutions of nitrite (NO_2^-) were prepared by dissolving appropriate amounts of sodium nitrite in acid saline to produce a 3.3 mM stock solution (i.e. identical to the estimated stock concentration of the NO saturated solutions). The stock solutions of NO_2^- were prepared in open, ambient air-exposure tubes. The NO and NO_2^- solutions were stored on ice and used within 3 to 4 h. The present fluorophotometric method is highly sensitive with a resolution of less than 5 pmol of NO. The method is about 100 times more sensitive for NO than for NO_2^-.

Purification of cNOS

Purification of cNOS from keratinocyte cytosol was achieved by the method described by Bredt & Snyder (1990). Cells were homogenized by sonication in 5 ml of ice-cold buffer containing: 50 mM Tris HCl pH 7.4; 1 mM EDTA; antipain 10 mg l^{-1}; leupeptin 10 mg l^{-1}; soybean trypsin inhibitor 10 mg l^{-1}; pepstatin 10 mg l^{-1}; chymostatin 10 mg l^{-1} and phenylmethylsulphonylfluoride 100 mg l^{-1}. The cytosol of keratinocytes, obtained as described above, (12 ml) was added to 2 ml of 2',5'-ADP-agarose equilibrated in a buffer containing: 50 mM Tris HCl (pH 7.4) 1 mM EDTA and 1 mM dithiothreitol. After a 10 min incubation, the suspension was poured into a fritted column which was washed with 20 ml of 50 mM Tris HCl containing 1 mM dithiothreitol and 500 mM NaCl and 50 ml of 50 mM Tris-HCl containing 1 mM dithiothreitol. cNOS was eluted with 8 ml of 50 mM Tris-HCl containing 1 mM dithiothreitol and 10 mM NADPH and applied to an anion exchange column packed with DEAE-BioGel A (0.5×1 cm). After washing the column with 50 mM Tris-HCl containing 1 mM dithiothreitol and 80 mM NaCl, cNOS was eluted with 6 ml of 50 mM Tris-HCl containing 1 mM dithiothreitol and 120 mM NaCl. In some cases residual Tris-HCl, dithiothreitol and NADPH were removed from purified cNOS by washing with HBSS-EDTA (1 mM) pH 7.4 in a Centricon-30 microconcentrator (Amicon, Danvers, MA, U.S.A.). Protein concentration was measured by the Bradford method (Bradford, 1976) with reagents from Bio-Rad (Richmond, CA, U.S.A.) and bovine serum albumin as a standard.

Assay of cNOS

Purified cNOS activity was measured by monitoring either NO or [^{3}H]-L-citrulline production.

NO determination

Reactions (1 ml sample volumes) were carried out for 5 min at 37°C. Standard reaction mixtures contained: HBSS–EDTA 1 mM, cNOS (1 μg), NADPH 100 μM and various combinations of FAD 5 μM, FMN 5 μM, tetrahydrobiopterin 5 μM and calmodulin 1 μM. L-NMMA (1 mM) was added where indicated. Reactions were terminated by adding 10 u of L-lactic dehydrogenase and 100 μl of Na pyruvate (10 mM). NO determination was carried out by mixing the incubates with 100 μl of the sulphanilamide-scopoletin reagent.

L-Citrulline determination

L-Citrulline was measured in 50 mM HEPES (pH 7.4) containing the same cofactors as described for NO measurements in the presence of cNOS (1 μg). [^{3}H]-L-arginine (100,000 c.p.m.) was mixed with cold L-arginine (100 μM) in a final volume of 200 μl. After incubation for 15 min at 37°C, assays were terminated with 2 ml of 20 mM Dowex AG50W-X8 (Na^+ form), which was eluted with 2 ml of water. [^{3}H]-L-citrulline was measured in a liquid scintillation counter. Blank values were determined in the absence of added enzyme.

Purification of sGC

sGC from keratinocytes was purified by GTP-agarose chromatography. Samples of cytosol (10 mg protein) in 12 ml of HBSS containing 10 mM $MnCl_2$ were added to a GTP-agarose column (1.8 × 9 cm) pre-equilibrated with 25 mM Tris HCl buffer pH 7.6, containing 250 mM sucrose and 10 mM $MnCl_2$. After application of the sample, the column was washed with 5 column volumes of equilibration buffer. sGC was then eluted from the column with 5 ml equilibration buffer plus 10 mM GTP. The eluted enzyme was immediately concentrated using Centricon-30 microconcentrators and resuspended in 25 mM Tris HCl, pH 7.6 containing 250 mM sucrose.

Cyclic GMP determination

Concentrations of cyclic GMP were determined by radioimmunoassay after acetylation of the samples with acetic anhydride. The reaction mixture contained triethanolamine/HCl 50 mM, creatine phosphate 5 mM, $MgCl_2$ 3 mM, isobutylmethylxanthine 1 mM, creatine kinase 0.6 u, GTP 1 mM, keratinocytes 10^6 cells or keratinocyte cytosol 200 μg or 0.085–1.0 μg purified soluble guanylate cyclase; the total volume was 150 μl. The reactions were initiated by the addition of GTP and samples were incubated for 10 min at 37°C. The incubation medium was aspirated and cyclic GMP was extracted by the addition of ice-cold HCl (0.1 M). After 10 min, the samples were transferred to a new plate, dried, and reconstituted in 5 mM sodium acetate (pH 4.75) for cyclic GMP determination. Cyclic GMP formation was determined with a cyclic GMP assay kit (Amersham).

Description of the incubation chamber

For the determination of NO released by purified NOS, we designed and fabricated a chamber with two compartments of 2.5 cm diameter, from solid rods of clear Plexiglas, which were hollowed out from one end with a machine-lathe to create an identical conical cavity within each of the plexiglas rods. They were then further machined and polished at the open ends, creating a very tight fit between the two conical cavities. A thin square of Teflon sheet (poly-tetrafluorethylene 0.0015 inches in thickness) was sandwiched between the assemblies which were recompressed with the thumbscrews. The two tube-access-parts at either side of the membrane allows biologically active samples and reactive substances to be injected into, withdrawn from, or modified at either side of the membrane during biological reactions (Figure 7, insert).

In vivo experiments: estimation of protection factor (PF)

Hartley guinea-pigs weighing 200 to 300 g were used. The day before the experiment hair removal was carried out with cold depilatory wax; talc was lightly applied to the surface of the skin and the animals were left for 24 h. On the following day the animals were lightly anaesthetized with ketamine (100 mg kg^{-1}, i.p.). A formulation containing L-NMMA (2% w/w) in an emulsified cream, consisting of phospholipids, glyceryl stearate, glycerol, squalene, cetyl alcohol, acrylium gel, triethanolamine buffer pH 6 in 90% water, was applied topically at a dose of 0.02 ml cm^{-2}.

A system comprising a fluorescent u.v.B lamp emitting from 280 nm to 320 nm with a peak at 315 nm was used. The wattage was 5.6 W and an electronic time was used to ensure automatic exposure at precise times. The lamp was placed at right angle to the lower part of the back from which hair had been removed. The test was carried out on 5 guinea-pigs in order to determine: (a) the minimum erythema dose (MED); and (b) the Protection Factor (PF).

Scoring scale of erythema was: 0 = no erythema, 1 = barely visible spots, 2 = obvious erythema, 3 = very visible erythema. MED is the radiation dose that promotes the appearance of a minimum erythema with a score of 1. Animals were exposed for periods of time that are multiples of the MED and in arithmetic progression with respect to the MED (18, 21.6, 25.9 and 31.1 min). The erythema was evaluated 6 h after application of the formulation and irradiation of animals and the PF was determined. A comparison was made between the control spot MED (cream base only treated skin areas) and the spots that had developed for each radiation dose corresponding to times that were multiples of this MED. The sum of scores equal to zero corresponds to 100% protection for the dose studied and the percentage protection is then calculated with respect to the control erythema MED (score of 10) according to the formula:

$$\frac{\text{Control erythema-treated erythema}}{\text{Control erythema}} \times 100 = \%$$

The upper 100% evaluation corresponds to the coefficient investigated.

$$\text{Protection Factor} = \frac{\text{Exposure duration for minimum erythema in protected skin}}{\text{Exposure duration for minimum erythema in unprotected skin}}$$

Statistical analysis

All values are expressed as means ± s.d. The data are derived from triplicate incubations of three or four independent experiments. Wilcoxon test for unpaired measurements (Wilcoxon rank sum test) was used. The 5% level of statistical significance was used in all experiments.

Materials

[^{3}H]-L-arginine (54 Ci $mmol^{-1}$; 1 Ci = 37 GBq) and cyclic GMP radioimmunoassay kit were obtained from the Radiochemical Centre, Amersham, Bucks, UK; NO (99.99% pure) was obtained from Messer Griesheim (Germany). 2',5'-ADP-agarose and GTP-agarose were obtained from Sigma

Chemical Co, St. Louis, Mo, U.S.A.; DEAE-Bio-Gel A and Dowex AG 50WX8 (Na^+ form) were obtained from Bio-Rad-Chemical Division, Richmond, Ca, U.S.A. L-NMMA and superoxide dismutase (SOD) were obtained from Calbiochem (Switzerland). Other reagents, solvents and salts were of analytical grade and were obtained from Sigma Chemical Co., St. Louis, Mo, U.S.A.

Results

NO and cyclic GMP determination after u.v.B radiation of keratinocytes

Figure 1a demonstrates that radiation of human keratinocytes with u.v.B evoked a dose-dependent increase in detectable NO release. The response occurred with doses of energy known to elicit erythema production in intact human skin (Pentland *et al.*, 1990). The rate of NO formation was decreased by the NOS inhibitor L-NMMA (1 mM). L-NMMA was added 15 min before irradiation to intact keratinocytes to allow it to penetrate into the cells and then complete its inhibitory action on NOS activity. Similarly, u.v.B treatment resulted in a three fold increase in cellular cyclic GMP at a dose of 100 mJ cm^{-2}. L-NMMA (1 mM) also decreased cyclic GMP formation (Figure 1b). Cyclic GMP accumulation provides a sensitive index of NO production because of the ability of NO to activate soluble guanylate cyclase directly (Stamler *et al.*, 1992). Table 1 shows that the production of NO by keratinocyte cytosol in the presence of a saturating concentration of L-arginine (100 μM) (Standard Reaction Mixture; SRM), was 525 ± 65 pmol NO min^{-1} mg^{-1}. This production was dependent on NADPH. In the presence of unsaturated concentrations of NADPH (10 μM and 50 μM) 52% and 61% decreases of NO production, respectively were obtained, when compared to the SRM (control) value ($P<0.02$). Concentrations of NADPH up to 1 mM did not increase the production of NO beyond that seen with 100 μM NADPH (SRM). The amount of NO produced after the addition of 2 mM ATP was the same as that obtained in the absence of ATP ($P>0.05$). Addition of D-arginine (100 μM), L-lysine (100 μM), L-guanidine (100 μM) and L-citrulline (100 μM) caused no statistically significant difference in NO production when compared to SRM from which L-arginine had been omitted ($P>0.05$) and a statistically significant difference when compared to SRM ($P<0.01$). These results suggest that D-arginine, L-lysine, L-guanidine and L-citrulline failed to stimulate enzyme activity, indicating the specificity of the activation to L-arginine. Table 1 also shows that sGC stimulation by L-arginine (100 μM) contained in the SRM was maximal in the presence of exogenous NADPH (100 μM) (6.25 ± 0.65 pmol cyclic GMP min^{-1} mg^{-1}) and concentrations of NADPH up to 1 mM did not increase the sGC activity beyond that seen with 100 μM NADPH. When the specificity of the activation of sGC by L-arginine was examined it was found that D-arginine (100 μM), L-lysine (100 μM), L-guanidine (100 μM) and L-citrulline (100 μM) failed to increase the sGC activity when compared to SRM from which L-arginine had been omitted ($P>0.05$), while a P value of less than 0.01 was obtained when compared to SRM. Table 2 shows that the synthesis of NO by the cytosol was completely Ca^{2+}/calmodulin and tetrahydrobiopterin-dependent. In a Ca^{2+}-free solution containing 1 mM EDTA, the activity of cNOS in the presence of 100 μM NADPH was very low (25.5 ± 2 pmol NO min^{-1} mg^{-1} cytosolic protein). Results from standard incubations without adjustment of the free Ca^{2+} concentration did not differ from those incubations in which the Ca^{2+} concentration was 10 μM or in which calmodulin (1 μM) was added, indicating that standard incubation mixtures contained sufficient Ca^{2+} and calmodulin in the keratinocyte cytosol ($P>0.05$). The calmodulin antagonist R24571 (25 μM) completely inhibited NOS activity.

NO and cyclic GMP determination after u.v.B radiation of keratinocyte cytosol

Figure 2a and b shows NO production and sGC activation after u.v.B radiation of keratinocyte cytosol. The amount of NO production increased four fold after a 50 mJ cm^{-2} dose of u.v.B radiation, accompanied by a four fold increase in the activity of sGC. L-NMMA (1 mM) added to the cell cytosol during the u.v.B radiation, resulted in an approximate 50% reduction of either NO formation or sGC activation. Concentrations of water soluble L-NMMA (up to 5 mM) did not inhibit the production of either NO or cyclic GMP beyond that seen with 1 mM L-NMMA (data not shown). The effectiveness of L-NMMA in partially inhibiting

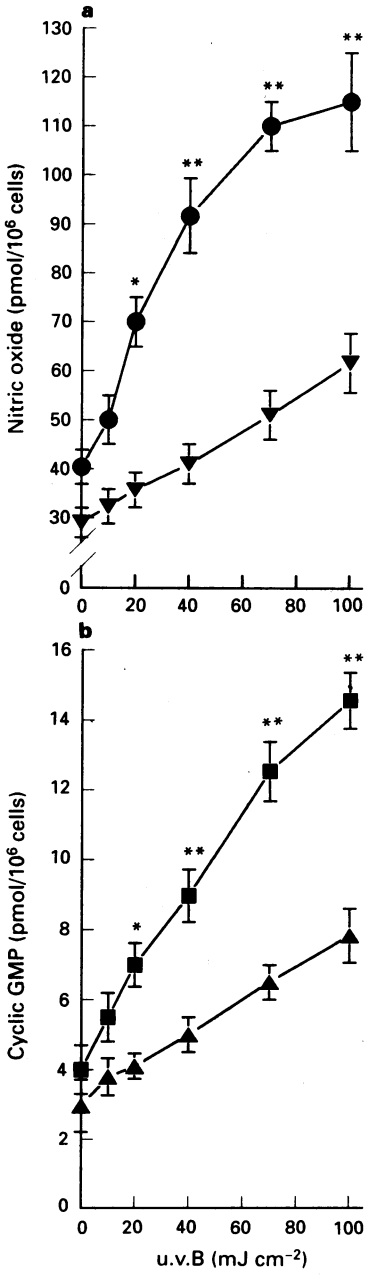

Figure 1 Effect of various doses of u.v.B radiation (290–320 nm) on (a) NO release and (b) cyclic GMP production by human keratinocytes: (●) NO release; (▼) NO release in the presence of L-NMMA (1 mM); (■) cyclic GMP production and (▲) cyclic GMP production in the presence of L-NMMA (1 mM). L-NMMA was added 15 min before the irradiation of the cells. Each point represents the mean ± s.d. of four independent experiments. A statistically significant difference from keratinocytes in the presence of L-NMMA was determined (*$P<0.01$, **$P<0.001$).

the NO and cyclic GMP production by u.v.B-irradiated keratinocytes or their cytosol prompted us to test whether stores of nitrite ions (NO_2^-) could be present in the keratinocytes. The generation of NO by u.v. radiation of NO_2^- in aqueous solutions has been studied (Zafiriou & Mcfarland, 1980; Bauer & Fung, 1993). To test this possibility we inactivated cNOS by boiling the keratinocyte cytosol at 100°C for 3 min. Although L-NMMA (1 mM) inhibited the NOS activity by almost 100%, we decided to denature the enzyme in order to exclude the possibility of an effect of u.v. irradiation on the dissociation of the NOS-L-NMMA complex and to ensure complete inactivation of the enzyme. Following u.v.B radiation (50 mJ cm^{-2}) of the denatured cytosol, the NO production was almost equal (0.78 ± 0.08 nmol NO mg^{-1} protein min^{-1}; $n = 4$) to the non-inhibitable NO production by L-NMMA suggesting the possible existence of stores of NO_2^- ions within the keratinocytes. Furthermore after dialysis (membrane dialysis, Diachema A.G. Switzerland) of the denatured keratinocyte cytosol for 24 h against phosphate buffered saline (PBS) pH 7.4 followed by u.v.B radiation (50 mJ cm^{-2}), the NO production was 0.020 ± 0.008 nmol NO mg^{-1} protein min^{-1} ($n = 4$), supporting the view that NO_2^- stores exist in keratinocytes.

Table 1 Effect of various agents on nitric oxide (NO) and cyclic GMP production by keratinocyte cytosol

Conditions	*NO* (pmol min^{-1} mg^{-1})	*Cyclic GMP* (pmol min^{-1} mg^{-1})
Standard reaction mixture (SRM)	525 ± 65	6.25 ± 0.65
NADPH (10 μM)	252 ± 37*	2.88 ± 0.28*
NADPH (50 μM)	324 ± 42*	4.14 ± 0.45*
NADPH (1 nM)	544 ± 68	6.08 ± 0.61
ATP (2 nM)	532 ± 66	6.42 ± 0.70
L-Arginine omitted	75 ± 8*	0.71 ± 0.05*
D-Arginine (50 μM)	82 ± 12*	0.89 ± 0.06*
D-Arginine (100 μM)	77 ± 7*	0.82 ± 0.05*
L-Lysine (100 μM)	64 ± 6*	0.93 ± 0.07*
L-Guanidine (100 μM)	87 ± 9*	0.78 ± 0.05*
L-Citrulline (100 μM)	71 ± 8*	0.83 ± 0.05*

Keratinocytes were harvested, homogenized and cytosolic fractions were prepared as described in the Methods section. Standard reaction mixture (SRM) contained all compounds except the omitted cofactors or substrates. Enzyme activities were determined as described in the Methods section. Data are mean ± s.d. of triplicate incubations of three independent experiments.
*Statistically significant difference ($P < 0.05$) compared to SRM.

Table 2 Characterization of NO-synthase activity in keratinocyte cytosol

Conditions	*NO* (pmol min^{-1} mg^{-1})
Standard reaction mixture (SRM)	525 ± 65
NADPH omitted	202 ± 31*
Flavins omitted	298 ± 49*
BH_4 omitted	165 ± 24*
Ca^{2+} free	25 ± 2*
Ca^{2+} (10 μM)	512 ± 63
Ca^{2+}/calmodulin (1 μM)	517 ± 67
Ca^{2+}/R24571 (25 μM)	28 ± 2*
Ca^{2+}/calmodulin/R24571	18 ± 2*

Enzyme incubation mixtures contained all compounds expect the omitted cofactor. For changing the Ca^{2+} concentration or testing the effects of calmodulin, EDTA buffers were included (Segal, 1986). Enzyme activities were determined as described in the Methods section. Data are mean ± s.d. of triplicate incubations of three independent experiments.
BH_4: tetrahydrobiopterin.
*Statistically significant difference ($P < 0.05$) compared to SRM.

Citrulline production by keratinocyte cytosol

Figure 3 demonstrates that incubation of the keratinocyte cytosol with 100 μM L-arginine mixed with [^{3}H]-L-arginine (100,000 c.p.m.) and 100 μM NADPH, resulted in the synthesis of [^{3}H]-L-citrulline at the rate of 725 ± 95 pmol mg^{-1}

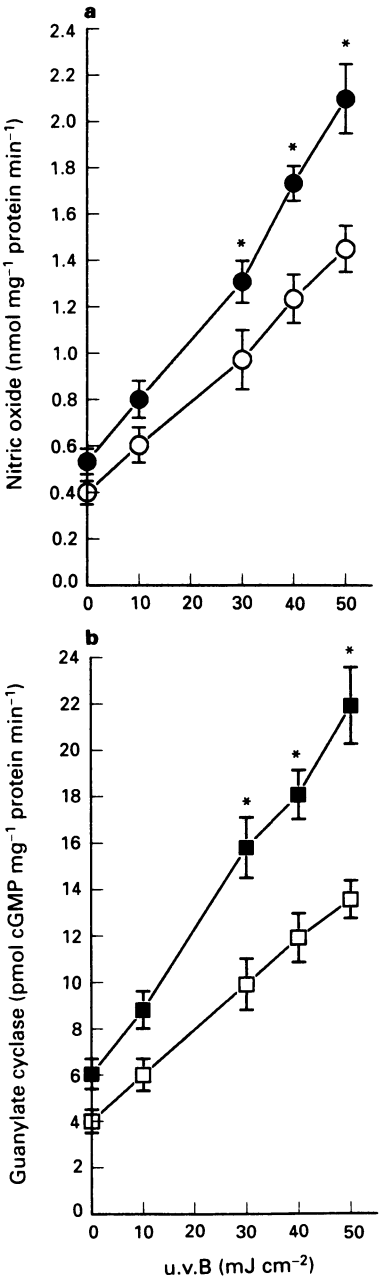

Figure 2 Effect of various doses of u.v.B (290–320 nm) radiation on (a) NO (●) and (b) cyclic GMP (■) production by the cytosol of human keratinocytes. Keratinocyte cytosol (200 μg ml^{-1}) enriched with L-arginine (100 μM); NADPH (100 μM); FAD (5 μM); FMN (5 μM) and tetrahydrobiopterin (5 μM) was incubated at 37°C for 5 min and the reaction was terminated by adding 10 u of L-lactic dehydrogenase and 100 μl of Na^+ pyruvate (10 mM). The effect of L-NMMA (1 mM) on both NO (○) and cyclic GMP (□) production is shown. Each point represents the mean ± s.d. of four independent experiments. A statistically significant difference from the cytosol in the presence of L-NMMA was determined (*$P < 0.02$).

protein min^{-1}. L-Citrulline formation increased four fold after irradiation with 50 mJ cm^{-2} u.v.B. The maximum stimulation of L-citrulline by u.v.B was inhibited by 90% in the presence of L-NMMA (1 mM).

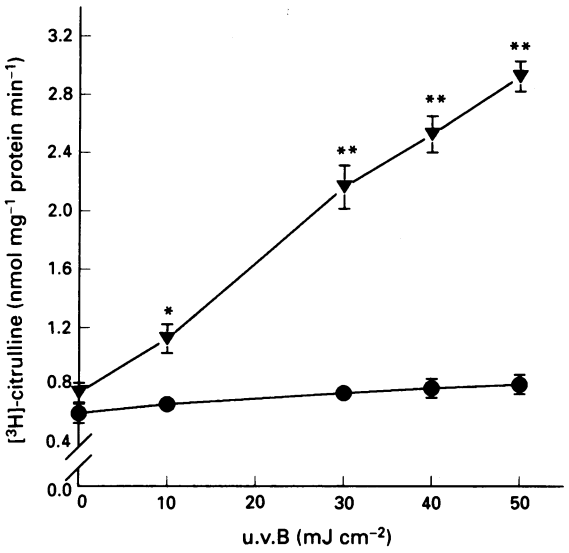

Figure 3 Effect of u.v.B (290–320 nm) radiation on [^{3}H]-L-citrulline (▼) formation by keratinocyte cytosol. The reaction mixture contained: [^{3}H]-L-arginine (100,000 c.p.m.) mixed with cold L-arginine (100 μM), NADPH (100 μM), FAD (5 μM), FMN (5 μM), tetrahydrobiopterin (5 μM), L-NMMA (1 mM) and cytosolic protein (200 μg). L-NMMA (1 mM) (●) inhibited [^{3}H]-L-citrulline formation by approximately 90%. Each point represents the mean ± s.d. of three independent experiments. A statistically significant difference from the cytosol in the presence of L-NMMA was determined (*$P<0.01$, **$P<0.001$).

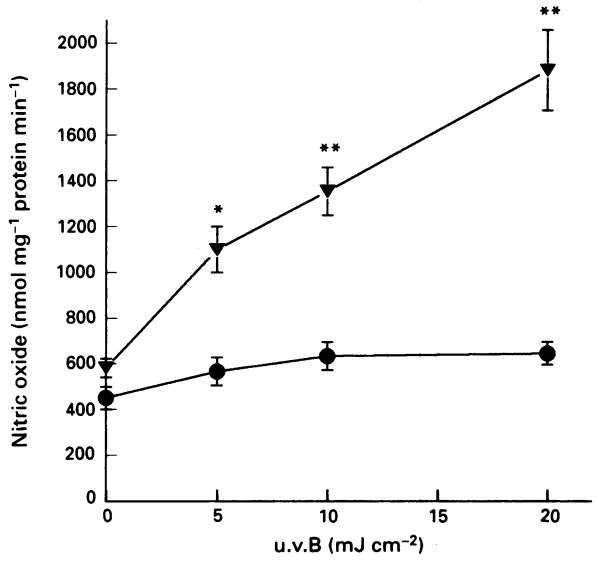

Figure 4 Effect of u.v.B (290–320 nm) radiation on NO production (▼) by purified cNOS isolated from keratinocyte cytosol. The reaction mixture (1 ml) contained HBSS-1 mM EDTA, pH 7.4, 1 μg of purified cNOS, 100 μM NADPH, 100 μM L-arginine, 1 μM calmodulin, 5 μM FAD, 5 μM FMN, 5 μM tetrahydrobiopterin and 1 mM L-NMMA. Incubations were carried out at 37°C for 5 min and the reaction was quenched by the addition of lactic dehydrogenase (10 u) and 100 μl of Na pyruvate (10 mM). The amount of NO produced was determined as described in the Methods section. L-NMMA (●) inhibited NO formation by approximately 90%. Each point represents the mean ± s.d. of four independent experiments. A statistically significant difference from the cNOS in the presence of L-NMMA was determined (*$P<0.01$, **$P<0.001$).

NO, cyclic GMP and citrulline production by purified NOS

cNOS purified approximately 1000 fold from the keratinocyte cytosol (525 ± 65 pmol mg^{-1} cytosolic protein min^{-1}) showed a specific activity of 575 ± 60 nmol NO mg^{-1} protein min^{-1}. Figure 4 shows the effect of various doses of u.v.B on NO formation by purified cNOS (1 μg) with the appropriate cofactors. u.v.B up to 20 mJ cm^{-2} caused a three fold increase in NO formation. L-NMMA (1 mM) inhibited the enzyme activity by approximately 90%. As sGC is the physiological effector system of L-arginine-derived NO, reconstitution experiments with purified cNOS and sGC were performed. Figure 5 shows that u.v.B radiation increased the activity of purified sGC by four fold, consistent with the increased cNOS activity by the u.v.B irradiation. In the absence of cNOS or L-arginine, u.v.B failed to increase the activity of sGC. Figure 6 (a and b) shows the quantities of NO and L-citrulline detected in samples obtained over a 60 min period following stimulation of purified cNOS by u.v.B radiation (20 mJ cm^{-2}). L-NMMA (1 mM) inhibited both L-citrulline and NO formation by approximately 90%.

NO and cyclic GMP determination with an incubation chamber

Figure 7 shows the amounts of NO detected when purified cNOS and HBSS were placed in two adjacent compartments of a chamber which were separated by a thin teflon membrane (poly-tetrafluoroethylene, 0.0015 inches in thickness, Dupont, Wilmington, Delaware, U.S.A.) permitting only NO diffusion through the membrane. The amounts of NO produced by cNOS with and without u.v.B irradiation, were monitored periodically. A time-dependent increase of NO in the compartment containing HBSS was observed to reach an equilibrium with NO present in the adjacent compartment containing cNOS within 50 min. When purified cNOS was

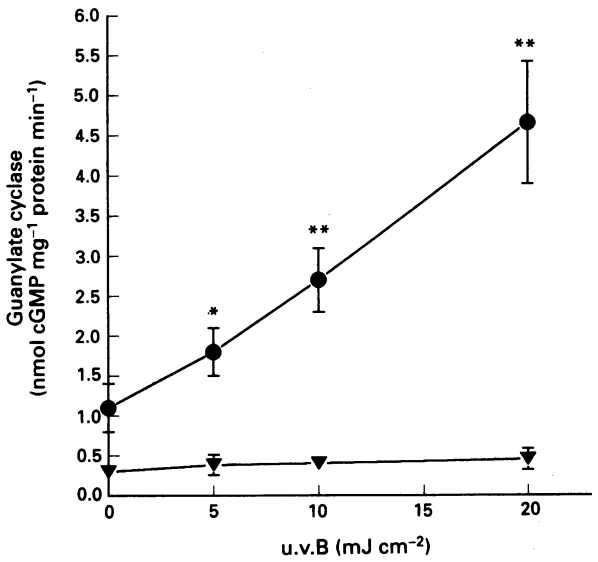

Figure 5 Effect of u.v.B (290–320 nm) radiation on the activity of sGC in the presence (●) and absence (▼) of purified cNOS, in reconstitution experiments consisting of purified sGC (1 μg) and cNOS (1 μg) in 50 mM triethanolamine/HCl buffer pH 7.4, L-arginine (100 μM), NADPH (100 μM), FAD (5 μM), FMN (5 μM), tetrahydrobiopterin (5 μM), Ca^{2+} (10 μM) and calmodulin (1 μM). The appropriate co-factors for the estimation of sGC were used as described in the Methods section. Incubations were carried out at 37°C for 5 min and cyclic GMP formed was determined by radioimmunoassay using a cyclic GMP kit (Amersham). Each point represents the mean ± s.d. of three independent experiments. A statistically significant difference sGC in the absence of cNOS was determined (*$P<0.01$, **$P<0.001$).

subjected to u.v.B irradiation (20 mJ cm^{-2}), the accumulation of NO in the HBSS compartment doubled, as was seen in the absence of u.v.B radiation. Finally, HBSS in the first compartment was replaced by purified sGC for periodic bioassay of NO activity over a 50 min period. In the absence of u.v.B irradiation, we noted that diffusion of NO across the teflon membrane into the sGC compartment resulted in the production of a significant amount of cyclic GMP (1.82 ± 0.12 nmol mg^{-1} protein min^{-1}). When the procedure was repeated with cNOS irradiated with 20 mJ cm^{-2} of u.v.B, a two fold increase in cyclic GMP production was observed, as compared to non-irradiated cNOS.

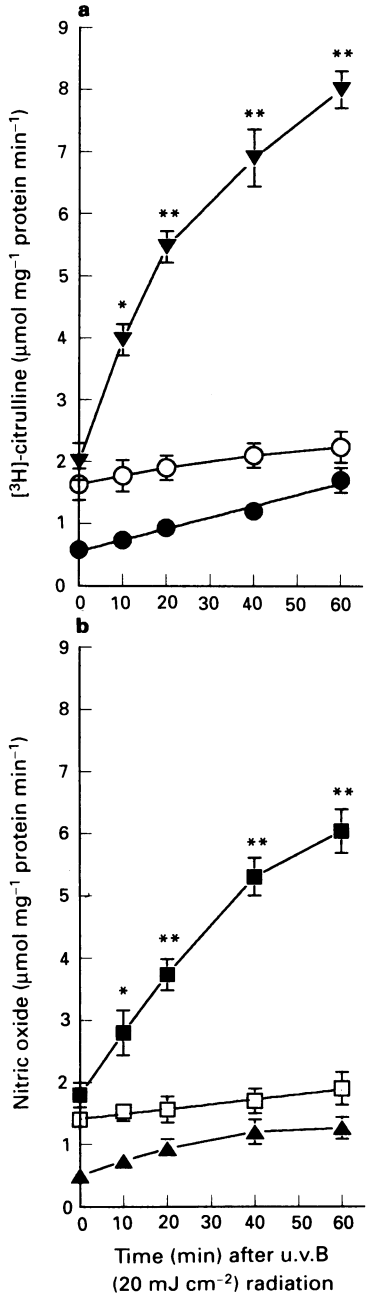

Figure 6 Time course experiments on (a) [^{3}H]-L-citrulline (▼) and (b) NO (■) formation by purified cNOS isolated from keratinocyte cytosol. The reaction mixture was as described in the legends to Figures 3 and 4. Purified cNOS was irradiated with 20 mJ cm^{-2} u.v.B. NO (▲) and [^{3}H]-L-citrulline (●) production by non-irradiated cNOS (control experiments) is also shown. L-NMMA (1 mM) included in the incubation mixture inhibited both NO (□) and [^{3}H]-L-citrulline (○) production by approximately 90%. The data represent the mean ± standard deviation of four independent experiments. At 60 min the difference between the two curves (●) and (○) in (a) and (▲) and (□) in (b) were found to be not statistically significant ($P > 0.05$). A statistically significant difference from cNOS in the presence of L-NMMA was determined (*$P < 0.01$, **$P < 0.001$).

Estimation of protection factor (PF)

In vivo experiments were then conducted where Hartley guinea-pigs were subjected to timed exposure to u.v.B irradiation. Prior to exposure a new formulation containing L-NMMA (2% w/w) in an emulsified cream base (consisting of: phospholipids, glyceryl stearate, glycerol, squalene, acetyl alcohol, acrylium gel, triethanolamine buffer pH 6 in 90% water), was applied to the skin as described in the Methods section. The treated side of the animals was exposed to multiples of the MED in geometric progression 1.2. Treated areas immediately after the application of the cream were exposed at times 18, 21.6, 25.9 and 31.1 min. Skin areas treated with the active ingredient were compared with the cream base-treated adjacent skin areas. According to the FDA recommendations, the PF calculated was 8.71 ± 2.85 ($n = 5$). The PF of the cream base as compared to untreated skin areas was 1.7 ± 0.5.

Discussion

Our present study has shown that u.v.B radiation, which is known to cause erythema in human skin, activates NO release with subsequent cyclic GMP production in keratinocytes (Figure 1). Erythema is a consequence of various inflammatory stimuli, including sunlight. It is thought to result from an increase in blood volume in both the superficial and deep vascular plexi of the dermis. The mechanism of human sunburn is poorly understood but its characteristic features include the development of visible redness following threshold doses of u.v.A and u.v.B, after a latent period of 4–8 h that is maximal at 16–24 h and fades slowly thereafter (Cavallo & Deleo, 1986). Keratinocytes SCC-13, a cell line derived from a human epidermal squamous cell carcinoma, express a constitutive form of the enzyme NOS which converts L-arginine into NO and L-citrulline in the presence of Ca^{2+}/calmodulin; NO is responsible for elevating cyclic GMP levels in keratinocytes or their cytosol (Figures 1 and 2). We confirmed that both NO and cyclic GMP production by keratinocytes or their cytosol were inhibited by L-NMMA, which inhibits the NOS activity (Schmidt *et al.*, 1992). u.v.B radiation used in the present experiments not only stimulated cNOS to produce NO, but also generated NO from NO_2^- in the keratinocyte cytosol, suggesting the existence of NO_2^- stores in keratinocytes. NO production by the purified cNOS can be achieved in a defined system containing L-arginine, NADPH, Ca^{2+}/calmodulin and tetrahydrobiopterin. Exogenous FAD (5 μM) and FMN (5 μM) increased the rate of NO synthesis by purified cNOS, and is consistent with a co-factor role. NADPH provides reducing equivalents to cNOS (Stamler *et al.*, 1992) and NADPH oxidation is coupled to NO synthesis through a FAD-containing flavoprotein and tetrahydrobiopterin (Schmidt *et al.*, 1992).

The physiological role of the constitutive forms of the NOS in keratinocytes may be the production of small quantities of NO that are important in maintaining the vascular tone of the skin blood vessels. NO release may also restore the normal blood flow in extreme cases of vasoconstriction of the cutaneous microvasculature. Alternatively, NO may act as an autacoid in keratinocytes inhibiting ribonucleotide reductase as well as mitochondrial respiration and DNA synthesis, events that control cellular proliferation (Henry *et al.*, 1993).

Our findings in this study demonstrating that, in a defined reconstitution system consisting of purified cNOS and purified sGC, the formation of cyclic GMP was increased

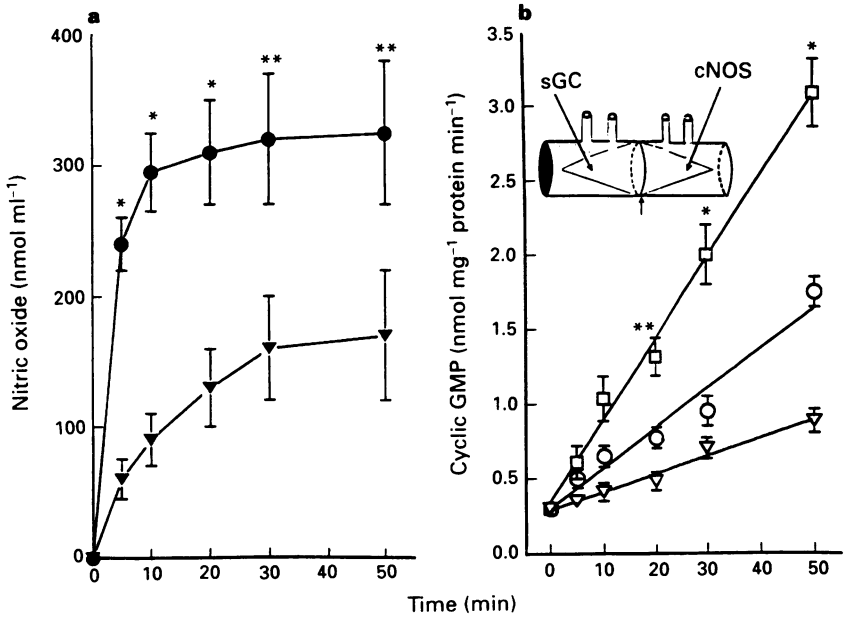

Figure 7 Purified cNOS isolated from keratinocyte cytosol and HBSS was placed in two compartments of a chamber separated by a thin teflon membrane (poly-tetrafluoroethylene 0.0015 inches in thickness), a membrane which permits only NO diffusion. NO was determined in HBSS when cNOS was placed in the opposite compartment (▼). u.v.B radiation (20 mJ cm^{-2}) of cNOS resulted in a two fold increase in the amount of NO that diffused into the HBSS compartment (●). Replacement of HBSS with sGC resulted in a two fold increase of cyclic GMP in the compartment containing sGC (○). When u.v.B (20 mJ cm^{-2}) irradiated purified cNOS was present in the opposite compartment of the chamber a further two fold increase in cyclic GMP production was observed (□). The basal activity of sGC (in the absence of cNOS in the opposite compartment of the chamber) is also illustrated (▽). Each point represents the mean ± s.d. of three independent experiments. A statistically significant difference from non-irradiated cNOS (control) was determined (*$P<0.01$; **$P<0.05$).

after u.v.B radiation, are consistent with the widespread signal transduction system which involves Ca^{2+}/calmodulin-regulated NO formation and activation of sGC (Schmidt *et al.*, 1993). These reconstitution experiments were also verified by placing purified NOS and purified sGC in a special incubation chamber with two compartments separated by a thin teflon membrane through which only NO gas could pass. Cyclic GMP increased approximately two fold, when u.v.B irradiated purified cNOS was placed in the opposite compartment (Figure 7). These experiments clearly suggest that the NO released from u.v.B irradiated keratinocytes is identical to gaseous NO and not to any nitrosothiol compound (Myers *et al.*, 1990) and it is consistent with the observations that glutathione is necessary in endothelial cells for NO synthesis rather than for the NO effect on sGC (Ghigo *et al.*, 1993). In *in vivo* experiments using experimental animals we tried to determine the PF of a cream formulation containing 2% L-NMMA. According to FDA recommendations, the PF calculated was 8.71 ± 2.85.

Prior studies have suggested the role of eicosanoids in the pathogenesis of sunburn since perfusates of radiated erythematous human skin contain increased amounts of vasodilator prostaglandins that can be diminished by pretreatment with nonsteroidal antiinflammatory agents such as aspirin and indomethacin (Snyder, 1976). In this respect, the cyclo-oxygenase enzymes are potential targets for NO because they contain an iron haeme centre at their active sites and indeed the vast majority of the effects mediated by NO are a consequence of its interaction with iron or iron containing enzymes (Salvemini *et al.*, 1993). NO enhances cyclo-oxygenase activity through a mechanism independent of cyclic GMP and in conditions in which both the NOS and cyclo-oxygenase systems are present there is a NO-mediated increase in the produciton of proinflammatory prostaglandins that may result in an exacerbated inflammatory response (Salvemini *et al.*, 1993). It has been shown that primary cultures of human keratinocytes and a mouse keratinocyte cell line respond to γ-interferon and lipopolysaccharide or tumour necrosis factor-α by producing NO at nanomolar concentrations, suggesting the expression of the inducible type of NOS in response to inflammatory stimuli. It is proposed that NO produced by keratinocytes may function in nonspecific host defence during wound healing, and that this may occur because NO, either alone and/or in combination with reactive oxygen intermediates, is toxic (Heck *et al.*, 1992). It was recently published that u.v.B irradiation of rat skin caused delayed onset vasodilatation and by 18 h basal blood flow increased. L-NAME injected locally 17.5 h after u.v.B irradiation abolished the 18 h increase in blood flow (Warren *et al.*, 1993). Our present studies indicating that human keratinocytes possess a constitutive NOS, and that they are capable of releasing NO for prolonged time periods following exposure to u.v. radiation, provide evidence that once NO is released by these cells the gas may continue to be produced and released even after the stimulus is removed (Figure 6). NO acting as EDRF would then diffuse abluminally to smooth muscle cells thereby leading to activation of sGC and enhance the intracellular levels of cyclic GMP that mediates the relaxation response (Deliconstantinos & Villiotou, 1992). Our data also raise the intriguing possibility that NO released by keratinocytes can directly augment sGC activity in smooth muscle cells and bypass the conventional abluminal pathway. Such a phenomenon could provide an explanation for the vasodilatation that accompanies human sunburn erythema and suggests that it may be possible to diminish the risk of the sunburn reaction in man by developing pharmacological agents that diminish epidermal NO production.

This project was supported by 'Europe Against Cancer' Grand EEC File NO 92CVV01276-0-Item B3-4300, and a Grant from the University of Athens, Greece.

References

BAUER, J.A. & FUNG, H.L. (1993). Photochemical generation of nitric oxide from nitro-containing compounds: possible relation to vascular photorelaxation phenomena. *Life Sci.*, **54**, PL1–4.

BRADFORD, M.M. (1976). Rapid and sensitive method for quantitation of microgram quantities of protein utilizing principle of protein-dye binding. *Anal. Biochem.*, **72**, 248–254.

BREDT, D.S. & SNYDER, S.H. (1990). Isolation of nitric oxide synthase, a calmodulin-requiring enzyme. *Proc. Natl. Acad. Sci. U.S.A.*, **87**, 682–685.

BUSSE, R. & MULSCH, A. (1990). Calcium-dependent nitric oxide synthesis in endothelial cytosol is mediated by calmodulin. *FEBS Lett.*, **265**, 133–136.

CAVALLO, J. & DELEO, V.A. (1986). Sunburn. *Dermatol Clin. North Am.*, **4**, 181–187.

DELICONSTANTINOS, G. & VILLIOTOU, V. (1992). Modulation of nitric oxide (NO) production by active oxygen species in keratinocytes. In *Biology of Nitric Oxide* ed. Moncada, S., Marletta, M.A., Hibbs, J.B. Jr & Higgs, E.A., pp. 182–185. Portland Press.

DELICONSTANTINOS, G., VILLIOTOU, V. & FASSITSAS, C.H. (1992). Ultraviolet radiated human endothelial cells elaborate nitric oxide that may evoke vasodilatory response. *J. Cardiovasc. Pharmacol.*, **20**, S63–S65.

DELICONSTANTINOS, G., VILLIOTOU, V. & STAVRIDES, J.C. (1993). Transplant rejection and endothelium-derived relaxing factor (EDRF) nitric oxide (NO). In *Liver Transplantation in Children.* ed. Willital, G.H., pp. 101–122. Wolfgang Pabst Verlag.

DELICONSTANTINOS, G., VILLIOTOU, V. & STAVRIDES, J.C. (1994). Pathophysiology of nitric oxide in cancer. *Cancer Mol. Biol.*, **1**, 77–86.

FURCHGOTT, R.F. (1988). Studies on relaxation of rabbit aorta by sodium nitrite: the basis for the proposal that the acid-activatable inhibitory factor from retractor penis is inorganic nitrite and endothelium-derived relaxing factor is nitric oxide. In *Vasodilatation: Vascular Smooth Muscle, Peptides, Autonomic Nerves and Endothelium.* ed. Vanhoutte, P.M., pp. 401–414. New York: Raven Press.

GHIGO, D., ALESSIO, P., FOCO, A., BUSSOLINO, F., COSTAMAGNA, C., HELLER, R., GARBARINO, G., PESCARMONA, G.P. & BOSIA, A. (1993). Nitric oxide synthesis is impaired in glutathione-depleted human umbilical vein endothelial cells. *Am. J. Physiol.*, **265**, C728–C732.

GREAVES, M.W. (1986). Ultraviolet erythema: causes and consequences. *Curr. Probl. Dermatol.*, **15**, 18–24.

HECK, D.E., LASKIN, D.L., GARDNER, C.R. & LASKIN, J.D. (1992). Epidermal growth factor suppresses nitric oxide and hydrogen peroxide production by keratinocytes. *J. Biol. Chem.*, **267**, 21277–21280.

HENRY, Y., LEPOIVRE, M., DRAPIER, J.C., DUCROCQ, C., BOUCHER, J.L. & GUISSANI, A. (1993). EPR characterization of molecular targets for NO in mammalian cells and organelles. *FASEB J.*, **7**, 1124–1134.

IGNARRO, L.J. (1990). Haem-dependent activation of guanylate cyclase and cyclic GMP formation by endogenous nitric oxide: a unique transduction mechanism for transcellular signaling. *Pharmacol. Toxicol.*, **67**, 1–7.

KEANEY, J.F., SIMON, D.I., STAMLER, J.S., JARAKI, O., SCHARFSTEIN, J., VITA, J.A. & LOSCALZO, J. (1993). NO forms an adduct with serum albumin that has endothelium-derived relaxing factor-like properties. *J. Clin. Invest.*, **91**, 1582–1589.

KIECHLE, F.L. & MALINSKI, T. (1993). Nitric oxide: biochemistry pathophysiology and detection. *Am. J. Clin. Pathol.*, **100**, 567–575.

LOWENSTEIN, C.J., DINERMAN, J.L. & SNYDER, S.H. (1994). Nitric oxide: a physiologic messenger. *Ann. Intern. Med.*, **120**, 227–237.

MAYER, B., SCHMIDT, K., HUMBERT, R. & BOHME, E. (1989). Biosynthesis of endothelium-derived relaxing factor: a cytosolic enzyme in porcine aortic endothelial cells Ca^{2+}-dependently converts L-arginine into an activator of soluble guanylyl cyclase. *Biochem. Biophys. Res. Commun.*, **164**, 678–685.

MONCADA, S., PALMER, R.M.J. & HIGGS, E.A. (1991). Nitric oxide: physiology, pathophysiology and pharmacology. *Pharmacol. Rev.*, **43**, 109–142.

MYERS, P.R., MINOR, R.L., Jr., GUERRA, R., Jr, BATES, J.N. & HARRISON, D.G. (1990). Vasorelaxant properties of the endothelium-derived relaxing factor more closely resemble S-nitrosocysteine than nitric oxide. *Nature*, **345**, 161–163.

PALMER, R.M., FERRIGE, A.G. & MONCADA, S. (1987). Nitric oxide release accounts for the biological activity of endothelium-derived relaxing factor. *Nature*, **327**, 524–526.

PENTLAND, A.P., MAHONEY, M., JACOBS, S.C. & HOTZMAN, M.J. (1990). Enhanced prostaglandin synthesis after ultraviolet injury is mediated by endogenous histamine stimulation. A mechanism for irradiation erythema. *J. Clin. Invest.*, **86**, 566–574.

PUFAHL, R.A. & MARLETTA, M.A. (1993). Oxidation of N^G-hydroxy-L-arginine by nitric oxide synthase: evidence for the involvement of the heme in catalysis. *Biochem. Biophys. Res. Commun.*, **193**, 963–970.

SALVEMINI, D., MISKO, T.P., MASFERRER, J.L., SEIBERT, K., CURRIE, M.G. & NEEDLEMAN, P. (1993). Nitric oxide activates cyclooxygenase enzymes. *Proc. Natl. Acad. Sci. U.S.A.*, **90**, 7240–7244.

SCHMIDT, H.H.H.W., LOHMAN, S.M. & WALTER, U. (1993). The nitric oxide and cGMP signal transduction system: regulation and mechanism of action. *Biochim. Biophys. Acta*, **1178**, 153–175.

SCHMIDT, K., WERNER, E.R., MAYER, B., WACHTER, H. & KUKOVETZ, W.R. (1992). Tetrahydrobiopterin-dependent formation of endothelium-derived relaxing factor (nitric oxide) in aortic endothelial cells. *Biochem. J.*, **281**, 277–300.

SEGAL, J. (1986). Lanthanum increases the rat thymocyte cytoplasmic free calcium concentration by enhancing calcium influx. *Biochim. Biophys. Acta*, **886**, 267–271.

SHIKANO, K., OHLSTEIN, E.H. & BERKOWITZ, B.A. (1987). Differential selectivity of endothelium-derived relaxing factor and nitric oxide in smooth muscle. *Br. J. Pharmacol.*, **92**, 483–485.

SNYDER, D.S. (1976). Effect of topical indomethacin on UVR-induced redness and prostaglandin E levels in sunburn guinea pig skin. *Prostaglandins*, **11**, 631–643.

STAMLER, J.S., SINGEL, D.J. & LOSCALZO, J. (1992). Biochemistry of nitric oxide and its redox-activated forms. *Science*, **258**, 1898–1902.

WARREN, J.B., LOI, R.K. & COUGHLAN, M.L. (1993). Involvement of nitric oxide synthase in the delayed vasodilator response to ultraviolet light irradiation of rat skin *in vivo*. *Br. J. Pharmacol.*, **109**, 802–806.

ZAFIRIOU, O.C. & MCFARLAND, M. (1980). Determination of trace levels of nitric oxide in aqueous solutions. *Anal. Chem.*, **52**, 1662–1667.

(Received June 10, 1994
Revised November 18, 1994
Accepted November 25, 1994)

British Journal of Pharmacology (1995) 114, 1266-1272

Effects of tyrosine kinase inhibitors on the contractility of rat mesenteric resistance arteries

[1]Catalin Toma, Peter E. Jensen, [2]Dolores Prieto, [3]Alun Hughes, Michael J. Mulvany & [4]Christian Aalkjær

Department of Pharmacology and Danish Biomembrane Center, The Bartholin Building, Aarhus University, 8000 Aarhus C, Denmark

1 A pharmacological characterization of tyrosine kinase inhibitors (TKI) belonging to two distinct groups (competitors at the ATP-binding site and the substrate-binding site, respectively) was performed, based on their effects on the contractility of rat mesenteric arteries.

2 Both the ATP-site competitors (genistein and its inactive analogue, daidzein) and the substrate-site competitors (tyrphostins A-23, A-47 and the inactive analogue, A-1) reversibly inhibited noradrenaline (NA, (10 μM)) and KCl (125 mM) induced contractions, concentration-dependently. Genistein was slightly but significantly more potent than daidzein; the tyrphostins were all less potent than genistein, and there were no significant differences between the individual potencies. The tyrosine kinase substrate-site inhibitor *bis*-tyrphostin had no inhibitory effect.

3 Genistein, daidzein, A-23 and A-47 each suppressed the contraction induced by Ca^{2+} (1 μM) in α-toxin permeabilized arteries. A-1 and *bis*-tyrphostin had little or no effect on contraction of the permeabilized arteries.

4 Genistein was significantly more potent than daidzein with respect to inhibition of the contraction induced by 200 nM Ca^{2+} in the presence of NA (100 μM) and GTP (3 μM). The effect of A-23, A-47, A-1 and *bis*-tyrphostin was similar in permeabilized arteries activated with Ca^{2+} (200 nM) + NA (100 μM) + GTP (3 μM) and permeabilized arteries activated with 1 μM Ca^{2+}.

5 Genistein (30 μM) reduced the fura-2 measured intracellular calcium activity ($[Ca^{2+}]_i$) in arteries stimulated with NA but had no effect on $[Ca^{2+}]_i$ in arteries stimulated with KCl (125 mM).

6 The potent effect of the TKIs in this study is consistent with a role for tyrosine kinases in the mechanisms which regulate both cytoplasmic Ca^{2+} levels and the effect of Ca^{2+} on the contractile apparatus in smooth muscle cells in resistance arteries. However, the results must be interpreted cautiously because the enzyme inhibitors may have a poor specificity in intact tissues and because the presumed inactive analogues had potent effects.

Keywords: Tyrosine kinase inhibitors: vascular smooth muscle; tyrphostin; genistein; daidzein; rat mesenteric resistance arteries

Introduction

During the last decade it has become clear that tyrosine phosphorylation of proteins plays a major role in the diverse cellular signalling pathways which are involved in cell proliferation and transformation (Bishop, 1987; Draetta *et al.*, 1988), cellular interactions with the extracellular matrix (Schaller & Parsons, 1993) and the regulation of neurotransmitter receptors (O'Dell *et al.*, 1991): for review see Glenney (1991). Against this background, tyrosine kinase inhibitors (TKIs) have recently been developed. Two groups of TKIs have been described: compounds interacting with the ATP binding site, such as genistein, a quercetin derivative (Akiyama *et al.*, 1987; Casnellie, 1991) and those which interact with the substrate binding site, such as the tyrphostins, which are synthetic analogues of erbstatin (Levitzki & Gilon, 1991; Casnellie, 1991). Inactive analogues with respect to the epidermal growth factor receptor kinase are also now available for each group, namely daidzein and tyrphostin A-1, respectively.

In smooth muscle cells, growth factors activate tyrosine kinases (Auger *et al.*, 1989; Yang *et al.*, 1992; Weiss & Nuccitelli, 1992), and also have agonistic effects with respect to force development (Berk *et al.*, 1986; Yang *et al.*, 1992). Conversely, classical constrictor agonists like angiotensin II, vasopressin and carbachol have been shown to activate smooth muscle tyrosine kinase and cause tyrosine phosphorylation (Tsuda *et al.*, 1991), and have growth promoting effects. Thus, the tyrosine phosphorylation associated with the application of these hormones could be of importance for both the growth response and the contractile response of these cells.

Much of the evidence indicating that tyrosine kinase activity influences force development is based on the potent antagonistic effect of TKIs against growth factor-induced force development in smooth muscles (see, Hollenberg, 1994). For the classical constrictor agonists such evidence is less clear. For some agonists, like carbachol and bradykinin, the inhibitory potency of the TKIs is reported to be low (Yang *et al.*, 1992; 1993), while for others, like angiotensin II, the potency is high (Yang *et al.*, 1993). Moreover, in a recent study, TKIs were shown to have an inhibitory effect in moderately high concentrations against carbachol- and noradrenaline (NA)-induced contraction (DiSalvo *et al.*, 1993), while in another study they were without effect against phenylephrine- and phorbol ester-induced contraction (Sauro & Thomas, 1993). This prompted us to investigate a range of TKIs for their concentration-dependent effect on the calcium-dependent and independent regulation of tone in rat isolated small mesenteric arteries. Experiments were also performed to determine the effect of TKIs on the intracellular calcium activity ($[Ca^{2+}]_i$) in these vessels.

Present address: [1] Department of Physiology, University of Medicine and Pharmacy Isai, Universitatii Str. 16, Isai 6600, Romania. [2] Departmento de Fisiologia, Facultad de Veterinaria, Universidad Complutense, Ciudad Universitaria, 28040 Madrid, Spain. [3] Department of Clinical Pharmacology, St Mary's Hospital Medical School, London W2 1NY. [4] Author for correspondence.

Methods

Preparation

Mesenteric resistance arteries (second or third order branches of the superior mesenteric artery) from male Wistar rats (12–15 weeks old) killed with CO_2 were used for all experiments. The procedures used to isolate the arteries and the myograph for isometric force measurements have been described previously (Mulvany & Halpern, 1977). Briefly, the arteries were dissected free from the surrounding connective tissue. Segments, approximately 2 mm long, were mounted in an isometric myograph (JP-trading, Denmark), as ring preparations. The internal circumference of the vessels was set to 0.9 times the circumference the vessels have at 100 mmHg, based on the passive length-tension curve (Mulvany & Halpern, 1977). At this setting, the arteries had an internal diameter of about 200 μm and develop near maximal active tension during stimulation (Mulvany & Halpern, 1977). In all experiments, except those where the arteries were permeabilized, pretreatment with 6-hydroxydopamine (Aprigliano & Hermsmeyer, 1976), or 100 μM guanethidine for 20 min, was used to eliminate the effect of endogenous NA. N^G-nitro-L-arginine methyl ester (L-NAME, 10 μM) was added 30 min before the experimental procedure and during experiments to avoid possible interference from NO release from endothelial cells. All experiments were started by repetitively stimulating vessels with a solution of 125 mM K^+ (KPSS, for composition see below) containing 10 μM NA for 2 min with 10 min between stimulations, until reproducible contractions were elicited.

Experimental procedure

The effects of different TKIs on contractions induced by 10 μM NA or KPSS were assessed 10 min after inducing contractions. Cumulative concentration-response curves were obtained for tyrphostin A-1, A-23, A-47, *bis*-tyrphostin, genistein and daidzein. All TKIs were dissolved in dimethylsulphoxide (DMSO). Time control experiments where the vehicle was added, were made before and after the application of TKI. The maximal DMSO concentration in the bath was 1.27% (for 100 μM TKI).

Permeabilization with α-toxin

The procedure used to permeabilize these vessels with α-toxin was described by Jensen (1994). The arteries were mounted as described above and stimulated once with KPSS at room temperature (experiments with permeabilized preparations were always conducted at room temperature). The bubbling was changed to 100% O_2 and the arteries were incubated for 15–20 min in relaxing solution (for composition see below). Permeabilization was made by incubating the arteries 10–15 min in 10 μl relaxing solution with 1 μM free Ca^{2+} and 1000 u ml^{-1} α-toxin. After permeabilization, the arteries were held in relaxing solution. They were stimulated twice with 10 μM free Ca^{2+} before further experimental procedures. The effect of the different TKIs was assessed on contractions induced with 1 μM free Ca^{2+} to give near maximal contraction or with 200 nM free Ca^{2+} after pretreatment of the arteries with 100 μM NA and 3 μM GTP for 10 min, which gave the same contraction as 1 μM free Ca^{2+}. Time control experiments where the vehicle was added, were carried out before and after the application of TKI.

Simultaneous measurements of cytoplasmic free calcium and force

We have previously described this technique and the calibration of the fluorescence signal in detail (Jensen *et al.*, 1992; 1993). Briefly, arteries mounted in the myograph were loaded with fura-2. The arteries were stimulated every 10 s with 347 and 380 nm light. The emitted light was measured by a photomultiplier through a 500–530 nm filter and a cut-off (<720 nM) filter. The system was controlled by a computer, and both force and the two emission signals (F_{347} and F_{380}) were stored for subsequent analysis. At the end of the experiment fura-2 signals were calibrated, based on the determination of the maximal (R_{max}) and minimal (R_{min}) fluorescence ratio and the ratio (β) between the maximal and minimal fluorescence at 380 nM (Grynkiewicz *et al.*, 1985; Jensen *et al.*, 1992). Background fluorescence was determined after quenching with 20 mM $MnCl_2$. With this setup the only inhibitor we could use was genistein, because the other TKIs quenched more than 90% of the fura-2 signals.

Solutions

The physiological saline solution (PSS) had the following composition (mM): NaCl 119, KCl 4.7, KH_2PO_4 1.18, $MgSO_4$ 1.17, $NaHCO_3$ 25, $CaCl_2$ 2.5, ethylenediaminetetraacetic acid (EDTA) 0.026 and glucose 5.5. The PSS was bubbled with 95% O_2 and 5% CO_2 (pH = 7.45–7.50 at 37°C). PSS containing high K^+ (KPSS, 125 mM K^+) was prepared by iso-osmolar substitution of NaCl with KCl. Relaxing solution had the following composition (mM): EGTA 2, potassium methane sulphonate 130, $MgCl_2$ 4, Tris maleate 20, Na_2ATP 4, creatine phoshate 10 and creatine phosphokinase 1 mg ml^{-1}. pH was adjusted to 7.15 with KOH and the solution was gassed with 100% O_2.

Chemicals

Fura-2AM and pluronic F127 (Molecular Probes, Oregon, U.S.A.), α-toxin (GIBCO, U.S.A.), tyrphostins, genistein and daidzein (Calbiochem, California, U.S.A.), cremophor EL, noradrenaline, nigericin, ionomycin, guanethidine, L-NAME and 6-hydroxydopamine (Sigma Chemicals, Poole, Dorset, U.K.) were used. The high purity EGTA (>99%) used in solutions for *in situ* calibration of fura-2 was from Fluka (Buchs, Switzerland). The TKIs were prepared as 10 mM stock solutions in DMSO.

Statistics

All results are shown as arithmetric means ± s.e.mean, n is the number of arteries, except for the mean $[Ca^{2+}]_i$ values, which are given as geometric means. Student's two-tailed t test or one way ANOVA test followed by Bonferroni test were used for statistical comparisons. $P<0.05$ was considered as a significant difference.

Results

Effects of TKIs on contraction induced with NA and KPSS

The effects of TKIs on tonic contractions induced with either 10 μM NA or KPSS were assessed. The results are presented in two main groups, according to the two different mechanisms for inhibition of the tyrosine kinases.

In the first group (Figure 1a and b), genistein and daidzein caused similar concentration-dependent relaxations of the active tension induced with both NA and KPSS. The pIC_{50}s ($-\log IC_{50}$, where IC_{50} is the concentration of the compounds causing a 50% inhibition of the contraction) of genistein and daidzein in arteries activated with KPSS were 4.65 ± 0.01 and 4.47 ± 0.03, $n = 4$, respectively ($P<0.05$). The pIC_{50}s of genistein and daidzein in arteries activated with 10 μM NA were 4.86 ± 0.10 and 4.56 ± 0.08, $n = 4$, respectively ($P<0.05$). A slight but significantly greater potency of genistein compared to daidzein was thus observed both in vessels activated with NA and with KPSS.

In the second group, the effects of four tyrphostins were assessed. Tyrphostin A-23, A-47 and A-1 caused concentration-dependent relaxations of contraction induced with both NA and KPSS (Figure 1c and d), but *bis*-tyrphostin had no significant effect on contractions. Tyrphostin A-23 in a concentration of 100 μM caused a complete inhibition of the force development and pIC_{50} was 4.30 ± 0.06, $n = 6$ and 4.43 ± 0.13, $n = 6$ for arteries activated with KPSS and 10 μM NA, respectively. The inhibitory effect of tyrphostin A-47 and A-1 was too small, in the concentration-range tested, to calculate the IC_{50}. After washout of genistein, daidzein, tyrphostin A-23, A-47 and A-1 the response to NA and KPSS almost completely recovered (data not shown except for genistein see Figure 2).

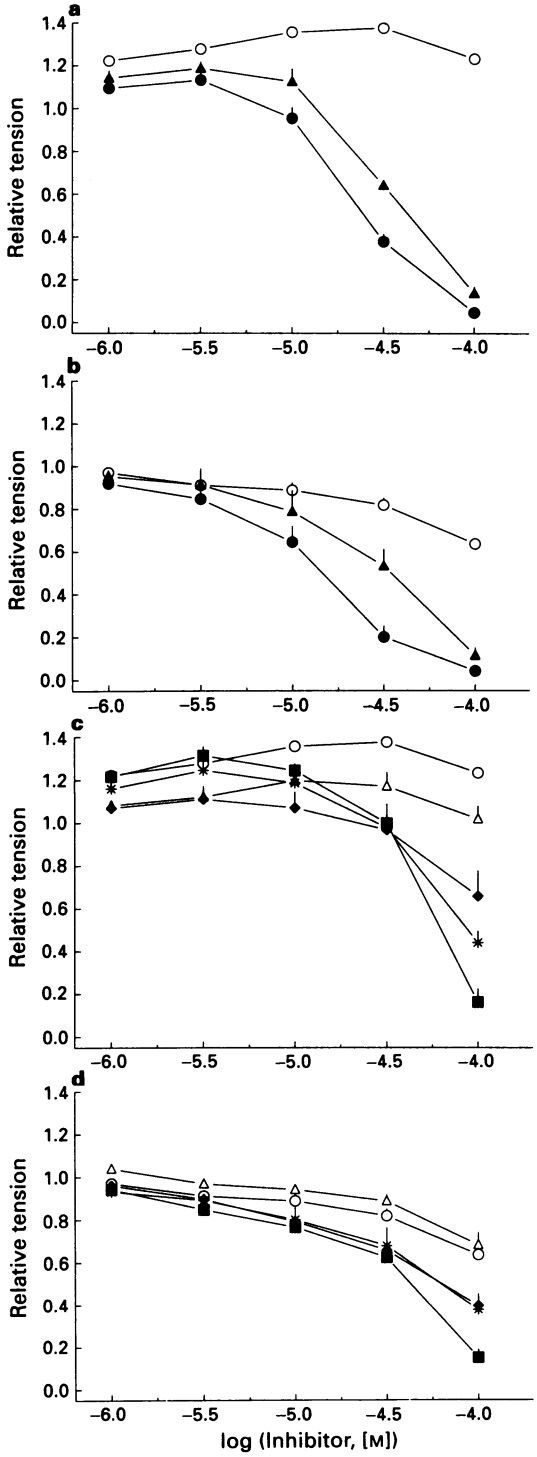

Figure 1 Effects of tyrosine kinase inhibitors (TKIs) on potassium-induced contraction (a and c) and noradrenaline-induced (10 μM) contraction (b and d) in intact arteries. The responses are expressed relative to the contraction immediately before the first concentration of drug or vehicle was added. Each point represents mean (with s.e.mean of 4–6 vessels where they exceed the size of the symbols). (a and b): (○) Vehicle; (●) genistein; (▲) daidzein. (c and d): (○) Vehicle; (△) *bis*-tyrphostin; (◆) A-47; (*) A-1; (■) A-23.

Effects of genistein on force and $[Ca^{2+}]_i$ during stimulation with NA and KPSS

Arteries were pretreated for 10 min with 30 μM genistein before stimulation with NA or KPSS. When genistein was added to the medium, both the F_{347} and the F_{380} signals

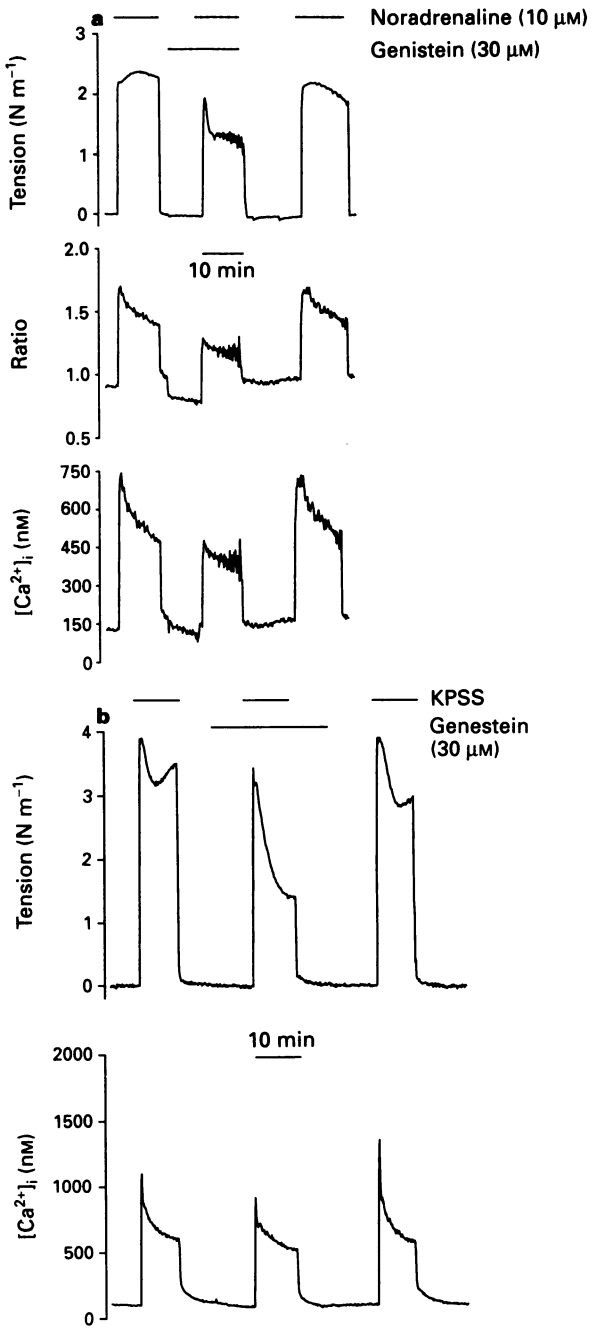

Figure 2 Recording of measurements of contraction and $[Ca^{2+}]_i$ during activation with noradrenaline (NA) (a) and high K^+ physiological saline solution (KPSS) (b). Where indicated 30 μM genistein was present. In (a) the middle trace shows the ratio of fura-2 fluorescence before correction for genistein-induced quenching of the fluorescence.

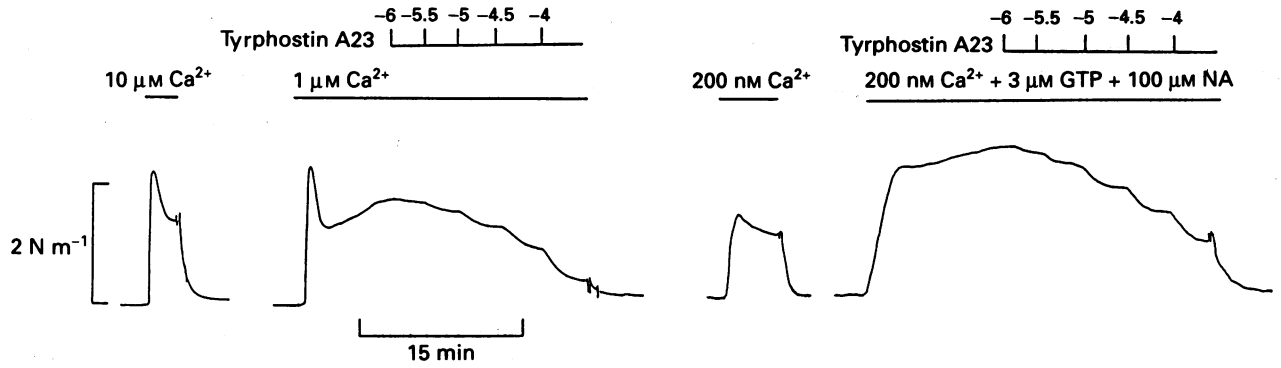

Figure 3 Trace showing the contraction in α-toxin-permeabilized mesenteric small arteries during stimulation with 1 μM Ca^{2+} and with 200 nM Ca^{2+} in the presence of 100 μM noradrenaline (NA) and 3 μM guanosine 5'-triphosphate (GTP). Where indicated, tyrphostin A-23 was added in increasing concentrations.

dropped significantly, and also the ratio was reduced (Figure 2a) as previously reported (Sargean *et al.*, 1993). The effect was quickly reversible after washout of genistein. At the end of experiments after fura-2 signals had been quenched by Mn^{2+}, 100 μM genistein had little effect on the remaining background signals (data not shown). This indicated that genistein quenched some of the Ca^{2+}-sensitive signals of fura-2, and could also reflect an effect of genistein on the K_d of fura-2 for $[Ca^{2+}]_i$. However, if 30 μM genistein was added to the acid form of fura-2 in PSS, there was little effect on fura-2 signals, indicating that genistein affected only the fura-2 signals from the cells. To circumvent these problems, the Ca^{2+}-sensitive fluorescence signals in the presence of genistein were calibrated using a R_{max}, R_{min} and β which were determined in the presence of genistein. Secondly, the K_d of the fura-2 Ca^{2+} complex in the presence of genistein was determined in the cells as described previously (Jensen *et al.*, 1993) and found not to be different from the K_d in the absence of genistein. For calibration of the fura-2 signals we therefore used the previously determined K_d of 342 nM (Jensen *et al.*, 1993).

Figure 2 depicts the effect of 30 μM genistein on active tension and $[Ca^{2+}]_i$ during stimulation with NA (Figure 2a) and during stimulation with KPSS (Figure 2b). In the presence of genistein, active tension after 10 min stimulation was significantly lower with both NA activation (2.35 ± 0.15 Nm^{-1} and 0.96 ± 0.21 Nm^{-1}, $n = 6$; control and genistein treated, respectively) and KPSS activation (2.72 ± 0.40 Nm^{-1} and 1.27 ± 0.32 Nm^{-1}, $n = 4$; control and genistein-treated, respectively). However, $[Ca^{2+}]_i$ at this time was significantly affected by genistein only during stimulation with NA ($p([Ca^{2+}]_i)$: 6.272 ± 0.048 and 6.592 ± 0.127, $n = 6$; control and genistein-treated, respectively); during KPSS activation no difference in $[Ca^{2+}]_i$ was observed ($p([Ca^{2+}]_i)$: 6.153 ± 0.037 and 6.163 ± 0.043, $n = 4$; control and genistein, respectively).

Effects of TKI on tension of α-toxin permeabilized arteries

Figure 3 illustrates the protocol used in the experiments with α-toxin permeabilized preparations. After α-toxin permeabilization, the arteries developed an active tension of 1.81 ± 0.07 N m^{-1} ($n = 50$) when maximally stimulated with 10 μM free Ca^{2+}. This response was $52 \pm 2\%$ of the response to KPSS (3.53 ± 0.12 N m^{-1}, $n = 50$) in the preparations before permeabilization. Since the response of rat mesenteric small arteries to KPSS is reduced to about 55% with denervation or in the presence of an α-adrenoceptor blocker (see e.g. Jensen *et al.*, 1992) this suggests that probably all of the smooth muscles in the preparation are activated by the 10 μM free Ca^{2+} and therefore presumably permeabilized. The effects of the two groups of TKIs on the contraction induced by a submaximal free Ca^{2+} concentration (1 μM) are shown in Figure 4a and b, and their inhibitory potencies are given in Table 1. Ca^{2+} (1 μM) elicited, in most preparations, a biphasic response with an initial transient and a second sustained phase which reached a plateau after 10–15 min (Figure 3). The plateau tension was 1.09 ± 0.09 N m^{-1} ($n = 28$), and this response was $60.1 \pm 0.5\%$ of the maximal tension elicited by 10 μM free Ca^{2+}.

Tyrosine kinase inhibitors relaxed in a concentration-dependent and reversible manner the contraction induced by Ca^{2+}. At the highest concentration used (100 μM), the maximal inhibitions elicited by genistein and daidzein were $93 \pm 2\%$ ($n = 5$) and $90 \pm 4\%$ ($n = 5$), respectively, of the Ca^{2+}-induced contraction (Figure 4a). The relaxations evoked by tyrphostin A-23 and tyrphostin A-47 were $62 \pm 8\%$ ($n = 6$) and $80 \pm 4\%$ ($n = 6$) (Figure 4b), respectively. In contrast, 100 μM tyrphostin A-1 induced only a slight inhibition of the contraction induced by Ca^{2+}, whereas the effect of *bis*-tyrphostin was not significantly different from that of the vehicle. There were no significant differences among the inhibitory potencies of the active compounds on the contractions induced by 1 μM free Ca^{2+} (Table 1).

Effects on contraction induced with Ca^{2+} in the presence of NA and GTP

Addition of 100 μM NA and 3 μM GTP 10 min before stimulation, increased the contraction to 200 nM Ca^{2+} from 0.54 ± 0.06 N m^{-1} ($n = 26$) to 1.31 ± 0.13 N m^{-1} ($n = 26$). These responses were $29 \pm 6\%$ and $70 \pm 3\%$ of the maximal tension elicited by 10 μM free Ca^{2+}, respectively. Figure 4c and d shows the effects of TKIs on contraction induced by Ca^{2+} in the presence of NA and GTP. The maximal relaxations evoked by genistein and daidzein were $96 \pm 2\%$ ($n = 5$) and $93 \pm 2\%$ ($n = 5$) of the initial contraction, respectively (Figure 4c). The maximal relaxations elicited by tyrphostin A-23 and tyrphostin A-47 were $68 \pm 2\%$ ($n = 4$) and $87 \pm 2\%$ ($n = 6$), respectively (Figure 4d). The effect of *bis*-tyrphostin on contraction to Ca^{2+} in the presence of NA and GTP was not significantly different from that of the vehicle. Tyrphostin A-1 evoked a slight inhibitory effect at the highest concentrations used (Figure 4d).

Genistein was more potent in inhibiting contractions elicited by Ca^{2+} in the presence of NA and GTP, than contraction elicited by Ca^{2+} alone (Table 1), while for the other TKIs no significant difference was observed.

Discussion

In the present study, the effects of two structurally and pharmacologically distinct groups of TKIs on active tension

in mesenteric small arteries have been characterized. In the discussion we first focus on the potency of these substances and secondly we discuss the possible role of tyrosine kinases for the excitation-contraction coupling in small arteries.

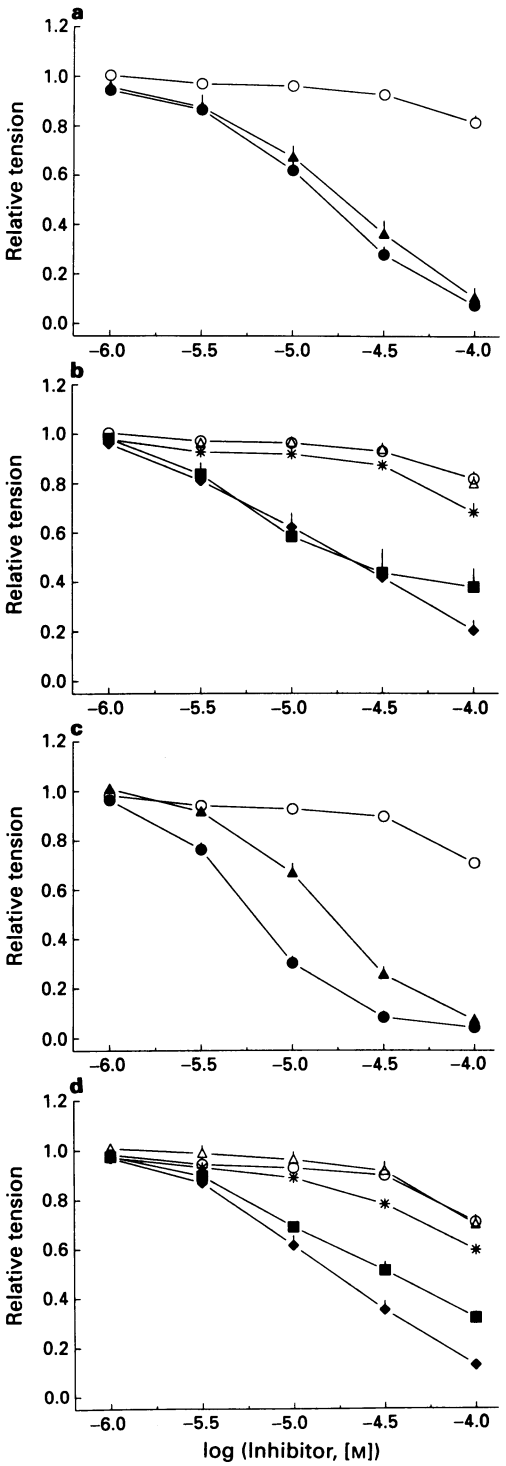

Figure 4 Effects of tyrosine kinase inhibitors (TKI) on Ca^{2+} (a, b) and Ca^{2+} + noradrenaline (NA) + guanosine 5'-triphosphate (GTP) (c, d) induced contraction of α-toxin-permeabilized mesenteric small arteries. Concentration-response curves for the inhibitory action of genistein and daidzein (a, c) and tyrphostins (b, d) are shown. Responses are expressed as percentage of the contraction just prior to the addition of the inhibitor or vehicle. Each point represents mean (with s.e.mean where they exceed the size of the symbols) of 4–10 vessels. (a and c): (○) Vehicle; (●) genistein; (▲) daidzein. (b and d): (○) Vehicle; (△) *bis*-tyrphostin; (◆) A-47; (*) A-1; (■) A-23.

Potency of tyrosine kinase inhibitors in resistance arteries

Genistein, which binds to the ATP binding site of tyrosine kinase, inhibited contraction with a potency that is consistent with it acting through inhibition of tyrosine kinase. Particularly in the α-toxin-permeabilized preparation, the potency of genistein (IC_{50} ca. 6 μM) is in the same range or lower than that reported for the inhibitory effect of genistein on angiotensin II (Yang *et al.*, 1993) or epidermal growth factor (EGF) induced contraction (Yang *et al.*, 1992) in guinea-pig stomach muscle. However, in the intact preparation, genistein was also potent with an IC_{50} of about 20 μM. On the other hand, the supposedly inactive analogue of genistein, daidzein, also potently inhibited the contraction both in the intact preparation and in the α-toxin-permeabilized preparation. Therefore, although the potency of daidzein was about two times less than that of genistein towards NA activated vessels, it is possible that genistein and daidzein also affect a tyrosine kinase independent pathway in these vessels, or that the tyrosine kinase in the smooth muscle cells of the resistance arteries is susceptible to daidzein in low concentrations.

Of the four tyrphostins tested in this study, A-1 is the supposedly inactive analogue and was indeed inactive in the permeabilized preparation in the sense that it had no effect at concentrations up to 100 μM. However, in the intact preparation 100 μM A-1 did cause an inhibition of both the K^+- and the NA-induced force development. This could be accounted for by an inhibitory effect of tyrphostin A-1 on the voltage-activated calcium channels, which we have previously reported (Wijetunge *et al.*, 1992). *Bis*-tyrphostin, which has a specificity towards EGF-receptor tyrosine kinase, had no effect on either K^+-induced or NA-induced responses, and was also inactive in the permeabilized preparation in concentrations up to 100 μM. This suggests that *bis*-tyrphostin may be used as an inactive analogue in the vessels studied here. In the rabbit ear artery though, one of us (Hughes, 1994) has shown, that 5 μM *bis*-tyrphostin inhibits the PDGF-induced tension. With respect to the active analogues, both A-23 and A-47 caused an inhibition of force development. In the α-toxin-permeabilized preparation, the IC_{50} of these two drugs was about 12–18 μM. This indicates a slightly less potent effect than reported for the EGF-activated guinea-pig gastric muscle (Yang *et al.*, 1992), for the EGF-activated rabbit

Table 1 Inhibitory potencies of tyrosine-kinase inhibitors on the contractions induced by 1 nM Ca^{2+} and by 200 nM Ca^{2+} in the presence of noradrenaline (NA) plus guanosine 5'-triphosphate (GTP) in α-toxin-permeabilized mesenteric resistance arteries

	Ca^{2+} (1 μM)		*Ca^{2+}* (0.2 μM) + *GTP* (3 μM) + *NA* (100 μM)	
	pIC_{50}	*n*	pIC_{50}	*n*
Genistein	4.82 ± 0.06	(5)	5.23 ± 0.03[1,2]	(5)
Daidzein	4.75 ± 0.08	(6)	4.83 ± 0.05	(5)
Tyr A-1	NC	(7)	NC	(6)
Tyr A-23	4.93 ± 0.19	(6)	4.74 ± 0.07	(4)
Tyr A-47	4.76 ± 0.13	(6)	4.76 ± 0.11	(6)
Bis-Tyr	NC	(4)	NC	(4)

Values are expressed as means ± s.e.mean. *n* indicates the number of vessels, NC means not calculated. The inhibitory potency of each compound is expressed as $pIC_{50} = -\log IC_{50}$, where IC_{50} is the concentration of the compounds causing a 50% inhibition of the contraction induced by either Ca^{2+} alone or Ca^{2+} plus NA and GTP. [1]Indicates significant differences between the pIC_{50} for genistein and daidzein (one-way ANOVA, posterio Bonferroni test). [2]Indicates significant differences between the pIC_{50} of genistein towards Ca^{2+} and Ca^{2+} plus NA and GTP activated vessels.

aorta (Merkel *et al.*, 1993) and for the PDGF-activated rat aorta (Sauro & Thomas, 1993), but in the same range as that reported for the angiotensin II-activated guinea-pig gastric muscle (Yang *et al.*, 1993) and probably consistent with these drugs acting through inhibition of tyrosine kinase. In the intact preparation, the potency of the TKIs was less than in the α-toxin-permeabilized preparations. It has been suggested (Lyall *et al.*, 1989) that it may take up to 16 h for the full effect of the tyrphostins to develop in intact cells. It is possible therefore that the lower apparent potency in the intact preparation, where the effect was assessed a few minutes after the TKIs were added, reflected poor penetration of the TKIs. This may point to difficulties in using TKIs for acute pharmacological experiments in membrane-intact preparations.

Effect of tyrosine kinase inhibitors on calcium-mediated contraction

One of the important aspects of this study was to assess which parts of the excitation-contraction coupling was potentially dependent on tyrosine phosphorylation. One way this was addressed was by comparing the effect of the TKIs on contraction induced by K^+ and by NA. It has previously been reported (DiSalvo *et al.*, 1993) that 50 μM tyrphostin A-47 inhibits the contraction of guinea-pig mesenteric small arteries to NA by about 80%, while the K^+-induced contraction was inhibited only by 20%. An apparent selectivity for the NA-induced contraction was not confirmed in this study, where the NA-induced response and the K^+-induced response was inhibited with almost the same potency and maximal effect by the tyrphostins. This observation was supported by the similar potency of the tyrphostins against the contraction induced by calcium and by calcium plus GTP and NA in the α-toxin-permeabilized preparation. It may not be surprising that agonist independent contraction (K^+-induced contraction of the intact arteries and calcium-induced contraction of the α-toxin permeabilized preparation) was inhibited by TKIs, since it has been shown in cultured vascular smooth muscle cells (Tsuda *et al.*, 1991) that the calcium ionophore, ionomycin, can induce tyrosine phosphorylation. In fact, the tyrosine phosphorylation pattern induced by the ionophore was not dissimilar to that induced by vasoconstrictors including NA (Tsuda *et al.*, 1991). There seems therefore good evidence that calcium can induce a tyrosine kinase activity in vascular smooth muscles. Also genistein had a potent effect on the KPSS-induced contraction and the calcium-induced contraction in the permeabilized arteries which supports this suggestion. In contrast to the tyrphostins, genistein was, however, more potent towards the NA-induced than to the KPSS-induced contraction. This would suggest that in addition to the calcium-induced tyrosine kinase activity, NA may induce a tyrosine kinase activity with a slightly higher susceptibility to genistein. The finding that genestein was also more potent towards the permeabilized arteries activated with calcium in the presence of NA and GTP compared to the arteries activated with calcium alone might suggest that the additional tyrosine kinase activity may play a role in the steps involved in agonist-induced modulation of the effectiveness of $[Ca^{2+}]_i$. On the other hand, the observation that the relaxant effect of genestein was associated with a decrease of $[Ca^{2+}]_i$ in NA-activated arteries, but not in potassium-activated arteries, indicates that the additional tyrosine kinase activated by NA may also be involved in regulation of $[Ca^{2+}]_i$ (see below).

Effect of genistein on the control of $[Ca^{2+}]_i$

We have previously shown that the calcium current in rabbit ear artery smooth muscle cells can be inhibited by genistein (IC_{50}, 36 μM), tyrphostin A-23 (IC_{50}, 88 μM) and tyrphostin A-1 (IC_{50}, 110 μM), although daidzein had no effect in concentrations below 300 μM (Wijetunge *et al.*, 1992). As pointed out above, the relaxant effect of tyrphostin A-1 in the non-permeabilized preparation could be explained by the inhibition of the potential sensitive calcium channels. However, it was unexpected that 30 μM genestein did not reduce $[Ca^{2+}]_i$ in potassium-activated vessels, in view of the above findings on the rabbit ear artery smooth muscle cells. Although we have no explanation for this, it is possible that the potency of genestein is different in the rabbit ear artery smooth muscle and in the rat mesenteric resistance arteries, either as a consequence of species differences or due to the fact that the voltage clamp experiments were done on isolated cells while the $[Ca^{2+}]_i$ measurements were made in whole tissue. In contrast, $[Ca^{2+}]_i$ was reduced by 30 μM genestein in NA-activated rat mesenteric arteries. In these vessels, the effect of NA on $[Ca^{2+}]_i$ is thought to be mediated almost exclusively by depolarization with a consequent opening of voltage-dependent calcium channels (Nilsson *et al.*, 1994). It is therefore a possibility that a tyrosine kinase is affecting the signal leading from stimulation of the adrenoceptor to membrane depolarization.

In conclusion, these data support a role for tyrosine kinases in the force development to classical vasoconstrictors. It is likely that the steps involved may include the NA-induced modulation of $[Ca^{2+}]_i$, the ability of calcium to induce force and perhaps also the agonist/GTP mediated modulation of the effectiveness of $[Ca^{2+}]_i$. On the other hand, these data also indicate that caution is needed in the interpretation of the effects of the tyrphostins in acute pharmacological experiments. Also the potent effect of the so called inactive analogues for the TKIs may indicate that the TKIs have potent effects on pathways unrelated to inhibition of tyrosine kinase, or that tyrosine kinases with a high susceptibility to the inactive analogues of the TKIs may play a role in excitation-contraction coupling.

This work was supported by the Danish Medical Research Council and The Novo Foundation. We thank Dr Dragomir N. Serban for helpful discussion of the manuscript. C.T. was a recipient of a fellowship from SOROS Foundation for an Open Society, Iasi, Romania, D.P. was supported by a grant from Comunidad de Madrid, Spain and M.J.M. was supported by the Danish Heart Foundation.

References

AKIYAMA, T., ISHIDA, J., NAKAGAWA, S., OGAWARA, H., WATANABE, S., ITOH, N., SHIBUYA, M. & FUKAMI, Y. (1987). Genistein, a specific inhibitor of tyrosine-specific protein kinases. *J. Biol. Chem.*, **262**, 5592–5595.

APRIGLIANO, O. & HERMSMEYER, K. (1976). *In vitro* denervation of the portal vein and caudal artery of the rat. *J. Pharmacol. Exp. Ther.*, **198**, 568–577.

AUGER, K.R., SERUNIAN, L.A., SOLTOFF, S.P., LIBBY, P. & CANTLEY, L.C. (1989). PDGF-dependent tyrosine phosphorylation stimulates production of novel polyphosphoinositides in intact cells. *Cell*, **57**, 167–175.

BERK, B.C., ALEXANDER, R.W., BROCK, T.A., GIMBRONE, Jr, M.A. & WEBB, R.C. (1986). Vasoconstriction, a new activity for platelet-derived growth factor. *Science*, **234**, 87–89.

BISHOP, J.M. (1987). The molecular genetics of cancer. *Science*, **235**, 305–311.

CASNELLIE, J.E. (1991). Protein kinase inhibitors: probes for the functions of protein phosphorylation. *Adv. Pharmacol.*, **22**, 167–205.

DI SALVO, J., STEUSLOFF, A., SEMENCHUK, L., SATOH, S., KOLQUIST, K. & PFITZER, G. (1993). Tyrosine kinase inhibitors suppress agonist-induced contraction in smooth muscle. *Biochem. Biophys. Res. Commun.*, **190**, 968–974.

DRAETTA, G., PIWNICA-WORMS, H., MORRISON, D., DRUCKER, B., ROBERTS, T. & BEACH, D. (1988). *Nature*, **336**, 738–744.

GLENNEY, J.R. (1991). Tyrosine-phosphorylated proteins: mediators of signal transduction from the tyrosine kinases. *Biochem. Biophys. Acta*, **1134**, 113–127.

GRYNKIEWICZ, G., POENIE, M. & TSIEN, R.Y. (1985). A new generation of Ca^{2+} indicators with greatly improved fluorescence properties. *J. Biol. Chem.*, **260**, 3440–3450.

HOLLENBERG, M.D. (1994). Tyrosine kinase pathways and the regulation of smooth muscle contractility. *Trends Pharmacol. Sci.*, **15**, 108–114.

HUGHES, A.D. (1994). Increase in tone and intracellular Ca^{2+} in rabbit isolated ear artery by platelet-derived growth factor. *Br. J. Pharmacol.*, (in press).

JENSEN, P.E. (1994). α-toxin permeabilization of rat mesenteric small arteries and effects of stretch. In: *The Resistance Arteries, Integration of the Regulatory Pathways.* ed. Halsern, W., Bevan, J.A., Brayden, J., Dustan, H., Nelson, M. & Osol, G. pp. 23–29. Totowa, New Jersey: Humana Press.

JENSEN, P.E., MULVANY, M.J. & AALKJÆR, C. (1992). Endogenous and exogenous agonist-induced changes in the coupling between $[Ca^{++}]_i$ and force in rat resistance arteries. *Eur. J. Physiol. Plügers Arch.*, **420**, 536–543.

JENSEN, P.E., MULVANY, M., AALKJÆR, C., NILSSON, H. & YAMAGUCHI, H. (1993). Free cytosolic Ca^{2+} measured with Ca^{2+}-selective electrodes and Fura-2 in rat mesenteric resistance arteries. *Am. J. Physiol.*, **265**, H741–H746.

LEVITZKI, A. & GILON, C. (1991). Tyrphostins as molecular tools and potential antiproliferative drugs. *Trends Pharmacol. Sci.*, **12**, 171–173.

LYALL, R.M., ZELBERSTEIN, A., GAZIT, A., GILON, C., LEVITZKI, A. & SCHLESSINGLER, J. (1989). Tyrphostins inhibit epidermal growth factor (EGF)-receptor tyrosine kinase activity in living cells and EGF-stimulated cell proliferation. *J. Biol. Chem.*, **264**, 14503–14509.

MERKEL, L.A., RIVERA, M.L., COLUSSI, D.J. & PERRONE, M.H. (1993). Inhibition of EGF-induced vasoconstriction in isolated rabbit aortic rings with the tyrosine kinase inhibitor RG50864. *Biochem. Biophys. Res. Commun.*, **192**, 1319–1326.

MULVANY, M.J. & HALPERN, W. (1977). Contractile properties of small arterial resistance vessels in spontaneously hypertensive and normotensive rats. *Circ. Res.*, **41**, 19–26.

NILSSON, H., JENSEN, P.E. & MULVANY, M.J. (1994). Minor role for direct adrenoceptor-mediated calcium entry in rat mesenteric small arteries. *J. Vasc. Res.*, **31**, 314–321.

O'DELL, T.J., KANDEL, E.R. & GRANT, S.G. (1991). Long-term potentiation in the hippocampus is blocked by tyrosine kinase inhibitors. *Nature*, **353**, 558–560.

SARGEAN, P., FARNDALES, R.W. & SAGE, S.O. (1993). ADP- and thapsigargin-evoked Ca^{2+} entry and protein-tyrosine phosphorylation are inhibited by the tyrosine kinase inhibitors genistein and nethyl-2,5-dihydroxycinnamate in fura-2-loaded human platelets. *J. Biol. Chem.*, **268**, 18151–18156.

SAURO, M.D. & THOMAS, B. (1993). Tyrphostin attenuates platelet-derived growth factor-induced contraction in aortic smooth muscle through inhibition of protein tyrosine kinase(s). *J. Pharmacol. Exp. Ther.*, **267**, 1119–1125.

SCHALLER, M.D. & PARSONS, J.T. (1993). Focal adhesion kinase: an integrin-linked protein tyrosine kinase. *Trends Cell Biol.*, **3**, 258–262.

TSUDA, T., KAWAHARA, Y., SHII, K., KOIDE, M., ISHIDA, Y. & YOKOHAMA, M. (1991). Vasoconstrictor induced protein-tyrosine phosphorylation in cultured vascular smooth muscle cells. *FEBS Lett.*, **285**, 44–48.

WEISS, R.H. & NUCCITELLI, R. (1992). Inhibition of tyrosine phosphorylation prevents thrombin-induced mitogenises, but not intracellular free calcium release, in vascular smooth muscle cells. *J. Biol. Chem.*, **267**, 5608–5613.

WIJETUNGE, S., AALKJÆR, C., SCHACHTER, M. & HUGHES, A. (1992). Tyrosine kinase inhibitors block calcium channel currents in vascular smooth muscle cells. *Biochem. Biophys. Res. Commun.*, **189**, 1620–1623.

YANG, S-G., SAIFEDDINE, M. & HOLLENBERG, M.D. (1992). Tyrosine kinase inhibitors and the contractile action of epidermal growth factor -urogastrone and other agonists in gastric smooth muscle. *Can. J. Physiol. Pharmacol.*, **70**, 85–93.

YANG, S-G., SAIFEDDINE, M., LANIYONU, A. & HOLLENBERG, M.D. (1993). Distinct signal transduction pathways for angiotensin-II in guinea-pig gastric smooth muscle: Differential blockade by indomethacin and tyrosine kinase inhibitors. *J. Pharmacol. Exp. Ther.*, **264**, 958–966.

(Received August 15, 1994
Revised October 27, 1994
Accepted November 22, 1994).

British Journal of Pharmacology (1995) 114, 1273-1281

Glibenclamide-induced inhibition of the expression of inducible nitric oxide synthase in cultured macrophages and in the anaesthetized rat

Chin-Chen Wu, [1]Christoph Thiemermann & John R. Vane

The William Harvey Research Institute, St. Bartholomew's Hospital Medical College, Charterhouse Square, London, EC1M 6BQ

1 We have investigated whether glibenclamide, an inhibitor of ATP-sensitive potassium channels, influences the induction of the calcium-independent isoform of nitric oxide synthase (iNOS) in cultured J774.2 macrophages activated by bacterial endotoxin (*E.coli* lipopolysaccharide; LPS), as well as in the lung and aorta of rats with endotoxic shock.

2 Pretreatment of J774.2 macrophages with glibenclamide (10^{-7} to 10^{-5} M for 30 min) dose-dependently inhibited the accumulation of nitrite caused by LPS (1 $\mu g\,ml^{-1}$). In contrast, pretreatment of macrophages with tetraethylammonium (10^{-4} to 10^{-2} M for 30 min), a non-selective inhibitor of potassium channels, did not affect the rise in nitrite caused by LPS. At the highest concentration (10^{-5} M) used, cromakalim, an opener of ATP-sensitive potassium channels, caused a small, but significant inhibition of nitrite formation in macrophages activated with LPS, while lower concentrations (10^{-7} to 3×10^{-6} M) were without effect.

3 The inhibition by glibenclamide (3 μM) of the increase in nitrite induced by LPS in J774.2 macrophages was weaker when glibenclamide was given several hours after LPS, indicating that glibenclamide inhibits the induction, but not the activity, of iNOS. In contrast, the degree of inhibition of nitrite formation caused by the nitric oxide synthase (NOS) inhibitor N^{ω}-nitro-L-arginine methyl ester (L-NAME) was similar when this agent was given up to 10 h after LPS.

4 In anaesthetized rats, LPS caused a fall in mean arterial blood pressure (MAP) from 120 ± 4 (time 0) to 98 ± 4 mmHg at 180 min ($P<0.05$, $n=6$). Treatment of LPS-rats with glibenclamide (1 mg kg^{-1}, i.v. at 60 min after LPS) caused a rapid and sustained rise in MAP (e.g. MAP at 180 min after LPS: 122 ± 4 mmHg; $n=6$, $P<0.05$ when compared to LPS-rats). The maximum of the rise in MAP produced by glibenclamide (1 mg kg^{-1}, i.v.) was similar when the drug was given either at 60 or 180 min after LPS. However, the duration of the pressor response was significantly longer when glibenclamide was given at 60 min, rather than at 180 min after LPS.

5 LPS-treatment caused a significant reduction of the pressor responses elicited by noradrenaline (NA, 1 $\mu g\,kg^{-1}$, i.v.) from 35 ± 2 to 19 ± 1 mmHg at 60 min and 20 ± 2 mmHg at 180 min ($P<0.05$). Treatment of LPS-rats with glibenclamide (1 mg kg^{-1}, i.v. at 60 min) caused a significant restoration of the pressor responses elicited by NA from 19 ± 1 mmHg at 60 min (prior to glibenclamide injection) to 29 ± 3 mmHg at 180 min ($P<0.05$).

6 Endotoxaemia for 180 min resulted in a significant increase in a calcium-independent NOS activity (which was taken to represent iNOS activity) in the lung from 0.17 ± 0.1 (control, $n=4$) to 6.21 ± 0.48 pmol $mg^{-1}\,min^{-1}$ ($n=6$, $P<0.05$). Injection of glibenclamide (1 mg kg^{-1}, i.v.) at 60 min after LPS attenuated the increase in iNOS activity caused by endotoxaemia in the lung by $43 \pm 7\%$ ($n=6$, $P<0.05$). In contrast, injection of glibenclamide at 180 min after LPS did not result in a significant inhibition of iNOS activity ($n=6$, $P<0.05$).

7 Thoracic aortae obtained from rats at 180 min after LPS showed a significant reduction in the contractions elicited by noradrenaline (NA, 10^{-9} to 10^{-6} M). Treatment of LPS-rats with glibenclamide (1 mg kg^{-1}, i.v. at 60 min after LPS) significantly alleviated this LPS-induced hyporeactivity to NA *ex vivo*. In contrast, when aortic rings from LPS-rats were incubated *in vitro* with glibenclamide (10 μM for 20 min), glibenclamide did not reverse the vascular hyporeactivity to NA. However, L-NAME (300 μM for 20 min) significantly enhanced the contractile response to NA in aortic rings obtained from LPS-rats ($P<0.05$, $n=6$).

8 No significant amounts of tumour necrosis factor-α (TNFα) were detectable in the plasma before the injection of LPS. Endotoxaemia for 90 min resulted in a significant rise in plasma TNFα levels (0.05 ± 0.05 ng ml^{-1} at time 0, 3.78 ± 0.24 ng ml^{-1} at 90 min, $n=6$, $P<0.05$). Treatment of LPS-rats with glibenclamide (1 mg kg^{-1}, i.v. at 15 min prior to LPS, $n=5$) did not significantly reduce the rise in plasma TNFα levels caused by endotoxin.

9 Thus, glibenclamide inhibits the induction, but not the activity, of iNOS *in vitro* and *in vivo*. This inhibition of iNOS induction may contribute to the beneficial haemodynamic effects of glibenclamide in endotoxic shock.

Keywords: Nitric oxide synthase; glibenclamide; lipopolysaccharide, endotoxic shock

Introduction

Nitric oxide (NO) is a potent, endogenous vasodilator produced from L-arginine by NO synthase (NOS). Three different isoforms of NOS have been isolated, cloned, sequenced, and expressed. Under physiological conditions, the release of NO by the constitutive NOS present in the vascular endothelium (eNOS) dilates blood vessels, and, in

[1] Author for correspondence.

concert with vasoconstrictors such as catecholamines, regulates blood vessel diameter, organ blood flow and blood pressure. Immunological stimuli including cytokines and endotoxin cause the expression of an inducible isoform of NOS (iNOS) which, once expressed, produces large amounts of NO. When produced in high local concentrations e.g. by cytokine-activated macrophages, NO is a cytotoxic molecule which kills bacteria and tumour cells. Thus, induction of iNOS in macrophages plays an important role in host defence (see Moncada & Higgs, 1993 for review).

Circulatory shock is characterized by severe hypotension, hyporeactivity of the vasculature to vasoconstrictor agents (vascular hyporeactivity), myocardial dysfunction, maldistribution in organ blood flow, and reduced tissue oxygen extraction, which ultimately lead to multiple organ failure and death (see Altura *et al.*, 1983). There is now good evidence that an enhanced formation of NO due to activation of eNOS (acute phase of shock) and induction of iNOS (delayed phase of shock) in the vascular smooth muscle makes an important contribution to hypotension and vascular hyporeactivity to catecholamines in various animal models of septic shock (see Thiemermann, 1994 for review). The induction of iNOS in septic shock is secondary to the stimulation by endotoxin (lipopolysaccharide, LPS) of the cytokines tumour necrosis factor-α (TNFα; Pittner & Spitzer, 1992; Thiemermann *et al.*, 1993) and interleukin-1 (IL-1; Moldawer *et al.*, 1993; Szabo *et al.*, 1993d) as well as the lipid mediator platelet-activating factor (PAF; Szabo *et al.*, 1993e), which either alone or in concert cause the expression of iNOS *in vivo*. The beneficial haemodynamic effects in animal models of septic shock of various drugs including dexamethasone (Wright *et al.*, 1992), monoclonal antibodies to TNFα (Thiemermann *et al.*, 1993), the endogenous IL-1 receptor antagonist (Szabo *et al.*, 1993d), the PAF receptor antagonist WEB 2086 (Szabo *et al.*, 1993e), and dihydropyridine-type calcium channel antagonists (Szabo *et al.*, 1993c) are, at least, in part due to the inhibition by these agents of the induction of iNOS *in vivo*.

Glibenclamide, an inhibitor of ATP-sensitive potassium (K^+_{ATP}) channels, exerts beneficial haemodynamic effects in dogs with septic shock (Landry & Oliver, 1992). Here, we investigate the effects of glibenclamide on the induction of iNOS caused by LPS in cultured macrophages and in the anaesthetized rat. To elucidate whether some of the observed effects of glibenclamide are due to the inhibition of K^+_{ATP} channels, we have compared the effects of glibenclamide on iNOS induction in macrophages activated with LPS with those elicited by tetraethylammonium, a non-selective inhibitor of potassium channels (see Robertson & Steinberg, 1990) and cromakalin, a potent activator of K^+_{ATP} potassium channels (Sanguinetti *et al.*, 1988).

An account of some of this work was recently presented to the British Pharmacological Society (Wu *et al.*, 1994).

Methods

Cell culture

The mouse macrophage cell line J774.2 was cultured and prepared as previously described (Szabo *et al.*, 1993d).

Nitrite production

Nitrite production, an indicator of NO synthesis, was measured in the supernatant of J774.2 macrophages as described previously (Gross *et al.*, 1991). Briefly, the cells were cultured in 96-well plates with 200 μl of culture medium until cells reached confluence (approximately 60,000 cells per well). In order to induce iNOS, fresh culture medium containing LPS (1 μg ml^{-1}) was added. Nitrite accumulation in the medium was measured at 24 h after the application of LPS. To assess their effects on nitrite production, glibenclamide (10^{-7} to 10^{-5} M), tetraethylammonium (10^{-4} to 10^{-2} M) or cromakalim (10^{-7} to 10^{-5} M) was added at 30 min prior to LPS to cells.

In order to elucidate whether the inhibition of nitrite formation by glibenclamide in J774.2 macrophages activated with LPS is due to inhibition of iNOS induction or inhibition of iNOS activity, separate experiments were performed in which glibenclamide (3 μM) was given either together with LPS (1 μg ml^{-1}) or at 2, 4, 6 or 10 h after LPS. Agents which inhibit the induction of iNOS lose over time their ability to inhibit the increase in nitrite formation afforded by LPS, because the expression of iNOS in these cells is maximal after 6 to 10 h (Szabo *et al.*, 1993a). For comparison, we have also investigated the effect of the NOS inhibitor, N^{ω}-nitro-L-arginine methyl ester (L-NAME), on the formation of nitrite by LPS-activated J774.2 macrophages. In these experiments, L-NAME (300 μM) was also given either together with LPS (1 μg ml^{-1}) or at 2, 4, 6 or 10 h after LPS.

Nitrite was measured by adding 100 μl of Griess reagent (1% sulfanilamide and 0.1% naphthylethylenediamide in 5% phosphoric acid) to 100 μl samples of medium. The optical density at 550 nm (OD_{550}) was measured with a Molecular Devices microplate reader (Richmond, CA, U.S.A.). Nitrite concentrations were calculated by comparison with OD_{550} of standard solutions of sodium nitrite prepared in culture medium.

Cell respiration

Cell respiration, an indicator of cell viability, was assessed by mitochondrial-dependent reduction of MTT [3-(4,5-dimethylthiazol-2-yl)-2,5-diphenyltetrazolium bromide] to formazan (Gross & Levi, 1992). Cells in 96-well plates were incubated (37°C) with MTT (0.2 mg ml^{-1} for 60 min). Culture medium was removed by aspiration and cells were solubilized in dimethylsulphoxide (100 μl). The extent of reduction of MTT to formazan within cells was quantitated by measurement of OD_{550}.

Measurement of haemodynamic changes

Male Wistar rats (240–320 g; Glaxo Laboratories Ltd., Greenford, Middx.) were anaesthetized with thiopentone sodium (Trapanal; 120 mg kg^{-1}, i.p.). The trachea was cannulated and connected to facilitate respiration and rectal temperature was maintained at 37°C with a homeothermic blanket (BioSciences, Sheerness, Kent). The right carotid artery was cannulated to a pressure transducer (P23XL, Spectramed, Statham, U.S.A.) for the measurement of phasic and mean arterial blood pressure (MAP) which were displayed on a Grass model 7D polygraph recorder (Grass Instruments, Quincy, MA, U.S.A.). The left femoral vein was cannulated for the administration of drugs. Upon completion of the surgical procedure, cardiovascular parameters were allowed to stabilize for 20 min. After recording baseline haemodynamic parameters, the pressor response to noradrenaline (NA 1 μg kg^{-1}, i.v.) was recorded. Ten minutes after injection of NA, animals were given *E.coli* lipopolysaccharide (LPS, 10 mg kg^{-1}, i.v.) as a slow injection over 10 min. The pressor responses to NA were reassessed at 60 min (immediately prior to injection of vehicle or glibenclamide), 120 min and 180 min. At 60 min after the injection of LPS, vehicle (10% dimethylsulphoxide, $n = 6$) or glibenclamide (1 mg kg^{-1}, i.v., $n = 6$) was administered to the rat as a single bolus injection and the haemodynamic parameters were monitored for another 120 min. A similar dose of glibenclamide exerts beneficial haemodynamic effects in dogs with endotoxic shock (Landry & Oliver, 1992). Assuming a blood volume of 60–70 ml kg^{-1} (16.8–19.6 ml of blood per rat), the injection of 1 mg kg^{-1} of glibenclamide should result in peak plasma concentrations of the drug of approximately 50–60 μg ml^{-1}. This plasma concentration of glibenclamide

is more than 100 fold higher than the one reported in patients with non-insulin-dependent diabetes mellitus treated with glibenclamide (2.5 mg day^{-1}, orally) (Ikegami *et al.*, 1986).

In a separate set of experiments, the magnitude and the duration of the rise in blood pressure elicited by glibenclamide (1 mg kg^{-1}, i.v.) were determined in rats treated with LPS (10 mg kg^{-1}, i.v.) for 180 min. To provide an indication of the duration of the pressor responses afforded by glibenclamide when given either at 60 or 180 min after LPS, we have defined the biological 'half life' ($t_{1/2}$) of the pressor response as the time which elapsed until the blood pressure had returned to 50% of the maximal response.

Organ bath experiments

At 180 min after the injection of LPS, thoracic aortae were obtained from sham-operated controls as well as from rats treated either with vehicle or with glibenclamide (1 mg kg^{-1}, i.v. at 60 min after LPS). The vessels were cleared of adhering periadventitial fat and the thoracic aortae were cut into rings of 3–4 mm width. The endothelium was removed by gently rubbing the intimal surface. The lack of a relaxation to acetylcholine (1 μM) following precontraction of rings with noradrenaline (NA; 1 μM) was considered as evidence that the endothelium had been removed. The rings were mounted in 10 ml organ baths filled with warmed (37°C), oxygenated (95% O_2/5% CO_2) Krebs solution (pH 7.4) consisting of (mM): NaCl 118, KCl 4.7, KH_2PO_4 1.2, $MgSO_4$ 1.17, $CaCl_2$ 2.5, $NaHCO_3$ 25 and glucose 5.6. Indomethacin (5.6 μM) was added to prevent the production of prostanoids. Isometric force was measured with Grass FT03 type transducers (Grass Instruments, Quincy, MA, U.S.A.) and recorded on a Grass model 7D polygraph recorder (Grass Instruments, Quincy, MA, U.S.A.). A tension of 2 g was applied and the rings were equilibrated for 60 min. Dose-response curves to NA (10^{-9} to 10^{-6} M) in the presence or absence of L-NAME (300 μM) or glibenclamide (10 μM) were obtained in all experimental groups.

Nitric oxide synthase assay

Lungs from LPS-treated rats given vehicle (control) or glibenclamide (1 mg kg^{-1}, i.v. at 60 min after LPS) were removed at 180 min and frozen in liquid nitrogen. In separate experiments, rats were treated with LPS (10 mg kg^{-1}, i.v.) for 180 min and then received glibenclamide (1 mg kg^{-1}, i.v.). After evaluating the $t_{1/2}$ of the pressor response elicited by glibenclamide (approx. 25 min), these animals were killed and the lungs were removed for the measurement of NOS activity. Lungs from sham-operated rats were also prepared for determination of baseline NOS activity. Lungs were stored for no more than 2 weeks at −80°C before assay. Frozen lungs were homogenized on ice with an Ultra-Turrax T 25 homogenizer (Janke & Kunkel, IKA Labortechnik, Staufen i. Br., Germany) in a buffer composed of: Tris-HCl 50 mM, EDTA 0.1 mM, EGTA 0.1 mM, 2-mercaptoethanol 12 mM and phenylmethylsulphonyl fluoride 1 mM (pH 7.4). Conversion of [^{3}H]-L-arginine to [^{3}H]-L-citrulline was measured in the homogenates as described by Szabo *et al.* (1993d). Briefly, tissue homogenates (30 μl, approx. 60 μg protein) were incubated in the presence of [^{3}H]-L-arginine (10 μM, 5 kBq/tube), NADPH (1 mM), calmodulin (30 nM), tetrahydrobiopterin (5 μM) and calcium (2 mM) for 25 min at 25°C in HEPES buffer (pH 7.5). Reactions were stopped by dilution with 1 ml of ice cold HEPES buffer (pH 5.5) containing EGTA (2 mM) and EDTA (2 mM). Reaction mixtures were applied to Dowex 50W (Na^+ form) columns and the eluted [^{3}H]-L-citrulline activity was measured by scintillation counting (Beckman, LS3801; Fullerton, CA, U.S.A.). Experiments performed in the absence of NADPH determined the extent of [^{3}H]-L-citrulline formation independent of a specific NOS activity. Experiments in the presence of NADPH, without calcium and with 5 mM EGTA, measured the calcium-independent NOS activity, which was taken to represent iNOS activity.

Protein concentration was measured spectrophotometrically in 96-well plates with Bradford reagent (Bradford, 1976), with bovine serum albumin used as standard.

Measurement of plasma levels of tumour necrosis factor-α (TNFα)

Rats were anaesthetized and instrumented as above. Upon completion of the surgical procedure, cardiovascular parameters were allowed to stabilize for 20 min. Thereafter, 0.6 ml of blood was collected from a catheter placed in the carotid artery to measure the plasma levels of TNFα. Animals were treated with vehicle (10% dimethylsulphoxide) or glibenclamide (1 mg kg^{-1}, i.v.). At 15 min after the injection of drugs, LPS (10 mg kg^{-1}, i.v.) was administered as a slow injection over 10 min. Another blood sample (0.6 ml) for the measurement of plasma TNFα levels was obtained at 90 min after the injection of LPS, a time point at which the rise in TNFα after LPS is maximal (Lechner *et al.*, 1993). The amounts of TNFα in the plasma were measured by an enzyme linked immunoadsorbent assay (ELISA) as previously described (Lechner *et al.*, 1992).

Materials

Calmodulin, bacterial lipopolysaccharide (*E.coli* serotype 0.127:B8), NADPH, acetylcholine chloride, cromakalim, noradrenaline bitartrate, N^{ω}-nitro-L-arginine methyl ester, tetraethylammonium acetate and Dowex 50W anion exchange resin were obtained from Sigma Chemical Co. (Poole, Dorset). Glibenclamide was purchased from Research Biochemical International (Natick, MA, U.S.A.). The Factor-Test-X Mouse TNFα ELISA Kit (Code 80-2802-00) was purchased from Genzyme Co. (Cambridge, MA, U.S.A.). Glibenclamide and cromakalim were dissolved in dimethysulphoxide then further diluted with saline or distilled water (final concentrations of dimethylsulphoxide are less than 10%). All other solutions were made in saline or distilled water. L-[2,3,4,5-^{3}H]-arginine hydrochloride was obtained from Amersham (Buckinghamshire). Tetrahydrobiopterin (6R-L-erythro-5,6,7,8-tetrahydrobiopterin) was obtained from Dr B. Schircks Laboratories (Jona, Switzerland).

Statistical evaluation

All values in the figures and text are expressed as mean ± s.e.mean of n observations, where n represents the number of animals or plates (3 wells in each plate) studied. A one-way or two-way analysis of variance (ANOVA) followed, if appropriate, by a Bonferroni's test for multiple comparisons was used to compare means between groups. A P value less than 0.05 was considered to be statistically significant.

Results

Glibenclamide reduces the increase in nitrite caused by LPS in the supernatant of cultured macrophages

Activation of J774.2 macrophages with LPS (1 μg ml^{-1}) resulted in a significant increase in nitrite concentration in the cell supernatant from 1.5 ± 0.4 μM (control cells treated with vehicle, but not LPS) to 50.8 ± 2.5 μM at 24 h after addition of LPS. Pretreatment of cells with glibenclamide (10^{-7} to 10^{-5} M at 30 min prior to LPS) reduced the increase in nitrite formation caused by LPS in a dose-dependent manner (Figure 1a). In contrast, pretreatment of macrophages with tetraethylammonium (10^{-14} to 10^{-2} M at

30 min prior to LPS) did not affect the increase in nitrite concentration in the supernatant of cells activated with LPS (Figure 1b). Pretreatment of cells with the highest dose of cromakalim used (10^{-5} M), caused a small, but significant inhibition of the increase in nitrite concentration afforded by LPS, while lower concentrations of this activator of K^+_{ATP} potassium channels (10^{-7} to 3×10^{-6} M) were without effect (Figure 1c). Glibenclamide, tetraethylammonium or cromakalim did not affect the viability of J774.2 macrophages (as determined by the MTT assay) when given alone or in combination with LPS (data not shown).

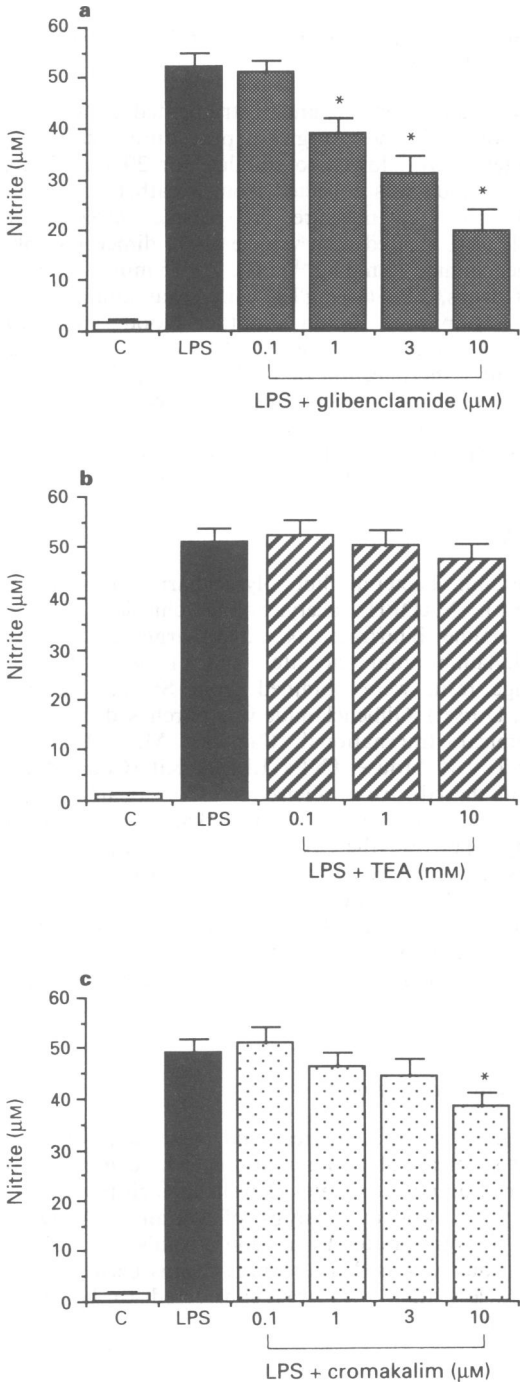

Figure 1 Glibenclamide causes a dose-dependent inhibition of nitrite formation caused by *E.coli* lipopolysaccharide (LPS). Nitrite formation was measured in J774.2 macrophages which were cultured in 96-well plates to confluence and incubated with LPS (1 μg ml^{-1} for 24 h). Depicted is nitrite formation by J774.2 macrophages incubated with culture medium alone (control, C; open columns; $n = 5$) for 24 h or cells treated with LPS alone (solid columns; $n = 5$) or with LPS plus treatment with glibenclamide (a: stippled columns; 10^{-7} to 10^{-5} M at 30 min prior to LPS, $n = 5$), tetraethylammonium (b: TEA; hatched columns; 10^{-4} to 10^{-2} M at 30 min prior to LPS, $n = 5$), or cromakalim (c: dotted columns; 10^{-7} to 10^{-5} M at 30 min prior to LPS, $n = 5$). Data are expressed as mean ± s.e.mean of $n = 5$ independent experiments. $^*P < 0.05$ represents significant difference between cells subjected to LPS with and without glibenclamide or cromakalim.

Glibenclamide inhibits the induction of iNOS, but not its activity

The inhibition by glibenclamide (3 μM; approx. EC_{50}) of the increase in nitrite formation became progressively weaker when glibenclamide was added to the cells at 2, 4, 6 or 10 h after LPS (Figure 2a). Although the addition of glibenclamide at 2 or 4 h after LPS still caused a partial inhibition of the accumulation of nitrite, addition of glibenclamide at 6 or 10 h after LPS had no effect on the increase in nitrite in the supernatant of macrophages activated with LPS (Figure 2a). In contrast, the NOS inhibitor L-NAME caused a similar degree of inhibition of nitrite accumulation when given either together with or at 2, 4, 6 or 10 h after LPS (Figure 2b).

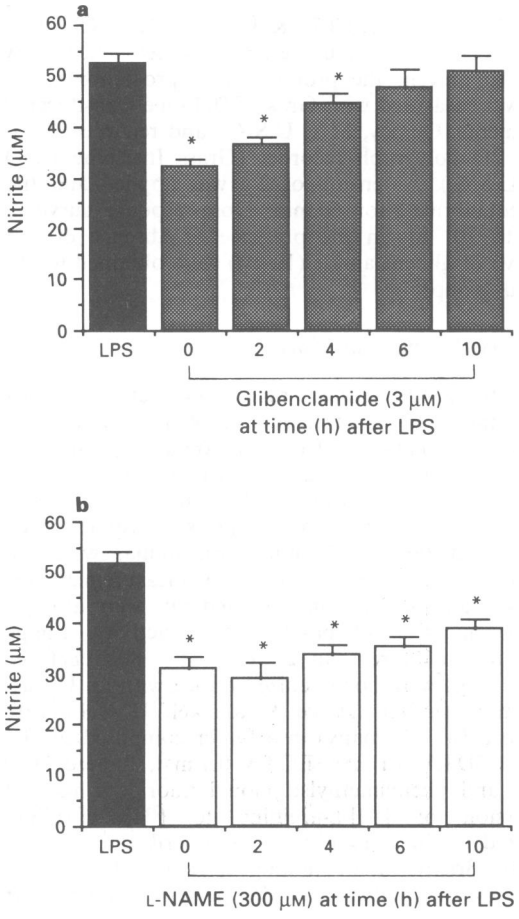

Figure 2 The inhibition by glibenclamide of the nitrite formation produced by *E.coli* lipopolysaccharide (LPS) is time-dependent. Nitrite formation was significantly increased in J774.2 macrophages incubated with LPS (1 μg ml^{-1} for 24 h; solid column; $n = 5$). In separate experiments, glibenclamide (a: 3 μM; stippled columns) or N^G-nitro-L-arginine methyl ester (L-NAME) (b: L-NAME, 300 μM; open columns) was given either together with LPS, or at 2, 4, 6 or 10 h after LPS ($n = 5$ at each time point). Data are expressed as mean ± s.e.mean of $n = 5$ independent experiments. $^*P < 0.05$ represents significant difference between cells treated with LPS with and without glibenclamide or L-NAME.

Glibenclamide exerts beneficial haemodynamic effects in rats with endotoxic shock

Baseline values of MAP ranged from 120 ± 4 to 126 ± 4 mmHg and heart rate from 375 ± 25 to 388 ± 15 beats min^{-1} and were not significantly different between any of the experimental groups studied. The injection of LPS (10 mg kg^{-1}, i.v.) resulted in a rapid fall of MAP from 120 ± 4 mmHg (time 0, prior to the injection of LPS) to 83 ± 5 mmHg at 10 min ($P<0.05$, $n=6$). Thereafter, MAP remained significantly lower than baseline in LPS-rats and hence, was 98 ± 4 mmHg at 180 min after the injection (Figure 3a). Three hours of endotoxaemia was, however, not associated with a significant tachycardia (time 0: 375 ± 25, time 180 min: 399 ± 21 beats min^{-1}, $P>0.05$, $n=6$). In addition, endotoxaemia resulted in a substantial attenuation of the pressor responses elicited by NA (1 μg kg^{-1}, i.v.) from 35 ± 2 mmHg (before LPS) to 17 ± 1 mmHg at 60 min and 20 ± 2 mmHg at 180 min after LPS injection ($P<0.05$, Figure 3b).

Administration of glibenclamide (1 mg kg^{-1}, i.v.) at 60 min after the onset of endotoxaemia resulted in a rapid (within 5 min) and sustained increase in MAP (Figure 3a). Thus, the MAP of LPS-rats treated with glibenclamide was significantly higher than in the LPS-control group at 65, 90, 120, 150 and 180 min. Although glibenclamide caused a small rise in heart rate, the heart rate of LPS-rats treated with glibenclamide was not significantly different from the heart rate in vehicle-treated LPS-rats (the former: 406 ± 11 beats min^{-1}, the latter: 364 ± 29 beats min^{-1}, $P>0.05$, $n=6$). In the glibenclamide-treated group, injection of LPS also caused an attenuation of the pressor responses elicited by NA from 38 ± 2 mmHg (before LPS) to 19 ± 1 mmHg at 60 min (before glibenclamide). Treatment of LPS-rats with glibenclamide enhanced the pressor responses afforded by NA at 180 min, but not at 120 min after injection of LPS (Figure 3b). Thus, the rise in MAP caused by NA at 180 min in LPS-rats treated with glibenclamide was significantly greater than in animals treated with LPS alone ($P<0.05$). When compared to the pressor responses elicited by NA prior to injection of LPS, however, the increase in MAP caused by NA at 180 min after LPS in rats treated with glibenclamide was still significantly reduced ($P<0.05$, Figure 3b).

In order to evaluate whether, and to what degree, the rise in MAP afforded by glibenclamide is due to inhibition of iNOS induction, rats were treated with LPS for 180 min, since this period of endotoxaemia results in a near maximal induction of iNOS activity in the lung of the rat (Szabo *et al.*, 1993d). In these experiments, the injection of LPS caused a fall in MAP from 122 ± 4 to 94 ± 6 mmHg by 180 min. The subsequent injection of glibenclamide (1 mg kg^{-1}, i.v.) resulted in a rapid, but relatively transient rise in MAP. The maximum of the rise in MAP afforded by glibenclamide when given at 180 min after LPS (23 ± 3 mmHg, $n=5$) was not different from the maximal pressor response caused by this agent when given at 60 min after LPS (25 ± 4 mmHg, $n=6$, $P>0.05$). However, the duration of this pressor response was significantly longer when glibenclamide was given at 60 min (biological half life, $t_{1/2}>120$ min) rather than at 180 min after the injection of LPS ($t_{1/2}$: 22 ± 2 min, $P<0.05$).

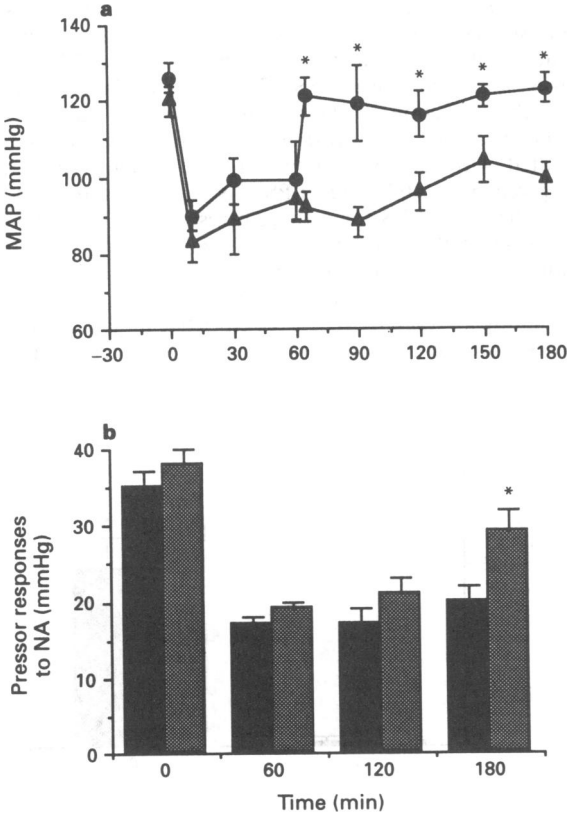

Figure 3 Glibenclamide ameliorates the delayed hypotension caused by endotoxin in the anaesthetized rat. Depicted are the changes in (a) mean arterial blood pressure (MAP) and (b) pressor responses to noradrenaline (NA; 1 μg kg^{-1}, i.v.) in rats treated with *E.coli* lipopolysaccharide (LPS) (10 mg kg^{-1}, i.v. at time 0). Different groups of animals were treated with vehicle (10% dimethylsulphoxide, ▲ or solid column; $n=6$) or glibenclamide (1 mg kg^{-1} i.v., ● or stippled column; $n=6$) at 60 min after LPS. Data are expressed as mean ± s.e.mean of n observations. $^*P<0.05$ represents significant difference when compared to LPS-controls at the same time point.

Glibenclamide attenuates the induction of iNOS in lungs from rats with endotoxic shock

A small calcium-independent iNOS activity was detectable in lung homogenates obtained from sham-operated animals. Endotoxaemia for 180 min was associated with a significant increase of iNOS activity in lung homogenates. However, the iNOS activity in lung homogenates obtained from LPS-rats which had received glibenclamide (1 mg kg^{-1}, i.v. at 60 min after LPS) was significantly lower than that in rats treated with LPS alone. In contrast, the injection of glibenclamide at

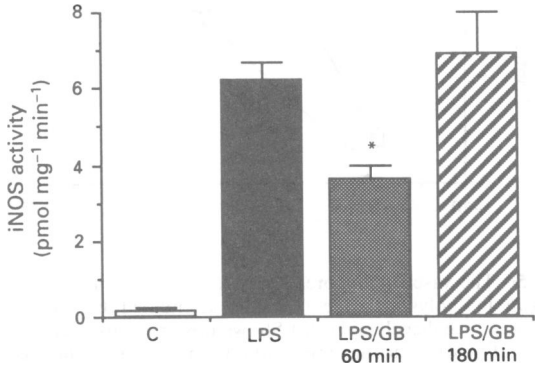

Figure 4 Treatment of rats with glibenclamide inhibits the induction of a calcium-independent iNOS activity in lung homogenates obtained from rats with endotoxaemia. Calcium-independent iNOS activity was measured in lung homogenates obtained from sham-operated control rats (C, open column; $n=4$) or rats treated with *E.coli* lipopolysaccharide (LPS, 10 mg kg^{-1}, i.v.) for 180 min. Different groups of LPS-rats were treated with vehicle (LPS, solid column; $n=6$) or with glibenclamide (LPS/GB; 1 mg kg^{-1}, i.v.) given either at 60 min (stippled column; $n=6$) or at 180 min (hatched column; $n=6$) after LPS. Data are expressed as mean ± s.e.mean of n observations. $^*P<0.05$ represents a significant reduction in iNOS activity when compared to LPS-rats.

180 min after the onset of endotoxaemia did not reduce the degree of iNOS activity in the lung when compared to rats treated with LPS alone (Figure 4).

Treatment of rats with glibenclamide attenuates the vascular hyporeactivity of rat aortic rings to noradrenaline ex vivo

In rat aortic rings obtained from sham-operated control rats, NA (10^{-9} to 10^{-6} M) caused a dose-related increase in vascular tone (Figure 5). The contractions induced by NA were significantly reduced in aortic rings obtained from rats at 180 min after the injection of LPS (Figure 5). In contrast, treatment of LPS-rats with glibenclamide (1 mg kg^{-1}, i.v. at 60 min after injection of LPS) caused a partial, but not complete, reduction of this vascular hyporeactivity to NA ($P<0.05$, when compared to LPS-controls).

Treatment of rat aortic rings obtained from sham-operated control animals with either glibenclamide (10 μM) or the NOS inhibitor, L-NAME (300 μM) *in vitro* did not affect the contractions elicited by NA (data not shown). Incubation of rat aortic rings obtained from LPS-rats with glibenclamide (10 μM for 20 min) *in vitro* did not enhance the contraction to NA in these vessels and hence, did not affect the vascular hyporeactivity caused by LPS. In contrast, L-NAME (300 μM for 20 min) significantly enhanced the contractile response to NA in aortic rings obtained from LPS-rats ($P<0.05$, Figure 5b).

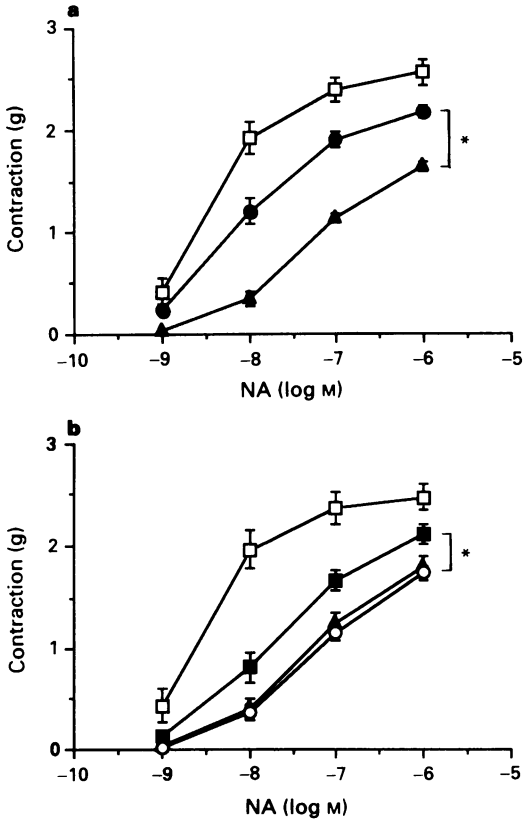

Figure 5 The vascular hyporeactivity to noradrenaline (NA) caused by *E.coli* lipopolysaccharide (LPS) is attenuated by treatment of LPS-rats with glibenclamide. (a) Shows dose-response curves to NA (10^{-9} to 10^{-6} M) in aortic rings without endothelium obtained from sham-operated rats (□; $n=6$), from rats treated with LPS (10 mg kg^{-1}, i.v.) for 180 min (▲; $n=6$) or from LPS-rats treated with glibenclamide (1 mg kg^{-1}, i.v. at 60 min after LPS, ●; $n=6$). (b) Depicts dose-response curves to NA (10^{-9} to 10^{-6} M) in aortic rings obtained from sham-operated rats (□; $n=6$), from rats treated with LPS (10 mg kg^{-1}, i.v.) for 180 min which were subsequently treated *in vitro* with vehicle (▲; $n=6$), glibenclamide (10 μM for 20 min, ○; $n=6$) or N^G-nitro-L-arginine methyl ester (L-NAME) (300 μM for 20 min, ■; $n=6$). Data are expressed as mean ± s.e.mean of n observations. *$P<0.05$ represents significant differences between LPS-rats treated with vehicle and those treated with glibenclamide (a) or between aortic rings obtained from LPS-rats treated with vehicle and L-NAME *in vitro* (b).

Glibenclamide does not affect the rise of TNFα levels caused by endotoxaemia

The surgical procedure alone did not result in a significant rise in plasma TNFα levels, because no significant amounts of TNFα were detectable at the end of the stabilization period. Endotoxaemia for 90 min, however, resulted in a significant rise in plasma TNFα levels (Figure 6). Treatment of LPS-rats with glibenclamide (1 mg kg^{-1}, i.v. at 15 min prior to LPS) did not affect the rise in plasma TNFα levels caused by endotoxin (Figure 6).

Discussion

Here we demonstrate that glibenclamide, an inhibitor of K^+_{ATP} channels, inhibits the induction of iNOS caused by LPS in cultured macrophages and in the anaesthetized rat. In addition, we demonstrate that the beneficial haemodynamic effects produced by glibenclamide in rats with septic shock are, in part, due to inhibition of iNOS induction.

Activation of J774.2 macrophages with LPS results in the accumulation of nitrite, one of the metabolites of NO, in the supernatant of these cells. This accumulation of nitrite reflects an enhanced formation of NO due to the induction of iNOS by LPS in these cells (Szabo *et al.*, 1993a). This study demonstrates that glibenclamide dose-dependently inhibits the accumulation of nitrite in the medium of J774.2 macrophages activated with LPS. Thus, glibenclamide inhibits either the induction or the activity of iNOS. The inhibition by glibenclamide of the formation of nitrite by macrophages activated with LPS was, however, lost when glibenclamide was given 6 or 10 h after LPS. As the exposure of J774.2 macrophages to LPS for 6 to 10 h results in a near maximal expression of iNOS in these cells (Szabo *et al.*, 1993a), this finding shows that glibenclamide inhibits the induction, but not the activity, of iNOS. This conclusion is supported by our finding that L-NAME, a competitive inhibitor of NOS activity (Moore *et al.*, 1990), caused a similar degree of

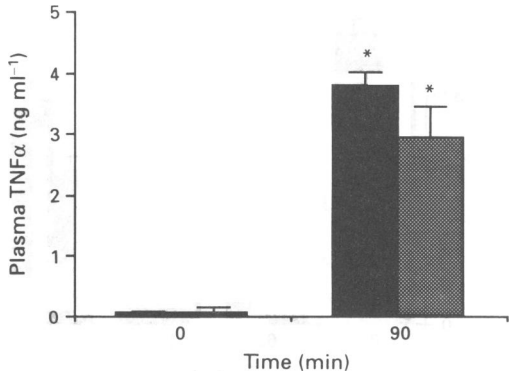

Figure 6 The increase in plasma tumour necrosis factor α (TNFα) levels caused by endotoxin is not affected by pretreatment of *E.coli* lipopolysaccharide (LPS)-rats with glibenclamide. Depicted are the changes in plasma TNFα levels in rats treated with LPS (10 mg kg^{-1}, i.v.). Different groups of animals were pretreated either with vehicle (10% dimethylsulphoxide, solid columns; $n=6$) or glibenclamide (1 mg kg^{-1}, i.v. at 15 min prior to LPS, stippled columns; $n=5$). Note that injection of LPS causes a significant increase in the plasma levels of TNFα; and that this increase was not significantly affected by pretreatment of rats with glibenclamide. Data are expressed as mean ± s.e.mean of n observations. *$P<0.05$ represents significant differences when compared to LPS-controls at time 0.

inhibition of nitrite accumulation in macrophages activated with LPS when given either together with LPS or at 2, 4, 6 or 10 h after LPS. Similarly, other inhibitors of iNOS induction including dexamethasone (Szabo *et al.*, 1993a), interleukin-10 (Cunha *et al.*, 1992), dihydropyridine-type calcium channel antagonists (Szabo *et al.*, 1993c) or spermine (Szabo *et al.*, 1994b) are also less potent in inhibiting the formation of nitrite by cells activated with LPS or cytokines when given several hours after the stimulus of iNOS expression.

Prolonged periods of endotoxaemia in the anaesthetized rat result in the induction of iNOS in several organs including the lung (Knowles *et al.*, 1990; Szabo *et al.*, 1993b), and the consequent enhanced formation of NO by iNOS in the vascular smooth muscle contributes importantly to the delayed hypotension and the vascular hyporeactivity to vasoconstrictor agents (Szabo *et al.*, 1993b). Injection of glibenclamide at 60 min after LPS attenuated the increase in iNOS activity in the lung seen in animals treated with LPS alone. This effect of glibenclamide is due to inhibition of iNOS induction rather than inhibition of iNOS activity, as injection of glibenclamide at 180 min after LPS, a time point at which a near maximal induction of iNOS has already occurred (Szabo *et al.*, 1993b), did not reduce iNOS activity in the lung. In contrast, inhibitors of NOS activity including N^G-methyl-L-arginine (Szabo *et al.*, 1993a), aminoguanidine (Wu *et al.*, 1995) or S-methyl-isothiourea sulphate (Szabo *et al.*, 1994a) also inhibit iNOS activity in the lung of rats when given several hours after the injection of LPS. In addition, treatment of rats with glibenclamide *in vivo* (at 60 min after LPS) also prevented the vascular hyporeactivity to noradrenaline in rat aortic rings *ex vivo*. Again, this effect of glibenclamide is due to inhibition of iNOS induction, rather than activity, because treatment *in vitro* of aortic rings obtained from LPS-treated rats with the NOS inhibitor, L-NAME, but not with glibenclamide, partially restored the contractile response caused by NA.

There is a good correlation between the degree of iNOS induction in the lung and the magnitude of the fall in blood pressure caused by endotoxaemia in the rat (Szabo *et al.*, 1993e). Moreover, the beneficial haemodynamic effects in animal models of septic shock given by dexamethasone (Wright *et al.*, 1992), PAF-receptor antagonists (Szabo *et al.*, 1993e), antibodies to TNFα (Thiemermann *et al.*, 1993), IL-1 receptor antagonists (Szabo *et al.*, 1993d) or dihydropyridine-type calcium channel antagonists (Szabo *et al.*, 1993c) are partly due to inhibition of iNOS induction *in vivo*. Thus, the beneficial haemodynamic effects caused by glibenclamide may be, at least in part, due to inhibition of iNOS induction. This hypothesis is supported by our findings that (i) the duration of the rise in blood pressure caused by glibenclamide in rats with septic shock was significantly longer (> 120 min) when the potassium channel antagonist was given at 60 min, rather than at 180 min after LPS; (ii) that glibenclamide prevented the induction of iNOS when given at 60 min, but not when given at 180 min after LPS; and (iii) that glibenclamide restored the pressor responses to NA at 180 min after LPS *in vivo*. There is now a substantial amount of evidence that this delayed (at 180 min after LPS) vascular hyporeactivity to NA is due to an enhanced formation of NO due to the induction of iNOS (see Thiemermann, 1994). Moreover, agents which prevent the induction of iNOS including dexamethasone (Szabo *et al.*, 1993b), antibodies to TNFα (Thiemermann *et al.*, 1993), IL-1 receptor antagonists (Szabo *et al.*, 1993d), PAF receptor antagonists (Szabo *et al.*, 1993e) or dihydropyridine-type calcium channel antagonists (Szabo *et al.*, 1993c) prevent the development of this delayed vascular hyporeactivity to NA. Thus, the inhibition of iNOS expression contributes to the improved haemodynamics (rise in blood pressure, restoration of pressor responses to NA) caused by glibenclamide at 180 min after LPS injection.

In addition, our findings (i) that injection of glibenclamide at 180 min after LPS did not attenuate the induction of iNOS in the lung, but still caused a transient rise in blood pressure and (ii) that at 60 min after injection of glibenclamide (120 min after LPS) the blood pressure was rapidly elevated, but the vascular hyporeactivity to NA was unaffected, clearly demonstrate that the early rise in blood pressure caused by glibenclamide in septic rats is partly due to effects other than inhibition of iNOS induction. This is not surprising, since (i) septic shock causes inadequate tissue perfusion, anaerobic metabolism and acidosis (Hopkins *et al.*, 1965; Kaufman *et al.*, 1984; Keung & Li, 1991); (ii) a decrease in intracellular ATP (anaerobic metabolism) (Noma, 1983; Deutsch *et al.*, 1991) or intracellular acidosis (Davies, 1990; Cuevas *et al.*, 1991) facilitates the activation of K^+_{ATP} channels; and (iii) activation of K^+_{ATP} channels results in vasodilatation (Standen *et al.*, 1989). Thus, it has been suggested that the beneficial haemodynamic effects of glibenclamide in dogs with septic shock are due to inhibition of the activation of K^+_{ATP} channels occurring secondary to lactic acidosis (Landry & Oliver, 1992). Interestingly, the rise in systemic vascular resistance caused by glibenclamide is significantly greater in dogs with septic shock than in dogs with lactic acidosis caused by hypoxia (Landry & Oliver, 1992), although both conditions lead to lactic acidosis and, hence, presumably the activation of K^+_{ATP} channels. In contrast to septic shock, ischaemia of the kidney which also causes local lactic acidosis does not result in the induction of iNOS in the rat (Cristol *et al.*, 1993). Thus, it is conceivable that the rise in systemic vascular resistance and, hence, blood pressure caused by glibenclamide in animals with septic shock (Landry & Oliver, 1992; this study) is due to a combination of inhibition of iNOS induction and inhibition of K^+_{ATP} channels. The relatively small and transient increase in systemic vascular resistance afforded by glibenclamide in dogs with hypoxic lactic acidosis (Landry & Oliver, 1992) or in rats with prolonged periods (> 180 min) of endotoxaemia, on the other hand, may well be due to inhibition of K^+_{ATP} channels.

Endotoxaemia in the rat causes the expression of cyclooxygenase-2 (COX-2) (Swierkosz *et al.*, 1994), which results in an enhanced formation of prostaglandins (PGs) and/or thromboxane A_2. Interestingly, glibenclamide (0.3 μM) attenutated the vasodilator effects of prostacyclin, PGE_2 and PGD_2 in the isolated perfused heart of the rat (Jackson *et al.*, 1993; Bouchard *et al.*, 1994). In isolated ring segments of the circumflex coronary artery of the dog, glibenclamide (1 to 30 μM) also caused a concentration-dependent reduction in both spontaneous isometric force and contractions induced by the thromboxane A_2-mimetic, U46619, suggesting that glibenclamide is a relatively potent and selective antagonist of thromboxane A_2 receptors (Cocks *et al.*, 1990). Thus, it is possible that some of the beneficial effects of glibenclamide in animal models with septic shock are due to the inhibition by glibenclamide of either the vasoactive effects of vasodilator PGs and/or thromboxane A_2 or even prevention of COX-2 induction.

What is the mechanism by which glibenclamide inhibits the induction of iNOS *in vitro* and *in vivo*? One could argue that this effect of glibenclamide is due to inhibition of K^+_{ATP} channels. This, however, cannot be the case, for (i) tetraethylammonium, a non-selective inhibitor of potassium channels (Robertson & Steinberg, 1990), did not inhibit the induction of iNOS caused by LPS in cultured macrophages; and (ii) cromakalim (at the highest concentration used), an activator of K^+_{ATP} channels (Sanguinetti *et al.*, 1988), caused a small, but significant inhibition of iNOS induction in these cells. Thus, the inhibition of iNOS induction afforded by glibenclamide *in vitro* is independent of the effects of this agent on K^+_{ATP} channels. Another possibility by which glibenclamide might inhibit the induction of iNOS afforded by LPS *in vivo*, would be the prevention of the release of cytokines such as TNFα and IL-1, because these cytokines mediate the induction of iNOS caused by LPS in the rat (Szabo *et al.*, 1993d; Thiemermann *et al.*, 1993). We demonstrate here, however, that pretreatment of rats with gliben-

clamide did not attenuate the rise in plasma TNFα levels caused by LPS. Taken together with our *in vitro* results, we speculate that glibenclamide inhibits the transcription or translation of iNOS.

Thus, glibenclamide inhibits the induction of iNOS caused by LPS in cultured macrophages and in the anaesthetized rat. The mechanism of this effect is unclear, but is not due to inhibition by glibenclamide of (i) K^+_{ATP} channels or (ii) the release of TNFα caused by LPS *in vivo*. The beneficial haemodynamic effects caused by glibenclamide in rats with septic shock are, in part, due to inhibition of iNOS induction.

This work was supported by Cassella AG, Frankfurt, Germany. We gratefully acknowledge the help of Dr P Klemm (Cassella AG) in setting up the assay for the measurement of TNFα. C.C.W. is supported by the National Defense Medical Centre of Taiwan. C.T. is supported by a grant from the Commission of the European Communities (Biomed I, BMHI, CT 92/1893).

References

ALTURA, B.M., LEFER, A.M. & SCHUMER, W. ed. (1983). *Handbook of Shock and Trauma*, Vol. 1: *Basic Science*. New York: Raven Press.

BOUCHARD, J.F., DUMONT, E. & LAMONTAGNE, D. (1994). Evidence that prostaglandins I_2, E_2, and D_2 may activate ATP sensitive potassium channels in the isolated rat heart. *Cardiovasc. Res.*, **28**, 901–905.

BRADFORD, M.M. (1976). A rapid and sensitive method for the quantification of protein dye binding. *Anal. Biochem.*, **72**, 248–254.

COCKS, T.M., KING, S.J. & ANGUS, J.A. (1990). Glibenclamide is a competitive antagonist of the thromboxane A_2 receptor in dog coronary artery *in vitro*. *Br. J. Pharmacol.*, **100**, 375–378.

CRISTOL, J.P., THIEMERMANN, C., MITCHELL, J.A., WALDER, C.E. & VANE, J.R. (1993). Support of renal blood flow after ischemic-reperfusion injury by endogenous formation of nitric oxide and of vasodilator cyclo-oxygenase metabolites. *Br. J. Pharmacol.*, **109**, 188–194.

CUEVAS, J., BASSETT, A.L., CAMERON, J.S., FURUKAWA, T., MYERBURG, R.J. & KIMURA, S. (1991). Effect of H^+ on ATP-regulated K^+ channels in feline ventricular myocytes. *Am. J. Physiol.*, **261**, H755–H761.

CUNHA, F.Q., MONCADA, S. & LIEW, F.Y. (1992). Interleukin-10 (IL-10) inhibits the induction of nitric oxide synthase by interferon-γ in murine macrophages. *Biochem. Biophys. Res. Commun.*, **182**, 1155–1159.

DAVIES, N.W. (1990). Modulation of ATP-sensitive K^+ channels in skeletal muscle by intracellular protons. *Nature*, **343**, 375–377.

DEUTSCH, N., KILTZNER, T.S., LAMP, S.T. & WEISS, J.N. (1991). Activation of cardiac ATP-sensitive K^+ current during hypoxia: correlation with tissue ATP levels. *Am. J. Physiol.*, **261**, H671–H676.

GROSS, S.S., JAFFE, E.A., LEVI, R. & KILBOURN, R.G. (1991). Cytokine-activated endothelial cells express an isotype of nitric oxide synthase which is tetrahydrobiopterin-dependent, calmodulin-independent and inhibited by arginine analogues with a rank order of potency characteristic of activated macrophages. *Biochem. Biophys. Res. Commun.*, **170**, 823–829.

GROSS, S.S. & LEVI, R. (1992). Tetrahydrobiopterin synthesis: An absolute requirement for cytokine-induced nitric oxide generation by vascular smooth muscle. *J. Biol. Chem.*, **267**, 25722–25729.

HOPKINS, R.W., SABGA, G., PENN, I. & SIMCONE, F.A. (1965). Haemodynamic aspects of haemorrhagic and septic shock. *J. Am. Med. Ass.*, **191**, 731–735.

IKEGAMI, H., SHIMA, K., TANAKA, A., TAHARA, Y., HIROTA, M. & KUMAHARA, Y. (1986). Interindividual variation in the absorption of glibenclamide in man. *Acta Endocrinol.*, **11**, 528–532.

JACKSON, W.F., KONIG, A., DAMBACHER, T. & BUSSE, R. (1993). Protacyclin-induced vasodilation in rabbit heart is mediated by ATP-sensitive potassium channels. *Am. J. Physiol.*, **264**, H238–H243.

KAUFMAN, B.S.E., RACKOW, E.C. & FALK, J.L. (1984). The relationship between oxygen delivery and consumption during fluid resuscitation of hypovolemic and septic shock. *Chest*, **85**, 336–340.

KEUNG, E.C. & LI, Q. (1991). Lactate activates ATP-sensitive potassium channels in guinea-pig ventricular myocytes. *J. Clin. Invest.*, **88**, 1772–1777.

KNOWLES, R.G., SALTER, M., BROOKS, S.L. & MONCADA, S. (1990). Anti inflammatory glucocorticoids inhibit the induction by endotoxin of nitric oxide synthase in the lung, liver and aorta of the rat. *Biochem. Biophys. Res. Commun.*, **189**, 392–397.

LANDRY, D.W. & OLIVER, J.A. (1992). The ATP-sensitive K^+ channel mediates hypotension in endotoxaemia and hypoxic lactic acidosis in dog. *J. Clin. Invest.*, **89**, 2071–2074.

LECHNER, A.J., ROUBEN, L.R., POTTHOFF, L.H., TREDWAY, T.L. & MATUSCHAK, G.M. (1993). Effects of pentoxifylline on tumour necrosis factor production and survival during lethal *E. coli* sepsis vs. disseminated candidiasis with fungal septic shock. *Circ. Shock*, **39**, 306–315.

LECHNER, A.J., TREDWAY, T.L., BRINK, D.S., KLEIN, C.A. & MATUSCHAK, G.M. (1992). Differential systemic and intrapulmonary TNF-alpha production in Candida sepsis during immunosuppression. *Am. J. Physiol.*, **263**, L526–L535.

MOLDAWER, L.L., FISCHER, E., VAN ZEE, K., THOMPSON, W.A. & LOWRY, S.F. (1993). A role of interleukin-1 in septic shock. In *Shock, Sepsis and Organ Failure*. ed. Schlag, G., Redl, H. & Traber, D.L. pp. 18–33. Berlin: Springer-Verlag.

MONCADA, S. & HIGGS, A. (1993). The L-arginine-nitric oxide pathway. *N. Engl. J. Med.*, **329**, 2002–2012.

MOORE, P.K., AL-SWAYEH, O.A., CHONG, N.W.S., EVANS, R.A. & GIBSON, A. (1990). N^G-nitroarginine (L-NOARG), a novel L-arginine reversible inhibitor of endothelium-dependent vasodilation *in vitro*. *Br. J. Pharmacol.*, **99**, 408–412.

NOMA, A. (1983). ATP-regulated K^+ channels in cardiac muscle. *Nature*, **305**, 147–148.

PITTNER, R.A. & SPITZER, J.A. (1992). Endotoxin and TNFα directly stimulate nitric oxide formation in cultured rat hepatocytes from chronically endotoxaemic rats. *Biochem. Biophys. Res. Commun.*, **185**, 430–435.

ROBERTSON, D.W. & STEINBERG, M.I. (1990). Potassium channel modulators: Scientific applications and therapeutic promise. *J. Med. Chem.*, **33**, 1529–1541.

SANGUINETTI, M.C., SCOTT, A.L., ZINGARO, G.J. & SIEGL, P.K.S. (1988). BRL 34915 (cromakalim) activated ATP-sensitive K^+ current in cardiac muscle. *Proc. Natl. Acad. Sci. U.S.A.*, **85**, 8360–8364.

STANDEN, N.B., QUAYLE, J.M., DAVIES, N.W., BRAYDEN, J.E., HUANG, Y. & NELSON, M.T. (1989). Hyperpolarizing vasolidators activate ATP-sensitive K^+ channels in arterial smooth muscle. *Science* (Wash. DC), **245**, 177–180.

SWIERKOSZ, T.A., MITCHELL, J.A., TOMLINSON, A., WARNER, T.D., THIEMERMANN, C. & VANE, J.R. (1995). Co-release and interactions of nitric oxide and prostanoids *in vitro* and *in vivo* following exposure to bacterial lipopolysaccharide. In *Biology of Nitric Oxide*. ed. Moncada, S., Feelisch, M. & Higgs, E.A. London: Portland Press (in press).

SZABO, C., MITCHELL, J.A., GROSS, S.S. THIEMERMANN, C. & VANE, J.R. (1993a). Nifedipine inhibits the induction of nitric oxide synthase by bacterial lipopolysaccharide. *J. Pharmacol. Exp. Ther.*, **265**, 674–680.

SZABO, C., MITCHELL, J.A., THIEMERMANN, C. & VANE, J.R. (1993b). Nitric oxide-mediated hyporeactivity to noradrenaline precedes the induction of nitric oxide synthase in endotoxin shock. *Br. J. Pharmacol.*, **108**, 786–792.

SZABO, C., SOUTHAN, G.J. & THIEMERMANN, C. (1994a). Beneficial effects and improved survival in rodent models of septic shock with S-methyl-isothiourea sulfate, a novel, potent and selective inhibitor of inducible nitric oxide synthase. *Proc. Natl. Acad. Sci. U.S.A.*, (in press).

SZABO, C., SOUTHAN, G.J. WOOD, E., THIEMERMANN, C. & VANE, J.R. (1994b). Inhibition by spermine of the induction of nitric oxide synthase in J774.2 macrophages: requirement of a serum factor. *Br. J. Pharmacol.*, **112**, 355–356.

SZABO, C., THIEMERMANN, C. & VANE, J.R. (1993c). Dihydropyridine antagonists and agonists of calcium channels inhibit the induction of nitric oxide synthase by endotoxin in cultured macrophages. *Biochem. Biophys. Res. Commun.*, **196**, 825–830.

SZABO, C., WU, C.C., GROSS, S.S., THIEMERMANN, C. & VANE, J.R. (1993d). Interleukin-1 contributes to the induction of nitric oxide synthase by endotoxin *in vivo*. *Eur. J. Pharmacol.*, **250,** 157–160.

SZABO, C., WU, C.C., MITCHELL, J.A., GROSS, S.S., THIEMERMANN, C. & VANE, J.R. (1993e). Platelet-activating factor contributes to the induction of nitric oxide synthase by bacterial lipopolysaccharide. *Circ. Res.*, **73,** 991–999.

THIEMERMANN, C. (1994). The role of the L-arginine: nitric oxide pathway in circulatory shock. *Adv. Pharmacol.*, **28,** 45–79.

THIEMERMANN, C., WU, C.C., SZABO, C., PERRETTI, M. & VANE, J.R. (1993). Role of tumour necrosis factor in the induction of nitric oxide synthase in a rat model of endotoxin shock. *Br. J. Pharmacol.*, **110,** 177–182.

WRIGHT, C.E., REES. D.D & MONCADA, S. (1992). Protective and pathological roles of nitric oxide in endotoxin shock. *Cardiovasc. Res.*, **26,** 48–57.

WU, C.C., CHEN, S.J., SZABO, C., THIEMERMANN, C. & VANE, J.R. (1995). Aminoguanidine attenuates the delayed circulatory failure and improves survival in rodent models of endotoxic shock. *Br. J. Pharmacol.* (in press).

WU, C.C., THIEMERMANN, C. & VANE, J.R. (1994). Glibenclamide inhibits the induction of nitric oxide synthase by lipopolysaccharide in cultured macrophages and in the anaesthetized rat. *Br. J. Pharmacol.*, **113,** 38P.

(Received October 19, 1994
Revised November 22, 1994
Accepted December 1, 1994)

British Journal of Pharmacology (1995) 114, 1282-1288

Enhancement of cyclic AMP accumulation mediated by 5-HT after chronic amitriptyline treatment in NG 108-15 cells

[1]Masami Shimizu, Akira Nishida, Hiroyuki Fukuda, Hiroshi Saito & *Shigeto Yamawaki

[1]Department of Psychiatry and Neuroscience, Institute of Clinical Research, Kure National Hospital, 3-1 Aoyama, Kure 737, Japan and *Department of Psychiatry and Neurosciences, Hiroshima University School of Medicine, Japan

1 The effects of chronic *in vitro* administration of amitriptyline, a tricyclic antidepressant, on 5-hydroxytryptamine (5-HT) receptor-mediated adenylyl cyclase activity was studied in the neuroblastoma × glioma hybrid cell line, NG 108-15.

2 Treatment of NG 108-15 cells with 8 μM amitriptyline for 3 days increased forskolin-stimulated (0.1 μM) adenosine 3':5'-cyclic monophosphate (cyclic AMP) accumulation. Addition of 5-HT (0.1 – 100 μM) increased forskolin-stimulated cyclic AMP accumulation in amitriptyline-treated cells in a concentration-dependent manner. However, 5-HT did not affect forskolin-stimulated cyclic AMP accumulation in untreated cells.

3 The 5-HT_4 receptor agonist, 5-methoxytryptamine, significantly enhanced forskolin-stimulated cyclic AMP accumulation in amitriptyline-treated cells. In contrast, amitriptyline treatment failed to modify 8-hydroxy-2-(di-n-propylamine) tetralin-induced inhibition of forskolin-stimulated cyclic AMP accumulation.

4 Pretreatment of cells with pertussis toxin did not affect the 5-HT-induced enhancement of cyclic AMP accumulation.

5 The 5-HT-induced enhancement of cyclic AMP accumulation in amitriptyline-treated cells was attenuated by the 5-HT_4 receptor antagonists, GR 113808 and ICS 205-930, with relatively low potency. However, spiperone, SCH 23390, and pindolol were completely ineffective against this 5-HT-induced enhancement.

6 Chronic treatment with amitriptyline did not modify the cyclic AMP production stimulated by prostaglandin E_1 or cholera toxin. This treatment also had no effect on GTPγS-, NaF-, and Mn^{2+}-stimulated cyclic AMP accumulation in isolated cell membranes.

7 Chronic treatment with the 5-HT receptor antagonists, pindolol or ICS 205-930, did not inhibit the 5-HT-induced enhancement of cyclic AMP accumulation.

8 Chronic treatment with other antidepressant drugs, imipramine, mianserin or paroxetine, elicited the 5-HT-induced enhancement of cyclic AMP accumulation.

9 Taken together, these results suggest that chronic amitriptyline treatment of NG 108-15 cells causes 5-HT to enhance forskolin-stimulated cyclic AMP accumulation by enhancing 5-HT receptor-mediated stimulation of adenylyl cyclase and not by reducing 5-HT-mediated inhibition of adenylyl cyclase. The 5-HT-induced enhancement of cyclic AMP accumulation in amitriptyline-treated cells may result from changes at the level of the 5-HT receptor rather than at the level of G_s proteins or adenylyl cyclase. It is unlikely that this enhancement of cyclic AMP accumulation is caused by long-term antagonism of the 5-HT receptor by amitriptyline.

Keywords: Adenylyl cyclase; amitriptyline; antidepressant; cyclic AMP; 5-HT; 5-HT receptor; forskolin; NG 108-15 cell

Introduction

Clinical efficacy of antidepressant drugs requires chronic administration, suggesting that the therapeutic effects are produced by the long-term development of adaptive changes in neurotransmission, rather than by acute biochemical changes such as blockade of monoamine reuptake. Several lines of evidence suggest that antidepressant drugs may exert their clinical effects by producing adaptive changes in the number or function of central 5-hydroxytryptamine (5-HT) receptor subtypes (Peroutka & Snyder, 1980; Willner, 1985). Pharmacological studies have shown that chronic administration of antidepressants leads to a down-regulation of 5-HT_{2A} receptors in the cerebral cortex of rats (Peroutka & Snyder, 1980; Kellar *et al.*, 1981) and a decrease in 5-HT_{2A} receptor-mediated activation of phosphoinositide turnover (Kendal & Nahorski, 1985). However, other studies have shown that chronic administration of selective 5-HT reuptake inhibitors did not cause a down-regulation of cortical 5-HT_{2A} receptors (Hyttel *et al.*, 1984; Sanders-Bush *et al.*, 1989).

The effect of chronic antidepressant treatment on 5-HT receptors that are coupled to adenylyl cyclase signal transduction, such as 5-HT_{1A} and 5-HT_{1B} receptors, has also been studied. Recent reports have shown that 5-HT_{1A} receptor-mediated inhibition of adenylyl cyclase in rat hippocampus is either attenuated (Newman & Lerer, 1988; Newman *et al.*, 1992) or unaffected (Varrault *et al.*, 1991) by antidepressant treatments. Such treatments also have no effect on the density of 5-HT_{1A} receptor binding sites (Peroutka & Snyder, 1980; Welner *et al.*, 1989; Newman *et al.*, 1990). In addition, no changes in the density and affinity of 5-HT_{1B} receptor binding sites have been found after chronic treatment with any one of several antidepressants (Montero *et al.*, 1991). The range of conflicting reports of the effect of chronic administration of antidepressants on 5-HT_1 and 5-HT_2 receptor families suggests that antidepressant drugs may exert their effects by inducing changes in some other 5-HT receptor subtype.

Recent studies have described several new categories of 5-HT receptor subtypes (5-HT_4, 5-HT_6 and 5-HT_7), in both the peripheral and the central nervous system, that are

[1] Author for correspondence.

positively coupled to adenylyl cyclase but are distinct from 5-HT_{1A} or 5-HT_{1B} receptors (Dumuis *et al.*, 1988; Bard *et al.*, 1993; Monsma *et al.*, 1993). In mouse colicular neurones and guinea-pig hippocampal membranes, 5-HT stimulates adenylyl cyclase activity, but selective 5-HT_1 and 5-HT_2 receptor agonists do not. Similarly, this stimulatory effect of 5-HT is not blocked by 5-HT_1 or 5-HT_2 receptor antagonists (Dumuis *et al.*, 1988; Bockaert *et al.*, 1990). However, there have been no studies of the effects of chronically administered tricyclic antidepressants on this type of 5-HT-stimulated adenylyl cyclase activity. Therefore, we examined the chronic effect of tricyclic antidepressants on 5-HT-stimulated adenylyl cylcase signal transduction in the neuroblastoma × glioma hybrid cell line, NG 108-15.

Methods

Cell culture

NG 108-15 cells were cultured in Dulbecco's modified Eagle's medium (DMEM) supplemented with 10% foetal bovine serum, 100 μM hypoxanthine and 16 μM thymidine in a humidified atmosphere of 90% air, 10% CO_2 at 37°C. Confluent cultures were subcultured at ratios of 1:10 to 1:20 in 35-mm culture dishes or 100-mm culture dishes (for the membrane preparation), and were exposed to vehicle or amitriptyline (0.25–10 μM) for 1–5 days. Media were replaced 2 days after the subculture.

Cyclic AMP determination

The DMEM was removed, and the cells (35-mm dish) were washed twice with 2.5 ml of HEPES-buffered Krebs-Ringer solution (composition, mM; NaCl 150, KCl 5, $MgSO_4$ 1, $CaCl_2$ 2, glucose 10, HEPES 10, pH 7.4) at 37°C and were incubated with 1.0 ml of buffer containing various agents for 10 min at 37°C. The reactions were terminated by adding 250 μl of ice-cold 20% perchloric acid and the mixtures were kept on ice for 20 min. The cells were removed by scraping and transferred into tubes. The extracts were centrifuged at 2000 *g* for 15 min at 4°C. The supernatants were neutralized with 1.53 M KOH containing 75 mM HEPES and were kept on ice for 60 min. Then the solutions were centrifuged at 2000 *g* for 15 min at 4°C, and the concentration of cyclic AMP in the supernatant was measured by radioreceptor binding assay (Amersham kit).

For cyclic AMP determination in membrane fractions, the cells (100-mm dish) were washed with phosphate buffered saline and harvested. A membrane fraction was prepared after centrifugation at 4°C at 900 *g* for 5 min and resuspension by homogenization with a polytron (Kinematica) in 10 mM Tris buffer containing 2 mM EGTA (pH 7.4). The resulting homogenate was centrifuged at 48 000 *g* for 20 min and the membrane pellet was resuspended in 10 mM Tris buffer containing 2 mM EGTA. The reaction buffer contained 80 mM Tris buffer (pH 7.4), 5 mM $MgSO_4$, 0.5 mM EGTA, 0.5 mM IBMX, 0.3% bovine serum albumin, 5 mM phosphocreatine, 50 units ml^{-1} creatine phosphokinase, 0.5 mM ATP and either GTPγS, NaF, forskolin or $MnCl_2$, and was preincubated for 3 min at 37°C. After preincubation, reactions were initiated by the addition of the membrane fraction and incubated for an additional 10 min at 37°C. Reactions were stopped by boiling for 3 min. Samples were centrifuged at 13 000 *g* for 5 min and the concentration of cyclic AMP was measured by radioreceptor binding assay.

Protein assay

After removal of the reaction mixtures, the culture dishes were rinsed with 1.0 ml of water and the rinses were added to the pellets which remained in the tubes. The tubes were centrifuged again at 2000 *g* for 15 min at 4°C. Protein determinations were performed in the resulting pellet with the Pierce BCA protein assay kit (Pierce, Rockford, IL, U.S.A.).

Materials

5-HT, 5-methoxytryptamine (5-MeOT), carbachol and prostaglandin E_1 (PGE_1) were obtained from Sigma Chem. Co. (St. Louis, MO, U.S.A.). Amitriptyline, imipramine, mianserin, noradrenaline (NA) and forskolin were obtained from Wako Pure Chem. (Osaka, Japan). Pindolol, R(+)-7-chloro-8-hydroxy-3-methyl-1-phenyl-2,3,4,5-tetrahydro-1H-3-benzazepine (SCH 23390), spiperone, 8-hydroxy-2-(di-n-propylamino)tetralin (8-OH-DPAT) and clonidine were obtained from Research Biochemicals Inc. (Natick, MA, U.S.A.). 3-Isobutyl-1-methylxanthine (IBMX) was obtained from Aldrich Chemical Co. (Milwaukee, WI, U.S.A.). Guanosine 5'-(3-*O*-thio)triphosphate (GTPγS) was obtained from Boehringer-Mannheim (Mannheim, Germany). Pertussis toxin was obtained from Kaken Seiyaku Co. (Tokyo, Japan). Cholera toxin was obtained from List Biological Laboratories Inc. (Campbell, CA, U.S.A.). Cyclic AMP assay kits were obtained from Amersham Co. (Arlington Heights, IL. U.S.A.). (3α-Tropanyl)-1H-indole-3-carboxylic acid ester (ICS 205-930) was donated by Sandoz Ltd. (Basel, Switzerland). {1-[2-(Methylsulphonylamino)ethyl]-4-piperidinyl} methyl 1-methyl-1H-indole-3-carboxylate (GR 113808A) was donated by Glaxo (Middlesex, U.K.). Paroxetine was donated by SmithKline Beecham (Surrey, U.K.). All other chemicals used were of analytical grade.

Data analysis

Data are shown as mean ± s.e.mean of the number (*n*) of separate experiments. The differences in cyclic AMP content stimulated by agonists between control and amitriptyline-treated were determined by Student's *t* test. Comparisons of the data expressed as the percentage of control were made using the Mann-Whitney U-test.

Results

Forskolin (0.01 to 10 μM) stimulated cyclic AMP accumulation in a dose-dependent manner in NG 108-15 cells. When the cells were treated with 8 μM amitriptyline for 1 to 5 days, forskolin-stimulated cyclic AMP accumulation increased markedly, with the maximal increase occurring after 3 days of treatment (data not shown). After 3 days of 8 μM amitriptyline treatment, exposure to 0.1 μM forskolin for 10 min increased cyclic AMP levels by 720%, while untreated (control) cells responded to this same forskolin treatment with only a 470% increase (Figure 1). In treated cells, the addition of 10 μM 5-HT enhanced this forskolin-stimulated cyclic AMP accumulation by 64% over the effect of forskolin alone. In control cells, the addition of 5-HT to the forskolin-stimulated cells did not significantly change the levels of the forskolin response (Figure 1). Amitriptyline treatment caused a slight, but statistically insignificant, increase in basal cyclic AMP levels. Protein contents per dish were not altered by the treatment with amitriptyline up to 10 μM (data not shown).

When the cells were treated with various concentrations of amitriptyline (0.25–10 μM), significant increases in cyclic AMP accumulation stimulated by forskolin in the presence of 5-HT were obtained even with low concentrations of amitriptyline (0.5–2 μM) (Figure 2). These low amitriptyline concentrations are similar to those required for clinical efficacy. On the other hand, significant increases of the forskolin response in the absence of 5-HT were obtained on treatment with >4 μM amitriptyline. Therefore, 8 μM amitriptyline was used in the majority of the experiments to maximise the increase of cyclic AMP accumulation. In amitriptyline-treated cells,

the 5-HT induced enhancement of forskolin-stimulated cyclic AMP accumulation was concentration-dependent over a range of 1 μM to 100 μM 5-HT (Figure 3).

To investigate the ability of various receptors, including 5-HT receptor subtypes, to modulate cyclic AMP production in amitriptyline-treated cells, we examined the effects of the following substances on forskolin-stimulated cyclic AMP accumulation: 5-MeOT (a 5-HT_4 receptor agonist), 8-OH-DPAT (a 5-HT_{1A} receptor agonist), carbachol (a muscarinic receptor agonist), clonidine (an α_2-adrenoceptor agonist) and NA. The addition of 5-MeOT (10 μM) to the forskolin exposure significantly increased cyclic AMP accumulation in amitriptyline-treated cells (22.8% over the control; Figure 4). On the other hand, the application of 8-OH-DPAT (10 μM) reduced forskolin-stimulated cyclic AMP accumulation in control and amitriptyline-treated cells by 39.3% and 29.4%, respectively, indicating that the effects of 8-OH-DPAT were not modified by amitriptyline treatment. The application of either carbachol (1 mM), clonidine (10 μM), or NA (10 μM) also inhibited forskolin-stimulated cyclic AMP accumulation to the same extent in both control and amitriptyline-treated cells.

To determine whether the 5-HT-induced enhancement of cyclic AMP accumulation is due to a decrease in the inhibition of adenylyl cyclase by an inhibitory guanine nucleotide binding regulatory protein (Gi protein), cells were preincubated for 20 h with pertussis toxin, 100 ng ml^{-1}. There was no significant difference in the degree of 5-HT-induced enhancement of forskolin-stimulated cyclic AMP accumulation between control and toxin-treated cells (Table 1). However, treatment with pertussis toxin abolished the ability of 8-OH-DPAT to inhibit forskolin-stimulated cyclic AMP accumulation.

The effects of various 5-HT receptor antagonists on 5-HT-induced enhancement of cyclic AMP accumulation in amitriptyline-treated cells were examined. Recent reports have

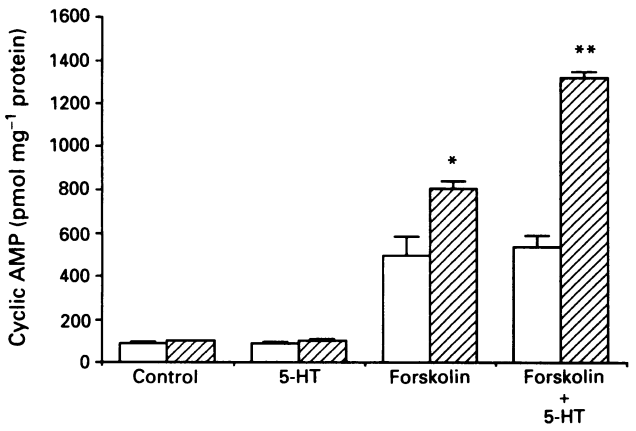

Figure 1 Modulation by 5-hydroxytryptamine (5-HT) of forskolin-stimulated cyclic AMP accumulation in NG 108-15 cells treated with amitriptyline. Cells were treated with (hatched columns) or without (open columns) 8 μM amitriptyline for 3 days. The media were replaced with HEPES-buffered Krebs-Ringer solution and the cells were incubated with 10 μM 5-HT, 0.1 μM forskolin alone, or forskolin plus 5-HT for 10 min at 37°C. Data represent the mean ± s.e.mean values of nine separate experiments. $^*P<0.05$, $^{**}P<0.01$ versus amitriptyline-untreated.

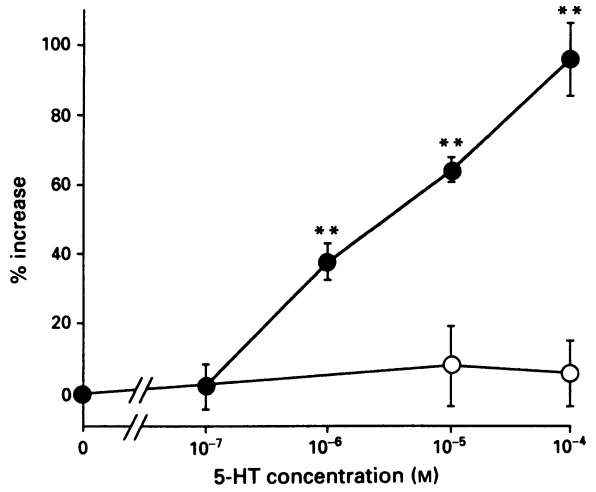

Figure 3 Concentration-dependent increases by 5-hydroxytryptamine (5-HT) of cyclic AMP accumulation in amitriptyline-treated NG 108-15 cells. Cells were treated with (●) or without (○) 8 μM amitriptyline for 3 days. The cells were incubated with 0.1 μM forskolin alone, or forskolin plus 5-HT (0.1 to 100 μM) for 10 min at 37°C. Data are presented as percentages of the values obtained with forskolin alone of control or amitriptyline-treated cells, and are mean ± s.e.mean values for three to five separate experiments. $^{**}P<0.01$ versus forskolin alone of amitriptyline-treated cell.

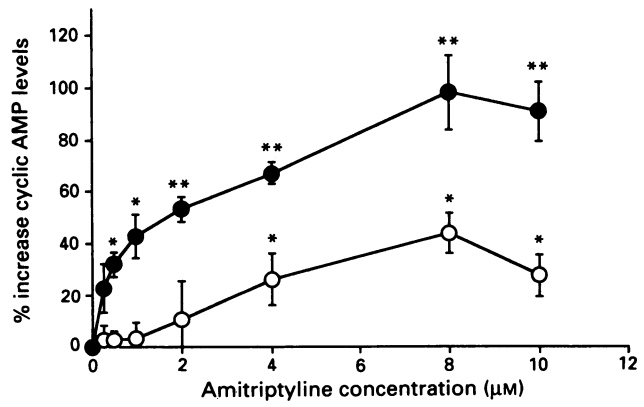

Figure 2 Effect of various amitriptyline concentrations on enhancement by 5-hydroxytryptamine (5-HT) of forskolin-stimulated cyclic AMP accumulation in NG 108-15 cells. Cells were treated with various concentrations (0.25 to 10 μM) of amitriptyline for 3 days. The cells were incubated with 0.1 μM forskolin alone (○), or forskolin plus 10 μM 5-HT (●) for 10 min at 37°C. Data are presented as percentages of the values obtained with forskolin alone or forskolin plus 5-HT of control cells, and are mean ± s.e.mean values for three to six separate experiments. $^*P<0.05$, $^{**}P<0.01$ versus control.

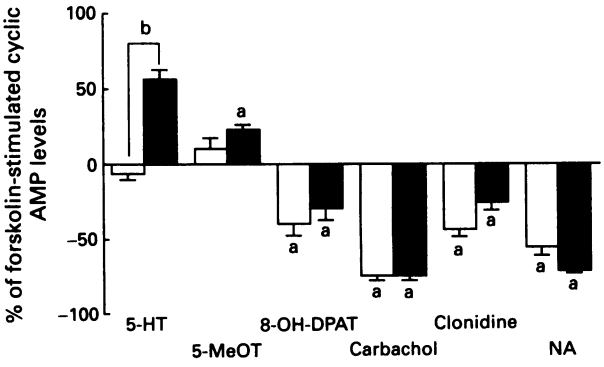

Figure 4 Effects of chronic amitriptyline treatment on regulation of forskolin-stimulated cyclic AMP accumulation by 5-hydroxytryptamine (5-HT) receptor, muscarinic receptor and adrenoceptor agonists in NG 108-15 cells. Cells were treated with (solid columns) or without (open columns) 8 μM amitriptyline for 3 days, and then incubated with 5-HT (10 μM), 5-MeOT (10 μM), 8-hydroxy-2-(di-n-propylamino) tetralin (8-OH-DPAT) (10 μM), carbachol (1 mM), clonidine (10 μM), or noradrenaline (NA, 10 μM), in the presence of 0.1 μM forskolin. Data are expressed as percentages of forskolin-stimulated cyclic AMP levels in control or amitriptyline-treated cells, and are mean ± s.e.mean values for three to six separate experiments. $^aP<0.05$ versus forskolin alone, $^bP<0.01$ versus control.

Table 1 Effect of pertussis toxin pretreatment on regulation by 5-hydroxytryptamine (5-HT) or 8-hydroxy-2-(di-n-propylamino) tetralin (8-OH-DPAT) of forskolin-stimulated cyclic AMP accumulation in amitriptyline-treated NG 108-15 cells

	Cyclic AMP (pmol mg^{-1} protein)			
Treatment				
Amitriptyline (−)	(+)		(−)	(+)
Pertussis toxin (−)	(−)		(+)	(+)
Basal	74 ± 5	76 ± 6	75 ± 6	74 ± 6
Forskolin	473 ± 26 (100)	680 ± 48 (100)	480 ± 25 (100)	696 ± 32 (100)
Forskolin + 5-HT	520 ± 36 (110)	1149 ± 68 (169)[a]	499 ± 10 (104)	1127 ± 37 (162)[a]
Forskolin + 8-OH-DPAT	330 ± 23 (69.8)[b]	488 ± 27 (71.8)[b]	514 ± 23 (107)[c]	807 ± 68 (116)[c]

Cells were treated with or without 8 μM amitriptyline for 3 days, and treated with pertussis toxin (100 ng ml^{-1}) in the presence or absence of amitriptyline for 20 h at the end of amitriptyline treatment. After the treatment, the cells were incubated with 0.1 μM forskolin alone, forskolin plus 10 μM 5-HT, or forskolin plus 10 μM 8-OH-DPAT. Data represent the mean ± s.e.mean values of three separate experiments. Numbers in parentheses are cyclic AMP levels as a percentage of the respective forskolin values. [a]$P<0.01$ versus forskolin, [b]$P<0.05$ versus forskolin, [c]$P<0.01$ versus (−) pertussis toxin.

demonstrated that GR 113808 is a highly potent antagonist of the 5-HT$_4$ receptor in guinea-pig and rat brain membranes (Grossman *et al.*, 1993; Kaumann, 1993). In addition, high concentrations of ICS 205-930 have been shown to antagonize competitively the 5-HT$_4$ receptor in many neuronal and peripheral tissues (Dumuis *et al.*, 1988; Kaumann *et al.*, 1990; Craig & Clarke, 1990). We found that GR 113808 (>5 μM) significantly attentuated 5-HT-induced enhancement of forskolin-stimulated cyclic AMP accumulation. However, the maximum inhibition by GR 113808 was only 65%, even at a concentration of 30 μM. In addition, ICS 205-930 (30 μM) decreased the 5-HT-induced enhancement by 47% (Figure 5). However, spiperone (an antagonist of 5-HT$_1$ and 5-HT$_2$ receptors), SCH23390 (an antagonist of the 5-HT$_2$ receptor) and pindolol (an antagonist of the 5-HT$_1$ receptor) all failed to inhibit the 5-HT-induced enhancement, even at concentrations of up to 30 μM.

The effects of amitriptyline treatment on cyclic AMP accumulation induced by the activation of other receptors that are positively coupled to adenylyl cyclase activity were examined. Cyclic AMP accumulation in NG 108-15 cells was strongly stimulated by PGE$_1$ (0.1 μM), but the amount of cyclic AMP accumulation was not altered by amitriptyline treatment. The addition of 10 μM 5-HT to the PGE$_1$ exposure did not modify the PGE$_1$-stimulated cyclic AMP accumulation in either control or amitriptyline-treated cells (Table 2). In addition, the possible involvement of post-receptor components of signal transduction was examined by studying the effects of amitriptyline treatment on cholera toxin-induced cyclic AMP production. Cholera toxin stimulates adenylyl cyclase by the ADP-ribosylation of α subunit of a stimulatory guanine nucleotide binding regulatory protein (Gs protein). We found that amitriptyline treatment failed to modify the amount of cyclic AMP produced by cholera toxin (Table 2). We also examined the effect of chronic amitriptyline treatment on the direct stimulation of G proteins by GTPγS or NaF in membranes of NG 108-15 cells. Neither the cyclic AMP produced by GTPγS (10 μM) nor NaF (10 mM) was affected by amitriptyline treatment. The addition of 10 μM 5-HT to the GTPγS exposure did not modify the GTPγS-stimulated cyclic AMP accumulation in either control or treated membranes (Table 2). Direct activation of adenylyl cyclase by 20 mM Mn^{2+} was also unaffected by amitriptyline treatment. However, amitriptyline treatment enhanced forskolin-stimulated cyclic AMP accumulation in the presence and absence of 10 μM 5-HT in both isolated membranes and intact cells.

To determine whether chronic amitriptyline treatment up-regulates the 5-HT receptors by receptor antagonism, cells were chronically treated with pindolol or ICS 205-930 in the presence or absence of amitriptyline for 3 days. Neither pindolol nor ICS 205-930 affected forskolin-stimulated cyclic AMP accumulation in either the presence or absence of 5-HT.

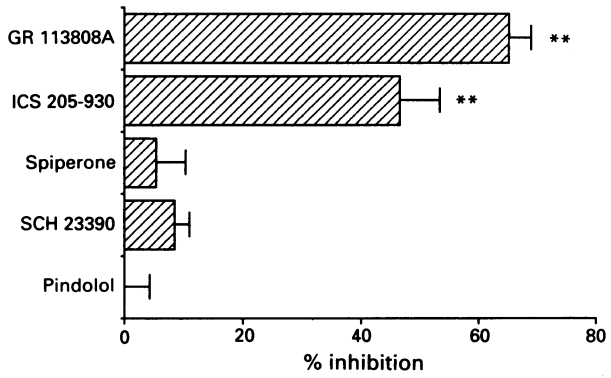

Figure 5 Effect of various 5-hydroxytryptamine (5-HT) receptor antagonists on 5-HT-induced enhancement of cyclic AMP accumulation in amitriptyline-treated cells. Cells were treated with or without 8 μM amitriptyline for 3 days. After washing, the cells were preincubated with GR 113808A (30 μM), ICS 205-930 (30 μM), spiperone (30 μM), SCH 23390 (30 μM), or pindolol (30 μM) for 10 min and then were stimulated with 0.1 μM forskolin alone, or forskolin plus 10 μM 5-HT for 10 min at 37°C in the presence of each antagonist. The addition of these antagonists did not affect the forskolin responses. Data are expressed as percentages of the values obtained with forskolin plus 5-HT in the absence of the antagonist, and are mean ± s.e. mean values for three separate experiments. **$P<0.01$ versus forskolin plus 5-HT of amitriptyline-treated cell.

Neither of these drugs also altered the effects of amitriptyline treatment (Table 3).

We examined the ability of chronic treatment with the antidepressant drugs, imipramine, mianserin, or paroxetine, to modify forskolin-stimulated cyclic AMP accumulation and its enhancement by 5-HT. Each of these antidepressants (8 μM for 3 days) mimicked the effect of amitriptyline on forskolin-stimulated cyclic AMP accumulation and its enhancement by 5-HT (Figure 6).

Discussion

In the present study, chronic amitriptyline treatment of NG 108-15 cells was found to cause 5-HT to enhance forskolin-stimulated cyclic AMP accumulation. This 5-HT-induced enhancement was not affected by pertussis toxin treatment. The application of 5-MeOT, a 5-HT receptor agonist, also significantly enhanced forskolin-stimulated cyclic AMP accumulation in amitriptyline-treated cells. These findings suggest that the 5-HT-induced enhancement of cyclic AMP accumulation in amitriptyline-treated cells may occur through the activation of a 5-HT receptor subtype that is positively coupled to adenylyl cyclase. Such a 5-HT receptor subtype in NG 108-15 cells has not been described pre-

Table 2 Effect of amitriptyline treatment on cholera toxin-, prostaglandin E_1-, GTPγS-, NaF-, and Mn^{2+}-stimulated cyclic AMP accumulation in NG 108-15 cells and isolated membranes

	Cyclic AMP (pmol mg^{-1} protein)	
	Control	*Amitriptyline-treated*
Intact cells		
Basal	86.9 ± 7.5	95.5 ± 8.8
Cholera toxin 1 μg ml^{-1}	349.0 ± 22.7	324.4 ± 30.3
Prostaglandin E_1 0.1 μM	318.6 ± 11.9	292.7 ± 18.8
+5-HT 10 μM	291.8 ± 10.6	296.1 ± 7.5
Membrane		
Basal	162.7 ± 18.2	209.4 ± 15.9
GTPγS 10 μM	1326.8 ± 71.6	1540.4 ± 90.0
+5-HT 10 μM	1374.8 ± 78.1	1575.4 ± 73.0
Forskolin 0.1 μM	786.0 ± 29.7	977.8 ± 78.8*
+5-HT 10 μM	842.6 ± 45.1	1218.1 ± 52.2**
NaF 10 mM	755.2 ± 99.2	794.4 ± 24.2
$MnCl_2$ 20 mM	4173.3 ± 554.8	4949.5 ± 383.9

Cells were treated with or without 8 μM amitriptyline for 3 days. The media were replaced with HEPES-buffered Krebs-Ringer solution, and the cells were incubated with 1 μg ml^{-1} cholera toxin for 30 min, or 0.1 μM prostaglandin E_1, or prostaglandin E_1 plus 10 μM 5-HT for 10 min at 37°C. Membranes were prepared as described in Methods, and were incubated with 10 μM GTPγS, 20 mM NaF, 0.1 μM forskolin, or 20 mM $MnCl_2$ for 10 min at 37°C. Data represent the mean ± s.e.mean values of three separate experiments. $*P<0.05$. $**P<0.01$ versus control.

Table 3 Effect of chronic treatment with pindolol or ICS 205-930 in the presence or absence of amitriptyline on regulation by 5-hydroxytryptamine (5-HT) of forskolin-stimulated cyclic AMP accumulation

	Cyclic AMP level (% of control)	
	Forskolin	*Forskolin+5-HT*
Control	100	100
Pindolol 10 μM	116 ± 8	108 ± 10
ICS 205-930 10 μM	117 ± 10	84 ± 4
Amitriptyline 8 μM	167 ± 11**	231 ± 14**
+Pindolol	162 ± 11**	220 ± 12**
+ICS 205-930	161 ± 8**	208 ± 10**

Cells were treated with or without 10 μM pindolol or 10 μM ICS 205-930 in the presence or absence of 8 μM amitriptyline for 3 days, and then incubated with 0.1 μM forskolin alone, or forskolin plus 10 μM 5-HT. Data represent percentages of the control values obtained in forskolin alone or forskolin plus 5-HT and are mean ± s.e.mean values of three separate experiments. $**P<0.01$ versus control.

viously. However, we observed that 5-MeOT increased basal cyclic AMP levels in the absence of forskolin (data not shown), suggesting the existence of a 5-HT receptor subtype positively coupled to adenylyl cyclase in NG 108-15 cells. The fact that 5-HT alone had no effect on cyclic AMP levels may be due to coincident stimulation and inhibition of adenylyl cyclase by 5-HT.

The presence of 5-HT-induced stimulation of cyclic AMP accumulation suggests the involvement of a 5-HT_4 receptor (Bockaert *et al.*, 1992). Several studies have indicated that the 5-HT_4 receptor positively coupled to adenylyl cyclase is neither a member of the 5-HT_1 nor the 5-HT_2 receptor families, and that it exists in various tissues, including nervous tissue (Ford & Clarke, 1993). In mouse colicular neurones and guinea-pig hippocampal membranes, the 5-HT_4 receptor-mediated activation of adenylyl cyclase was not blocked by antagonists for the 5-HT_{1A}, 5-HT_{1C}, 5-HT_{1D}, 5-HT_2, or 5-HT_3 receptors, with the exception of ICS 205-930, which blocked the 5-HT_4 receptor-mediated effect with low

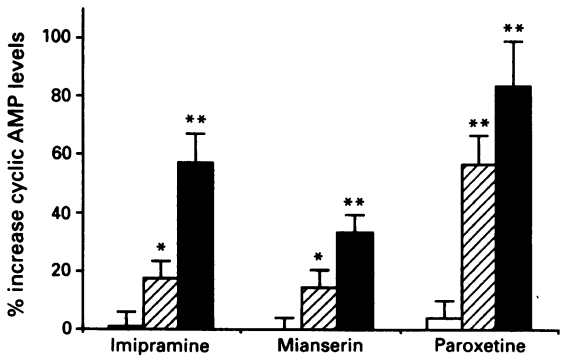

Figure 6 Effect of imipramine, mianserin or paroxetine treatment on regulation by 5-hydroxytryptamine (5-HT) of forskolin-stimulated cyclic AMP accumulation in NG 108-15 cells. Cells were treated with either 8 μM imipramine, 8 μM mianserin, or 8 μM paroxetine for 3 days. Then the cells were incubated with vehicle (open columns), 0.1 μM forskolin (hatched columns), or forskolin plus 10 μM 5-HT (solid columns) for 10 min at 37°C. Data are expressed as percentages of the values obtained with vehicle, forskolin alone or forskolin plus 5-HT of control cells, and are mean ± s.e.mean values for three separate experiments. $*P<0.05$, $**P<0.01$ versus control.

potency (Shenker *et al.*, 1987; Dumuis *et al.*, 1988; Bockaert *et al.*, 1990). The finding that 5-HT-induced enhancement of cyclic AMP accumulation in amitriptyline-treated cells was not inhibited by pindolol, spiperone, or SCH 23390, is consistent with the pharmacological profile of the 5-HT_4 receptor. However, the relatively low potency of ICS 205-930 and GR 113808 on the 5-HT-induced enhancement precludes the involvement of the 5-HT_4 receptor. We attempted to measure 5-HT_4 receptor binding in membranes from NG 108-15 cells using [^{3}H]-GR 113808 (Grossman *et al.*, 1993). However, little specific binding of [^{3}H]-GR 113808 was observed in either control or amitriptyline-treated membranes when either 5-HT or GR 113808 were used to define nonspecific binding (data not shown). This inability to measure specific binding to 5-HT_4 receptors may be due to a low density of these receptors on NG 108-15 cells.

On the other hand, there are a number of reports describing other 5-HT receptors positively coupled to adenylyl cyclase, which are pharmacologically different from the 5-HT_4 receptor, such as: the 5-HT_6 receptor (Monsma *et al.*, 1993), 5-HT_7 receptor (Bard *et al.*, 1993), neuroblastoma NCB20 5-HT receptor (Conner & Mansour, 1990), and mouse 5-HT_x receptor (Plassat *et al.*, 1993). Interestingly, some of these receptors exhibit relatively high affinity for psychotropic drugs such as clozapine, amoxipine, or amitriptyline (Monsma *et al.*, 1993; Plassat *et al.*, 1993). More recently, 5-HT-mediated adenylyl cyclase activation has been observed in mouse neuroblastoma N18TG2 cells, and it exhibited a pharmacological profile resembling some aspects of the 5-HT_6 receptor (Unsworth & Molinoff, 1994). Since NG 108-15 cells are derived by fusing cells from N18TG2 cells and C6Bu-1 cells, it is possible that the same kind of 5-HT receptors found in N18TG2 cells may also exist in NG 108-15 cells.

We investigated whether the 5-HT-induced enhancement of cyclic AMP accumulation caused by amitriptyline treatment was due to decreased activation of a 5-HT receptor-G_i protein pathway. We found that the inhibition of forskolin-stimulated cyclic AMP accumulation by 8-OH-DPAT (an agonist for G_i protein-coupled 5-HT receptor) was not affected by amitriptyline treatment. This is consistent with previous reports that 5-HT_{1A} receptor-induced inhibition of adenylyl cyclase is not altered by chronic desipramine treatment in rat forebrain and hippocampus (De Montigny & Aghajanian, 1978; Varrault *et al.*, 1991). We also found that amitriptyline treatment did not modify carbachol-, clonidine-, or NA-induced inhibition of forskolin-stimulated cyclic AMP

accumulation. Moreover, pretreatment with 100 ng ml^{-1} pertussis toxin had no effect on the 5-HT enhancement of forskolin-stimulated cyclic AMP accumulation in either control or amitriptyline-treated cells. These results indicate that a 5-HT receptor coupled to G_i proteins does not participate in the 5-HT-induced enhancement of cyclic AMP accumulation in amitriptyline-treated cells.

It is possible that chronic amitriptyline treatment produces the 5-HT-induced enhancement through an increase in G_s protein activity. However, the present study shows that the cyclic AMP accumulation produced by cholera toxin and NaF was not affected by amitriptyline treatment. The GTPγS-stimulated cyclic AMP accumulation was slightly, but not significantly, increased in amitriptyline-treated membranes. These findings indicate that chronic amitriptyline treatment may not induce quantitative or functional changes in G_s proteins. Furthermore, PGE_1-stimulated cyclic AMP accumulation was also unaffected by amitriptyline treatment. Taken together, it is most likely that the 5-HT-induced enhancement of forskolin-stimulated cyclic AMP accumulation in amitriptyline-treated cells is due to modifications at the level of the 5-HT receptor rather than at the level of the G_s protein.

The present study shows that chronic amitriptyline treatment of NG 108-15 cells caused an increase in forskolin-stimulated cyclic AMP accumulation. This is consistent with previous reports that demonstrate that chronic antidepressant treatment enhances forskolin-stimulated cyclic AMP production in rat cerebral cortex and limbic system (Ozawa & Rasenick, 1989; De Montis *et al.*, 1990; Jolas *et al.*, 1994). Our results also showed that Mn^{2+}-induced adenylyl cyclase activation was not modified by amitriptyline treatment. In isolated membranes of NG 108-15 cells, [^{3}H]-forskolin binding seems to be biphasic, with one binding site exhibiting a high affinity (K_d = 18 nM) for the complex of adenylyl cyclase and $G_s\alpha$ proteins (Kim *et al.*, 1994). At a concentration of 0.1 μM (as used in this study), forskolin predominantly recognizes the high affinity binding site, indicating that the increase of forskolin-stimulated cyclic AMP accumulation by amitriptyline treatment may reflect an increase of the complex of adenylyl cyclase and Gs proteins rather than an increase in the population of the cyclase. In fact, Ozawa & Rasenick (1989) suggested that chronic *in vivo* treatment with antidepressants induces an increased coupling between G_s proteins and the catalytic subunits of adenylyl cyclase in rat cerebral cortex. This increased coupling between G_s proteins and adenylyl cyclase could contribute to the G protein-mediated stimulation of adenylyl cyclase. However, we did not find significant increases in GTPγS- and NaF-stimulated cyclic AMP accumulation in amitriptyline-treated membranes. With regard to this discrepancy, it should be considered that forskolin acts on adenylyl cyclase by G protein-mediated mechanisms unlike Mn^{2+} (Seamon *et al.*, 1981) and that the interaction between G_s proteins and adenylyl cyclase is complicated, e.g., multiple subtypes of α subunit with differential coupling efficiencies to different isoforms of adenylyl cyclase (Tang *et al.*, 1991; Tang & Gilman, 1992; Ishikawa *et al.*, 1993). Nonetheless, it is still questionable that the 5-HT-induced enhancement in amitriptyline-treated cells occurs only in the presence of forskolin. However, it is notable that treatment with lower concentrations of amitriptyline (<2 μM) causes 5-HT to enhance significantly forskolin-stimulated cyclic AMP accumulation despite an unchanged forskolin response. This result indicates that amitriptyline treatment may exert its effects on 5-HT receptor function and the forskolin response through distinctly different mechanisms.

If chronic amitriptyline treatment increases 5-HT receptor function, it is possible that the 5-HT receptors are up-regulated due to receptor antagonism by amitriptyline. However, chronic treatment with pindolol or ICS 205-930 did not cause the enhancement of cyclic AMP accumulation by 5-HT. Neither pindolol nor ICS 205-930 affected 5-HT-induced enhancement of cyclic AMP accumulation produced by amitriptyline treatment. Thus, it is not likely that the effect of amitriptyline treatment is due to 5-HT receptor antagonism.

Chronic treatment with either the tricyclic antidepressant, imipramine, or other types of antidepressants such as mianserin and paroxetine, mimicked the effects of amitriptyline. Mianserin, a weak monoamine uptake inhibitor, also caused 5-HT to enhance forskolin-stimulated cyclic AMP accumulation, suggesting that the blockade of monoamine reuptake may not be involved in the 5-HT-induced enhancement of cyclic AMP accumulation. The therapeutic plasma concentrations of tricyclic antidepressants are estimated at about 0.5~1 μM under normal conditions, rising to >3 μM during an overdose (Braithwaite *et al.*, 1979; Friedel, 1982). The present study demonstrates that 5-HT can significantly potentiate cyclic AMP accumulation in the presence of similarly low antidepressant concentrations. This suggests that the effect of antidepressants on 5-HT-modulated cyclic AMP production may contribute to some of the therapeutic or adverse effects of antidepressants.

In the present study, we demonstrated that chronic amitriptyline treatment of NG 108-15 cells caused 5-HT to enhance forskolin-stimulated cyclic AMP accumulation, and that this enhancement was unaffected by pretreatment with pertussis toxin and insensitive to 5-HT_1 and 5-HT_2 receptor antagonists. In contrast, chronic amitriptyline treatment did not affect 8-OH-DPAT-induced inhibition of cyclic AMP accumulation. Cyclic AMP production by direct stimulation of G proteins and adenylyl cyclase was also unaffected by amitriptyline treatment. These results suggest that this 5-HT-induced enhancement of cyclic AMP accumulation may be due to increased activity of the 5-HT receptor that is positively coupled to adenylyl cyclase, and that this increased activity may result from the changes at the level of the 5-HT receptor rather than at the level of the G_s proteins or adenylyl cyclase. It is unlikely that the enhancement of cyclic AMP accumulation is caused by a reduction in the inhibition of adenylyl cyclase or by long-term antagonism of the 5-HT receptor by amitriptyline.

We are grateful to Dr H. Higashida of Kanazawa University and Dr A. Kagaya of Hiroshima University for providing NG 108-15 cells.

References

BARD, J.A., ZGOMBICK, J., ADHAM, N., VAYSSE, P., BRANCHEK, T.A. & WEINSHANK, R.L. (1993). Cloning of a novel human serotonin receptor (5-HT_7) positively linked to adenylate cyclase. *J. Biol. Chem.*, **268**, 23422–23426.

BOCKAERT, J., SEBBEN, M. & DUMUIS, A. (1990). Pharmacological characterization of 5-hydroxytryptamine$_4$ (5-HT_4) receptors positively coupled to adenylate cyclase in adult guinea-pig hippocampal membranes: effect of substituted benzamide derivatives. *Mol. Pharmacol.*, **37**, 408–411.

BRAITHWAITE, R.A., CROME, P. & DAWLING, S. (1979). Amitriptyline overdose: plasma concentrations and clinical features. *Br. J. Clin. Pharmacol.*, **8**, 388–389.

CONNER, D.A. & MANSOUR, T.E. (1990) Serotonin receptor-mediated activation of adenylate cyclase on the neuroblastoma NCB.20: a novel 5-hydroxytryptamine receptor. *Mol. Pharmacol.*, **37**, 742–751.

CRAIG, D.A. & CLARKE, D.E. (1990). Pharmacological characterization of a neuronal receptor for 5-hydroxytryptamine in guinea pig ileum with properties similar to the 5-hydroxytryptamine$_4$ receptor. *J. Pharmacol. Exp. Ther.*, **252,** 1378–1386.

DE MONTIGNY, C. & AGHAJANIAN, G.K. (1978). Tricyclic antidepressants: long term treatment responsivity of rat forebrain neurons to serotonin. *Science*, **202,** 1303–1306.

DE MONTIS, G.M., DEVOTO, P., GESSA, G.L. PORCELLA, A., SERRA, G. & TAGLIAMONTE, A. (1990). Selective adenylate cyclase increase in the limbic area of long-term imipramine-treated rats. *Eur. J. Pharmacol.*, **180,** 169–174.

DUMUIS, A., BOUHELAL, R., SEBBEN, M., CORY, R. & BOCKAERT, J. (1988). A nonclassical 5-hydroxytryptamine receptor positively coupled with adenylate cyclase in the central nervous system. *Mol. Pharmacol.*, **34,** 880–887.

FRIEDEL, R.O. (1982). The relationship of therapeutic response to antidepressant plasma levels: an update. *J. Clin. Psychiatry*, **43,** 37–43.

FORD, A.P.D.W. & CLARKE, D.E. (1993). The 5-HT$_4$ receptor. *Med. Res. Rev.*, **13,** 633–662.

GROSSMAN, C.J., KILPATRICK, G.J. & BUNCE, K.T. (1993). Development of a radioligand binding assay for 5-HT$_4$ receptors in guinea-pig and rat brain. *Br. J. Pharmacol.*, **109,** 618–624.

HYTTEL, J., OVERO, K.F. & ARNT, J. (1984). Biochemical and drug levels in rats after long-term treatment with the specific 5-HT-uptake inhibitor, citalopram. *Psychopharmacol.*, **83,** 20–27.

ISHIKAWA, Y., KATSUSHIKA, S., KAWABE, J., IWAMI, G. & HOMCY, C.J. (1993). Adenylylcyclase: multiple mechanisms to generate the diversity. *Clin. Res.*, **41,** 146–151.

JOLAS, T., HAJ-DAHMANE, S., KIDD, E.J., LANGLOIS, X., LANFUMEY, L., FATTACCINI, C.M., VANTALON, V., LAPORTE, A.M., ADRIEN, J., GOZLAN, H. & HAMON, M. (1994). Central pre- and postsynaptic 5-HT$_{1A}$ receptors in rats treated chronically with a novel antidepressant, cericlamine. *J. Pharmacol. Exp. Ther.*, **268,** 1432–1443.

KAUMANN, A.J. (1993). Blockade of human atrial 5-HT$_4$ receptors by GR 113808. *Br. J. Pharmacol.*, **110,** 1172–1174.

KAUMANN, A.J., SANDERS, L., BROWN, A.M., MURRAY, K.J. & BROWN, M.J. (1990). A 5-hydroxytryptamine receptor in human atrium. *Br. J. Pharmacol.*, **100,** 879–885.

KELLAR, K.J., CASCIO, C.S., BUTLER, J.A. & KURTZKE, R.N. (1981). Differential effects of electroconvulsive shock and antidepressant drugs on serotonin-2 receptors in rat brain. *Eur. J. Pharmacol.*, **69,** 515–518.

KENDAL, D.A. & NAHORSKI, S.R. (1985). 5-Hydroxytryptamine-stimulated inositol phospholipid hydrolysis in rat cerebral cortex slices, Pharmacological characterization and effects of antidepressants. *J. Pharmacol. Exp. Ther.*, **233,** 473–479.

KIM, G.-D., ADIE, E.J. & MILLIGAN, G. (1994). Quantitative stoichiometry of the proteins of the stimulatory arm of the adenylyl cyclase cascade in neuroblastoma x glioma hybrid, NG108-15 cells. *Eur. J. Biochem.*, **219,** 135–143.

MONSMA, F.J., SHEN, Y., WARD, R.P., HAMBLIN, M.W. & SIBLEY, D.R. (1993). Cloning and expression of a novel serotonin receptor with high affinity for tricyclic psychotropic drugs. *Mol. Pharmacol.*, **43,** 320–327.

MONTERO, D., FELIPE, M.C. & DEL RIO, J. (1991). Acute or chronic antidepressants do not modify [^{125}I]cyanopindolol binding to 5-HT$_{1B}$ receptors in rat brain. *Eur. J. Pharmacol.*, **196,** 327–329.

NEWMAN, M.E., DRUMMER, D. & LERER, B. (1990). Single and combined effects of desipramine and lithium on serotoninergic receptor number and second messenger function in rat brain. *J. Pharmacol. Exp. Ther.*, **252,** 826–831.

NEWMAN, M.E. & LERER, B. (1988). Chronic electroconvulsive shock and desipramine reduce the degree of inhibition by 5-HT and carbachol of forskolin-stimulated adenylate cyclase in rat hippocampal membranes. *Eur. J. Pharmacol.*, **148,** 257–260.

NEWMAN, M.E., SHAPIRA, B. & LERER, B. (1992). Regulation of 5-hydroxytryptamine$_{1A}$ receptor function in rat hippocampus by short- and long-term administration of 5-hydroxytryptamine$_{1A}$ agonists and antidepressants. *J. Pharmacol. Exp. Ther.*, **260,** 16–20.

OZAWA, H. & RASENICK, M.M. (1989). Coupling of the stimulatory GTP-binding protein Gs to rat synaptic membrane adenylate cyclase is enhanced subsequent to chronic antidepressant treatment. *Mol. Pharmacol.*, **36,** 803–808.

PEROUTKA, S.J. & SNYDER, S.H. (1980). Long-term antidepressant treatment decreases spiroperidol-labeled serotonin receptor binding. *Science*, **210,** 88–90.

PLASSAT, J.-L., AMLAIKY, N. & HEN, R. (1993). Molecular cloning of a mammalian serotonin receptor that activates adenylate cyclase. *Mol. Pharmacol.*, **44,** 229–236.

SANDERS-BUSH, E., BREEDING, M. & TSUTSUMI, M. (1989). Sertraline-induced desensitization of the serotonin 5-HT2 receptor transmembrane signaling system. *Psychopharmacol.*, **99,** 64–69.

SEAMON, K.B., PADGETT, W. & DALY, J.W. (1981). Forskolin: unique diterpene activator of adenylate cyclase in membrane and in intact cells. *Proc. Natl. Acad. Sci. U.S.A.*, **78** 3363–3367.

SHENKER, A., MAAYANI, S., WEINSTEIN, H. & GREEN, J.P. (1987). Pharmacological characterization of two 5-hydroxytryptamine receptors coupled to adenylate cyclase in guinea pig hippocampal membranes. *Mol. Pharmacol.*, **31,** 357–367.

TANG, W.-J. & GILMAN, A.G. (1992). Adenylate cyclases. *Cell*, **70,** 869–872.

TANG, W.-J., KRUPINSKI, J. & GILMAN, A.G. (1991). Expression and characterization of calmodulin-activated (type I) adenylylcyclase. *J. Biol. Chem.*, **266,** 8595–8603.

UNSWORTH, C.D. & MOLINOFF, P.B. (1994). Characterization of a 5-hydroxytryptamine receptor in mouse neuroblastoma N18TG2 cells. *J. Pharmacol. Exp. Ther.*, **269,** 246–255.

VARRAULT, A., LEVIEL, V. & BOCKAERT, J. (1991). 5-HT$_{1A}$-sensitive adenylyl cyclase of rodent hippocampal neurons: effects of antidepressant treatments and chronic stimulation with agonists. *J. Pharmacol. Exp. Ther.*, **257,** 433–438.

WELNER, S.A., DE MONTIGNY, C., DESROCHES, J., DESJARDINS, P. & SURANYL-CADOTTE, B.E. (1989). Autoradiographic quantification of serotonin-1A receptors in rat brain following antidepressant drug treatment. *Synapse*, **4,** 347–352.

WILLNER, P. (1985). Antidepressants and serotonergic neurotransmission: an integrative review. *Psychopharmacol.*, **85,** 387–392.

(Received August 22, 1994
Revised November 4, 1994
Accepted November 25, 1994)

British Journal of Pharmacology (1995) 114, 1289-1295

Effects of semotiadil fumarate, a novel Ca^{2+} antagonist, on cytosolic Ca^{2+} level and force of contraction in porcine coronary arteries

[1]Masaaki Kageyama, [2]Teruyuki Yanagisawa & Norio Taira

Department of Pharmacology, Tohoku University School of Medicine, 2-1 Seiryo-machi, Aoba-ku, Sendai 980, Japan

1 The mechanisms of action of semotiadil fumarate, a novel Ca^{2+} antagonist, were examined by measuring the cytosolic Ca^{2+} level ($[Ca^{2+}]_i$) and force of contraction in porcine coronary arteries, and by determining [^{3}H]-pyrilamine binding to bovine cerebellar membranes.

2 Semotiadil or verapamil (0.1 and 1 μM) inhibited both the high KCl-induced increases in $[Ca^{2+}]_i$ and force in a concentration-dependent manner.

3 Histamine (30 μM) produced transient increases followed by sustained increases in $[Ca^{2+}]_i$ and force, which were inhibited by semotiadil and verapamil (1 and 10 μM). The agents were different in that semotiadil reduced the maximum $[Ca^{2+}]_i$ and force responses to histamine, but not pD_2 values, whereas verapamil did reduce the pD_2 values for histamine, but not the maximum responses.

4 Verapamil (10 μM), but not semotiadil, inhibited histamine-induced increases in $[Ca^{2+}]_i$ and force in Ca^{2+}-free solution. Neither semotiadil nor verapamil affected the increases in $[Ca^{2+}]_i$ and force induced by caffeine. Semotiadil even at the higher concentration (10 μM) did not displace specific binding of [^{3}H]-pyrilamine to bovine cerebellar membranes.

5 These results suggest that semotiadil inhibits both KCl- and histamine-induced contractions mainly by blocking voltage-dependent L-type Ca^{2+} channels.

Keywords: Semotiadil; verapamil; Ca^{2+} antagonists; fura-2; cytosolic Ca^{2+} level; force of contraction; porcine coronary arteries

Introduction

Semotiadil fumarate, (SD-3211, (+)-(**R**)-2-[5-methoxy-2-[3-[methyl[2-[3,4-(methylenedioxy)phenoxy]ethyl]amino]propoxy] phenyl]-4-methyl-2*H*-1,4-benzothiazine-3(4H)-one hydrogen fumarate) (chemical structure shown in Figure 1), was reported to be an orally active Ca^{2+} antagonist with antihypertensive (Kageyama *et al.*, 1991b; Takada *et al.*, 1991) and antianginal activities (Mori *et al.*, 1990a; 1991). Semotiadil has a quite different chemical structure from dihydropyridine Ca^{2+} antagonists but like the dihydropyridines, it is vasoselective compared with other non-dihydropyridine Ca^{2+} antagonists such as verapamil and diltiazem (Yoneyama *et al.*, 1990; Nishimura *et al.*, 1990; Miyawaki *et al.*, 1991). Semotiadil has been shown to decrease the plateau of the fast action potential without affecting the maximum upstroke velocity and to depress the slow action potential induced by isoprenaline in guinea-pig isolated papillary muscles (Miyawaki *et al.*, 1990). Semotiadil has also been shown to inhibit, in a heterotropic and allosteric manner, the binding of [^{3}H]-PN200-110, a dihydropyridine, [^{3}H]-verapamil and [^{3}H]-diltiazem in porcine coronary arterial membranes (Nakayama *et al.*, 1992). These results suggested that semotiadil dilated arteries by inhibiting Ca^{2+} channels by binding to a site other than those occupied by Ca^{2+} antagonists currently available. However, the exact mechanisms underlying semotiadil-induced arterial dilatation are still unclear.

In the present study, we examined the effects of semotiadil on high KCl- or histamine-induced increases in the cytosolic Ca^{2+} level ($[Ca^{2+}]_i$) and force by simultaneous measurement of both variables to clarify further its vasodilator mechanisms in comparison with a classical Ca^{2+} antagonist verapamil. To measure $[Ca^{2+}]_i$, porcine coronary arterial rings were loaded with fura-2, an indicator of $[Ca^{2+}]_i$ (Grynkiewicz *et al.*, 1985). In addition, the effect of semotiadil on histamine H_1 receptors was examined by the [^{3}H]-pyrilamine binding assay.

Methods

Tissue preparation

Fresh porcine hearts were obtained from a slaughter house and transported on ice to the laboratory. Small coronary arteries (1-2 mm in outer diameter, second and third branches of the anterior descending artery) were excised and cleaned of excess fat and connective tissues in physiological salt solution (PSS) under a binocular microscope. The arteries were cut into rings 1 mm in width and everted with the luminal side outwards. The endothelium was removed by rubbing gently the luminal surface with a pair of forceps. Removal of endothelium was verified by the absence of relaxation after applications of acetylcholine (1 μM) or bradykinin (0.1 μM).

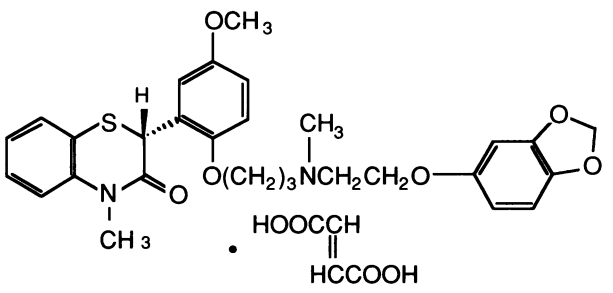

Figure 1 The chemical structure of semotiadil fumarate.

[1] Present address: Developmental Research Laboratories, Santen Pharmaceutical Co., Ltd., Osaka 533, Japan

[2] Author for correspondence.

Measurements of fluorescence and force of contraction

Fluorescence and force of contraction were measured simultaneously by the method described previously (Yanagisawa *et al.*, 1989; Mori *et al.*, 1990b; Kageyama *et al.*, 1991a). Briefly, coronary arterial rings were incubated in PSS containing 10 μM fura-2 acetoxymethyl ester (AM) and 0.1% w/v Pluronic F-127, a non-cytotoxic detergent, for 5–7 h at room temperature. After the fura-2 loading, the rings were rinsed with PSS for more than 1 h to remove excess dye on the tissue surface. They were mounted between two tungsten hooks, one of which was connected to a force displacement transducer (Shinko UL2GR, Minebea Co., Ltd., Nagano, Japan) under a resting tension of about 5 mN. The rings were placed horizontally in a 0.4 ml organ bath, which was attached to the stage of an inverted microscope (TMD-8, Nikon, Tokyo, Japan) and perfused at a rate of 4 ml min^{-1} with PSS warmed at 37°C. An equilibration period of at least 30 min was allowed before each protocol was started.

Fluorescence was measured by a fluorimeter equipped with a dual wavelength excitation device (CAM-200 or CAM-220, Japan Spectroscopic, Tokyo, Japan) connected to the microscope. Smooth muscle cells in the medial layers of rings were illuminated for 2 s every 10 s alternately with wavelengths of 340 and 380 nm by chopping at a frequency of 100 Hz. Fluorescence at excitation with 340 nm (F_{340}) and 380 nm (F_{380}) through a 500 nm filter was detected by a photomultiplier. After each experiment was completed, autofluorescence derived from tissues was obtained by adding a detergent, Triton X-100, and $MnCl_2$ and this was subtracted from each of the photosignals. A ratio of corrected F_{340} and F_{380} was calculated and used as an index of $[Ca^{2+}]_i$. Force, F_{340}, F_{380} and their ratio were continuously recorded on the thermal pen recorder (Recti-Horiz 8K, NEC-San-ei, Tokyo, Japan). At the beginning of each experiment, tissues were perfused with PSS containing 90 mM KCl (90 mM KCl-PSS) for 10 min. Changes in $[Ca^{2+}]_i$ and force induced by each agent are expressed as a percentage of those induced by the 90 mM KCl-PSS at 10 min.

Binding assay

The method of Chang *et al.* (1979) was used for the binding assay, carried out by Nova Pharmaceuticals (Baltimore, MD, U.S.A.) as contract work. Briefly, the bovine cerebellum were homogenized with a Brinkmann Kinematica Polytron in ice-cold 50 mM Na-KPO_4 (pH 7.5). The homogenate was centrifuged at 50,000 *g* for 10 min, and then the pellets were resuspended in the same volume of fresh buffer. After the suspension was centrifuged again, the final pellets were resuspended to a concentration of 37.5 mg wet tissue weight ml^{-1}. The membrane fraction (15 mg wet tissue weight/each tube) was incubated with [^{3}H]-pyrilamine in 50 mM NaH_2PO_4-K_2HPO_4 buffer (pH 7.5) at 25°C for 30 min. The reaction was terminated by rapid vacuum filtration of the reaction contents through glass fibre filters with a Brandell 48 well Cell Harvester. The filtration was followed by 10 to 15 ml washes per well. Radioactivity trapped on the filters was determined by liquid scintillation counting (LS3801, Bechman Instruments Inc., Fullerton, CA, U.S.A.) Non-specific binding was determined in the presence of 10 μM triprolidine.

Drugs and solutions

PSS contained (in mM): NaCl 140, KCl 5, $CaCl_2$ 2.5, $MgCl_2$ 2.5, glucose 11.1 and 4-(2-hydroxyethyl)-1-piperazineethanesulphonic acid 3 (HEPES, pH 7.4). The PSS containing high concentrations of KCl was made by substituting NaCl with equimolar KCl. Ca^{2+}-free PSS was made by removing $CaCl_2$ from normal PSS and by adding 1 mM ethyleneglycol-*bis*(b-aminoethylether)-*N*,*N*,*N*',*N*'-tetraacetic acid (EGTA).

The following drugs were used: semotiadil fumarate (Santen Pharmaceutical Co., Ltd., Osaka, Japan), (±)-verapamil hydrochloride and triprolidine (Sigma Chemical, Co., St. Louis, MO, U.S.A.), bradykinin (Peptide Institute Osaka, Japan), acetylcholine chloride, histamine dihydrochloride, caffeine, dimethyl sulphoxide (DMSO), Triton X-100 (Wako Pure Chemical Co., Osaka, Japan), fura-2 AM, Pluronic F-127 and HEPES (Dojin Chemical Co., Kumamoto, Japan), [^{3}H]-pyrilamine (New England Nuclear Co., Boston, MA, U.S.A.). Semotiadil was dissolved in DMSO at a concentration of 10 mM. Triprolidine was also dissolved in DMSO. Verapamil, acetylcholine, bradykinin and histamine were dissolved in distilled water at a concentration of 10 mM. Fura-2 AM and Pluronic F-127 were dissolved in DMSO at 1 mM and 25% (w/v), respectively. These stock solutions were diluted to the desired concentrations with PSS. Caffeine was dissolved in PSS at a concentration of 25 mM.

Analysis of concentration-response curves and statistical analysis

Each value represents the mean ± s.e. Concentration-response curves for the effects of KCl and histamine on $[Ca^{2+}]_i$ and force in the absence or presence of semotiadil or verapamil were computer-fitted to a logistic equation:

$$E = M \times A^P/(A^P + K^P)$$

where E is the normalized response, M is the maximum response. A is the concentration of KCl or histamine, K is

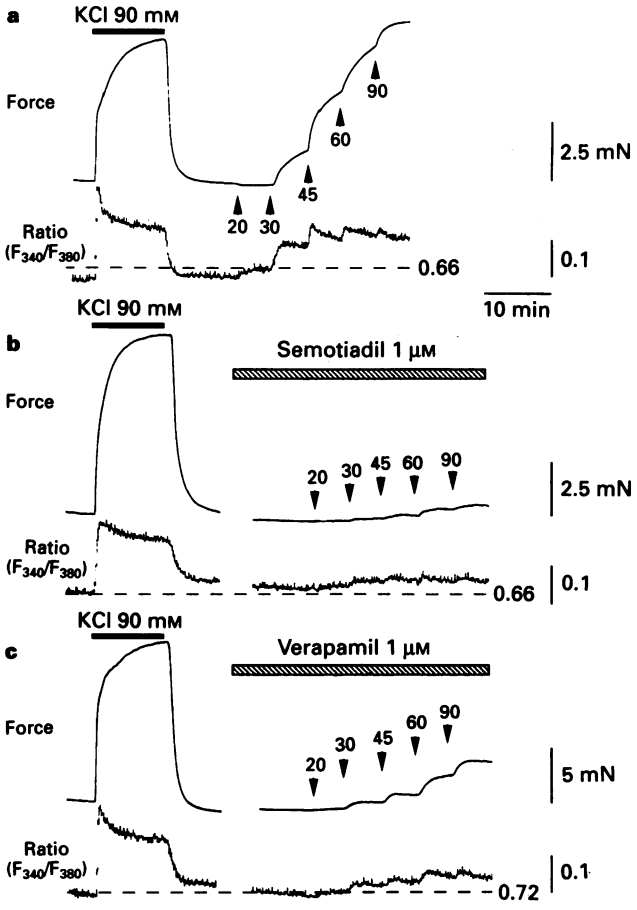

Figure 2 Typical recordings of changes in $[Ca^{2+}]_i$ (indicated by fluorescence ratio) and force induced by increasing concentrations of KCl-PSS in the absence (upper traces) or presence of semotiadil (middle traces) or verapamil (lower traces) in porcine coronary arteries loaded with fura-2. Semotiadil or verapamil was applied 20 min before cumulative applications of KCl-PSS. In this protocol, the changes in fluorescence ratio and force of contraction induced by perfusion of 90 mM KCl-PSS for 10 min were 0.35 ± 0.03 and 7.7 ± 0.6 mN, respectively ($n = 31$).

the EC_{50} of KCl or histamine and is the slope parameter. The EC_{50} of histamine was expressed as the pD_2 ($-\log EC_{50}$) value. Statistical significance was determined by a one-way analysis of variance followed by Dunnett's multiple comparison test, or by Kruskal-Wallis's test followed by Dunnett-type multiple comparison test after Bartlett's test. If $P<0.05$, the value was considered statistically significant.

Results

Effects of semotiadil or verapamil on KCl-induced contraction

Both semotiadil and verapamil decreased slightly basal $[Ca^{2+}]_i$ and force. Figures 2 and 3 show the effects of semotiadil and verapamil (0.1 and 1 μM) on changes in $[Ca^{2+}]_i$ and force induced by cumulatively increasing concentrations of KCl-PSS in porcine coronary arteries. Perfusion of 90 mM KCl-PSS rapidly increased $[Ca^{2+}]_i$ and force. $[Ca^{2+}]_i$ reached a peak within 2 min and then decreased gradually during the perfusion. Force reached a peak 10 min after the start of the perfusion. Following the 90 mM KCl-PSS perfusion, in the absence of each vasodilator, cumulative applications of KCl-PSS from 5 to 90 mM resulted in concentration-dependent increases in $[Ca^{2+}]_i$ and force. After applications of semotiadil or verapamil (0.1 and 1 μM) for 20 min, both of the increases in $[Ca^{2+}]_i$ and force induced by KCl-PSS were attenuated in a concentration-dependent manner. Both agents reduced the maximum KCl-induced increases in $[Ca^{2+}]_i$ and force, and increased the EC_{50} values for KCl (Table 1).

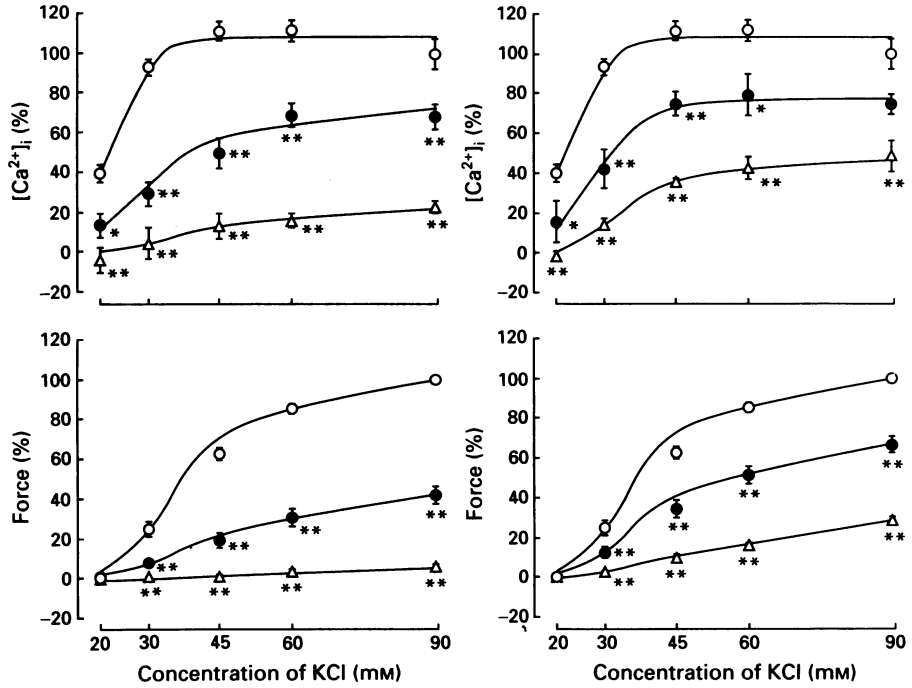

Figure 3 Effects of semotiadil (left panels) and verapamil (right panels) on increases in $[Ca^{2+}]_i$ and force induced by cumulative applications of KCl-PSS in porcine coronary arteries loaded with fura-2. Semotiadil or verapamil was applied 20 min before cumulative applications of KCl-PSS. (○) Control; (●) 0.1 μM semotiadil or 0.1 μM verapamil; (△) 1 μM semotiadil or 1 μM verapamil. Changes in $[Ca^{2+}]_i$ and force induced by each concentration of KCl are expressed as a percentage of those induced by the 90 mM KCl-PSS for 10 min. Concentration-response curves were computer-fitted using mean values of the data. $*P<0.05$; $**P<0.01$, compared with control. Each value represents the mean ± s.e.mean of 5 to 9 different experiments.

Table 1 The maximum responses and pD_2 values for the KCl- and histamine-induced increases in $[Ca^{2+}]_i$ and force in the absence or presence of vasodilators

		$[Ca^{2+}]_i$		Force	
KCl	n	*Maximum response* (%)	EC_{50} (mM)	*Maximum response* (%)	EC_{50} (mM)
Control	(5)	108.0 ± 5.7	21.7 ± 0.6	102.0 ± 1.9	40.4 ± 1.3
Semotiadil 0.1 μM	(9)	76.9 ± 7.1*	34.9 ± 4.0	49.2 ± 5.5*	52.5 ± 4.5
1 μM	(5)	24.3 ± 3.8**	44.8 ± 6.8**	8.4 ± 1.6**	69.5 ± 10.6**
Verapamil 0.1 μM	(5)	77.9 ± 7.2*	27.6 ± 2.4	72.1 ± 5.2	47.1 ± 3.5
1 μM	(7)	50.1 ± 8.2**	37.1 ± 2.5*	35.9 ± 4.0**	59.2 ± 4.5*
Histamine	n	*Maximum response* (%)	pD_2 (-logM)	*Maximum response* (%)	pD_2 (-logM)
Control	(7)	72.5 ± 7.4	5.83 ± 0.06	88.5 ± 14.5	5.46 ± 0.12
Semotiadil 1 μM	(7)	37.9 ± 8.1*	5.82 ± 0.42	57.7 ± 13.0	5.37 ± 0.14
10 μM	(5)	30.1 ± 9.2*	5.16 ± 0.29	34.7 ± 9.9	5.42 ± 0.18
Verapamil 1 μM	(6)	69.0 ± 15.9	5.48 ± 0.23	91.3 ± 28.9	5.44 ± 0.16
10 μM	(5)	57.1 ± 6.7	4.79 ± 0.18*	61.4 ± 6.6	4.77 ± 0.09**

Each value represents the mean ± s.e.mean. The numbers of experiments (n) are shown in parentheses. $*P<0.05$; $**P<0.01$, statistically significant compared with control in the absence of vasodilators.

Effects of histamine on $[Ca^{2+}]_i$ and force

Figure 4 shows typical recordings of the effects of histamine (30 μM) on $[Ca^{2+}]_i$ and force in porcine coronary arteries. On perfusion of histamine, $[Ca^{2+}]_i$ and force increased rapidly and reached a peak around 1 min after the application and force reached a peak within 3 min (the first phase). $[Ca^{2+}]_i$ and force decreased gradually to a level higher than the resting level 10 min after the perfusion of histamine (the second phase). Perfusion of Ca^{2+}-free 5 mM KCl-PSS containing 1 mM EGTA for 10 min decreased the resting $[Ca^{2+}]_i$, whereas force was decreased very slightly. When histamine (30 μM) was applied in the absence of extracellular Ca^{2+}, $[Ca^{2+}]_i$ and force increased transiently and $[Ca^{2+}]_i$ or force reached a peak around 1 min or within 2 min after the application, respectively. Then $[Ca^{2+}]_i$ and force returned to the decreased resting level within 3 min. Thus, removal of extracellular Ca^{2+} markedly reduced the first phase of the histamine-induced increases in $[Ca^{2+}]_i$ and force, and it abolished the second phase of the increase in $[Ca^{2+}]_i$.

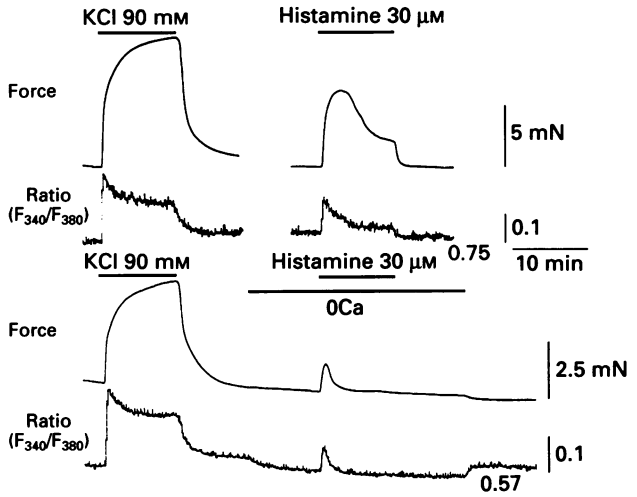

Figure 4 Typical recordings of the effects of histamine (30 μM) on $[Ca^{2+}]_i$ (indicated by fluorescence ratio) and force in the presence (upper traces) or absence of extracellular Ca^{2+} (lower traces) in porcine coronary arteries loaded with fura-2. Extracellular Ca^{2+} was removed by perfusion with Ca^{2+}-free PSS containing 1 mM EGTA 10 min before the application of histamine (0Ca).

Effects of semotiadil or verapamil on histamine-induced contraction

An application of semotiadil at 1 and 10 μM for 20 min before the addition of histamine inhibited both first and second phases of the increases in $[Ca^{2+}]_i$ and force induced by histamine (30 μM) in a concentration-dependent manner (Figure 5). The second phase of the increase in $[Ca^{2+}]_i$ was almost abolished by semotiadil at 1 μM. Verapamil (1 and 10 μM) also inhibited the histamine-induced increases in $[Ca^{2+}]_i$ and force, but its inhibitory effects were less potent than those of semotiadil.

Figure 6 shows the concentration-response curves for the first phase of histamine-induced increases in $[Ca^{2+}]_i$ and force in the absence or presence of semotiadil or verapamil. Semotiadil (1 and 10 μM) flattened the concentration-response curves for the increases in $[Ca^{2+}]_i$ and force induced by histamine (1 to 300 μM). On the other hand, verapamil at 1 μM did not affect the concentration-response curves for histamine. At the higher concentration (10 μM) verapamil shifted rightward the concentration-response curves for histamine. As shown in Table 1, the maximum responses of this histamine-induced increase in $[Ca^{2+}]_i$ were significantly reduced in the presence of 1 and 10 μM semotiadil, but were not affected by verapamil even at the higher concentration (10 μM). In contrast, pD_2 values of the histamine-induced increases in $[Ca^{2+}]_i$ and force were significantly reduced by verapamil at 10 μM, but not 1 μM, whereas they were not altered by semotiadil at either concentration.

As shown in Figure 7, semotiadil (1 and 10 μM) did not

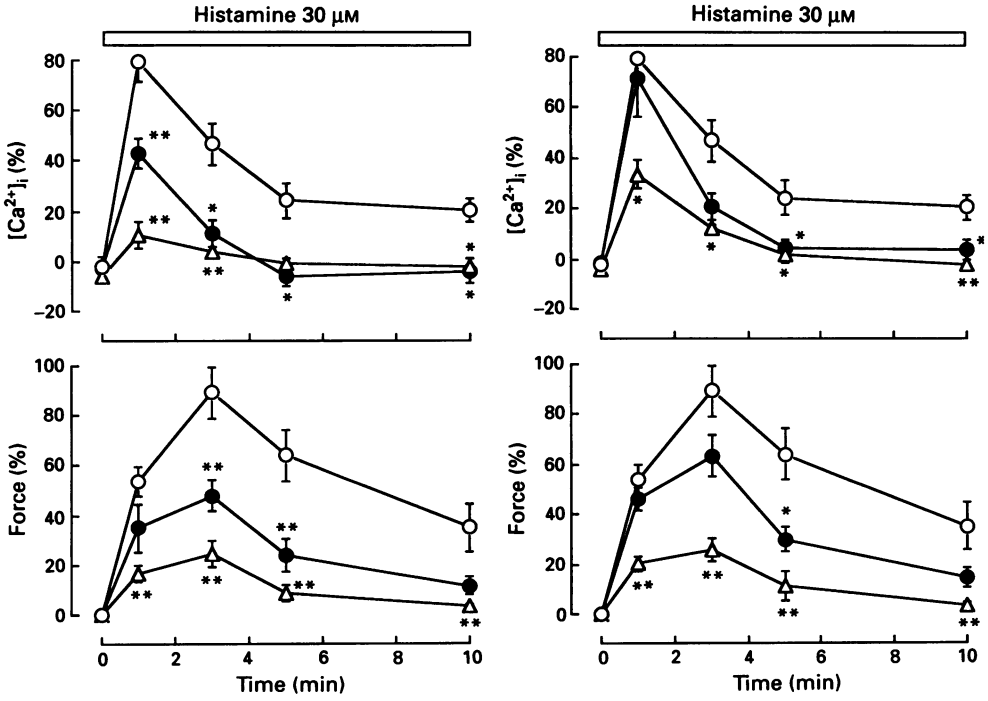

Figure 5 Effects of semotiadil (left panel) and verapamil (right panel) on increases in $[Ca^{2+}]_i$ and force induced by histamine (30 μM) in porcine coronary arteries loaded with fura-2. Semotiadil or verapamil was applied 20 min before the application of histamine. (○) Control; (●) 1 μM semotiadil or 1 μM verapamil; (△) 10 μM semotiadil or 10 μM verapamil. Changes in $[Ca^{2+}]_i$ and force induced by histamine are expressed as a percentage of those induced by 90 mM KCl-PSS for 10 min. $^*P<0.05$; $^{**}P<0.01$, compared with control. Each value represents the mean ± s.e.mean of 4 to 6 different experiments.

change the transient increases in $[Ca^{2+}]_i$ and force induced by histamine in Ca^{2+}-free PSS containing 1 mM EGTA. In contrast, verapamil at 10 μM inhibited significantly the $[Ca^{2+}]_i$ and contractile responses to histamine ($P<0.05$), but at 1 μM it did not affect them. Neither semotiadil nor verapamil (0.1 to 10 μM) had a statistically significant effect on the increases in $[Ca^{2+}]_i$ and force induced by 25 mM caffeine (data not shown).

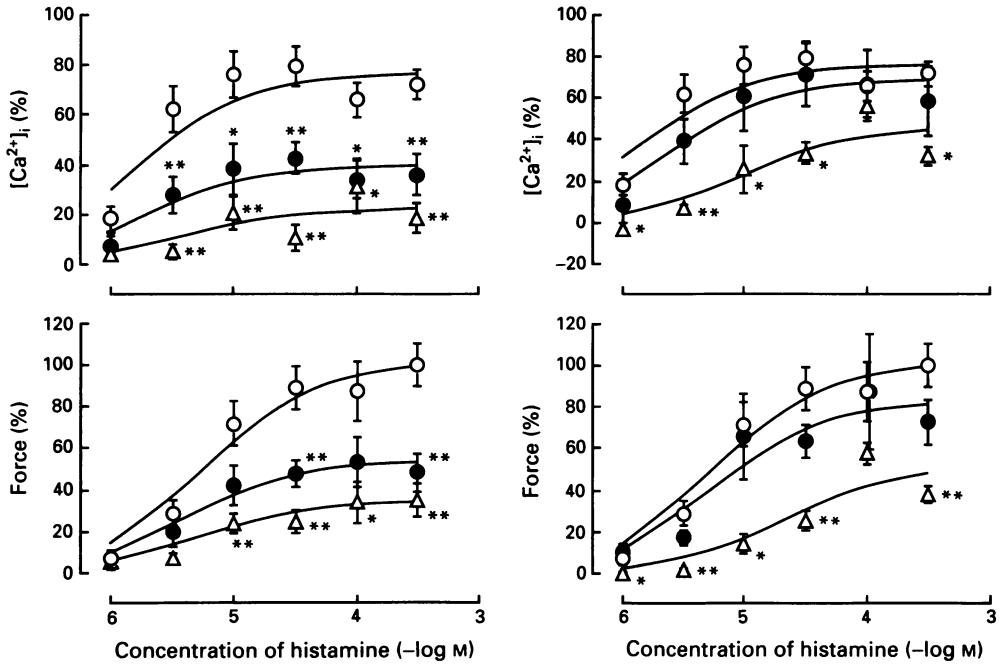

Figure 6 Concentration-response curves for the first phase of the response to histamine on $[Ca^{2+}]_i$ and force in the absence (○) or presence of 1 μM semotiadil or 1 μM verapamil (●) and 10 μM semotiadil or 10 μM verapamil (△) in porcine coronary arteries loaded with fura-2. Semotiadil or verapamil was applied 20 min before the application of each concentration of histamine. The histamine-induced increases in $[Ca^{2+}]_i$ and force in the first phase are defined as those observed at 1 and 3 min after the application of histamine, respectively. Changes in $[Ca^{2+}]_i$ and force induced by histamine are expressed as a percentage of those induced by 90 mM KCl-PSS for 10 min. The concentration-response curves were computer-fitted using mean values of the data. $*P<0.05$; $**P<0.01$, compared with control. Each value represents the mean ± s.e.mean of 4 to 7 different experiments.

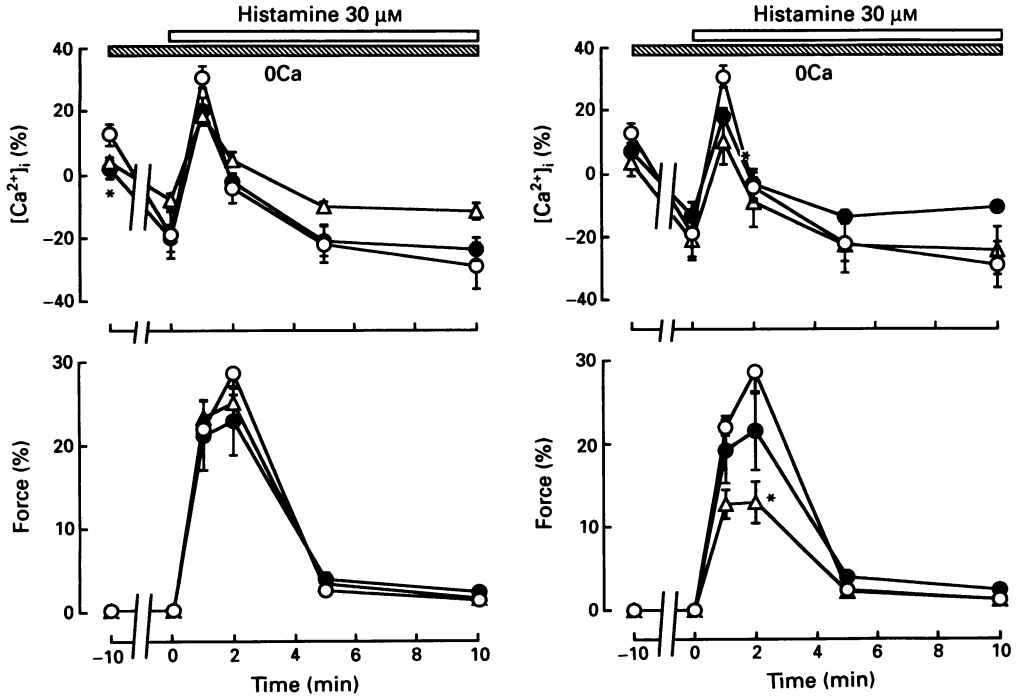

Figure 7 Effects of semotiadil (left panel) and verapamil (right panel) on increases in $[Ca^{2+}]_i$ and force induced by histamine (30 μM) in the absence of extracellular Ca^{2+} in porcine coronary arteries loaded with fura-2. Extracellular Ca^{2+} was removed by perfusion with Ca^{2+}-free PSS containing 1 mM EGTA before the application of histamine (0Ca). (○) Control; (●) 1 μM semotiadil or 1 μM verapamil; (△) 10 μM semotiadil or 10 μM verapamil. Changes in $[Ca^{2+}]_i$ and force induced by histamine are expressed as percentage of those induced by the 90 mM KCl-PSS for 10 min. $*P<0.05$, compared with control. Each value represents the mean ± s.e.mean of 4 to 5 different experiments.

Effect of semotiadil on [^{3}H]-pyrilamine binding

Verapamil has been demonstrated to bind to histamine H_1 receptors in membrane fractions from porcine aorta with a dissociation constant (K_i) of 7.1 ± 1.9 μM (Matsumoto *et al.*, 1989). Therefore, we tried to clarify whether or not semotiadil inhibits the histamine-induced contraction by interacting with histamine H_1 receptors. The specific binding of [^{3}H]-pyrilamine to bovine cerebellar membrane was saturable, and non-specific binding was only 20% of total binding. The binding affinity (K_d value) was 1.3 nM, and receptor density (B_{max}) was 6.2 pmol g^{-1} wet weight of tissue. Triprolidine (1 pM to 300 nM) displaced the specific [^{3}H]-pyrilamine binding with the K_i value of 1.0 nM, and the displacement at 100 nM was complete. Semotiadil even at 10 μM had little effect on the specific [^{3}H]-pyrilamine binding, and the inhibition by semotiadil was only 10.9% ($n = 2$).

Discussion

In the present study, semotiadil and verapamil each inhibited both the KCl-induced increases in $[Ca^{2+}]_i$ and force in porcine coronary arteries. They also inhibited the histamine-induced increases in $[Ca^{2+}]_i$ and force. However, in the absence of extracellular Ca^{2+}, semotiadil had no effect on the $[Ca^{2+}]_i$ and force responses to histamine, whereas verapamil inhibited them. These results suggest that in coronary arteries contracted with KCl, the vasodilator mechanisms of semotiadil and verapamil are the same, but semotiadil differs from verapamil in the mechanisms for inhibition of the histamine-induced contraction.

As extracellular KCl concentration was increased, force of contraction increased even after $[Ca^{2+}]_i$ had reached a peak level. If membrane depolarization with KCl increases an apparent sensitivity of contractile elements to cytosolic Ca^{2+}, a contraction should develop without a further increase in $[Ca^{2+}]_i$. Our recent studies have demonstrated that the apparent Ca^{2+} sensitivity is increased by membrane depolarization with KCl (Yanagisawa & Okada, 1994) and is decreased by hyperpolarization with K^+ channel openers (Okada *et al.*, 1993). These results suggest that membrane potential is one of the regulators of the apparent Ca^{2+} sensitivity. Thus, one possible explanation of the present results seems to be increased Ca^{2+} sensitivity of the contractile elements by KCl.

Semotiadil like verapamil inhibited increases in $[Ca^{2+}]_i$ as well as force induced by elevation of extracellular KCl concentrations. In a similar way, in canine basilar arteries contracted with KCl, semotiadil also decreased both $[Ca^{2+}]_i$ and force (Nakayama *et al.*, 1992). Such a simultaneous inhibition of the KCl-induced increases in $[Ca^{2+}]_i$ and force is a common characteristic of Ca^{2+} antagonists (Sato *et al.*, 1988; Yanagisawa *et al.*, 1989). Recently, the inhibition by semotiadil of voltage-dependent Ca^{2+} currents has been shown in the smooth muscle cells of rabbit portal vein (Teramoto, 1993). Thus, as seen with verapamil, the inhibition by semotiadil of the KCl-induced contraction may be due to blockade of voltage-dependent L-type Ca^{2+} channels in porcine coronary arteries.

Histamine is a strong spasmogen which contracts atherosclerotic porcine (Shimokawa *et al.*, 1983) and human coronary arteries (Kalsner & Richards, 1984). When histamine is applied in the presence of extracellular Ca^{2+}, $[Ca^{2+}]_i$ rapidly increases, reaches a maximum level (the first phase), and then decreases to a level higher than the resting level (the second phase, Rembold & Murphy, 1988; Mori *et al.*, 1990c). The histamine-induced change in $[Ca^{2+}]_i$ precedes the increase in force as seen with other agonists such as noradrenaline (Sato *et al.*, 1988) and carbachol (Himpens & Somlyo, 1988). In the present study, histamine also produced biphasic changes in $[Ca^{2+}]_i$ and force. The first phase of the $[Ca^{2+}]_i$ and contractile responses to histamine was greatly reduced, but still obtainable in the absence of extracellular Ca^{2+}. This means that the first phase is partially mediated by the release of Ca^{2+} from intracellular stores. Actually, histamine has been shown to produce inositol 1,4,5-trisphosphate (Donaldson & Hill, 1985), which releases Ca^{2+} from intracellular stores (Berridge & Irvine, 1984). The second phase of the histamine-induced increase in $[Ca^{2+}]_i$ was abolished and that of force was greatly reduced by removing extracellular Ca^{2+}. Therefore, histamine may stimulate both Ca^{2+} release and influx in the first phase, and only Ca^{2+} influx in the second phases.

To clarify the pathways of Ca^{2+} influx in the first and second phases, we examined the effects of verapamil on the histamine-induced increase in $[Ca^{2+}]_i$. We observed that verapamil inhibited, in a concentration-dependent manner, both the first and second phases of $[Ca^{2+}]_i$ and force responses to histamine. In an earlier study using porcine coronary arteries (Hirano *et al.*, 1990), diltiazem also attenuated these responses to histamine. Furthermore, it has been reported that the stimulation of histamine H_1 receptors increases L-type Ca^{2+} currents in rabbit coronary artery cells (Ishikawa *et al.*, 1993). Therefore, Ca^{2+} may enter into the cytosol through voltage-dependent L-type Ca^{2+} channels in the first and second phases.

We found that verapamil caused rightward shifts in the concentration-response curves for the first phase of histamine responses: the pD_2 value for histamine was reduced by verapamil, whereas the maximum response was not affected. Furthermore, verapamil at 10 μM attenuated the $[Ca^{2+}]_i$ and force responses to histamine in Ca^{2+}-free PSS, but not those to caffeine, suggesting that it does not act directly on intracellular Ca^{2+} stores. Therefore, verapamil at 10 μM may antagonize histamine at histamine H_1-receptors. This notion is directly supported by the earlier study indicating that verapamil displaces the [^{3}H]-mepyramine binding to porcine aortic membranes with a K_i of 7.1 μM (Matsumoto *et al.*, 1989). In contrast, the concentration-response curves for histamine responses were non-competitively inhibited by semotiadil (1 and 10 μM), which reduced the maximum responses without affecting the pD_2 values. Semotiadil did not affect the $[Ca^{2+}]_i$ and force responses to histamine in Ca^{2+}-free PSS and those to caffeine, and the binding of [^{3}H]-pyrilamine. These results suggest that semotiadil inhibits the histamine-induced contraction mainly by blocking Ca^{2+} influx through voltage-dependent L-type Ca^{2+} channels, whereas verapamil acts by both Ca^{2+} channel blockade and H_1-receptor antagonism.

In conclusion, semotiadil like verapamil may inhibit both KCl-induced and histamine-induced contractions by blocking voltage-dependent L-type Ca^{2+} channels in porcine coronary arteries. Semotiadil may be different from verapamil in that it does not bind to histamine H_1-receptors.

We are grateful to Santen Pharmaceutical Co., Ltd. for a kind gift of semotiadil. This work was supported by Grants-in-Aid for Scientific Research of Priority Area (No. 04263103) and for Scientific Research (No. 04670106, 05670082) from the Ministry of Education, Science and Culture, Japan.

References

BERRIDGE, M.J. & IRVINE, R.F. (1984). Inositol trisphosphate, a novel second messenger in cellular signal transduction. *Nature*, **312**, 315–321.

CHANG, R.S.L., TRAN, V.T. & SNYDER, S.H. (1979). Heterogeneity of histamine H_1-receptors: Species variations in [^{3}H]mepyramine binding of brain membranes. *J. Neurochem.*, **32**, 1653–1663.

DONALDSON, J. & HILL, S.J. (1985). Histamine-induced inositol phospholipid breakdown in the longitudinal smooth muscle of guinea-pig ileum. *Br. J. Pharmacol.*, **85**, 499–512.

GRYNKIEWICZ, G., POENIE, M. & TSIEN, R.Y. (1985). A new generation of Ca^{2+} indicators with greatly improved fluorescence properties. *J. Biol. Chem.*, **260**, 3440–3450.

HIMPENS, B. & SOMLYO, A.P. (1988). Free-calcium and force transients during depolarization and pharmacomechanical coupling in guinea-pig smooth muscle. *J. Physiol.*, **395**, 507–530.

HIRANO, K., KANAIDE, H., ABE, S. & NAKAMURA, M. (1990). Effects of diltiazem on calcium concentrations in the cytosol and on force of contractions in porcine coronary arterial strips. *Br. J. Pharmacol.*, **101**, 273–280.

ISHIKAWA, T., HUME, J. & KEEF, K.D. (1993). Modulation of K^+ and Ca^{2+} channels by histamine H_1-receptor stimulation in rabbit coronary artery cells. *J. Physiol.*, **468**, 379–400.

KAGEYAMA, M., MORI, T., YANAGISAWA, T. & TAIRA, N. (1991a). Is staurosporine a specific inhibitor of protein kinase C in intact porcine coronary arteries? *J. Pharmacol. Exp. Ther.*, **259**, 1019–1026.

KAGEYAMA, M., NISHIMURA, K., TAKADA, T., MIYAWAKI, N. & YAMAUCHI, H. (1991b). SD-3211, a novel bezothiazine calcium antagonist, alone and in combination with a beta-adrenoceptor antagonist, produces antihypertensive effects without affecting heart rate and atrioventricular conduction in conscious renal hypertensive dogs. *J. Cardiovasc. Pharmacol.*, **17**, 102–107.

KALSNER, S. & RICHARDS, R. (1984). Coronary arteries of cardiac patients are hyperreactive and contain stores of amines: A mechanism for coronary spasm. *Science (Wash. DC)*, **223**, 1435–1437.

MATSUMOTO, T., KANAIDE, H., NISHIMURA, J., KUGA, T., KOBAYASHI, S. & NAKAMURA, M. (1989). Histamine-induced calcium transients in vascular smooth muscle cells: effects of verapamil and diltiazem. *Am. J. Physiol.*, **257**, H563–H570.

MIYAWAKI, N., FURUTA, T., SHIGEI, T., YAMAUCHI, H. & ISO, T. (1990). Electrophysiological properties of SD-3211, a novel putative Ca^{2+} antagonist, in isolated guinea pig and rabbit hearts. *J. Cardiovasc. Pharmacol.*, **16**, 769–775.

MIYAWAKI, N., FURUTA, T., SHIGEI, T., YAMAUCHI, H. & ISO, T. (1991). Cardiovascular characterization of SD-3211, a novel benzothiazine calcium channel blocker, in isolated rabbit hearts. *Life Sci.*, **48**, 1903–1909.

MORI, T., IRIE, K., ISHII, F. & ASHIDA, S. (1990a). Prevention of coronary vasospasm by a novel Ca^{++} antagonist, SD-3211 (semotiadil) in rats. *Jpn. J. Pharmacol.*, **52**, (Suppl. I), 213p.

MORI, T., YANAGISAWA, T. & TAIRA, N. (1990b). Phorbol 12,13-dibutyrate increases vascular tone but has a dual action on intracellular calcium levels in porcine coronary arteries. *Naunyn-Schmied. Arch. Pharmacol.*, **341**, 251–255.

MORI, T., YANAGISAWA, T. & TAIRA, N. (1990c). Histamine increases vascular tone and intracellular calcium level using both intracellular and extracellular calcium in porcine coronary arteries. *Jpn. J. Pharmacol.*, **52**, 263–271.

MORI, T., IRIE, K. & ASHIDA, S. (1991). Inhibitory effects of SD-3211, a novel long-acting Ca^{++} antagonist, on vasopressin induced ST segment depression in rats. *Jpn. J. Pharmacol.*, **55**, (Suppl. I), 328p.

NAKAYAMA, K., MORIMOTO, K., NOZAWA, Y. & TANAKA, Y. (1992). Calcium antagonistic and binding properties of semotiadil (SD-3211), a benzothiazine derivative, assessed in cerebral and coronary arteries. *J. Cardiovasc. Pharmacol.*, **20**, 380–391.

NISHIMURA, K., MIYAWAKI, N., YAMAUCHI, H. & ISO, T. (1990). Tissue selectivity of the novel calcium antagonist semotiadil fumarate in isolated smooth muscles and cardiac muscles. *Arzneim. Forsch./Drug Res.*, **40**, 224–248.

OKADA, Y., YANAGISAWA, T. & TAIRA, N. (1993). BRL38227 (levcromakalim)-induced hyperpolarization reduces the sensitivity to Ca^{2+} of contractile elements in canine coronary artery. *Naunyn-Schmied. Arch. Pharmacol.*, **347**, 438–444.

REMBOLD, C.M. & MURPHY, R.A. (1988). Myoplasmic $[Ca^{2+}]$ determines myosin phosphorylation in agonist-stimulated swine arterial smooth muscle. *Circ. Res.*, **63**, 593–603.

SATO, K., OZAKI, H. & KARAKI, H. (1988). Changes in cytosolic calcium level in vascular smooth muscle strip measured simultaneously with contraction using fluorescent calcium indicator fura 2. *J. Pharmacol. Exp. Ther.*, **246**, 294–300.

SHIMOKAWA, H., TOMOIKE, H., NABEYAMA, S., YAMAMOTO, H., ARAKI, H., NAKAMURA, M., ISHI, Y. & TANAKA, K. (1983). Coronary artery spasm induced in atherosclerotic miniature swine. *Science (Wash. DC)*, **221**, 560–562.

TAKADA, T., MIYAWAKI, N., KAGEYAMA, M., MATSUNO, K., ISHIDA, N., YAMAUCHI, H. & ISO, T. (1991). Antihypertensive effect of a novel calcium antagonist, SD-3211, in experimental hypertensive rats. *J. Cardiovasc. Pharmacol.*, **18**, 855–862.

TERAMOTO, N. (1993). Mechanisms of the inhibitory action of semotiadil fumarate, a novel Ca antagonist, on the voltage-dependent Ca current in smooth muscle cells of the rabbit portal vein. *Jpn. J. Pharmacol.*, **61**, 183–195.

YANAGISAWA, T., KAWADA, M. & TAIRA, N. (1989). Nitroglycerin relaxes canine coronary arterial smooth muscle without reducing intracellular Ca^{2+} concentrations measured with fura-2. *Br. J. Pharmacol.*, **98**, 469–482.

YANAGISAWA, T. & OKADA, Y. (1994). KCl depolarization increases Ca^{2+} sensitivity of contractile elements in coronary arterial smooth muscle. *Am. J. Physiol.*, **267**, H614–H621.

YONEYAMA, F., YAMADA, H., SATOH, K. & TAIRA, N. (1990). Cardiac versus coronary dilator effects of SD-3211 a new nondihydropyridine calcium antagonist, in isolated, blood-perfused dog hearts. *Cardiovasc. Drugs Ther.*, **4**, 1469–1476.

(Received August 31, 1994
Revised November 14, 1994
Accepted November 29, 1994)

British Journal of Pharmacology (1995) 114, 1296–1302

Subgroups among μ-opioid receptor agonists distinguished by ATP-sensitive K^+ channel-acting drugs

María Ocaña, Esperanza Del Pozo, Manuel Barrios & [1]José M. Baeyens

Department of Pharmacology and Neurosciences Institute, School of Medicine, University of Granada, E-18012 Granada, Spain

1 We evaluated the effects of the i.c.v. administration of different K^+ channel blockers (gliquidone, 4-aminopyridine and tetraethylammonium) and an opener of K^+ channels (cromakalim) on the antinociception induced by several μ-opioid receptor agonists in a tail flick test in mice.

2 The s.c. administration of all agonists of μ-opioid receptors tested (morphine, 1–16 mg kg^{-1}; methadone, 1–6 mg kg^{-1}; buprenorphine, 0.04–0.64 mg kg^{-1}; fentanyl, 0.02–0.32 mg kg^{-1} and levorphanol, 0.2–3.2 mg kg^{-1}) elicited a dose-dependent antinociceptive effect.

3 The ATP-sensitive K^+ channel blocker, gliquidone (0.06–16 μg per mouse, i.c.v.) antagonized the antinociception induced by buprenorphine, morphine and methadone. In contrast, gliquidone (0.25–160 μg per mouse) did not modify the antinociceptive effects of fentanyl and levorphanol.

4 Cromakalim (4–64 μg per mouse, i.c.v.), an opener of ATP-sensitive K^+ channels, enhanced the antinociception produced by buprenorphine, morphine, and methadone, and did not significantly modify the antinociceptive effects of fentanyl and levorphanol.

5 The i.c.v. administration of the K^+ channel blockers tetraethylammonium (10 μg per mouse) or 4-aminopyridine (25 ng per mouse) did not significantly modify the antinociception induced by any μ-opioid receptor agonist tested.

6 These results suggest that the opening of ATP-sensitive K^+ channels is involved in the antinociceptive effect of morphine, buprenorphine and methadone, but not in that of fentanyl or levorphanol. Consequently, we suggest that at least two subgroups can be distinguished among μ-opioid receptor agonists, each inducing antinociception through different effector mechanisms.

Keywords: Antinociception; μ-opioid receptor agonists; ATP-sensitive K^+ channels; morphine; fentanyl; cromakalim; gliquidone; 4-aminopyridine; tetraethylammonium.

Introduction

Many electrophysiological studies have demonstrated that agonists of μ-opioid receptors open K^+ channels in neurones (for a review see North, 1989). We have tested the hypothesis that the opening of K^+ channels plays a role in the antinociceptive effect of morphine and found that the i.c.v. administration of glibenclamide, a sulphonylurea that specifically blocks ATP-sensitive K^+ (K_{ATP}) channels (Amoroso *et al.*, 1990), dose-dependently antagonizes morphine-induced antinociception (Ocaña *et al.*, 1990). This observation was later confirmed with different sulphonylureas and several nociceptive tests (Wild *et al.*, 1991; Narita *et al.*, 1992a; Ocaña *et al.*, 1993a; Roane & Boyd, 1993; Welch & Dunlow, 1993). In addition, K_{ATP} channel blockers also antagonize morphine-induced hyperthermia (Narita *et al.*, 1992b) and hypermotility (Ocaña *et al.*, 1993b), as well as the exacerbation by morphine of bicuculline-induced convulsions (Narita *et al.*, 1993a). Consequently, the opening of K_{ATP} channels may represent an important step in the mechanism of action of morphine.

It is not known whether the opening of K_{ATP} channels is also involved in the effects induced by other agonists at μ-opioid receptors. This information is of interest because μ-opioid receptor agonists are not a functionally homogeneous group of drugs. For example, [D-$Pen^{2,5}$]enkephalin enhances antinociception induced by morphine, normorphine and codeine but not that induced by sufentanil, [D-Ala^2, $MePhe^4$, Gly-ol^5]enkephalin (DAMGO) and other μ-opioid receptor agonists (Heyman *et al.*, 1989; Jiang *et al.*, 1990). On the other hand, droperidol enhances fentanyl- and sufentanil-induced, but not morphine-induced, antinociception (Statile *et al.*, 1988). In addition, lithium and meptazinol differentially antagonize morphine-, sufentanil- and DAMGO-induced antinociception (Dray *et al.*, 1986; Raffa *et al.*, 1992). Other effects of μ-opioid receptor agonists also suggest functional heterogeneity within this group of drugs. Thus, [D-$Pen^{2,5}$]enkephalin enhances, whereas several κ-opioid receptor agonists (U50,488H, tifluadon, ethylketocyclazocine, dynorphin A) antagonize, the centrally-mediated inhibition of rat urinary bladder motility induced by morphine and normorphine, but not the inhibition due to meperidine, sufentanil, DAMGO and other μ-opioid receptor agonists (Sheldon *et al.*, 1987; 1988a,b).

In this study, to evaluate whether the opening of K^+ channels underlies the antinociception induced by several μ-opioid receptor agonists, we tested the effects of a blocker (gliquidone) and an opener (cromakalim) of neuronal K_{ATP} channels (Amoroso *et al.*, 1990; Schmid-Antomarchi *et al.*, 1990) on the antinociception induced by five agonists of μ-opioid receptors. Furthermore, since the antinociception induced by some drugs, such as the $GABA_B$ receptor agonist, baclofen, is not modified by K_{ATP} channel blockers but is antagonized by other K^+ channel blockers such as 4-aminopyridine (4-AP) and tetraethylammonium (TEA) (Ocaña & Baeyens, 1993), we also tested whether 4-AP and TEA affected the antinociception induced by the different agonists at μ-opioid receptors.

Methods

Female CD-1 mice (Charles River, Barcelona, Spain) weighing 25–30 g were used for all the experiments, The animals were housed in a temperature-controlled room (21 ± 1°C)

[1] Author for correspondence.

with air exchange every 20 min and an automatic 12 h light/dark cycle (lights on at 08 h 00 min and off at 20 h 00 min)). The experiments were performed from 09 h 00 min to 15 h 00 min. Food and water were freely available until the beginning of the experiments. Naive animals were used throughout. Mice were always handled in accordance with current guidelines for the care of laboratory animals and the ethical guidelines for investigations of experimental pain in conscious animals (Zimmermann, 1983).

The drugs used as μ-opioid receptor agonists and their suppliers were: morphine hydrochloride (General Directorate of Pharmacy and Drugs, Spanish Health Ministry), buprenorphine hydrochloride (Laboratorios Dr. Esteve, S.A., Barcelona, Spain), methadone hydrochloride, fentanyl citrate and levorphanol tartrate (Sigma Quimica, Madrid, Spain). The K^+ channel-acting drugs were: gliquidone (Europharma S.A., Madrid, Spain), cromakalim, tetraethylammonium bromide (TEA) and 4-aminopyridine (4-AP) (Sigma Química, Madrid, Spain). All μ-opioid receptor agonists were dissolved in demineralized water and injected subcutaneously (s.c.) in a volume of 5 ml kg^{-1}. All K^+ channel-acting drugs were dissolved in 1% Tween 80 in demineralized water, and were injected intracerebroventricularly (i.c.v.) in a volume of 5 μl per mouse. Control animals received the same volume of vehicle. The s.c. injections were made in the interscapular region. The i.c.v. injections were made in the lateral cerebral ventricle of nonanaesthetized mice according to the method described previously (Ocaña *et al.*, 1993a). Briefly, the injection site was identified according to the method by Haley & McCormick (1957) and the drug solution was injected with a 10 μl Hamilton syringe with a sleeve around the needle to prevent the latter from penetrating more than 3 mm into the skull. After the experiments were done, the position of the injection was evaluated in each brain, and the results from animals in which the tip of the needle did not reach the lateral ventricle were discarded.

The tail flick test was used to evaluate the antinociceptive effects of the drugs. The test was performed as previously described (Ocaña *et al.*, 1993a). Briefly, the animals were restrained in a plexiglass tube and placed on the tail flick apparatus (LI 7100, Letica, S.A., Barcelona, Spain). A noxious beam of light was focussed on the tail about 4 cm from the tip, and the latency to removal was recorded automatically to the nearest 0.1 s. The intensity of the radiant heat source was adjusted to yield baseline latencies between 3 and 5 s; this intensity was never changed and any animal in which baseline latency was outside the pre-established limits was excluded from the experiments. The cut-off time was 10 s.

Baseline tail flick latencies were recorded 10 min before and immediately before all injections. Once baseline latencies were obtained the animals received an s.c. injection of a μ-opioid receptor agonist or its solvent, and immediately thereafter an i.c.v. injection of one of the K^+ channel-acting drugs or its solvent. The end of the last injection was considered as time 0; from this time tail flick latencies were measured again 10, 20, 30, 45, 60, 90 and 120 min after the injections. When the effects of K^+ channel-acting drugs *per se* (i.e. not associated with μ-opioid receptor agonists) were

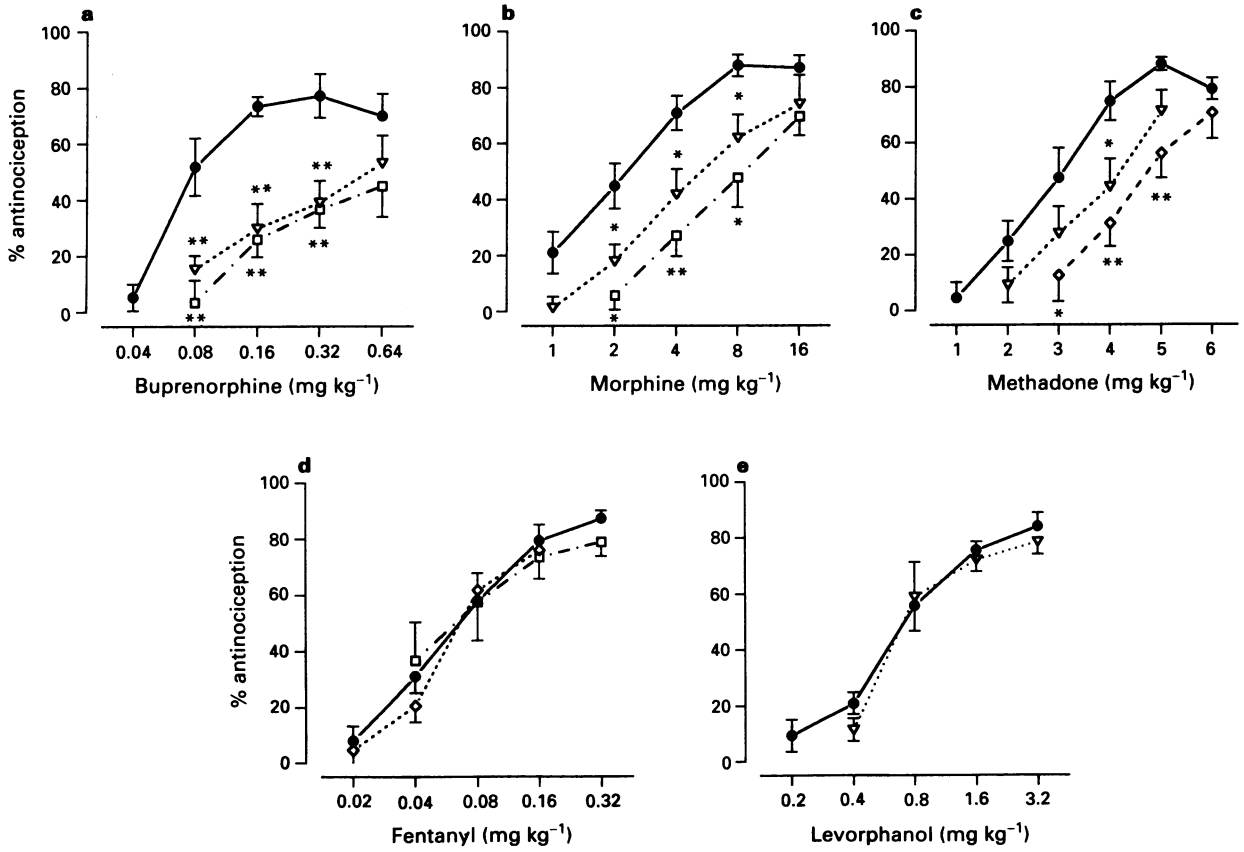

Figure 1 Effects of i.c.v. treatment with different doses of gliquidone on the antinociception induced by several μ-opioid receptor agonists in a tail flick test in mice. (a) Effects of buprenorphine + vehicle (●); buprenorphine + gliquidone 1 μg per mouse (▽); and buprenorphine + gliquidone 4 μg per mouse (□). (b) Effects of morphine + vehicle (●); morphine + gliquidone 1 μg per mouse (▽); and morphine + gliquidone 4 μg per mouse (□). (c) Effects of methadone + vehicle (●); methadone + gliquidone 1 μg per mouse (▽); and methadone + gliquidone 16 μg per mouse (◇). (d) Effects of fentanyl + vehicle (●); fentanyl + gliquidone 4 μg per mouse (◇); and fentanyl + gliquidone 160 μg per mouse (□). (e) Effects of levorphanol + vehicle (●); and levorphanol + gliquidone 64 μg per mouse (▽). Each point represents the mean ± s.e.mean of the values obtained in 8–12 animals. Statistically significant differences in comparison with vehicle-treated group: $*P<0.05$; $**P<0.01$ (Newman Keuls test in a–d and Student's *t* test in e).

tested, baseline tail flick latencies were determined, the drug under study was injected i.c.v. at time 0, and tail flick latencies were determined during 2 h at the times indicated above. To obtain a global value of the antinociception induced over the 2 h experimental period, the area under the curve of antinociception against time (AUC) was calculated for each animal according to the method of Tallarida & Murray (1987). The degree of antinociception in each animal was calculated according to the formula: % antinociception = $[(AUC_t - AUC_c)\ (AUC_{max} - AUC_c)^{-1}] \times 100$, where AUC_t and AUC_c are the areas under the curve for treated and control animals respectively, and AUC_{max} is the area under the curve of maximum possible antinociception (10 s in each determination).

Comparisons between the means of two groups were made with Student's t test for non-paired data. Values in the control group were compared against those obtained in the groups of animals treated with different doses of each K^+ channel-acting compound by one-way analysis of variance (ANOVA) followed by Newman Keuls test. The differences between means were considered significant when the value of P was below 0.05.

Results

Effects of gliquidone on the antinociception induced by μ-opioid receptor agonists

The subcutaneous administration of all μ-opioid receptor agonists tested (buprenorphine, 0.04–0.64 mg kg^{-1}; morphine, 1–16 mg kg^{-1}; methadone, 1–6 mg kg^{-1}; fentanyl, 0.02–0.32 mg kg^{-1} and levorphanol, 0.2–3.2 mg kg^{-1}) elicited a dose-dependent antinociceptive effect (Figure 1).

The K_{ATP} channel blocker, gliquidone, differentially affected the antinociception induced by the μ-opioid receptor agonists tested. Gliquidone (1–16 μg per mouse, i.c.v.) displaced the dose-response lines of morphine, methadone and buprenorphine to the right (Figure 1a–c). On the other hand, gliquidone (4–160 μg per mouse), i.e. even at doses greater than those used in the previous experiments, did not significantly shift the dose-response lines of fentanyl or levorphanol (Figure 1d–e). The differential effect of gliquidone against the antinociception induced by the μ-opioid receptor agonists was not due to the differential time-course of their antinociceptive effects, because gliquidone antagonized buprenorphine-, morphine- and methadone-induced antinociception at all times of study (from 10 to 120 min after injection), whereas the antinociception produced by fentanyl and levorphanol was not modified by gliquidone at any time throughout the study (data not shown).

When a wide range of doses of gliquidone (0.06–160 μg per mouse, i.c.v.) was tested against the antinociception induced by equieffective doses of the μ-opioid receptor agonists differential sensitivity to the K_{ATP} channel blocker was also observed. The antinociceptive effect of buprenorphine (0.16 mg kg^{-1}), morphine (4 mg kg^{-1}) and methadone (4 mg kg^{-1}) was antagonized by gliquidone (0.06–16 μg per mouse, i.c.v.) (Figure 2). Maximal antagonism by gliquidone was observed at 16 μg per mouse (data not shown). On the other hand, the antinociception induced by fentanyl (0.16 mg kg^{-1}) and levorphanol (1.6 mg kg^{-1}) was not modified by gliquidone (0.25-160 μg per mouse, i.c.v.) (Figure 2).

Gliquidone itself (i.e. not associated with μ-opioid receptor agonists) did not significantly modify tail flick latency at any of the doses tested. For example, the i.c.v. administration of gliquidone at doses of 0.25, 4 and 64 μg per mouse produced -7.4 ± 7.7, -3.0 ± 3.2 and $+9.16 \pm 4.9$% antinociception respectively ($P > 0.05$ in comparison to control value, Newman Keuls test).

Effects of cromakalim on the antinociception induced by μ-opioid receptor agonists

The effect of a wide range of doses of the K_{ATP} channel opener cromakalim (4–64 μg per mouse, i.c.v.) on the antinociception induced by the different μ-opioid receptor agonists was also tested. Cromakalim enhanced the antinociceptive effects of buprenorphine (0.04 mg kg^{-1}), morphine (1 mg kg^{-1}) and methadone (2 mg kg^{-1}) (Figure 3). In contrast, cromakalim did not significantly modify fentanyl (0.04 mg kg^{-1}) and levorphanol (0.4 mg kg^{-1}) induced antinociception (Figure 3).

When a fixed dose of cromakalim (32 μg per mouse) was tested with different doses of each μ-opioid receptor agonist, different interactions were also observed. Cromakalim displaced to the left the dose-response lines of buprenorphine, morphine and methadone, without increasing their maximum antinociceptive effects (Figure 4a–c). In contrast, this dose of cromakalim did not significantly modify the dose-response relationships of fentanyl or levorphanol (Figure 4d–e).

None of the doses of cromakalim tested significantly modified tail flick latency in control animals. For example the i.c.v. administration of cromakalim at doses of 32 and 64 μg per mouse produced 11.0 ± 6.3 and 8.2 ± 4.6% antinociception respectively ($P > 0.05$ in comparison to control value, Newman Keuls test).

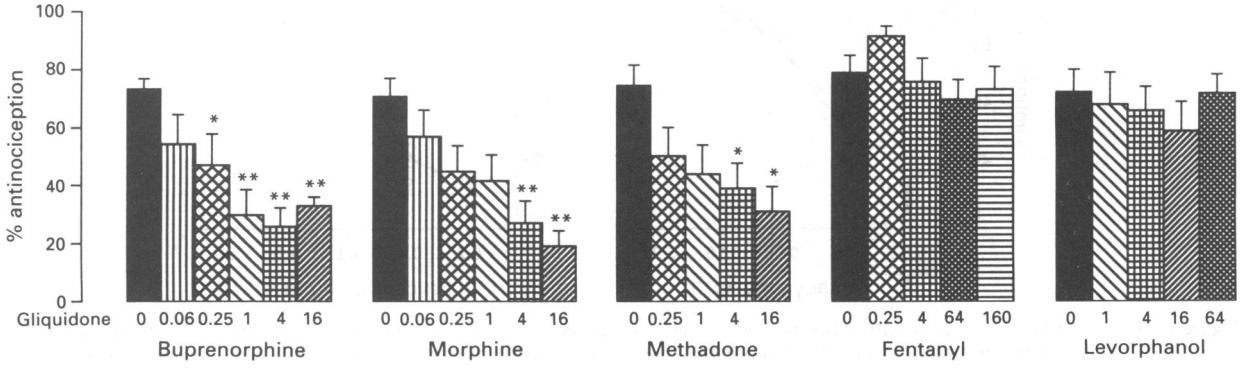

Figure 2 Comparison of the effects of different doses of gliquidone on the antinociception induced by the s.c. administration of buprenorphine (0.16 mg kg^{-1}), morphine (4 mg kg^{-1}), methadone (4 mg kg^{-1}), fentanyl (0.16 mg kg^{-1}) and levorphanol (1.6 mg kg^{-1}). The solid columns represent the effect of each μ-opioid receptor agonist plus gliquidone solvent. The doses of gliquidone (μg per mouse, i.c.v.) are shown below the columns. Each column represents the mean ± s.e.mean of the values obtained in 8-12 animals. Statistically significant differences in comparison with vehicle-treated group: $^*P < 0.05$; $^{**}P < 0.01$ (Newman Keuls test).

Effects of 4-aminopyridine and tetraethylammonium on the antinociception induced by μ-opioid receptor agonists

Neither 4-AP (25 ng per mouse, i.c.v.), nor TEA (10 μg per mouse, i.c.v.) significantly modified the antinociception induced by the μ-opioid receptor agonists tested (Table 1). These doses of 4-aminopyridine and tetraethylammonium did not significantly modify tail flick latency in control animals (Table 1).

Discussion

Our results show that gliquidone differentially antagonized, and cromakalim differentially enhanced, the antinociception induced by several μ-opioid receptor agonists in mice. We also found that neither 4-AP nor TEA modified the antinociceptive effect of these drugs.

All agonists of opioid receptors that we used induce antinociception through the activation of μ-opioid receptors

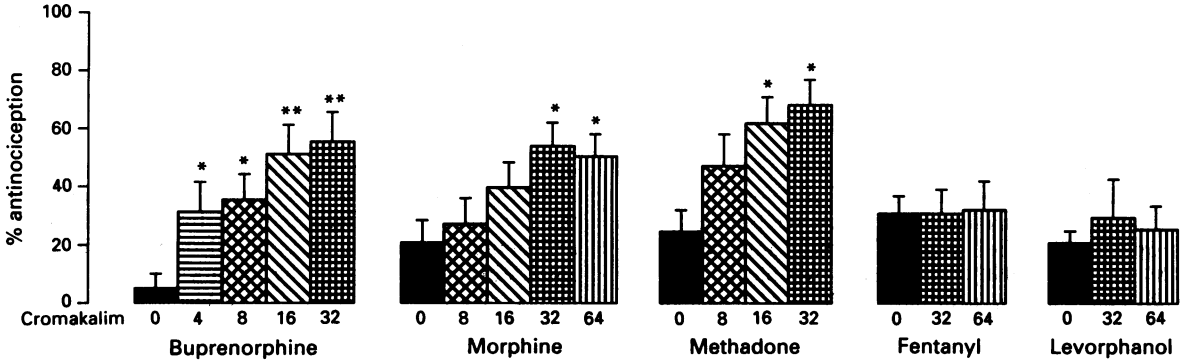

Figure 3 Comparison of the effects of different doses of cromakalim on the antinociception induced by the s.c. administration of buprenorphine (0.04 mg kg^{-1}), morphine (1 mg kg^{-1}), methadone (2 mg kg^{-1}), fentanyl (0.04 mg kg^{-1}) and levorphanol (0.4 mg kg^{-1}). The solid columns represent the effect of each μ-opioid receptor agonist plus cromakalim solvent. The doses of cromakalim (μg per mouse, i.c.v.) are shown below the columns. Each column represents the mean ± s.e.mean of the values obtained in 8–12 animals. Statistically significant differences in comparison with vehicle-treated group: $*P<0.05$; $**P<0.01$ (Newman Keuls test).

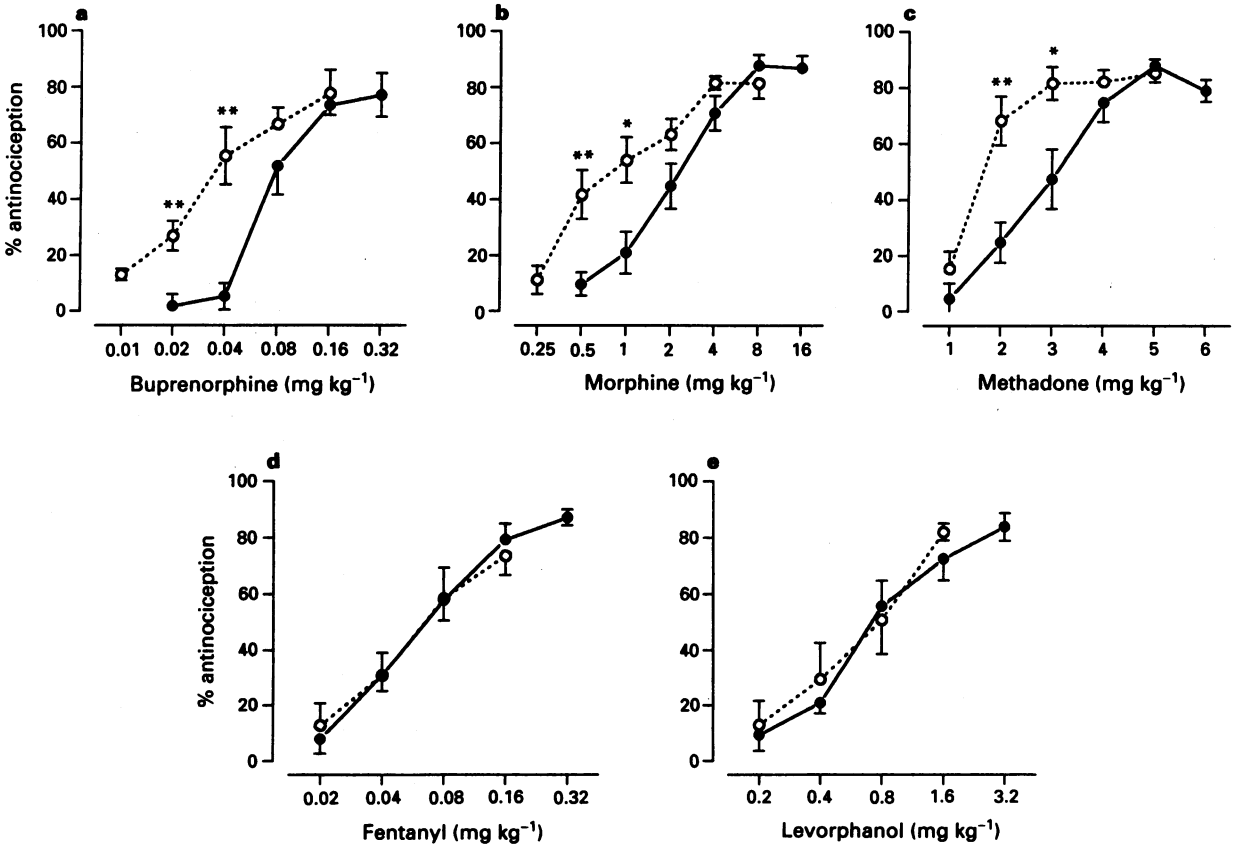

Figure 4 Effects of i.c.v. treatment with cromakalim (32 μg per mouse) on the antinociception induced by several μ-opioid receptor agonists in a tail flick test in mice. (a) Effects of buprenorphine + vehicle (●); and buprenorphine + cromakalim (○). (b) Effects of morphine + vehicle (●); and morphine + cromakalim (○). (c) Effects of methadone + vehicle (●); and methadone + cromakalim (○). (d) Effects of fentanyl + vehicle (●); and fentanyl + cromakalim (○). (e) Effects of levorphanol + vehicle (●); and levorphanol + cromakalim (○). Each point represents the mean ± s.e.mean of the values obtained in 8–12 animals. Statistically significant differences in comparison with vehicle-treated group: $*P<0.05$, $**P<0.01$ (Student's t test for non-paired data).

Table 1 Effects of 4-aminopyridine (25 ng per mouse, i.c.v.) and tetraethylammonium (10 μg per mouse, i.c.v.) on the antinociception induced by the s.c. administration of different agonists of μ-opioid receptors

Treatment	*Dose*[a]	*%antinociception*[b] *+ Vehicle*	*+ 4-Aminopyridine*	*+ Tetraethylammonium*
Saline		0.0 ± 3.0	−1.6 ± 3.0	8.1 ± 4.7
Buprenorphine	0.16	67.1 ± 7.9	68.2 ± 6.9	62.6 ± 6.7
Morphine	4	71.1 ± 8.9	64.0 ± 6.3	65.6 ± 9.1
Methadone	4	74.8 ± 6.9	69.1 ± 7.3	68.6 ± 8.1
Fentanyl	0.16	73.5 ± 9.0	85.1 ± 4.5	83.2 ± 4.0
Levorphanol	1.6	72.5 ± 7.6	78.5 ± 8.8	66.8 ± 7.2

[a]The numbers represent the dose (mg kg^{-1}) of each opiate administered s.c.
[b]The values represent the mean ± s.e.mean of the results obtained in 8–12 animals in each group. No statistically significant differences in comparison to opiate + vehicle were found in any case (Student's *t* test for non-paired data).

(Magnan *et al.*, 1982; Zimmerman *et al.*, 1987; Adams *et al.*, 1990). Morphine and other agonists of μ-opioid receptors open K^+ channels in neurones (for a review see North, 1989), and this opening may be involved in their antinociceptive effects (Ocaña *et al.*, 1990). TEA and 4-AP block different types of K^+ channels in neurones, such as Ca^{2+}-activated and voltage-dependent K^+ channels, although they are not selective for any of them in particular (Cook & Quast, 1990; Halliwell, 1990). Our results show that neither 4-AP nor TEA, administered i.c.v., significantly modified the antinociception induced by the μ-opioid receptor agonists tested. This lack of effect cannot be traced to any methodological failure, since a previous study using the same doses and methods demonstrated that both 4-AP and TEA antagonize baclofen-induced antinociception (Ocaña & Baeyens, 1993). Consequently, the K^+ channels blocked by 4-AP and TEA are apparently not involved in μ-opioid receptor-mediated antinociception. The present results are not surprising, as the lack of effect of i.c.v. TEA on morphine-induced antinociception has been reported previously (Ocaña *et al.*, 1990; Wild *et al.*, 1991; Narita *et al.*, 1992a), and the intrathecal (i.t.) administration of 4-AP and TEA did not antagonize morphine antinociception (Welch & Dunlow, 1993). Furthermore, electrophysiological studies have shown that the K^+ channels opened by μ-opioid receptor agonists are not sensitive to 4-AP and TEA (North & Williams, 1985).

Gliquidone and other hypoglycaemic sulphonylureas block K_{ATP} channels in neurones (for a review see Edwards & Weston, 1993). Recently, sulphonylureas have also been shown to block two other (non-K_{ATP}) types of K^+ channels (Reeve *et al.*, 1992; Crépel *et al.*, 1993). These channels are blocked both by sulphonylureas and by 4-AP or TEA. Because neither 4-AP nor TEA modified the antinociceptive effects of μ-opioid receptor agonists in our study, these sulphonylurea-sensitive non-K_{ATP} channels are unlikely to be involved in μ-opioid-mediated antinociception. All sulphonylureas tested to date, whether administered i.c.v. or i.t., dose-dependently antagonized morphine-induced antinociception (Ocaña *et al.*, 1990; 1993a; Wild *et al.*, 1991; Narita *et al.*, 1992a; Roane & Boyd, 1993; Welch & Dunlow, 1993). The order of potency of sulphonylureas in blocking K_{ATP} channels in neurones (gliquidone>glipizide>glibenclamide >tolbutamide) (Amoroso *et al.*, 1990; Schmid-Antomarchi *et al.*, 1990) is the same as their order of potency in blocking morphine-induced antinociception (Ocaña *et al.*, 1993a), which suggests that the opening of K_{ATP} channels underlies the antinociceptive effect of morphine. This idea is further supported by the fact that pinacidil and cromakalim, two openers of K_{ATP} channels (Longman & Hamilton, 1992), dose-dependently enhanced morphine-induced antinociception (Vergoni *et al.*, 1992; Narita *et al.*, 1993b). Our results confirm the antagonism by gliquidone, and the enhancement by cromakalim, of the antinociceptive effect of morphine. In addition, we show that the antinociception induced by methadone and buprenorphine is similarly antagonized by gliquidone and enhanced by cromakalim. These results suggest that the opening of K_{ATP} channels underlies the antinociceptive effects induced by morphine, methadone and buprenorphine (henceforth called 'morphine-like drugs'). Interestingly, 20–30% of the antinociception induced by the higher doses of morphine-like drugs remains insensitive to gliquidone (see Figure 2). This indicates that both K_{ATP} channel opening and other(s) unknown mechanism(s) are involved in the antinociceptive effects of morphine-like drugs. On the other hand, fentanyl- and levorphanol-induced antinociception was not modified by gliquidone or cromakalim, which suggests that K_{ATP} channels play no role in the antinociceptive effects of fentanyl and levorphanol (henceforth called 'fentanyl-like drugs'). These differences, particularly between fentanyl and morphine, were not totally unexpected as previous studies suggested dissimilarities between the mechanisms involved in the antinociceptive effects of fentanyl (and/or its analogue sufentanil) and morphine (see the second paragraph of the Introduction for references). Consequently, our results add new evidence in favour of the idea that μ-opioid receptor agonists are not a functionally homogeneous group of drugs, and particularly suggest that this heterogeneity may be due to the involvement of different effector mechanisms.

Theoretically, the activation of different effector mechanisms by two agonists of a receptor may be due to their action on different subtypes of the receptor, or to their action on the same receptor coupled to different transducer proteins (see Milligan, 1993). Both possibilities may be considered in explaining our data.

Two different types of μ-opioid receptors, called μ_1 and μ_2 have been described (for a review see Pasternak, 1988); both types are involved in the antinociceptive effects of μ-opioid agonists (Heyman *et al.*, 1988; Paul *et al.*, 1989; Pick *et al.*, 1993). Consequently, one explanation for our results might be that μ_1 and μ_2 receptors are differentially coupled to K_{ATP} channels, and that morphine-like drugs act on one of these receptors whereas fentanyl-like drugs act on the other. However, this does not appear to be the case because the antinociception induced by i.c.v. morphine, a predominantly μ_1-mediated effect (Heyman *et al.*, 1988; Pick *et al.*, 1993), and i.t. morphine, a predominantly μ_2-mediated effect (Heyman *et al.*, 1988; Pick *et al.*, 1993), are both antagonized by the K_{ATP} channel blocker, glibenclamide (Narita *et al*, 1992a; Welch & Dunlow, 1993). In addition, the antinociception elicited by the peripheral administration of morphine and fentanyl is due mostly to activation of μ_1 receptors (Ling *et al.*, 1985; Jang & Yoburn, 1991), but is differentially modified by K_{ATP} channel-acting drugs. Consequently, our results cannot be explained by differences in the effects of morphine-like and fentanyl-like drugs on μ_1 and μ_2 opioid receptors.

Alternatively, morphine-like and fentanyl-like drugs may act on isoforms of μ-opioid receptors with similar ligand-binding properties but coupled to different transducer proteins and effector mechanisms, as recently proposed for the

variants of EP_3 prostanoid receptors (see Milligan, 1993 for a review). Several facts support this idea. Firstly, μ-opioid receptors may exist in at least two different forms separately coupled to G_i and G_o proteins (Ueda *et al.*, 1988; 1990). Secondly, pertussis toxin and N-ethylmaleimide, two drugs that inactivate G_i/G_o proteins, differentially reduce the antinociception induced by several μ-opioid receptor agonists (Sanchez Blazquez & Garzón, 1988; 1991; Sanchez-Blazquez *et al.*, 1989). Thirdly, a $G_i2\alpha$ antisense oligodeoxyribonucleotide antagonizes morphine- but not sufentanil-induced antinociception (Raffa *et al.*, 1994).

Finally, μ-opioid receptor agonists show marked differences in their intrinsic activities (Zimmerman *et al.*, 1987; Adams *et al.*, 1990). These differences have been cited to explain the differential degree of cross-tolerance between the antinociceptive effects of several μ-opioid receptor agonists (Paronis & Holtzman, 1992), as well as the differential effects of lithium against morphine and sufentanil antinociception (Raffa *et al.*, 1992). However, these differences in intrinsic activity do not appear to explain our results. The intrinsic activity of the μ agonists tested is fentanyl>methadone>morphine=levorphanol>buprenorphine (Adams *et al.*, 1990; Zimmerman *et al.*, 1987). Therefore, fentanyl and levorphanol should have shown opposite sensitivities to K_{ATP} channel-acting drugs, but this was not seen.

In summary, we have found that a K_{ATP} channel blocker antagonizes, and a K_{ATP} channel opener enhances, the antinociception induced by morphine, methadone and buprenorphine; however, none of the K_{ATP} channel-acting drugs modified the antinociceptive effects of fentanyl or levorphanol. These results suggest that at least two μ-opioid receptor agonist subgroups, can be distinguished, which use different effector mechanisms to induce antinociception.

This study was supported in part by grants from CICYT (SAF 93-0559) and Laboratorios Dr. Esteve S.A. We thank Ms Karen Shashok for revising the English style of the manuscript.

References

ADAMS, J.U., PARONIS, C.A. & HOLTZMAN, G. (1990). Assessment of relative intrinsic activity of mu-opioid analgesics in vivo by using β-funaltrexamine. *J. Pharmacol. Exp. Ther.*, **255**, 1027–1032.

AMOROSO, S., SCHMID-ANTOMARCHI, H., FOSSET, M. & LAZDUNSKI, M. (1990). Glucose, sulfonylureas, and neurotransmitter release: Role of ATP-sensitive K^+ channels. *Science*, **247**, 852–854.

COOK, N.S. & QUAST, U. (1990). Potassium channel pharmacology. In *Potassium Channels: Structure, Classification, Function and Therapeutic Potential.* ed. Cook, N.S.. pp. 181–255. Chichester: Ellis Horwood Limited.

CRÉPEL, V., KRNJEVIC, K. & BEN-ARI, Y. (1993). Sulphonylureas reduce the slowly inactivating D-type outward current in rat hippocampal neurons. *J. Physiol.*, **466**, 39–54.

DRAY, A., NUNA, L. & WIRE, W. (1986). Meptazinol: unusual in vivo opioid receptor activity at supraspinal and spinal sites. *Neuropharmacology*, **25**, 343–349.

EDWARDS, G. & WESTON, A.H. (1993). The pharmacology of ATP-sensitive potassium channels. *Annu. Rev. Pharmacol. Toxicol.*, **33**, 597–637.

HALEY, T.J. & MCCORMICK, W.G. (1957). Pharmacological effects produced by intracerebral injection of drugs in the conscious mouse. *Br. J. Pharmacol. Chemother.*, **12**, 12–15.

HALLIWELL, J.V. (1990). K^+ channels in the central nervous system. In *Potassium Channels: Structure, Classification, Function and Therapeutic Potential.* ed. Cook, N.S. pp. 348–381. Chichester: Ellis Horwood Limited.

HEYMAN, J.S., WILLIAMS, C.L., BURKS, T.F., MOSBERG, H.I. & PORRECA, F. (1988). Dissociation of opioid antinociception and central gastrointestinal propulsion in the mouse: studies with naloxonazine. *J. Pharmacol. Exp. Ther.*, **245**, 238–243.

HEYMAN, J.S., VAUGHT, J.L., MOSBERG, H.I., HAASETH, R.C. & PORRECA, F. (1989). Modulation of μ-mediated antinociception by δ agonists in the mouse: selective potentiation of morphine and normorphine by [D-Pen^2,D-Pen^5]enkephalin. *Eur. J. Pharmacol.*, **164**, 1–10.

JANG, Y. & YOBURN, B.C. (1991). Evaluation of receptor mechanisms mediating fentanyl analgesia and toxicity. *Eur. J. Pharmacol.*, **197**, 135–141.

JIANG, Q., MOSBERG, H.I. & PORRECA, F. (1990). Modulation of the potency and efficacy of mu-mediated antinociception by delta agonists in the mouse. *J. Pharmacol. Exp. Ther.*, **254**, 683–689.

LING, G.S.F., SPIEGEL, K., LOCKHART, S.H. & PASTERNAK, G.W. (1985). Separation of opioid analgesia from respiratory depression: evidence for different receptor mechanisms. *J. Pharmacol. Exp. Ther.*, **232**, 149–155.

LONGMAN, S.D. & HAMILTON, T.C. (1992). Potassium channel activator drugs: mechanism of action, pharmacological properties, and therapeutic potential. *Med. Res. Rev.*, **12**, 73–148.

MAGNAN, J., PATERSON, S.J., TAVANI, A. & KOSTERLITZ, H.W. (1982). The binding spectrum of narcotic analgesic drugs with different agonist and antagonist properties. *Naunyn Schmied Arch. Pharmacol.*, **319**, 197–205.

MILLIGAN, G. (1993). Mechanisms of multifunctional signalling by G protein-linked receptors. *Trends Pharmacol. Sci.*, **14**, 239–244.

NARITA, M., SUZUKI, T., MISAWA, M., NAGASE, H., NABESHIMA, A., ASHIZAWA, T., OZAWA, H., SAITO, T. & TAKAHATA, N. (1992a). Role of central ATP-sensitive potassium channels in the analgesic effect and spinal noradrenaline turnover-enhancing effect of intracerebroventricularly injected morphine in mice. *Brain Res.*, **596**, 209–214.

NARITA, M., SUZUKI, T., MISAWA, M. & NAGASE, H. (1992b). Role of central ATP-sensitive potassium channels in the hyperthermic effect of morphine in mice. *Psychopharmacology*, **109**, 239–240.

NARITA, M., TAKAHASHI, Y., SUZUKI, T., MISAWA, M. & NAGASE, H. (1993). An ATP-sensitive potassium channel blocker abolishes the potentiating effect of morphine on the bicuculline-induced convulsion in mice. *Psychopharmacology*, **110**, 500–502.

NARITA, M., TAKAMORI, K., KAWASHIMA, N., FUNADA, M., KAMEI, J., SUZUKI, T., MISAWA, M. & NAGASE, H. (1993b). Activation of central ATP-sensitive potassium channels produces the antinociception and spinal noradrenaline turnover-enhancing effect in mice. *Psychopharmacology*, **113**, 11–14.

NORTH, R.A. (1989). Drug receptors and the inhibition of nerve cells. *Br. J. Pharmacol.*, **98**, 13–28.

NORTH, R.A. & WILLIAMS, J.T. (1985). On the potassium conductance increased by opioids in rat locus coeruleus neurones. *J. Physiol.*, **364**, 265–280.

OCAÑA, M. & BAEYENS J.M. (1993). Differential effecs of K^+ channel blockers on antinociception induced by α_2-adrenoceptor, $GABA_B$ and κ-opioid receptor agonists. *Br. J. Pharmacol.*, **110**, 1049–1054.

OCAÑA, M., DEL POZO, E. & BAEYENS, J.M. (1993a). ATP-dependent K^+ channel blockers antagonize morphine- but not U-50488H-induced antinociception. *Eur. J. Pharmacol.*, **230**, 203–207.

OCAÑA, M., DEL POZO, E. & BAEYENS, J.M. (1993b). Gliquidone, an ATP-dependent K^+ channel antagonist, antagonizes morphine-induced hypermotility. *Eur. J. Pharmacol.*, **239**, 253–255.

OCAÑA, M., DEL POZO, E., BARRIOS, M., ROBLES, L.I. & BAEYENS, J.M. (1990). An ATP-dependent potassium channel blocker antagonizes morphine analgesia. *Eur. J. Pharmacol.*, **186**, 377-378.

PARONIS, C.A. & HOLTZMAN, S.G. (1992). Development of tolerance to the analgesic activity of mu agonists after continuous infusion of morphine, meperidine and fentanyl. *J. Pharmacol. Exp. Ther.*, **262**, 1–9.

PASTERNAK, G.W. (1988). Multiple morphine and enkephalin receptors and the relief of pain. *J. Am. Med. Ass.*, **259**, 1362-1367.

PAUL, D., BODNAR, R.J., GISTRAK, M.A. & PASTERNAK, G.W. (1989). Different μ receptor subtypes mediate spinal and supraspinal analgesia in mice. *Eur. J. Pharmacol.*, **168**, 307–314.

PICK, C.G., NEJAT, R.J. & PASTERNAK, G.W. (1993). Independent expression of two pharmacologically distinct supraspinal mu analgesic systems in genetically different mouse strains. *J. Pharmacol. Exp. Ther.*, **265**, 166–171.

RAFFA, R.B., CONNELLY, C.D. & MARTINEZ, R.P. (1992). Opioid efficacy is linked to the LiCl-sensitive, inositol-1,4,5-triphosphate-restorable pathway. *Eur. J. Pharmacol.*, **217**, 221–223.

RAFFA, R.B., MARTINEZ, R.P. & CONNELLY, C.D. (1994). G-protein antisense oligodeoxyribonucleotides and μ-opioid supraspinal antinociception. *Eur. J. Pharmacol.*, **258**, R5–R7.

REEVE, H.L., VAUGHAN, P.F.T. & PEERS, C. (1992). Glibenclamide inhibits a voltage-gated K^+ current in the human neuroblastoma cell line SH-SY5Y. *Neurosci. Lett.*, **135**, 37–40.

ROANE, D.S. & BOYD, N.E. (1993). Reduction of food intake and morphine analgesia by central glybenclamide. *Pharmacol. Biochem. Behav.*, **46**, 205–207.

SANCHEZ-BLAZQUEZ, P. & GARZON, J. (1988). Pertussis toxin differentially reduces the efficacy of opioids to produce supraspinal analgesia in the mouse. *Eur. J. Pharmacol.*, **152**, 357–361.

SANCHEZ-BLAZQUEZ, P. & GARZON, J. (1991). Cholera toxin and pertussis toxin on opioid- and α_2-mediated supraspinal analgesia in mice. *Life Sci.*, **48**, 1721–1727.

SANCHEZ-BLAZQUEZ, P., ULIBARRI, I. & GARZON, J. (1989). Intracerebroventricular N-ethylmaleimide differentially reduced supraspinal opioid analgesia in mice. *Eur. J. Pharmacol.*, **166**, 193–200.

SCHMID-ANTOMARCHI, H., AMOROSO, S., FOSSET, M. & LAZDUNSKI, M. (1990). K^+ channel openers activate brain sulfonylurea-sensitive K^+ channels and block neurosecretion. *Proc. Natl. Acad. Sci. U.S.A.*, **87**, 3489–3492.

SHELDON, R.J., NUNAN, L. & PORRECA, F. (1987) Mu antagonist properties of kappa agonists in a model of rat urinary bladder motility in vivo. *J. Pharmacol. Exp. Ther.*, **243**, 234–240.

SHELDON, R.J., NUNAN, L. & PORRECA, F. (1988a). U50,488H differentially antagonizes the bladder effects of μ agonists at spinal sites. *Eur. J. Pharmacol.*, **146**, 229–235.

SHELDON, R.J., NUNAN, L. & PORRECA, F. (1988b). Differential modulation by [D-Pen^2,D-Pen^5]enkephalin and dynorphin A-(1-17) of the inhibitory bladder motility effects of selected mu agonists in vivo. *J. Pharmacol. Exp. Ther.*, **249**, 462–469.

STATILE, L., PUIG, M.M., WARNER, W., BANSINATH, M., LOVITZ, M. & TURNDORF, H. (1988). Droperidol enhances fentanyl and sufentanil, but not morphine, analgesia. *Gen. Pharmacol.*, **19**, 451–454.

TALLARIDA, R.J. & MURRAY, R.B. (1987). *Manual of Pharmacologic Calculations with Computer Programs.* Berlin: Springer.

UEDA, H., HARADA, H., NOZAKI, M., KATADA, T., UI, M., SATOH, M. & TAKAGI, H. (1988). Reconstitution of rat brain mu opioid receptors with purified guanine nucleotide binding regulatory proteins, G_i and G_o. *Proc. Natl. Acad. Sci. U.S.A.*, **85**, 7013–7017.

UEDA, H., MISAWA, H., KATADA, T., UI, M., TAKAGI, H. & SATOH, M. (1990). Functional reconstruction of purified G_i and G_o with mu-opioid receptors in guinea pig striatal membranes pretreated with micromolar concentrations of N-ethylmaleimide. *J. Neurochem.*, **54**, 841–848.

VERGONI, A.V., SCARANO, A. & BERTONINI, A. (1992). Pinacidil potentiates morphine analgesia. *Life Sci.*, **50**, PL135–PL138.

WELCH, S.P. & DUNLOW, L.D. (1993). Antinociceptive activity of intrathecally administered potassium channel openers and opioid agonists: a common mechanism of action? *J. Pharmacol. Exp. Ther.*, **267**, 390–399.

WILD, K.D., VANDERAH, T., MOSBERG, H.I. & PORRECA, F. (1991). Opioid δ receptor subtypes are associated with different potassium channels. *Eur. J. Pharmacol.*, **193**, 135–136.

ZIMMERMANN, M. (1983). Ethical guidelines for investigations of experimental pain in conscious animals. *Pain*, **16**, 109–110.

ZIMMERMAN, D.M., LEANDER, J.D., REEL, J.K. & HYNES, M.D. (1987). Use of β-funaltrexamine to determine mu opioid receptor involvement in the analgesic activity of various opioid ligands. *J. Pharmacol. Exp. Ther.*, **241**, 374–378.

(Received June 1, 1994
Revised November 3, 1994
Accepted November 28, 1994)

British Journal of Pharmacology (1995) 114, 1303-1309

The effect of nitric oxide donors on haemodynamics and blood flow distribution in the porcine carotid circulation

[1]E. Marcel van Gelderen, Emile L.E. De Bruijne, Hendrik J. Agteresch & [2]Pramod R. Saxena

Department of Pharmacology, Dutch Migraine Research Group, Cardiovascular Research Institute COEUR, Faculty of Medicine and Health Sciences, Erasmus University Rotterdam, P.O. Box 1738, 3000 DR Rotterdam, The Netherlands

1 The role of nitric (NO) in the regulation of capillary and arteriovenous anastomotic blood flow was evaluated in the carotid circulation of the pig. For this purpose, the effect of intracarotid (i.c.) infusions of saline and two NO donors, nitroprusside sodium (NPR) and S-nitroso-*N*-acetylpenicillamine (SNAP) in concentrations of 3–100 $\mu g\,min^{-1}$ was studied on systemic haemodynamics and carotid blood flow and its distribution in anaesthetized pigs with low arteriovenous anastomotic blood flow, by use of the radioactive microsphere method.

2 Apart from heart rate, which increased after both NPR and SNAP, no major changes in systemic haemodynamic variables were observed. In contrast to saline, both NPR and SNAP increased common carotid blood flow, vascular conductance and vascular pulsations dose-dependently.

3 The distribution of the carotid artery blood flow over capillary and arteriovenous anastomotic fraction remained stable after saline infusions. Both NPR and SNAP enhanced total capillary blood flow and conductance. In contrast to NPR, arteriovenous anastomotic blood flow and conductance were increased by SNAP.

4 At the tissue level, capillary blood flow increases following NPR or SNAP were reflected by an increase in both extracerebral and dural blood flow without changes in total brain blood flow.

5 These results indicate that both NO donors cause arteriolar dilatation together with enhanced vascular pulsations in the carotid circulation of the pig. Probably by way of a 'steal' phenomenon, this pronounced arteriolar dilatation limits the effect of NO donors on arteriovenous anastomoses.

6 The results of the present investigation support the contention that dilatation of intra- and extracranial arteries and arteriovenous anastomoses leads to increased vascular pulsations, which (rather than increased blood flow) could, at least in part, be responsible for the headache caused by nitrovasodilators.

Keywords: Arteriovenous anastomoses; endothelium; headache; migraine; nitric oxide; sodium nitroprusside; pig carotid circulation; S-nitroso-*N*-acetylpenicillamine

Introduction

Nitric oxide (NO) released from endothelial cells by numerous stimuli participates in the regulation of vascular tone (see Moncada *et al.*, 1991). A dilatation of large (extra) cranial arteries and arteriovenous anastomoses has been implicated in the pathogenesis of migraine, though the mechanism involved is not fully clear (Saxena, 1978; 1994; Humphrey & Feniuk, 1991; Ferrari & Saxena, 1993). Recent observations in both animals and man have led to the suggestion that NO may also be involved in migraine. Inhibition of NO-biosynthesis resulted in a reduced blood flow through systemic and cranial arteriovenous anastomoses of the pig, thus indicating a NO-dependent vasodilator tone in these shunt vessels (Van Gelderen *et al.*, 1993; Van Gelderen & Saxena, 1994a). Histamine, known to relax isolated cranial blood vessels via release of NO from vascular endothelium (Toda, 1990; Fujiwara *et al.*, 1992), induced pulsatile headache in migraine patients (Krabbe & Olesen, 1980). Nitrovasodilators, such as nitroglycerin and isosorbide mononitrate, which are generally thought to act as NO donors, caused dose-dependent temporal artery dilatations and headache in man (Iversen, 1992; Iversen *et al.*, 1992). Moreover, patients with migraine appeared to be more sensitive to nitroglycerin as demonstrated by a more pronounced headache and cerebral artery dilatation relative to non-migraine subjects (Olesen *et al.*, 1993; Thompson *et al.*, 1993).

The present investigation was devoted to study the effect of NO donors on the carotid haemodynamics and the distribution of the common carotid artery blood flow over arteriovenous and capillary (tissue) fractions in the anaesthetized pig. Some reports suggest that S-nitrosothiols may account, as an intermediate, for the NO-induced vasorelaxant actions (Ignarro, 1990; Myers *et al.*, 1990; Rubanyi *et al.*, 1991). Therefore, we investigated both sodium nitroprusside (NPR), known to release NO spontaneously (Feelisch & Noack, 1987), and the NO-'precursor' S-nitroso-*N*-acetylpenicillamine (SNAP; Ignarro *et al.*, 1981). To preserve the constrictor tone in cranial arteriovenous anastomoses, necessary to study mechanisms involved in opening arteriovenous anastomoses, a recently described anaesthetic regimen was used (Den Boer *et al.*, 1993).

Some of these results were presented at the winter meeting of the British Pharmacological Society (Van Gelderen *et al.*, 1994).

Methods

General

Domestic pigs (Yorkshire × Landrace; 15–17 kg) were anaesthetized with i.m. injection of ketamine (25 $mg\,kg^{-1}$) and midazolam (0.3 $mg\,kg^{-1}$). Following injection of thiopentone (6 $mg\,kg^{-1}$), the animals were intubated and connected to a respirator (Bear 2E, BeMeds AG, Baar, Switzerland) for

[1] Author for reprint request.
[2] Author for correspondence.

intermittent positive pressure ventilation with a mixture of room air and oxygen. By adjusting oxygen supply, respiratory rate and tidal volume, arterial blood gas values were kept within physiological range (pH 7.39–7.49; P_{CO_2} 37–44; P_{O_2} 100–130). Anaesthesia was maintained by a continuous i.v. infusion with a mixture of fentanyl (18–38 $\mu g\,kg^{-1}\,h^{-1}$) and thiopentone (6–12 $mg\,kg^{-1}\,h^{-1}$). Due to differences in sensitivity of individual animals, infusion rate was adjusted in each animal according to two criteria: (i) absence of blinking reflex, indicative of appropriate anaesthesia and (ii) venous oxygen saturation values below 60%, indicative of low arteriovenous anastomotic blood flow.

A catheter was introduced into the aortic arch via the left femoral artery, connected to a pressure transducer (Statham P23, Hato Rey, Puerto Rico) for measurement of arterial blood pressure and blood sample withdrawal to determine blood gases (ABL-510, Radiometer, Copenhagen, Denmark). Cardiac output and pulmonary arterial blood pressure were measured with a 6F-Swan-Ganz thermodilution catheter (Corodyn, Braun Melsungen AG, Melsungen, Germany) introduced into the pulmonary artery via the left femoral vein and connected to a cardiac output computer (WTI, Rotterdam, The Netherlands) as well as to a pressure transducer. Mean arterial (MAP) and mean pulmonary artery (MPAP) pressures were calculated from respectively systolic (SBP) and diastolic (DBP) blood pressures as: MAP or MPAP = DBP = (SBP-DBP)/3. Heart rate was triggered from the blood pressure signals using a tachograph as well as counted directly from these signals over a 30 s recording interval. Systemic vascular conductance was calculated by dividing cardiac output by MAP. The right common carotid artery was dissected free and the total carotid blood flow on the ipsilateral side was measured with a flow probe (internal diameter: 2.5 or 3 mm) connected to a sine-wave electromagnetic flow meter (Transflow 600-system, Skalar, Delft, The Netherlands). Vascular pulsations were calculated from the flow signals as the difference in systolic and diastolic blood flow values. Two hubless needles (external diameter 0.5 mm), bent at right angles and connected to a polyethylene tubing, were inserted into the common carotid artery against the direction of the blood flow for administration of radioactive microspheres or drugs. The right jugular vein was cannulated to collect venous blood samples to determine venous blood gases. All catheters were filled with a heparin sodium solution (80 iu ml^{-1}) to prevent blood clotting. During the experiment, physiological saline was infused to compensate for fluid loss and body temperature was kept between 37–38°C. The animals were allowed to stabilize for at least 45 min before the start of experiments.

Distribution of common carotid artery blood flow

The distribution of common carotid artery blood flow was measured using repeated injections of radioactive microspheres (mean ± s.d. diameter: 15 ± 1 μm; NEN Company, Dreieich, Germany) with different labels (^{141}Ce, ^{113}Sn, ^{103}Ru, ^{95}Nb or ^{46}Sc) (Johnston & Saxena, 1978). A suspension of approximately 250,000 microspheres was vortexed before each measurement and injected into the common carotid artery against the direction of the blood flow to ensure uniform mixing. At the end of the experiment the animals were killed and the heart, kidneys, lungs and the different intra- and extracranial tissues were dissected out, weighed and put in vials. The radioactivity in these vials was counted for 10 min in a γ-scintillation counter (Packard, Minaxi Autogamma 5000) using suitable windows for discriminating between the different isotypes. Radioactivity was counted in entire tissues, except in the case of bone, fat and skin, where aliquots (more than 50% of total weight) were analysed.

Tissue (capillary) blood flow was calculated by multiplying the ratio of tissue and total radioactivity by total carotid blood flow at the time of injection. Since radioactivity was absent in the heart and kidneys, all radioactive microspheres reaching the venous side of the circulation had passed through arteriovenous anastomoses to be ultimately sieved in the lungs (see Johnston & Saxena, 1978; Saxena & Verdouw, 1982). Therefore, the amount of radioactivity in the lungs represents the arteriovenous anastomotic fraction of common carotid blood flow.

Experimental protocol

After the stabilization period, animals were randomly assigned to either control or treatment groups. At the start of the experiments, baseline haemodynamic parameters, blood gases as well as the distribution of the common carotid artery blood flow were measured. Thereafter, the first group was treated four times with i.c. infusions of saline (control; $n = 6$). The second group was treated with either three (10, 30, 100 $\mu g\,min^{-1}$; $n = 4$) or four increasing doses of NPR (3, 10, 30 and 100 $\mu g\,min^{-1}$; $n = 4$). In the third group, the potential effect of the solvent (20% v/v ethanol in saline) was measured, followed by three doses of SNAP (3, 10, 30 $\mu g\,min^{-1}$; $n = 6$). Additionally in this group, three animals were treated with SNAP (100 $\mu g\,min^{-1}$) to determine the effect on carotid and systemic haemodynamic values. The amount of ethanol infused during the experimental period (75 min) ranged from 0.97 to 1.1 ml, depending on the weight of the animal. Since solvent infusion did not induce significant effects, SNAP-induced responses were compared with responses observed in the saline (control) group. In all groups, infusion rate (125 $\mu l\,min^{-1}$ 15 kg^{-1}) was adjusted to correct for differences in animal weight. Each dose was infused for 15 min in which time period the carotid blood flow signal and systemic haemodynamic parameters stabilized; during the last 5 min of each infusion all parameters were reassessed and blood samples collected.

Data presentation and analysis

All data, calculated with a personal computer (Olivetti PCS 286) using a set of specially developed computer programmes (Saxena *et al.*, 1980), are presented in the text as mean ± s.e.mean. The effect of treatment was analysed in each group by repeated measurement analysis of variance. When the samples represented different populations, the values after the different treatments were compared to baseline values by use of Duncan's new multiple range test. Subsequently, the percentage changes from baseline values among the groups were tested by Duncan's test for multiple comparisons. Statistical significance was accepted at a level of $P \leqslant 0.05$.

Chemicals

The chemicals used in this study were: fentanyl citrate (Janssen Pharmaceutica, Beerse, Belgium), heparin sodium (Heparin Leo, LEO pharmaceutical products B.V., Weesp, The Netherlands), ketamine HCl (Apharmo, Arnhem, The Netherlands), midazolam (Dormicum, Roche, Mijdrecht, The Netherlands), nitroprusside sodium (Pharmacy Department, University Hospital Dijkzigt, Rotterdam, The Netherlands), S-nitroso-*N*-acetylpenicillamine (SNAP; RBI, Natick, U.S.A.), thiopentone sodium (Rhône-Poulenc Rorer, Amstelveen, The Netherlands). All chemicals were dissolved in sterile saline, except fentanyl citrate and SNAP. Fentanyl citrate was dissolved in propylene glycol and subsequently diluted in distilled water. SNAP was dissolved in a mixture containing 20% v/v ethanol (70%) in saline to reach a concentration of 100 μg 125 μl^{-1} (highest dose used). This stock solution was subsequently diluted with sterile saline to obtain the lower concentrations (3, 10 and 30 $\mu g\,ml^{-1}$). All doses refer to their respective salts.

Results

Systemic haemodynamics

The systemic haemodynamic variables of all groups at baseline and followed by either saline, solvent, NPR or SNAP are depicted in Table 1. There were no significant differences between the three groups in systemic haemodynamic values at baseline. Neither saline nor solvent (ethanol/saline, 20% v/v) induced any change in the systemic haemodynamic variables. Both NPR (100 $\mu g\,min^{-1}$) and SNAP (30 and 100 $\mu g\,min^{-1}$) increased heart rate significantly; with the highest dose heart rate increased by $57 \pm 15\%$ and $44 \pm 17\%$, respectively. Mean arterial blood pressure tended to decrease following NPR and SNAP, being significantly different from baseline values with the highest dose of NPR only. Neither drug significantly affected other systemic haemodynamic variables.

Carotid haemodynamics

Carotid blood flow remained stable throughout the saline infusions (Figure 1). Likewise, no changes were observed in baseline carotid blood flow (52 ± 6 ml min^{-1}) in the SNAP group following solvent infusion (51 ± 8 ml min^{-1}; not shown in figure). Both NPR and SNAP induced a dose-dependent increase in carotid blood flow. The maximum increase from baseline, observed with the highest dose (100 $\mu g\,min^{-1}$) of the two compounds, was $79 \pm 9\%$ and $85 \pm 18\%$, respectively. The increase in carotid blood flow was associated partly with enhanced vascular pulsations, which were increased from baseline by a maximum of $59 \pm 17\%$ (NPR) and $109 \pm 45\%$ (SNAP) (Figure 1).

At baseline, $23 \pm 4\%$ ($n = 20$) of the total carotid blood flow was shunted through arteriovenous anastomoses and no differences between groups were observed. The extent of shunting in pigs anaesthetized with fentanyl and thiopentone is much less than that (~75%) previously observed in pigs anaesthetized with pentobarbitine (Saxena & Verdouw, 1982; Den Boer *et al.*, 1990; Villalón *et al.*, 1990; Van Gelderen & Saxena, 1994a). The NPR-induced carotid blood flow increase was reflected by a dose-dependent increase in total capillary blood flow; maximum increase from baseline was $100 \pm 11\%$. No changes were observed in the arteriovenous anastomotic fraction (Figure 2). In contrast to NPR, SNAP increased both total capillary blood flow and arteriovenous anastomotic blood flow. Total capillary blood flow was increased by $71 \pm 19\%$ from baseline, being significantly different from saline-treated animals from 10 $\mu g\,min^{-1}$ onwards. Arteriovenous anastomotic blood flow increased significantly from baseline following SNAP (10 and 30 $\mu g\,min^{-1}$); the maximum increase ($245 \pm 151\%$) was observed with the highest dose (Figure 2).

Both NPR and SNAP increased carotid vascular conductance from baseline by a maximum of $127 \pm 15\%$ and $178 \pm 66\%$, respectively; being significantly different from the saline group from 10 $\mu g\,min^{-1}$ onwards (Figure 3). Arteriovenous anastomotic conductance was essentially unaffected by NPR (maximum increase $72 \pm 40\%$; NS), whereas SNAP enhanced the conductance significantly from

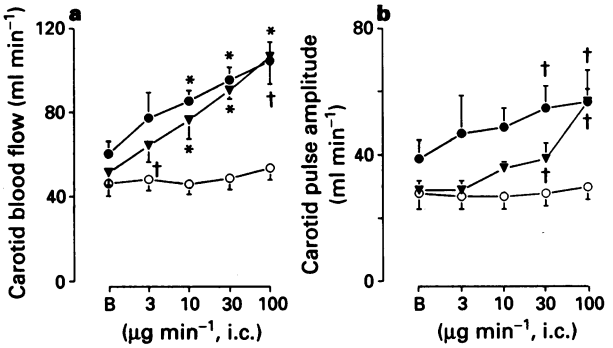

Figure 1 Carotid blood flow (a) and pulse amplitude (b) at baseline (B) and after intracarotid infusions with either saline (125 $\mu l\,min^{-1}$, 4 times; $n = 6$), sodium nitroprusside (NPR; 3 $\mu g\,min^{-1}$, $n = 4$, and 10, 30 and 100 $\mu g\,min^{-1}$, $n = 8$ each) or S-nitroso-*N*-acetylpenicillamine (SNAP; 3, 10, 30 $\mu g\,min^{-1}$; $n = 6$ each, and 100 $\mu g\,min^{-1}$; $n = 3$). In case of SNAP solvent values (not shown) were not different from baseline values. In both panels, (○), (●) and (▼) represent saline, NPR and SNAP, respectively. Values are given as mean ± s.e.mean. †$P < 0.05$ versus baseline (B); *$P < 0.05$ versus saline.

Table 1 Systemic haemodynamic variables measured at baseline and after intracarotid infusions with saline (control; $n = 6$), nitroprusside sodium (NPR; $n = 8$, except 3 $\mu g\,min^{-1}$ $n = 4$) and solvent (S) followed by S-nitroso-*N*-acetylpenicillamine (SNAP; $n = 6$, except 100 $\mu g\,min^{-1}$ $n = 3$)

			Saline, NPR or SNAP ($\mu g\,min^{-1}$)			
	Baseline	*S*	*3*	*10*	*30*	*100*
HR (beats min^{-1})						
Saline	77 ± 7	–	77 ± 7	79 ± 8	81 ± 9	81 ± 10
NPR	85 ± 5	–	87 ± 10	88 ± 5	98 ± 4	130 ± 12*†
SNAP	80 ± 8	81 ± 8	87 ± 10	100 ± 19	117 ± 19†	124 ± 27†
MAP (mmHg)						
Saline	94 ± 5	–	93 ± 6	93 ± 6	91 ± 6	89 ± 7
NPR	91 ± 5	–	90 ± 5	86 ± 5	81 ± 5	74 ± 6†
SNAP	82 ± 3	84 ± 6	88 ± 7	85 ± 6	74 ± 6	74 ± 10
MPAP (mmHg)						
Saline	21 ± 1.4	–	22 ± 1.2	22 ± 1.2	22 ± 1.3	22 ± 1.4
NPR	23 ± 0.6	–	22 ± 1.5	22 ± 1.0	22 ± 0.9	20 ± 1.0
SNAP	20 ± 0.8	21 ± 1	21 ± 0.7	20 ± 1.1	19 ± 1.3	20 ± 1.9
CO (l min^{-1})						
Saline	1.4 ± 0.1	–	1.4 ± 0.1	1.4 ± 0.2	1.4 ± 0.2	1.5 ± 0.2
NPR	1.7 ± 0.2	–	1.7 ± 0.3	1.7 ± 0.2	1.8 ± 0.2	1.9 ± 0.2
SNAP	1.4 ± 0.1	1.3 ± 0.1	1.3 ± 0.1	1.3 ± 0.1	1.4 ± 0.1	1.9 ± 0.2
SVC (ml min^{-1} $mmHg^{-1}$)						
Saline	15 ± 1	–	15 ± 1	15 ± 2	15 ± 2	16 ± 1
NPR	19 ± 2	–	19 ± 4	21 ± 3	22 ± 2	26 ± 3
SNAP	17 ± 2	16.2	15 ± 1	16 ± 3	19 ± 1	26 ± 2

Data are given as mean ± s.e.mean. †$P < 0.05$ versus baseline; *$P < 0.05$ versus saline. HR, heart rate; MAP, mean arterial blood pressure; MPAP, mean pulmonary artery pressure; CO, cardiac output; SVC, systemic vascular conductance.

baseline by 284 ± 160%. Total capillary conductance was equally increased by NPR and SNAP; 30 μg min^{-1} of either NPR or SNAP increased conductance by 89 ± 7% and 91 ± 21%, respectively (Figure 3).

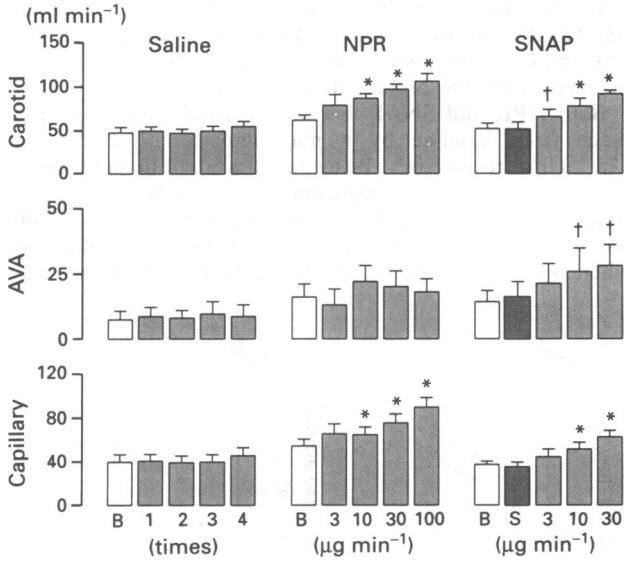

Figure 2 Total carotid, arteriovenous anastomotic (AVA) and capillary blood flow at baseline (B) and after intracarotid infusions with either saline (125 μl min^{-1}, 4 times; $n = 6$), sodium nitroprusside (NPR; 3 μg min^{-1}; $n = 4$, and 10, 30 and 100 μg min^{-1}; $n = 8$ each) or S-nitroso-*N*-acetylpenicillamine (SNAP; 3, 10 and 30 μg min^{-1}; $n = 6$). In each set of panels, open and hatched columns represent baseline values and values after increasing doses of saline, NPR or SNAP, respectively; in the case of SNAP cross-hatched columns represent values after the solvent (S). Data are given as mean ± s.e.mean. †$P < 0.05$ versus baseline; *$P < 0.05$ versus saline.

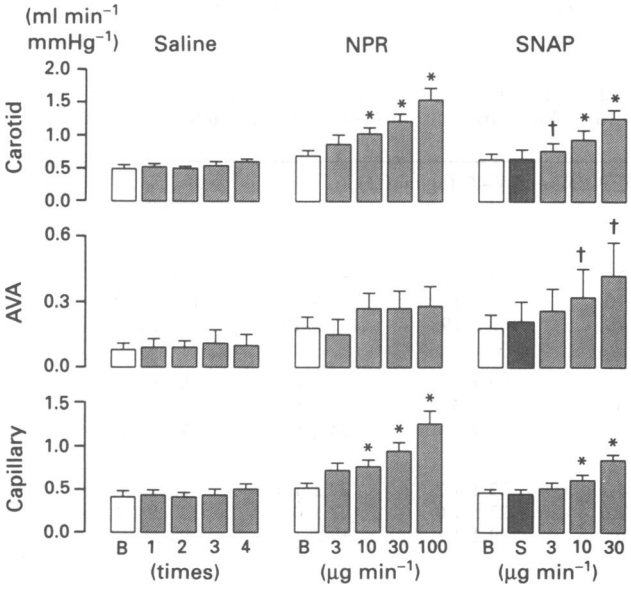

Figure 3 Total carotid, arteriovenous anastomotic (AVA) and capillary conductance at baseline (B) and after intracarotid infusions with either saline (125 μl min^{-1}, 4 times; $n = 6$), sodium nitroprusside (NPR; 3 μg min^{-1}; $n = 4$, and 10, 30 and 100 μg min^{-1}; $n = 8$ each) or S-nitroso-*N*-acetylpenicillamine (SNAP; 3, 10 and 30 μg min^{-1}; $n = 6$). In each set of panels, open and hatched columns represent baseline values and values after increasing doses of saline, NPR or SNAP, respectively; in the case of SNAP cross-hatched columns represent values after the solvent (S). Data are given as mean ± s.e.mean. †$P < 0.05$ versus baseline; *$P < 0.05$ versus saline.

Regional carotid blood flow

As depicted in Figure 4, neither saline infusions nor solvent infusion affected blood flow distribution to either the total brain, extracerebral or dural tissues. Both NPR and SNAP failed to affect total brain blood flow. In contrast, a significant increase in extracerebral blood flow was observed following NPR (10, 30 and 100 μg min^{-1}) and SNAP (10 and 30 μg min^{-1}); maximum increases were 106 ± 12% and 84 ± 17%, respectively. Dural blood flow was enhanced dose-dependently by NPR, 30 and 100 μg min^{-1}, with a maximum increase of 368 ± 96%. Likewise, SNAP (10 and 30 μg min^{-1}) enhanced dural blood flow from baseline (154 ± 57%).

A number of extracerebral tissues (bones, ear, muscle and skin) showed enhanced blood flows following both NPR and SNAP (Figure 5). Furthermore, SNAP increased blood flow to the fat (Figure 5) and to the eyes from a baseline value of 30 ± 5 ml min^{-1} to a maximum of 75 ± 20 ml min^{-1} with the highest dose (100 μg min^{-1}).

Arteriovenous oxygen saturation difference

In all groups, venous oxygen and carbon dioxide tension remained stable throughout the experiments. In contrast to saline, NPR and SNAP reduced the arterial partial oxygen pressure by 24 ± 2% and 9 ± 2%, respectively (Table 2). The difference in arteriovenous oxygen saturation was reduced from baseline with the highest dose of NPR, whereas no changes were observed in either saline- or SNAP-treated animals (Table 2).

Discussion

General

This study aimed to investigate the effect of exogenous NO on the carotid circulation of the anaesthetized pig with low arteriovenous anastomotic blood flow. In the conscious state

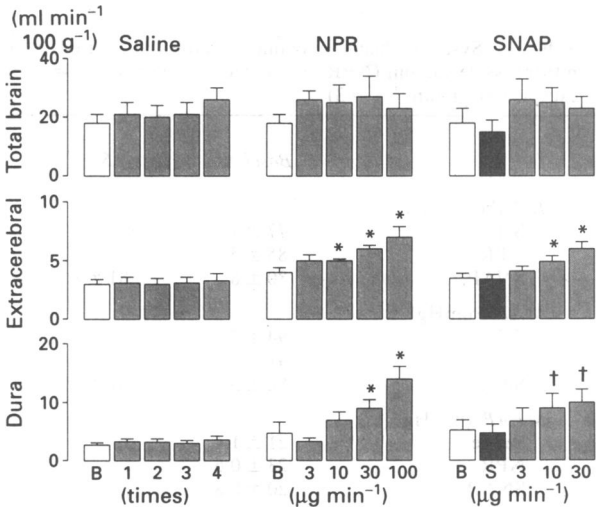

Figure 4 Blood flow distribution to cerebral and extracerebral tissues and to dura mater at baseline (B) and after intracarotid infusions with either saline (125 μl min^{-1}, 4 times; $n = 6$), sodium nitroprusside (NPR; 3 μg min^{-1}; $n = 4$, and 10, 30 and 100 μg min^{-1}; $n = 8$ each) or S-nitroso-*N*-acetylpenicillamine (SNAP; 3, 10 and 30 μg min^{-1}; $n = 6$). In each set of panels, open and hatched columns represent baseline values and values after increasing doses of saline, NPR or SNAP, respectively; in the case of SNAP cross-hatched columns represent values after the solvent (S). Data are given as mean ± s.e.mean. †$P < 0.05$ versus baseline; *$P < 0.05$ versus saline.

arteriovenous anastomoses are under a predominantly sympathetic constrictor tone and, as a consequence, less than 5% of intracardially injected microspheres are sieved in the lungs (Van Woerkens *et al.*, 1990). During anaesthesia, arteriovenous shunting is increased substantially limiting comparison with conscious animals. Recently, a mixture of fentanyl and thiopentone was reported to preserve tone in arteriovenous anastomoses, enabling the investigation of effects on arteriovenous anastomoses under conditions which resemble the conscious state (Den Boer *et al.*, 1993). In accord with the latter study, we observed that approximately 20% of the carotid blood flow was directed to arteriovenous anastomoses. It is to be noted that, as seems to be the case in man (Heyck, 1969), basal arteriovenous shunting is higher in the carotid vascular bed than in the systemic vascular bed, which may be explained by the relatively greater skin area, together with higher density of arteriovenous anastomoses in the head skin, perfused by the carotid circulation (Saxena & Verdouw, 1985).

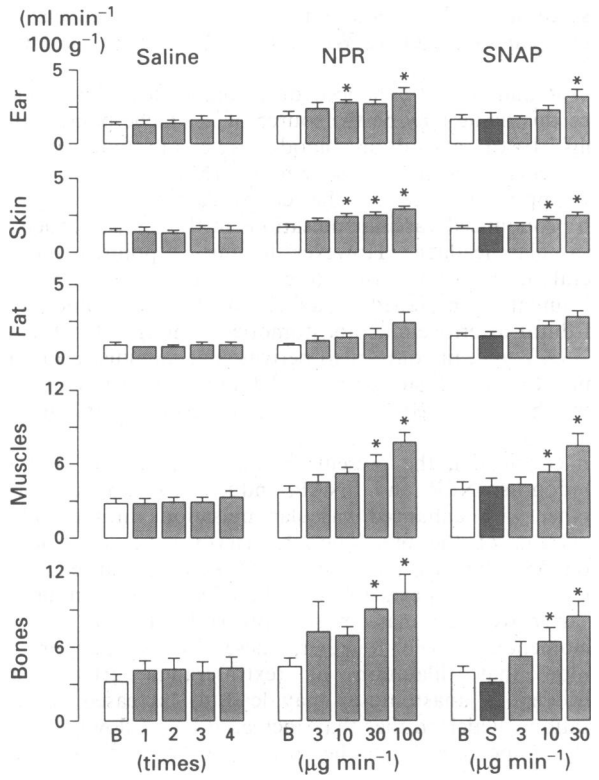

Figure 5 Blood flow to extracerebral tissues at baseline (B) and after intracarotid infusions with either saline (125 μl min^{-1}, 4 times; $n = 6$), nitroprusside sodium (NPR; 3 μg min^{-1}; $n = 4$, and 10, 30 and 100 μg min^{-1}; $n = 8$ each) or S-nitroso-*N*-acetylpenicillamine (SNAP; 3, 10 and 30 μg min^{-1}; $n = 6$). In each set of panels, open and hatched columns represent baseline values and values after increasing doses of saline, NPR or SNAP, respectively; in the case of SNAP, cross-hatched columns represent values after the solvent (S). Data are given as mean ± s.e.mean. *$P < 0.05$ versus baseline.

Systemic and carotid haemodynamics

Following intracarotid infusions of NPR and SNAP, systemic haemodynamic variables were not much affected indicating that the drug effects were primarily confined to the carotid part of the circulation. However, we cannot fully exclude a systemic contribution as heart rate increased (NPR: 100 μg min^{-1}; SNAP: 30 and 100 μg min^{-1}) and MAP tended to decrease with NPR. The increase in heart rate is probably reflex-mediated to compensate for the expected fall in systemic blood pressure, although additional effects may be involved. For example, hypercapnia is associated with tachycardia presumably via activation of chemoreceptors in the carotid body. Interestingly, NO synthase-containing fibres have been demonstrated in the carotid body of rats (Wang *et al.*, 1993; Höhler *et al.*, 1994) and cats (Prabhakar *et al.*, 1993). Moreover, NPR increases cyclic GMP formation in the carotid body arterioles (Wang *et al.*, 1991), whereas inhibition of the endogenous NO biosynthesis increases chemoreceptor outflow and reduces cyclic GMP formation (Prabhakar *et al.*, 1993). So far, it is not yet known whether exogenous NO stimulates chemoreceptors to reduce their outflow.

Both NO donors induced similar increases in carotid blood flow which were accompanied by enhanced vascular pulsations. Likewise, enhanced pulsatility was observed in the human carotid and cerebral artery with the NO donor nitroglycerin (MacDonald *et al.*, 1989; Thomsen *et al.*, 1993). The mechanism underlying these enhanced pulsations is not clear, but it may be related to changes in vascular compliance following vasodilatation. Since pulsatility is also increased by calcitonin gene-related peptide (MacDonald *et al.*, 1989; Van Gelderen & Saxena, 1994b), an exclusively NO-dependent phenomenon is precluded.

Carotid blood flow distribution

Both NPR and SNAP showed a similar arteriolar dilatation as reflected by the increase in capillary blood flow and conductance, whereas in contrast to NPR, only SNAP enhanced blood flow through arteriovenous anastomoses. The latter

Table 2 Arterial Po_2 (*A* Po_2), jugular venous blood Po_2 (*V* Po_2) and difference in arterial and jugular venous oxygen saturation, measured at baseline and after intracarotid injection of either saline (control; $n = 6$), nitroprusside sodium (NPR; $n = 8$, except 3 μg min^{-1} $n = 4$) and solvent (S) followed by S-nitroso-*N*-acetylpenicillamine (SNAP; $n = 6$)

			Saline, NPR or SNAP (μg min^{-1})			
	Baseline	*S*	*3*	*10*	*30*	*100*
A Po_2 (mmHg)						
Saline	121 ± 8	–	123 ± 7	121 ± 7	117 ± 7	114 ± 8
NPR	117 ± 4	–	119 ± 3	109 ± 4	103 ± 4†	89 ± 3†
SNAP	115 ± 4	116 ± 3	118 ± 5	109 ± 2	104 ± 3†	ND
V Po_2 (mmHg)						
Saline	37 ± 3	–	38 ± 2	39 ± 2	38 ± 2	37 ± 2
NPR	35 ± 2	–	39 ± 5	37 ± 2	38 ± 2	41 ± 3
SNAP	41 ± 6	39 ± 5	42 ± 6	40 ± 6	42 ± 5	ND
A-V o_2 *sat* (%)						
Saline	45 ± 7	–	42 ± 7	41 ± 6	42 ± 7	43 ± 6
NPR	50 ± 5	–	45 ± 10	42 ± 4	40 ± 4	35 ± 4†
SNAP	38 ± 9	38 ± 8	36 ± 9	37 ± 8	34 ± 7	ND

Data represent means ± s.e.mean. ND: not determined. †$P < 0.05$ versus baseline value.

finding is in accord with our previous observations demonstrating that endogenous NO may participate in the regulation of shunt flow in the carotid circulation (Van Gelderen & Saxena, 1994a). However, the lack of effect on arteriovenous anastomoses with NPR conflicts with this observation and the previously reported tendency of NPR to increase blood flow through systemic arteriovenous anastomoses in rabbits (Hof & Hof, 1989). This discrepancy may be explained partly by the concomitant rise in capillary blood flow which could lead to a redirection of carotid blood flow towards the capillaries to negate the increase in arteriovenous anastomotic blood flow ('steal' phenomenon). Recent experiments in man (Bruning, 1994) have shown that NPR, infused into the brachial artery but in a much lower concentration ($5\ ng\ kg^{-1}\ min^{-1}$), also failed to increase arteriovenous anastomotic blood flow in the fingers.

The differences observed in the present experiments between NPR and SNAP may be explained by differences in the amount of NO released from these compounds. At 37°C, approximately $0.2\ \mu mol\ min^{-1}$ is released spontaneously from NPR (Feelisch & Noack, 1987), whereas under similar conditions SNAP releases approximately six times more NO (Kodja *et al.*, 1994). Moreover, it has been suggested that nitrosothiols may be actively degraded at vascular membranes (Kowaluk & Fung, 1990) and SNAP has been shown to have an *in vitro* chemical half life of 70 min (Mathews & Kerr, 1993), although the rate of formation and degradation may differ significantly in biological fluids. Therefore, it is conceivable that following repeated infusions SNAP accumulates at arteriovenous anastomoses, thus providing sufficient local concentration of NO to cause vasodilatation.

A reduced difference between arterial and venous oxygen saturation has been observed in migraine patients (Heyck, 1969), suggesting enhanced shunting of arterial blood towards the venous side of the circulation. Likewise, after inhibition of NO synthesis this difference was increased together with a reduction in blood flow through arteriovenous anastomoses in anaesthetized pigs (Van Gelderen & Saxena, 1994a). In the present study, the ability of SNAP to enhance arteriovenous blood flow is not reflected by a concomitant reduction in the difference in arteriovenous oxygen saturation. Since both NPR and SNAP induced a marked arteriolar dilatation, an increase in oxygen consumption at the capillary level may partially account for this lack of effect. Additionally, a reduced arterial oxygen supply may have limited the amount of oxygen shunted towards the venous side. Indeed, a significant reduction in partial oxygen pressure together with a slight reduction in arterial oxygen saturation was observed with NPR and SNAP.

Regional carotid blood flow distribution

Both NO donors enhanced extracerebral blood flow without changing brain blood flow, suggesting that these drugs do not interfere with autoregulatory processes. However, the absence of cerebral blood flow changes does not *per se* rule out middle cerebral artery dilatation as reported in migraine (Friberg *et al.*, 1991), because such large vessel dilatations cannot be detected with radioactive microspheres. Although, the role of extracranial dilatation in migraine headache is often disregarded, dilatation and increased pulsations in the extracranial blood vessels have been observed on the side of headache (Ray & Wolff, 1940; Iversen *et al.*, 1990). Manual pressure as well as ergotamine oppose these effects and relieve pain (Graham & Wolff, 1938; Drummond & Lance, 1988).

NPR and SNAP enhanced dural blood flow significantly. Since this tissue may be the source of headache pain (Ray & Wolff, 1940), and dural blood vessels are innervated by perivascular trigeminal sensory nerves (Mayberg *et al.*, 1984), it is tempting to speculate that enhanced blood flow together with pronounced vascular pulsations in this tissue participate in vascular headache. However, it must be pointed out that several antimigraine drugs (ergotamine, dihydroergotamine and sumatriptan) failed to affect porcine dural blood flow and dural arteriovenous anastomotic shunting (Den Boer *et al.*, 1992), and, in contrast to perivascular administration, i.v. administration of sumatriptan did not constrict feline pial artery, but increased carotid vascular resistance (Connor *et al.*, 1992).

In conclusion, the present findings demonstrate that the NO donors, NPR and SNAP, induce arteriolar dilatation together with enhanced vascular pulsations in the carotid circulation of the pig. Though arteriovenous anastomotic blood flow did increase with SNAP, the pronounced arteriolar dilatation appears to limit the effect of exogenous NO on arteriovenous anastomoses, probably due to a 'steal' phenomenon. Taken together, these findings support the opinion that dilatation of (extra)cranial arteries and arteriovenous anastomoses may lead to increased vascular pulsations, which (rather than increased blood flow) could be partly responsible for the headaches caused by nitrovasodilators.

The authors wish to thank Mr Jan Heiligers for his skilful technical assistance.

References

BRUNING, T.A. (1994). Serotonergic and muscarinic receptors mediating vascular effects in the human foreman. *Thesis, The State University of Leiden*, pp. 135–150.

CONNOR, H.E., STUBBS, C.M., FENIUK, W. & HUMPHREY, P.P.A. (1992). Effect of sumatriptan, a selective 5-HT1-like receptor agonist, on pial vessel diameter in anaesthetised cats. *J. Cereb. Blood Flow Metab.*, **12**, 514–519.

DEN BOER, M.O., SOMERS, J.A.E. & SAXENA, P.R. (1992). Lack of effect of the antimigraine drugs, sumatriptan, ergotamine and dihydroergotamine on arteriovenous anastomotic shunting in the dura mater of the pig. *Br. J. Pharmacol.*, **107**, 577–583.

DEN BOER, M.O., VILLALÓN, C.M., HEILIGERS, J.P.C., HUMPHREY, P.P.A. & SAXENA, P.R. (1990). Role of 5-HT_1-like receptors in the reduction of porcine cranial arteriovenous anastomotic shunting by sumatriptan. *Br. J. Pharmacol.*, **102**, 323–330.

DEN BOER, M.O., VAN WOERKENS, L.J., SOMERS, J.A.E., DUNCKER, D.J., LACHMANN, B., SAXENA, P.R. & VERDOUW, P.D. (1993). On the preservation and regulation of vascular tone in arteriovenous anastomoses during anaesthesia. *J. Appl. Physiol.*, **75**, 782–789.

DRUMMOND, P.D. & LANCE, J.W. (1988). Contribution of the extracranial circulation to the pathophysiology of headache. In *Basic Mechanisms of Headache*. ed. Olesen, J. & Edvinsson, L. pp. 321–330. Amsterdam: Elsevier.

FEELISCH, M. & NOACK, E. (1987). Correlation between nitric oxide formation during degradation of organic nitrates and activation of guanylate cyclase. *Eur. J. Pharmacol.*, **139**, 19–30.

FERRARI, M.D. & SAXENA, P.R. (1993). Clinical and experimental effects of sumatriptan in humans. *Trends Pharmacol. Sci.*, **14**, 129–133.

FRIBERG, L., OLESEN, J., IVERSEN, H.K. & SPERLING, B. (1991). Migraine pain associated with middle cerebral artery dilatation: reversal by sumatriptan. *Lancet*, **338**, 13–17.

FUJIWARA, M., USUI, H., KURAHASHI, K., JINO, H., SHIRAHASE, H. & MEKATA, F. (1992). Endothelium-dependent contraction produced by acetylcholine and relaxation produced by histamine in monkey basilar arteries. *J. Cardiovasc. Pharmacol.*, **20**, S114–S116.

GRAHAM, J.R. & WOLFF, H.G. (1938). Mechanism of migraine headache and action of ergotamine tartrate. *Arch. Neurol. Psychiatr.*, **39**, 737–763.

HEYCK, H. (1969). Pathogenesis of migraine. *Res. Clin. Stud. Headache*, **2**, 1–28.

HOF, R.P. & HOF, A. (1989). Differential effects of antihypertensive drugs on nutritive and nonnutritive blood flow in anaesthetized rabbits. *J. Cardiovasc. Pharmacol.*, **13**, 565–571.

HÖHLER, B., MAYER, B. & KUMMER, W. (1994). Nitric oxide synthase in the rat carotid body and carotid sinus. *Cell. Tissue Res.*, **276**, 559–564.

HUMPHREY, P.P.A. & FENIUK, W. (1991). Mode of action of the anti-migraine drug sumatriptan. *Trends Pharmacol. Sci.*, **12**, 444–446.

IGNARRO, L.J. (1990). Biosynthesis and metabolism of endothelium-derived nitric oxide. *Annu. Rev. Pharmacol. Toxicol.*, **30**, 535–560.

IGNARRO, L.J., LIPPTON, H., EDWARDS, J.C., BARICOS, W.H., HYMAN, A.L., KADOWITZ, P.J. & GRUETTER, C.A. (1981). Mechanism of vascular smooth muscle relaxation by organic nitrates, nitrites, nitroprusside and nitric oxide: evidence for the involvement of S-nitrosothiols as active intermediates. *J. Pharmacol. Exp. Ther.*, **218**, 739–749.

IVERSEN, H.K. (1992). N-acetylcysteine enhances nitroglycerin-induced headache and cranial arterial responses. *Clin. Pharmacol. Ther.*, **52**, 125–133.

IVERSEN, H.K., NIELSEN, T.H., GARRE, K., TFELT-HANSEN, P. & OLESEN, J. (1992). Dose-dependent headache response and dilatation of limb and extracranial arteries after three doses of 5-isosorbide-mononitrate. *Eur. J. Clin. Pharmacol.*, **42**, 31–35.

IVERSEN, H.K., NIELSEN, T.H., OLESEN, J. & TFELT-HANSEN, P. (1990). Arterial responses during migraine headache. *Lancet*, **336**, 837–839.

JOHNSTON, B.M. & SAXENA, P.R. (1978). The effect of ergotamine on tissue blood flow and the arteriovenous shunting of radioactive microspheres in the head. *Br. J. Pharmacol.*, **63**, 541–549.

KODJA, G., JANSEN, D., STROHBACH, H. & NOACK, E. (1994). Induction of vascular tolerance to glyceryl trinitrate by spontaneous nitric oxide donor S-nitroso-N-acetyl-D,L-penicillamine (SNAP). *Naunyn-Schmied Arch. Pharmacol.*, **349**, R25.

KOWALUK, E.A. & FUNG, H.-L. (1990). Spontaneous liberation of nitric oxide cannot account for *in vitro* vascular relaxation by S-nitrosothiols. *J. Pharmacol. Exp. Ther.*, **255**, 1256–1264.

KRABBE, A.A. & OLESEN, J. (1980). Headache provocation by continuous intravenous infusion of histamine, clinical results and receptor mechanisms. *Pain*, **8**, 253–259.

MACDONALD, N.J., BUTTERS, L., O'SHAUGHNESSY, D.J., RIDDEL, A.J. & RUBIN, P.C. (1989). A comparison of the effects of human alpha calcitonin gene-related peptide and glyceryl trinitrate on regional blood velocity in man. *Br. J. Clin. Pharmacol.*, **28**, 257–261.

MATHEWS, W.R. & KERR, S.W. (1993). Biological activity of S-nitrosothiols: The role of nitric oxide. *J. Pharmacol. Exp. Ther.*, **267**, 1529–1537.

MAYBERG, M.R., ZERVAS, N.T. & MOSKOWITZ, M.A. (1984). Trigeminal projections to supratentorial pial and dural blood vessels in cats demonstrated by horseradish peroxidase histochemistry. *J. Comp. Neurol.*, **223**, 46–56.

MONCADA, S., PALMER, R.M.J. & HIGGS, E.A. (1991). Nitric oxide: physiology, pathophysiology and pharmacology. *Pharmacol. Rev.*, **43**, 109–118.

MYERS, P.R., MINOR, R.L., GUERRA, R., BATES, J.N. & HARRISON, D.G. (1990). Vasorelaxant properties of the endothelium-derived relaxing factor more closely resemble S-nitrosocysteine than nitric oxide. *Nature*, **345**, 161–163.

OLESEN, J., IVERSEN, H.K. & THOMSEN, L.L. (1993). Nitric oxide supersensitivity: a possible molecular mechanism of migraine pain. *Neuroreport*, **4**, 1027–1030.

PRABHAKAR, N.R., KUMAR, G.K., CHANG, C.H., AGANI, F.H. & HAXHIU, M.A. (1993). Nitric oxide in the sensory function of the carotid body. *Brain Res.*, **625**, 16–22.

RAY, B.S. & WOLFF, H.G. (1940). Experimental studies on headache: pain sensitive structures of the head and their significance in headache. *Arch. Surg.*, **41**, 813–856.

RUBANYI, G.M., JOHNS, A., WILCOX, D., BATES, F.N. & HARRISON, D. (1991). Evidence that a S-nitrosothiol, but not nitric oxide, may be identical with endothelium-derived relaxing factor. *J. Cardiovasc. Pharmacol.*, **17**, S41–S45.

SAXENA, P.R. (1978). Arteriovenous shunting and migraine. *Res. Clin. Stud. Headache*, **6**, 89–102.

SAXENA, P.R. (1994). The pathogenesis and pharmacology of migraine. *Rev. Comtemp. Pharmacother.*, **5**, 259–269.

SAXENA, P.R., SCHAMHARDT, H.C., FORSYTH, R.P. & LOEVE, J. (1980). Computer programs for the radioactive microsphere technique. *Comp. Progr. Biomed.*, **12**, 63–84.

SAXENA, P.R. & VERDOUW, P.D. (1982). Redistribution by 5-hydroxytryptamine of carotid arterial blood at the expense of arteriovenous anastomotic blood flow. *J. Physiol.*, **332**, 501–520.

SAXENA, P.R. & VERDOUW, P.D. (1985). Tissue blood flow and localization of arteriovenous anastomoses in pigs with microspheres of four different sizes. *Pflügers Arch.*, **403**, 128–135.

THOMSEN, L.L., IVERSEN, H.K., BRINCK, T.A. & OLESEN, J. (1993). Arterial supersensitivity to nitric oxide (nitroglycerin) in migraine sufferers. *Cephalalgia*, **13**, 395–399.

TODA, N. (1990). Mechanism underlying responses to histamine of isolated monkey and human cerebral arteries. *Am. J. Physiol.*, **258**, H311–317.

VAN GELDEREN, E.M., DE BRUIJNE, E.L.E., AGTERESCH, H.J. & SAXENA, P.R. (1994). Different effect of nitric oxide donors on the distribution of the common carotid blood flow in the cranial circulation of the pig. *Br. J. Pharmacol.*, **112**, 70P.

VAN GELDEREN, E.M., DEN BOER, M.O. & SAXENA, P.R. (1993). N^G-nitro-L-arginine methyl ester: systemic and pulmonary haemodynamics, tissue blood flow and arteriovenous shunting in the pig. *Naunyn-Schmied Arch. Pharmacol.*, **348**, 417–423.

VAN GELDEREN, E.M. & SAXENA, P.R. (1994a). Inhibition of nitric oxide biosynthesis and carotid arteriovenous anastomotic shunting in the pig. *Br. J. Pharmacol.*, **111**, 961–967.

VAN GELDEREN, E.M. & SAXENA, P.R. (1994b). The effects of calcitonin gene-related peptide on the carotid blood flow distribution in the anaesthetized pig. *Can. J. Physiol. Pharmacol.*, **72**, 409.

VAN WOERKENS, L.J., DUNCKER, D.J., HUIGEN, R.J., VAN DER GIESSEN, W.J. & VERDOUW, P.D. (1990). Redistribution of cardiac output caused by opening of arteriovenous anastomoses by a combination of azaperone and metomidate. *Br. J. Anaesth.*, **65**, 393–399.

VILLALÓN, C.M., BOM, A.H., HEILIGERS, J., DEN BOER, M.O. & SAXENA, P.R. (1990). Constriction of porcine arteriovenous anastomoses by indorenate is unrelated to 5-HT_{1A}, 5-HT_{1B}, 5-HT_{1C} or 5-HT_{1D} receptor subtype. *Eur. J. Pharmacol.*, **190**, 167–176.

WANG, Z.-Z., BREDT, D.S., FIDONE, S.J. & STENSAAS, L.J. (1993). Neurons synthesizing nitric oxide innervate the mammalian carotid body. *J. Comp. Neurol.*, **336**, 419–432.

WANG, Z.-Z., STENSAAS, L.J., DE VENTE, J., DINGER, B. & FIDONE, S.J. (1991). Immunocytochemical localization of cAMP and cGMP in cells of the rat carotid body following natural and pharmacological stimulation. *Histochem.*, **96**, 523–530.

(Received September 12, 1994
Revised November 11, 1994
Accepted November 28, 1994)

British Journal of Pharmacology (1995) 114, 1310-1316

Effects of the tachykinin NK_1 receptor antagonist, RP 67580, on central cardiovascular and behavioural effects of substance P, neurokinin A and neurokinin B

[1]Juraj Culman, Brigitte Wiegand, Heidi Spitznagel, Sabine Klee & Thomas Unger

German Institute for High Blood Pressure Research and Department of Pharmacology, University of Kiel, 24105 Kiel, Germany

1 We have investigated the effects of the non-peptide NK_1 tachykinin receptor antagonist, RP 67580, and its inactive enantiomer, RP 68651, on the cardiovascular and behavioural responses to substance P (SP), neurokinin A (NKA) and neurokinin B (NKB) injected intracerebroventricularly (i.c.v.) in conscious rats.

2 The SP and NKA (25 pmol)-induced increases in blood pressure (BP) and heart rate (HR) were of the same magnitude. The cardiovascular responses to both peptides were associated with excessive grooming behaviour and wet dog shakes (WDS). Relative to SP, NKA was weaker in inducing hindquarter grooming (HG), but more effective in eliciting WDS. The cardiovascular response to NKB (50 pmol) comprised an increase in BP and HR, while the behavioural response was weak.

3 RP 67580 (100 pmol), injected 10 or 30 min prior to SP, effectively inhibited the cardiovascular and behavioural responses to the peptide whereas lower doses were ineffective. Pretreatment with 500 pmol of RP 67580, 10 or 30 min prior to SP, reduced the BP response. Of the behavioural manifestations, only face washing was attenuated when the antagonist was injected 10 min before SP. At 2500 pmol, the antagonist exaggerated the BP response to the peptide without affecting the behavioural response. RP 68651 (100 or 2500 pmol) did not modify the central responses to SP.

4 Neither RP 67580 nor RP 68651 (100 pmol), affected the cardiovascular and behavioural responses to NKA or NKB.

5 Our results indicate that RP 67580 is a selective and high affinity antagonist at central NK_1 tachykinin receptors in the rat.

Keywords: Substance P; neurokinin A; neurokinin B; RP 67580; blood pressure; heart rate; behaviour; central actions

Introduction

Substance P (SP), neurokinin A (NKA) and neurokinin B (NKB) represent the principal tachykinins in mammals and are widely distributed in the central nervous system (CNS) and peripheral tissues (Maggio, 1988). The physiological actions exerted by tachykinins are mediated by three types of receptors referred to as NK_1, NK_2 and NK_3. SP binds preferentially to NK_1 receptors, whereas NKA and NKB display highest affinity for NK_2 and NK_3 receptors, respectively (for review see Helke *et al.*, 1990; Guard & Watson, 1991; Nakanishi, 1991; Maggi *et al.*, 1993).

In recent years, several non-peptide antagonists for tachykinin receptors have been developed. CP-96,345 was the first selective and high affinity non-peptide antagonist described for NK_1 receptors (Snider *et al.*, 1991). Functional and binding studies revealed that CP-96,345 displayed a higher affinity for NK_1 receptors in man and guinea-pig than in mouse and rat (Snider *et al.*, 1991; Beresford *et al.*, 1991; Barr & Watson, 1993; Fardin *et al.*, 1993). In addition to possessing high affinity for the NK_1 receptors, CP-96,345 binds to L-type calcium channels and displays a variety of non-specific effects that are not stereoselective (Wang & Hakanson, 1992; Griesbacher *et al.*, 1992; Donnerer *et al.*, 1992; Guard *et al.*, 1993).

Recently, another specific non-peptide NK_1 receptor antagonist, RP 67580, (3a**R**, 7a**R**)-7,7-diphenyl-2-[1-imino-2-(2-methoxyphenyl)-ethyl] perhydroisoindol-4-one), has been described which is selective for the rodent NK_1 receptor type (Garret *et al.*, 1991). This antagonist was shown to inhibit binding of [^{3}H]-SP to NK_1 receptors in a competitive manner in membranes or crude synaptosomes prepared from rat brain (Garret *et al.*, 1991; Beaujoan *et al.*, 1993). RP 65780 also inhibited the plasma extravasation induced by SP in the urinary bladder or by antidromic electrical stimulation of the saphenous nerve in the hind paw skin of the rat. When injected peripherally, the antagonist induced a dose-dependent inhibition of nociceptive responses to formalin in the rat paw as well as the facilitation of the spinal reflex by various conditioning stimuli in the rat. In contrast, the 3aS, 7aS enantiomer of RP 67580, RP 68651, was inactive in these assays (Garret *et al.*, 1991; 1993; Laird *et al.*, 1993). Non-peptide antagonists for NK_1 receptors such as RP 67580 may thus represent a novel group of drugs for the treatment of neurogenic inflammation and pain (Garret *et al.*, 1991; Moussaoui *et al.*, 1993).

Tachykinins in the brain are thought to be involved in the regulation of a variety of physiological processes (Helke *et al.*, 1990; Otsuka & Yoshioka, 1993). Peripherally administered non-peptide antagonists generally cross the blood-brain-barrier and may therefore modify central tachykinin actions.

Of the biological effects induced by stimulation of central tachykinin receptors, the cardiovascular and behavioural responses appear to be the most prominent (Unger *et al.*, 1988; Itoi *et al.*, 1992).

In the present study, we have investigated the effects of RP 67580 on central cardiovascular and behavioural responses evoked by endogenous mammalian tachykinins. SP, NKA and NKB were used because these tachykinin neuropeptides represent the natural agonists for tachykinin receptors. The peptides and the non-peptide antagonist were injected intracerebroventricularly (i.c.v.) in conscious rats. The effects of RP 67580 were compared with those of its inactive enantiomer, RP 68651.

[1] Author for correspondence at Department of Pharmacology.

Methods

Implantation of cannulae and catheters and measurement of cardiovascular and behavioural parameters

Male Wistar rats (Dr Karl Thomae, Biberach, Germany) weighing 320–350 g were used. The animals were allowed free access to food and water and maintained on a 12 h light/dark cycle.

For i.c.v. injections, chronic polyethylene cannulae (PP 20) were implanted into the left lateral brain ventricle 7 days before experiments. Five days were allowed for recovery, and then femoral artery catheters (PP 50) were implanted. The surgical procedures have been described previously (Itoi *et al.*, 1992). Experiments were performed 48 h after the femoral artery cannulation.

All experiments were carried out in conscious, freely moving rats. On each test day, rats were placed in the test cages which were of the same size as the home cages and habituated to the new environment at least for 1 h. Then, the femoral artery catheter was connected to the transducer. The experiments were started when the animals were resting and when basal mean arterial pressure (MAP) and heart rate (HR) were stable. SP and NKA, dissolved in isotonic saline, were injected i.c.v. in 1 μl and flushed with 4 μl of saline. NKB, dissolved in acidic saline (approximate pH 3.5), was injected i.c.v. in 1 μl together with 4 μl of phosphate buffered saline (pH 7.4). I.c.v. injection procedure for RP 67580 and for RP 68651 was the same as for NKB (see Materials).

Measurements of MAP and HR were performed via the arterial catheters using a Statham P23Db pressure transducer connected to a Gould Brush 2400 recorder. Analogue output signals of MAP and HR from the blood pressure computer were digitalized and then processed using a computerized programme (Stauss *et al.*, 1990). The MAP and HR are expressed as the area under the curve (AUC) (MAP: mmHg × min; HR: b.p.m. × min). These values represent the sum of MAP and HR changes integrated in time, i.e. one number quantitatively characterizes the whole response. The values have been calculated for a period of 20 min starting at the time point of the i.c.v. injection using a computerized calculation programme developed in our laboratory (Stauss *et al.*, 1990; Itoi *et al.*, 1992).

Behavioural responses were recorded in test cages with grid cage tops removed over a 20 min period starting immediately following the i.c.v. injections. The frequency of the following behavioural manifestations: face washing/head scratching (FW) (movement of forepaws over the nose, eyes and ears or scratching the head with the forepaws), hindquarter grooming/biting (HG) (licking or biting the caudal part of the body including the hindlimbs) and wet dog shakes (WDS) (whole body shaking) was determined according to the 15 s sampling procedure of Gispen *et al.* (1975). During every consecutive period of 15 s, a score of 1 or 0 was given depending on whether the animals showed the specific type of behavioural manifestation or not, regardless of the intensity or the duration of the response. Summation of scores for 20 min following the i.c.v. injection gave the total behavioural score. The maximum theoretical score was 80.

Experimental protocols

Effects of RP 67580 and of its inactive enantiomer, RP 68651, on the cardiovascular and behavioural responses induced by i.c.v. SP The central responses to the same dose of tachykinins may vary from animal to animal. The cardiovascular and behavioural responses to SP obtained after pretreatment with RP 67580 or RP 68651 were, therefore, compared to the responses induced by the same dose of the peptide after vehicle pretreatment in each animal.

Seven groups of rats were used in the first set of experiments. On the first day, rats were pretreated i.c.v. with vehicle (1 μl of acidic saline, approximate pH 4, injected together with 4 μl phosphate buffered saline, pH 7.4). Ten min thereafter, SP (25 pmol) was injected i.c.v. and the cardiovascular and behavioural responses were recorded. Two days later, rats were pretreated i.c.v. with RP 67580 (5 groups of rats) or RP 68651 (2 groups of rats). Ten min later, SP (25 pmol) was injected i.c.v. and the cardiovascular and behavioural responses were recorded. Each rat received only one dose of RP 67580 or RP 68651. Five doses of RP 67580 (25, 50, 100, 500 and 2500 pmol) and two doses of its inactive enantiomer, RP 68651 (100 and 2500 pmol) were used.

On the basis of the results obtained in the first set of experiments, it appeared possible that RP 67580, especially in higher doses, displayed some intrinsic activity. Therefore, in the second set of experiments, the time interval between the i.c.v. pretreatment with the antagonist and the i.c.v. SP injection was increased to 30 min. These experiments were conducted to investigate the intrinsic activity of the antagonist by measuring the cardiovascular and behavioural effects induced by the antagonist itself and to dissociate the cardiovascular effects induced by SP from those induced by the antagonist.

Three experimental groups of rats were used. On the first day of experiment, all rats received SP (25 pmol, i.c.v.) 30 min after i.c.v. pretreatment with vehicle (see above). Two days later, the first group was pretreated i.c.v. with 25 pmol, the second group with 100 pmol and the third group with 500 pmol of RP 67580. BP and HR were monitored and the behavioural manifestations were recorded starting immediately following the antagonist injection. SP (25 pmol) was injected i.c.v. 30 min after the antagonist, and the cardiovascular and behavioural responses to the peptide were recorded.

The intrinsic activity of the highest dose of RP 67580 (2500 pmol) and the intrinsic activity of its inactive enantiomer, RP 68651 were examined in separate experiments.

Effects of RP 67580 and of its inactive enantiomer, RP 68651, on the cardiovascular and behavioural responses induced by i.c.v. NKA and NKB The first group of rats was pretreated i.c.v. with vehicle (see above), the second with RP 67580 (100 pmol, i.c.v.) and the third with RP 68651 (100 pmol, i.c.v.). Ten min thereafter, NKA (25 pmol) was injected i.c.v. and the cardiovascular and behavioural responses to the peptide were recorded.

In a further protocol, rats received an i.c.v. injection of NKB (50 pmol) instead of NKA (25 pmol).

Materials

RP 67580 (3a**R**, 7a**R**)-7,7-diphenyl-2[1-imino-2(2-methoxyphenyl)-ethyl] perhydroisoindol-4-one) and its (3a**S**, 7a**S**) enantiomer, RP 68651, were kind gifts from Dr C. Garret, Rhône-Poulenc Rorer, France. RP 67580 and RP 68651 were dissolved in a small volume of 0.1 M HCl (1/10 of the final volume of the stock solution). Saline was added to obtain the final volume in the stock solution (5000 pmol/1 μl). On the day of experiment, the stock solution was further diluted with saline to obtain the desired concentration of the compounds. One μl of the solution containing either RP 67580 or RP 68651 (approximate pH 3.5) was injected i.c.v., together with 4 μl of phosphate buffered saline, pH 7.4.

SP, NKA and NKB were purchased from Bachem, Biochemica GmbH, Heidelberg, Germany. SP and NKA were dissolved in isotonic saline. NKB was dissolved in a minimal volume of 50% acetic acid. After a short (15–20 s) sonication of the solution in an ultrasound bath, saline was added to obtain the stock solution (500 pmol/1 μl).

The stock solutions of the peptides (500 pmol/1 μl) were divided in aliquots and stored at −20°C no longer than two weeks. On the day of experiment, the stock solution was further diluted with saline to obtain the desired concentration of the peptide.

Statistical analysis of data

All values are expressed as means ± s.e.mean. The data obtained in experiments employing SP were analysed by Student's *t* test for paired samples since the cardiovascular and behavioural responses to SP after pretreatment with the vehicle and those after pretreatment with RP 67580 or RP 68651 were always obtained from the same animal. When more than one comparison was made, the data were subjected to a one-way analysis of variance (ANOVA) followed by a *post hoc* Bonferroni test. A significance level of $P<0.05$ was accepted.

Results

I.c.v. injections of RP 67580 (25, 100, 500 and 2500 pmol, i.c.v.) and RP 68651 (25, 100 and 2500 pmol, i.c.v.) were without appreciable effects on cardiovascular parameters (Table 1). Similarly, when administered i.c.v. at the above doses, the behavioural responses to both drugs did not differ from vehicle (data not shown).

Effects of RP 67580 and of its inactive enantiomer, RP 68651, on the cardiovascular and behavioural responses induced by i.c.v. SP

I.c.v. administration of SP resulted in increases in MAP and HR which reached a maximum at 2–5 min and then returned gradually to basal values within 15–20 min. The cardiovascular responses to the peptide were associated with increased behavioural activity. In agreement with our previous findings (Culman *et al.*, 1993), FW and HG were the most dominant behavioural manifestations.

I.c.v. pretreatment with 25 or 50 pmol RP 67580, 10 min prior to SP, did not modify the cardiovascular and behavioural responses to the peptide (Figure 1, Table 2). The dose of 100 pmol RP 67580, injected 10 min prior to SP, significantly reduced the BP and HR responses (by about 60%–75%) to values which did not differ significantly from values obtained in i.c.v. saline-treated control rats (Figure 1). FW and HG, which represent the most prominent behavioural manifestations evoked by SP, as well as WDS, were also antagonized (Table 2). I.c.v. pretreatment with 500 pmol RP 67580 markedly reduced only the BP response to SP while the HR response remained unaffected (Figure 1). Of all behavioural manifestations, only FW was inhibited (Table 2). The highest dose of the antagonist, 2500 pmol injected 10 min prior to SP, increased the BP responses to the peptide (Figure 1), whereas the HR responses and the behavioural effects were not altered (Figure 1, Table 2).

Similar results were obtained when RP 67580 was injected i.c.v. 30 min prior to SP. The dose of 25 pmol of the antagonist did not affect the cardiovascular and the behavioural responses to SP. RP 67580 injected i.c.v. at a dose of 100 pmol, 30 min prior to SP, reduced the BP and HR response to the peptide to values that were not significantly different from those obtained in i.c.v. saline-treated controls (Figure 2). This dose of antagonist also effectively inhibited all behavioural manifestations elicited by SP (Table 2). I.c.v. pretreatment with 500 pmol RP 67580 resulted solely in a reduction of the BP response to the peptide, whereas the behavioural effects were not altered (Figure 2, Table 2).

A dose of 100 pmol RP 67580 most effectively inhibited the central cardiovascular and behavioural responses to SP. The same dose of its inactive enantiomer, RP 68651, injected i.c.v. 10 min before SP, failed to affect these responses. Similarly, the dose of 2500 pmol RP 68651 did not alter the central effects of SP (Figure 3, Table 3).

Table 1 Effects of RP 67580 and RP 68651 injected i.c.v. on mean arterial pressure (MAP) and heart rate (HR)

Treatment (i.c.v.)		n	*MAP* (AUC)	*HR* (AUC)
Vehicle		9	15.7 ± 4.4	66 ± 18
RP 67580	(25 pmol)	7	11.4 ± 6.3	85 ± 51
RP 67580	(100 pmol)	7	22.7 ± 7.2	133 ± 38
RP 67580	(500 pmol)	8	20.4 ± 7.5	144 ± 42
RP 67580	(2500 pmol)	7	15.9 ± 7.4	71 ± 19
RP 68651	(25 pmol)	7	12.5 ± 13	166 ± 80
RP 68651	(100 pmol)	8	13.2 ± 5.2	102 ± 39
RP 68651	(2500 pmol)	6	28.0 ± 4.5	157 ± 82

Values represent the means ± s.e.mean of (*n*) rats. MAP and HR are expressed as area under the curve (AUC) (MAP: mmHg × min; HR: b.p.m. × min). RP 67580 and RP 68651 were injected i.c.v. at indicated doses. AUC was calculated for a period of 20 min starting at the time point of the i.c.v. injection. Statistical comparison to vehicle treatment was made with ANOVA. No statistically significant differences were observed.

Effects of RP 67580 and RP 68651 on the central cardiovascular and behavioural responses induced by i.c.v. NKA and NKB

The cardiovascular and behavioural effects observed following i.c.v. NKA and NKB administration are thought to be immediated by NK_2 and NK_3 receptors, respectively (Takano *et al.*, 1990; Tschöpe *et al.*, 1992). To test the selectivity of RP 67580 for the NK_1 receptor *in vivo*, the effects of pretreat-

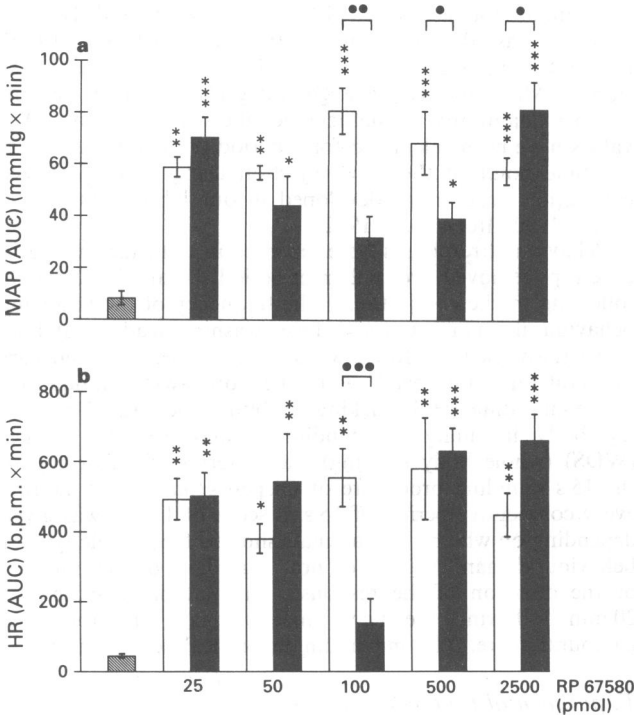

Figure 1 Cardiovascular responses to substance P (SP, 25 pmol, i.c.v.) injected 10 min after i.c.v. pretreatment with RP 67580 (solid columns; 25 pmol: $n=9$; 50 pmol: $n=8$; 100 pmol: $n=8$; 500 pmol: $n=7$; 2500 pmol: $n=10$) or vehicle (open columns); saline (hatched columns). MAP (a) and HR (b) are expressed as area under the curve (AUC). AUC was calculated for a period of 20 min starting at the time point of the i.c.v. injection of SP or saline. Values are given as means ± s.e.mean. $^{*}P<0.05$, $^{**}P<0.01$, $^{***}P<0.001$ statistical comparison to saline, calculated with one-way ANOVA followed by a *post-hoc* Bonferroni test. $^{\bullet}P<0.05$, $^{\bullet\bullet}P<0.01$, $^{\bullet\bullet\bullet}P<0.001$ statistical comparison to the respective vehicle-pretreated group, calculated with Student's *t* test for paired samples.

Table 2 Effect of RP 67580 (i.c.v.) on behavioural responses induced by substance P (SP, 25 pmol, i.c.v)

Pretreatment (i.c.v.)		*Agonist* (i.c.v.)	*Time interval* (min) *between i.c.v.-injections*	n	*Face washing*	*Hind-quarter grooming*	*Wet-dog shakes*
–		Saline	10	9	0.8 ± 0.3	0.5 ± 0.5	0.6 ± 0.3
Vehicle		SP	10	9	8.7 ± 1.4**	6.0 ± 1.1*	3.9 ± 1.4
RP 67580	(25 pmol)	SP	10	9	6.7 ± 1.0*	5.8 ± 1.8*	3.9 ± 1.0
Vehicle		SP	10	8	5.9 ± 1.0*	6.1 ± 1.3*	2.5 ± 0.7
RP 67580	(50 pmol)	SP	10	8	5.6 ± 2.1	5.3 ± 2.2	1.6 ± 0.8
Vehicle		SP	10	8	10.3 ± 1.5***	9.3 ± 2.1**	3.2 ± 0.8
RP 67580	(100 pmol)	SP	10	8	3.3 ± 0.8[b]	2.3 ± 1.4[a]	0.8 ± 0.4[a]
Vehicle		SP	10	7	9.5 ± 1.1**	8.3 ± 1.0**	3.3 ± 1.3
RP 67580	(500 pmol)	SP	10	7	5.4 ± 1.4[a]	8.1 ± 2.7*	1.3 ± 0.7
Vehicle		SP	10	10	7.7 ± 1.4**	7.6 ± 2.0**	1.7 ± 0.7
RP 67580	(2500 pmol)	SP	10	10	8.5 ± 1.8	9.9 ± 2.1**	2.0 ± 0.7
Vehicle		SP	30	10	7.4 ± 1.4**	6.1 ± 1.3*	4.0 ± 1.2
RP 67580	(25 pmol)	SP	30	10	6.0 ± 1.5*	6.8 ± 2.0*	3.1 ± 1.2
Vehicle		SP	30	7	7.7 ± 1.8**	8.1 ± 2.8**	4.3 ± 0.9
RP 67580	(100 pmol)	SP	30	7	1.9 ± 0.6[a]	2.6 ± 1.3[a]	1.0 ± 0.3[b]
Vehicle		SP	30	10	8.1 ± 2.0**	6.6 ± 1.6*	3.6 ± 1.3
RP 67580	(500 pmol)	SP	30	10	4.1 ± 1.2	3.5 ± 1.0	3.9 ± 1.0

Values represent the frequency of individual behavioural manifestations for 20 min and are indicated by the means ± s.e.mean of (*n*) rats. RP 67580 was injected i.c.v. at indicated doses 10 or 30 min prior to SP (25 pmol, i.c.v.)
*$P<0.05$; **$P<0.01$; ***$P<0.001$, statistical comparison to saline, calculated with one-way ANOVA followed by a *post hoc* Bonferroni test.
[a]$P<0.05$, [b]$P<0.01$, statistical comparison to the respective, vehicle-pretreated group, calculated with Student's *t* test for paired samples.

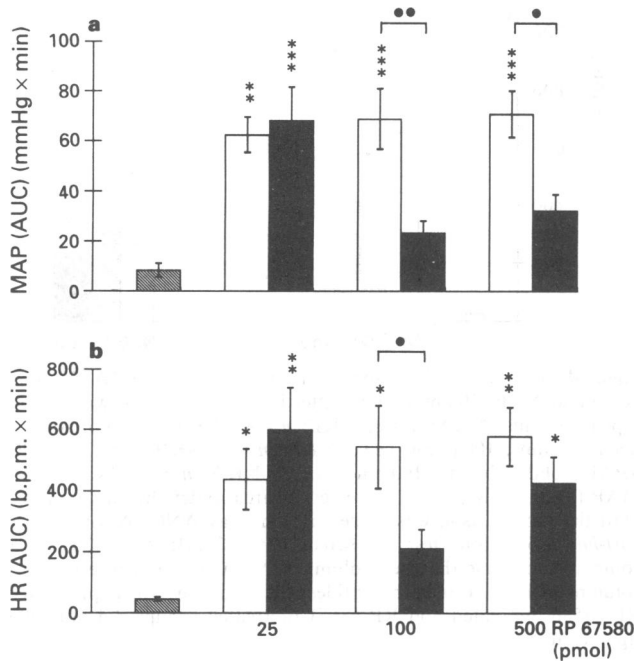

Figure 2 Cardiovascular responses to substance P (SP, 25 pmol, i.c.v.) injected 30 min after i.c.v. pretreatment with RP 67580 (solid columns; 25 pmol: $n = 10$; 100 pmol: $n = 7$; 500 pmol: $n = 10$) or vehicle (open columns); saline (hatched columns). For further details see the legend to Figure 1.

ment with RP 67580 (100 pmol) on the cardiovascular and behavioural effects induced by i.c.v. NKA and NKB were investigated. The cardiovascular responses to NKA were practically identical with those of an equimolar dose of SP (Figure 1, Figure 4). In agreement with our previous findings (Culman *et al.*, 1993), NKA was as potent as SP in eliciting FW. Relative to SP, NKA was weaker in inducing HG behaviour, but more effective in eliciting WDS (Table 2, Table 4). The cardiovascular response to i.c.v. NKB (50 pmol) comprised an increase in BP and HR, while the behavioural response to NKB was less prominent compared to behavioural effects induced by SP or NKA. The NK_1 receptor antagonist, RP 67580, and its inactive enantiomer, RP 68651, did not significantly alter the cardiovascular and behavioural responses either to NKA or NKB (Figure 4, Table 4).

Discussion

In the present study, we examined the effects of RP 67580 on central cardiovascular and behavioural responses induced by the endogenous mammalian tachykinin peptides, SP, NKA and NKB. These peptides represent the preferred endogenous ligands for NK_1, NK_2 and NK_3 receptors, respectively (Guard & Watson, 1991; Maggi *et al.*, 1993). Since it is likely that most areas of the CNS contain more than one type of tachykinin receptor, it is difficult to characterize exactly the effects mediated by specific tachykinin receptor types in the CNS. In the present study, peptides and antagonist were administered i.c.v. Recent studies have demonstrated that all three types of tachykinin receptor are present in periventricular areas of rat brain (Takano *et al.*, 1990; Itoi *et al.*, 1992; Tschöpe *et al.*, 1992; Culman *et al.*, 1993). It has been suggested that, at low concentrations, SP, NKA and NKB, are selective for particular tachykinin receptor binding sites (Helke *et al.*, 1990). This idea is consistent with our recent finding demonstrating that patterns of the behavioural responses induced by low doses of SP and NKA differ and that the observed differences may be ascribed to the activation of different types of tachykinin receptors (Culman *et al.*, 1993). Low doses of SP, NKA and NKB were also used in the present study.

The cardiovascular and behavioural responses induced by i.c.v. injections of SP, NKA and NKB were evaluated for a period of time of 20 min since we have shown previously that increased BP and HR after i.c.v. injections of 25 pmol SP or NKA returned to baseline within 15 min (Tschöpe *et al.*, 1992).

Table 3 Effect of RP 68651 (i.c.v.) on behavioural responses induced by substance P (SP, 25 pmol, i.c.v)

Pretreatment (i.c.v.)	*Agonist* (i.c.v.)	*Time interval* (min) *between i.c.v.-injections*	n	*Face washing*	*Hind-quarter grooming*	*Wet-dog shakes*
–	Saline	10	9	0.8 ± 0.3	0.5 ± 0.5	0.6 ± 0.3
Vehicle	SP	10	6	7.5 ± 1.3**	6.2 ± 1.8*	3.5 ± 1.0
RP 68651 (100 pmol)	SP	10	6	12.0 ± 2.8***	9.8 ± 2.1***	6.8 ± 2.3*
Vehicle	SP	10	8	7.6 ± 0.9**	6.1 ± 1.2*	2.8 ± 0.8
RP 68651 (2500 pmol)	SP	10	8	6.4 ± 1.0*	5.9 ± 1.3*	3.6 ± 0.6

Values represent the frequency of individual behavioural manifestations for 20 min and are indicated by the means ± s.e.mean of (*n*) rats. RP 68651 was injected i.c.v. at indicated doses 10 min prior to SP (25 pmol, i.c.v.)
*$P<0.05$; **$P<0.01$; ***$P<0.001$, statistical comparison to saline, calculated with one-way ANOVA followed by a *post hoc* Bonferroni test. Statistical significance of the differences between RP 68651-pretreated groups and their respective, vehicle-pretreated controls was evaluated with Student's *t* test for paired samples. No significant differences were observed.

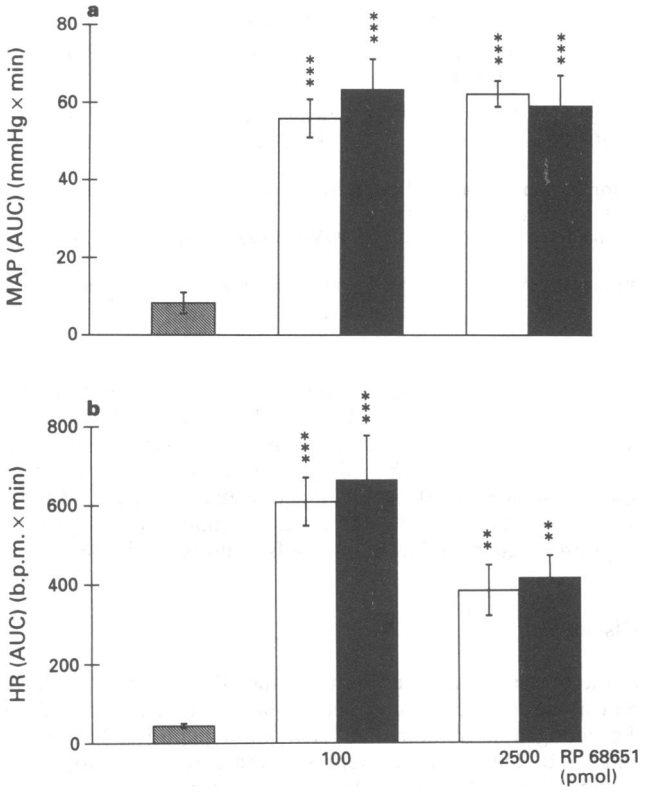

Figure 3 Cardiovascular responses to substance P (SP, 25 pmol, i.c.v.) injected 10 min after i.c.v. pretreatment with RP 68651 (solid columns; 100 pmol: $n=6$; 2500 pmol: $n=8$) or vehicle (open columns); saline (hatched columns). **$P<0.01$, ***$P<0.001$ statistical comparison to saline calculated with one-way ANOVA followed by a *post-hoc* Bonferroni test. No statistical differences were found between RP 68651-pretreated groups and their respective vehicle-pretreated controls (Student's *t* test for paired samples). For further details see the legend to Figure 1.

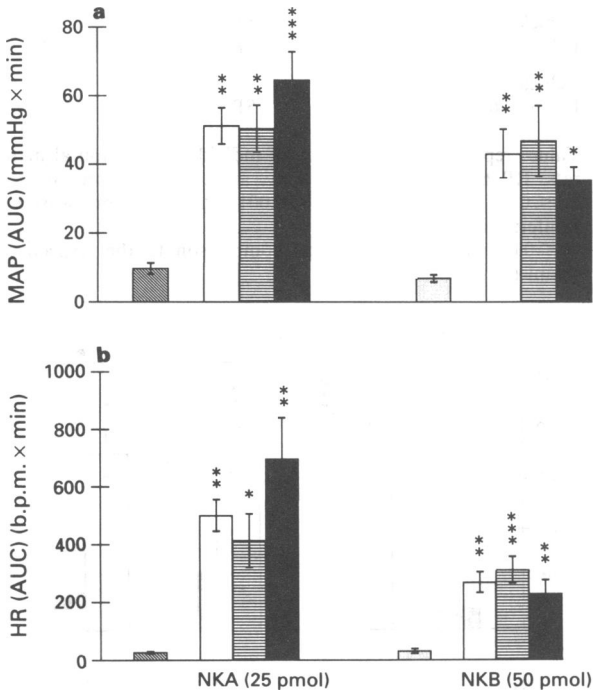

Figure 4 Cardiovascular responses to neurokinin A (NKA, 25 pmol, i.c.v.) and NKB (50 pmol, i.c.v.) after i.c.v. pretreatment with vehicle (open columns; NKA: $n=8$; NKB: $n=8$), RP 67580 (horizontally lined columns; 100 pmol, i.c.v., NKA: $n=8$; NKB: $n=7$) and RP 68651 (solid columns; 100 pmol, i.c.v.; NKA: $n=7$; NKB: $n=7$). MAP (a) and HR (b) are expressed as area under the curve (AUC). Statistical comparison was made with one-way ANOVA followed by *post-hoc* Bonferroni test. *$P<0.05$; **$P<0.01$; ***$P<0.001$ as compared to saline (hatched columns) (NKA) or to vehicle (stippled columns) (NKB). For both peptides, the values in vehicle-pretreated, RP 67580-pretreated and RP 68651-pretreated groups did not differ significantly.

In the present study, we observed that pretreatment with a dose of 100 pmol of RP 67580 effectively inhibited the cardiovascular responses and the behavioural manifestations induced by 25 pmol of SP. Previous studies have shown that a 50 times higher dose of (±)-CP-96,345 was necessary to achieve an inhibition of the cardiovascular responses to the same dose of the peptide. Of the behavioural manifestations, only FW was abolished by (±)-CP-96,345 (Tschöpe *et al.*, 1992). These findings are consistent with recent data demonstrating that RP 67580 is more potent than CP-96,345 in inhibiting the specific binding of [^{3}H]-SP to NK_1 receptors in rat brain tissue or in antagonizing NK_1 receptor-stimulated hydrolysis of inositol phospholipids in rat glial cells (Fardin *et al.*, 1993; Barr & Watson, 1993; Beaujouan *et al.*, 1993).

RP 67580 has been reported to inhibit the nociceptive response to formalin injection into the hind paw or plasma extravasation in rats after various stimuli in a dose-dependent manner (Garret *et al.*, 1993; Moussaoui *et al.*, 1993). In contrast to these studies, in our experiments RP 67580 did not inhibit the central responses to SP in a dose-dependent manner. Regardless of whether RP 67580 was injected 10 or 30 min before SP, 100 pmol RP 67580 very potently inhibited both the cardiovascular and behavioural responses to the peptide, while lower doses were ineffective. A higher dose of RP 67580 (500 pmol) was less potent in

Table 4 Effect of RP 67580 and RP 68651 (i.c.v.) on behavioural responses induced by neurokinin A (NKA, 25 pmol, i.c.v) and NKB (50 pmol, i.c.v.)

Pretreatment (i.c.v.)		*Agonist* (i.c.v.)	*Time interval* (min) *between i.c.v.-injections*	n	*Face washing*	*Hind-quarter grooming*	*Wet-dog shakes*
–		Saline	10	6	0.5 ± 0.3	0.7 ± 0.3	0.7 ± 0.3
Vehicle		NKA	10	8	6.8 ± 0.9**	3.6 ± 0.8	6.1 ± 1.4*
RP 67580	(100 pmol)	NKA	10	8	5.9 ± 0.9*	6.0 ± 1.7	3.8 ± 0.9
RP 68651	(100 pmol)	NKA	10	7	6.3 ± 2.1*	3.2 ± 0.9	4.9 ± 1.6
–		Vehicle	10	8	0.3 ± 0.2	0.5 ± 0.3	0.4 ± 0.2
Vehicle		NKB	10	8	3.4 ± 1.1	1.6 ± 0.5	1.8 ± 0.6
RP 67580	(100 pmol)	NKB	10	7	2.7 ± 1.1	2.8 ± 1.2	3.0 ± 0.8*
RP 68651	(100 pmol)	NKB	10	7	2.0 ± 0.7	0.3 ± 0.3	1.6 ± 0.6

Values represent the frequency of individual behavioural manifestations for 20 min and are shown as means ± s.e.mean of (*n*) rats. RP 67580 (100 pmol) and RP 68651 (100 pmol) were injected i.c.v. 10 min prior to NKA (25 pmol) or NKB (50 pmol). Statistical comparison was made with ANOVA followed by a post-hoc Bonferroni test, separately for each peptide. $*P<0.05$; $**P<0.01$ as compared to saline (NKA) or vehicle (NKB). For both peptides, the values in vehicle-pretreated, RP 67580-pretreated and RP 68651-pretreated groups did not differ significantly.

antagonizing the SP responses than 100 pmol, whereas the highest dose of the antagonist used in the present study (2500 pmol) even potentiated the SP-induced increase in BP without affecting the behavioural responses to the peptide.

This response pattern could occur if RP 67580 acts as a partial agonist at the NK_1 receptor. However, RP 67580, in addition to blocking NK_1 receptors, has been reported to exert action unrelated to the inhibition of NK_1 receptors including an interaction with calcium channels and non-specific inhibitory effects on neurotransmission by a mechanism similar to that of local anaesthetics (Wang *et al.*, 1994; Lombet & Spedding, 1994). The sensitization phenomenon of the highest dose of RP 67580 on SP-induced increase in BP may therefore result from such non-specific effects of the compound on neurotransmission or neuronal excitability in neural circuits related to the central BP regulation. The fact that the potentiation of the BP responses to SP after pretreatment with the highest dose of RP 67580 was not accompanied by a corresponding exaggeration of the behavioural responses would argue in favour of such a non-specific interaction.

On the other hand, the inactive enantiomer, RP 68651, at both doses tested, did not affect the central responses to SP. The decreased ability of higher doses of RP 67580 to inhibit the central responses to SP and the potentiation of the BP response to the peptide by the highest dose of the antagonist therefore appears to be enantioselective and may result from specific interactions of RP 67580 with central NK_1 receptors. In contrast to CP-96,345, the molecular interactions between RP 65780 and the NK_1 receptor have not yet been described. However, it has been suggested that RP 67580 and CP-96,345 bind to overlapping but not identical sites at the NK_1 receptor (Gether *et al.*, 1993b; Fong *et al.*, 1993; Fardin *et al.*, 1993). Both non-peptide antagonists have been considered to act as allosteric inhibitors which alter the formation of the high affinity binding site for the natural agonist (Gether *et al.*, 1993a). If the potentiation of the blood pressure response results from a specific interaction of RP 67580 with central NK_1 receptors, our data suggest that the molecular interaction of RP 67580 with the brain NK_1 receptors *in vivo* may at least partly depend on the concentration of the agonist. RP 67580 at lower doses behaves as a full antagonist for central NK_1 receptors, whereas higher concentrations of this compound seem to sensitize these receptors to SP.

The dose of 100 pmol RP 67580 was most effective in inhibiting the cardiovascular and behavioural responses to SP. To test the selectivity of RP 67580 at central tachykinin receptors *in vivo* we investigated the effects of the same dose of RP 67580 and of its inactive enantiomer, RP 68651, on the cardiovascular and behavioural responses induced by the natural agonists for NK_2 and NK_3 receptors, NKA and NKB, respectively.

Compared to senktide, a specific agonist for NK_3 receptors, the cardiovascular response to an equimolar dose of NKB was weaker. The cardiovascular response induced by stimulation of central NK_3 receptors is brought about by increased release of vasopressin into the circulation rather than by stimulation of sympathetic activity (Takano *et al.*, 1990). As with senktide, the initial increase in BP was accompanied by a slight bradycardia followed by tachycardia. The behavioural response to NKB was weak and, in contrast to senktide, WDS did not represent the prominent behavioural manifestation (Itoi *et al.*, 1992). Compared to senktide, the faster degradation of NKB in the ventricular system or in periventricular tissues may explain the weaker potency of the peptide in inducing the cardiovascular and behavioural effects. Nevertheless, NKB was employed in the present study because we intended to investigate the effect of RP 67580 on central effects induced by the natural agonists for tachykinin receptors. The failure of RP 67580 to affect the central effects of NKB is not surprising since among the three tachykinin receptors, NK_1 and NK_3 receptors show the most distinct differences in their peptide binding profile (Regoli *et al.*, 1987; Helke *et al.*, 1990).

However, the same is not true for central NK_1 and NK_2 receptors. The central effects of SP are predominantly mediated by NK_1 receptors and those of NKA solely by NK_2 receptors (Tschöpe *et al.*, 1992). However, recent studies have demonstrated that SP can also interact with NK_2 receptors and that NKA, in turn, may desensitize one of the two proposed subtypes of central NK_1 receptors (Culman *et al.*, 1993). In the present study, the central responses to NKA remained unaffected after pretreatment with either RP 67580 or with RP 68651, suggesting that RP 67580 does not interact with central NK_2 receptors.

In conclusion, we have shown that RP 67580 but not its inactive enantiomer, RP 68651, potently inhibits in a relatively narrow range of effective doses the cardiovascular and behavioural effects induced by SP without affecting those induced by NKA or NKB. Hence, our data demonstrate that RP 67580 is a selective high affinity antagonist at central NK_1 tachykinin receptors in the rat. High doses of RP 67580 stereoselectively potentiated the blood pressure response to SP. The present data do not allow any definite conclusion regarding the nature of this phenomenon.

We are grateful to Dr C. Garret from Rhône-Poulenc Rorer, France who generously provided RP 67580 and RP 68651.

References

BARR, A.J. & WATSON, S.P. (1993). Non-peptide antagonists, CP-96,345 and RP 67580, distinguish species variants in tachykinin NK_1 receptors. *Br. J. Pharmacol.*, **108**, 223–227.

BEAUJOUAN, J.-C., HEUILLET, E., PETITET, F., SAFFROY, M., TORRENS, Y. & GLOWINSKI, J. (1993). Higher potency of RP 67580, in the mouse and in the rat compared with other nonpeptide and peptide tachykinin NK_1 antagonists. *Br. J. Pharmacol.*, **108**, 793–800.

BERESFORD, I.J.M., BIRCH, P.J., HAGAN, R.M. & IRELAND, S.J. (1991). Investigation into species variants in tachykinin NK_1 receptors by use of the non-peptide antagonist, CP-96,345. *Br. J. Pharmacol.*, **104**, 292–293.

CULMAN, J., TSCHÖPE, C., JOST, N., ITOI, K. & UNGER, TH. (1993). Substance P and neurokinin A induced desensitization to cardiovascular and behavioral effects: evidence for the involvement of different tachykinin receptors. *Brain Res.*, **625**, 75–83.

DONNERER, J., STARK, U., TRITTHART, H.A. & LEMBECK, F. (1992). CP-96,345, a non-peptide antagonist of substance P. III. Cardiovascular effects in mammals unrelated to actions on substance P receptors. *Naunyn-Schmied. Arch. Pharmacol.*, **346**, 328–332.

FARDIN, V., FOUCAULT, F., BOCK, M.D., JOLLY, A., FLAMAND, O., CLERC, F. & GARRET, C. (1993). Variations in affinities for the NK_1 receptor: differences between the non-peptide substance P antagonists RP 67580 and CP-96,345 and the agonist septide. *Regul. Pept.*, **46**, 300–303.

FONG, T.M., CASCIERI, M.A., YU, H., BANSAL, A., SWAIN, C. & STRADER, C.D. (1993). Amino-aromatic interaction between histidine 197 of the neurokinin-1 receptor and CP 96345. *Nature*, **362**, 350–353.

GARRET, C., CARRUETTE, A., FARDIN, V., MOUSSAOUI, S., PEYRONEL, J.-F., BLANCHARD, J.-C. & LADURON, P.M. (1991). Pharmacological properties of a selective nonpeptide substance P antagonist. *Proc. Natl. Acad. Sci. U.S.A.*, **88**, 10208–10212.

GARRET, C., CARRUETTE, A., FARDIN, V., MOUSSAOUI, S., MONTIER, F., PEYRONEL, J.-F. & LADURON, P.M. (1993). Antinociceptive properties and inhibition of neurogenic inflammation with potent SP antagonists belonging to perhydroisoindolones. *Regul. Pept.*, **46**, 24–30.

GETHER, U., JOHANSEN, T.E., SNIDER, R.M., LOWE III, J.A., EMONDS-ALT, X., YOKOTA, Y., NAKANISHI, S. & SCHWARTZ, T.W. (1993a). Binding epitopes for peptide and non-peptide ligands on the NK_1 (substance P) receptor. *Regul. Pept.*, **46**, 49–58.

GETHER, U., JOHANSEN, T.E., SNIDER, R.M., LOWE III, J.A., NAKANISHI, S. & SCHWARTZ, T.W. (1993b). Different binding epitopes on the NK_1 receptor for substance P and a non-peptide antagonist. *Nature*, **362**, 345–348.

GISPEN, W.H., WIEGANT, V.M., GREVEN, H.M. & DE WIED, D. (1975). The induction of excessive grooming in the rat by intraventricular application of peptides derived from ACTH: structure-activity studies. *Life Sci.*, **17**, 645–652.

GRIESBACHER, T., DONNERER, J., LEGAT, F.J. & LEMBECK, F. (1992). CP-96,345, a non-peptide antagonist of substance P: II. Actions on substance P-induced hypotension and bronchoconstriction, and on depressor reflexes in mammals. *Naunyn-Schmied. Arch. Pharmacol.*, **346**, 323–327.

GUARD, S. & WATSON, S.P. (1991). Tachykinin receptor types: classification and membrane signalling mechanisms. *Neurochem. Int.*, **18**, 149–165.

GUARD, S., BOYLE, S.J., TANG, K.-W., WATLING, K.J., MCKNIGHT, A.T. & WOODRUFF, G.N. (1993). The interaction of the NK_1 receptor antagonist CP-96,345 with L-type calcium channels and its functional consequences. *Br. J. Pharmacol.*, **110**, 385–391.

HELKE, C.J., KRAUSE, J.E., MANTYH, P.W., COUTURE, R. & BANNON, M.J. (1990). Diversity in mammalian tachykinin peptidergic neurons: multiple peptide, receptors, and regulatory mechanisms. *FASEB J.*, **4**, 1606–1615.

ITOI, K., TSCHÖPE, C., JOST, N., CULMAN, J., LEBRUN, C., STAUSS, B. & UNGER, TH. (1992). Identification of the central tachykinin receptor subclass involved in substance P-induced cardiovascular and behavioral responses in conscious rats. *Eur. J. Pharmacol.*, **219**, 435–444.

LAIRD, J.M.A., HARGREAVES, R.J. & HILL, R.G. (1993). Effect of RP 67580, a non-peptide neurokinin$_1$ receptor antagonist, on facilitation of a nociceptive spinal flexion reflex in the rat. *Br. J. Pharmacol.*, **109**, 713–718.

LOMBET, A. & SPEDDING, M. (1994). Differential effects of non-peptidic tachykinin receptor antagonists on Ca^{2+} channels. *Eur. J. Pharmacol. Molec. Pharmacol. Section*, **267**, 113–115.

MAGGI, C.A., PATACCHINI, R., ROVERO, P. & GIACHETTI, A. (1993). Tachykinin receptors and tachykinin receptor antagonists. *J. Auton. Pharmacol.*, **13**, 23–93.

MAGGIO, J.E. (1988). Tachykinins. *Annu. Rev. Neurosci.*, **11**, 13–28.

MOUSSAOUI, S.M., MONTIER, F., CARRUETTE, A., BLANCHARD, J.C., LADURON, P.M. & GARRET, C. (1993). A non-peptide NK_1-receptor antagonist, RP 67580, inhibits neurogenic inflammation postsynaptically. *Br. J. Pharmacol.*, **109**, 259–264.

NAKANISHI, S. (1991). Mammalian tachykinin receptors. *Annu. Rev. Neurosci.*, **14**, 123–126.

OTSUKA, M. & YOSHIOKA, K. (1993). Neurotransmitter functions of mammalian tachykinins. *Physiol. Rev.*, **73**, 229–308.

REGOLI, D., DRAPEAU, G., DION, S. & D'ORLÉANS-JUSTE, P. (1987). Pharmacological receptors for substance P and neurokinins. *Life Sci.*, **40**, 109–117.

SNIDER, M.R., CONSTANTINE, J.W., LOWE III, J.A., LONGO, K.P., LEBEL, W.S., WOODY, H.A., DROZDA, S.E., DESAI, M.C., VINICK, F.J., SPENCER, R.W. & HESS, H. (1991). A potent, non-peptide antagonist of the substance P (NK_1) receptor. *Science*, **251**, 435–437.

STAUSS, B., ITOI, K., STAUSS, H. & UNGER, TH. (1990). A novel inexpensive computer system to record and analyse hemodynamic data in conscious animals. *Eur. J. Pharmacol.*, **183**, 863.

TAKANO, Y., NAGASHIMA, A., HAGIO, T., TATEISHI, K. & KAMIYA, H. (1990). Role of central tachykinin peptides in cardiovascular regulation in rats. *Brain Res.*, **528**, 231–237.

TSCHÖPE, C., PICARD, P., CULMAN, J., PRAT, A., ITOI, K., REGOLI, D., UNGER, TH. & COUTURE, R. (1992). Use of selective antagonists to dissociate the central cardiovascular and behavioural effects of tachykinins on NK_1 and NK_2 receptor in the rat. *Br. J. Pharmacol.*, **107**, 750–755.

UNGER, TH., CAROLUS, S., DEMMERT, G., GANTEN, D., LANG, R.E., MASER-GLUTH, C., STEINBERG, H. & VEELKEN, R. (1988). Substance P induces a cardiovascular defense reaction in the rat: pharmacological characterization. *Circ. Res.*, **63**, 812–820.

WANG, Z.-Y. & HÅKANSON, R. (1992). (±)-CP-96,345, a selective tachykinin NK_1 receptor antagonist has non-specific actions on neurotransmission. *Br. J. Pharmacol.*, **107**, 762–765.

WANG, Z.-Y., TUNG, S.R., STRICHARTZ, G.R. & HÅKANSON, R. (1994). Non-specific actions of the non-peptide tachykinin receptor antagonists, CP-96,345, RP 67580 and SR 48968, on neurotransmission. *Br. J. Pharmacol.*, **111**, 179–184.

(Received April 11, 1994
Revised October 4, 1994
Accepted December 5, 1994)

British Journal of Pharmacology (1995) 114, 1317-1323

Delayed circulatory failure due to the induction of nitric oxide synthase by lipoteichoic acid from *Staphylococcus aureus* in anaesthetized rats

Sjef J. De Kimpe, Melanie L. Hunter, Clare E. Bryant, [1]Christoph Thiemermann & John R. Vane

The William Harvey Research Institute, St. Bartholomew's Hospital Medical College, Charterhouse Square, London EC1M 6BQ

1 This study investigates the effect of lipoteichoic acid (LTA) from the cell wall of *Staphylococcus aureus*, a micro-organism without endotoxin, on haemodynamics and induction of nitric oxide synthase (iNOS) in the anaesthetized rat.

2 Intravenous injection of LTA (10 mg kg^{-1}) resulted in a decrease in blood pressure from 123 ± 1 mmHg to 83 ± 7 mmHg after 270 min ($P<0.001$) and a reduction of the pressor response to noradrenaline (1 μg kg^{-1}) from 33 ± 1 mmHg.min to 23 ± 3 mmHg.min after 270 min ($P<0.05$).

3 The delayed circulatory failure (hypotension and vascular hyporeactivity) caused by LTA was prevented by pretreatment of rats with dexamethasone (10 mg kg^{-1}, 60 min prior to LTA) or the nitric oxide synthase inhibitor N^G-monomethyl-L-arginine (L-NMMA, 10 mg kg^{-1}h^{-1}, i.v. infusion starting 30 min prior to LTA).

4 In contrast, treatment of rats with polymyxin B (0.05 mg kg^{-1}), an agent which binds endotoxin (lipopolysaccharides, LPS), did not affect the delayed circulatory failure caused by LTA. Polymyxin B, however, attenuated the hypotension and vascular hyporeactivity to noradrenaline afforded by endotoxaemia (2 mg kg^{-1} LPS, i.v.) for 270 min.

5 The delayed circulatory failure caused by LTA was associated with a time-dependent increase in (i) the expression of iNOS protein in the lung (Western blot analysis), and (ii) iNOS activity. This increase in iNOS protein and activity was prevented by pretreatment of LTA-rats with dexamethasone (10 mg kg^{-1}).

6 Intravenous injection of LTA resulted in an increase in serum tumour necrosis factor (TNF)-α (maximum at 90 min after LTA), which was attenuated by pretreatment of rats with dexamethasone (10 mg kg^{-1}, 60 min prior to LTA). The magnitude of the rise in TNF-α caused by LTA was similar to the one elicited by LPS (10 mg kg^{-1}, i.v.).

7 Thus, an enhanced formation of nitric oxide following the induction of iNOS contributes importantly to the delayed vascular failure (hypotension and vascular hyporeactivity) caused by LTA in the anaesthetized rat. We suggest that the endogenous release of TNF-α contributes to the induction of iNOS caused by LTA *in vivo*.

Keywords: Nitric oxide; lipoteichoic acid; gram-positive shock; circulatory shock; hypotension; noradrenaline

Introduction

Nitric oxide (NO) is a potent endogenous vasodilator produced from the guanidino nitrogen group of L-arginine by nitric oxide synthase (NOS). Different isoforms of NOS have recently been sequenced, cloned and expressed (for review, see Nathan, 1992; Knowles and Moncada, 1994). Under physiological conditions, the release of NO from endothelial cells by the constitutive NOS (eNOS) causes dilatation of the underlying vascular smooth muscle and contributes importantly to the regulation of organ blood flow and blood pressure (Moncada *et al.*, 1991). In addition, bacterial lipopolysaccharides (LPS, endotoxin) and a number of cytokines, such as tumour necrosis factor (TNF)-α, cause the expression of a distinct, inducible isoform of NOS (iNOS) in a wide variety of cells including macrophages, endothelial and vascular smooth muscle cells (for review, see Moncada *et al.*, 1991; Thiemermann, 1994). In contrast to eNOS, iNOS is calcium-independent and produces large amounts of NO for relatively long periods. The NO released following induction of iNOS in activated macrophages is cytostatic/cytotoxic to certain microbial pathogens and tumour cells. Overproduction of NO following iNOS induction in vascular smooth muscle cells makes an important contribution to the circulatory failure (hypotension and vascular hyporeactivity to vasoconstrictor agents) in endotoxin shock and to the delayed vascular decompensation in haemorrhagic shock (for review, see Thiemermann, 1994).

There are numerous studies which have used LPS in animals and man to elucidate the sequence of the pathophysiological events which lead to the 'systemic inflammatory response syndrome' (SIRS) and ultimately circulatory shock. Although these studies help to gain a better understanding of the pathophysiology of gram-negative shock, they may only provide a limited insight into the pathophysiology of circulatory shock caused by gram-positive bacteria, for these organisms do not contain endotoxin. However, the prevalence of sepsis resulting from gram-positive organisms has risen markedly in the last decade, and it is possible that cases of gram-positive sepsis may predominate in the years to come (Bone, 1994). A gram-positive organism contains various not very well characterized substances, that may initiate the release of cytokines, SIRS, or shock (Bone, 1993). Moreover, little is known about the pathophysiological importance of NO in gram-positive sepsis. Lipoteichoic acid (LTA), a cell-wall component from gram-positive bacteria, causes an enhanced

[1] Author for correspondence.

release of NO due to induction of iNOS in cultured vascular smooth muscle cells (Auguet *et al.*, 1992; Lonchampt *et al.*, 1992) and in murine peritoneal macrophages (Cunha *et al.*, 1993). LTA also stimulates the release of cytokines, such as TNF-α, from human isolated blood monocytes (Lindermann *et al.*, 1988; Bhakdi *et al.*, 1991) and murine peritoneal macrophages (Kuwano *et al.*, 1993). This study investigates the effect of LTA isolated from the gram-positive bacterium, *Staphylococcus aureus*, on haemodynamics and induction of iNOS in anaesthetized rats.

Methods

Haemodynamic measurements

Animal experiments were performed in accordance with the Home Office regulations. Male Wistar rats (200–300 g, Glaxo Laboratories Ltd, Greenford, Middlesex) were anaesthetized with thiopentone sodium (Trapanal, 3% solution, 120 mg kg^{-1}, i.p.). The trachea was cannulated to facilitate respiration, and rectal temperature was maintained at 37°C with a homeothermic blanket (BioSciences, Sheerness, Kent). The right carotid artery was cannulated with a catheter filled with heparinised saline (50 iu ml^{-1} heparin in 0.9 M NaCl) and connected to a pressure transducer (model P23XL, Spectramed, Stratham, NH, U.S.A) for the measurement of phasic and mean arterial blood pressure (MAP) and heart rate, which were registered on a polygraph recorder (model 7D, Grass Instruments, Quincy, MA, U.S.A). The right femoral and right jugular veins were cannulated for the administration of drugs.

After the surgical procedure, cardiovascular parameters were allowed to stabilize for 20 min. After recording baseline haemodynamic parameters, the pressor response to noradrenaline (1 μg kg^{-1}, i.v.) was determined. Subsequently, animals received vehicle (0.2 ml 0.9% NaCl) or LTA from *Staphylococcus aureus* (10 mg kg^{-1}) as a slow intravenous injection over 2 min. The pressor responses to noradenaline were reassessed at 60, 120, 180, 240, 300, 360 min after the administration of LTA. At the end of the experiment, lung, spleen, liver, heart and brain were removed, snap frozen in liquid nitrogen and stored at −80°C for the measurement of iNOS activity (see below).

To investigate the role of NO in the haemodynamic changes elicited by LTA, rats were (i) pretreated with the glucocorticosteroid dexamethosone (10 mg kg^{-1}, i.v., 60 min prior to LTA), a potent inhibitor of the induction of iNOS (Radomski *et al.*, 1990), or (ii) treated with the competitive NOS inhibitor N^G-monomethyl-L-arginine (L-NMMA, 10 mg kg^{-1} h^{-1}, i.v. starting 30 min prior to the injection of LTA and continuing until the end of the experiments). In these experiments, the pressor responses to noradrenaline (1 μg kg^{-1}, i.v.) were assessed 10 min before the administration of LTA and 60 and 270 min after LTA. To exclude the possibility that endotoxaemia accounts for the haemodynamic effects afforded by LTA, a separate group of animals was treated with LTA together with polymyxin B (0.05 mg kg^{-1}, i.v.), which binds and inactivates endotoxin. To ensure that this dose of polymyxin B is sufficient to attenuate the haemodynamic effects caused by endotoxin (positive control), rats received polymyxin B (0.05 mg kg^{-1}, i.v.) together with LPS (2 mg kg^{-1}, i.v.).

In a separate set of experiments, rats were treated with either vehicle (control) or LTA (10 mg kg^{-1}, i.v.) for 90, 180 or 270 min. At the end of each experiment, blood samples were obtained to measure white blood cell counts, TNF-α levels in serum and nitrite concentration in plasma. Subsequently, all animals were killed and the lung was removed and snap frozen in liquid nitrogen in order to evaluate the time-dependent changes in iNOS protein expression [Western (immuno)blot analysis] and iNOS activity.

Serum TNF-α levels

TNF-α levels were measured in the serum with a mouse TNF-α enzyme-linked immunoabsorbent assay (ELISA) kit from Genzyme (Cambridge, MA, U.S.A) which has also been used successfully to quantitate natural rat TNF-α (Pizarro *et al.*, 1993). The samples were measured according to the instruction delivered with the ELISA kit by the supplier. For comparison, TNF-α levels were also measured in the serum obtained from LPS-treated rats at 90 min and 180 min after injection of LPS (10 mg kg^{-1}, i.v.).

Plasma nitrite concentration

Nitrite is the primary oxidation product of NO and, hence, the nitrite concentration in plasma was determined as an indicator of changes in NO production. Nitrite was assayed by adding 0.8 ml Griess reagent (4% sulphonilamide and 0.2% naphtylenediamide in 10% phosphoric acid) to 0.2 ml plasma. After centrifugation, the difference in optical density between 540 mm and 600 nm was measured with a spectrophotometer. Nitrite concentrations (μM) were calculated by comparison with the optical density of standard solutions of sodium nitrite prepared in plasma.

NOS activity assay

Frozen organs (lung, spleen, liver, heart, brain) were homogenized on ice with an Ultra-Turrax T 25 in a Tris-buffer (pH = 7.4) composed of (mM) Tris-HCl 50, EDTA 0.1, EGTA 0.1, 2-mercaptoethanol 12 and phenylmethylsulphonylfluoride 1. Conversion of [^{3}H]-L-arginine to [^{3}H]-L-citrulline was measured in the homogenates as previously described (Szabó *et al.*, 1993a). Briefly, tissue homogenates (30 μl, approximately 100 μg protein) were incubated in the presence of L-arginine/[^{3}H]-L-arginine (10 μM, 7.4 kBq per tube), NADPH (1 mM), calmodulin (300 u ml^{-1}), tetrahydrobiopterin (5 μM), L-valine (50 mM) and calcium (1 mM) for 30 min at room temperature in Tris-buffer (total reaction volume 100 μl). Reactions were stopped by addition of 1 ml ice-cold HEPES buffer (pH = 5.5) containing HEPES (20 mM), EDTA (2 mM) and EGTA (2 mM). Reaction mixtures were applied to DOWEX 50W (sodium form) columns, and the eluted [^{3}H]-L-citrulline activity was measured by scintillation counting (model, Beckman Instruments Inc, Fullerton, California). Experiments performed in the absence of NADPH determined the extent of [^{3}H]-L-citrulline formation independent of NOS activity. Experiments in calcium-free buffer containing NADPH and EGTA (1 mM) determined the calcium-independent (i.e., induced) NOS activity. Protein concentrations were measured spectrophotometrically in 96-well plates by the method of Bradford with bovine serum albumin used as standard (Bradford, 1976).

Western (immuno)blot analysis

Lungs were homogenized on ice with an Ultra-Turrax T 25 homogenizer in an extraction buffer (pH = 7.4) consisting of 50 mM Tris-HCl, 10 mM EDTA, 1% v/v Triton X-100, and the protease inhibitors pepstatin A 50 μM, leupeptin 0.2 mM and phenylmethylsulphonylfluoride 1 mM. The homogenates were centrifuged (5000 *g*) for 15 min at 4°C and the supernatant was boiled for 10 min with gel-loading buffer (Tris 20 mM, EDTA 2 mM, SDS 2% w/v, glycerol 20% v/v, 2-mercaptoethanol 10% v/v, bromophenol blue 2 mg ml^{-1}, pH = 6.8) in a ratio of 1:1 (v/v). Cell extracts from bovine aortic endothelial cells in culture and murine macrophages (J774 cell line) activated with LPS (1 μg ml^{-1} for 24 h) were used as a positive control for the presence of eNOS and iNOS protein, respectively. The proteins in the samples were resolved by one dimensional gel electrophoresis (7.5% SDS gel) with molecular weight markers (SDS-7B; Sigma). After transfer to nitrocellulose by electrophoresis, the membranes

were primed overnight at 4°C with a polyclonal antibody raised to macrophage iNOS developed in rabbits (a generous gift from Eurodiagnostica, Sweden) or a monoclonal mouse antibody raised to constitutive, endothelial NOS (Affinity Research Products Ltd., U.K.). The blots were then incubated as appropriate with either anti-rabbit or anti-mouse IgG linked to horseradish peroxidase. All antibodies were used at a 1:1000 dilution. Subsequently, the Western blots were developed with diaminobenzamine used as a substrate.

Drugs

Unless stated otherwise, all compounds were purchased from Sigma (Dorset). Heparin (Multiparin) was obtained from Evans Medical (Middlesex) U.K. and thiopentone sodium (Intraval Sodium) from Rhône Mérieux Ltd. (Harlow, Essex). Solutions for injection were prepared in nonpyrogenic saline (0.9% NaCl; Baxter Healthcare Ltd., Thetford, Norfolk) and care was taken to prevent endotoxin contamination.

Data analysis

All data are presented as mean ± standard error of the mean (s.e.mean) of n independent experiments. The vasopressor response to noradrenaline was evaluated determining the area under the curve and was expressed in mmHg·min. Statistical analysis was performed by (one- or two-way) analysis of variance (ANOVA). If appropriate, this was followed by Bonferroni's test (one-way ANOVA) or Fisher's test (two-way ANOVA) for multiple comparison of single means.

Results

Circulatory failure induced by LTA

Injection of LTA (10 mg kg^{-1}) resulted in an initial fall in MAP from 123 ± 1 mmHg (time 0, control) to 101 ± 3 mmHg at 60 min ($P<0.01$). This was followed by a second fall in MAP from 104 ± 6 mmHg at 150 min to 83 ± 7 mmHg at 270 min. Thereafter, the MAP only gradually declined reaching 79 ± 4 mmHg at 360 min after LTA injection. The decrease in MAP observed in LTA-treated rats was significantly greater than the one observed in vehicle-treated rats (Figure 1a), in which the MAP showed a small, gradual decline from 122 ± 3 mmHg (at time 0) to 106 ± 7 mmHg at 360 min after injection of vehicle. There was no significant effect of LTA on heart rate (results not shown). In addition, the pressor response elicited by noradrenaline (1 μg kg^{-1}) was significantly reduced at 60, 120, 300 and 360 min in LTA-treated rats, but not in rats receiving vehicle (Figure 1b).

All subsequent experiments designed to elucidate the mechanism of the circulatory failure elicited by LTA were limited to 270 min, as both hypotension and vascular hyporeactivity to noradrenaline were near maximal at this time point. Injection of polymyxin B (0.05 mg kg^{-1}) together with LTA (10 mg kg^{-1}) neither inhibited hypotension to LTA (Figure 2a) nor the vascular hyporeactivity to noradrenaline (Figure 2b). When given together with LPS (2 mg kg^{-1}),

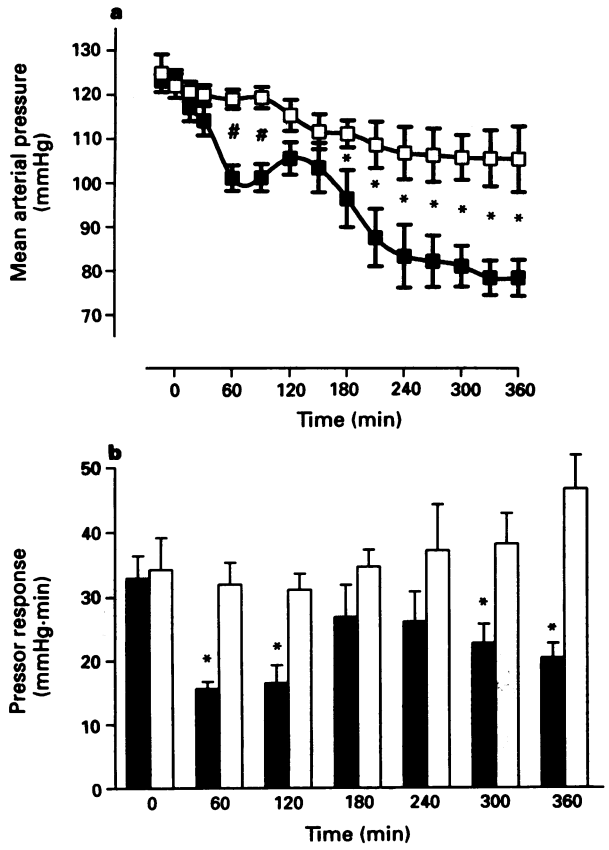

Figure 1 Hypotension (a) and attenuation of the pressor response to noradrenaline (b) (1 μg kg^{-1}, i.v.) elicited by lipoteichoic acid (LTA, 10 mg kg^{-1}, i.v.). Rats were treated with LTA (a: ■; b: solid columns, $n=8$) or vehicle (a: □; b: open columns, $n=5$). Results are expressed as mean ± s.e.mean. *$P<0.05$, *$P<0.01$ LTA vs. vehicle (two-way ANOVA followed by Fisher's test).

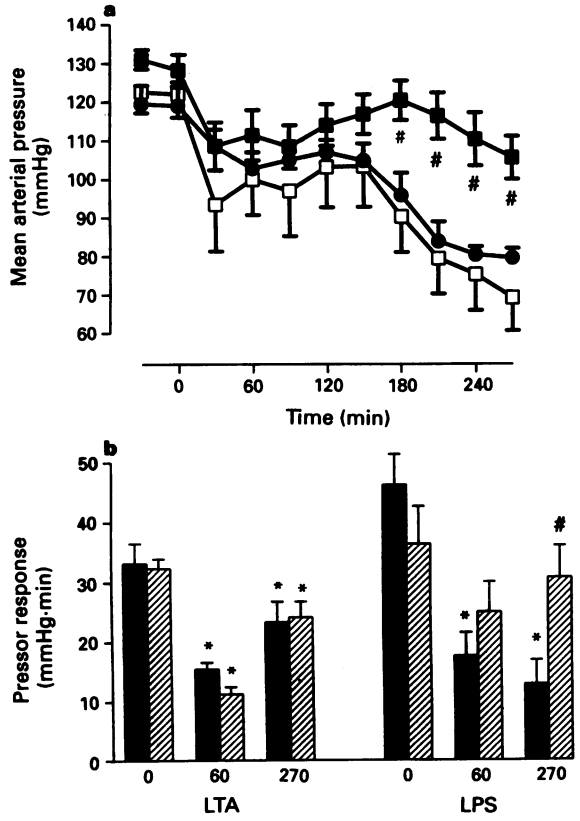

Figure 2 The delayed hypotension (a) and the vascular hyporeactivity to noradrenaline (b) elicited by endotoxin (lipopolysaccharide, LPS, 10 mg kg^{-1}, i.v.), but not by lipoteichoic acid (LTA, 10 mg kg^{-1}, i.v.) is inhibited by polymyxin B (0.05 mg kg^{-1}, i.v.). Rats were treated with LPS (a) □, b: solid columns), LPS and polymyxin B (a: ■, b: hatched columns), LTA (a: not shown -see Figure 3a, b: solid columns), or LTA and polymyxin B (a: ●, b: hatched columns). Results are expressed as mean ± s.e.mean. # $P<0.01$ (a), $P<0.05$ (b) LPS vs. LPS plus polymyxin B (two-way ANOVA followed by Fisher's test) and *$P<0.05$ vs time 0 (B only; one-way ANOVA followed by Bonferroni's test).

however, polymyxin B (0.05 mg kg^{-1}) attenuated both the fall in MAP as well as the vascular hyporeactivity to noradrenaline (at time 270 min) elicited by LPS (Figure 2). Although LPS in the presence of polymyxin B still caused some immediate decrease in MAP and vascular hyporeactivity to noradrenaline (60 min), this was no longer statistically significant compared to time 0 (just prior to LPS injection).

Inhibition of LTA-induced circulatory failure

Pretreatment of the animals with dexamethasone (10 mg kg^{-1}, i.v., 1 h prior to LTA) prevented the early and the delayed fall in MAP elicited by LTA (Figure 3a). In addition, dexamethasone pretreatment prevented the hyporeactivity to noradrenaline observed at 60 and 270 min after LTA injection (Figure 3b). Surprisingly, in control (vehicle treated)-rats pretreated with dexamethasone, the pressor responses to noradrenaline (measured as area under the curve) increased over time from 32 ± 6 mmHg·min (time 0), 35 ± 7 mmHg·min at 60 min to 51 ± 8 mmHg·min at 270 min ($P<0.05$) after injection of vehicle. There was no significant difference in the pressor response to noradrenaline between dexamethasone pretreated rats receiving vehicle or LTA.

Infusion of the NOS inhibitor L-NMMA (10 mg kg^{-1} h^{-1}) caused within 30 min a significant increase in MAP from 126 ± 4 mmHg to 141 ± 4 mmHg ($P<0.05$). The subsequent administration of LTA resulted in a fall in MAP to 118 ± 3 mmHg at 60 min ($P<0.01$). However, the delayed hypotension caused by LTA was significantly attenuated by infusion of L-NMMA (Figure 3a). In addition, infusion of L-NMMA also prevented the LTA-induced vascular hyporeactivity to noradrenaline (Figure 3b).

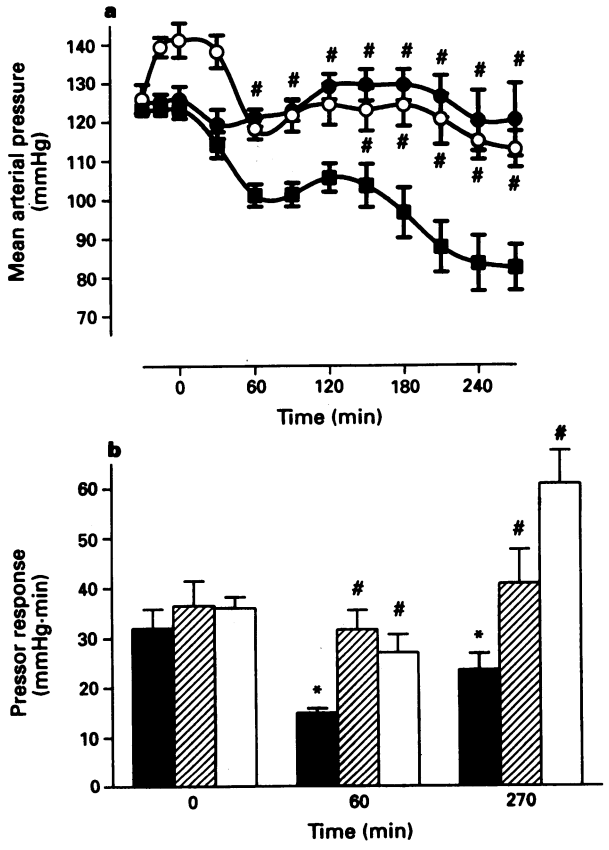

Figure 3 Inhibition of the hypotension (a) and vascular hyporeactivity to noradrenaline (b) elicited by lipoteichoic acid (LTA, 10 mg kg^{-1}, i.v.) by treatment of rats with dexamethasone (10 mg kg^{-1}, i.v., 1 h before LTA) or N^G-monomethyl-L-arginine (L-NMMA, 10 mg kg^{-1} h^{-1}, i.v., continuous infusion starting 30 min before LTA). Rats were treated with LTA (a: ■, b: solid columns), LTA and L-NMMA (a: ○, b: hatched columns), or LTA and dexamethasone (a: ●, b: open columns). Results are expressed as mean ± s.e.mean. #$P<0.01$ LTA vs LTA plus treatment (dexamethasone or L-NMMA) (two-way ANOVA followed by Fisher's test), and *$P<0.05$ vs time 0 (b only; one-way ANOVA followed by Bonferroni's test).

Induction of NOS by LTA

At 360 min after LTA injection, there was a significant increase in total NOS and calcium-independent iNOS activity in organ homogenates prepared from lung, spleen and liver (Figure 4). In contrast, no iNOS activity was found in homogenates from either brain or heart of rats treated for 360 min with LTA. The constitutive, neuronal NOS activity measured in brain homogenates was similar in LTA- and vehicle-treated rats (Figure 4).

The time-course of the expression of iNOS activity elicited by LTA is depicted in Figure 5. No significant increase in iNOS activity was observed in lungs obtained from rats treated with LTA for 90 min. However, a significant and progressive increase in iNOS activity was observed in lungs obtained from rats treated with LTA for 180 or 270 min. Similarly, plasma nitrite levels were not significantly elevated at 90 min after LTA administration, while a significant increase in plasma nitrite was observed at 180 and 270 min (Figure 5). Western blot analysis demonstrated a protein of approximately 130 kDa which was recognised by the iNOS antibody. A time-dependent expression of a 130 kDa protein recognised by the iNOS antibody was demonstrated by Western blot analysis in homogenates from lung obtained from rats treated with LTA (Figure 6). The iNOS antibody showed some cross reactivity with eNOS, but the protein recognised by the iNOS antibody was not recognised by the eNOS antibody. Furthermore, treatment of rats with LTA did not result in any alteration in the expression of eNOS protein (results not shown). Dexamethasone (10 mg kg^{-1}, i.v., 1 h prior to LTA) inhibited the expression of iNOS protein in the lung (Figure 6). Moreover, dexamethasone prevented the increase in iNOS activity caused by LTA (at 270 min) in the lung (LTA alone: 113 ± 10, and LTA plus dexamethasone: 2 ± 6 pmol L-citrulline 30 min^{-1} mg^{-1} protein; $P<0.001$).

Increase in serum TNF-α levels caused by LTA

Serum TNF-α levels were below the detection limit (35 pg ml^{-1}) in serum obtained from rats prior to the injection of LTA. However, after the injection of LTA, serum TNF-α levels rose markedly to 3834 ± 330 pg ml^{-1} at 90 min

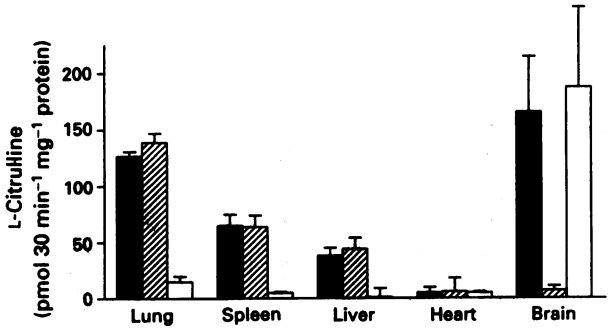

Figure 4 Induction of nitric oxide synthase activity (iNOS) by lipoteichoic acid (LTA, 10 mg kg^{-1}, i.v.) The conversion of [^{3}H]-L-arginine to [^{3}H]-L-citrulline was measured in homogenates from organs obtained from rats 6 h after treatment with vehicle (open columns) or LTA (solid columns). Hatched columns represent iNOS activity in the absence of calcium and in the presence of EGTA (1 mM) in homogenates from organs obtained from LTA-treated rats. Results are expressed as mean ± s.e.mean.

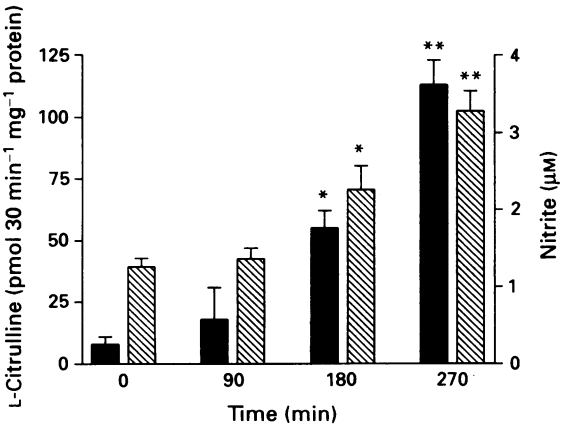

Figure 5 Time course of the induction of nitric oxide synthase activity (iNOS, solid columns) and the increase in plasma nitrite concentration (hatched columns) by lipoteichoic acid (LTA, 10 mg kg^{-1}, i.v.). The conversion of [^{3}H]-L-arginine to [^{3}H]-L-citrulline was measured in the absence of calcium and in the presence of EGTA (1 mM) in homogenates from lungs. Lungs and plasma were obtained at time 0 (control) or 90, 180 or 270 min after injection of LTA. Results are expressed as mean ± s.e.mean. *$P<0.05$ and **$P=0.01$ LTA vs. time 0 (control) (one-way ANOVA followed by Bonferroni's test).

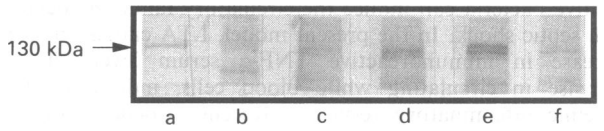

Figure 6 Time course of the expression of inducible nitric oxide synthase (iNOS) protein by lipoteichoic acid (LTA, 10 mg kg^{-1}, i.v.) determined by Western (immuno)blot analysis of homogenates from lung. The iNOS antibody recognised a protein at a molocular weight of approximately 130 kDa. The immunoblot presents in lane (a) endotoxin (1 μg ml^{-1}) activated murine macrophages (J774 cell line) (positive control), (b) time 0 (control rats), (c) LTA for 90 min, (d) LTA for 180 min, (e) LTA for 270 min, and (f) LTA for 270 min plus dexamethasone (10 mg kg^{-1}, i.v. 1 h before LTA). This immunoblot is representative for 3 separate experiments.

after which they rapidly declined to 498 ± 225 pg ml^{-1} at 180 and to 102 ± 12 pg ml^{-1} at 270 min ($n=6$). Pretreatment of rats with dexamethasone (10 mg kg^{-1}, i.v., 60 min prior to LTA) markedly attenuated the maximum increase in serum TNF-α levels caused by LTA (639 ± 275 pg ml^{-1}, $n=4$, $P<0.01$). Like LTA, injection of LPS (10 mg kg^{-1}) caused a time-dependent increase in serum TNF-α levels from undetectable levels (time 0) to 3553 ± 111 pg ml^{-1} at 90 min and 498 ± 183 pg ml^{-1} at 180 min ($n=3$–4).

Fall in white blood cell counts caused by LTA

Intravenous injection of LTA (10 mg kg^{-1}) caused a significant decrease in total white blood cell counts from 4.1 ± 0.3 × 10^6 ml^{-1} (time 0) to 1.8 ± 0.1 × 10^6 ml^{-1} at 90 min after LTA ($P<0.01$, $n=6$). This leukopenia was maintained throughout the experiment (180 min: 2.1 ± 0.2 × 10^6 ml^{-1}; 270 min: 3.0 ± 0.2 × 10^6 ml^{-1}).

Discussion

This study demonstrates that LTA from *Staphylococcus aureus* causes hypotension and vascular hyporeactivity to noradrenaline (circulatory failure) in the anaesthetized rat. Furthermore, LTA treatment resulted in a time-dependent increase in the expression of iNOS protein and activity, which coincided with an increase in plasma nitrite concentration. Thus, there is an enhanced formation of the vasodilator nitric oxide following the induction of iNOS after LTA. The time course of iNOS induction and plasma nitrite elevation reflect the delayed alterations in haemodynamics seen after LTA. The circulatory failure elicited by LTA occurs in two distinct phases. The first fall in blood pressure after LTA injection levels off after 60 min and is followed by a delayed, second drop in blood pressure starting approximately 150 min after LTA. Similarly, the pressor response to noradenaline was only significantly attenuated during the first (60 to 120 min) and the delayed (from 270 min) fall in blood pressure. Thus, only the delayed circulatory failure after LTA is associated with an elevated NO production following the induction of iNOS. Dexamethasone inhibited the induction of iNOS protein and activity elicited by LTA, explaining its beneficial haemodynamic effects on the circulatory failure elicited by LTA. The NOS inhibitor L-NMMA prevented the second fall in blood pressure and the delayed vascular hyporeactivity, providing further evidence that an enhanced formation of NO contributes to the delayed circulatory failure elicited by LTA.

The early hypotension and vascular hyporeactivity to vasoconstrictor agents in animals with LPS-shock is due to an enhanced formation of NO by the constitutive NOS (Julou-Schaeffer *et al.*, 1990; Kilbourn *et al.*, 1990; Thiemermann & Vane, 1990; Szabó *et al.*, 1993a). Here, NO release due to activation of the constitutive NOS also accounts for the acute vascular hyporeactivity caused by LTA in the anaesthetized rat, for (i) this vascular hyporeactivity was abolished by L-NMMA and (ii) no induction of iNOS in the lung was demonstrated within the first 90 min after LTA injection. Infusion of L-NMMA attenuated, but not abolished, the immediate hypotension caused by LTA. As L-NMMA caused a significant rise in blood pressure prior to injection of LTA, this effect of L-NMMA may in part be due to a functional antagonism. Dexamethasone prevented both the acute hypotension and acute vascular hyporeactivity elicited by LTA. As dexamethasone prevents the formation of prostanoids (Flower & Blackwell, 1979) and platelet-activating factor (Braquet *et al.*, 1987), an enhanced release of these inflammatory mediators may well mediate the early haemodynamic effects caused by LTA *in vivo*.

How gram-positive organisms initiate an inflammatory response is not yet clear. Animal models of sepsis have usually employed endotoxin, a constituent of the cell wall of gram-negative bacteria, which is regarded as the primary initiator of gram-negative septic shock (Suffredini *et al.*, 1989; Danner *et al.*, 1991). In the present study, LTA from the cell wall of *Staphylococcus aureus* induced a sustained decrease in blood pressure and a hyporeactivity to noradrenaline, that was not affected by the LPS neutralising agent, polymyxin B. In contrast, the delayed circulatory failure elicited by LPS was inhibited by polymyxin B. Thus, a rise in plasma LPS caused by contamination of LTA or by bacterial translocation from the intestine, is unlikely to account for the delayed hypotension and hyporeactivity to noradrenaline observed after LTA. Similarly, by using a well-characterized canine model of septic shock, Natanson *et al.* (1989) demonstrated that *Staphylococcus aureus* in the absence of endotoxaemia, induced the same cardiovascular abnormalities of septic shock as did *Escherichia coli*. Heat-killed *Staphylococcus epidermis* (a gram-positive organism) also induces a shock-like state without causing endotoxaemia in anaesthetized rabbits (Wakabayashi *et al.*, 1991). Thus, the present results further demonstrate that circulatory failure associated with septic shock can occur in the absence of endotoxin. Moreover, the present study shows that one component of the cell wall from gram-positive bacteria, LTA, may alone be sufficient to elicit cardiovascular abnormalities which are similar to those observed in septic shock.

Little is known about the mechanism by which gram-

positive bacteria can induce the circulatory failure associated with septic shock. In the present model, LTA causes an early increase in immunoreactive TNF-α serum levels and a decrease in circulating white blood cells, indicative of a systemic inflammatory response. Recent evidence indicates that inflammatory cytokines, such as TNF-α and interleukin (IL)-1, are key mediators of some of the pathophysiological events in septic shock caused by gram-positive bacteria. In a murine model of septic shock employing gram-positive bacteria, a causal relationship between the release of TNF-α and mortality has been reported (Freudenberg & Galanos, 1991) and, in the anaesthetized rabbit, release of interleukin-1 has been implicated in the hypotension induced by *Staphylococcus epidermis* (Aiura *et al.*, 1993). In the anaesthetized rat, IL-1 receptor antagonists and antibodies against TNF-α reduce not only the circulatory failure elicited by LPS, but also the induction of iNOS (Szabó *et al.*, 1993b; Thiemermann *et al.*, 1993). Interestingly, in the present study, expression of iNOS protein and activity followed the initial elevation in serum TNF-α and both effects were markedly attenuated by pretreatment with dexamethasone. Therefore, we suggest that the release of inflammatory cytokines such as TNF-α caused by LTA initiates translation and *de novo* iNOS protein synthesis resulting in an elevated release of NO.

The incidence of sepsis by gram-positive organisms has risen markedly and may predominate in the coming years (Bone, 1994). Therefore, it is important to develop animal models without endotoxaemia in order to elucidate the pathophysiological events leading to the circulatory failure caused by gram-positive organisms. These models are also useful to evaluate the effects of novel therapeutics which are potentially useful in septic shock. The demonstration that novel therapeutics exert beneficial effects in septic shock caused by gram-negative and gram-positive bacteria is of particular importance, for these agents are often (in clinical trials) given to patients regardless of the type of infectious organism. Thus, an enhanced release of NO following the induction of iNOS by LTA from *Staphylococcus aureus* is important for the delayed circulatory failure associated with septic shock.

This work was supported by a grant from Casella A.G. (Frankfurt, Germany). S.J.D.K. is a recipient of a travel fellowship from the commission of the European Union. C.E.B. is a Wellcome veterinary research fellow. C.T. is supported by a grant from the commission of the European Union (Biomed I, BMHI, 92/1893).

References

AIURA, K., GELFAND, J.A., BURKE, J.F., THOMPSON, R.C. & DINARELLO, C. (1993). Interleukin-1 (IL-1) receptor antagonist prevents *staphylococcus epidermis*-induced hypotension and reduces circulating levels of tumor necrosis factor and IL-1β in rabbits. *Inf. Immun.*, **61**, 3342–3350.

AUGUET, M., LONCHAMPT, M.-O., DELAFLOTTE, S., GOULIN-SCHULZ, J., CHABRIER, P.E. & BRAQUET, P. (1992). Induction of nitric oxide synthase by lipoteichoic acid from *Staphylococcus aureus* in vascular smooth muscle cells. *FEBS Lett.*, **297**, 183–185.

BHAKDI, S., KLONISCH, T., NUBER, P. & FISCHER, W. (1991). Stimulation of monokine production by lipoteichoic acids. *Inf. Immun.*, **59**, 4614–4620.

BONE, R.C. (1993). How gram-positive organisms cause sepsis. *J. Crit. Care*, **8**, 51–59.

BONE, R.C. (1994). Gram-positive organisms and sepsis. *Arch. Intern. Med.*, **154**, 26–34.

BRADFORD, M.M. (1976). A rapid and sensitive method for quantitation of microgram quantities of protein utilizing the principle of protein-dye binding. *Anal. Biochem.*, **72**, 248.

BRAQUET, P., TOUQUI, L., SHEN, T.Y. & VARGAFTIG, B.B. (1987). Perspectives in platelet-activating factor research. *Pharmacol. Rev.*, **39**, 97–145.

CUNHA, F.Q., MOSS, D.W., LEAL, L.M.C.C., MONCADA, S. & LIEW, F.Y. (1993). Induction of macrophage parasiticidal activity by *Staphylococcus aureus* and exotoxins through the nitric oxide synthesis pathway. *Immunology*, **78**, 563–567.

DANNER, R.L., ELIN, R.J., HOSSEINI, J.M., WESLEY, R.A., REILLY, J.M. & PARILLO, J.E. (1991). Endotoxemia in human septic shock. *Chest*, **99**, 169–175.

FLOWER, R.J. & BLACKWELL, G.J. (1979). Anti-inflammatory steroids induce biosynthesis of a phospholipase A_2 inhibitor which prevents prostaglandin generation. *Nature*, **278**, 456–459.

FREUDENBERG, M.A. & GALANOS, C. (1991). Tumor necrosis factor alpha mediates lethal activity of killed gram-negative and gram-positive bacteria in (D)-galactosamine-treated mice. *Inf. Immun.*, **59**, 2110–2115.

JULOU-SCHAEFFER, G., GRAY, G.A., FLEMING, I., SCHOTT, C., PARRATT, J.R. & STOCKLETT, J.-C. (1990). Loss of responsiveness induced by endotoxin involves L-arginine pathway. *Am. J. Physiol*, **259**, H1038–H1043.

KILBOURN, R.G., JUBRAN, A., GROSS, S.S., GRIFFITH, O.W., LEVI, R., ADAMS, J. & LODATO, R.F. (1990). Reversal of endotoxin-mediated shock by N^G-methyl-L-arginine, an inhibitor of nitric oxide synthesis. *Biochem. Biophys. Res. Commun.*, **172**, 1132–1138.

KNOWLES, R.G. & MONCADA, S. (1994). Nitric oxide synthases in mammals. *Biochem. J.*, **298**, 249–258.

KUWANO, K., AKASHI, A., MATSU-URA, I., NISHIMOTO, M. & ARAI, S. (1993). Induction of macophage-mediated production of tumor necrosis factor alpha by an L-form derived from *Staphylococcus aureus*. *Inf. Immun.*, **61**, 1700–1706.

LINDERMANN, R.A., ECONOMOU, J.S. & TOTHERMAL, H. (1988). Production of interleukin-1 and tumour necrosis factor by human monocytes activated by peridontal bacterial and extracted lipopolysaccharides. *J. Dent. Res.*, **67**, 1131–1135.

LONCHAMPT, M.O., AUGUET, M., DELAFLOTTE, S., GOULIN-SCHULZ, J., CHABRIER, P.E. & BRAQUET, P. (1992). Lipoteichoic acid: a new inducer of nitric oxide synthase. *J. Cardiovasc. Pharmacol.* **20**, (Suppl. 12), S145–S147.

MONCADA, S., PALMER, R.M.J. & HIGGS, E.A. (1991). Nitric oxide: physiology, pathophysiology, and pharmacology. *Pharmacol. Rev.*, **43**, 109–142.

NATANSON, C., DANNER, R.L., ELIN, R.J., HOSSEINI, J.M., PEART, K.W., BANKS, S.M., MACVITTIE, J.T., WALKER, R.I. & PARILLO, J.E (1989). Role of endotoxemia in cardiovascular dysfunction and mortality: *Escherichia coli* and *Staphylococcus aureus* challenges in a canine model of human shock. *J. Clin. Invest.*, **83**, 243–251.

NATHAN, C. (1992). Nitric oxide as a secretory product of mammalian cells. *FASEB J.*, **6**, 3051–3064.

PIZARRO, T.T., MALINOWSKA, K., KOVACS, E.J., CLANCY, J., Jr, ROBINSON, J.A. & PICCININI, L.A. (1993). Induction of TNFÂ and TNFβ gene expression in rat cardiac transplants during allograft rejection. *Transplantation*, **56**, 399–404.

RADOMSKI, M.W., PALMER, R.M.J. & MONCADA, S. (1990). Glucocorticoids inhibit expression of an inducible, but not the constitutive nitric oxide synthase in vascular endothelial cells. *Proc. Natl. Acad. Sci. U.S.A.*, **87**, 10043–10047.

SUFFREDINI, A.F., FROMM, R.E., PARKER, M.M., BRENNER, M., KOVACS, J.A., WESLEY, R.A. & PARILLO, J.E. (1989). The cardiovascular response of normal humans to the administration of endotoxin. *N. Engl. J. Med.*, **321**, 280–287.

SZABO, C., MITCHELL, J.A., THIEMERMANN, C. & VANE, J.R. (1993a). Nitric oxide-mediated hyporeactivity to noradrenaline precedes the induction of nitric oxide synthase in endotoxin shock. *Br. J. Pharmacol.*, **108**, 786–792.

SZABO, C., WU, C.-C., GROSS, S.S., THIEMERMANN, C. & VANE, J.R. (1993b). Interleukin-1 contributes to the induction of nitric oxide synthase by endotoxin *in vivo*. *Eur. J. Pharmacol.* **250**, 157–160.

THIEMERMANN, C. (1994). The role of arginine: nitric oxide pathway in circulatory shock. *Adv. Pharmacol.*, **28**, 45–79.

THIEMERMANN, C. & VANE, J. (1990). Inhibition of nitric oxide synthesis reduces the hypotension induced by bacterial lipopolysaccharides in the rat in vivo. *Eur. J. Pharmacol.*, **182,** 591–595.

THIEMERMANN, C., WU, C.-C., SZABO, C., PERETTI, M. & VANE, J.R. (1993). Role of tumour necrosis factor in the induction of nitric oxide synthase in a rat model of endotoxic shock. *Br. J. Pharmacol.*, **110,** 177–182.

WAKABAYASHI, G., GELFAND, J.A., JUNG, W.K., CONNOLY, R.J., BURKE, J.F. & DINARELLO, C.A. (1991). *Staphylococcus epidermis* induces complement activation tumor necrosis factor and inerleukin-1, a shock-like state and tissue injury in rabbits without endotoxemia. *J. Clin. Invest.*, **87,** 1925–1935.

(Received October 17, 1994
Revised December 5, 1994
Accepted December 6, 1994)

Erratum

Br. J. Pharmacol. (1994) **113,** 439–444

R. Gniadecki, M. Gniadecki & J. Serup. Inhibition of glucocorticoid-induced epidermal and dermal atrophy with KH 1060-a potent 20-epi analogue of 1,25-dihydroxyvitamin D_3

In the above paper, the legend to Figure 6 was published incorrectly. The publishers would like to apologise for any inconvenience this may have caused. The correct version is reproduced below.

Figure 6 Effect of KH 1060 on incorporation of [^{35}S]-sulphate into glycosaminoglycans and synthesis of hydroxyproline from [^{3}H]-proline in the skin treated with betamethasone-17-valerate. Skin was treated on the contralateral sides of the back with 2.5 nmol cm^{-2} betamethasone and 2.5 nmol cm^{-2} betamethasone and KH 1060 (0.625–6.25 pmol cm^{-2}). Open and cross-hatched columns represent respectively: ^{35}S and ^{3}H labelling of the control skin treated only with betamethasone-17-valerate. Hatched and solid columns show ^{35}S and ^{3}H-labelling in the KH 1060 treated sites, respectively. Each column represents mean ($n = 6$) with s.e.mean. Ordinate: specific radioactivity in disintegrations per minute per cm^2 of the skin. $^*P < 0.05$ vs control.

British Journal of Pharmacology

VOLUME 114 (6) MARCH 1995

SPECIAL REPORTS

S. Mariotto, L. Cuzzolin, A. Adami, P. Del Soldato, H. Suzuki & G. Benoni. Inhibition by sodium nitroprusside of the expression of inducible nitric oxide synthase in rat neutrophils 1105

C. Davidson & J.A. Stamford. Evidence that 5-hydroxytryptamine release in rat dorsal raphé nucleus is controlled by 5-HT_{1A}, 5-HT_{1B} and 5-HT_{1D} autoreceptors 1107

PAPERS

A.P. Davenport, G. O'Reilly & R.E. Kuc. Endothelin ET_A and ET_B mRNA and receptors expressed by smooth muscle in the human vasculature: majority of the ET_A sub-type 1110

R. Cirillo, A.R. Renzetti, P. Cucchi, M. Guelfi, A. Salimbeni, S. Caliari, A. Castellucci, S. Evangelista, A. Subissi & A. Giachetti. Pharmacology of LR-B/081, a new highly potent, selective and orally active, nonpeptide angiotensin II AT_1 receptor antagonist 1117

S.J. Bailey & S.M.O. Hourani. Effects of suramin on contractions of the guinea-pig vas deferens induced by analogues of adenosine 5'-triphosphate 1125

G.B. Willars & S.R. Nahorski. Quantitative comparisons of muscarinic and bradykinin receptor-mediated Ins(1,4,5)P_3 accumulation and Ca^{2+} signalling in human neuroblastoma cells 1133

S. Boehm, S. Huck, K. Schwarz, E. Agneter, H. Drobny & E.A. Singer. Rapid, agonist-induced desensitization of α_2-autoreceptors modulating transmitter release 1143

P. Santicioli, G. Carganico, S. Meini, S. Giuliani, A. Giachetti & C.A. Maggi. Modulation by stereoselective inhibition of cyclo-oxygenase of electromechanical coupling in the guinea-pig isolated renal pelvis 1149

M. Lipartiti, R. Arban, E. Fadda, A. Zanotti & P. Giusti. Characterization of [^{3}H]-imidazenil binding to rat brain membranes 1159

T. Ohta, K. Kawai, S. Ito & Y. Nakazato. Ca^{2+} entry activated by emptying of intracellular Ca^{2+} stores in ileal smooth muscle of the rat 1165

D. Salvemini, S.L. Settle, J.L. Masferrer, K. Seibert, M.G. Currie & P. Needleman. Regulation of prostaglandin production by nitric oxide; an *in vivo* analysis 1171

J.G. De Man, G.E. Boeckxstaens, B.Y. De Winter, T.G. Moreels, M.E. Misset, A.G. Herman & P.A. Pelckmans. Comparison of the pharmacological profile of S-nitrosothiols, nitric oxide and nitrergic neurotransmitter in the canine ileocolonic junction 1179

S.E. Telford, A.I. Smith, R.A. Lew, R.B. Perich, A.C. Madden & R.G. Evans. Role of angiotensin converting enzyme in the vascular effects of an endopeptidase 24.15 inhibitor 1185

S. Farkas & H. Ono. Participation of NMDA and non-NMDA excitatory amino acid receptors in the mediation of spinal reflex potentials in rats: an *in vivo* study 1193

P. Valeri, L.A. Morrone, L. Romanelli & M.C. Amico. Acute withdrawal after bremazocine and the interaction between μ- and κ-opioid receptors in isolated gut tissues 1206

C.H. Gill, J.A. Peters & J.J. Lambert. An electrophysiological investigation of the properties of a murine recombinant 5-HT_3 receptor stably expressed in HEK 293 cells 1211

T. Kobayashi, G. Mikala & A. Yatani. A novel enhancing effect of clofilium on transient outward-type cloned cardiac K^+ channel currents 1222

S.-M. Yu, Z.-J. Cheng & S.-C. Kuo. Antiproliferative effects of A02011-1, an adenylyl cyclase activator, in cultured vascular smooth muscle cells of rat 1227

G.M. James & W.C. Hodgson. Potentiation by endothelin-1 of 5-hydroxytryptamine responses in aortae from streptozotocin-diabetic rats: a role for thromboxane A_2 1236

M.H. Richards & P.L.M. van Giersbergen. Human muscarinic receptors expressed in A9L and CHO cells: activation by full and partial agonists 1241

A. Ueno, H. Ishida & S. Oh-ishi. Comparative study of endotoxin-induced hypotension in kininogen-deficient rats with that in normal rats 1250

G. Deliconstantinos, V. Villiotou & J.C. Stavrides. Release by ultraviolet B (u.v.B) radiation of nitric oxide (NO) from human keratinocytes: a potential role for nitric oxide in erythema production 1257

C. Toma, P.E. Jensen, D. Prieto, A. Hughes, M.J. Mulvany & C. Aalkjær. Effects of tyrosine kinase inhibitors on the contractility of rat mesenteric resistance arteries 1266

C.-C. Wu, C. Thiemermann & J.R. Vane. Glibenclamide-induced inhibition of the expression of inducible nitric oxide synthase in cultured macrophages and in the anaesthetized rat 1273

M. Shimizu, A. Nishida, H. Fukuda, H. Saito & S. Yamawaki. Enhancement of cyclic AMP accumulation mediated by 5-HT after chronic amitriptyline treatment in NG 108-15 cells 1282

M. Kageyama, T. Yanagisawa & N. Taira. Effects of semotiadil fumarate, a novel Ca^{2+} antagonist, on cytosolic Ca^{2+} level and force of contraction in porcine coronary arteries 1289

M. Ocaña, E. Del Pozo, M. Barrios & J.M. Baeyens. Subgroups among μ-opioid receptor agonists distinguished by ATP-sensitive K^+ channel-acting drugs 1296

E.M. van Gelderen, E.L.E. De Bruijne, H.J. Agteresch & P.R. Saxena. The effect of nitric oxide donors on haemodynamics and blood flow distribution in the porcine carotid circulation 1303

J. Culman, B. Wiegand, H. Spitznagel, S. Klee & T. Unger. Effects of the tachykinin NK_1 receptor antagonist, RP 67580, on central cardiovascular and behavioural effects of substance P, neurokinin A and neurokinin B 1310

S.J. De Kimpe, M.L. Hunter, C.E. Bryant, C. Thiemermann & J.R. Vane. Delayed circulatory failure due to the induction of nitric oxide synthase by lipoteichoic acid from *Staphylococcus aureus* in anaesthetized rats 1317

STOCKTON

BRITISH JOURNAL OF PHARMACOLOGY

The *British Journal of Pharmacology* welcomes contributions in all fields of experimental pharmacology including neuroscience, biochemical, cellular and molecular pharmacology. The Board of Editors represents a wide range of expertise and ensures that well-presented work is published as promptly as possible, consistent with maintaining the overall quality of the journal.

Edited for the British Pharmacological Society by

A.T. Birmingham
(Chairman)

R.W. Horton **W.A. Large**
(Secretaries)

Submission of manuscripts: Manuscripts (two copies) should be sent to The Editorial Office, British Journal of Pharmacology, St. George's Hospital Medical School, Cranmer Terrace, London SW17 0RE.

Authors should consult the Instructions to Authors and the Nomenclature Guidelines for Authors in Vol. **114,** 245–255. These Instructions and Guidelines also appear with the journal Index for Volumes **111–113**, 1994. A checklist of the essential requirements is summarised in each issue of the journal, or as the last page of the issue.

The *British Journal of Pharmacology* is published by Stockton Press, a division of Macmillan Press Ltd. It is the official publication of the British Pharmacological Society.

Scope The *British Journal of Pharmacology* is published twice a month. It welcomes contribution in all field of experimental pharmacology including neuroscience, biochemical, cellular and molecular pharmacology. The Board of Editors represents a wide range of expertise and ensures that well-presented work is published as promptly as possible, consistent with maintaining the overall quality of the journal

This journal is covered by Current Contents, Excerpta Medica, BIOSIS and Index Medicus.

Editorial Manuscripts (plus two copies) and all editorial correspondence should be sent to: The Editorial Office, British Journal of Pharmacology, St George's Hospital Medical School, Cranmer Terrace, London SW17 0RE, UK. Tel: +44 (0)181 767 6765; Fax: +44 (0)181 767 5645.

Advertisements Enquiries concerning advertisements should be addressed to: Michael Rowley, Hasler House, High Street, Great Dunmow, Essex CM6 1AP, UK. Tel: +44 (0)1371 874613; Fax: +44 (0)1371 872273.

Publisher All business correspondence, supplement enquiries and reprint requests should be addressed to British Journal of Pharmacology, Stockton Press, Houndmills, Basingstoke, Hampshire RG21 2XS, UK. Tel: +44 (0)1256 29242; Fax: +44 (0)1256 810526. Publisher: Marija Vukovojac. Editorial Assistant: Alice Ellingham. Production Controller: Tony Holton.

Subscriptions – EU/Rest of World Subscription price per annum (3 volumes, 24 issues) £620, rest of world £820 (Airmail), £685 (Surface mail) or equivalent in any other currency. Orders must be accompanied by remittance. Cheques should be made payable to Macmillan Magazines and sent to: The Subscription Department, Macmillan Press Ltd, Houndmills, Basingstoke, Hampshire RG21 2XS, UK. Where appropriate, subscribers may make payments into UK Post Office Giro Account No. 519 2455. Full details must accompany the payment. Subscribers from EU territories should add sales tax at the local rate.

Subscriptions – USA USA subscribers call toll free 1-800-221-2123 or send check/money order/credit card details to: Stockton Press, 49, West 24th Street, New York, NY 10010; Tel: 212 627 5757, Fax: 212 627 9256. USA annual subscription rates: $1230 Airmail; $1030 Surface (Institutional/Corporate); $225 (Individual making personal payment).

British Journal of Pharmacology (ISSN 0007–1188) is published twice a month by Macmillan Press Ltd, c/o Mercury Airfreight International Ltd, 2323 Randolph Avenue, Avenel, NJ 07001, USA. Subscription price for institutions is $1030 per annum (surface). 2nd class postage is paid at Rahway NJ. Postmaster: send address corrections to Macmillan Press Ltd, c/o Mercury Airfreight International Ltd, 2323 Randolph Avenue, Avenel NJ 07001.

Reprints of any article in this journal are available from Stockton Press, Houndmills, Basingstoke, Hampshire RG21 2XS, UK. Tel: +44 (0)1256 29242; Fax: +44 (0)1256 810526.

ISSN 0007–1188

PREPARATION OF MANUSCRIPTS

Authors are strongly recommended to read the full *Instructions to Authors* and *Nomenclature Guidelines for Authors* (*Br. J. Pharmacol.* 1995, **114,** 245–255) before submitting a manuscript for publication in the *British Journal of Pharmacology*. The manuscript and cover letter should be checked against the following list before mailing.

The original and one copy of the manuscript must be supplied. Manuscripts must be typed in double-line spacing on one side of A4 paper, in type not smaller than 12 characters per inch or 10 point. Both copies to include Tables and a set of labelled Figures. One set of Figures without numbers or letters is also to be included. The text to be arranged in the following subsections:

1. **Title**—To have no more than 150 characters on a separate page, which should also include a Short Title (50 characters maximum) and the name and address of the author for correspondence.
2. **Summary**—To be arranged in numbered paragraphs (Full Papers) or a single paragraph (Special Reports).
   —to include aims, principal results and conclusions.
   —to include Key words (10 maximum) at end of summary.
3. **Introduction**—To contain concise statements of the problem and the aims of the investigation.
4. **Methods**—To have brief but adequate account of the procedures; *full names of drugs (including those referred to by manufacturer's code)*, sources of drugs and statistical tests to be stated.
5. **Results**—To have no repetition of data in Figures, Tables and text.
6. **Discussion**—Findings and conclusions to be placed in context of other relevant work.
   NB Simple repetition of results and unwarranted speculation are not acceptable.
7. **Acknowledgements**—Sources of support. Sources of drugs not widely available commercially.
8. **References**—All references in the text to be included in the Reference List and *vice versa*. References in alphabetical order with complete citations; Journals publishing 'in press' papers identified.
   References to manuscripts submitted to other journals but not yet accepted are not allowed.
9. **Tables**—Each on a separate page and prepared in accordance with current requirements of the Journal.
10. **Figures**—Both labelled and non-labelled Figures to be prepared in accordance with current requirements of the Journal (see *Instructions to Authors*, 1995, **114,** 245–251) and provided with Figure Number and Authors' names on back (*in pencil*).
    —each legend to be typed on a separate page and carrying keys to symbols.
    —keys to symbols and histograms must not appear on the figures themselves, but in the respective legends.
    —'box style' figures are not in keeping with the Journal style; line drawings etc must have only left-hand and bottom axes.
11. **Manuscripts**—To be accompanied by a declaration signed by each author that
    (a) results are original
    (b) approval of all persons concerned has been given to submit manuscripts for consideration (see also 12b)
    (c) the same material is neither 'in press' (i.e. is in proof or has definitely been accepted for publication) nor under consideration elsewhere. Furthermore it will not be submitted or published elsewhere before a decision has been reached by the Editorial Board of the *British Journal of Pharmacology* and will not be submitted elsewhere if accepted by the *British Journal of Pharmacology*.
    (d) Copyright assignment is included.
12. **Cover letter**—To state clearly
    (a) Corresponding author's full postal address, telephone, telex or Fax number
    (b) where appropriate, that *either* ethical approval has been given for investigation *or* Company or Institutional permission to publish work has been received.
13. **Reminder**—Packaging to be sufficiently robust to protect Figures and to withstand mailing.

Failure to comply with *Instructions to Authors* may lead to substantial delays in processing, review and publication and may even jeopardize acceptance of the manuscript.

NOMENCLATURE

Authors are reminded that accepted receptor and associated terminology is laid out in *Nomenclature Guidelines for Authors*, as published in the *British Journal of Pharmacology*, *Br. J. Pharmacol.*, 1995, **114,** 253–255.

SPECIAL REPORTS

The purpose of *Special Reports* is to provide rapid publication for **new** and **important** results which the Editorial Board considers are likely to be of special pharmacological significance. *Special Reports* will have publication priority over all other material and so authors are asked to consider carefully the status of their work before submission.

In order to speed publication there is normally no revision allowed beyond very minor typographical or grammatical corrections. If significant revision is required, the Board may either invite rapid re-submission or, more probably, propose that it be re-written as a Full Paper and be re-submitted for consideration. In order to reduce delays, proofs of *Special Reports* will be sent to authors but **essential corrections must reach the Production Office within 48 hours of receipt.** Authors should ensure that their submitted material conforms exactly to the following requirements.

Special Reports should normally occupy no more than two printed pages of the Journal; two illustrations (Figures or Tables, with legends) are permitted. As a guideline, with type face of 12 pitch and double-line spacing, a page of A4 paper could contain about 400 words. The absolute maximum length of the *Special Report* is 1700 words. For each Figure or Table, please deduct 200 words. The manuscript should comprise a Title page with key words (maximum of 10), a Summary consisting of a single short paragraph, followed by Introduction, Methods, Results, Discussion and References (maximum of 10). In all other respects, the requirements are the same as for Full Papers (see current 'Instructions to Authors').

BRITISH JOURNAL OF PHARMACOLOGY VOLUME 114 (6) 1995

SPECIAL REPORTS

S. Mariotto, L. Cuzzolin, A. Adami, P. Del Soldato, H. Suzuki & G. Benoni. Inhibition by sodium nitroprusside of the expression of inducible nitric oxide synthase in rat neutrophils 1105

C. Davidson & J.A. Stamford. Evidence that 5-hydroxytryptamine release in rat dorsal raphé nucleus is controlled by 5-HT_{1A}, 5-HT_{1B} and 5-HT_{1D} autoreceptors 1107

PAPERS

A.P. Davenport, G. O'Reilly & R.E. Kuc. Endothelin ET_A and ET_B mRNA and receptors expressed by smooth muscle in the human vasculature: majority of the ET_A sub-type 1110

R. Cirillo, A.R. Renzetti, P. Cucchi, M. Guelfi, A. Salimbeni, S. Caliari, A. Castellucci, S. Evangelista, A. Subissi & A. Giachetti. Pharmacology of LR-B/081, a new highly potent, selective and orally active, nonpeptide angiotensin II AT_1 receptor antagonist 1117

S.J. Bailey & S.M.O. Hourani. Effects of suramin on contractions of the guinea-pig vas deferens induced by analogues of adenosine 5'-triphosphate 1125

G.B. Willars & S.R. Nahorski. Quantitative comparisons of muscarinic and bradykinin receptor-mediated $Ins(1,4,5)P_3$ accumulation and Ca^{2+} signalling in human neuroblastoma cells 1133

S. Boehm, S. Huck, K. Schwarz, E. Agneter, H. Drobny & E.A. Singer. Rapid, agonist-induced desensitization of α_2-autoreceptors modulating transmitter release 1143

P. Santicioli, G. Carganico, S. Meini, S. Giuliani, A. Giachetti & C.A. Maggi. Modulation by stereoselective inhibition of cyclo-oxygenase of electromechanical coupling in the guinea-pig isolated renal pelvis 1149

M. Lipartiti, R. Arban, E. Fadda, A. Zanotti & P. Giusti. Characterization of [^{3}H]-imidazenil binding to rat brain membranes 1159

T. Ohta, K. Kawai, S. Ito & Y. Nakazato. Ca^{2+} entry activated by emptying of intracellular Ca^{2+} stores in ileal smooth muscle of the rat 1165

D. Salvemini, S.L. Settle, J.L. Masferrer, K. Seibert, M.G. Currie & P. Needleman. Regulation of prostaglandin production by nitric oxide; an *in vivo* analysis 1171

J.G. De Man, G.E. Boeckxstaens, B.Y. De Winter, T.G. Moreels, M.E. Misset, A.G. Herman & P.A. Pelckmans. Comparison of the pharmacological profile of S-nitrosothiols, nitric oxide and nitrergic neurotransmitter in the canine ileocolonic junction 1179

S.E. Telford, A.I. Smith, R.A. Lew, R.B. Perich, A.C. Madden & R.G. Evans. Role of angiotensin converting enzyme in the vascular effects of an endopeptidase 24.15 inhibitor 1185

S. Farkas & H. Ono. Participation of NMDA and non-NMDA excitatory amino acid receptors in the mediation of spinal reflex potentials in rats: an *in vivo* study 1193

P. Valeri, L.A. Morrone, L. Romanelli & M.C. Amico. Acute withdrawal after bremazocine and the interaction between μ- and κ-opioid receptors in isolated gut tissues 1206

C.H. Gill, J.A. Peters & J.J. Lambert. An electrophysiological investigation of the properties of a murine recombinant 5-HT_3 receptor stably expressed in HEK 293 cells 1211

T. Kobayashi, G. Mikala & A. Yatani. A novel enhancing effect of clofilium on transient outward-type cloned cardiac K^+ channel currents 1222

S.-M. Yu, Z.-J. Cheng & S.-C. Kuo. Antiproliferative effects of A02011-1, an adenylyl cyclase activator, in cultured vascular smooth muscle cells of rat 1227

G.M. James & W.C. Hodgson. Potentiation by endothelin-1 of 5-hydroxytryptamine responses in aortae from streptozotocin-diabetic rats: a role for thromboxane A_2 1236

M.H. Richards & P.L.M. van Giersbergen. Human muscarinic receptors expressed in A9L and CHO cells: activation by full and partial agonists 1241

A. Ueno, H. Ishida & S. Oh-ishi. Comparative study of endotoxin-induced hypotension in kininogen-deficient rats with that in normal rats 1250

G. Deliconstantinos, V. Villiotou & J.C. Stavrides. Release by ultraviolet B (u.v.B) radiation of nitric oxide (NO) from human keratinocytes: a potential role for nitric oxide in erythema production 1257

C. Toma, P.E. Jensen, D. Prieto, A. Hughes, M.J. Mulvany & C. Aalkjær. Effects of tyrosine kinase inhibitors on the contractility of rat mesenteric resistance arteries 1266

C.-C. Wu, C. Thiemermann & J.R. Vane. Glibenclamide-induced inhibition of the expression of inducible nitric oxide synthase in cultured macrophages and in the anaesthetized rat 1273

M. Shimizu, A. Nishida, H. Fukuda, H. Saito & S. Yamawaki. Enhancement of cyclic AMP accumulation mediated by 5-HT after chronic amitriptyline treatment in NG 108-15 cells 1282

M. Kageyama, T. Yanagisawa & N. Taira. Effects of semotiadil fumarate, a novel Ca^{2+} antagonist, on cytosolic Ca^{2+} level and force of contraction in porcine coronary arteries 1289

M. Ocaña, E. Del Pozo, M. Barrios & J.M. Baeyens. Subgroups among μ-opioid receptor agonists distinguished by ATP-sensitive K^+ channel-acting drugs 1296

E.M. van Gelderen, E.L.E. De Bruijne, H.J. Agteresch & P.R. Saxena. The effect of nitric oxide donors on haemodynamics and blood flow distribution in the porcine carotid circulation 1303

J. Culman, B. Wiegand, H. Spitznagel, S. Klee & T. Unger. Effects of the tachykinin NK_1 receptor antagonist, RP 67580, on central cardiovascular and behavioural effects of substance P, neurokinin A and neurokinin B 1310

S.J. De Kimpe, M.L. Hunter, C.E. Bryant, C. Thiemermann & J.R. Vane. Delayed circulatory failure due to the induction of nitric oxide synthase by lipoteichoic acid from *Staphylococcus aureus* in anaesthetized rats 1317

STOCKTON

Typeset by Elite Typesetting Techniques, Eastleigh, Hants
and printed in Great Britain by Unwin Brothers Ltd., The Gresham Press, Old Woking, Surrey